frontiers | Research Topics

# Can traditional Chinese medicines affect endocrine diseases via effects on the intestinal flora?

**Edited by**
Zhoujin Tan, Xinhua Shu
and Guang Chen

**Published in**
Frontiers in Endocrinology

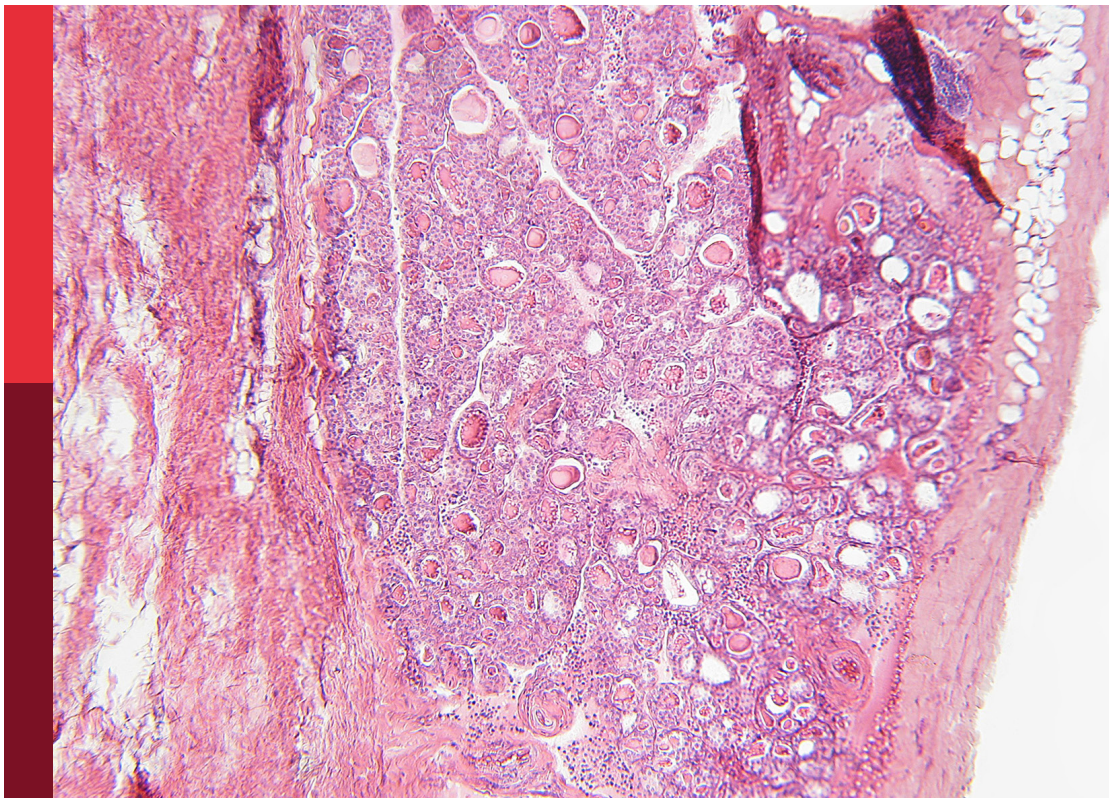

ISSN 1664-8714
ISBN 978-2-8325-4448-8
DOI 10.3389/978-2-8325-4448-8

## About Frontiers

Frontiers is more than just an open access publisher of scholarly articles: it is a pioneering approach to the world of academia, radically improving the way scholarly research is managed. The grand vision of Frontiers is a world where all people have an equal opportunity to seek, share and generate knowledge. Frontiers provides immediate and permanent online open access to all its publications, but this alone is not enough to realize our grand goals.

## Frontiers journal series

The Frontiers journal series is a multi-tier and interdisciplinary set of open-access, online journals, promising a paradigm shift from the current review, selection and dissemination processes in academic publishing. All Frontiers journals are driven by researchers for researchers; therefore, they constitute a service to the scholarly community. At the same time, the *Frontiers journal series* operates on a revolutionary invention, the tiered publishing system, initially addressing specific communities of scholars, and gradually climbing up to broader public understanding, thus serving the interests of the lay society, too.

## Dedication to quality

Each Frontiers article is a landmark of the highest quality, thanks to genuinely collaborative interactions between authors and review editors, who include some of the world's best academicians. Research must be certified by peers before entering a stream of knowledge that may eventually reach the public - and shape society; therefore, Frontiers only applies the most rigorous and unbiased reviews. Frontiers revolutionizes research publishing by freely delivering the most outstanding research, evaluated with no bias from both the academic and social point of view. By applying the most advanced information technologies, Frontiers is catapulting scholarly publishing into a new generation.

## What are Frontiers Research Topics?

Frontiers Research Topics are very popular trademarks of the *Frontiers journals series*: they are collections of at least ten articles, all centered on a particular subject. With their unique mix of varied contributions from Original Research to Review Articles, Frontiers Research Topics unify the most influential researchers, the latest key findings and historical advances in a hot research area.

Find out more on how to host your own Frontiers Research Topic or contribute to one as an author by contacting the Frontiers editorial office: frontiersin.org/about/contact

# Can traditional Chinese medicines affect endocrine diseases via effects on the intestinal flora?

**Topic editors**

Zhoujin Tan — Hunan University of Chinese Medicine, China
Xinhua Shu — Glasgow Caledonian University, United Kingdom
Guang Chen — Huazhong University of Science and Technology, China

**Citation**

Tan, Z., Shu, X., Chen, G., eds. (2024). *Can traditional Chinese medicines affect endocrine diseases via effects on the intestinal flora?* Lausanne: Frontiers Media SA. doi: 10.3389/978-2-8325-4448-8

# Table of contents

frontiers | Frontiers in Endocrinology

TYPE Editorial
PUBLISHED 16 May 2023
DOI 10.3389/fendo.2023.1193396



OPEN ACCESS

EDITED AND REVIEWED BY
Jeff M. P. Holly,
University of Bristol, United Kingdom

*CORRESPONDENCE
Xinhua Shu
Xinhua.Shu@gcu.ac.uk
Zhoujin Tan
tanzhjin@sohu.com

RECEIVED 24 March 2023
ACCEPTED 04 May 2023
PUBLISHED 16 May 2023

CITATION
Shu X, Chen G and Tan Z (2023) Editorial: Can traditional Chinese medicines affect endocrine diseases via effects on the intestinal flora? *Front. Endocrinol.* 14:1193396. doi: 10.3389/fendo.2023.1193396



# Editorial: Can traditional Chinese medicines affect endocrine diseases via effects on the intestinal flora?

Xinhua Shu[1,2,3]*, Guang Chen[4] and Zhoujin Tan[5]*

[1]Pu Ai Medical School, Shaoyang University, Shaoyang, China, [2]Department of Biological and Biomedical Sciences, Glasgow Caledonian University, Glasgow, United Kingdom, [3]Department of Vision Science, Glasgow Caledonian University, Glasgow, United Kingdom, [4]Department of Integrated Traditional Chinese and Western Medicine, Tongji Hospital, Tongji Medical College, Huazhong University of Science and Technology, Wuhan, China, [5]College of Chinese Medicine, Hunan University of Chinese Medicine, Changsha, Hunan, China

KEYWORDS

**endocrine disorder, traditional Chinese medicine, gut microbiota, therapy, molecular mechanisms**

Editorial on the Research Topic
Can traditional Chinese medicines affect endocrine diseases via effects on the intestinal flora?

Human gut microbiota is a complex and dynamic ecosystem, containing over 1500 microbial species and comprising appropriately 9.9 million microbial genes (1, 2). The diversity of human gut microbiota rapidly expands from infancy to early childhood, then the expansion slows down during preadolescence; the diversity remains quite stable in adulthood but gradually decreases with ageing (3). Various factors, including host genetic features and environmental influences, regulate gut microbiota diversity, among which diet is considered to be a predominant factor. Gut microbiota has multiple functions, including maintenance of the structural integrity of the gut mucosal barrier; suppression of pathogen overgrowth; regulation of host immune response, endocrine and neurologic signalling pathways; metabolism of host nutrients, bile salts and xenobiotic substances; elimination of exogenous toxins; and synthesis of neurotransmitters, vitamins and other uncharacterized compounds (3). Disruption of gut microbiota diversity and function, termed as dysbiosis, is associated with a wide range of human diseases, such as endocrine and neurodegenerative diseases (3).

Traditional Chinese medicine (TCM) has been widely used for the prevention and treatment of human disease in China and other Asian countries over thousands of years (4). Currently, TCM is recognized as the most important alternative to Western medicine. TCM formulas contain a variety of functional compounds, particularly polysaccharides and polyphenols. Oral administration of TCM leads directly or indirectly to interaction between TCM and gut microbiota. TCM bioactive ingredients can regulate the diversity and function of gut microbiota, while enzymes produced by gut microbiota participate in the metabolization of TCM. The resultant metabolites have shown therapeutic effects in a wide range of diseases, including endocrine conditions (4). However, the underlying mechanisms are not fully understood. The current Research Topic aims to collect recent

progress in elucidating the functional interplay between TCM and gut microbiota in treating endocrine diseases. We welcomed original research and review papers concerning the molecular mechanisms and protective effects of TCM-mediated treatments in animal models and/or patients with endocrine diseases. We collected 6 review articles and 14 original research papers.

Diabetes mellitus is the commonest endocrine disease and is characterized by deficient insulin production or insulin resistance. There are two types of diabetes: type 1 and type 2 diabetes. In the former, destruction of pancreatic beta cells results in reduced insulin production; in the latter, less insulin is produced or the insulin is less effective. Gut microbiota also plays an important role in diabetes. TCM treatment has been shown to regulate gut microbiota composition and function. Su et al. discussed the correlation of gut microbiota with type 2 diabetes, and the effects of individual Chinese herb ingredients (polysaccharides, saponins, polyphenols, alkaloids and flavonoids) and medicinal plant extracts (licorice and *Sargassum fusiforme*) on gut microbiota balance in diabetic rodent models. The authors also give examples of TCM formulas, including Huang-Lian-Jie-Du decoction, Xie-Xin decoction, Ge-Gen-Qin-Lian decoction, Pi-Dan-Jian-Qing decoction, Shen-Ling-Bai-Zhu powder, Shen-Qi compound, Liu-Wei-Di-Huang pills, San-Huang-Yi-Shen capsule and Tang-Nai-Kang, which have been show to effectively counteract diabetes in diabetic rodent models, at least in part *via* positive regulation of gut microbiota. He et al. further discussed the protective function of berberine, a member of the alkaloid group, against type 2 diabetes. The antidiabetic capacity of berberine is at least in part mediated by the regulation of gut microbiota. Berberine can inhibit opportunistic pathogen growth, induce death of harmful gut microbiota, and promote proliferation of beneficial bacteria. Berberine treatment can increase synthesis of short chain fatty acid (SCFA) in the intestine and help to maintain the integrity and function of the intestinal barrier. Furthermore, berberine can enhance metabolism of bile acid and amino acids in the intestine. The authors also updated the literature related to the protective effects of berberine against diabetes-associated metabolic disorders in clinical trials. Li et al. reported that Huang Lian extract, which contains multiple functional compounds, including berberine, had protective effects against type 2 diabetes *via* a shifting of the composition of the gut microbiota by enriching bacterial species associated with bile acid metabolism. In addition, *Inonotus obliguus* extract and individual compound (chlorogenic acid) demonstrated similar protection against diabetes in db/db mice by regulating gut microbiota composition (Yan et al.; Ye et al.). Additionally, Shi et al. and Huang et al. demonstrated that salidroside (the predominant active component isolated from Rhodiola) and Zuogui Jiangtang Shuxin formula alleviated, respectively, diabetic cardiomyopathy and improved myocardial function in diabetic mouse models, possibly in part mediated by remodelling the structure of gut microbiota. Obesity is closely associated with type 2 diabetes. Extensive evidence suggests that obesity is linked to disruption of gut microbiota and impairment of gut barrier function. Li et al. reviewed literature concerning the regulation of gut microbiota by TCM in obesity. TCM ingredients can enhance the abundance of gut microbiota and the generation of beneficial metabolites, regulate lipid metabolism and decrease fat accumulation, and counteract high-fat-induced inflammation. Hu reported that *Grifola frondosa* powder had anti-obesity capacity by regulating the structure and composition of gut microbiota and increasing production of SCFA.

Non-alcoholic fatty liver disease (NAFLD) is the most common chronic liver disease and is characterized by the presence of steatosis in the absence of over-consumption of alcohol. NAFLD is a complex disease, associated with other metabolic disorders such as obesity, diabetes and hyperlipidemia (5). Data from NAFLD patients and rodent models has shown dysbiosis is associated with NAFLD (Guo et al.). Individual TCM compounds or TCM decoctions can repair intestinal barrier function, inhibit growth of pathogenic bacteria in the intestine, suppress inflammation, and decrease lipid deposition in the liver, leading to alleviated liver steatosis in NAFLD animal models (Guo et al.). Lv et al. reported the protective effect of Qingrequzhuo capsule against nonalcoholic steatohepatitis (NASH), a type of NAFLD, in mice fed with methionine and choline deficient diet. The diversity of gut microbiota was decreased in NASH mice; Qingrequzhuo treatment reversed the effect. Colonic permeability was significantly reduced in Qingrequzhuo-treated NASH mice, compared to untreated NASH mice. Qingrequzhuo treatment also downregulated expression of proinflammatory cytokines in the liver of NASH mice *via* inactivation of the TLR4/NF-kB signalling pathway (Lv et al.). In a clinical trial, Hui et al. assessed the beneficial effect of a 'spleen-strengthening' and 'liver-draining' herbal formula in NAFLD patients. The authors found that the formula improved liver function and glycolipid metabolism, and alleviated fatigue symptom. These protective effects of this formula were mediated by regulating the disturbance of gut microbiota in NAFLD patients (Hui et al.). Additionally, Liu et al. demonstrated that a combination of polysaccharides from *Astragalus membranaceus* and *Hippophae rhamnoides* alleviated liver pathology and repaired disturbance of gut microbiota in mice with alcoholic fatty liver disease.

This Research Topic also collected papers related to other endocrine-associated disorders. Liu et al. reviewed the literature concerning the relation between gut microbiota and polycystic ovary syndrome (PCOS), a common reproductive endocrine disorder. PCOS is associated with hyperandrogenemia, insulin resistance, obesity, and chronic inflammation. It is well documented that gut microbiota regulates these PCOS-associated risk factors, so indicating that gut microbiota has a direct and/or indirect relationship with PCOS (Liu et al.). Ping et al. investigated the effect of *Atractylodis macrocephalae rhizoma* polysaccharide on mammary gland hyperplasia and found that polysaccharide treatment exhibited therapeutic effects against mammary gland hyperplasia in rats by decreasing the production of estradiol and prolactin, increasing the progesterone level, and regulating the diversity and abundance of gut flora; the same group also developed microneedles loaded with aqueous extract of *Atractylodis macrocephalae rhizome* and found that the microneedles had similar protective effects on mammary gland

hyperplasia and on gut microbiota as the polysaccharide (Ping et al.). Xia et al. evaluated the effect of Si-Jun-Zi decoction (SJZD) on diarrhoea-predominant irritable bowel syndrome (IBS-D) by co-culturing SJZD with intestinal microbiota from healthy controls and IBS-D patients. The authors found that co-culture with SJZD reversed IBS-D associated dysbiosis and regulated the production of bacterial metabolites that are functionally linked to IBS-D-associated neurotransmitters. Shang et al. compared the difference in gut microbiota in patients with metabolic syndromes associated with TCM: specifically, qi-yin deficiency syndrome (QYDS) or phlegm-dampness syndrome (PDS). QYDS refers to the damage of both Yang Qi and Yin liquid in the body and is characterized by shortness of breath, chest pain, spontaneous sweating, and fatigue; PDS refers to spleen deficiency and formation of phlegm overtime with main symptoms of coughing, phlegm accumulation and chest tightness. The authors found that there was significant difference in gut microbiota structure between the two patient groups. The authors also noticed that there was correlation between gut microbiota genera and clinical phenotypes in both patient groups. Aging is a complex metabolic process that is associated with dynamic changes in host gut microbiota. Liu et al. showed an anti-aging capacity of *Dubosiella newyorkensis* in aged mice by inhibiting oxidative stress and inflammation and promoting growth of beneficial genus.

In summary, the articles in this Research Topic collection provide novel insights into the functions and underlying mechanisms of TCM in treating endocrine disorders. The Research Topic will contribute to the development of new TCM treatment for a wide range of endocrine disorders and strengthen the dissemination of TCM knowledge to the international community.

## Author contributions

XS wrote the editorial. ZT and GC read and revised the editorial. All authors contributed to the article and approved the submitted version.

## Acknowledgments

We thank all the reviewers for their effort to assess these manuscripts for this Research Topic collection. We acknowledge funding support from the Locus Scholarship Program of Hunan Province, China (2019-23 to XS), the TENOVUS Scotland (S20-02 to XS), the Chief Scientist Office/the RS Macdonald Charitable Trust (SNRF2021 to XS) and the Sight Research UK (SAC037 to XS).

## Conflict of interest

The authors declare that the research was conducted in the absence of any commercial or financial relationships that could be construed as a potential conflict of interest.

## Publisher's note



## References

1. Lagier JC, Khelaifia S, Alou MT, Ndongo S, Dione N, Hugon P, et al. Culture of previously uncultured members of the human gut microbiota by culturomics. *Nat Microbiol* (2016) 1(12):16203. doi: 10.1038/nmicrobiol.2016.203

2. Li J, Jia H, Cai X, Zhong H, Feng Q, Sunagawa S, et al. An integrated catalog of reference genes in the human gut microbiome. *Nat Biotechnol* (2014) 32(8):834–41. doi: 10.1038/nbt.2942

3. Lynch SV, Pedersen O. The human intestinal microbiome in health and disease. *N Engl J Med* (2016) 375(24):2369–79. doi: 10.1056/NEJMra1600266

4. Feng W, Ao H, Peng C, Yan D. Gut microbiota, a new frontier to understand traditional Chinese medicines. *Pharmacol Res* (2019) 142:176–91. doi: 10.1016/j.phrs.2019.02.024

5. Powell EE, Wong VWS, Rinella M. Non-alcoholic fatty liver disease. *Lancet* (2021) 397(10290):2212–24. doi: 10.1016/S0140-6736(20)32511-3

frontiers | Frontiers in Endocrinology

TYPE Original Research
PUBLISHED 23 September 2022
DOI 10.3389/fendo.2022.1014577



OPEN ACCESS

EDITED BY
Zhoujin Tan,
Hunan University of Chinese Medicine, China

REVIEWED BY
Xueying Tao,
Nanchang University, China
Hongxia Zhang,
Yantai University, China

*CORRESPONDENCE
Tian Hang Feng
f_tianhang@163.com
Jin Shang
935516165@qq.com

†These authors have contributed equally to this work

SPECIALTY SECTION
This article was submitted to Gut Endocrinology, a section of the journal Frontiers in Endocrinology

RECEIVED 08 August 2022
ACCEPTED 29 August 2022
PUBLISHED 23 September 2022

CITATION
Shi J, Zhao Q, Hao DD, Miao HX, Wan S, Zhou CH, Wang SY, Chen SY, Shang J and Feng TH (2022) Gut microbiota profiling revealed the regulating effects of salidroside on iron metabolism in diabetic mice. *Front. Endocrinol.* 13:1014577. doi: 10.3389/fendo.2022.1014577



# Gut microbiota profiling revealed the regulating effects of salidroside on iron metabolism in diabetic mice

Jing Shi[1†], Qin Zhao[1†], Dou Dou Hao[1], Hong Xia Miao[2], Sha Wan[1], Chao Hua Zhou[1], Si Yu Wang[1], Si Yuan Chen[1], Jin Shang[3*] and Tian Hang Feng[3*]

[1]Hospital of Chengdu Office of People's Government of Tibetan Autonomous Region (Hospital.C.T.), Chengdu, China, [2]Department of Laboratory Medicine, Qingdao Central Hospital, Qingdao, China, [3]Sichuan Provincial People's Hospital, University of Electronic Science and Technology of China, Chengdu, China

**Background:** Diabetes is a common metabolic disease that is associated with gut microbiota dysbiosis and iron metabolism. Salidroside (SAL) is the main ingredient of the traditional Chinese herb Rhodiola, previous studies have shown that SAL could reshape the gut microbiota and limit iron accumulation. Therefore, it is possible that SAL can act as an alternative therapy for diabetes, and its underlying mechanism is worth exploring.

**Methods:** SAL was used to treat diabetic db/db mice. Serum glucose and iron levels and the histopathology of myocardial fibres were evaluated. The gut microbiota composition was determined by 16S rRNA Illumina sequencing technology.

**Results:** Treatment with SAL significantly reduced blood glucose and ameliorated diabetic cardiomyopathy in diabetic db/db mice, which was accompanied by inhibited ferroptosis and iron accumulation. Furthermore, the 16S rRNA sequencing results showed that SAL induced a change in the gut microbiota composition. Overall, SAL could increase the proportion of probiotic bacteria and decrease Lactobacillus to improve gut microbiota. Specifically, SAL increased the ratio of Bacteroidetes to Firmicutes in diabetic mice. The most significant biomarker was the genus Lactobacillus between the MD group and the SAL group. In addition, COG and KEGG analyses suggested that SAL mainly participated in nutrient metabolism, among them iron metabolism was associated with the abundance of Lactobacillus.

**Conclusions:** SAL could reduce the glucose level and protect against diabetic cardiomyopathy in diabetic mice, which might be mediated by the change in the gut microbiota and the regulation of iron metabolism. The findings suggested that SAL was a promising complementary option for diabetes therapy.

KEYWORDS

**salidroside, diabetes, gut microbiota, iron metabolism, lactobacillus**

# Introduction

Diabetes mellitus (DM) is a chronic disease with a high disability rate, and DM is the ninth leading cause of death. The International Diabetes Federation estimated that 1 in 11 adults aged 20–79 years (463 million adults) had DM worldwide in 2019 and that the number would increase to 578 million by 2030 and, surprisingly, 700 million by 2045. Moreover, according to previous reports, the actual prevalence of DM is often underestimated, and the global prevalence of DM might be even grimmer (1). Type 2 diabetes mellitus (T2DM) accounts for the vast majority (approximately 90%) of DM cases. T2DM is characterized by a combination of relative insulin deficiency and insulin resistance. In terms of pathophysiological manifestations, blood glucose is elevated, and the metabolism of a range of nutrients can also be affected (2). Among the risk factors for T2DM, such as genetic factors and high caloric intake, the role of the gut microbiota in the progression of T2DM has been gradually revealed (3).

The gut microbiota is recognized as a key factor in human health. Previous studies have shown that many chronic diseases might lead to gut microbiota disorders (4). A healthy gut microbiota is beneficial for the host, but gut microbiota changes are associated with a range of metabolic dysbioses, including diabetes and obesity (5). Gut microbiota dysbiosis in diabetes patients is linked to inflammation status, oxidative stress, and toxin release. Hence, probiotics might represent a novel, economical approach for managing T2DM (6). In addition, the gut microbiota is associated with other factors involved in T2DM, such as nutrient metabolism.

Iron is an important nutrient with extensive physiological functions for both the host and the gut microbiota (7). Iron overload can lead to the formation of toxic oxygen free radicals (hydroxyl radicals) through the Fenton reaction. Thus, iron metabolism needs to be tightly regulated at the cellular and organism levels (8). Abnormal iron metabolism in T2DM has been observed in a large number of cross-sectional surveys and further verified by emerging cohort studies (9). Iron metabolism has been reported to play an important role in reshaping the gut microbiota in T2DM (10). Therefore, the regulation of both the gut microbiota composition and iron metabolism is essential in ameliorating insulin resistance and improving the prognosis of T2DM.

Rhodiola is a kind of traditional Chinese herb that is recorded in the Ming Dynasty classics Compendium of Materia Medica. It is mainly grown at altitudes of 1600~4000 metres and is commonly distributed in Chinese Tibet (11). Rhodiola rosea has a long history of use as an adaptogen in traditional Chinese medicine and is also called “Tibetan ginseng”. The function and application prospect of Rhodiola as a Chinese herb were first summarized in 2007 (12). Salidroside (SAL) is one of the most potent bioactive constituents isolated from Rhodiola. Recent studies have shown that SAL has many attractive physiological functions, including reducing the risk of T2DM (13). Regarding the mechanism by which SAL reduces the risk of T2DM, SAL was reported to significantly reduce the level of oxygen free radicals by inhibiting the oxidative stress response; for example, SAL showed a protective effect in myocardial cells, with changes in a range of antioxidant enzymes. The antioxidant enzymes were also reported to be involved in iron metabolism (14). On the other hand, SAL exhibited functions in regulating the living environment of the gut microbiota so that the proportion of beneficial bacteria was increase (15). Therefore, SAL potentially has an effect on the regulation of both the gut microbiota and iron metabolism. The role and mechanism of SAL in DM is worthy of exploration. Here, we designed the present study to explore the effect and concrete mechanism of SAL on the gut microbiota and iron metabolism in T2DM, aiming to provide new ideas for the prevention and treatment of T2DM.

# Materials and methods

## Chemicals and reagents

Salidroside was purchased from Chengdu Refines Biotechnology Co., Ltd. (Chengdu, China). Anti-GPX4 rabbit monoclonal antibody (ab125066), anti-SCL7A11 rabbit monoclonal antibody (ab175186) and anti-cTNT rabbit monoclonal antibody (ab209813) were purchased from Abcam (Cambridge, UK), and anti-GAPDH rat monoclonal antibody was purchased from Affinity (USA).

## Animal experiments

Twenty male BKS-Leprem2Cd479/Gpt (db/db)(C57bl/KS diabetic mice with knockdown of the Leptin receptor gene) and ten male BKS-Leprem2Cd479/Gpt (wt/wt) (C57bl/KS wild-type normal mice), the standard was 8 weeks of age, were purchased from Jiangsu Jicui Yaokang Biotechnology Co., Ltd. (Jiangsu, China). The db/db mice with blood glucose levels that were over 16.7 mmol/L, as measured by an Accu-Chek Performa glucometer (Roche Diagnostics, Mannheim, Germany), for 3 days were considered diabetic mice. The experiment was started after a 1-week period of acclimation to laboratory conditions. Ten wt/wt mice were normal controls (the WT group), and twenty db/db mice were randomized into 2 groups, namely, (1) the SAL group and (2) the T2DM model group (MD group), with ten mice in each group. The SAL group was intragastrically administered SAL (1.5 g/kg) for 5 weeks, whereas the MD and WT groups were both administered the same amount of normal saline. The dosage of SAL was determined according to a previous SAL toxicity study (16). The animals of each group

were provided with their corresponding diet and were allowed free access to tap water. Body weight and blood glucose were measured weekly. At the end of the experiments, animals were intraperitoneally injected with 6% chloral hydrate (0.5 mL/10 g), and blood was taken from the veins. Serum was separated and then stored at −80°C for biochemical estimations. The heart was dissected and stored at −80°C for further analysis, and the faeces of mice were stored at −80°C for intestinal microflora analysis. All experiments performed were approved by the ethics committee of the Hospital of the Chengdu Office of the People's Government of the Tibetan Autonomous Region.

## Sequencing of the gut microbiota

Faeces were collected from animals before they were dissected. Then,DNA extraction kit was purified by the Zymo Research BioMICS DNA Microprep Kit(Cat# D4301), and the DNA concentration was quantified. The 16S rRNA V4 region of the sample was amplified, detected, purified and quantified. Then, New England BioLabs NEBNext Ultra II DNA Library Prep Kit for Illumina (NEB#E7645L) and a HiSeq Rapid SBS Kit v2 (FC-402-4023 500 Cycle) and Illumina sequencing technology were used for sequencing (17). Finally, the data obtained by sequencing were used for bioinformatics analysis using Usearch and QIIME1.9.0 (18).

## Determination of the biochemical parameters

Serum levels of iron, ferritin and transferrin were detected by the Hospital of the Chengdu Office of the People's Government of the Tibetan Autonomous Region using the corresponding colorimetric kit according to the manufacturer's instructions.

## Pathology analysis

Heart tissues were fixed in 4% paraformaldehyde for 48 h. Fixed tissues were processed for dehydration and paraffin embedding, and 3-μm-thick sections were prepared for histopathological and immunohistochemical examinations. Heart sections were stained with haematoxylin and eosin (H&E) for routine histopathological examination as well as morphometric analysis with a light microscope (Nikon, Japan) at 200× magnification and a panoramic slice scanner (3DHISTECH, Hungary). The specimens were placed under a high-power optical microscope, and 20 fields were randomly selected. Then, the mean value of the grading of myocardial injury was taken based on the following scale: Grade 0 – the muscle fibres were neatly arranged, the transverse lines were clear, the nuclei were obvious, and there was no cell swelling; Grade I – scattered point-like necrosis of the myocardium, mainly coagulative necrosis, confined to the subendocardial; Grade II – the myocardial necrosis foci were distributed in sheets without connections, and the lesions did not involve the whole layer of the heart wall; and Grade III – extensive patchy necrotic of the myocardium, interconnecting with the heart and involving the whole pericardium. Immunohistochemical examination was used to detect the GPX4 and cTNT content and distribution. The sections were observed at 200× magnification. Then, the optical density value (IOD) and the pixel area (AREA) of the brown-coloured immunostained area were measured.

## Western blot analysis

The heart tissue was washed 2-3 times with cold PBS to remove blood, was cut into small pieces and placed in a homogenizer. Then, RIPA lysis solution at 10 times the tissue weight was added, and the tissue was homogenized thoroughly on ice and centrifuged at 12,000 × g for 10 min. The supernatant was collected to form the total protein solution. The protein concentrations were measured by a BCA protein assay kit (Biosharp, Shanghai, China). Frozen protein sample was removed and thawed on ice, and a 4× volume of the total protein was loaded onto a 10% SDS acrylamide gel and then electrotransferred to a polyvinylidene fluoride (PVDF) membrane (Millipore, ISEQ00010, USA). After blocking with 5% skim milk (TBST preparation) for 1 h at room temperature, the membranes were incubated overnight at 4°C with the primary antibody against the target protein and then for 1 h with the corresponding secondary antibody. The PVDF-membrane-bound protein was placed on the sample tray and detected with an ECL Plus kit according to the operating guidelines. Then, images were collected under a chemiluminescence imaging system (ChemiScope 6100, Shang Hai, China), and the density of each target band was quantified by Image Pro-Plus 6.0 software (Media Cybernetics, Inc., Rockville, MD, USA), with the optical density normalized to that of GAPDH.

## Transmission electron microscopy

The heart tissue of the animal was fixed in glutaraldehyde (3%) and then fixed again in 1% osmium tetroxide. Subsequently, the samples were stepwise dehydrated, permeabilized, and embedded in Araldite. Then, the tissues were cut into ultrathin sections (50 nm) using an ultramicrotome (Leica EM UC7, Solms, Germany) and placed onto a copper grid. Subsequently, the thin slices on the copper grid were stained with uranyl acetate (2%) and lead citrate at room temperature for 15-20 min and observed under a transmission electron microscope (JEM-1400FLASH, JEOL, Japan).

## Statistical analysis

All animal data are expressed as the mean ± standard deviation (SD). For between-group comparisons in this study, we used one-way analysis of variance (ANOVA) followed by Tukey's *post hoc* test. All data were analysed using the statistical program SPSS version 21 (SPSS Inc., Chicago, IL, USA). Graphs were created using GraphPad Prism version 8 (San Diego, CA, USA). Differences with a P value < 0.05 were considered statistically significant differences.

# Results

## SAL reduced the levels of blood glucose and protected against diabetic cardiomyopathy in db/db mice

Ten wt/wt mice formed the WT group, and twenty db/db mice were randomized into 2 groups, namely, (1) the SAL group and (2) the T2DM model group (MD), with 10 mice in each group. After 35 days, there were two mice that died in the MD group and three mice that died in the SAL group. SAL did not exhibit toxicity to mice in the SAL group compared with the control group. The levels of baseline glucose in db/db mice in the MD group and the SAL group were similar and significantly higher than those in wt/wt mice in the WT group. The treatment of db/db mice with SAL reduced their blood glucose during the intervention period. A significant reduction in blood glucose was observed in the SAL group after week 4 when compared with that in the MD group (Figure 1A). The weight of db/db mice in the SAL group was slightly lower than that of the MD group, but the difference was not significant, suggesting that treatment with SAL tended to reduce the weight of db/db mice (Figure 1A). These results showed that SAL could alleviate elevated blood glucose in diabetic mice.

The histopathology of myocardial fibres was observed, and the heart tissues of each mouse were used to make paraffin sections. The H&E staining results showed that no pathological changes existed in normal mice in the WT group. The myocardial cell boundaries were clear, the shape was consistent, and the grade of myocardial injury was Garde 0. Uniform and unstructured coagulation of necrotic myofibrils was found in db/db mice in the MD group (Figure 1B, green arrow). A number of irregular myocardial fibres and obscure intercellular borders were also found in db/db mice in the MD group (Figure 1B, black arrow); the myocardial cell nucleus was hyperchromatic, fragmented or dissolved, and the cytoplasm was eosinophilic (Figure 1B, red arrow). The grade of myocardial injury was Grade I. In contrast, SAL ameliorated the myocardial necrosis of diabetic myocardial tissue in db/db mice. Necrotic myofibrils and obscure intercellular borders were rarely found in db/db mice in the SAL group, and the grade of myocardial injury was Grade 0.

To further observe the effect of SAL on myocardial cells in diabetic mice, 6 mice in each group were randomly selected to observe the changes in myocardial cell microstructure by TEM. The results showed that the morphology and structure of cardiomyocytes in the WT group were normal, the myofibrils were arranged neatly, and the M and Z lines of the dark band were clear and straight. In contrast, in the MD group, most mitochondria between myocardial fibres were swollen, the cristae were broken and dissolved, myofibrillary dissolution existed in some regions, the Z line of the dark zone was clear and straight, and there were many lipid droplets and a few secondary lysosomes. In the SAL group, the myofibrils of db/db mice were arranged neatly, the sarcomere structure was intact, and the mitochondria between the myofibrils were normal in shape without obvious lesions (Figure 1C). A characteristic of ferroptosis is mitochondrial dysfunction, including mitochondrial swelling and cristae dissolution. The results indicated that the alleviation effect of SAL on mitochondrial injury was associated with ferroptosis.

## SAL inhibited ferroptosis by reducing iron overload in db/db mice

To further investigate the influence of SAL on ferroptosis in diabetic mice, immunohistochemistry analysis of cTNT and GPX4 was conducted (Figure 2A). The expression of cTNT was higher in the MD group than in the WT group ($p$=0.000) and SAL group ($p$=0.001) (Figure 2B). This finding indicated that diabetic myocardial damage was present in the diabetic mice. The expression of GPX4 was lower in the MD group than in the WT group ($p$=0.002) and SAL group($p$=0.045) (Figure 2C). GPX4 is an inhibitor protein of ferroptosis. This finding indicated that SAL could inhibit ferroptosis.

The occurrence of ferroptosis depends on iron overload and oxidative stress injury. To further explore the effect of SAL on iron metabolism, the levels of serum iron and transferrin were detected. The results showed that transferrin and serum iron were higher in the MD group than in the WT group. The levels of serum iron and transferrin were significantly lower in the SAL group than in the MD group (Figure 3A, B). This finding indicated that SAL could reduce iron overload in diabetic mice. Western blotting of two protein markers of iron metabolism, SLC7A11 and LC3II, was conducted. The results showed that the expression of LC3II was higher in the MD group than in the WT group. SAL reduced the expression of LC3II in

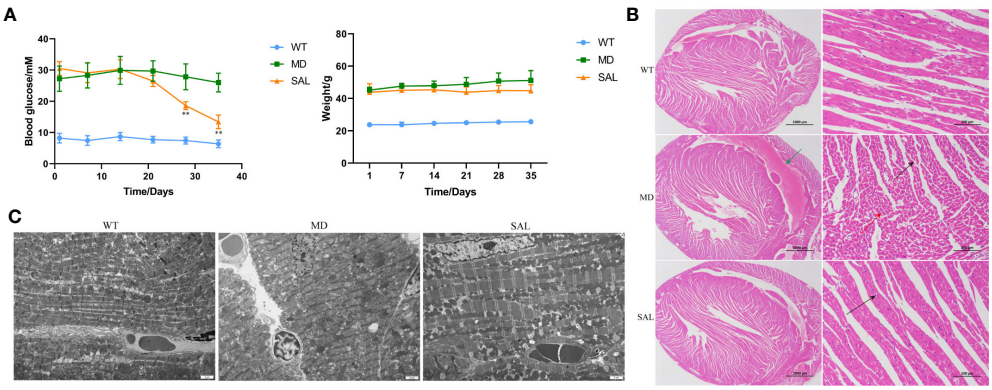


FIGURE 1
Influence of SAL on glucose regulation and diabetic cardiomyopathy in diabetic mice. **(A)**, Changes in the blood glucose and weight of db/db mice during the period of SAL treatment. (**$p$ < 0.05 as MD group vs SAL group). **(B)**, H&E staining of myocardial tissue sections. **(C)**, Transmission electron microscopy of myocardial cells.Green arrow: extravasation of the heart cavity; black arrow: irregularly shaped cavities; red arrow: necrotic cardiomyocytes.

diabetic mice (Figure 3C). Moreover, SAL tended to reduce SLC7A11 expression *via* grey value analysis (Figure 3D).

## SAL exerted a probiotic effect in the regulation of the gut microbiota in db/db mice

To analyse the effect of SAL on the gut microbiota of diabetic mice, 16S rRNA sequencing was conducted. The sequencing data have been published in NCBI (https://www.ncbi.nlm.nih.gov/sra/PRJNA868147) and the code is PRJNA868147. We obtained a total of 756,702 clean tags from 768,415 raw tags. The results showed that the most abundant phylum in any group was Bacteroidetes, which can benefit hosts by preventing infection with potential pathogens in most instances (19). The proportion of Bacteroidetes was decreased in diabetic mice in the MD group compared with mice in the WT group, while SAL ameliorated the reduction in Bacteroidetes in diabetic mice in the SAL group. The second most abundant phylum was Firmicutes. The proportion of Firmicutes was increased in diabetic mice in the MD group compared with mice in the WT group, while SAL ameliorated the up-regulation of Firmicutes in diabetic mice in the SAL group. The ratio of Bacteroidetes to Firmicutes was decreased in the MD

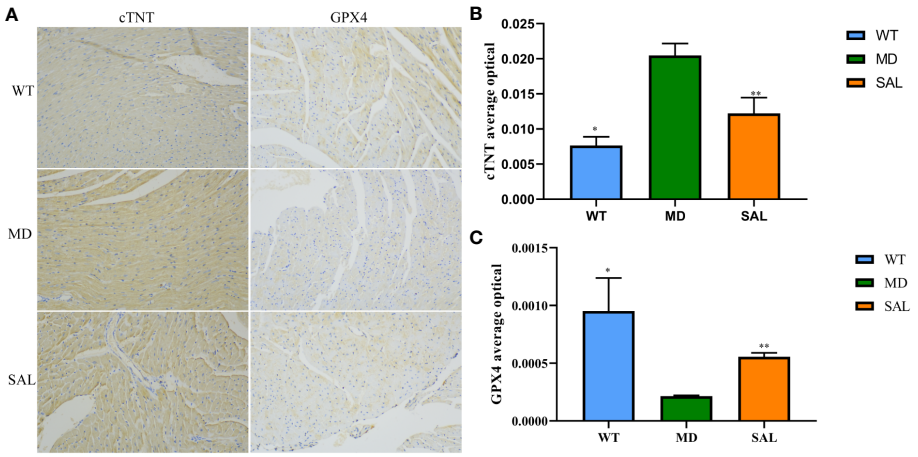


FIGURE 2
Influence of SAL on the expression of myocardial injury markers in diabetic mice. **(A)**, Immunohistochemistry of cTNT and GPX4 in myocardial tissue. **(B)**, The optical density value (IOD) of the brown colour of cTNT staining in myocardial tissue. **(C)**, The IOD value of the brown colour of GPX4 staining in myocardial tissue. (ns, no statistical significance; *$p$ < 0.05 as MD group vs WT group; **$p$ < 0.05 as MD group vs SAL group).

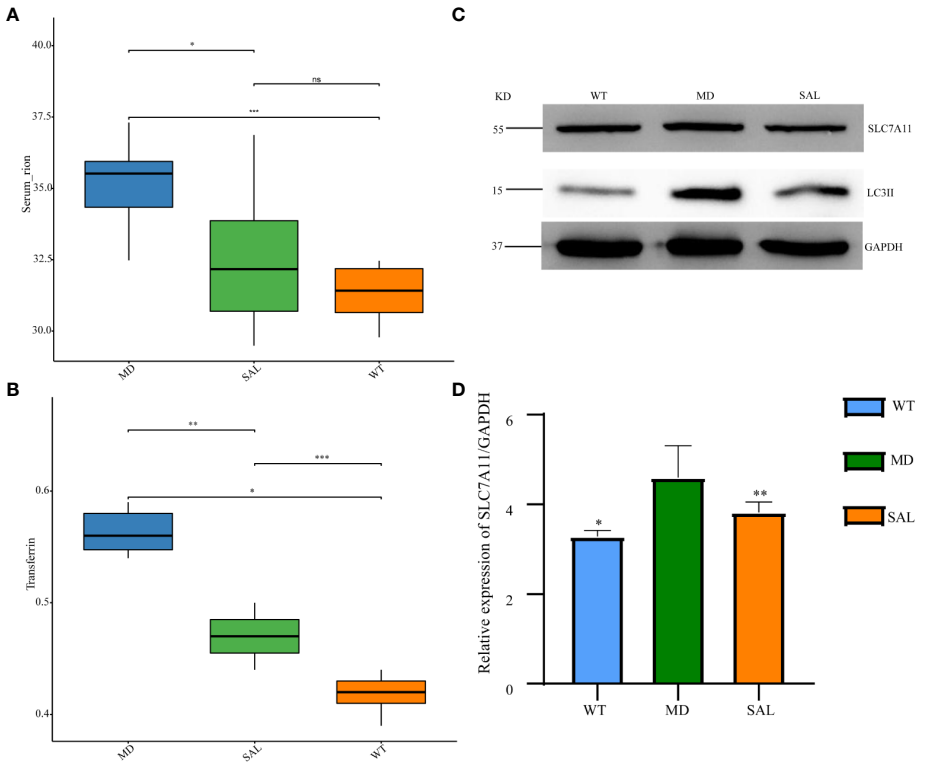


FIGURE 3
Influence of SAL on iron metabolism in diabetic mice. **(A)**, The serum iron levels of mice in the different groups; **(B)**, The transferrin levels of mice in the different groups; **(C)** Western blot analysis of the protein expression of SLC7A11, LC3II, and GAPDH in myocardial tissue; **(D)** Grey value analysis of the western blot results. (ns, no statistical significance; *$p < 0.05$ as MD group vs WT group; **$p < 0.05$ as MD group vs SAL group). ***means that SAL group compared with WT group is difference significant.

group, while the ratio was increased after SAL treatment in the SAL group. Other abundant phyla included Verrucomicrobia, Proteobacteria, Actinobacteria, Tenericutes, Desferribacteres, Cyanobacteria and several unclassified bacteria (Figure 4A). A decrease in Bacteroidetes or an increase in Firmicutes or a decrease in the ratio of Bacteroidetes to Firmicutes contributes to the promotion of obesity and increases the risk of diabetes (20). Therefore, this result showed that the SAL could reduce the risk of diabetes.

At the bacterial genus level, the genera *Enterobacter*, *Lactobacillus,bacteroides, lachnospiraceae NK4A136 group and alistipes accounted for a larger proportion*. Among these, *Enterobacter* and *Lactobacillus* were increased, *bacteroides* and *alistipes* were decreased in the MD group compared with the SAL group, while SAL ameliorated the up-regulation of the genera *Enterobacter* and *Lactobacillus* in diabetic mice in the SAL group (Figure 4B). So, we speculated that SAL could up-regulate the proportion of probiotic bacteria (*bacteroides* and *alistipes)* and reduce the proportion of pathogenic bacteria (*Enterobacter)* in diabetic mice, and also has a unique down-regulation effect on *Lactobacillus*.

## *Lactobacillus* was a potential biomarker of SAL treatment

To further explore the key biomarkers associated with SAL treatment, random forest analysis was conducted. The results showed that the proportions of *Lactobacillus* was significantly higher in the MD group than in either the WT group or the SAL group. In contrast, the proportions of *Odoribacter*, *Ruminococcaceae UCG-010*, and *Lachnospiraceae UCG-004* were significantly lower than those in either the WT group or the SAL group (Figure 5A). Moreover, the linear discriminant analysis (LDA) effect size (LEfSe) method was performed. The histogram of the distribution of LDA values (LDA > 2.5) showed the significantly different biomarkers ($p < 0.05$). The results showed that *Lactobacillus* was the most significant difference and could be used as a biomarker of diabetes by comparing the MD group with the SAL ($p$=0.002), which coincidentally indicated that *Lactobacillus* was significantly down-regulated in SAL group after SAL treatment (Figure 5B). Therefore, the above results suggested that members of the genus *Lactobacillus* were the unique target bacteria of SAL treatment.

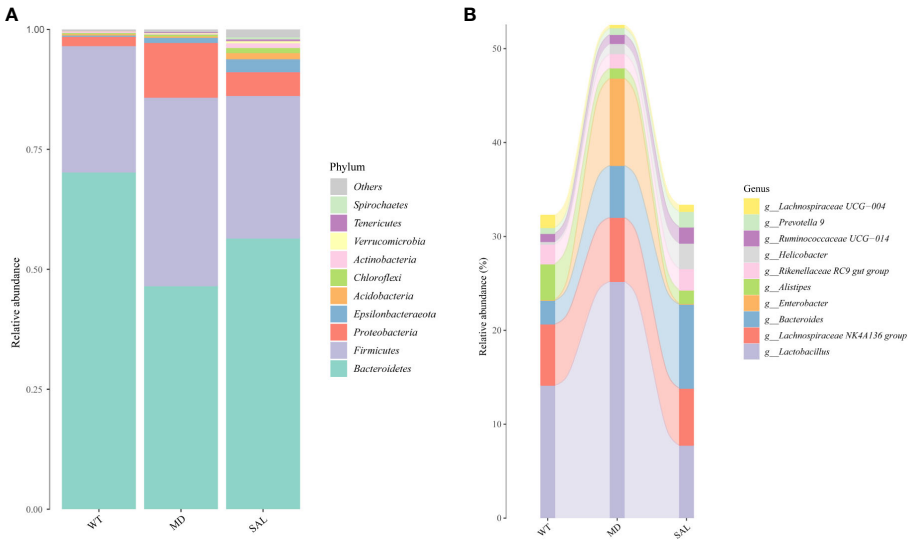


FIGURE 4
Changes in the gut microbiota of mice in the different groups. **(A)**, The overall composition of the gut microbiota at the phylum level. **(B)**, Sankey plot of the changes in the composition of the gut microbiota at the genus level.

## *Lactobacillus* was associated with iron metabolism

To explore iron metabolism-related bacteria, the Cluster of Orthologous Groups of proteins (COG) and the Kyoto Encyclopedia of Genes and Genomes (KEGG) pathway databases were used to make functional predictions. The significant differences in species between each group were analysed by LEfSe. The threshold values of LDA > 2.5 and $p < 0.05$ were used. The results showed that SAL mainly participated in nutrient metabolism, such as glycan biosynthesis and metabolism and lipid metabolism, at level 2. Furthermore, oxidative phosphorylation, starch and sucrose metabolism, and amino sugar and nucleotide sugar metabolism were involved in SAL treatment at level 3. According to the KEGG database, the significantly different functional pathways were similar to those in the COG categories. Briefly, genes related to nutrient metabolism were enriched in the SAL-treated group (Figure 6A).

To further investigate the relationship between the gut microbiota and iron metabolism, correlation analyses between the

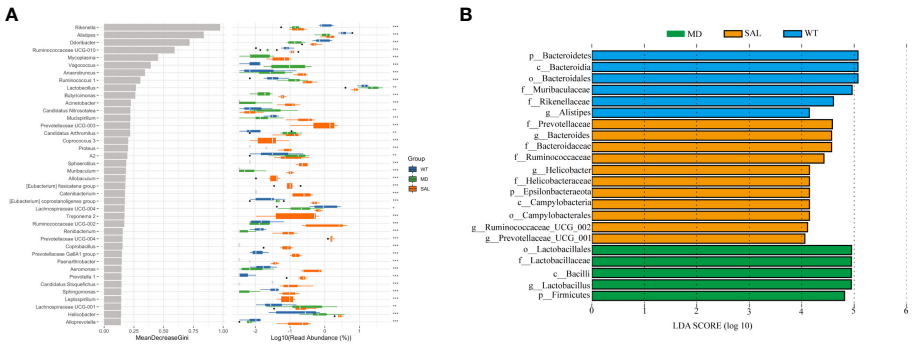


FIGURE 5
Assessment of significantly different species between groups. **(A)**, Random forest analysis was combined with a difference test indicating significant differences in different groups and the importance of classification between groups. The * on the right represents the significance of the difference between groups (Kruskal–Wallis rank-sum test) (***$p < 0.001$; **$p < 0.01$; *$p < 0.05$). **(B)**, LDA scores plot. The horizontal coordinates were the logarithmic scores of LDA for each classfication unit. The vertical coordinates were the classfication units with signficant difference between groups. The longer the length, the more signficant the difference was.

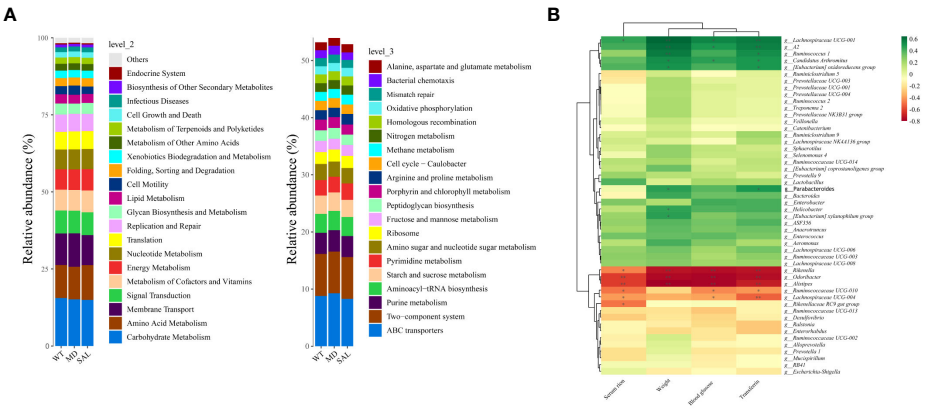


FIGURE 6
Functional prediction and analysis of SAL-related bacteria. **(A)**, Kyoto Encyclopedia of Genes and Genomes (KEGG) pathways by Tax4Fun tools at level 2 and level 3. **(B)**, Correlation analysis between high-abundance genera and iron metabolism and glucose metabolism. Color depth indicates correlation, the more red indicates the stronger negative correlation, the more green indicates the stronger positive correlation, and the asterisk indicates significance (**$p < 0.01$; *$p < 0.05$).

abundances of different bacterial species and serum iron, transferrin, blood glucose and weight were conducted. The results showed that *Rikenella*, *Alistipes*, *Odoribacter*, etc., were negatively correlated with serum iron, blood glucose, weight and transferrin. In contrast, *Lachnospiraceae UCG-001, Ruminococcus-1, Candidatus Arthromitus, Enterobacter, Lactobacillus*, etc., were positively correlated with serum iron, blood glucose, weight and transferrin (Figure 6B). Among them, only *Lactobacillus* was down-regulated in diabetic mice after SAL treatment (Figure 4B), and also *Lactobacillus* was a biomarker between the MD group and SAL group, and SAL had a down-regulation effect on it (Figure 5B). *Lachnospiraceae UCG-001, Ruminococcus-1, Candidatus Arthromitus, Enterobacter* despite showing a positively correlation with iron metabolism, did not show a statistical difference during the comparison between the SAL and MD groups. Among the bacteria commonly related to glucose metabolism and iron metabolism, the abundance of *Lactobacillus* was significantly higher in diabetic mice with serum iron load, which is consistent with the biomarker screening results of SAL treatment. The above results showed that SAL could alleviate iron overload in diabetes by reducing the abundance of *Lactobacillus* in the gut microbiota.

## Discussion

DM involves an array of metabolic dysfunctions due to hyperglycaemia, and these metabolic dysfunctions lead to a series of complications, such as diabetic retinopathy, diabetic nephropathy, diabetic cardiopathy, diabetic coma, and diabetic foot (21). The number of people with DM worldwide continues to increase, which poses an increased risk of all-cause mortality (22). Novel therapeutic strategies that reduce the complications of DM are still worth exploring.

In the present study, we evaluated the function of SAL in treating diabetic mice. *In vivo* tests showed that SAL could reduce the blood glucose level and alleviate diabetic cardiomyopathy in diabetic mice. These results were in accordance with the results of previous studies (22–24). To further investigate the mechanism of SAL, the effects of SAL on ferroptosis occurrence and iron metabolism were evaluated. We found that SAL inhibited the expression of cTNT and GPX4 in the myocardial tissue of diabetic mice. cTNT is an indicator of myocardial injury, while the expression of GPX4 is an inhibitor of ferroptosis and is involved in iron metabolism (25). Furthermore, we found that SAL could limit iron accumulation in diabetic mice and inhibit the expression of SLC7A11 and LC3II. SLC7A11 and LC3II were identified as iron metabolism-related genes (26, 27). This finding indicated that the preventative effect of SAL on diabetic cardiomyopathy was associated with iron metabolism regulation.

Increasing evidence suggests that iron metabolism and the gut microbiota are frequently linked, and dysfunctions of both have been observed in patients with T2DM (28). Moreover, the gut microbiota was reported to act as a regulator of metabolic diseases such as DM. Currently, there are few studies on the relationship between SAL and the gut microbiota in diabetes. Therefore, we explored the gut microbiota composition using 16S rRNA sequencing and evaluated iron metabolism-related intestinal bacterial indicators. In our study, SAL increased *Bacteroides* and reduced *Lactobacillus*. Studies indicated that *Bacteroides* played a beneficial role on glucose metabolism in humans and experimental animals (29).It had also been reported that *Lactobacillus* was increased in T2DM and nonalcoholic fatty

liver disease (30). Which indicated that SAL could up-regulate the proportion of probiotic bacteria and down-regulated *Lactobacillus* to improved the gut microbiota. Moreover, at the bacterial genus level, members of the genus *Lactobacillus* were the unique target bacteria of SAL treatment. It is interesting that *Lactobacillus casei* could act as a probiotic in diabetes (31). However, *Lactobacillus* has been reported to increase ferric iron (32). To clarify the association between the gut microbiota and iron metabolism, correlation analysis was conducted between different flora and related indicators of iron metabolism. The results indicated that SAL could alleviate iron overload in diabetes by reducing the abundance of *Lactobacillus*. Therefore, the results of the present study showed that SAL was found to reduce T2DM-associated pathogenic bacteria and that it had a potential effect on preventing diabetic cardiomyopathy by regulating iron metabolism-associated bacteria.

Gut microbiota-targeted therapy is a promising new therapeutic strategy in T2DM patients. Oral administration of probiotics, prebiotics or faecal microbiota could improve gut metabolic functions during the treatment of T2DM. However, the use of antibiotics restricts their efficacy (33). On the other hand, no-drug therapy, including diet modification and exercise, could also benefit T2DM patients by influencing the gut microbiota. For example, animal-based diets decrease the levels of *Firmicutes*, which metabolize plant polysaccharides, while increasing the abundance of bile-tolerant microorganisms (34). The efficacy of no-drug therapy is restricted by the lifestyle of T2DM patients. Therefore, more gut microbiota-targeting drugs are worth exploring. The safety of SAL has been widely verified in clinical trials (35, 36). The function of SAL in regulating glucose and iron metabolism by affecting the gut microbiota in the present study indicated that SAL could be effective in treating T2DM along with already known treatments.

In conclusion, the present study showed that SAL could reduce glucose levels and protect against diabetic cardiomyopathy in diabetic mice. The therapeutic effect of SAL on diabetes might be mediated by changes in the gut microbiota the regulation of iron metabolism. The findings suggested that SAL was a promising complementary option for diabetes. The efficacy and safety of SAL are worth investigating in the clinic in the future.

## Data availability statement

The datasets presented in this study can be found in online repositories. The names of the repository/repositories and accession number(s) can be found below: https://www.ncbi.nlm.nih.gov/, PRJNA868147.

## Ethics statement

The animal study was reviewed and approved by the ethics committee of Hospital of Chengdu Office of People's Government of Tibetan Autonomous Region.

## Author contributions

JShi designed the experiments and prepared the manuscript. QZ helped with experiments. DH performed the data analysis. HM designed the detection index. SW collected mouse faeces. CZ, SYW and SC helped with sample storage and extraction. TF and JSha revised the manuscript. All authors contributed to the article and approved the submitted version.

## Funding

This work was supported by the Natural Science Foundation of Tibet Autonomous Region (XZ202101ZR0101G); the Key Research Projects of the Hospital of Chengdu Office of People's Government of Tibetan Autonomous Region (Hospital.C.T.) (QH-1(2019)-03); and the Research Project of Sichuan Medical Association (S19072).

## Acknowledgments

The authors are grateful to all members of the laboratory for their continuous technical advice and helpful discussion.

## Conflict of interest

The authors declare that the research was conducted in the absence of any commercial or financial relationships that could be construed as a potential conflict of interest.

## Publisher's note

# References

1. Refardt J. Diagnosis and differential diagnosis of diabetes insipidus: Update. *Best Pract Res Clin Endocrinol Metab* (2020) 34(5):101398. doi: 10.1016/j.beem.2020.101398

2. Wu Y, Ding Y, Tanaka Y, Zhang W. Risk factors contributing to type 2 diabetes and recent advances in the treatment and prevention. *Int J Med Sci* (2014) 11(11):1185–200. doi: 10.7150/ijms.10001

3. Muñoz-Garach A, Diaz-Perdigones C, Tinahones FJ. Gut microbiota and type 2 diabetes mellitus. *Endocrinol Nutr* (2016) 63(10):560–8. doi: 10.1016/j.endonu.2016.07.008

4. Salgaço MK, Oliveira LGS, Costa GN, Bianchi F, Sivieri K. Relationship between gut microbiota, probiotics, and type 2 diabetes mellitus. *Appl Microbiol Biotechnol* (2019) 103(23-24):9229–38. doi: 10.1007/s00253-019-10156-y

5. Hu Y, Xu J, Sheng Y, Liu J, Li H, Guo M, et al. Pleurotus ostreatus ameliorates obesity by modulating the gut microbiota in obese mice induced by high-fat diet. *Nutrients* (2022) 14(9):1868. doi: 10.3390/nu14091868

6. Hu Y, Xu J, Sheng Y, Liu J, Li H, Guo M, et al. Gut microbiota as a trigger for metabolic inflammation in obesity and type 2 diabetes. *Front Immunol* (2020) 11:571731. doi: 10.3389/fimmu.2020.571731

7. Rusu IG, Suharoschi R, Vodnar DC, Pop CR, Socaci SA, Vulturar R, et al. Iron supplementation influence on the gut microbiota and probiotic intake effect in iron deficiency-a literature-based review. *Nutrients* (2020) 12(7):1993. doi: 10.3390/nu12071993

8. Lal AA-O. Iron in health and disease: An update. *Indian J Pediatr* (2020) 87 (1):58–65. doi: 10.1007/s12098-019-03054-8

9. Jung DH, Hong KW, Park B, Lee YJ. Dietary iron to total energy intake ratio and type 2 diabetes incidence in a longitudinal 12-year analysis of the Korean genome and epidemiology cohort study. *Eur J Nutr* (2021) 60(8):4453–61. doi: 10.1007/s00394-021-02596-y

10. Sachinidis A, Doumas M, Imprialos K, Stavropoulos K, Katsimardou A, Athyros VG. Dysmetabolic iron overload in metabolic syndrome. *Curr Pharm Des* (2020) 26(10):1019–24. doi: 10.2174/1381612826666200130090703

11. Magani SKJ, Mupparthi SD, Gollapalli BP, Shukla D, Tiwari AK, Gorantala J, et al. Salidroside - can it be a multifunctional drug? *Curr Drug Metab* (2020) 21 (7):512–24. doi: 10.2174/1389200221666200610172105

12. Jafari M, Felgner JS, Bussel II, Hutchili T, Khodayari B, Rose MR, et al. Rhodiola: a promising anti-aging Chinese herb. *Rejuvenation Res* (2007) 10 (4):587–602. doi: 10.1089/rej.2007.0560

13. Zhao CC, Wu XY, Yi H, Chen R, Fan G. The therapeutic effects and mechanisms of salidroside on cardiovascular and metabolic diseases: An updated review. *Chem Biodivers* (2021) 18(7):e2100033. doi: 10.1002/cbdv.202100033

14. Chen H, Zhu J, Le Y, Pan J, Liu Y, Liu Z, et al. Salidroside inhibits doxorubicin-induced cardiomyopathy by modulating a ferroptosis-dependent pathway. *Phytomedicine* (2022) 99:153964. doi: 10.1016/j.phymed.2022.153964

15. Yuan Y, Wu X, Zhang X, Hong Y, Yan H. Ameliorative effect of salidroside from rhodiola rosea l. on the gut microbiota subject to furan-induced liver injury in a mouse model. *Food Chem Toxicol* (2019) 125:333–40. doi: 10.1016/j.fct.2019.01.007

16. Zhu J, Wan X, Zhu Y, Ma X, Zheng Y, Zhang T. Evaluation of salidroside *in vitro* and *in vivo* genotoxicity. *Drug Chem Toxicol* (2010) 33(2):220–6. doi: 10.3109/01480540903373654

17. Kuczynski J, Lauber CL, Walters WA, Parfrey LW, Clemente JC, Gevers D, et al. Experimental and analytical tools for studying the human microbiome. *Nat Rev Genet* (2012) 13:47–58. doi: 10.1038/nrg3129

18. Caporaso JG, Kuczynski J, Stombaugh J, Bittinger K, Bushman FD, Costello EK, et al. QIIME allows analysis of high-throughput community sequencing data. *Nat Meth* (2010) 7:335–6. doi: 10.1038/nmeth.f.303

19. Global, regional, and national incidence, prevalence, and years lived with disability for 354 diseases and injuries for 195 countries and territorie –2017: a systematic analysis for the global burden of disease study 2017. *Lancet* (2018) 392 (10159):1989–1858 doi: 10.1016/S0140-6736(18)32279-7

20. Magne FA-O, Gotteland M, Gauthier L, Zazueta A, Pesoa S, Navarrete P, et al. The Firmicutes/Bacteroidetes ratio: A relevant marker of gut dysbiosis in obese patients? *Nutrients* (2020) 12(5):1474. doi: 10.3390/nu12051474

21. Karaa A, Goldstein A. The spectrum of clinical presentation, diagnosis, and management of mitochondrial forms of diabetes. *Pediatr Diabetes* (2015) 16(1):1–9. doi: 10.1111/pedi.12223

22. Zheng Y, Ley SH, Hu FB. Global aetiology and epidemiology of type 2 diabetes mellitus and its complications. *Nat Rev Endocrinol* (2018) 14(2):88–98. doi: 10.1038/nrendo.2017.151

23. Xie RY, Fang XL, Zheng XB, Lv WZ, Li YJ, Ibrahim Rage H, et al. Salidroside and FG-4592 ameliorate high glucose-induced glomerular endothelial cells injury *via* HIF upregulation. *BioMed Pharmacother* (2019) 118:109175. doi: 10.1016/j.biopha.2019.109175

24. Lu H, Li Y, Zhang T, Liu M, Chi Y, Liu S, et al. Salidroside reduces high-Glucose-Induced podocyte apoptosis and oxidative stress *via* upregulating heme oxygenase-1 (HO-1) expression. *Med Sci Monit* (2017) 23:4067–76. doi: 10.12659/MSM.902806

25. Seibt TM, Proneth B, Conrad M. Role of GPX4 in ferroptosis and its pharmacological implication. *Free Radic Biol Med* (2019) 133:144–52. doi: 10.1016/j.freeradbiomed.2018.09.014

26. Tang B, Zhu J, Li J, Fan K, Gao Y, Cheng S, et al. The ferroptosis and iron-metabolism signature robustly predicts clinical diagnosis, prognosis and immune microenvironment for hepatocellular carcinoma. *Cell Commun Signal* (2020) 18 (1):174. doi: 10.1186/s12964-020-00663-1

27. Masaldan S, Clatworthy SAS, Gamell C, Meggyesy PM, Rigopoulos AT, Haupt S, et al. Iron accumulation in senescent cells is coupled with impaired ferritinophagy and inhibition of ferroptosis. *Redox Biol* (2018) 14:100–15. doi: 10.1016/j.redox.2017.08.015

28. Botta A, Barra NG, Lam NH, Chow S, Pantopoulos K, Schertzer JD, et al. Iron reshapes the gut microbiome and host metabolism. *J Lipid Atheroscler* (2021) 10(2):160–83. doi: 10.12997/jla.2021.10.2.160

29. Gurung M, Li Z, You H, Rodrigues R, Shulzhenko N. Role of gut microbiota in type 2 diabetes pathophysiology. *EBioMedicine* (2020) 51:102590. doi: 10.1016/j.ebiom.2019.11.051

30. Yang G, Wei P, Liu Q, Zhang Y, Tian G, Hou L, Meng Y, Xin , Jiang X, et al. Role of the gut microbiota in type 2 diabetes and related diseases. *Metabolism* (2021) 117:154712. doi: 10.1155/2018/8597897

31. Khalili L, Alipour B, Jafar-Abadi MA, Faraji I, Hassanalilou T, Mesgari Abbasi M, et al. The effects of lactobacillus casei on glycemic response, serum Sirtuin1 and fetuin-a levels in patients with type 2 diabetes mellitus: A randomized controlled trial. *Iran BioMed J* (2019) 23(1):68–77. doi: 10.29252/ibj.23.1.68

32. Sandberg AA-O, Önning G, Engström N, Scheers N. Iron supplements containing lactobacillus plantarum 299v increase ferric iron and up-regulate the ferric reductase DCYTB in human caco-2/HT29 MTX Co-cultures. *Nutrients* (2018) 10(12):1949. doi: 10.3390/nu10121949

33. Adeshirlarijaney A, Gewirtz AT. Considering gut microbiota in treatment of type 2 diabetes mellitus. *Gut Microbes* (2020) 11:253–64. doi: 10.1080/19490976.2020.1717719

34. David LA, Maurice CF, Carmody RN, Gootenberg DB, Button JE, Wolfe BE, et al. Diet rapidly and reproducibly alters the human gut microbiome. *Nature* (2014) 505:559–63. doi: 10.1038/nature12820

35. Lewicki S, Skopińska-Różewska E, Lewicka A, Lewicka A, Zdanowski R. Longterm supplementation of rhodiola kirilowii extracts during pregnancy and lactation does not affect mother health status, J. *Matern. Fetal. Neonatal. Med* (2019) 32(5):838–44. doi: 10.1080/14767058.2017.1393069

36. Edwards D, Heufelder A, Zimmermann A. Therapeutic effects and safety of rhodiola rosea extract WS® 1375 in subjects with life-stress symptoms-results of an open-label study, phytother. *Res* (2012) 26(8):1220–5.

frontiers | Frontiers in Endocrinology

TYPE Original Research
PUBLISHED 29 September 2022
DOI 10.3389/fendo.2022.1018557



OPEN ACCESS

EDITED BY
Zhoujin Tan,
Hunan University of Chinese Medicine, China

REVIEWED BY
Yueying Wu,
Other, China
Liang Liu,
Yangzhou University, China

*CORRESPONDENCE
Xiaoliang Li
lixiaoliang-1984@163.com
Hong Zhao
zhaohong1981@jmsu.edu.cn

SPECIALTY SECTION
This article was submitted to Gut Endocrinology, a section of the journal Frontiers in Endocrinology

RECEIVED 13 August 2022
ACCEPTED 02 September 2022
PUBLISHED 29 September 2022

CITATION
Liu J, Kong L, Shao M, Sun C, Li C, Wang Y, Chai X, Wang Y, Zhang Y, Li X and Zhao H (2022) Seabuckthorn polysaccharide combined with *astragalus* polysaccharide ameliorate alcoholic fatty liver by regulating intestinal flora.
*Front. Endocrinol.* 13:1018557.
doi: 10.3389/fendo.2022.1018557



# Seabuckthorn polysaccharide combined with *astragalus* polysaccharide ameliorate alcoholic fatty liver by regulating intestinal flora

Jiayue Liu[1], Lingzhou Kong[1], Mengting Shao[1], Changhai Sun[1], Changxu Li[1], Yanyan Wang[1], Xue Chai[1], Yuliang Wang[1], Yu Zhang[1], Xiaoliang Li[2*] and Hong Zhao[1*]

[1]College of Pharmacy, Heilongjiang Provincial Key Laboratory of New Drug Development and Pharmacotoxicological Evaluation, Jiamusi University, Jiamusi, China, [2]Key Laboratory of Tropical Translational Medicine of Ministry of Education, Hainan Provincial Key Laboratory for Research and Development of Tropical Herbs, Haikou Key Laboratory of Li Nationality Medicine, School of Pharmacy, Hainan Medical University, Haikou, China

**Background:** At present, the incidence of alcoholic fatty liver disease (AFLD) is increasing year by year, and numerous studies have confirmed that liver diseases are closely related to intestinal flora. Seabuckthorn and *Astragalus membranaceus*, as traditional Chinese medicine (TCM) with the homology of medicine and food, have good liver protection, and their polysaccharides can regulate the intestinal flora. Here, we studied the effects of HRP, APS and the combination of the two polysaccharides on the intestinal flora of AFLD mice, which provided scientific basis for the treatment of AFLD with the two polysaccharides.

**Materials and methods:** Thirty Kunming (KM) mice were randomly divided into the control group (Con), the model group (Mod), the HRP treatment group (HRP), the APS treatment group (APS), and HRP+APS treatment group (HRP+APS), with six mice in each group. The AFLD model was constructed by continuous intragastric administration of 42% vol Niulanshan ethanol solution for 28 days, and the mice in each polysaccharide group were given corresponding drugs. The levels of AST, ALT, TC and TG in serum of mice were measured. 16S rRNA amplicon sequencing technique was used to determine the diversity and richness of intestinal flora, and the relative abundance of intestinal flora at phylum level and genus level of the mice in each group.

**Results:** HRP, APS and HRP+APS could reduce the serum levels of AST, ALT, TC and TG in mice. In addition, HRP, APS and HRP + APS restored the diversity, relative abundance and community structure of intestinal mucosa bacteria in AFLD mice to a certain extent. Specifically, HRP, APS and HRP+APS remarkably decreased the ratio of *Firmicutes* to *Bacteroidetes*, and ultimately increased the abundance of beneficial bacteria and reduced the abundance of pathogenic bacteria.

**Conclusion:** HRP, APS, and HRP+APS can improve the intestinal microecology of AFLD model mice, alleviate liver injury, and maintain normal intestinal function in different degrees.

KEYWORDS

Seabuckthorn, *Astragalus*, polysaccharide, alcoholic fatty liver, intestinal flora

## Introduction

With the development of economy and the living standard, the culture of drinking is prevalent, and excessive drinking is increasingly the norm for many people (1). According to the World Health Organization, more than 3 million alcohol-related deaths occur globally each year, accounting for 5.3% of all deaths (2). The liver is the main place for the oxidative metabolism of alcohol, and long-term alcoholism will lead to a series of liver diseases. Alcoholic liver disease is one of the common diseases, which usually manifests as AFLD in the early stage (3, 4). Luckily, AFLD can be reversed, but without timely intervention, it will develop into more serious liver diseases, such as alcoholic hepatitis, liver fibrosis, cirrhosis, and even deteriorate into liver cancer (5). At present, the treatment of AFLD mainly includes abstinence, nutritional support and drug therapy (6). The drug treatment mainly includes metadoxine, glucocorticoids, glycyrrhizic acid preparation and other drugs, which are not suitable for long-term use and are not specific drugs for AFLD (7, 8). Therefore, the development of high-efficiency and low-toxicity therapeutic drugs for AFLD has become an urgent clinical need.

Long-term excessive drinking leads to disturbances in the composition and distribution of intestinal microbiota, the decrease of beneficial bacteria and the increase of harmful bacteria, which in turn increases the permeability of the intestinal wall and induces endotoxemia (9). Lipopolysaccharide (LPS) from Gram-negative bacteria in the gut enters the peripheral circulation through the damaged intestinal mucosal barrier and reaches the liver tissue through the portal vein blood (10). LPS overactivates Kuffer cells, which in turn induces the occurrence of inflammatory reactions and the release of inflammatory factors, ultimately leading to liver damage (11). Many studies (12, 13) have shown that intestinal dysbacteriosis and excessive expression of inflammatory factors play an important role in the occurrence and development of AFLD. TCM and its active ingredients are mostly orally entered into the body, while the active ingredients in drugs interact with intestinal flora after entering the gastrointestinal tract and exert therapeutic effects by affecting the intestinal microbiota (14–16).

Seabuckthorn, as a classic TCM for promoting blood circulation and dispersing blood stasis, can be combined with *Astragalus membranaceus* to strengthen spleen and Qi, nourish stomach and Yin. *Hippophae rhamnoides* polysaccharide (HRP), as one of the main active components of *Hippophae rhamnoides*, has been proved to have good liver protection (17). At the same time, *astragalus* polysaccharide (APS) was found to have significant anti-inflammatory, liver protection, anti-oxidation and immune-enhancing effects, and can significantly improve liver damage, which has potential therapeutic effects on AFLD (18, 19). These two polysaccharides have different degrees of liver protection. Whether the combination of the two produces can produce synergistic effects and whether the mechanism is related to the regulation of intestinal flora are the key issues to be solved.

In the present study, HRP and APS were used in an equal mass ratio to compare the therapeutic effects of HRP, APS and HRP+APS on AFLD mice. To evaluate its impact on the intestinal flora structure in AFLD mice, the 16S rRNA coding region of the mice intestinal contents were amplified and

**Abbreviations:** AFLD, Alcoholic fatty liver disease; TCM, traditional Chinese medicine; KM, Kunming; LPS, Lipopolysaccharide; ALT, Alanine aminotransferase; AST, Aspartate aminotransferase; TG, Triglyceride; TC, Total cholesterol; PCA, Principle component analysis; NMDS, Nonmetric multidimensional scaling; HRP, Hippophae rhamnoides polysaccharide; APS, Astragalus polysaccharide; H&E, Hematoxylin-eosin.

annotated by the NovaSeq 6000 system. This study laid an experimental foundation for solving the problem of limited activity of single polysaccharide and provided a new idea for the prevention and treatment of AFLD in the future.

# Materials and methods

## Animals and reagents

A total of 30 male Kunming mice of SPF grade, weighing 18-22 g, were purchased from Changchun Yisi Experimental Animal Technology Co., Ltd. (SCXK (Ji)-2018-0007). All experimental procedures involving animals were approved by Animal Ethics Committee of the Animal Experimental Center of Jiamusi University.

42% vol liquor of Niulanshan was purchased from Niulanshan distillery of Beijing Shunxin Agricultural Co., Ltd. Alanine aminotransferase (ALT), aspartate aminotransferase (AST), triglyceride (TG) and total cholesterol (TC) kits were obtained from Nanjing Jiancheng Bioengineering Institute (Nanjing, China).

## Preparation of polysaccharides

Seabuckthorn fruit was purchased from Jiamusi Minsheng pharmacy (batch number: 180312); *Astragalus* was purchased from Tongrentang pharmacy, Jiamusi City, Heilongjiang Province (batch number 170801).

After degreasing, sea buckthorn fruit was extracted three times with distilled water at the ratio of 1:23 g/ml at 90° for 3 h each time, and HRP with a polysaccharide content of 64.33% was obtained after further deproteinization. Similarly, the defatted *astragalus* was extracted 3 times with distilled water at 95°C with a ratio of 1:20 g/ml, each time for 3 h, and after deproteinization, APS with polysaccharide content of 62.73% was obtained.

## Modeling and treatment

After a week of acclimation, 30 male KM mice were divided into control group (Con), model group (Mod), HRP treatment group (HRP), APS treatment group (APS), and HRP+APS treatment group (HRP+APS) according to the random number table method, with 6 mice in each group. Except for the Con group, the mice in the other groups were orally administered 14 mL/kg 42% vol liquor of Niulanshan every day. After 6 h, mice in HRP and APS groups were given 22 mg/kg corresponding polysaccharide solution, and mice in HRP +APS treatment group were given 22 mg/kg mixed solution of HRP and APS. Con and mod groups were given the same amount of normal saline for 28 days. The body weight of mice in each group was recorded every 3 days during the experiment. Flowchart of the experimental design was shown in Figure 1.

## Hepatic tissue staining

After the experiment, liver tissues of mice were removed, fixed immediately in 10% neutral buffered formalin for 24h, and then embedded in paraffin. The liver tissues embedded in paraffin were cut into 5mm thick sections and stained with hematoxylin and eosin (H&E). The steatosis of liver tissue was examined under a light microscope at 400 magnifications.

## Serum biochemical analysis

Serum samples were isolated from eye blood of mice by centrifugation at 3000 rpm for 10 minutes at 4°. The level of AST, ALT, TC and TG in serum of mice were determined by automatic blood biochemical analyzer.

## 16S rRNA amplicon sequencing analyses

According to the instructions of the DNA kit, DNA was extracted from the intestinal contents of mice, quantified by Nanodrop, and the quality of DNA extraction was detected by 1.2% agarose gel electrophoresis. PCR amplification and sequencing were designed according to the V3-V4 region of 16S rRNA. The microbiota of intestinal contents of mice were sequenced using NovaSeq 6000 platform of Illumina, and the results were annotated with Green Genes 13.8 database. Sequencing was completed by Wuhan Frasergen Genomic Medicine Co., Ltd (Wuhan, China).

## Bioinformatics and statistical analysis

Non-repetitive sequences were clustered by OTU with 97% similarity using QIME2 software and compared with the SILVA database to obtain the species classification information corresponding to each OTU. Alpha diversity analysis including Chao1, ACE, Simpson and Shannon indices was calculated and analyzed using R 4.1.2. The structural variation of microbial communities across samples was investigated by the Beta diversity, including Principle component analysis (PCA) of UniFrac distance metrics and nonmetric multidimensional scaling (NMDS) (19).

SPSS 26.0 statistical software was used for data analysis. Differences between multiple groups were compared using Kruskal-Wallis and one-way ANOVA analysis, and differences between two groups were compared using T-test. The results

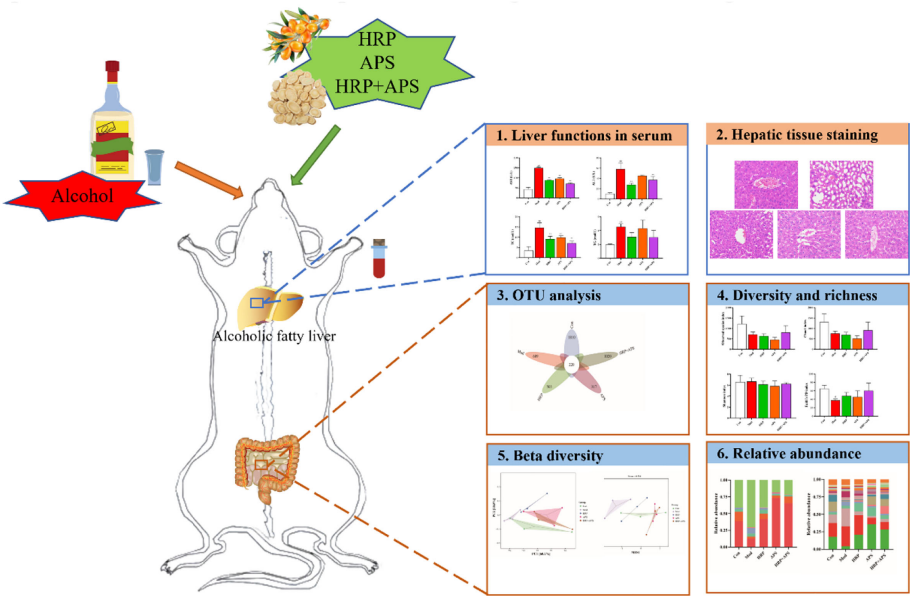


FIGURE 1
Flowchart of the experimental design.

were expressed as mean ± SD, and $P<0.05$ was considered statistically significant. Graphs were performed using R 4.2 and GraphPad Prism 8 software.

# Results

## Effects of the combination of HRP and APS on general characteristics and liver histopathological changes in AFLD mice

At the beginning of the experiment, all mice exhibited normal food intake, natural spirit, smooth shiny hair, and dry black fecal pellets that did not stick to hands when squeezed. As shown in Figure 2A, on the third day after the administration of Chinese Baijiu, the weight of mice in the model group decreased significantly ($P<0.01$), the food intake reduced, and the hair lost luster, while no obvious abnormalities were found in other groups. On the 27th day of the experiment, compared with the model group, the weight of mice in HRP administration group increased slightly ($P>0.05$), and the weight of mice in APS and HRP+APS groups increased remarkably ($P<0.01$). Meanwhile, after the polysaccharide intervention, the hair of mice in each group became thick and shiny, and the food intake and urine volume were normal.

As shown in Figure 2B, the liver tissue structure of mice in the blank group was complete, and the nuclei were round and orderly arranged. By contrast, chronic ethanol exposure caused disordered arrangement of hepatocytes, increased tissue vacuoles and fat accumulation in mice. After polysaccharides intervention, the abnormal structure of liver tissue of mice in each group was improved to varying degrees. Among them, the improvement effect of HRP+APS group was more significant, and some cells in the liver tissue of HRP and APS groups were still in disorder and fat accumulation. These results showed that the combination of HRP and APS could improve the weight loss and liver injury of AFLD mice.

## Analysis of serum biochemical indexes of mice

As shown in Figure 3, compared with the Con group, the contents of AST, ALT, TC and TG in the serum of mice in the model group were all significantly increased ($P<0.01$). Compared with the model group, AST, ALT and TC in serum of mice in HRP group were remarkably decreased ($P<0.01$), AST and TC in serum of mice in APS group were dramatically reduced ($P< 0.01$), and AST, ALT and TC in HRP + APS group were significantly decreased ($P<0.01$). After HRP and APS intervention, the serum TG content of mice decreased, but there was no significant difference. The above results implied that HRP, APS and HRP+APS had the regulating serum biochemical indexes of mice in AFLD mice.

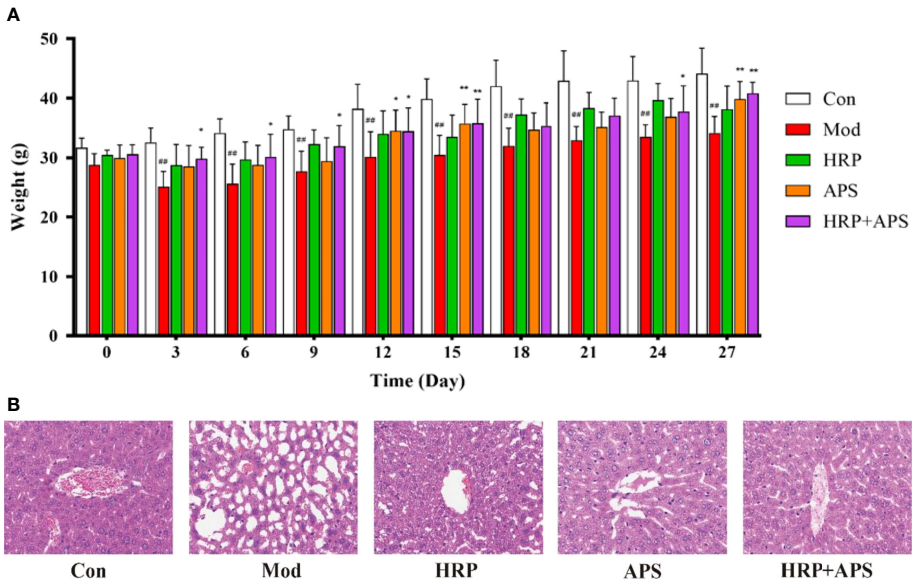


FIGURE 2
The effects of HRP, APS and the combination of HRP and APS on the body weight and histopathological change of liver in AFLD mice. **(A)** Weight changes of mice during the experiment. **(B)** Hematoxylin-eosin (H&E) staining of hepatocytes (Original magnification, ×400, n = 3). Data are presented as mean ± SD (n = 6). $^{\#\#}P < 0.01$ vs. Con; $^{*}P < 0.05$ and $^{**}P < 0.01$ vs. Mod.

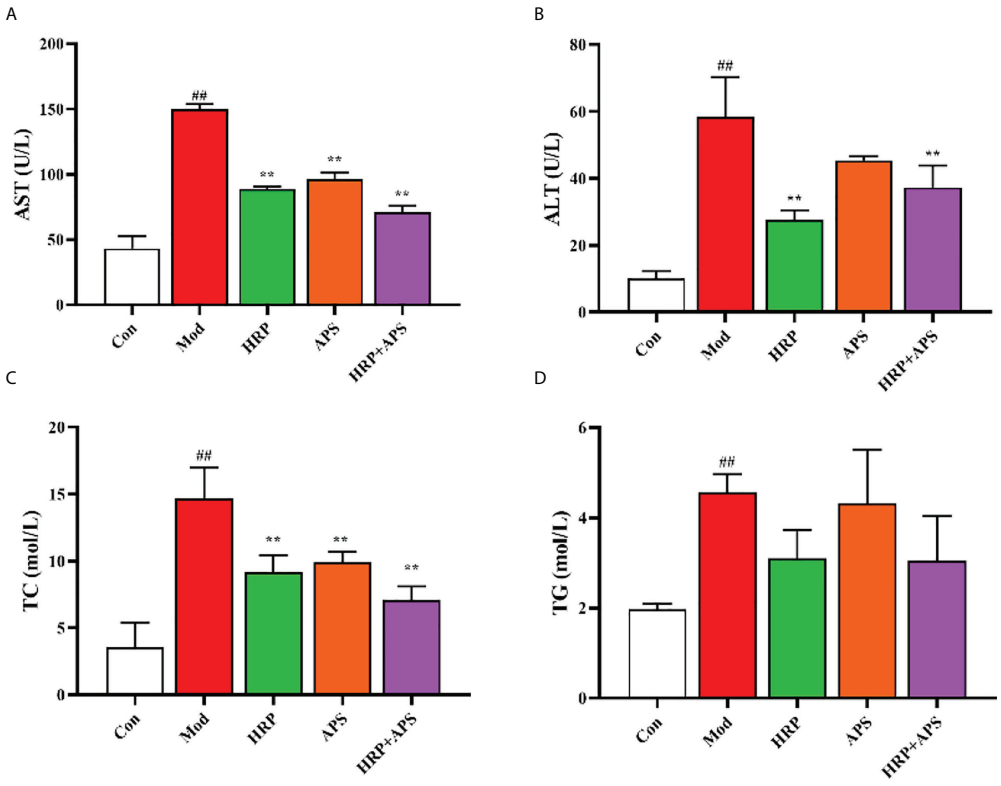


FIGURE 3
The effects of HRP, APS and the combination of HRP and APS on serum biochemical indexes of AFLD mice. **(A)** Serum AST. **(B)** Serum ALT. **(C)** Serum TC. **(D)** Serum TG. Data are presented as mean ± SD (n = 6). $^{\#\#}P < 0.01$ vs. Con; $^{**}P < 0.01$ vs. Mod.

## Effects of the combination of HRP and APS on bacterial OTU number and alpha diversity in the intestinal mucosa of AFLD mice

The analysis of OTUs are shown in Figure 4A, there were 220 OTUs in the five experimental groups, and the number of OTUs in blank group, model group, HRP group, APS group, and HRP+APS group were 1810, 609, 503, 317, and 1020, respectively. Compared with the blank group, the number of OTUs in the model group was significantly decreased, indicating that the intestinal flora of mice was disordered after drinking. After the intervention of different polysaccharides, the number of OTUs in the intestinal tract of mice increased, and the HRP+APS group was the closest to the blank group.

Alpha diversity refers to the diversity within a specific area or ecosystem, and is a comprehensive indicator reflecting richness and evenness. Observed species and Chao1 indices are used to evaluate richness, and the larger its values, the more abundant the total number of species in the environment. As two other indicators for assessing diversity, Shannon and Faith's PD index, the higher the value, the higher the diversity of species in the environment. As can be seen from Figures 4B-E, compared with the blank group, the Observed species and Chao1 in the intestinal flora of AFLD mice were decreased ($P>0.05$) and the Faith's PD was significantly decreased ($P<0.05$), which indicated that alcohol caused certain damage to the diversity and richness of the intestinal flora in mice. After the polysaccharide intervention, there was no significant difference in Observed species, Chao1, Shannon and Faith's PD index in the intestinal flora of mice in the HRP and APS groups. But, HRP + APS could increase the observed species, Chao1 and Faith's PD index in the intestinal flora of AFLD mice ($P>0.05$), indicating that HRP + APS could restore the richness and diversity of the intestinal flora of AFLD mice.

## Effects of the combination of HRP and APS on intestinal beta diversity in AFLD mice

Beta diversity, also known as between-habitat diversity, is used to study the species diversity relationship between communities, including unconstrained ordination, such as PCoA and NMDS. The PCA plot (Figure 5A) and NMDS plot (Figure 5B) showed that the gut microbiota structure of the model group was remarkably different from that of the blank group, which indicated that alcohol could alter the structure of the mice gut microbiota. As expected, each administration group was relatively concentrated and had a high similarity in community structure with the blank group after HRP, APS and HRP+APS treatment. Beta diversity analysis indicated that the structure of intestinal mucosal bacteria could be repaired and restored to normal state by the combined application of HRP and APS.

## Effects of the combination of HRP and APS on relative abundance of intestinal flora in AFLD mice

The relative abundance of intestinal mucosal bacteria at the phylum level in mice is shown in Figure 6A, in which *Firmicutes* and *Bacteroidetes* are the dominant phyla. Compared with the blank group, the relative abundance of *Firmicutes* in the intestinal flora of the model group was significantly increased

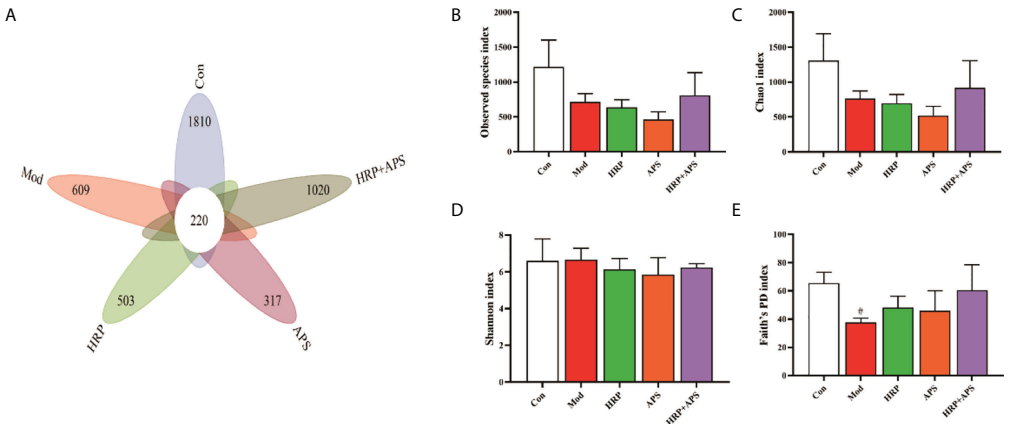


FIGURE 4
Effects of HRP, APS and the combination of HRP and APS on the number of OTUs and alpha diversity in mice intestinal mucosal bacteria. **(A)** The number of observed OTUs. **(B)** Observed species index. **(C)** Chao1 index. **(D)** Simpson index. **(E)** Faith's PD index. $^{\#}P < 0.05$ vs. Con.

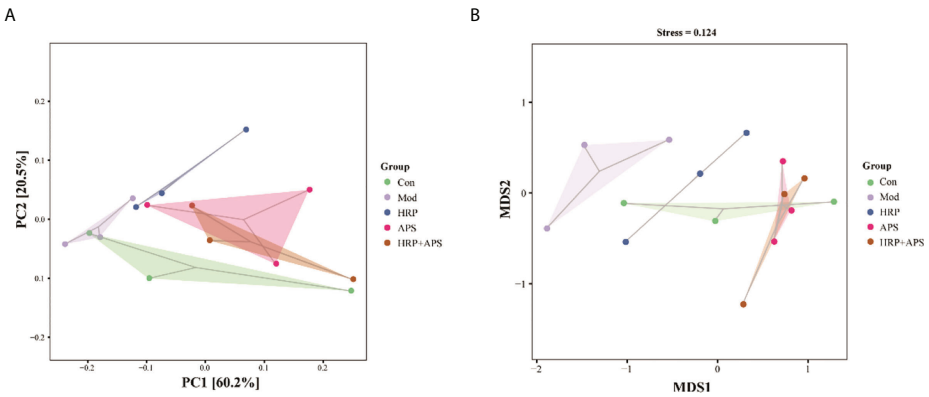


FIGURE 5
Effect of HRP, APS and the combination of HRP and APS on the beta diversity of mice intestinal mucosal bacteria. **(A)** PCA and **(B)** NMDS.

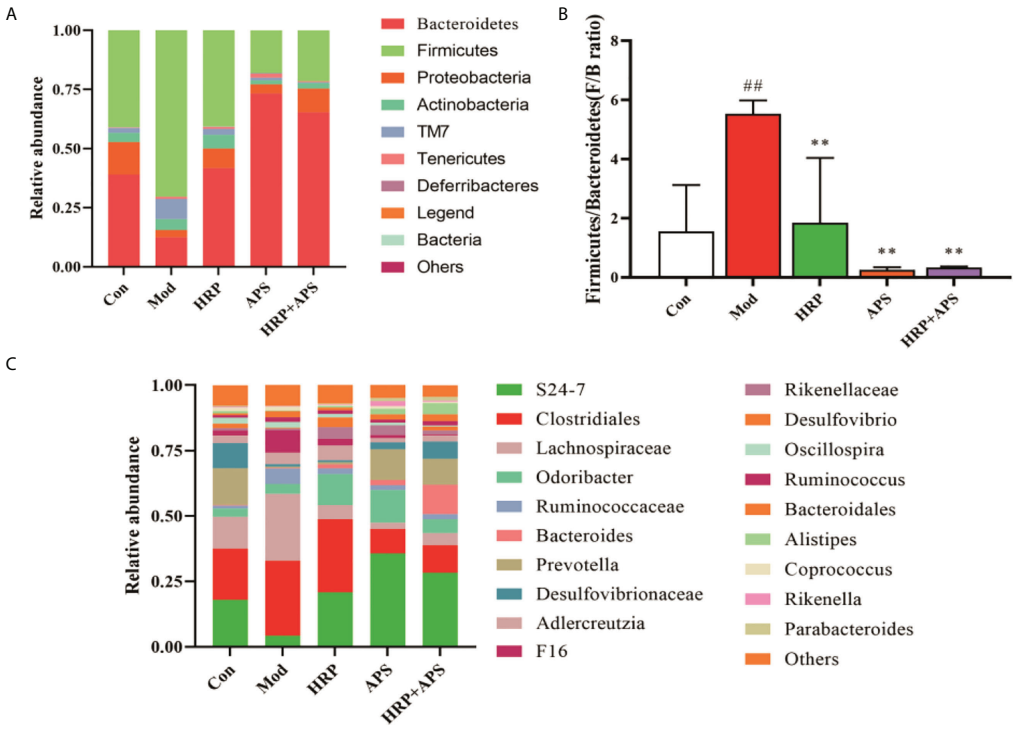


FIGURE 6
Effect of HRP, APS and the combination of HRP and APS on relative abundance of intestinal flora in AFLD mice. **(A)** Relative abundance at the phylum level. **(B)** Histogram of Firmicutes/Bacteroidetes ratio. **(C)** Relative abundance at the genus level. $^{\#\#}P < 0.01$ vs. Con; $^{**}P < 0.01$ vs. Mod.

($P$<0.01), and the relative abundance of *Bacteroidetes* was dramatically decreased ($P$<0.01). These trends were remarkably reversed after the intervention of all polysaccharide groups. As shown in Figure 6B, the F/B ratio of the model group was significantly increased ($P$<0.01), while the F/B ratio was significantly decreased after HRP, APS and HRP+APS treatment ($P$ <0.01).

The relative abundance of intestinal microbiota in mice at the genus level are shown in Figure 6C, in which *S24-7*, *Clostridiales*, and *Lachnospiraceae* are the dominant genera.

Compared with the blank group, the relative abundance of *S24-7* in the intestinal microbiota of mice in the model group was decreased, while the relative abundance of *Clostridiales* and *Lachnospiraceae* was increased, but there was no significant difference ($P>0.05$). After polysaccharide intervention, the relative abundance of *S24-7* in intestinal microbiota of mice in APS group and HRP+APS group was significantly increased compared with that in model group ($P<0.01$), and the relative abundance of *Clostridiales* and *Lachnospiraceae* was decreased in HRP, APS and HRP+APS groups ($P>0.05$).

## Correlation between gut microbiota and AFLD

To further determine the relationship between intestinal flora and AFLD induced by Chinese Baijiu exposure in mice, Spearman correlation analysis was performed in the current study. The relationship between liver function indicators including AST, ALT and blood lipid indicators including TC and TG and the top 20 genera in intestinal flora of mice was analyzed. As shown in Figure 7, The level of serum AST, ALT, TC and TG were positively correlated with *Firmicutes, TM7* and *Actinobacteria*. Among them, the serum AST, ALT and TC were positively correlated with *Ruminococcaceae* in *Firmicutes* ($P<0.05$). Moreover, the level of serum AST, ALT, TC and TG were negatively correlated with some genera in *Bacteroidetes*. Particularly, the serum AST was negatively correlated with *Desulfovibrio* in *Proteobacteria* ($P<0.05$).

# Discussion

The gut microbiota is the normal intestinal microbiota formed in the long-term evolution of the human body (20). They are distributed in the intestine with a certain regularity and form a defense barrier together with intestinal mucosa (21, 22). Many studies have shown that changes in the composition of gut microbiota affect host metabolism and are associated with diseases such as cirrhosis, diabetes, toxemia (23, 24). The gastrointestinal tract of the human body is the most important part of ethanol absorption and digestion, and long-term chronic drinking has adverse effects on the intestinal microecology. The accumulation of a large amount of ethanol in the intestinal tract will affect the intracellular signaling cascade and lead to the damage of various organs in the body. When the content of alcohol dehydrogenase in the body is low, the high concentration of ethanol cannot be metabolized, which will directly cause damage to the intestine and liver, including the bacterial translocation, the injury of intestinal barrier function, increased tissue inflammation, and the production of a large amount of endotoxin in the intestine (25). The liver and intestine are connected through the portal vein system, and a small amount of endotoxin enters the portal vein through the intestinal mucosa, which can maintain the hepatic reticuloendothelial system in an activated state. However, when the intestine is damaged, the imbalance of intestinal flora leads to a large amount of intestinal toxins entering the liver through the portal vein system, causing or aggravating liver injury (26, 27).

AST and ALT are important indicators to determine whether liver function is damaged, while TC and TG are the other two main indicators to measure liver lipid accumulation (28, 29). In the present study, the serum levels of AST, ALT, TC and TG in the administration group were significantly lower than those in the model group, indicating that the combination of HRP and APS can effectively regulate the liver function damage and lipid accumulation in AFLD mice. In addition, alpha diversity can reflect the diversity and richness of microbial communities *in vivo* (30, 31). 16S rRNA amplicon sequencing was used to decipher microbial diversity and abundance. Our study found that the Observed species, Chao1, Shannon and Faith's PD index in the intestinal tract of the model group were remarkably decreased, indicating that alcohol consumption had a certain inhibitory effect on the richness and diversity of the intestinal flora in mice. After

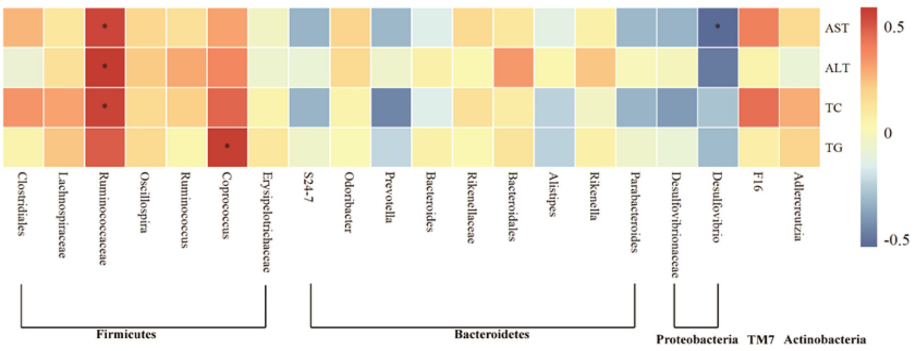


FIGURE 7
Heat map of the correlation of gut microbiota with indicators of liver injury in AFLD mice. Significant differences are indicated by asterisks, *$P < 0.05$.

the polysaccharide intervention, the Observed species, Chao1, Shannon and Faith's PD index in the intestinal tract of mice increased, and the HRP+APS group was close to the level of the blank group, which showed that combination of HRP and APS had a certain recovery effect on the intestinal microbial disturbance caused by alcohol consumption in mice.

By comparing the relative abundance changes of phylum levels in different groups of mice, we further analyzed how HRP+APS changed the intestinal microecology of AFLD mice. The change of relative abundance of *Fimicutes* and *Bacterodietes* is an important factor leading to the end-stage liver disease and other intestinal diseases. When the relative abundance of *Fimicutes* increases and the relative abundance of *Bacterodietes* decreases, inflammatory factors can be released and intestinal barrier is dysregulated. At the same time, the ratio of the relative abundance of *Fimicutes* and *Bacterodietes* can reflect the inflammatory state of samples. The results of this study showed that alcohol caused a significant increase in the F/B of the intestinal microbiota in mice, indicating that the intestinal microbiota in AFLD mice was dysregulated. After polysaccharide intervention, F/B decreased significantly, which was close to the blank group. It was speculated that HRP combined with APS was beneficial to the recovery of *Fimicutes* and *Bacterodietes* in AFLD mice. Both *Clostridiales* and *Lachnospiraceae* belong to the phylum *Fimicutes*. Among them, *Clostridiales* plays an important role in inducing and regulating immunity, mental diseases, puberty obesity and so on. At the same time, it plays an important role in intervening abnormal liver lipid metabolism and regulating fatty liver bile acid homeostasis, while *Ruminococcaceae* and *Lachnospiraceae* play a vital role in hepatic steatosis and lipid metabolism (32, 33). *Coprococcus* can actively ferment and decompose carbohydrates to produce such as butyric acid, acetic acid, formic acid, propionic acid, lactic acid, etc. Studies have shown that the change of *Coprococcus* is positively correlated with the changes of individual body weight, TC and TG (34). *S24-7* belongs to *Bacterodietes*, which can participate in the metabolism of human body. In the present study, correlation analysis indicated that the main changes of gut microbiota induced by alcohol treatment in mice were significantly positively correlated with hepatic steatosis. Furthermore, compared with the model group, HRP, APS and HRP + APS could increase the relative abundance of AFLD mice *S24-7* and reduce the relative abundance of *Lachnospiraceae*. Interestingly, APS was more likely to increase the relative abundance of *S24-7* in the gut of AFLD mice than HRP, and reduce the relative abundance of *Clostridiales* and *Lachnospiraceae* in the gut of AFLD mice. However, the combination of the two polysaccharides could reduce the effect of APS and make APS regulate the intestinal flora of AFLD mice more mildly.

## Conclusion

Excessive alcohol consumption can destroy the diversity and richness of intestinal microbiota in mice, and the combination of HRP and APS contribute to restore the diversity, relative abundance and community structure of intestinal mucosal bacteria to a certain extent. However, the effects of HRP and APS on intestinal microbiota of AFLD mice in dose and proportion need further study.

## Data availability statement

The original contributions presented in the study are publicly available. This data can be found here: https://github.com/lixiaoliang1894/Seabuckthorn-polysaccharide-combined-with-astragalus-polysaccharide-ameliorate-alcoholic-fatty-liver.git.

## Ethics statement

The animal study was reviewed and approved by Animal Ethics Committee of the Animal Experimental Center of Jiamusi University.

## Author contributions

HZ designed the study and revised the manuscript. LK, MS, JL, CS, and CL performed the experiments. YaW and XC analyzed the data. YuW and YZ supervised the work, and reviewed the manuscript. XL contributed to the study design and revised the manuscript. All authors reviewed the manuscript and approved the submitted version.

## Acknowledgments

This study was supported by the Foundation of Central Government Supports Local Universities (Grant No. 2019zyzcdf-01), Postdoctoral Research Special Fund of Heilongjiang Province (LBH-Q20185), North Medicine and Function Food Discipline of Heilongjiang Province (Grant No. 2018-TSXK-02), the Excellent Subject Team Project of Jiamusi University (Grant No. JDXKTD-2019005), and Scientific Research Support Project of Colleges and Universities in Hainan Province (Hnky2019ZD-24). The Technological Innovation Team Construction Project of Heilongjiang Provincial Department of Education (2021-KYYEF-0638).

## Conflict of interest

The authors declare that the research was conducted in the absence of any commercial or financial relationships that could be construed as a potential conflict of interest.

## Publisher's note



## References

1. Aslam S, Buggs J, Melo S, Ermekbaeva A, Rogers E, Shaw R, et al. The association between alcoholic liver disease and alcohol tax. *Am Surg* (2021) 87:92–6. doi: 10.1177/0003134820945223

2. Sepanlou SG, Safiri S, Bisignano C, Ikuta KS, Merat S, Saberifiroozi M, et al. The global, regional, and national burden of cirrhosis by cause in 195 countries and territories, 1990–2017: A systematic analysis for the global burden of disease study 2017. *Lancet Gastroenterol Hepatol* (2020) 5:245–66. doi: 10.1016/S2468-1253(19)30349-8

3. Han S, Yang ZH, Zhang T, Ma J, Chandler K, Liangpunsakul S. Epidemiology of alcohol-associated liver disease. *Clin Liver Dis* (2021) 25:483–92. doi: 10.1016/j.cld.2021.03.009

4. Higuera-de-la-Tijera F, Lira-Vera JE, Morales-Gutiérrez O, Martínez-Castillo M, Medina-Ávila Z, Servín-Caamaño A, et al. Alcoholic liver disease. *Clin Liver Dis (Hoboken)* (2022) 19:63–7. doi: 10.1002/cld.1164

5. Johnston MP, Patel J, Byrne CD. Causes of mortality in non-alcoholic fatty liver disease (NAFLD) and alcohol related fatty liver disease. *Curr Pharm Des* (2020) 26:1079–92. doi: 10.2174/1381612826666200128094231

6. Stickel F, Datz C, Hampe J, Bataller R. Pathophysiology and management of alcoholic liver disease: Update 2016. *Gut Liver* (2017) 11:173–88. doi: 10.5009/gnl16477

7. Sharma S, Maras JS, Das S, Hussain S, Mishra AK, Shasthry SM, et al. Pre-therapy liver transcriptome landscape in Indian and French patients with severe alcoholic hepatitis and steroid responsiveness. *Sci Rep* (2017) 7:6816. doi: 10.1038/s41598-017-07161-4

8. Zhang T, Li J, Liu CP, Guo M, Gao CL, Zhou LP, et al. Butyrate ameliorates alcoholic fatty liver disease *via* reducing endotoxemia and inhibiting liver gasdermin d-mediated pyroptosis. *Ann Transl Med* (2021) 9:873. doi: 10.21037/atm-21-2158

9. Guo KX, Xu SS, Zhang QL, Peng MJ, Yang ZY, Li WG, et al. Bacterial diversity in the intestinal mucosa of mice fed with asparagus extract under high-fat diet condition. *3 Biotech* (2020) 10:228. doi: 10.1007/s13205-020-02225-1

10. Li XY, Peng XX, Guo KX, Tan ZJ. Bacterial diversity in intestinal mucosa of mice fed with dendrobium officinale and high-fat diet. *3 Biotech* (2021) 11:22. doi: 10.1007/s13205-020-02558-x

11. Marshall JC. The gut as a potential trigger of exercise-induced inflammatory responses. *Can J Physiol Pharmacol* (1998) 76:479–84. doi: 10.1139/cjpp-76-5-479

12. Liu GH, Zhao QX, Wei HY. Characteristics of intestinal bacteria with fatty liver diseases and cirrhosis. *Ann Hepatol* (2019) 18:796–803. doi: 10.1016/j.aohep.2019.06.020

13. Lang S, Schnabl B. Microbiota and fatty liver disease-the known, the unknown, and the future. *Cell Host Microbe* (2020) 28:233–44. doi: 10.1016/j.chom.2020.07.007

14. Wang XM, Li XB, Peng Y. Impact of qi -invigorating traditional Chinese medicines on intestinal flora: A basis for rational choice of prebiotics. *Chin J Natural Medicines* (2017) 15:241–54. doi: 10.1016/S1875-5364(17)30041-9

15. He L, Liu YW, Guo YF, Shen KJ, Hui HY, Tan ZJ. Diversity of intestinal bacterial lactase gene in antibiotics-induced diarrhea mice treated with Chinese herbs compound qi wei bai Zhu San. *3 Biotech 8* (2017) 1–8. doi: 10.1007/s13205-017-1024-y

16. Hui HY, Wu Y, Zheng T, Zhou SN, Tan ZJ. Bacterial characteristics in intestinal contents of antibiotic-associated diarrhea mice treated with qiweibaizhu powder. *Med Sci Monit* (2020) 26:e921771. doi: 10.12659/MSM.921771

17. Liu H, Zhang W, Dong SC, Song L, Zhao SM, Wu CY, et al. Protective effects of sea buckthorn polysaccharide extracts against LPS/d-GalN-induced acute liver failure in mice *via* suppressing TLR4-NF-kappaB signaling. *J Ethnopharmacol* (2015) 176:69–78. doi: 10.1016/j.jep.2015.10.029

18. Zhou JX, Zhang NH, Zhao L, Wu W, Zhang LB, Zhou F, et al. Astragalus polysaccharides and saponins alleviate liver injury and regulate gut microbiota in alcohol liver disease mice. *Foods* (2021) 10:1–16. doi: 10.3390/foods10112688

19. Lv HW, Tang YQ, Zhang HH, Li SM, Fan ZY. Astragalus polysaccharide supplementation improves production performance, egg quality, serum biochemical index and gut microbiota in chongren hens. *Anim Sci J* (2021) 92: e13550. doi: 10.1111/asj.13550

20. Li CR, Zhou K, Xiao NQ, Peng MJ, Tan ZJ. The effect of qiweibaizhu powder crude polysaccharide on antibiotic-associated diarrhea mice is associated with restoring intestinal mucosal bacteria. *Front Nutr* (2022) 9:952647. eCollection 2022. doi: 10.3389/fnut.2022.952647

21. Wang R, Tang RQ, Li B, Ma X, Schnabl B, Tilg H. Gut microbiome, liver immunology, and liver diseases. *Cell Mol Immunol* (2021) 18:4–17. doi: 10.1038/s41423-020-00592-6

22. Li XY, Deng N, Zheng T, Qiao B, Peng MJ, Xiao NQ, et al. Importance of dendrobium officinale in improving the adverse effects of high-fat diet on mice associated with intestinal contents microbiota. *Front Nutr* (2022) 9:957334. eCollection 2022. doi: 10.3389/fnut.2022.957334

23. Ma QT, Li YQ, Li PF, Wang M, Wang JK, Tang ZY, et al. Research progress in the relationship between type 2 diabetes mellitus and intestinal flora. *BioMed Pharmacother* (2019) 117:109138. doi: 10.1016/j.biopha.2019.109138

24. Jin MC, Qian ZY, Yin JY, Xu WT, Zhou X. The role of intestinal microbiota in cardiovascular disease. *J Cell Mol Med* (2019) 23:2343–50. doi: 10.1111/jcmm.14195

25. Meroni M, Longo M, Dongiovanni P. Alcohol or gut microbiota: Who is the guilty? *Int J Mol Sci* (2019) 20:4568. doi: 10.3390/ijms20184568

26. Albillos A, de Gottardi A, Rescigno M. The gut-liver axis in liver disease: Pathophysiological basis for therapy. *J Hepatol* (2020) 72:558–77. doi: 10.1016/j.jhep.2019.10.003

27. Tripathi A, Debelius J, Brenner DA, Karin M, Loomba R, Schnabl B, et al. The gut-liver axis and the intersection with the microbiome. *Nat Rev Gastroenterol Hepatol* (2018) 15:397–411. doi: 10.1038/s41575-018-0011-z

28. Zhang YH, Tan XY, Cao Y, An X, Chen JH, Yang LN. Punicalagin protects against diabetic liver injury by upregulating mitophagy and antioxidant enzyme activities. *Nutrients* (2022) 14:1–16. doi: 10.3390/nu14142782

29. Liu MF, Jia HX, He Y, Huan Y, Kong Z, Xu N, et al. Preventive effects of ilex cornuta aqueous extract on high-fat diet-induced fatty liver of mice. *Evid Based Complement Alternat Med* (2022) 2022:7183471. doi: 10.1155/2022/7183471

30. Liu YY, Tan YY, Huang JQ, Wu C, Fan XT, Stalin A, et al. Revealing the mechanism of huazhi rougan granule in the treatment of nonalcoholic fatty liver through intestinal flora based on 16S rRNA, metagenomic sequencing and network pharmacology. *Front Pharmacol* (2022) 13:875700. eCollection 2022. doi: 10.3389/fphar.2022.875700

31. Zhao L, Ren PP, Wang ML, Wang JJ, He XY, Gu JY, et al. Changes in intestinal barrier protein expression and intestinal flora in a rat model of visceral hypersensitivity. *Neurogastroenterol Motil* (2022) 34:e14299. doi: 10.1111/nmo.14299

32. Shen F, Zheng RD, Sun XQ, Ding WJ, Wang XY, Fan JG. Gut microbiota dysbiosis in patients with non-alcoholic fatty liver disease. *Hepatobiliary Pancreat Dis Int* (2017) 16:375–81. doi: 10.1016/S1499-3872(17)60019-5

33. Ponziani FR, Bhoori S, Castelli C, Putignani L, Rivoltini L, Del Chierico F, et al. Hepatocellular carcinoma is associated with gut microbiota profile and inflammation in nonalcoholic fatty liver disease. *Hepatology* (2019) 69:107–20. doi: 10.1002/hep.30036

34. Zhou L, Ni ZX, Yu J, Cheng W, Cai ZL, Yu CQ. Correlation between fecal metabolomics and gut microbiota in obesity and polycystic ovary syndrome. *Front Endocrinol (Lausanne)* (2020) 11:628. eCollection 2020. doi: 10.3389/fendo.2020.00628

frontiers | Frontiers in Endocrinology

TYPE Original Research
PUBLISHED 09 November 2022
DOI 10.3389/fendo.2022.1063579



OPEN ACCESS

EDITED BY
Zhoujin Tan,
Hunan University of Chinese Medicine, China

REVIEWED BY
Tao Wu,
Shanghai University of Traditional Chinese Medicine, China
Lixin Zhu,
The Sixth Affiliated Hospital of Sun Yat-sen University, China

*CORRESPONDENCE
Zhonghai Yu
yuzhonghai0715@126.com
Yueqiong Ni
yueqiong.ni@leibniz-hki.de
Bing Wang
bingbrain@163.com

†These authors have contributed equally to this work and share first authorship

SPECIALTY SECTION
This article was submitted to Gut Endocrinology, a section of the journal Frontiers in Endocrinology

RECEIVED 07 October 2022
ACCEPTED 24 October 2022
PUBLISHED 09 November 2022

CITATION
Shang H, Zhang L, Xiao T, Zhang L, Ruan J, Zhang Q, Liu K, Yu Z, Ni Y and Wang B (2022) Study on the differences of gut microbiota composition between phlegm-dampness syndrome and qi-yin deficiency syndrome in patients with metabolic syndrome. *Front. Endocrinol.* 13:1063579. doi: 10.3389/fendo.2022.1063579



# Study on the differences of gut microbiota composition between phlegm-dampness syndrome and qi-yin deficiency syndrome in patients with metabolic syndrome

Haonan Shang[1†], Lu Zhang[2†], Tiegang Xiao[1†], Li Zhang[1], Jun Ruan[3], Qiang Zhang[1], Kaili Liu[1], Zhonghai Yu[1*], Yueqiong Ni[2*] and Bing Wang[1*]

[1]Department of Traditional Chinese Medicine, Shanghai Sixth People's Hospital Affiliated to Shanghai Jiao Tong University School of Medicine, Shanghai, China, [2]Systems Biology & Bioinformatics Unit, Leibniz Institute for Natural Product Research and Infection Biology - Hans Knöll Institute, Jena, Germany, [3]Shanghai municipal Hospital of Traditional Chinese Medicine, Shanghai University of Traditional Chinese Medicine, Shanghai, China

**Background:** Metabolic syndrome (MS) is a group of complex medical conditions that can lead to serious cardiovascular and cerebrovascular diseases. According to the theory of traditional Chinese medicine (TCM), MS can be divided into two main subtypes termed 'phlegm-dampness syndrome' (TSZE) and 'qi-yin deficiency syndrome' (QYLX). At present, the research into intestinal microbiota of different TCM syndromes of MS and its association with clinical manifestation is lacking.

**Materials and methods:** Using 16S rRNA sequencing, we performed a cross-sectional analysis of human gut microbiota between two different TCM syndromes (QYLX and TSZE, n=60) of MS, and their differences with healthy participants (n=30).

**Results:** We found that the QYLX and TSZE groups differ from the healthy control group in the overall gut microbiota composition, and some specific microbial taxa and functional pathways. Moreover, significantly differentially abundant taxa and distinct BMI-correlated taxa were observed between QYLX and TSZE groups, suggesting the potential contribution of gut microbiota to the distinction between the two TCM syndromes. The predicted functional profiles also showed considerable differences, especially pathways related to amino acid metabolism and lipopolysaccharide synthesis.

**Conclusion:** Our study highlights the gut microbiota's contribution to the differentiation between two TCM syndromes of MS and may provide the rationale for adopting different microbiota-directed treatment strategies for different TCM syndromes of MS in the future.

KEYWORDS

metabolic syndrome, traditional Chinese medicine, gut microbiota, phlegm-dampness syndrome, qi-yin deficiency

# Introduction

Metabolic syndrome (MS) is a clustering of risk factors, such as central obesity, insulin resistance, dyslipidaemia and hypertension that together culminate in the increased risk of type II diabetes mellitus and cardiovascular disease (1). Available evidences show that in most countries, 20% to 30% of the adult population can be described as suffering from metabolic syndromes, and the prevalence is even higher in some countries (2). Unlike modern medicine, the understanding of MS in TCM involves viscera, qi and blood, body fluid, yin and yang, and is related to many pathological products such as phlegm, dampness, heat and blood stasis (3, 4). According to TCM, the yin and yang in harmonious balance indicate healthiness, whereas imbalances towards either side indicate unhealthiness, which may result in diseases (5). The syndrome of TCM is the whole reflected state of pathology and physiology in the background of a disease (6). It is generally considered that metabolic syndrome has 5 TCM syndromes, among which the most common is qi-yin deficiency syndrome, followed by phlegm-dampness syndrome, yin deficiency heat excess syndrome, phlegm-stasis interaccumulation syndrome, and yin and yang deficiency syndrome (7, 8).

The collection of bacteria, archaea, viruses and eukaryote colonizing the gastrointestinal tract is termed 'gut microbiota'. It constitutes a huge and complex microecosystem that plays an important role in the host (9). In the long-term co-evolution of gut microbiota and human beings, there is always a dynamic balance between different microbial strains, hosts, and external environment (10), reaching finally a relatively stable 'internal environment'. This dynamic balance involves various ecological relationships such as mutualism and competition, and is similar to the theory of yin and yang balance in TCM, which includes the interdependence between yin and yang, the opposition and restriction of yin and yang, and the absence of single yin or yang. During health, the intestinal microbiota provides many benefits to the host and is generally resistant to colonization by new species; however, disruption of this complex community can lead to pathogen invasion, inflammation, and disease (11). Because the MS is a cluster of different conditions rather than a single symptom, its pathogenesis and clinical manifestations are complex. As such, studying the involvement of gut microbiota in MS, especially in relation to TCM, could increase our understanding of this complex systemic disease.

Previous studies have found differences in the TCM syndromes of some diseases compared with controls (12), as well as differences in gut microbiota between TCM syndromes, such as ulcerative colitis and colorectal cancer (13, 14), but there has been no study on intestinal microbiota of different syndrome types of MS. Therefore, we selected the two most common TCM syndromes of MS, phlegm-dampness syndrome and qi-yin deficiency syndrome, in order to study whether there exist differences in gut microbiota among MS patients with different TCM syndromes. We collected stool samples from 60 MS patients together with 30 healthy control participants and used 16S rRNA sequencing technology to investigate the overall microbiota composition and specific microbial abundances. We found significant differences in the gut microbiota between the TCM syndrome of MS and healthy participants, as well as between patients with the two different TCM syndromes, thus providing the rationale for adopting different microbiota-directed treatment strategies for different TCM syndromes. This study was approved by the Medical Ethics Committee of Shanghai Sixth People's Hospital (project acceptance number: SH6THHOSP-NDGZ-2019-035).

# Materials and methods

## Diagnosis of metabolic syndrome

Metabolic syndrome was diagnosed using the 2013 Chinese Diabetes Society criteria (15) (Diabetes Branch of Chinese Medical Association), by the presence of three or more following conditions: (1) central obesity: waist circumference (WC) (Chinese) for male ≥ 90 cm or female ≥ 85 cm; (2) hyperglycemia: fasting plasma glucose ≥ 6.1 mmol/L and/or 2 h plasma glucose ≥ 7.8 mmol/L, or previously diagnosed type II diabetes and receiving treatment; (3) hypertension: systolic blood pressure/diastolic blood pressure ≥

130/90 mmHg, or previously diagnosed hypertension and receiving treatment; (4) fasting plasma triglyceride ≥ 1.7 mmol/L (150mg/dL); (5) fasting plasma high-density lipoprotein cholesterol (HDL) < 1.04 mmol/L.

## Defining TCM syndromes of MS

By referring to Guiding principles for clinical research of new syndromic TCM drugs (16) from National Medical Products Administration, combined with clinical observation and literature reports, we selected two common syndromes of deficiency and/or excess: (1) Qi-yin deficiency syndrome (QYLX), with main symptoms being shortness of breath, fatigued spirit and weakness, chest discomfort and vague pain sometime, and minor symptoms being dizziness and palpitation, dysphoria in chest palms-soles, spontaneous sweating or night sweating, thirst with desire for drinks, short voidings of scant urine, dry and hard stool, red tongue with little coating or teeth-printed tongue, vacuous pulse or irregularly pulse; (2) Phlegm-dampness syndrome (TSZE), with main symptoms being heaviness of head, sense of suppression in the chest, numbness and heaviness in limbs, and minor symptoms including obesity, palpitation, tastelessness and poor appetite, nausea and salivation, sleepiness, facial distortion, tongue with white greasy or slippery fur, smooth pulse. Patients with MS were diagnosed with either QYLX or TSZE if two main symptoms or one main symptom plus two concurrent minor symptoms are present.

## Patient recruitment

From March 2018 to May 2019, 140 patients with MS were collected from the outpatient and inpatient departments of Shanghai Sixth People's Hospital Affiliated to Shanghai Jiao Tong University School of Medicine. All patients filled in the questionnaire for clinical information on TCM syndromes of metabolic syndrome and 60 patients who met all inclusion and exclusion criteria were enrolled in this clinical study. In addition, healthy control participants were recruited from participants undergoing health examination in Shanghai Sixth People's Hospital Affiliated to Shanghai Jiao Tong University School of Medicine (all healthy participants in the control group had no MS after medical diagnosis), including 16 males and 14 females. This study was approved by the Medical Ethics Committee of Shanghai Sixth People's Hospital (project acceptance number: SH6THHOSP-NDGZ-2019-035).

Detailed inclusion criteria were: (1) Men and women aged 18-65 (inclusive); (2) Non-pregnant and non-lactating; (3) Conformed to the diagnostic criteria for MS established in the above-mentioned western medicine standards; (4) Met the diagnostic criteria of qi-yin deficiency syndrome or phlegm-dampness syndrome in the TCM syndrome types of MS formulated in the above TCM standards; (5) No history of using microecological agents (probiotics or prebiotics) or antibiotics within 2 weeks before the sampling; (6) Willing to follow the sampling method of this study and to provide qualified samples; (7) Submitted the signed informed consent before the experiment and being cooperative in the whole process of the experiment.

Participant who has any one or more than one of the following conditions should be excluded from this study: (1) Has taken microecological agents (probiotics or prebiotics) or antibiotics within 2 weeks before sampling; (2) Infected with infectious diseases, or severe trauma or operation; (3) Contaminated specimens during or after sampling; (4) Pregnant or lactating women.

## Fecal sample collection

The fresh feces naturally discharged by all candidates were collected (more than 2g), quickly put into sterile sample tubes and then transported to the Spleen and Stomach Disease Laboratory of Longhua Hospital within 1 hour with ice bath. Samples were unpacked under sterile conditions and stored in -80°C ultra-low temperature refrigerator after cooling with liquid nitrogen.

## DNA extraction, library preparation and Illumina MiSeq PE250 sequencing

Microbial DNA was extracted from the samples using the QIAamp fast DNA stool Mini Kit (51604, Qiagen, Germany) according to the manufacturer's protocols. The V3-V4 regions of bacterial 16S ribosomal RNA genes were amplified with PCR (95°C for 3 minutes, followed by 30 cycles at 98°C for 20s, 58°C for 15s, 72°C for 20s and the last extension step at 72°C for 5 minutes) using primers 341F 5'-CCTACGGGRSGCAGCAG)-3' and 806R 5'-GGACTACVVGGGTATCTAATC-3'. PCR reactions were carried out in 30 μL of mixture containing 15 μL of 2 × Kapa Library Amplification ReadyMix, 1 μL of each primer (10 μM), 50ng template DNA and ddH2O.

Amplicons were extracted from 2% agarose gels and purified using the AxyPrep DNA Gel Extraction Kit (Axygen Biosciences, Union City, CA, U.S.) according to the manufacturer's instructions and quantified using Qubit®2.0 (Invitrogen, U.S.). After the preparation of library, these tags were sequenced on MiSeq platform (Illumina, Inc., CA, USA) for paired-end reads of 250bp. DNA extraction, library construction and sequencing were conducted at Realbio Genomics Institute (Shanghai, China).

## 16s rRNA sequencing data analysis

Tags, trimmed of barcodes and primers, were further checked on their rest lengths and average base quality. 16S tags were restricted between 220 bp and 500 bp such that the average Phred score of bases was not lower than 20 (Q20) and no more than 3 ambiguous N. The copy number of tags was enumerated and redundancy of repeated tags was removed. Only the tags with frequency of more than 1 were clustered into OTUs, each of which had a representative tag. Operational Taxonomic Units (OTUs) were clustered with 97% similarity using UPARSE (17) and chimeric sequences were identified and removed using Usearch (version 7.0) (18). Taxonomic assignment was done by RDP Classifier (19) against the RDP database (http://rdp.cme.msu.edu/) using confidence threshold of 0.8. OTU profiling table and alpha/beta diversity analyses were also achieved by python scripts from Qiime (20). The α-diversity indices evaluating gut microbial community richness (the Chao1 index) and community diversity (the Shannon and Simpson indexes) were calculated from rarefied data. Principal coordinate analysis (PCoA) based on UniFrac distance and permutational multivariate analysis of variance (PERMANOVA) with 999 permutations were performed to compare the global microbiota composition between groups at genus level. Linear discriminant analysis effect size (LEfSe) (21), with default parameters and the logarithmic LDA score threshold of 2.0, was employed for differential abundance analysis at various taxonomic levels without pre-filtering based on abundances. Spearman's rank-based correlations were used for assessing the correlations between microbial taxa and clinical metadata.

## Functional analysis of gut microbiota

PICRUSt (22) was used for predicting gut microbiota functional profiles as Kyoto Encyclopedia of Genes and Genomes (KEGG) Orthology and further collapse into KEGG pathways. LEfSe (21) was used to identify significantly enriched pathways ($p<0.05$, Kruskal-Wallis test) for the two TCM syndromes of MS and the healthy control group.

## Statistical analysis

Chi square test was used for comparisons of categorical data, Kruskal-Wallis test was used for comparing age (non-normally distributed) and one-way ANOVA followed by *post-hoc* Tukey's test was used for comparing body mass index (normally distributed) using R package *stats*. Kruskal-Wallis test and Wilcoxon rank sum test were used to compare microbial alpha diversity indexes of the metabolic syndrome groups and the control group, as well as between the two metabolic syndrome groups. LEfSe or Wilcoxon rank sum test of two tailed distribution was used to test for significantly different taxa between the metabolic syndrome groups and the control group, as well as between the two metabolic syndrome groups. Multiple hypothesis testing was corrected using false discovery rate (FDR) method (23), for Wilcoxon rank sum test to screen significant genera and for Spearman correlation analyses between genera and clinical indicators. Raw p value of 0.05 was deemed significant unless otherwise stated.

# Results

## Basic characteristics of study participants

From March 2018 to May 2019, 60 MS patients who met the inclusion criteria were collected from the outpatient and inpatient MS patients at Department of Traditional Chinese Medicine, Shanghai Sixth People's Hospital Affiliated to Shanghai Jiao Tong University School of Medicine. This included 29 cases of qi-yin deficiency syndrome (QYLX) and 31 cases of phlegm-dampness depression syndrome (TSZE). At the same time, 30 healthy participants were recruited, including 16 males and 14 females. All volunteers provided informed consent participating in the study. Clinical characteristics of the 90 human subjects are shown in Table 1. There was no significant difference in age or sex between the patients with MS and the control group ($p>0.05$). There was no significant difference in clinical indicators between the QYLX and the TSZE groups ($p>0.05$).

## Comparison of gut microbiota structure among patients of 2 TCM subtypes of MS and the healthy control participants

We then performed 16S rRNA sequencing for the 90 participants to investigate the differences of gut microbiota among QYLX, TSZE patients and healthy control participants. This generated a total of 3242982 clean reads (mean 36033; s.d. 1822) after quality control. The Good's coverage estimator for all samples was above 99.7%, indicating the sufficiency of sequencing depth to recover the vast majority of the microbiota community in all samples. The comparisons of microbiota alpha diversity indexes showed significant differences in chao1 index, observed species index and phylogenetic diversity (PD whole tree) between each MS group and the healthy control group (Figure 1) ($p<0.05$, Wilcoxon rank sum test), except for the comparison of phylogenetic diversity between QYLX and control ($p=0.053$). However, there were no significant differences in alpha diversity between the QYLX and the TSZE groups.

TABLE 1 Comparison of age, sex and clinical indicators between MS patients and control group.

| Variable | QYLX (n=29) | TSZE (n=31) | Control group (n=30) | *P* value |
|---|---|---|---|---|
| **Gender** | | | | |
| Male (%) | 11 (37.9%) | 13 (41.9%) | 16 (53.3%) | |
| Female (%) | 18 (62.1%) | 18 (58.1%) | 14 (46.7%) | |
| **Age (years)** | 54.93 ± 9.651 | 54.30 ± 8.871 | 43.97 ± 18.31 | 0.069[1] |
| **BMI (kg/m$^2$)** | 26.33 ± 0.62 | 25.28 ± 0.55 | 22.02 ± 0.49 | <0.001[2] |
| **Liver enzyme index** | | | | |
| ALT (U/L) | 26.61 ± 16.26 | 24.11 ± 13.95 | | 0.539 |
| AST (U/L) | 22.43 ± 7.21 | 22.07 ± 7.35 | | 0.855 |
| **Renal function index** | | | | |
| SCr (μmol/L) | 63.27 ± 13.69 | 64.00 ± 14.80 | | 0.849 |
| BUN (mmol/L) | 5.38 ± 1.33 | 5.87 ± 1.60 | | 0.219 |
| UA (μmol/L) | 357.85 ± 86.04 | 353.96 ± 98.35 | | 0.877 |
| **Blood lipid index** | | | | |
| TC (mmol/L) | 4.98 ± 1.09 | 5.21 ± 1.11 | | 0.433 |
| TG (mmol/L) | 1.93 ± 1.18 | 2.48 ± 1.69 | | 0.163 |
| HDL (mmol/L) | 1.21 ± 0.32 | 1.16 ± 0.37 | | 0.601 |
| LDL (mmol/L) | 3.01 ± 0.91 | 3.12 ± 1.10 | | 0.685 |
| **Glucose metabolism index** | | | | |
| FPG (mmol/L) | 5.89 ± 1.61 | 6.29 ± 1.67 | | 0.361 |

[1]Data do not conform to normal distribution; Kruskal-Wallis test p=0.069.
[2]Data conform to normal distribution; one-way ANOVA p=9.7e-07 (post-hoc Tukey's test: QYLX vs control: p=1.4e-06; TSZE vs control: p=1.9e-04; QYLX vs TSZE: p=0.378).
ALT, alanine aminotransferase; AST, aspartate aminotransferase; SCr, serum creatinine; BUN, blood urea nitrogen; UA, Uric Acid; TC, total cholesterol; TG, triglyceride; HDL, high density lipoprotein cholesterol; LDL, low density lipoprotein cholesterol; FPG, fasting plasma glucose. Student's t test was used for comparison of other data between the two MS groups.

To further investigate the differences in the overall gut microbiota composition among different groups, we calculated and compared genus-level beta diversities using both unweighted and weighted UniFrac distances. Principal coordinate analysis (PCoA) and PERMANOVA showed small, yet statistically significant differences between each of the MS groups and the control group (Supplementary Figure 1) (QYLX vs Control: p=0.001, $R^2$ = 0.051 for unweighted and p=0.032, $R^2$ = 0.049 for weighted UniFrac; TSZE vs Control: p=0.001, $R^2$ = 0.075 for unweighted and p=0.001, $R^2$ = 0.090 for weighted UniFrac). It was also observed that the TSZE group was more different to the healthy control group than the QYLX group, using either unweighted or weighted UniFrac (Supplementary Figure 1). Notably, the two TCM syndromes of MS showed significant differences (p=0.039, $R^2$ = 0.027, PERMANOVA) in intestinal microbiota structure when using unweighted UniFrac distance (Figure 2A), and specifically in the second principal coordinate of PCoA (p=0.004, Wilcoxon rank sum test). This association between microbiota diversity and different TCM subtypes of MS was not obvious with weighted UniFrac distance that considers microbial abundances (p=0.093, $R^2$ = 0.030, PERMANOVAs) (Figure 2B). This finding implies that the TSZE and QYLX groups may share more similarity in the highly abundant taxa but are more distinct in the low abundant genera.

## Differentially abundant taxa among patients with distinct TCM subtypes of MS and healthy control participants

Next, we performed pairwise differential abundance analysis among TSZE, QYLX and healthy control groups, aiming to identify specific bacterial taxa associated with different TCM syndromes of MS. Compared to the control group, LEfSe analysis identified 25 (10 enriched and 15 depleted) and 43 (28 enriched and 15 depleted) significant taxa in patients with QYLX and TSZE, respectively (Supplementary Figure 2, 3, Supplementary Table 1). The higher number in comparing TSZE against the control group is consistent with the observation from ecological diversity comparison above that the TSZE group was more different to the healthy control group than the QYLX group was. Moreover, some taxa are commonly enriched (e.g. *Flavonifractor* and *Epsilonproteobacteria*) or depleted (e.g. *Paraprevotella* and *Faecalibacterium*) in both TCM syndromes compared to the healthy control group, implying the shared intestinal microbiota and pathophysiological characteristics of the two MS subtypes.

However, there are also microbial signatures unique to either QYLX or TSZE. Indeed, a direct comparison between the two TCM syndromes revealed a cluster of significantly differentially abundant taxa (5 QYLX-enriched and 18 TSZE-enriched), some

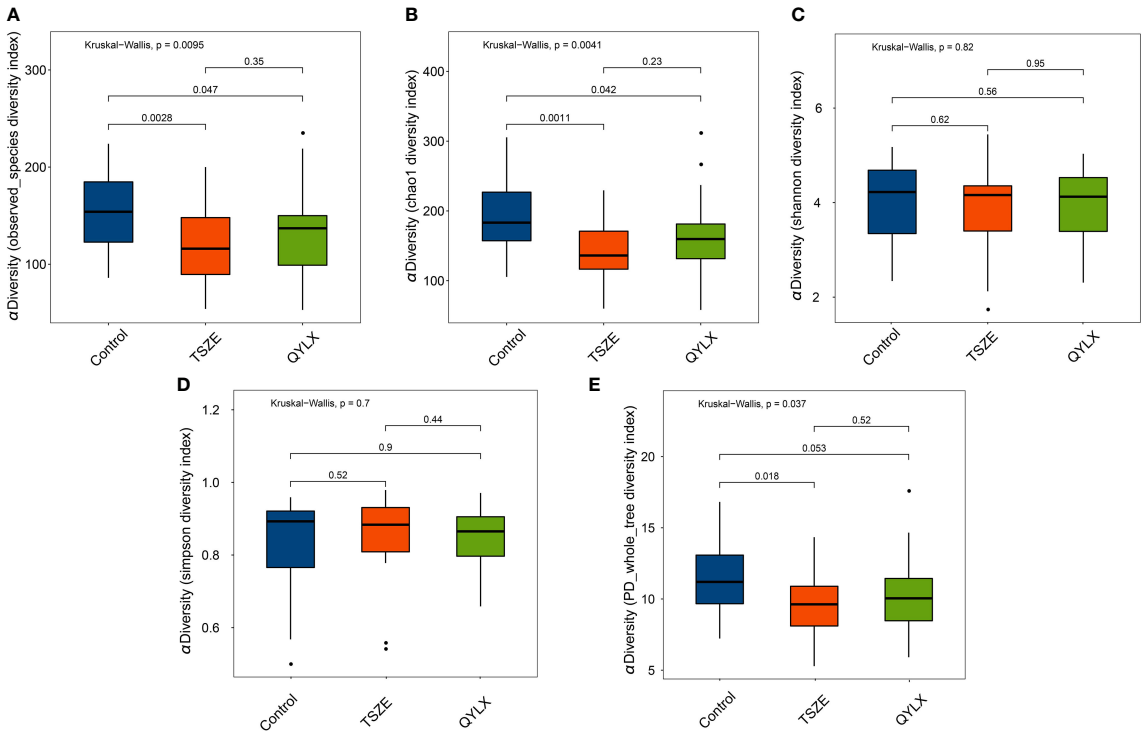


FIGURE 1
Comparison of microbiota alpha diversity among different TCM syndromes of MS and healthy control. Rarefied data are used to calculate different diversity indexes as **(A)** observed species; **(B)** Chao1 diversity; **(C)** Shannon diversity; **(D)** Simpson diversity; **(E)** phylogenetic diversity. Kruskal-Wallis test and Wilcoxon rank sum test were used for statistical comparison, and p value < 0.05 is considered statistical significance. Boxplots show median (centerlines), lower/upper quartiles (box limits), whiskers (the last data points 1.5 times interquartile range (IQR) from the lower or upper quartiles), and notches (95% confidence interval for the medians). QYLX, qi-yin deficiency syndrome; TSZE, phlegm-dampness syndrome.

of which are possibly related to the distinct clinical manifestations of the two TCM syndromes (Supplementary Table 1). According to Figure 3, the microbial taxa enriched in TSZE group with the highest LDA score was the class *Negativicutes* (p=0.012), followed by *Selenomonadales*, *Enterobacteriaceae*, *Enterobacteriales*, *Gammaproteobacteria*, *Proteobacteria*, etc. Conversely, the taxa enriched in QYLX group included the genus *Eubacterium*, the family *Fusobacteriaceae* and its affiliated higher taxonomic ranks.

In addition, we used Wilcoxon rank sum test to screen significantly differentially abundant genera between healthy and each TCM syndrome of MS, as well as between the two TCM syndromes. Similar conclusions were obtained regarding the differences in the intestinal microbiota mentioned above. Compared to the control group, this identified 7 and 11 significant genera after correcting for multiple hypothesis testing (FDR-correct p<0.05) in patients with QYLX and TSZE, respectively (Supplementary Figure 4, Supplementary Table 1). Even though patients of both TCM syndromes of MS differed considerably from healthy participants, *Akkermansia* was the only significant genus between them after FDR correction (FDR-corrected p<0.05).

## Gut microbiota genera correlated with MS-related clinical measurements differently in QYLX and TSZE

To identify the microbial taxa that are potentially associated with disease phenotypes and pathophysiology, we performed spearman correlation analysis between intestinal microbial genera and a panel of clinical metadata related to anthropometrics, liver and kidney functions, lipid metabolism, and glucose homeostasis. For the QYLX group, we observed 36 significant correlations from 15 genera; weight, alanine transaminase (ALT), and serum creatinine (SCr) had the top 3 highest number of related genera, while *Lachnospiracea incertae sedis*, *Coprococcus*, *Asaccharobacter*, *Enterococcus*, and *Coprobacillus* had the most correlations with clinical data (Figure 4). In comparison, the TSZE group had fewer correlations (n=24) from fewer genera (n=11); aspartate transaminase (AST), ALT, total cholesterol (TC), and low-density lipoprotein (LDL) were correlated with the highest number of genera, while *Weissella* had most correlations with clinical measures that were mainly related to lipid metabolism (Figure 5). Notably, almost no correlations were commonly found between the QYLX and the TSZE groups, except the correlation between

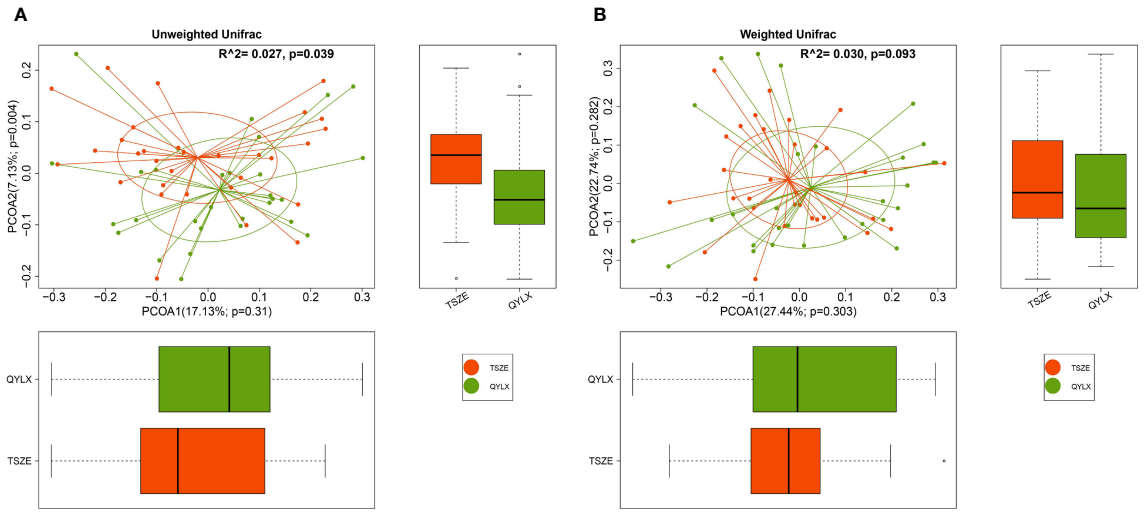


FIGURE 2
Principal coordinate analysis (PCoA) comparing microbiota beta diversity between the QYLX and TSZE groups. Genus-level abundance data are used for calculating both **(A)** unweighted and **(B)** weighted UniFrac distances. The horizontal and vertical box plots show the sample distribution on the first and second principal coordinates for each group, respectively. Statistical comparison of microbial communities and each principal coordinate between two groups were based on PERMANOVA and Wilcoxon rank sum test, respectively. P value < 0.05 is considered statistical significance. QYLX, qi-yin deficiency syndrome; TSZE, phlegm-dampness syndrome.

*Gemmiger* and SCr but with opposite direction. The highly distinct correlation patterns remained when we re-performed the correlation analysis using microbial abundances after centered log-ratio transformation that deals with data compositionality. Within the bacteria correlated to clinical profile, two genera (*Coprococcus* and *Haemophilus*) were also significantly differentially abundant between the QYLX group and healthy control (Supplementary Figure 4), while three genera (*Faecalibacterium*, *Gemmiger*, and *Prevotella*) were observed for the TSZE comparison. In summary, the QYLX and the TSZE groups differ in gut microbiota composition and microbial correlations with clinical measures related to MS, implying the association between gut microbiota and TCM manifestations of metabolic syndrome.

## Differential functions between TSZE and QYLX

Having compared the microbiota structure and compositions, we then ought to investigate the microbiota functional differences among the TSZE, QYLX and healthy control groups. The KEGG pathways were predicted with PICRUSt, followed by LEfSe to identify signature pathways of each group (Figure 6). In patients with QYLX, gut microbiota was enriched in functions related to carbohydrate metabolism (starch and sucrose metabolism; carbohydrate metabolism). In the TSZE group, microbiota functions related to lipopolysaccharide (LPS) synthesis (such as lipopolysaccharide biosynthetic protein and lipopolysaccharide biosynthesis) were more abundant, and the gut microbiota-derived LPS has been implicated in inflammation and obesity (24). The metabolism of cofactors and vitamins was also enriched in the TSZE group.

Moreover, the QYLX and TSZE groups showed large differences in amino acid metabolism of gut microbiota: alanine, aspartate and glutamate metabolism, as well as valine, leucine and isoleucine biosynthesis pathway were more abundant in QYLX group; while in TSZE patients, tryptophan metabolism, lysine degradation, valine leucine and isoleucine degradation, and phenylalanine metabolism were enriched. Such discrepancy in the amino acid metabolism of intestinal microbiota is possibly related to the different TCM syndromes of MS and their clinical manifestations.

# Discussion

In this study, we performed a cross-sectional analysis of human gut microbiota in patients with two different TCM syndromes (QYLX and TSZE) of MS, and compared their differences with healthy participants. Through high throughput 16S rRNA sequencing of fecal samples from 60 MS patients and 30 healthy control participants, it was found that the QYLX and TSZE groups differ from the healthy control group in the overall gut microbiota composition, and in specific microbial taxa and functional pathways. The TSZE group seemed to have higher dissimilarity from the healthy control group than the QYLX group regarding the microbiota composition and functionality. Moreover, significantly

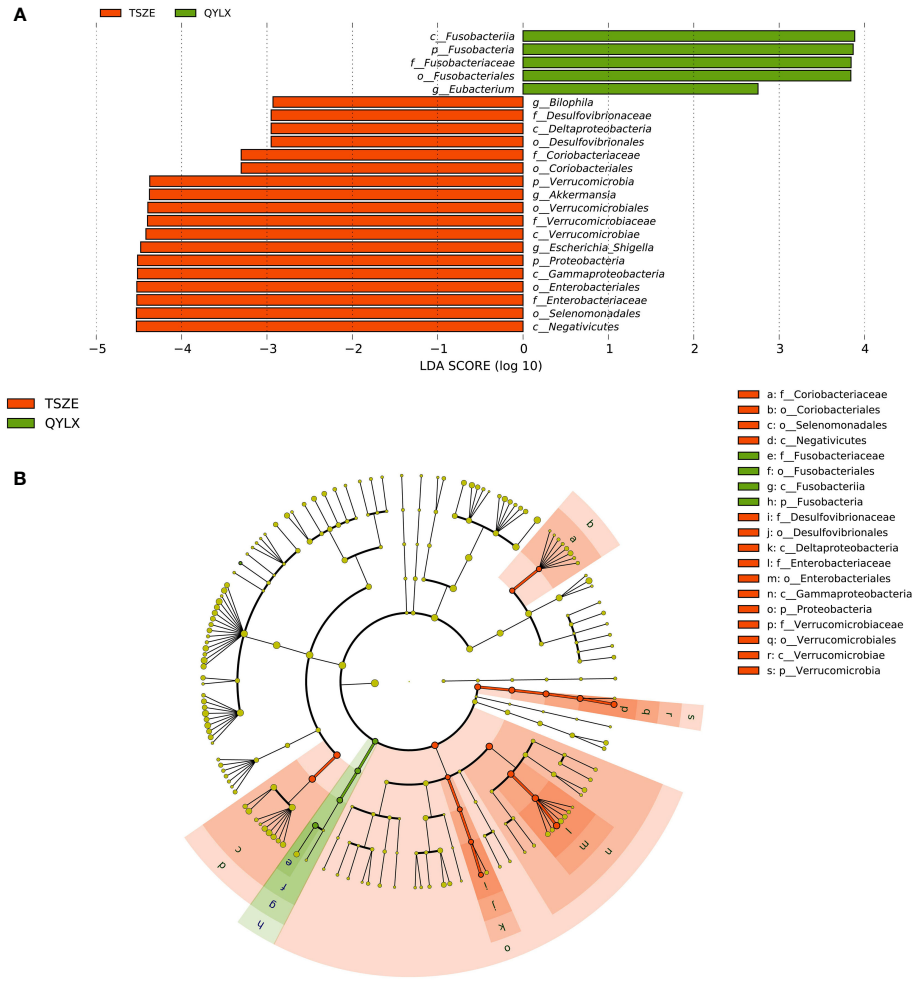


FIGURE 3
Specific microbiota taxa at various taxonomic ranks differentially enriched in QYLX and TSZE patients. **(A)** The full list of significant microbial taxa is identified with LefSe (linear discriminant analysis effect size), at p value < 0.05 and log10-transformed LDA score > 2. **(B)** A cladogram showing the enriched microbial taxa on a phylogenetic tree. The color indicates which branch of the phylogenetic tree more significantly represents a certain group. Green: microbial taxa enriched in QYLX group; orange: microbial taxa enriched in TSZE group. QYLX, qi-yin deficiency syndrome; TSZE, phlegm-dampness syndrome.

differentially abundant taxa and distinct BMI-correlated taxa were observed between QYLX and TSZE groups in our exploratory study. These findings, though remain to be confirmed by future studies on a larger scale, may suggest the potential contribution of gut microbiota to the distinction between the two TCM syndromes.

Despite numerous efforts to understand and treat MS, its exact pathogenesis is not clear yet (25). Previous studies have demonstrated the important regulatory role of intestinal microbiota in the pathogenesis of MS (26, 27).Specific changes in microbial taxa have been associated with MS, e.g. the increase of *Lactobacillus* and decrease of *Faecalibacterium* in patients with MS (26, 28), which were also observed in our QYLX and TSZE syndromes of MS, respectively. The relative abundance of *Akkermansia* was reported to be lower in MS patients (26, 29), but we observed here a significant increase in the patients with TSZE syndrome of MS compared to the healthy control participants. The change of gut microbiota can affect the host's metabolism through several routes such as gut barrier integrity, production of metabolites affecting satiety and insulin resistance, epigenetic factors, and bile acid metabolism and subsequent changes in metabolic signaling (30). Current research into different components of MS and gut microbiota is getting more and deeper, and our understanding of the pathophysiological mechanism of MS is constantly being updated. Central obesity is one of the main clinical manifestations of MS. Le Roy et al. (31) found seven bacterial genera related to visceral fat mass, of which *Coprococcus* and *Ruminococcus* showed significant negative correlations. Interestingly, *Coprococcus* and *Ruminococcus*

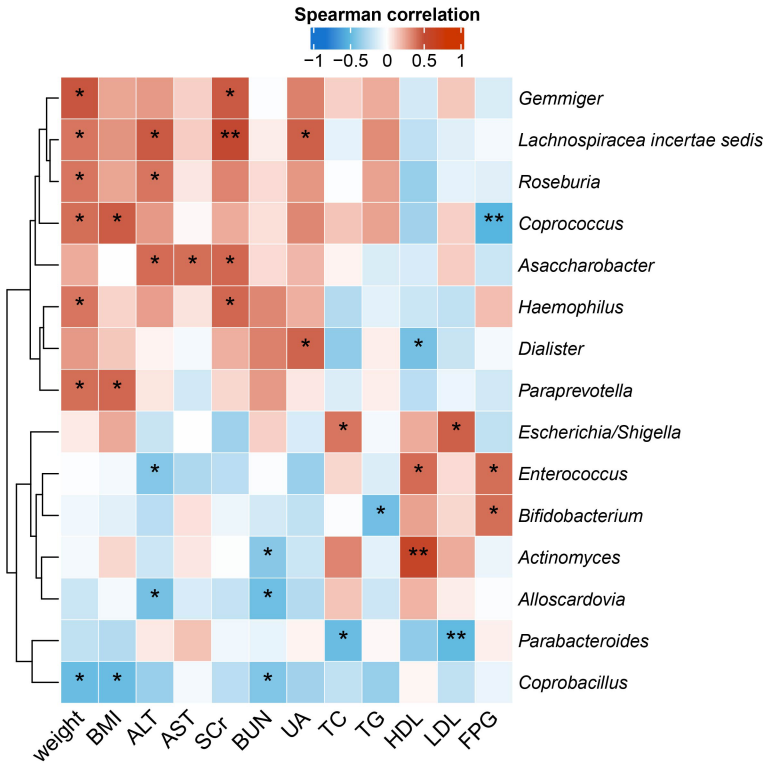


FIGURE 4
Correlations between specific genera and MS-related clinical measurements in the QYLX group. Spearman's rank-based correlations are calculated using samples from the QYLX group between each genus and clinical metadata related to anthropometrics, liver and kidney functions, lipid metabolism, and glucose homeostasis. Only genera with at least two significant correlation ($p < 0.05$) are included. Red, positive correlations; blue, negative correlations. *p< 0.05; **p< 0.01. ALT, alanine aminotransferase; AST, aspartate aminotransferase; SCr, serum creatinine; BUN, blood urea nitrogen; UA, Uric Acid; TC, total cholesterol; TG, triglyceride; HDL, high density lipoprotein cholesterol; LDL, low density lipoprotein cholesterol; FPG, fasting plasma glucose.

were reduced here in patients with both QYLX (though not statistically significant for *Ruminococcus*) and TSZE syndromes of MS (Supplementary Figure 4), and were also reported to be lower in elderly patients with MS (28). A recent metagenome-wide association study has demonstrated the strong connection between visceral fat, a hallmark of central obesity, with gut microbiota composition and functionality (32). Specifically, they found that the microbiota biosynthesis of phenylalanine and LPS are positively correlated with visceral fat area, waist and waist-to-hip ratio. In our study, both pathways were increased in the patients with TSZE syndrome of MS (Figure 6). The changes in microbiota metabolites or microbial components might be also responsible for the impaired intestinal mucosal barrier function and increased intestinal permeability in obese people (33–35). Microbial metabolism of tryptophan, which was shown to regulate gut barrier function *via* the aryl hydrocarbon receptor (36), was enriched in the TSZE syndrome of MS.

Diabetes, hyperlipidemia and hypertension are important parts of MS and their relationship with intestinal microbiota has been widely studied. Compared with non-diabetic patients, adult patients with type II diabetes patients have an imbalanced intestinal microecology and decreased abundance of butyrate-producing bacteria in the intestine (37, 38). Interestingly, the aforementioned genera *Coprococcus* and *Ruminococcus*, which were decreased in patients with the TCM syndromes of MS, are also butyrate-producing bacteria (34). Amino acids and their byproducts were suggested to play a key role in obesity and its complications including insulin resistance, hyperglycemia, and dyslipidemia (39). Here we found distinct pathways of amino acid metabolism to be enriched in patients with different TCM syndromes of MS (Figure 6). Through shotgun metagenomic analysis of a cohort of 196 Chinese individuals, Li et al. found decreased microbial richness and diversity, altered microbiota composition and functionality (increase in LPS biosynthesis and export, phenylalanine biosynthesis, phosphotransferase system, and

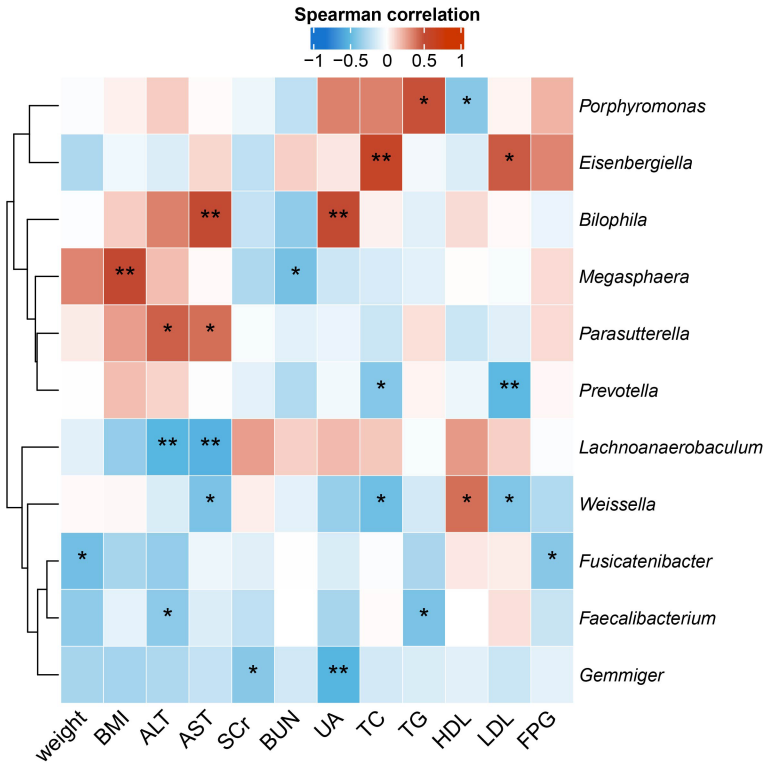


FIGURE 5
Correlations between specific genera and MS-related clinical measurements in the TSZE group. Spearman's rank-based correlations are calculated using samples from the TSZE group between each genus and clinical metadata related to anthropometrics, liver and kidney functions, lipid metabolism, and glucose homeostasis. Only genera with at least two significant correlation ($p < 0.05$) are included. Red, positive correlations; blue, negative correlations. *p< 0.05; **p< 0.01. ALT, alanine aminotransferase; AST, aspartate aminotransferase; SCr, serum creatinine; BUN, blood urea nitrogen; UA, Uric Acid; TC, total cholesterol; TG, triglyceride; HDL, high density lipoprotein cholesterol; LDL, low density lipoprotein cholesterol; FPG, fasting plasma glucose.

secretion system, among others), in both pre-hypertensive and hypertensive populations (40). They further transplanted fecal microbiota from hypertensive human donors to germ-free mice and observed elevated blood pressure, demonstrating the causal role of intestinal microbiota in the pathogenesis of hypertension. In our study, we also found decreased microbiota richness in patients with the two TCM syndromes of MS compared to healthy participants (Figure 1), although no significant differences were observed in Shannon or Simpson diversity. Microbial functions including LPS biosynthesis, phenylalanine metabolism, secretion system, and phosphotransferase system were enriched as well in patients with the TSZE syndrome of MS.

This pilot study demonstrates again the vital role of gut microbiota in metabolic syndrome, highlights its contribution to the differentiation between two TCM syndromes of MS, and offers functional insights into such differentiation based on inferred functions such as amino acid metabolism and LPS biosynthesis. Similar studies of gut microbiota have been performed in other TCM syndromes such as spleen-yang-deficiency syndrome (41), kidney-yang-deficiency syndrome (42), as well as different TCM syndromes of ulcerative colitis (13) and colorectal cancer (14). Future research may investigate the differences in microbiota metabolism of amino acids and the serum or stool amino acid levels in MS patients with different TCM syndromes, by employing shotgun metagenomics approach coupled with targeted or untargeted metabolomics analysis. The exploration of mechanistic differences can shed light on the personalized management of patients with metabolic syndrome and future intervention studies using TCM, especially for microbiota-targeted therapies. However, this study has also limitations. The lack of detailed information on medication usages such as antihypertensive drugs and hypoglycemic drugs is a major limitation. A longer absence period of antibiotics usage can be used in future studies to reduce its confounding effect. Future work may use shotgun metagenomic sequencing, together with a metabolomics, for deeper and more accurate

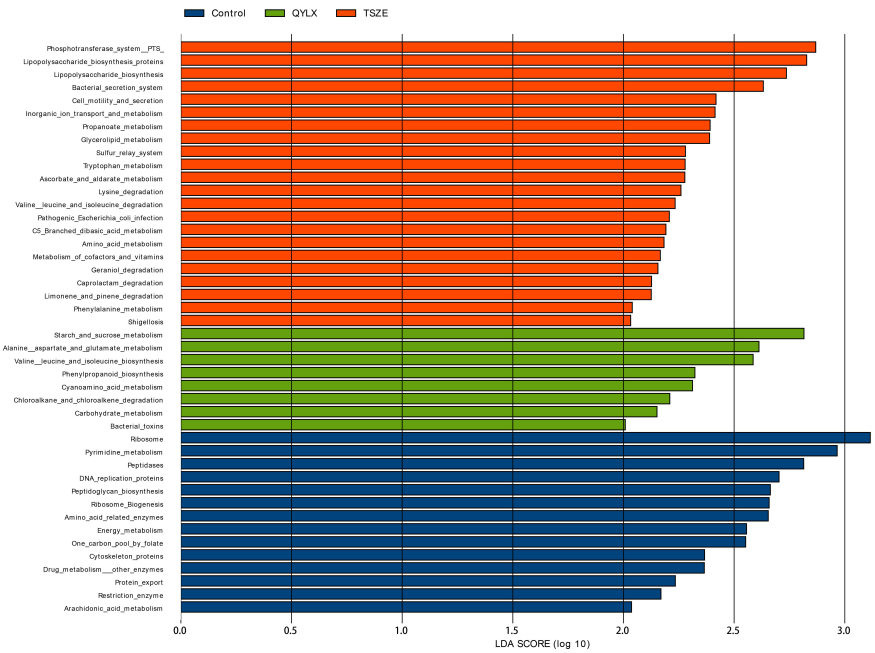


FIGURE 6
Specific microbiota functions differentially abundant among QYLX, TSZE patients and healthy control. The full list of significant KEGG pathways enriched in each of the 3 groups is identified with LefSe (linear discriminant analysis effect size), at p value < 0.05 and log10-transformed LDA score > 2. Green: microbial taxa enriched in QYLX group; orange: microbial taxa enriched in TSZE group; blue: microbial taxa enriched in healthy control, thus depleted in both TCM syndromes of MS. QYLX, qi-yin deficiency syndrome; TSZE, phlegm-dampness syndrome.

characterization of gut microbiota composition and functionality or functional readout. Given the limited sample size, larger cohorts with multi-center design are needed in the future for validation of our findings here.

## Data availability statement

The datasets presented in this study can be found in online repositories. The names of the repository/repositories and accession number(s) can be found below: https://www.ncbi.nlm.nih.gov/, PRJNA809501.

## Ethics statement

The clinical study was reviewed and approved by the ethics committee of Shanghai Sixth People's hospital. The patients/participants provided their written informed consent to participate in this study.

## Author contributions

BW, YN, and ZY designed and supervised the study. HS, LuZ, JR, QZ, KL, and LiZ finished data collection and analysis. TX, YN and BW provided technical guidance for the whole work. YN and HS. wrote the manuscript. All authors contributed to the study and approved the final version of the manuscript.

## Funding

This work was supported by Shanghai High-level Talents Leading Plan of Traditional Chinese Medicine, Three-year Action Plan (2021-2023) of Shanghai Municipality for Further Accelerating the Inheritance, Innovation and Development of Traditional Chinese Medicine [grant number: ZY(2021-2023)-0205-04], Construction of East China Area and Municipal TCM Specialist Disease Alliance [grant number: ZY(2021-2023)-0302] to BW.

## Conflict of interest

The authors declare that the research was conducted in the absence of any commercial or financial relationships that could be construed as a potential conflict of interest.

## Publisher's note

All claims expressed in this article are solely those of the authors and do not necessarily represent those of their affiliated organizations, or those of the publisher, the editors and the reviewers. Any product that may be evaluated in this article, or claim that may be made by its manufacturer, is not guaranteed or endorsed by the publisher.

## Supplementary material

The Supplementary Material for this article can be found online at: https://www.frontiersin.org/articles/10.3389/fendo.2022.1063579/full#supplementary-material

## References

1. O'Neill S, O'Driscoll L. Metabolic syndrome: A closer look at the growing epidemic and its associated pathologies. *Obes Rev* (2015) 16(1):1–12. doi: 10.1111/obr.12229

2. Grundy SM. Metabolic syndrome pandemic. *Arterioscler Thromb Vasc Biol* (2008) 28(4):629–36. doi: 10.1161/ATVBAHA.107.151092

3. Zhang CH, Sheng JQ, Xie WH, Luo XQ, Xue YN, Xu GL, et al. Mechanism and basis of traditional Chinese medicine against obesity: Prevention and treatment strategies. *Front Pharmacol* (2021) 12:615895. doi: 10.3389/fphar.2021.615895

4. Yin J, Zhang H, Ye J. Traditional Chinese medicine in treatment of metabolic syndrome. *Endocrine Metab Immune Disord Drug Targets* (2008) 8(2):99–111. doi: 10.2174/187153008784534330

5. Hu Q, Yu T, Li J, Yu Q, Zhu L, Gu Y. End-to-End syndrome differentiation of yin deficiency and yang deficiency in traditional Chinese medicine. *Comput Methods programs biomedicine* (2019) 174:9–15. doi: 10.1016/j.cmpb.2018.10.011

6. Dong Y, Li HZ, Zhu S, Li J, Wang J. [Theoretical discussion and clinical application of treating the same syndrome with different methods in "Treatise on febrile and miscellaneous diseases"]. *Zhongguo Zhong yao za zhi = Zhongguo zhongyao zazhi = China J Chin materia Med* (2019) 44(18):3890–4. doi: 10.19540/j.cnki.cjcmm.20190121.002

7. Liang Y, Xiong Y, Yan G. Distribution of tcm syndromes of metabolic syndrome. *Chin Med Res* (2012) 25(11):16–9. doi: 10.3969/j.issn.1001-6910.2012.11.008

8. Wang X, Niu Y, Zhang S. Distribution of tcm syndromes in metabolic syndrome based on the methods of modern literature research. *J Yunnan Univ Traditional Chin Med* (2019) 42(06):20–5. doi: 10.19288/j.cnki.issn.1000-2723.2019.06.004

9. Chen YZ, Yuan MY, Chen YL, Zhang X, Xu XT, Liu SL, et al. The gut microbiota and traditional Chinese medicine: A new clinical frontier on cancer. *Curr Drug Targets* (2021) 22(11):1222–31. doi: 10.2174/1389450122666210412141304

10. Guo N, Zhang Z, Han C, Chen L, Zheng X, Yu K, et al. Effects of continuous intravenous infusion of propofol on intestinal flora in rats. *Biomedicine pharmacotherapy = Biomedecine pharmacotherapie* (2021) 134:111080. doi: 10.1016/j.biopha.2020.111080

11. Gibson MK, Pesesky MW, Dantas G. The yin and yang of bacterial resilience in the human gut microbiota. *J Mol Biol* (2014) 426(23):3866–76. doi: 10.1016/j.jmb.2014.05.029

12. Zhu J, Li X, Deng N, Peng X, Tan Z. Diarrhea with deficiency kidney-yang syndrome caused by adenine combined with folium senna was associated with gut mucosal microbiota. *Front Microbiol* (2022) 13:1007609. doi: 10.3389/fmicb.2022.1007609

13. Zhang YL, Cai LT, Qi JY, Lin YZ, Dai YC, Jiao N, et al. Gut microbiota contributes to the distinction between two traditional Chinese medicine syndromes of ulcerative colitis. *World J Gastroenterol* (2019) 25(25):3242–55. doi: 10.3748/wjg.v25.i25.3242

14. Wang P, Ding S, Sun L, Feng Y, Guo K, Zhu Y, et al. Characteristics and differences of gut microbiota in patients with different traditional Chinese medicine syndromes of colorectal cancer and normal population. *J Cancer* (2020) 11(24):7357–67. doi: 10.7150/jca.50318

15. Chinese Diabetes Society. Chinese Guidelines for the prevention and treatment of type 2 Diabetes(2013 edition). *Chin J Diabetes* (2014) 22:42. doi: 10.3760/cma.j.issn.1674-2809.2014.07.004

16. National medical products Administration. Guiding principles for clinical research of new syndromic tcm drugs. (2018). https://www.nmpa.gov.cn/yaopin/ypggtg/ypqtgg/20181106155701473.html.

17. Edgar RC. Uparse: Highly accurate otu sequences from microbial amplicon reads. *Nat Methods* (2013) 10(10):996–8. doi: 10.1038/nmeth.2604

18. Edgar RC. Search and clustering orders of magnitude faster than blast. *Bioinf (Oxford England)* (2010) 26(19):2460–1. doi: 10.1093/bioinformatics/btq461

19. Wang Q, Garrity GM, Tiedje JM, Cole JR. Naive Bayesian classifier for rapid assignment of rrna sequences into the new bacterial taxonomy. *Appl Environ Microbiol* (2007) 73(16):5261–7. doi: 10.1128/aem.00062-07

20. Navas-Molina JA, Peralta-Sánchez JM, González A, McMurdie PJ, Vázquez-Baeza Y, Xu Z, et al. Advancing our understanding of the human microbiome using qiime. *Methods enzymology* (2013) 531:371–444. doi: 10.1016/b978-0-12-407863-5.00019-8

21. Segata N, Izard J, Waldron L, Gevers D, Miropolsky L, Garrett WS, et al. Metagenomic biomarker discovery and explanation. *Genome Biol* (2011) 12(6):R60. doi: 10.1186/gb-2011-12-6-r60

22. Douglas GM, Beiko RG, Langille MGI. Predicting the functional potential of the microbiome from marker genes using picrust. *Methods Mol Biol (Clifton NJ)* (2018) 1849:169–77. doi: 10.1007/978-1-4939-8728-3_11

23. Benjamini Y, Hochberg Y. Controlling the false discovery rate: A practical and powerful approach to multiple testing. *J R Stat Society: Ser B (Methodological)* (1995) 57(1):289–300. doi: 10.1111/j.2517-6161.1995.tb02031.x

24. Hersoug LG, Moller P, Loft S. Gut microbiota-derived lipopolysaccharide uptake and trafficking to adipose tissue: Implications for inflammation and obesity. *Obes Rev* (2016) 17(4):297–312. doi: 10.1111/obr.12370

25. McCracken E, Monaghan M, Sreenivasan S. Pathophysiology of the metabolic syndrome. *Clinics Dermatol* (2018) 36(1):14–20. doi: 10.1016/j.clindermatol.2017.09.004

26. Lim MY, You HJ, Yoon HS, Kwon B, Lee JY, Lee S, et al. The effect of heritability and host genetics on the gut microbiota and metabolic syndrome. *Gut* (2017) 66(6):1031–8. doi: 10.1136/gutjnl-2015-311326

27. Dabke K, Hendrick G, Devkota S. The gut microbiome and metabolic syndrome. *J Clin Invest* (2019) 129(10):4050–7. doi: 10.1172/JCI129194

28. Ni Y, Mu C, He X, Zheng K, Guo H, Zhu W. Characteristics of gut microbiota and its response to a Chinese herbal formula in elder patients with metabolic syndrome. *Drug Discovery Ther* (2018) 12(3):161–9. doi: 10.5582/ddt.2018.01036

29. Thingholm LB, Ruhlemann MC, Koch M, Fuqua B, Laucke G, Boehm R, et al. Obese individuals with and without type 2 diabetes show different gut microbial functional capacity and composition. *Cell Host Microbe* (2019) 26(2):252–64.e10. doi: 10.1016/j.chom.2019.07.004

30. Lee CJ, Sears CL, Maruthur N. Gut microbiome and its role in obesity and insulin resistance. *Ann New York Acad Sci* (2020) 1461(1):37–52. doi: 10.1111/nyas.14107

31. Le Roy CI, Beaumont M, Jackson MA, Steves CJ, Spector TD, Bell JT. Heritable components of the human fecal microbiome are associated with visceral fat. *Gut Microbes* (2018) 9(1):61–7. doi: 10.1080/19490976.2017.1356556

32. Nie X, Chen J, Ma X, Ni Y, Shen Y, Yu H, et al. A metagenome-wide association study of gut microbiome and visceral fat accumulation. *Comput Struct Biotechnol J* (2020) 18:2596–609. doi: 10.1016/j.csbj.2020.09.026

33. Ghosh S, Whitley CS, Haribabu B, Jala VR. Regulation of intestinal barrier function by microbial metabolites. *Cell Mol Gastroenterol Hepatol* (2021) 11 (5):1463–82. doi: 10.1016/j.jcmgh.2021.02.007

34. LeBlanc JG, Chain F, Martin R, Bermudez-Humaran LG, Courau S, Langella P. Beneficial effects on host energy metabolism of short-chain fatty acids and vitamins produced by commensal and probiotic bacteria. *Microb Cell Fact* (2017) 16(1):79. doi: 10.1186/s12934-017-0691-z

35. Nogal A, Louca P, Zhang X, Wells PM, Steves CJ, Spector TD, et al. Circulating levels of the short-chain fatty acid acetate mediate the effect of the gut microbiome on visceral fat. *Front Microbiol* (2021) 12:711359. doi: 10.3389/fmicb.2021.711359

36. Scott SA, Fu J, Chang PV. Microbial tryptophan metabolites regulate gut barrier function *Via* the aryl hydrocarbon receptor. *Proc Natl Acad Sci U.S.A.* (2020) 117(32):19376–87. doi: 10.1073/pnas.2000047117

37. Zhang X, Shen D, Fang Z, Jie Z, Qiu X, Zhang C, et al. Human gut microbiota changes reveal the progression of glucose intolerance. *PloS One* (2013) 8 (8):e71108. doi: 10.1371/journal.pone.0071108

38. Qin J, Li Y, Cai Z, Li S, Zhu J, Zhang F, et al. A metagenome-wide association study of gut microbiota in type 2 diabetes. *Nature* (2012) 490 (7418):55–60. doi: 10.1038/nature11450

39. Ejtahed HS, Angoorani P, Soroush AR, Hasani-Ranjbar S, Siadat SD, Larijani B. Gut microbiota-derived metabolites in obesity: A systematic review. *Biosci Microbiota Food Health* (2020) 39(3):65–76. doi: 10.12938/bmfh.2019-026

40. Li J, Zhao F, Wang Y, Chen J, Tao J, Tian G, et al. Gut microbiota dysbiosis contributes to the development of hypertension. *Microbiome* (2017) 5(1):14. doi: 10.1186/s40168-016-0222-x

41. Lin Z, Ye W, Zu X, Xie H, Li H, Li Y, et al. Integrative metabolic and microbial profiling on patients with spleen-Yang-Deficiency syndrome. *Sci Rep* (2018) 8(1):6619. doi: 10.1038/s41598-018-24130-7

42. Chen R, Wang J, Zhan R, Zhang L, Wang X. Fecal metabonomics combined with 16s rrna gene sequencing to analyze the changes of gut microbiota in rats with kidney-yang deficiency syndrome and the intervention effect of you-gui pill. *J ethnopharmacology* (2019) 244:112139. doi: 10.1016/j.jep.2019.112139

frontiers | Frontiers in Endocrinology

TYPE Original Research
PUBLISHED 14 November 2022
DOI 10.3389/fendo.2022.1053103



OPEN ACCESS

EDITED BY
Zhoujin Tan,
Hunan University of Chinese Medicine, China

REVIEWED BY
Xiaoliang Li,
Heilongjiang University of Chinese Medicine, China
Lv Chunyan,
Chengdu University, China

*CORRESPONDENCE
Weijun Ding
dingweijun@cdutcm.edu.cn

†These authors have contributed equally to this work

SPECIALTY SECTION
This article was submitted to Gut Endocrinology, a section of the journal Frontiers in Endocrinology

RECEIVED 25 September 2022
ACCEPTED 17 October 2022
PUBLISHED 14 November 2022

CITATION
Xia XW, Xie Y, Chen QQ, Ding D, Wang ZQ, Xu YJ, Wang YL, Wang XM and Ding WJ (2022) Cocultivation of Chinese prescription and intestine microbiota: SJZD alleviated the major symptoms of IBS-D subjects by tuning neurotransmitter metabolism. *Front. Endocrinol.* 13:1053103. doi: 10.3389/fendo.2022.1053103



# Cocultivation of Chinese prescription and intestine microbiota: SJZD alleviated the major symptoms of IBS-D subjects by tuning neurotransmitter metabolism

Xiuwen Xia[1†], Ya Xie[1†], Qiaoqiao Chen[1,2], Dou Ding[1,3], Zongqin Wang[4], Yaji Xu[1,5], Yili Wang[6], Xiumin Wang[1,7] and Weijun Ding[1*]

[1]School of Basic Medical Sciences, Chengdu University of Traditional Chinese Medicine, Chengdu, China, [2]Department of Fundamental Medicine, Neijiang Health Vocational College, Neijiang, China, [3]Department of Traditional Chinese Medicine, Zunyi Medical and Pharmaceutical College, Zunyi, China, [4]Department of Gastroenterology, Sichuan Hospital of Traditional Chinese Medicine, Chengdu, China, [5]Medical School, Chengdu University, Chengdu, China, [6]Innovative Institute of Chinese Medicine and Pharmacy, Chengdu University of Traditional Chinese Medicine, Chengdu, China, [7]Department of Proctology, Chengdu First People's Hospital, Chengdu, China

**Objective:** Diarrhea-predominant irritable bowel syndrome (IBS-D) is a recurrent and common disease featuring dysbiotic intestinal microbiota, with limited treatments. Si-Jun-Zi Decoction (SJZD), a classic Chinese prescription, has been extensively used for IBS-D. This work aimed to explore the *ex vivo* interactions of SJZD and IBS-D's intestinal microbiota.

**Methods:** Five samples of intestinal microbiota collected from IBS-D volunteers and five age-matched healthy controls were recruited from the Affiliated Hospital, Chengdu University of Traditional Chinese Medicine (TCM). A representative mixture of intestinal microbiota was composed of an equal proportion of these fecal samples. To simulate the clinical interaction, this microbiota was cocultivated with SJZD at clinical dosage in an anaerobic incubator at 37°C for 35 h. Microbiota and metabolic alterations were assessed by 16S rRNA gene sequencing in the V3/V4 regions and a nontargeted metabolome platform, respectively.

**Results:** After being cocultivated with SJZD, the dysbiotic intestine microbiota from IBS-D subjects was largely restored to those of the healthy controls. A total of 624 differentially expressed metabolites were detected by nontargeted metabolomics, of which 16 biomarkers were identified. These metabolites were then enriched into 11 pathways by KEGG, particularly those involved in neurotransmitter metabolism responses for the major symptom of IBS-D. Correlation analysis of bacterial metabolites demonstrated a synergistic

pattern of neurotransmitter metabolism between *Streptococcus* and *E. Shigella*.

**Conclusion:** *SJZD* rescued the dysbiotic intestinal microbiota and ameliorated the dysfunctional neurotransmitter metabolism involved in IBS-D's major symptoms.

KEYWORDS

diarrhea-predominant irritable bowel syndrome (IBS-D), Si-Jun-Zi decoction (SJZD), nontargeted metabolomics, 16S rRNA gene sequencing, microbiota-herbal cocultivation

# Introduction

Irritable bowel syndrome (IBS) is a common and recurrent disease, with an internationally pooled prevalence of 12.41% and limited treatments (1, 2). Diarrhea-predominant irritable bowel syndrome (IBS-D), as the major type of IBS, is characterized by perennial abdominal pain and diarrhea (3), with complex and diverse pathogenesis (4–6). Although its etiology remains unclear, microbial factors play key roles in IBS pathophysiology (7). Both the structure and function of the intestinal microbiota of IBS-D patients are intensively disturbed (8, 9). The multifactorial pathophysiology of IBS-D suggests multiple therapeutic approaches, such as altering intestine microbiota, visceral hypersensitivity, intestinal permeability, gut-brain interaction and psychological strategies (10). Therefore, complementary and alternative medicines such as traditional Chinese medicine (TCM) featuring synergistic effects may show special activities for IBS-D (11).

Few investigations have shown direct interactions between TCM formulas and gut microbiota. It is well known that oral administration is the major routine of TCM that inevitably interacts with the intestinal microbiota. The slight alterations of the construction and function in gut microbiota can significantly change the decomposition, transformation, and absorption of complex ingredients in Chinese herbs. Hence, directly detecting the potential molecular interactions between the intestinal microbiota and TCM herbs is pivotal for probing their interactive mechanisms. For instance, Si-Jun-Zi Decoction (SJZD) has been extensively used for IBS-D and other intestinal complaints for hundreds of years (11, 12). Unfortunately, the underlying mechanisms of SJZD *via* intestinal microbiota against IBS-D have not been fully described.

The *ex vivo* fermentation system is a promising platform for exploring the direct interactions between TCM formulas and intestinal microbiota. Accumulating publications have demonstrated that gut microbiota can transform ingredients in TCM herbs into diverse metabolites that show different bioavailability, bioactivity and/or toxicity (13), which can intensively impact the health and disease of mammalian hosts (14). A considerable amount of research has been performed to explore the interactions between intestinal microbiota (always from healthy volunteers) and the ingredients of certain TCM herbs (15, 16). However, few studies have explored the precise interactions of intestinal microbiota derived from particular patients and relevant TCM formulas (17, 18). Originally from long-term successful clinical practice, TCM formulas consisting of several herbs create a much more complicated mechanism because different active ingredients can work together to produce a more desired health effect or can cancel out the negative effects associated with a single herb, thereby minimizing side effects and retaining only the desired effect.

In the present work, an *ex vivo* cocultivation system will be established to determine the direct interactions of SJZD with the intestinal microbiota derived from IBS-D patients (19). To simulate the interactive regulation process between IBS-D intestine flora and effective TCM formulas, this anaerobic fermentation platform is of scientific significance for elucidating the interactive molecular mechanisms of a large number of TCM prescriptions and sparks a revolution in drug discovery based on Chinese formulas (20).

# Materials and methods

## Collection and preparation of samples

This work was approved by the Ethics Committee of the Chengdu University of TCM. Each participant signed an informed consent form before the experiment. Five representative IBS-D patients (group IBS-D) were diagnosed and recruited according to TCM standards (ZY/T001.9~001.9.94 & GB/T16751.2~1997) for the screen of Spleen-deficiency syndrome and Rome III diagnostic criteria

for IBS-D identification. Five age-matched healthy subjects were simultaneously enrolled as normal controls (NC group). All participants had a routine diet before sample collection. None of the volunteers had taken antibiotics for the last three months. All fecal samples were collected under sterile rule. A solution for sample preservation and transportation, composed of $KH_2PO_4$ (0.45%), $Na_2HPO_4$ (0.6%), Tween-80 (0.05%), and agar (0.1%), was prepared and applied for temporary storage and transit of collected samples.

## Preparation of SJZD solution

All herbs of SJZD formula were purchased from the Affiliated Hospital, Chengdu University of TCM. It consists of six herbs: *Codonopsis Tangshan Oliv.*, *Atractylodes macrocephala Koidz.*, *Poria cocos (Schw. Wolf*, *Glycyrrhiza uralensis Fisch*, *Citrus reticulata Blanco*, *Zingiber oj-jicinale Rosc.*, 30 g for each herb. This formula was prepared under the manufacturing rule of TCM decoction (21). The applied solution of SJZD was adjusted to 1 g/ml (W/V).

## Coculturation of SJZD with intestine microbiota

### Reagents

Tween-80 (Kemiou Chemical reagent, Tianjin, China), vitamin K1 (Solarbio Biotechnology, Beijing, China), and protohemin (Meilun Biotech, Dalian, China) were used in anaerobic culture. The culture medium, named General Anaerobic Medium (GAM) (Hopebiol Biotechnology, Qingdao, China), was composed of peptone 5.0 g, proteose peptone 5.0 g, enzymatically digested soybean meal 3.0 g, serum powder 10.0 g, beef extract 2.2 g, yeast extract 2.5 g, liver infusion 1.2 g, soluble starch 5.0 g, dextrose 0.5 g, sodium chloride 3.0 g, monopotassium phosphate 2.5 g, L-tryptophan 0.2 g, L-arginine 1.0 g, sodium thioglycollate 0.3 g, and L-cysteine monohydrochloride 0.3 g, and water was added up to 1000 mL. pH 7.3 was adjusted, sterilized at 121 °C for 20 min, and stored at 4°C for culture. The culture solution ($KH_2PO_4$ 4.5 g, $Na_2HPO_4$ 6 g, Tween-80 0.5 g, agar 1 g, added distilled water to 1000 ml) was mixed with GAM 3:7 (V/V) to obtain the transfer solution.

### Preparation of intestinal microbiota

Approximately 1 g of fecal sample was collected from each volunteer. The fecal sample was immediately put into a tube with 2 ml of the solution for sample preservation and transportation as described above. After slight mixing at 4°C for 5 min, 0.2 ml of the mixture was removed from each sample. The representative intestinal microbiota was then obtained by putting together five mixtures of groups IBS-D or NC and stored at -80°C.

### Cocultivation

The representative intestinal microbiota derived from the IBS-D and NC groups were resuscitated in GAM (1:9, V/V) at 37°C. A total of 10 ml of gut microbiota was mixed with 90 ml of drug-containing GAM (1:4, V/V) and cultured in a 250 ml flask located in an anaerobic airbag at 37°C for 35 h. NC0, NC6, NC12, NC24 and NC35 represent the coculture mixtures from group NC and sampled at 0, 6, 12, 24, and 35 h postincubation, respectively, while IBSD0, IBSD6, IBSD12, IBSD24, and IBSD35 represent those of group IBS-D. Three duplicated samples of each group were performed and centrifuged at 4000 g and 4°C for 10 min. The supernatant was collected, and three samples at each time point were equally mixed together and stored in a -80° C refrigerator.

### 16S rRNA gene sequencing

Cetyltrimethylammonium bromide (CTAB) and sodium dodecyl sulfate (SDS) were used to extract the total DNA from each sample of fermentation solution. The V3 and V4 regions of the 16S rRNA gene were amplified with a barcode (22) by a high-fidelity PCR master mix (New England Biolabs). The PCR products were then purified with a GeneJET gel extraction kit (Thermo Scientific). Sequencing libraries were generated using the NEB Next® Ultra™ DNA Library Prep Kit for Illumina (NEB, USA) following the manufacturer's recommendations, and index codes were added. Sequencing data were analyzed by a quantitative kit (Kapa Biosystems, KK4824) using an Illumina MiSeq platform for paired-end sequencing. The operational taxonomic units (OTUs) were selected through open reference OTU selection. Using LEfSe software, the LDA score was set to 4, and the community structure differences of the samples were analyzed. Metastatic analysis was carried out by R (Version 2.15.3) to analyze the differences between groups at each classification level, and the p value was obtained. Referring to Benjamin and Hochberg's false discovery rate, the Q value was obtained by correction of the p value (23). R (Version 2.15.3) was used to perform the t test between groups to determine the species with significant differences between groups and draw the map.

### Nontargeted metabolomics

Then, 400 µL of 80% methanol solution was added to 100 µL of fermentation, vortexed well, and centrifuged at 14000 g and 4°C for 20 min. Next, 300 µL of the supernatant was placed in a 1.5-ml centrifuge tube for LC–MS analysis. The supernatant was diluted to a final concentration of 53% methanol with LC–MS grade water. The samples were subsequently transferred to a fresh tube and centrifuged at 14000 g and 4°C for 20 min. Finally, the supernatant was injected into the LC–MS/MS system for further analysis. A Conquer UHPLC system (ThermoFisher) and a track rap Q extraction series mass spectrometer (ThermoFisher) were used in positive and negative modes. The original data generated by UHPLC–MS/MS were processed by peak pairing, peak selection, and quantification of each metabolite using compound

finder 3.1 (CD3.1, Thermo Fisher). Principal component analysis (PCA) and partial least squares discrimination analysis (PLS-DA) were used to analyze the significant differences in metabolites between the IBS-D and NC groups. Hierarchical clustering (HCA) and metabolite correlation analysis were used to reveal the relationship between metabolites and samples. Finally, the differentially expressed metabolites (DEMs) were matched with relevant biological processes based on the KEGG database.

### Network pharmacology forecast

Network pharmacology forecasting was performed by the "BATMAN-TCM" (Bioinformatics Analysis Tool for Molecular mechANism of Traditional Chinese Medicine) (24) to predict the compounds and corresponding targets in SJZD (set score = 20, $P <= 0.05$). Compared with the Therapeutic Target Database (TTD) and Online Mendelian Inheritance in Man (OMIM), targets and compounds related to IBS(-D) were obtained. The pathways that contact related targets were retrieved through the Kyoto Encyclopedia of Genes and Genomes (KEGG) database. Finally, the network diagram was drawn using Cytoscape 3.8.2 software.

### Statistical analysis

SPSS Software (V16.0; SPSS Inc., Chicago, IL) was used for statistical analyses. All data are expressed as the mean ± standard deviation (SD). Data were analyzed with one-way ANOVA. Differences between the groups were evaluated using Student's *t* test. Data were considered to be statistically significant with each value $^{*}P < 0.05$, $^{**}P < 0.01$. The correlation analysis was based on the cor() function in R (v3.1.3), and the Pearson correlation coefficient R ($1 \geq R \geq -1$) between all metabolites was calculated to analyze the correlation among the metabolites. The cor.test () function (FDR < 0.05) was used to test the significance of the correlation analysis.

## Results

From May 15 to August 04, 2018, ten stool samples, including five IBS-D subjects (IBS-D group) and five healthy subjects as normal controls (NC group), were collected from patients aged 18~35 years in the outpatient clinic of the Department of Gastroenterology, Sichuan Provincial Hospital of TCM.

### Differential microbiota between IBS-D and healthy individuals

The results of 16S rRNA gene sequencing showed that the dominant phyla in the cocultivations were Firmicutes, Proteobacteria, Actinobacteria and Bacteroidetes (Figure 1A), while *Streptococcus, E. Shigella, Lactobacillus, Clostridium, Paraclostridium and Bifidobacterium* were *the main* genera (Figure 1B). A total of 578 OTUs were identified from both groups (Figure 1C), and 103 were identified as core bacteria (Figure 1D). The T tests between groups showed that *Proteobacteria* and *Firmicutes* were significantly different at the phylum level (Figure 1E), and 6 microbiota were significantly different at the genus level (Figure 1F). LEfSe analysis of biomarkers (gate level to genus level) in each group revealed 10 biomarkers in the IBS-D group and 6 biomarkers in the NC group (Figure 1G).

The alpha diversity counted by the Shannon and Simpson indexes between the IBS-D and NC groups was significantly different ($^{*}P < 0.05$, $^{**}P < 0.01$), while the Ace and Chao1 indexes were not ($P > 0.05$) (Table 1 and Figures S1A–D). In addition, the beta diversities between the two groups also reached significant differences (Figure S1E).

### SJZD restored the dysbiotic microbiota of IBS-D subjects

SJZD restores the gut microbiota of IBS-D *in vitro*. The UPGMA clustering tree shows that with the development of time, the clustering distance between IBS-D samples cultured for 35 h and the NC group becomes shorter, and the difference between the IBS-D group and the NC group decreases (Figure 2A). SJZD mainly reduced the relative abundance of the phylum *Proteobacteria* and increased the relative abundance of *Firmicutes* (Figure 2A). Based on the screened differential microbiota from T test and LEfSe analysis and observing their dynamics from 0 through 35 h coculture time. We homogenized the differential microbiota using the Zscore to assess changes in microbiota abundance at different taxonomic levels in the samples before and after culture and found that most microbiota in the IBS-D group were more discrete than those in the NC group (Figure 2B). Among the top 10 genera, *Escherichia-Shigella* (Figure 2C), *Streptococcus* (Figure 2D), and *Paeniclostridium* (Figure 2E) were upregulated by SJZD. In addition, SJZD-upregulated *Bifidobacterium* was also the dominant group in the Top10 at the genus level (Figure 2F). The change in the ratio of *Escherichia-Shigella* to *Bifidobacterium* in the IBS-D group was less than that in the NC group (Figure 2G).

### IBS-D-derived metabolites are involved in neuroactive ligand–receptor interactions

The potential targets of 450 compounds of SJZD were predicted by the BATMAN-TCM platform (Table 2). We then compared the TTD database with the OMIM database to select compounds and targets associated with IBS (Table 3). Third, five target genes (HTR3A, HTR4, HTR6, CRHR1, HTR3B) of SJZD

10.3389/fendo.2022.1053103

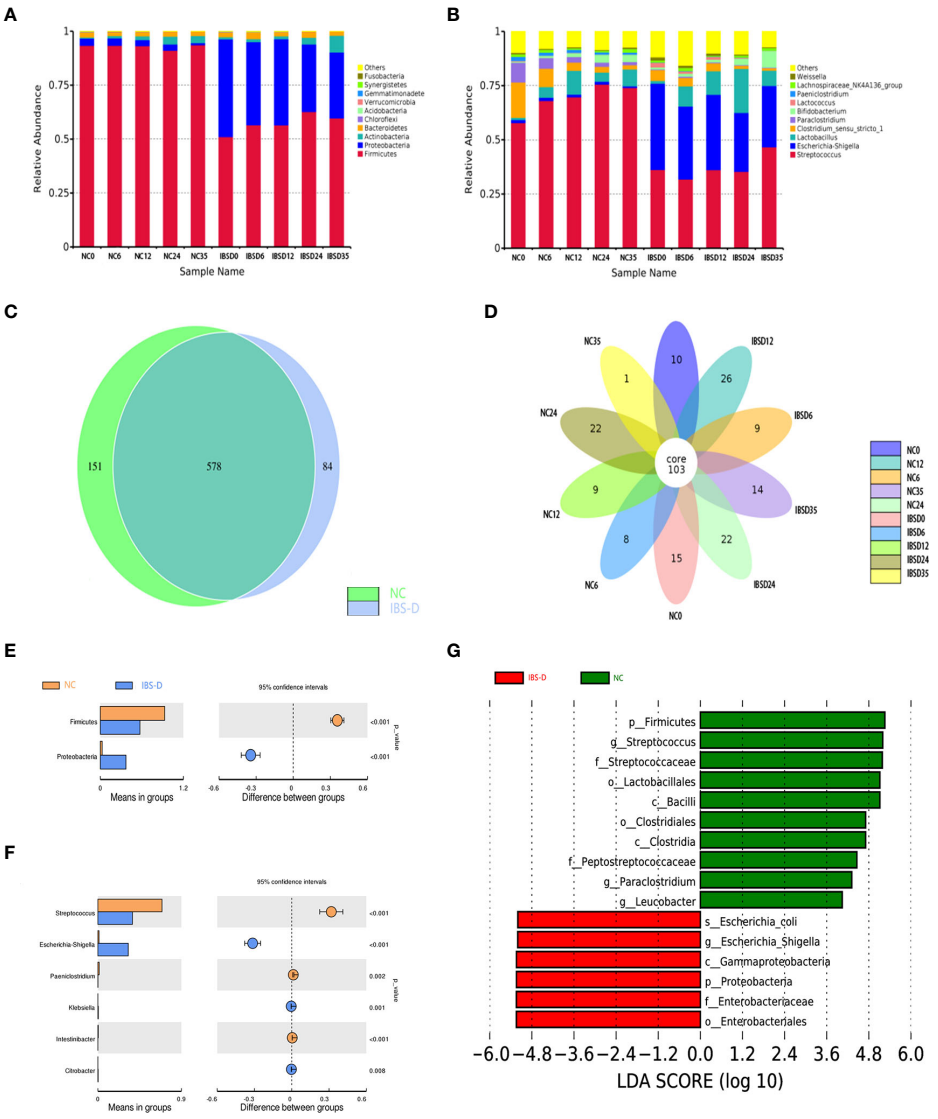


FIGURE 1
Basic characteristics of the cocultivated microbiota. **(A, B)** Histogram of relative abundance at the phylum **(A)** and genus **(B)** levels. The Arabic numerals within the sample name (0–35) indicate the culture time (hours). **(C, D)** Differentially expressed species between groups NC and IBS-D **(C)** and time series cocultivations **(D)**. **(E, F)** Differentially expressed taxa at the phylum **(E)** and genus **(F)** levels. **(G)** LEfSe analysis. LEfSe: LDA effect size analysis. LDA score: Linear discriminant analysis (LDA) affects the influence of species with significant differences in data. IBS-D: IBS-D group. NC: Normal control group. NC0-NC35: time series cocultivations of SJZD and intestine microbiota derived from the NC group. IBSD0-IBSD35: time series cocultivations of SJZD and intestine microbiota derived from the IBS-D group. SJZD: Si-Jun-Zi Decoction. IBS-D: diarrhea-predominant irritable bowel syndrome.

TABLE 1 Alpha diversity analysis of the cocultivated intestinal microbiota.

| Algorithm name | Wilcox (*p* value) | T test (*p* value) |
|---|---|---|
| Shannon | 0.01587* | 0.007274** |
| Simpson | 0.007937** | 0.001264** |
| Chao1 | 0.4206 | 0.3621 |
| Ace | 0.5476 | 0.4141 |

* *p* value <0.05, ** *p* value <0.01.

acting on IBS-D were screened after comparing the above results. Finally, these target genes were enriched in four pathways (i.e., serotonergic synapse, calcium signaling pathway, neuroactive ligand–receptor interaction, long-term depression.) based on the KEGG database.

Associated with the above virtual experiments, we analyzed the metabolites in the coculture system and found that the differentially expressed metabolites (DEM) were also enriched in neuroactive ligand–receptor interactions. A total of 458 DEMs

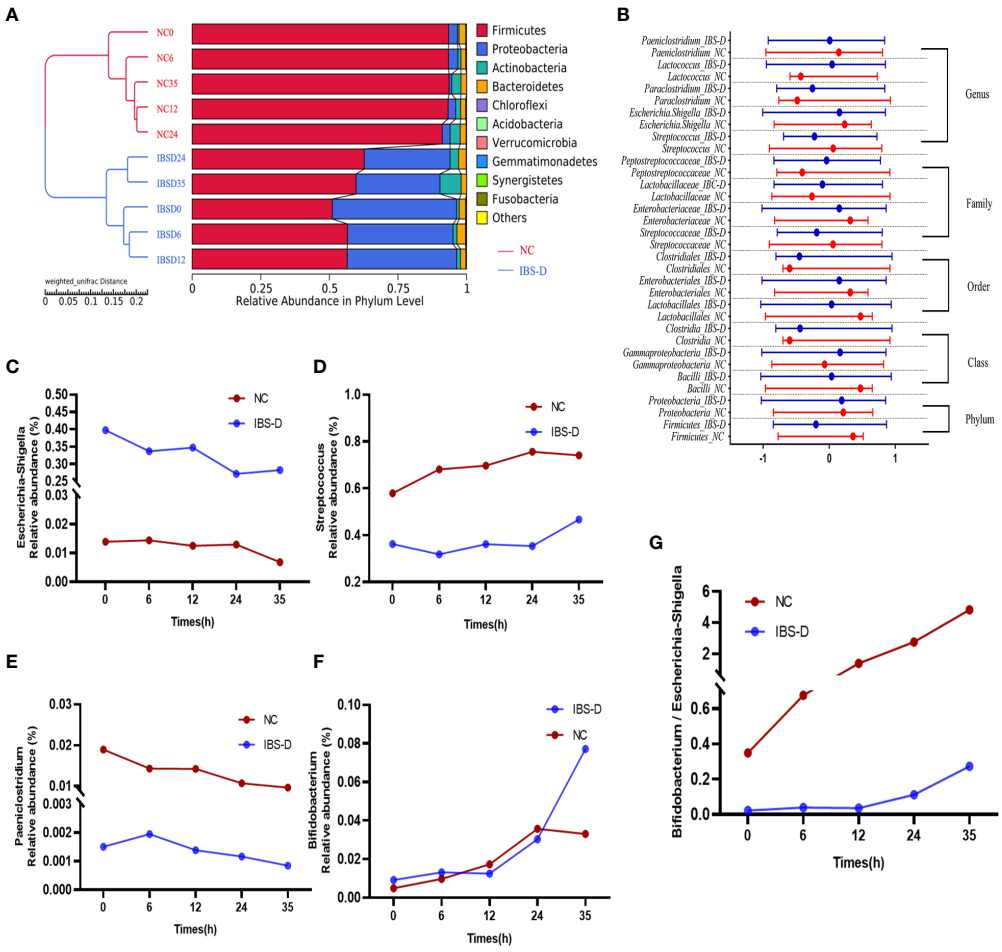


FIGURE 2
SJZD restored the dysbiotic intestinal microbiota of IBS-D subjects. **(A)** The unweighted pair-group method with arithmetic mean (UPGMA) clustering tree. **(B)** The Zscores of biomarkers at different taxa. The nodes in the graph show the median and interquartile ranges. Zscore = (x−μ)/σ (x: relative abundance of known bacteria, σ: standard difference, μ: average value). **(C-F)** Time series of relative abundances of *Escherichia-Shigella* **(C)**, *Streptococcus* **(D)**, *Paeniclostridium* **(E)**, and *Bifidobacterium* **(F)**. **(G)** *Bifidobacterium* to *Escherichia-Shigella ratio*. IBS-D: IBS-D group. NC: Normal controls. The Arabic numbers 0~35 indicate the coculture times (hours) of SJZD with the microbiota. SJZD: Si-Jun-Zi Decoction. IBS-D: diarrhea-predominant irritable bowel syndrome.

(Figure 3A, C) were detected in positive ion mode, and 166 DEMs (Figure 3B, D) were detected in negative ion mode (Table 4). Eleven KEGG pathways were statistically enriched based on the above DEMs ($p<0.05$), including 14 metabolites such as histamine, morphine, cytocine, tryptamine, and pyridoxamine (Table 5). It is worth mentioning that histamine, morphine and tryptamine are enriched in the neuroactive ligand–receptor interaction pathway.

## Neurotransmitter-related metabolites in cocultivations involved in IBS-D therapy

The gut microbiota showed a close correlation with intestinal DEMs (S2). Correlation analysis showed that five genera, *Proteobacteria* and *Paeniclostridium*, were significantly correlated with three DEMs (histamine, morphine and tryptamine) (Figure 4A). At the phylum level, SJZD mainly affected the relative abundance of *Firmicutes* (Figure 4B) and *Proteobacteria* (Figure 4C) in IBS-D subjects; *Proteobacteria* was negatively correlated with *Firmicutes* and positively correlated with histamine, morphine and tryptamine. At the genus level, *Escherichia-Shigella* was negatively correlated with *Streptococcus* and *Paeniclostridium* and positively correlated with histamine, morphine and tryptamine. Using Cytoscape 3.8.2 software, the crucial intestinal microbe-metabolite-SJZD-target network diagram was drawn (Figure 4D), particularly associated with the neuroactive ligand–receptor interaction pathway (hsa04080) and key intestinal microbiota.

TABLE 2 Target prediction of IBS-D based on SJZD.

| Gene name | Compound |
|---|---|
| HTR3A | 1,22-Docosanediol; 1-Heptadecanol; Nicotine; Isotrilobine; Ergotamine; Phenylic Acid; Hesperidin; N-Nonanol; Isoliensinine; Tetrahydropalmatine |
| HTR4 | Ergotamine; Hesperidin |
| HTR6 | Nicotine; Ergotamine; Tetrahydropalmatine; Alpha-Curcumene |
| CRHR1 | Ergotamine |
| HTR3B | 1,22-Docosanediol; 1-Heptadecanol; Ergotamine; Phenylic Acid; N-Nonanol |

TABLE 3 Targets to IBS predicted by the TTD and OMIM databases.

| Term ID | Term description | gene names |
|---|---|---|
| hsa04726 | Serotonergic synapse | HTR3A; HTR4; HTR6; HTR3B |
| hsa04020 | Calcium signaling pathway | HTR4; HTR6 |
| hsa04080 | Neuroactive ligand–receptor interaction | HTR4; HTR6; CRHR1 |
| hsa04730 | Long-term depression | CRHR1 |

## Discussion

Given that oral administration is the main approach in TCM, observation of the direct interactions between TCM formulas and gut microbiota is an extremely important and urgent research field. The intestinal microbiome of human beings is a diverse and dynamic collection of microorganisms that have much more metabolic potential than those of their mammalian host. Ever-increasing evidence indicates that the intestinal microbiota plays a pivotal role in TCM therapy by complicated interplay with Chinese components (25). This interplay includes activities such as intestinal microbiota biotransforming TCM components into metabolites with different bioavailability and bioactivity/toxicity from their precursors (15), improving the dysbiotic microbiota and consequently ameliorating associated pathological conditions (16) and mediating the synergistic and antagonistic interactions between the multiple chemicals in certain TCM formulas (26). However, the interactive mechanisms between TCM herbs/formula and relevant intestinal microbiota have always been distorted by gut ecology, such as mucosal immunity, the enteric nervous system and the hormonal environment.

This work aims to observe the direct interaction mechanism of a typical dysbiotic intestine microbiota and a TCM formula based on a cocultivation or fermentation system. IBS is a common but complex disease characterized by dysbiotic intestinal microbiota. Compared with healthy controls, the family *Enterobacteriaceae* (phylum *Proteobacteria*), family *Lactobacillaceae*, and genus *Bacteroides* were increased in IBS subjects, whereas *uncultured Clostridiales I*, genus *Faecalibacterium* and genus *Bifidobacterium* were decreased (27). On the other hand, the TCM formula SJZD has a long history of clinical application for functional dyspepsia and IBS-D. Therefore, we collected five intestinal microbiota samples derived from representative IBS-D subjects and five controls and established an *ex vivo* concultivation system to reveal the interaction pattern of SJZD compounds and the intestinal microbiota of IBS-D patients.

The results of 16S rRNA gene sequencing showed that SJZD effectively rescued intestinal dysbiosis in patients with IBS-D. Both alpha and beta diversities between the IBS-D and NC groups reached significant differences (Table 1 and Figure S1E) (28–31). Core taxa were observed in both groups (Figure 1B), consistent with other publications (32). The genera *Bifidobacteria* (33), *Lactobacillus* and *Streptococcus* (34) can ameliorate the symptoms of IBS; we observed that the relative abundances of these genera increased with cocultivation time. Interestingly, the abundance of the genus *Streptococcus* was significantly higher than that in the NC group at every time point. Previous studies have reported that the abundance of Streptococcus in constipated IBS (IBS-C) is relatively high (35), but the underlying mechanism is not clear. IBS-D is associated with increased abundances of *Escherichia-Shigella* (36–38). *Paeniclostridium* is related to intestinal injury and inflammation (39), whereas *Proteobacteria* is a negative factor for intestinal homeostasis (30–32). In summary, SJZD effectively rescued key abnormal bacteria in the intestinal microbiota of IBS-D patients.

Metabolome analysis revealed that SJZD beneficially tuned the altered metabolite profile of intestinal microbiota in IBS-D

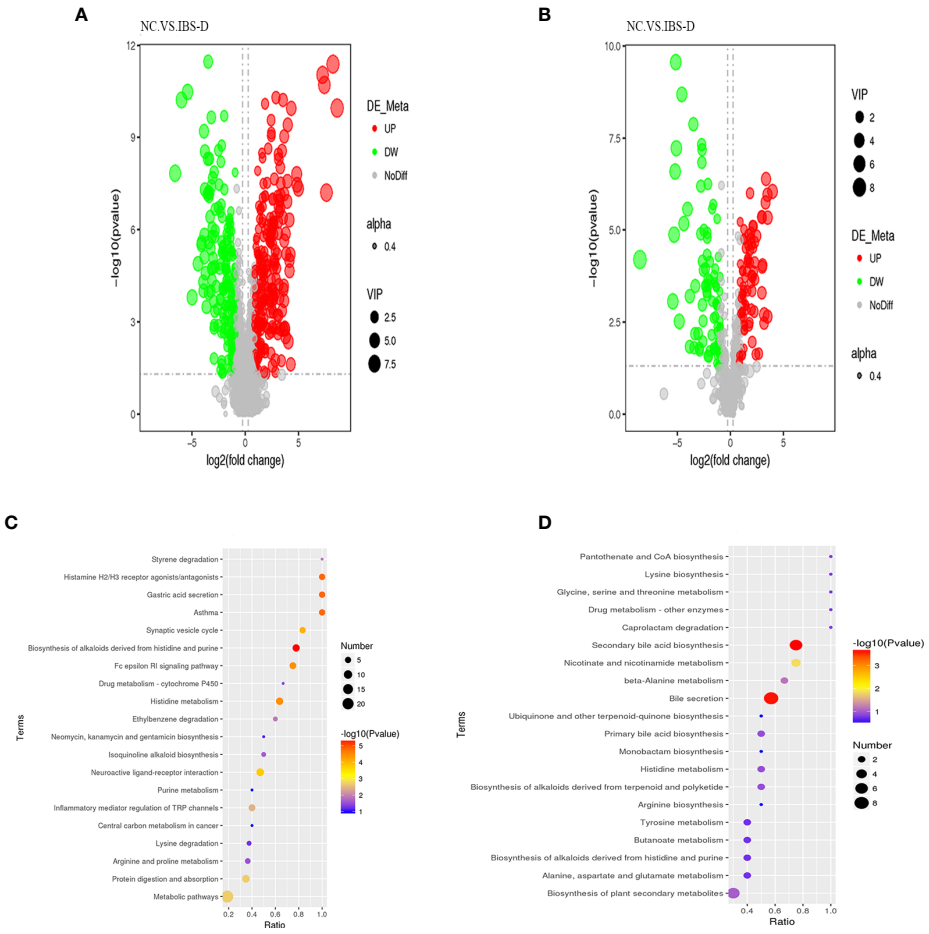


FIGURE 3
Nontargeted metabolites of the cocultured SJZD and intestine microbiota. **(A, B)** Volcano map of differentially expressed metabolites (DEM) from positive ion mode **(A)** and negative ion mode **(B)**. VIP: Variable importance in the projection. alpha: Transparency of dots. Black: the metabolite with no significant difference (nodiff), red: upregulated metabolite (up), green: downregulated metabolite (DW). **(C, D)** Bubble chart of enriched KEGG pathways, positive ion mode **(C)** and negative ion mode **(D)**. SJZD: Si-Jun-Zi Decoction. IBS-D: diarrhea-predominant irritable bowel syndrome.

subjects. Abdominal pain, as one of the predominant manifestations of IBS-D, is associated with the abnormal metabolism of enteric neurotransmitters such as tryptophan. Tryptamine, as the bacterial metabolite of tryptophan, plays a pivotal role in balancing intestinal immune tolerance and maintaining intestinal microbiota (40–44) and promoting intestinal functions (45). In this work, we observed significantly higher levels of tryptamine, morphine, arachidonic acid, and histamine in the IBS-D group (S3). The concentrations of these neurotransmitters and metabolites were positively correlated with

TABLE 4 Differentially expressed metabolites identified by LC−MS.

| Compared samples | Num. of total ident. | Num. of total sig. | Num. of Sig.down | Num. of Sig.up |
|---|---|---|---|---|
| IBSD.vs.NC_pos | 4042 | 458 | 262 | 196 |
| IBSD.vs.NC_neg | 1247 | 166 | 83 | 83 |

Num. Of Total Ident.: the total number of identified compounds. Num. Of Total Sig.: the number of metabolites detected as differentially expressed metabolites (DEM). Num. Of Sig.up: Number of upregulated DEMs. Num. Of Sig.down: the number of downregulated DEMs.

10.3389/fendo.2022.1053103

TABLE 5 KEGG pathways enriched by differentially expressed metabolites.

| Map ID | Map title | Adjusted *p* value | Metabolite names |
|---|---|---|---|
| map01065 | Biosynthesis of alkaloids derived from histidine and purine | 0.000304047 | Histamine; L-Histidine |
| map04971 | Gastric acid secretion | 0.000304047 | Histamine |
| map05310 | Asthma | 0.000304047 | Histamine |
| map07227 | Histamine H2/H3 receptor agonists/antagonists | 0.000304047 | Histamine |
| map00340 | Histidine metabolism | 0.000479862 | Histamine, L-Histidine |
| map04664 | Fc epsilon RI signaling pathway | 0.000479862 | Histamine, Arachidonic acid |
| map04721 | Synaptic vesicle cycle | 0.000954972 | Histamine |
| map04080 | Neuroactive ligand–receptor interaction | 0.001591021 | Histamine, Morphine, Tryptamine |
| map04974 | Protein digestion and absorption | 0.015358943 | Histamine, L-Histidine, Putrescine |
| map04750 | Inflammatory mediator regulation of TRP channels | 0.025307978 | Histamine, Arachidonic acid |
| map01100 | Metabolic pathways | 0.015358943 | Histamine, L-Histidine, Morphine, Tryptamine, Arachidonic acid, Putrescine, Guanine, Cytosine, Styrene, L-Tyrosine, Pipecolic acid, 1-Piperideine, Pyridoxamine, Agmatine |

Mapid: the ID of the enriched KEGG pathway. Maptitle: The name of the enriched KEGG pathway. Adjusted pV: corrected p value. Meta names: enriched in different metabolites related to this pathway. KEGG pathway significant enrichment.

*Escherichia-Shigella* but negatively correlated with *Streptococcus* (Figures 4B, D). Although morphine has the effect of slowing down movement in the large intestine (46) and arachidonic acid may improve gastrointestinal movement (47), our present work showed that the content of morphine is not statistically high in the IBS-D group. The histamine level was negatively correlated with L-histidine (Figures 4B, C), suggesting that histidine was converted to histamine in the IBS-D group (S3). In addition, our results indicated that the genera *Escherichia-Shigella* and *Streptococcus* may synergistically regulate histidine metabolism and suggest that foods rich in L-histidine may worsen the symptoms of IBS-D. In a sentence, histamine, morphine and tryptamine, as crucial metabolites enriched in the neuroactive ligand–receptor interaction pathway, were the essential neurotransmitters derived from the fermentation of SJZD and the intestinal microbiota of IBS-D subjects. These metabolites respond to abdominal pain, the crucial symptom of IBS-D patients. Therefore, our results indicated that SJZD facilitated the *ex vivo* modulation of the metabolite profiles, particularly those involved in the pathway of neuroactive ligand–receptor interaction.

Correlation analysis further revealed the network outline of intestine microbiota, intestine metabolites, SJZD compounds and targets for IBS-D patients (Figure 4D), particularly associated with the neuroactive ligand–receptor interaction pathway (hsa04080) and core taxa in the intestinal microbiota. The BATMAN-TCM network pharmacology and other correlation analysis platforms revealed that, in addition to metabolic modulation of the intestinal microbiota that leads to symptom amelioration, SJZD compounds showed regulatory targets for IBS-D therapy. Specifically, the correlation analysis demonstrated that five genera were significantly correlated with IBS-D-relevant neurotransmitters (i.e., histamine, morphine and tryptamine) (Figure 4A). These results could be used to determine the correlation between *SJZD* and the restoration of abnormal abundances of certain intestinal microbes. This finding indicates that the cocultivation of *SJZD* and gut microbiota originating from IBS-D volunteers is a useful platform to explore the direct interactions of TCM formula and complex intestine microbiota.

Some shortcomings exist in this work. First, our concultivation platform does not fully mimic the intestine microecology of human beings. For instance, apart from the majority of anaerobic bacteria, there are facultative and even aerobic bacteria living within our intestine. The dynamic growth of anaerobic, facultative and aerobic bacteria is one of the key mechanisms underlying the robust intestinal air environment. Hence, our anaerobic culture environment cannot fully simulate clinical gas conditions. Second, although we used an ex vivo fermentation system and observed a direct interaction between SJZD and the intestinal microbiota of IBS-D patients, the underlying molecular regulation mechanisms need to be further explored. Third, to detect more complete mechanisms of SJZD against IBS-D subjects, comparative studies between *in*

10.3389/fendo.2022.1053103

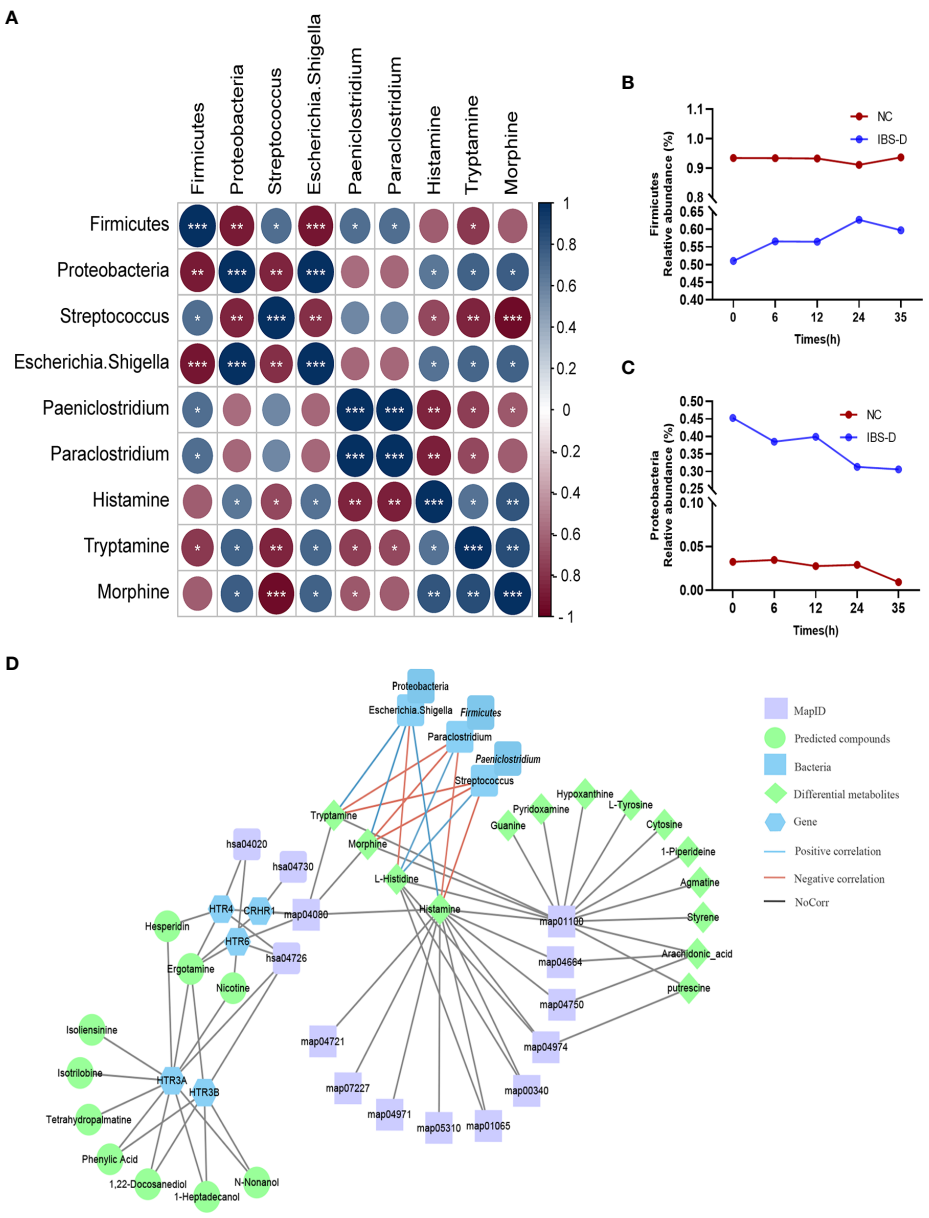


FIGURE 4
Significant correlations between microbiota and metabolites. **(A)** Correlation analysis of intestinal microbiota and differentially expressed metabolites. **(B, C)**. Time series of relative abundances of the phyla Proteobacteria **(B)** and Firmicutes **(C)** in a cocultivation system. **(D)** Compound-target network based on IBS-D microbiota-metabolome-SJZD compound analysis. SJZD: Si-Jun-Zi Decoction. IBS-D: diarrhea-predominant irritable bowel syndrome.

*vivo* and *ex vivo* models should also be executed. Finally, the representative samples of intestine microbiota were composed of only ten donors in this study. Given the marked individual diversities of the intestinal microbiota in IBS-D patients, a larger sample size might be required for further studies.

## Conclusion

Our work demonstrated that *SJZD* rescued the dysbiotic intestinal microbiota and ameliorated the dysfunctional neurotransmitter metabolism involved in the major symptoms

of IBS-D. The *ex vivo* coculture system could be extensively used to reveal the direct interactions between TCM formulas and complex gut microbiota.

## Data availability statement

The original contributions presented in the study are publicly available. This data can be found here: NCBI database; PRJNA898776; https://www.ncbi.nlm.nih.gov/bioproject/PRJNA898776.

## Ethics statement

The studies involving human participants were reviewed and approved by The Ethics Committee of the Chengdu University of TCM. The patients/participants provided their written informed consent to participate in this study.

## Author contributions

XWX: Writing - Original Draft, Data Curation. YX: Investigation, Data Curation, Visualization. QQC: Visualization. DD: Writing-Review and Editing. ZQW: Investigation. YJX: Investigation. YLW: Resources. XMW: Resources. WJD: Writing - Review and Editing, Project administration, Funding acquisition. All authors contributed to the article and approved the submitted version.

## Acknowledgments

The author would like to express their sincere gratitude to the experimental technical assistance provided by the Institute of Chinese Medicine Innovation, Chengdu University of Traditional Chinese Medicine.

## Conflict of interest

The authors declare that the research was conducted in the absence of any commercial or financial relationships that could be construed as a potential conflict of interest.

## Publisher's note

All claims expressed in this article are solely those of the authors and do not necessarily represent those of their affiliated organizations, or those of the publisher, the editors and the reviewers. Any product that may be evaluated in this article, or claim that may be made by its manufacturer, is not guaranteed or endorsed by the publisher.

## Supplementary material

The Supplementary Material for this article can be found online at: https://www.frontiersin.org/articles/10.3389/fendo.2022.1053103/full#supplementary-material

## References

1. Devanarayana NM, Rajindrajith S, Pathmeswaran A, Abegunasekara C, Gunawardena NK, Benninga MA. Epidemiology of irritable bowel syndrome in children and adolescents in Asia. *J Pediatr Gastroenterol Nutr* (2015) 60:792–8. doi: 10.1097/MPG.0000000000000714

2. Longstreth GF, Thompson WG, Chey WD, Houghton LA, Mearin F, Spiller RC. Functional bowel disorders. *Gastroenterology* (2006) 130:1480–91. doi: 10.1053/j.gastro.2005.11.061

3. Guilera M, Balboa A, Mearin F. Bowel habit subtypes and temporal patterns in irritable bowel syndrome: Systematic review. *Am J Gastroenterol* (2005) 100:1174–84. doi: 10.1111/j.1572-0241.2005.40674.x

4. Crowell MD, Harris L, Jones MP, Chang L. New insights into the pathophysiology of irritable bowel syndrome: Implications for future treatments. *Curr Gastroenterol Rep* (2005) 7:272–9. doi: 10.1007/s11894-005-0019-8

5. Hasler WL. Traditional thoughts on the pathophysiology of irritable bowel syndrome. *Gastroenterol Clin North Am* (2011) 40:21–43. doi: 10.1016/j.gtc.2010.12.004

6. Pimentel M, Chang C. Inflammation and microflora. *Gastroenterol Clin North Am* (2011) 40:69–85. doi: 10.1016/j.gtc.2010.12.010

7. Pimentel M, Lembo A. Microbiome and its role in irritable bowel syndrome. *Dig Dis Sci* (2020) 65:829–39. doi: 10.1007/s10620-020-06109-5

8. Distrutti E, Monaldi L, Ricci P, Fiorucci S. Gut microbiota role in irritable bowel syndrome: New therapeutic strategies. *World J Gastroenterol* (2016) 22:2219–41. doi: 10.3748/wjg.v22.i7.2219

9. Mohajeri MH, La Fata G, Steinert RE, Weber P. Relationship between the gut microbiome and brain function. *Nutr Rev* (2018) 76:481–96. doi: 10.1093/nutrit/nuy009

10. Nee J, Lembo A. Review article: Current and future treatment approaches for IBS with diarrhoea (IBS-d) and IBS mixed pattern (IBS-m). *Aliment Pharmacol Ther* (2021) 54 Suppl 1:S63–74. doi: 10.1111/apt.16625

11. Li L, Cui H, Li T, Qi J, Chen H, Gao F, et al. Synergistic effect of berberine-based Chinese medicine assembled nanostructures on diarrhea-predominant irritable bowel syndrome *In vivo*. *Front Pharmacol* (2020) 11:1210. doi: 10.3389/fphar.2020.01210

12. Wu Z-C, Zhao Z-L, Deng J-P, Huang J-T, Wang Y-F, Wang Z-P. Sanhuang shu'ai decoction alleviates DSS-induced ulcerative colitis *via* regulation of gut microbiota, inflammatory mediators and cytokines. *BioMed Pharmacother* (2020) 125:109934. doi: 10.1016/j.biopha.2020.109934

13. An X, Bao Q, Di S, Zhao Y, Zhao S, Zhang H, et al. The interaction between the gut microbiota and herbal medicines. *BioMed Pharmacother* (2019) 118:109252. doi: 10.1016/j.biopha.2019.109252

14. Sekirov I, Russell SL, Antunes LCM, Finlay BB. Gut microbiota in health and disease. *Physiol Rev* (2010) 90:859–904. doi: 10.1152/physrev.00045.2009

15. Chen F, Wen Q, Jiang J, Li H-L, Tan Y-F, Li Y-H, et al. Could the gut microbiota reconcile the oral bioavailability conundrum of traditional herbs? *J Ethnopharmacol* (2016) 179:253–64. doi: 10.1016/j.jep.2015.12.031

16. Li H, Zhou M, Zhao A, Jia W. Traditional Chinese medicine: Balancing the gut ecosystem. *Phytother Res* (2009) 23:1332–5. doi: 10.1002/ptr.2590

17. Peterson CT, Sharma V, Iablokov SN, Albayrak L, Khanipov K, Uchitel S, et al. 16S rRNA gene profiling and genome reconstruction reveal community metabolic interactions and prebiotic potential of medicinal herbs used in neurodegenerative disease and as nootropics. *PloS One* (2019) 14(3):e0213869. doi: 10.1371/journal.pone.0213869

18. Su L, Su Y, An Z, Zhang P, Yue Q, Zhao C, et al. Fermentation products of danshen relieved dextran sulfate sodium-induced experimental ulcerative colitis in mice. *Sci Rep* (2021) 11:16210. doi: 10.1038/s41598-021-94594-7

19. Wu R, Zhao D, An R, Wang Z, Li Y, Shi B, et al. Linggui zhugan formula improves glucose and lipid levels and alters gut microbiota in high-fat diet-induced diabetic mice. *Front Physiol* (2019) 10:918. doi: 10.3389/fphys.2019.00918

20. Jia W, Li H, Zhao L, Nicholson JK. Gut microbiota: A potential new territory for drug targeting. *Nat Rev Drug Discovery* (2008) 7:123–9. doi: 10.1038/nrd2505

21. Tian S, Song X, Wang Y, Wang X, Mou Y, Chen Q, et al. Chinese Herbal medicine baoyuan jiedu decoction inhibits the accumulation of myeloid derived suppressor cells in pre-metastatic niche of lung *via* TGF-β/CCL9 pathway. *Biomed Pharmacother* (2020) 129:110380. doi: 10.1016/j.biopha.2020.110380

22. Larsson E, Tremaroli V, Lee YS, Koren O, Nookaew I, Fricker A, et al. Analysis of gut microbial regulation of host gene expression along the length of the gut and regulation of gut microbial ecology through MyD88. *Gut* (2012) 61:1124–31. doi: 10.1136/gutjnl-2011-301104

23. White JR, Nagarajan N, Pop M. Statistical methods for detecting differentially abundant features in clinical metagenomic samples. *PloS Comput Biol* (2009) 5:e1000352. doi: 10.1371/journal.pcbi.1000352

24. Liu Z, Guo F, Wang Y, Li C, Zhang X, Li H, et al. BATMAN-TCM: A bioinformatics analysis tool for molecular mechANism of traditional Chinese medicine. *Sci Rep* (2016) 6:21146. doi: 10.1038/srep21146

25. Xu J, Chen H-B, Li S-L. Understanding the molecular mechanisms of the interplay between herbal medicines and gut microbiota. *Med Res Rev* (2017) 37:1140–85. doi: 10.1002/med.21431

26. Zhang M, Long Y, Sun Y, Wang Y, Li Q, Wu H, et al. Evidence for the complementary and synergistic effects of the three-alkaloid combination regimen containing berberine, hypaconitine and skimmianine on the ulcerative colitis rats induced by trinitrobenzene-sulfonic acid. *Eur J Pharmacol* (2011) 651:187–96. doi: 10.1016/j.ejphar.2010.10.030

27. Pittayanon R, Lau JT, Yuan Y, Leontiadis GI, Tse F, Surette M, et al. Gut microbiota in patients with irritable bowel syndrome-a systematic review. *Gastroenterology* (2019) 157:97–108. doi: 10.1053/j.gastro.2019.03.049

28. Si J-M, Yu Y-C, Fan Y-J, Chen S-J. Intestinal microecology and quality of life in irritable bowel syndrome patients. *World J Gastroenterol* (2004) 10:1802–5. doi: 10.3748/wjg.v10.i12.1802

29. Chey WD, Kurlander J, Eswaran S. Irritable bowel syndrome: A clinical review. *JAMA* (2015) 313:949–58. doi: 10.1001/jama.2015.0954

30. Wang Y, Zheng F, Liu S, Luo H. Research progress in fecal microbiota transplantation as treatment for irritable bowel syndrome. *Gastroenterol Res Pract* (2019) 2019:9759138. doi: 10.1155/2019/9759138

31. Kassinen A, Krogius-Kurikka L, Mäkivuokko H, Rinttilä T, Paulin L, Corander J, et al. The fecal microbiota of irritable bowel syndrome patients differs significantly from that of healthy subjects. *Gastroenterology* (2007) 133:24–33. doi: 10.1053/j.gastro.2007.04.005

32. Qin J, Li R, Raes J, Arumugam M, Burgdorf KS, Manichanh C, et al. A human gut microbial gene catalogue established by metagenomic sequencing. *Nature* (2010) 464:59–65. doi: 10.1038/nature08821

33. Parkes GC, Rayment NB, Hudspith BN, Petrovska L, Lomer MC, Brostoff J, et al. Distinct microbial populations exist in the mucosa-associated microbiota of sub-groups of irritable bowel syndrome. *Neurogastroenterol Motil* (2012) 24:31–9. doi: 10.1111/j.1365-2982.2011.01803.x

34. Lewis ED, Antony JM, Crowley DC, Piano A, Bhardwaj R, Tompkins TA, et al. Efficacy of lactobacillus paracasei HA-196 and bifidobacterium longum R0175 in alleviating symptoms of irritable bowel syndrome (IBS): A randomized, placebo-controlled study. *Nutrients* (2020) 12:E1159. doi: 10.3390/nu12041159

35. Matsumoto H, Shiotani A, Katsumata R, Fukushima S, Handa Y, Osawa M, et al. Mucosa-associated microbiota in patients with irritable bowel syndrome: A comparison of subtypes. *Digestion* (2021) 102:49–56. doi: 10.1159/000512167

36. Liu Y, Yuan X, Li L, Lin L, Zuo X, Cong Y, et al. Increased ileal immunoglobulin a production and immunoglobulin a-coated bacteria in diarrhea-predominant irritable bowel syndrome. *Clin Transl Gastroenterol* (2020) 11:e00146. doi: 10.14309/ctg.0000000000000146

37. Li J, Cui H, Cai Y, Lin J, Song X, Zhou Z, et al. Tong-Xie-Yao-Fang regulates 5-HT level in diarrhea predominant irritable bowel syndrome through gut microbiota modulation. *Front Pharmacol* (2018) 9:1110. doi: 10.3389/fphar.2018.01110

38. Carroll IM, Ringel-Kulka T, Siddle JP, Ringel Y. Alterations in composition and diversity of the intestinal microbiota in patients with diarrhea-predominant irritable bowel syndrome. *Neurogastroenterol Motil* (2012) 24:521–530, e248. doi: 10.1111/j.1365-2982.2012.01891.x

39. Tian S, Liu Y, Wu H, Liu H, Zeng J, Choi MY, et al. Genome-wide CRISPR screen identifies semaphorin 6A and 6B as receptors for paeniclostridium sordellii toxin TcsL. *Cell Host Microbe* (2020) 27:782–792.e7. doi: 10.1016/j.chom.2020.03.007

40. Leprun PMB, Clarke G. The gut microbiome and pharmacology: A prescription for therapeutic targeting of the gut-brain axis. *Curr Opin Pharmacol* (2019) 49:17–23. doi: 10.1016/j.coph.2019.04.007

41. Gao J, Xu K, Liu H, Liu G, Bai M, Peng C, et al. Impact of the gut microbiota on intestinal immunity mediated by tryptophan metabolism. *Front Cell Infect Microbiol* (2018) 8:13. doi: 10.3389/fcimb.2018.00013

42. Jennis M, Cavanaugh CR, Leo GC, Mabus JR, Lenhard J, Hornby PJ. Microbiota-derived tryptophan indoles increase after gastric bypass surgery and reduce intestinal permeability *in vitro* and *in vivo*. *Neurogastroenterol Motil* (2018) 30(2). doi: 10.1111/nmo.13178

43. Zucchi R, Chiellini G, Scanlan TS, Grandy DK. Trace amine-associated receptors and their ligands. *Br J Pharmacol* (2006) 149:967–78. doi: 10.1038/sj.bjp.0706948

44. Williams BB, Van Benschoten AH, Cimermancic P, Donia MS, Zimmermann M, Taketani M, et al. Discovery and characterization of gut microbiota decarboxylases that can produce the neurotransmitter tryptamine. *Cell Host Microbe* (2014) 16:495–503. doi: 10.1016/j.chom.2014.09.001

45. Bhattarai Y, Williams BB, Battaglioli EJ, Whitaker WR, Till L, Grover M, et al. Gut microbiota-produced tryptamine activates an epithelial G-Protein-Coupled receptor to increase colonic secretion. *Cell Host Microbe* (2018) 23:775–785.e5. doi: 10.1016/j.chom.2018.05.004

46. Corazziari E. Role of opioid ligands in the irritable bowel syndrome. *Can J Gastroenterol* (1999) 13 Suppl:A:71A–75A. doi: 10.1155/1999/598659

47. Zhang Q, Zhong D, Ren Y-Y, Meng Z-K, Pegg RB, Zhong G. Effect of konjac glucomannan on metabolites in the stomach, small intestine and large intestine of constipated mice and prediction of the KEGG pathway. *Food Funct* (2021) 12:3044–56. doi: 10.1039/d0fo02682d

frontiers | Frontiers in Endocrinology

TYPE Original Research
PUBLISHED 17 November 2022
DOI 10.3389/fendo.2022.1042044



OPEN ACCESS

EDITED BY
Xinhua Shu,
Glasgow Caledonian University,
United Kingdom

REVIEWED BY
Haoqing Shao,
Hunan University of Medicine, China
Yuli Li,
Hunan University of Chinese Medicine,
China

*CORRESPONDENCE
Xu Zhou
stu.hnucm.edu.cn

SPECIALTY SECTION
This article was submitted to
Gut Endocrinology,
a section of the journal
Frontiers in Endocrinology

RECEIVED 12 September 2022
ACCEPTED 31 October 2022
PUBLISHED 17 November 2022

CITATION
Yan Y, Li Q, Shen L, Guo K and Zhou X (2022) Chlorogenic acid improves glucose tolerance, lipid metabolism, inflammation and microbiota composition in diabetic db/db mice. *Front. Endocrinol.* 13:1042044. doi: 10.3389/fendo.2022.1042044



# Chlorogenic acid improves glucose tolerance, lipid metabolism, inflammation and microbiota composition in diabetic db/db mice

Yongwang Yan[1], Qing Li[2], Ling Shen[1], Kangxiao Guo[1,3] and Xu Zhou[4]*

[1]Pharmaceutical College, Changsha Health Vocational College, Changsha, China, [2]Department of Pathology, Changsha Health Vocational College, Changsha, China, [3]National Engineering Laboratory for Rice and By-Product Deep Processing, College of Food Science and Engineering, Central South University of Forestry and Technology, Changsha, China, [4]Department of Spleen, Stomach and Liver Diseases, Affiliated Hospital of Hunan Academy of Traditional Chinese Medicine, Changsha, China

**Introduction:** Chronic and acute chlorogenic acid (CGA) can improve glucose tolerance (GT) and insulin sensitivity (IS). However, whether acute administration of CGA has beneficial effects on hepatic lipid metabolism and cecal microbiota composition remains unclear.

**Methods:** In the current study, diabetic db/db mice were administered CGA or metformin, and db/m mice were used as controls to explore the effects of CGA on hepatic lipid metabolism, including fatty acid oxidation and transportation and triglyceride (TG) lipolysis and synthesis. Moreover, alterations in the inflammatory response and oxidative stress in the liver and gut microbe composition were evaluated.

**Results:** The results showed that CGA decreased body weight and improved glucose tolerance and insulin resistance, and these effects were similar to those of metformin. CGA decreased hepatic lipid content by increasing the expression of *CPT1a* (carnitine palmitoyltransferase 1a), *ACOX1* (Acyl-CoA oxidase 1), *ATGL* (adipose triglyceride lipase), and *HSL* (hormone-sensitive lipase) and decreasing that of *MGAT1* (monoacylglycerol O-acyltransferase 1), *DGAT1* (diacylglycerol O-acyltransferase), *DGAT2, CD36*, and *FATP4* (fatty acid transport protein 4). Additionally, CGA restored the expression of inflammatory genes, including *TNF-α* (tumor necrosis factor-alpha), *IL-1β (interleukin-1beta), IL-6*, and *IL-10*, and genes encoding antioxidant enzymes, including *SOD1* (superoxide dismutases 1), *SOD2* (superoxide dismutases 2), and *GPX1*

10.3389/fendo.2022.1042044

(glutathione peroxidase 1). Furthermore, CGA improved the bacterial alpha and beta diversity in the cecum. Moreover, CGA recovered the abundance of the phylum Bacteroidetes and the genera *Lactobacillus, Blautia*, and *Enterococcus*.

**Discussion:** CGA can improve the antidiabetic effects, and microbes may critically mediate these beneficial effects.

KEYWORDS

chlorogenic acid, hyperglycemia, hyperlipidemia, inflammation, oxidative stress

# Introduction

Chlorogenic acid (CGA), a member of the hydroxycinnamic acid family, is abundant in many plants, including coffee beans, apples, tea, and tobacco leaves (1). CGA has been proven to be one of the most promising phenolic acids, serving as either a food additive or nutraceutical due to its efficacy in alleviating oxidative stress, the inflammatory response, and glucose and lipid metabolism disorders (1–3). Based on these effects, the use of CGA for treating metabolic syndromes, such as type 2 diabetes mellitus and cardiovascular diseases, has been widely studied (4). Human and animal studies have confirmed that CGA can dramatically lower total cholesterol and total triglyceride levels (5, 6). In overweight patients, taking CGA twice a day can improve blood glucose, insulin sensitivity and other metabolic parameters (7). In high-fat diet (HFD)-fed mice, CGA exerts its protective effect on obesity and related metabolic syndrome by regulating gut microbiota structure, diversity, and changes in relative abundance at the phylum to genus levels (8). AMPK (AMP-activated protein kinase) signaling and gut microbes are involved in the anti-diabetic and anti-lipidemic effects of CGA (9). However, the detailed mechanisms require further investigation.

Gut microbes are considered to be important health regulators, and dietary components are one of the major factors determining the composition of the gut microbiota (10, 11). Approximately 30% of dietary CGA is absorbed in the small intestine (12, 13), indicating that CGA can reach the large intestine and exert direct effects on microbes. Numerous studies have demonstrated the modulatory effects of CGA on the diversity and composition of the microbiota. CGA can decrease the abundance of *Lachnospiraceae*, *Ruminococcaceae*, *Desulfovibrionaceae*, *and Erysipelotrichaceae* and increase that of *Lactobacillaceae* and *Bacteroidaceae* (14). Significantly, CGA improved the abundance of beneficial bacteria, including *Ruminococcaceae UCG-005, Akkermansia*, *Christensenellaceae R-7_group*, and *Rikenellaceae RC9_gut_group* (15) and short-chain fatty acid producers such as *Faecalibaculum*, *Romboutsia*, *Mucispirillum*, and *Dubosiella* (16). Meanwhile, CGA reduced the abundance of bacteria involved in inflammation, such as *Sutterella* species and those that cause intestinal dysfunction, such as *Escherichia coli* and other LPS-producers (17, 18). These changes in microbiota composition, induced by CGA, mediate the positive effects of CGA on metabolic disorders. However, whether CGA administration can recover the microbiota composition of diabetic mice has not been fully determined.

A previous study reported the acute effects of CGA on glucose tolerance (GT), insulin sensitivity (IS), gluconeogenesis, and fatty acid synthesis in $Lepr^{db}$ diabetic (db/db) mice (11). However, whether acute treatment with CGA affects fatty acid oxidation, inflammatory responses, and microbiota composition remains to be explored. Consequently, we investigated the acute effects of CGA on lipid metabolism and the inflammatory and antioxidative status in db/db diabetic mice. Furthermore, the involvement of intestinal microbes in the beneficial effects of CGA has been elucidated

# Materials and methods

## Animal experiments

Eighteen male diabetic db/db mice and six male db/m mice were provided by Gene&Peace Biotech Co., Ltd (Guangzhou, China). The db/db mice were assigned to the following treatment groups: (1) DB group, animals were orally gavaged with 0.1 mL PBS once a day; (2) CA group, animals were gavaged with 0.25 g CGA/kg body weight (BW) once a day; (3) MET, animals were gavaged with 0.25 g metformin/kg BW once a day. The concentration of CGA used was based on our preliminary experiment. The db/m mice were assigned as the control (CON). CGA and metformin were purchased from Sigma (Shanghai, China). The experiment lasted 18 days. All mice had free access to water and feed. Feed intake and BW were recorded during the experiment. Animals were treated humanely, using approved procedures in accordance with the guidelines of Changsha Health Vocational College. The study was approved by the Institutional Animal Care and Use Committee of Changsha Health Vocational College (2021053).

## Oral GT and IS tests

Fasting blood glucose was tested every 7 days, and it was significantly decreased on Day 14 after treatment with CGA or metformin. Then, oral GT and IS tests were performed. After fasting for 6 h, mice were either orally gavaged with a dose of 2.0 g glucose or intraperitoneally injected with a dose of 0.65 U insulin/kg BW. Blood was obtained from the tail vein, and the glucose concentration was analyzed at 0, 30, 60 and 120 min.

## Sample collection

First, blood was obtained from the retro-orbital sinus and serum samples were separated. Then, after cervical dislocation, liver, inguinal and epididymal adipose tissue were separated and weighed. Furthermore, liver samples were either fixed in formaldehyde solution or stored at −80°C for analysis of gene expression. Additionally, cecum content was obtained for the determination of gut microbiota.

## Serum biochemistry assay

The contents of glucose, high-density lipoprotein cholesterol (HDL-C), low-density lipoprotein cholesterol (LDL-C), total cholesterol (TC) and triglycerides (TGs), and the activities of alanine aminotransferase (ALT) and aspartate aminotransferase (AST) were determined by using commercial kits (Meimian, Nantong, China) as previously described (19).

## Hepatic histological and lipid content analyses

Fixed liver samples were paraffin embedded and sectioned into 8-μm thick sections; then, the samples were either subjected to H&E (hematoxylin–eosin) staining for histological observation or Oil Red O staining for the determination of lipid content as previously described (20).

## RT-qPCR

Total RNA was extracted using Trizol reagent (Invitrogen, Shanghai, China) and DNA was removed after treatment with DNase I (Takara, Beijing, China). Then, cDNA was synthesized using a RevertAid Reverse Transcription Kit (Thermo Scientific) as previously described (21). RT-qPCR was carried out by using SYBR Green mix (Applied Biosystems). The primers used for qPCR are shown in Supplementary Table 1.

## Gut microbiota profiling

DNA was extracted with cecum contents, and bacterial 16S rRNA gene sequences (V3–V4 regions) were amplified. PCRs were carried out with Phusion High-Fidelity PCR Master Mix (Thermo Fisher). Then, MiSeq Illumina sequencing was performed with products with a length of 400-450 bp. The Greengenes database with the RDP algorithm was used to analyze representative OTUs.

## Statistical analysis

Statistical analysis was performed using one-way ANOVA with Tukey's *post hoc* test using SPSS 18.0. All data were expressed as the means ± SEM, and significant differences were confirmed when $P < 0.05$.

# Results

## Effects of chlorogenic acid on body weight, feed intake and adipose tissue and liver weight in db/db mice

As shown in Table 1, the BW of db/db diabetic mice was significantly higher than that of db/m mice at the beginning of the experiments. The BW of mice in the CA and MET groups was significantly lower than that in the DB group, whereas it

TABLE 1 Effects of chlorogenic acid on body weight and feed intake in db/db mice.

| | CON | DB | CA | MET |
|---|---|---|---|---|
| Body weight (Day 0), g | 23.50 ± 2.15$^{b}$ | 38.20 ± 0.98$^{a}$ | 39.00 ± 0.80$^{a}$ | 39.00 ± 1.00$^{a}$ |
| Body weight (Day 7), g | 24.00 ± 2.17$^{b}$ | 41.78 ± 0.89$^{a}$ | 40.55 ± 0.82$^{a}$ | 40.48 ± 1.88$^{a}$ |
| Body weight (Day 14), g | 22.55 ± 1.97$^{c}$ | 41.27 ± 0.97$^{a}$ | 38.98 ± 0.70$^{b}$ | 38.63 ± 1.08$^{b}$ |
| Body weight (Day 18), g | 23.33 ± 1.68$^{c}$ | 41.30 ± 1.11$^{a}$ | 37.93 ± 0.65$^{b}$ | 37.90 ± 0.95$^{b}$ |
| Daily feed intake, g | 3.28 ± 0.17$^{c}$ | 5.62 ± 0.31$^{a}$ | 4.69 ± 0.36$^{b}$ | 4.41 ± 0.19$^{b}$ |

$^{a,b,c}$ Groups that share the same superscript letters are not significantly different from each other ($P < 0.05$). Data are expressed as the means ± SEMs, n=6.

10.3389/fendo.2022.1042044

remained significantly higher than that in the CON group on day 7, 14 and 18. Mice in the CA and MET group had lower daily feed intake than those in the DB group, whereas they had higher daily feed intake than those in the CON group. As shown in Table 2, the weights of inguinal fat and liver in mice in the CA and MET groups were significantly lower than those in the DB group, whereas they were significantly higher than those in the CON group. Epididymal fat weight was significantly lower in mice in the CON group than in the other three groups.

TABLE 2 Effects of chlorogenic acid on adipose tissue and liver weight in db/db mice.

| | CON | DB | CA | MET |
|---|---|---|---|---|
| Inguinal fat weight, g | 0.146 ± 0.014$^{c}$ | 1.617 ± 0.062$^{a}$ | 1.239 ± 0.094$^{b}$ | 1.127 ± 0.068$^{b}$ |
| Epididymal fat weight, g | 0.118 ± 0.010$^{b}$ | 1.541 ± 0.053$^{a}$ | 1.43 ± 0.062$^{a}$ | 1.504 ± 0.042$^{a}$ |
| Liver weight, g | 1.087 ± 0.072$^{c}$ | 2.595 ± 0.074$^{a}$ | 2.450 ± 0.072$^{b}$ | 2.407 ± 0.089$^{b}$ |

$^{a,b,c}$ Groups that share the same superscript letters are not significantly different from each other ($P < 0.05$). Data are expressed as the means ± SEMs, n=6.

## Effects of chlorogenic acid on GT and IS in db/db mice

According to Figure 1, either chlorogenic acid or metformin improved GT and IS in db/db mice, whereas all the db/db mice still showed lower GT and IS than the db/m mice.

## Effects of chlorogenic acid on serum biochemical indicators in db/db mice

As shown in Table 3, glucose and TG contents were significantly lower in mice in the CA and MET groups than in the DB group, whereas they were significantly higher than those in the CON group. Compared with those in the DB group, mice in the other three groups had significantly lower TC and LDL-C contents, and higher HDL-C contents. The activities of AST and ALT were significantly lower in mice in the CA and MET groups than in the DB group, whereas they were significantly higher in mice in the CA group than in the CON group.

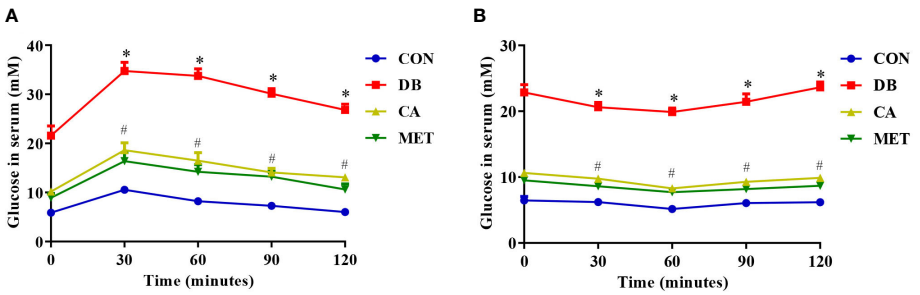


FIGURE 1
Effects of chlorogenic acid on glucose tolerance and insulin resistance in diabetic db/db mice. **(A)** Glucose tolerance; **(B)** Insulin resistance. Data are expressed as the means ± SEMs, n=6. *$P < 0.05$ (significant difference between mice in the DB group and mice in the other groups); #$P < 0.05$ (significant difference between mice in the CON group and mice in the CA and MET groups).

TABLE 3 Effects of chlorogenic acid on serum biochemical indicators in db/db mice.

| Index | CON | DB | CA | MET |
|---|---|---|---|---|
| Glucose, mM | 5.83 ± 0.57$^{c}$ | 23.67 ± 1.09$^{a}$ | 9.45 ± 0.64$^{b}$ | 8.73 ± 0.77$^{b}$ |
| TG, mM | 0.78 ± 0.22$^{c}$ | 2.02 ± 0.34$^{a}$ | 1.23 ± 0.22$^{b}$ | 1.17 ± 0.18$^{b}$ |
| TC, mM | 1.88 ± 0.32$^{b}$ | 5.68 ± 0.35$^{a}$ | 2.13 ± 0.45$^{b}$ | 1.83 ± 0.33$^{b}$ |
| LDL-C, mM | 0.36 ± 0.05$^{c}$ | 1.62 ± 0.11$^{a}$ | 0.56 ± 0.08$^{b}$ | 0.46 ± 0.12$^{bc}$ |
| HDL-C, mM | 2.32 ± 0.14$^{b}$ | 1.65 ± 0.16$^{a}$ | 2.24 ± 0.20$^{b}$ | 2.31 ± 0.15$^{b}$ |
| AST, U/L | 22.6 ± 3.0$^{c}$ | 54.2 ± 4.6$^{a}$ | 28.3 ± 5.8$^{b}$ | 27.5 ± 4.1$^{bc}$ |
| ALT, U/L | 22.7 ± 2.9$^{d}$ | 99.6 ± 8.7$^{a}$ | 43.1 ± 6.3$^{b}$ | 31.7 ± 5.6$^{c}$ |

$^{a,b,c,d}$ Groups that share the same superscript letters are not significantly different from each other ($P < 0.05$). Data are expressed as the means ± SEMs, n=6.

## Effects of chlorogenic acid on hepatic morphology and lipid content in db/db mice

According to Figure 2, H&E staining showed that liver morphology was significantly damaged (microvesicular fatty change) in db/db diabetic mice, whereas the administration of chlorogenic acid and metformin both alleviated the impairment, although the morphology was still not returned to normal. Oil red O staining showed that db/db diabetic mice had higher lipid accumulation in the liver, whereas the administration of chlorogenic acid and metformin both decreased hepatic lipid accumulation.

## Effects of chlorogenic acid on expression of lipid metabolism-related genes in live db/db mice

The expression of genes including *CPT1a*, *ACOX1* (Figure 3A), *ATGL* and *HSL* (Figure 3B) was significantly

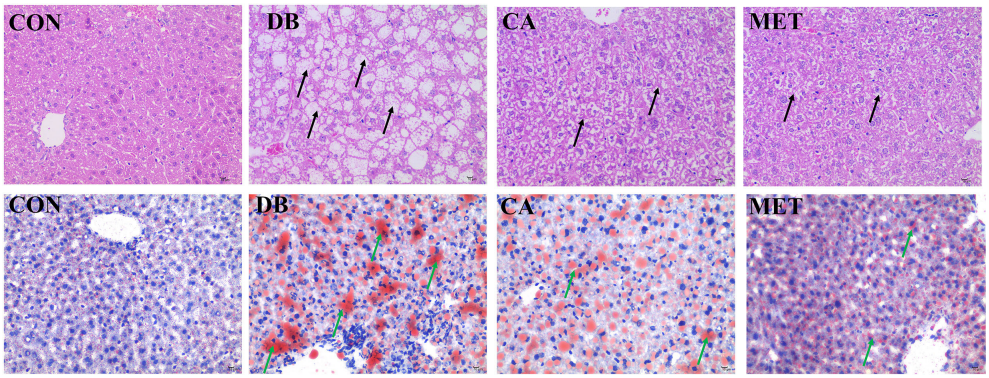


FIGURE 2
Effects of chlorogenic acid on liver morphology and lipid accumulation in diabetic db/db mice. Upper panel, representative results of H&E staining (400×); Lower panel, representative results of Oil red O staining (400×). Black arrows, damaged hepatocytes; green arrows, lipid droplets.

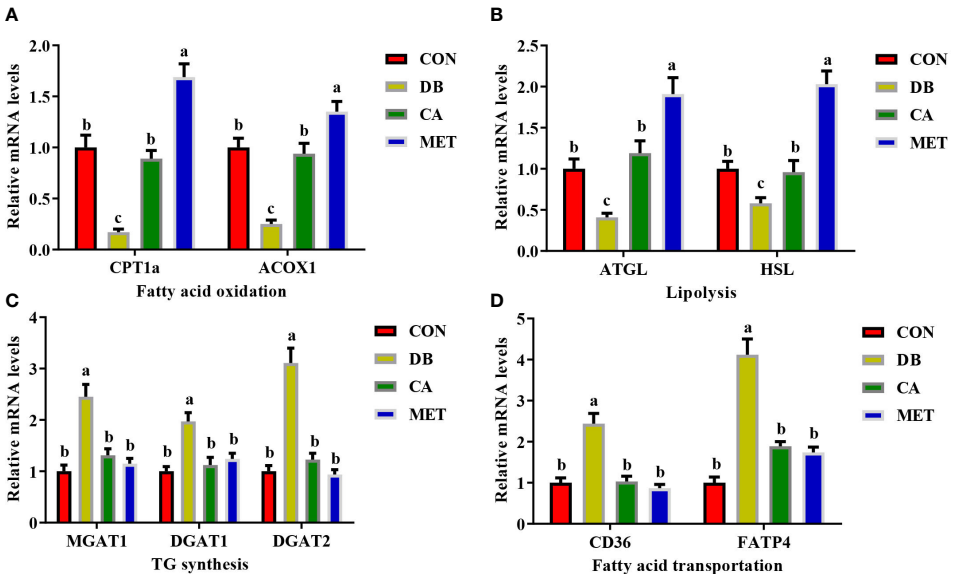


FIGURE 3
Effects of chlorogenic acid on the expression of genes involved in lipid metabolism in the livers of diabetic db/db mice. **(A)** Expression of genes involved in fatty acid oxidation; **(B)** Expression of genes involved in lipolysis; **(C)** Expression of genes involved in TG synthesis; **(D)** Expression of genes involved in fatty acid transportation. Data are expressed as the means ± SEMs, n=6. $^{a,b,c}$ Groups that share the same superscript letters are not significantly different from each other ($P < 0.05$).

lower in mice in the CON and CA groups than in the MET group, whereas they were significantly higher than those in the DB group. Compared with mice in the DB group, mice in the other three groups had significantly lower expression of genes involved in TG synthesis (*MGAT1*, *DGAT1* and *DGAT2*) (Figure 3C) and fatty acid transport (*CD36* and *FATP4*) (Figure 3D).

## Effects of chlorogenic acid on the expression of inflammation- and antioxidant ability-related genes in live db/db mice

Compared with mice in the DB group, mice in the other three groups had significantly lower expression of genes (*IL-1β*, *TNF-α* and *IL-6*) encoding proinflammatory cytokines and higher expression of the *IL10* gene encoding an anti-inflammatory cytokine (Figure 4A). Compared with mice in the DB group, mice in the other three groups had significantly higher expression of genes including *SOD1*, *SOD2* and *GPX1* (Figure 4B).

## Effects of chlorogenic acid on cecal microbiota composition in db/db mice

The alpha diversity of the microbial community, as indicated by the Shannon and Simpson index (Figures 5A, B), was significantly higher in mice in the CA and MET groups than in the DB group, whereas there was no significant difference among mice in the CA, MET and CON groups. Principal coordinates analysis (PCoA) showed that mice in the DB group were clearly separated from those in the other treatment groups (Figure 5C). Firmicutes, Proteobacteria and Bacteroidetes were the most abundant microbes at the phylum- level (Figure 5D). Compared with mice in the other groups, Bacteroidetes abundance was lower while Proteobacteria abundance was higher in mice of the DB group. Compared with mice in the other groups, *Lactobacillus* abundance at a genus-level taxonomy was lower while *Blautia*, *Robinsoniella* and *Enterococcus* abundance were higher in mice of the DB group (Figure 5E).

# Discussion

Db/db mice are commonly used models for studying diabetes. Chronic administration of a relatively low CGA concentration or acute administration of a high concentration in db/db mice improved GT and IS (22, 23). In the present study, CGA alleviated hyperglycemia, and hyperlipidemia and decreased hepatic lipid overaccumulation in db/db mice. Moreover, our results suggest that CGA alleviates the inflammatory response and enhances antioxidant activity. Furthermore, CGA improved microbiota diversity and recovered their composition in the cecum of db/db mice.

CGA can decrease lipid accumulation in obese individuals. In the present study, short-term administration of CGA reduced body weight, adipose tissue, and liver weight in db/db mice, although their weight was not comparable to that of control db/m mice. Previous studies have focused on the effects of CGA on gluconeogenesis and fatty acid synthesis (24–26), while our results suggest that CGA enhances hepatic lipolysis and reduces TG synthesis and fatty acid transportation in the liver of db/db mice. In addition, CGA improved the expression of genes involved in hepatic lipid metabolism in high-fat diet (HFD)-fed mice (27). These results suggest that CGA improves hepatic lipid metabolism in animal models of lipid metabolic disorders. Hepatic lipid overaccumulation is usually

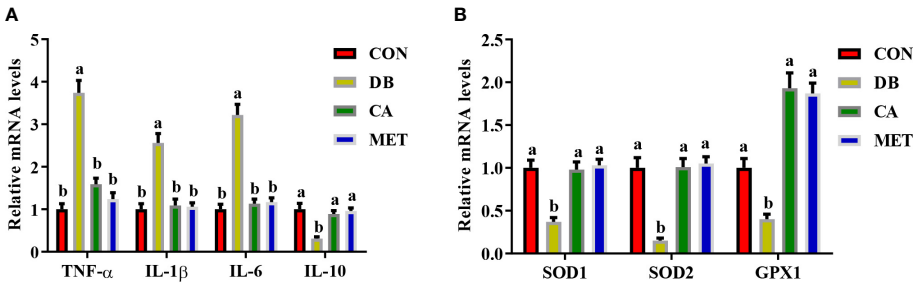


FIGURE 4
Effects of chlorogenic acid on the expression of genes encoding inflammatory cytokines and antioxidant enzymes in the livers of diabetic db/db mice. **(A)** Expression of genes encoding inflammatory cytokines; **(B)** Expression of genes encoding antioxidant enzymes. Data are expressed as the means ± SEMs, n=6. $^{a,b}$ Groups that share the same superscript letters are not significantly different from each other ($P < 0.05$).

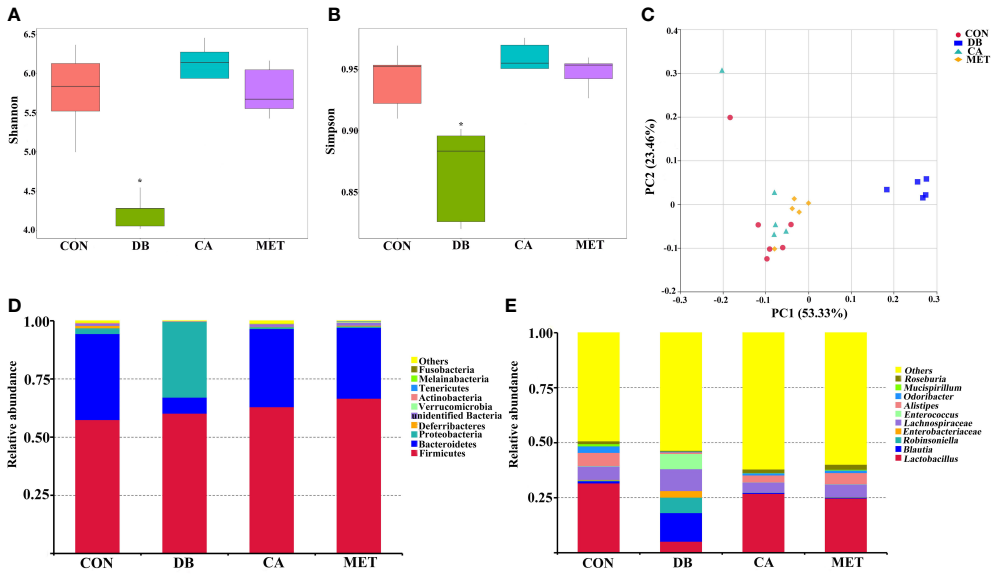


FIGURE 5
Effects of chlorogenic acid on cecal microbe composition in diabetic db/db mice. **(A)** Shannon index; **(B)** Simpson index; **(C)** PCoA plot of the microbiota based on an unweighted UniFrac metric; **(D)** Relative abundance of predominant bacteria at the phylum level; **(E)** Relative abundance of predominant bacteria at the genus level. *$P < 0.05$ (significant difference between mice in the DB group and mice in the other groups).

associated with activated inflammatory responses (28–30). Our results suggest that CGA alleviates inflammation, similar to a previous study in mice with HFD-induced obesity (31). HFD resulted in an imbalance in the oxidative status, which always accompanied by inflammation, and CGA administration recovered the antioxidant status in rats. The results confirmed the antioxidative ability of CGA, as indicated by the increased expression of genes encoding enzymes such as SOD and GPX (32, 33). Although our results showed the anti-inflammatory and anti-lipidemic effects of CGA in db/db mice, the specific targets of CGA and the possible signaling pathways that regulate the alteration in inflammation and lipid metabolism remain to be explored.

The gut microbiota can influence the differentiation and apoptosis of intestinal epithelial cells and positive regulation of the gut microbiota is conducive to alleviating metabolic syndromes (34–36). Some short-chain fatty acids among the metabolites of gut microbiota are capable of improving diet-induced obesity and insulin resistance (37). Several studies have demonstrated that the beneficial role of CGA is positively related to gut microbiota regulation (18, 38). For instance, CGA could increase the contents of *Bifidobacterium* and reduce *Escherichia coli* in NAFLD mice (17). CGA also exerts its antiobesity effects by ameliorating HFD-induced gut microbiota dysbiosis by inhibiting the growth of Desulfovibrionaceae, Ruminococcaceae, Lachnospiraceae, and Erysipelotrichaceae, and raising the growth of Bacteroidaceae, Lactobacill*aceae* (14, 39). However, studies have also demonstrated that CGA- treated mice showed microbial structures similar to those of the control group (40–43). According to these sudies and our results, we speculated that CGA could regulate gut microbiota structure under different pathological conditions in different ways. In our study, we found that CGA or metformin increased the α-diversity of the gut microbiota in db/db mice. Additionally, the β-diversity, as indicated by the PCoA, showed that mice administered CGA or metformin were similar to control mice but different from untreated db/db mice. These effects of CGA on the improvement of gut microbiota diversity were consistent with previous results using different models (44, 45). HFD-induced obesity and glucose and lipid metabolism disorders are often accompanied by increased abundance of Firmicutes and decreased abundance of Bacteroidetes and Proteobacteria (16). However, our results only showed similar results that Bacteroidetes abundance was decreased, whereas Firmicutes abundance was not changed and Proteobacteria abundance was increased in db/db mice. Another study showed that db/db mice did not show the alterations mentioned above when compared to wild-type m/m mice (46). These results suggest that different models of diabetic mice exhibit inconsistent changes in microbiota composition. Nevertheless, CGA restored the structure of the gut microbiota, and these effects were similar to those of metformin.

The most significant change at the genus level after CGA administration was the recovery of *Lactobacillus* abundance. This result suggested that CGA exerted beneficial effects, as most *Lactobacillus* species are considered to be beneficial microbes (47, 48). Surprisingly, *Blautia* abundance significantly increased in db/db mice, whereas CGA administration reduced this abundance. *Blautia* is a functional genus with probiotic properties, including improved metabolic function and host health (49). We speculated that the recovery of *Blautia* abundance by CGA could be an indirect effect and that *Blautia* may not be the critical genus mediating the beneficial effects of CGA. However, the underlying mechanisms need to be elucidated further. Additionally, the abundance of *Robinsoniella*, a spore-forming genus, was significantly increased in db/db mice, whereas CGA administration restored it. Alterations in the abundance of *Robinsoniella* are responsible for causing diseases such as nonalcoholic fatty liver and colitis (50, 51), indicating its role in lipid metabolism and inflammation. CGA administration notably decreased the abundance of *Enterococcus*, an important pathogen, when it reached a high density (24). These results indicate the modulatory effects of CGA on dysbiosis of the intestinal microbiota in diabetic db/db mice. However, the changes in microbes that contribute to the beneficial effects of CGA, especially the lipid-lowering effects, need to be further elucidated.

In conclusion, our results suggest that the acute administration of CGA improves GT and IS in diabetic db/db mice. CGA improved lipid metabolism by enhancing fatty acid oxidation and TG lipolysis and reducing TG synthesis and fatty acid transportation in the liver. Moreover, CGA alleviated the hepatic inflammatory response and oxidative stress. Significantly, CGA improved the diversity of the microbiota and promoted the recovery of microbiota composition. These data suggest that acute CGA treatment aids the anti-diabetic effect, and microbes may mediate these effects. Our results indicate that gut microbial alterations should be carefully monitored during the use of CGA in metabolic syndromes.

## Data availability statement

The data presented in the study are deposited in the NCBI repository, accession number PRJNA891362.

## Ethics statement

The animal study was reviewed and approved by Institutional Animal Care and Use Committee of Changsha Health Vocational College.

## Author contributions

YY and XZ designed the experiments. YY, QL, LS and KG performed the experiments, analyzed the data, and drafted the manuscript. XZ revised the manuscript. All authors contributed to the article and approved the submitted version.

## Funding

This work was supported by the Changsha Municipal Natural Science Foundation (grant number kq2014029) and Natural Science Foundation of Hunan Province (2022JJ60111).

## Conflict of interest

The authors declare that the research was conducted in the absence of any commercial or financial relationships that could be construed as a potential conflict of interest.

## Publisher's note



## Supplementary material

The Supplementary Material for this article can be found online at: https://www.frontiersin.org/articles/10.3389/fendo.2022.1042044/full#supplementary-material

SUPPLEMENTARY TABLE 1
Primer sequences. The table provided the sequences of primers used for RT-qPCR analysis.

# References


1. Miao M, Xiang L. Pharmacological action and potential targets of chlorogenic acid. *Adv Pharmacol* (2020) 87:71–88. doi: 10.1016/bs.apha.2019.12.002

2. Pimpley V, Patil S, Srinivasan K, Desai N, Murthy PS. The chemistry of chlorogenic acid from green coffee and its role in attenuation of obesity and diabetes. *Prep Biochem Biotechnol* (2020) 50(10):969–78. doi: 10.1080/10826068.2020.1786699

3. Yan Y, Zhou X, Guo K, Zhou F, Yang H. Use of chlorogenic acid against diabetes mellitus and its complications. *J Immunol Res* (2020) 2020:9680508. doi: 10.1155/2020/9680508

4. Santana-Gálvez J, Cisneros-Zevallos L, Jacobo-Velázquez DA. Chlorogenic acid: Recent advances on its dual role as a food additive and a nutraceutical against metabolic syndrome. *Molecules* (2017) 22(3):358. doi: 10.3390/molecules22030358

5. Rodriguez de Sotillo DV, Hadley M. Chlorogenic acid modifies plasma and liver concentrations of: Cholesterol, triacylglycerol, and minerals in (Fa/Fa) zucker rats. *J Nutr Biochem* (2002) 13(12):717–26. doi: 10.1016/s0955-2863(02)00231-0

6. Xu M, Yang L, Zhu Y, Liao M, Chu L, Li X, et al. Collaborative effects of chlorogenic acid and caffeine on lipid metabolism *via* the AMPKα-LXRα/SREBP-1c pathway in high-fat diet-induced obese mice. *Food Funct* (2019) 10(11):7489–97. doi: 10.1039/c9fo00502a

7. Rondanelli M, Riva A, Petrangolini G, Allegrini P, Bernardinelli L, Fazia T, et al. The metabolic effects of cynara supplementation in overweight and obese class I subjects with newly detected impaired fasting glycemia: A double-blind, placebo-controlled, randomized clinical trial. *Nutrients* (2020) 12(11):3298. doi: 10.3390/nu12113298

8. Ye X, Liu Y, Hu J, Gao Y, Ma Y, Wen D. Chlorogenic acid-induced gut microbiota improves metabolic endotoxemia. *Front Endocrinol (Lausanne)* (2021) 12:762691. doi: 10.3389/fendo.2021.762691

9. Ong KW, Hsu A, Tan BK. Anti-diabetic and anti-lipidemic effects of chlorogenic acid are mediated by ampk activation. *Biochem Pharmacol* (2013) 85 (9):1341–51. doi: 10.1016/j.bcp.2013.02.008

10. Shao H, Zhang C, Xiao N, Tan Z. Gut microbiota characteristics in mice with antibiotic-associated diarrhea. *BMC Microbiol* (2020) 20(1):313. doi: 10.1186/s12866-020-01999-x

11. Long CX, Wu JQ, Tan ZJ. Intestinal microbiota disturbance affects the occurrence of African swine fever. *Anim Biotechnol* (2021) 7:1–10. doi: 10.1080/10495398.2021.2010089

12. Gonthier MP, Verny MA, Besson C, Remesy C, Scalbert A. Chlorogenic acid bioavailability largely depends on its metabolism by the gut microflora in rats. *J Nutr* (2003) 133(6):1853–9. doi: 10.1093/jn/133.6.1853

13. Zhang X, Zhao Q, Ci X, Chen S, Xie Z, Li H, et al. Evaluation of the efficacy of chlorogenic acid in reducing small intestine injury, oxidative stress, and inflammation in chickens challenged with clostridium perfringens type a. *Poult Sci* (2020) 99(12):6606–18. doi: 10.1016/j.psj.2020.09.082

14. Wang Z, Lam KL, Hu J, Ge S, Zhou A, Zheng B, et al. Chlorogenic acid alleviates obesity and modulates gut microbiota in high-Fat-Fed mice. *Food Sci Nutr* (2019) 7(2):579–88. doi: 10.1002/fsn3.868

15. Chen F, Zhang H, Zhao N, Yang X, Du E, Huang S, et al. Effect of chlorogenic acid on intestinal inflammation, antioxidant status, and microbial community of young hens challenged with acute heat stress. *Anim Sci J* (2021) 92 (1):e13619. doi: 10.1111/asj.13619

16. Zhang XY, Chen J, Yi K, Peng L, Xie J, Gou X, et al. Phlorizin ameliorates obesity-associated endotoxemia and insulin resistance in high-fat diet-fed mice by targeting the gut microbiota and intestinal barrier integrity. *Gut Microbes* (2020) 12 (1):1–18. doi: 10.1080/19490976.2020.1842990

17. Shi A, Li T, Zheng Y, Song Y, Wang H, Wang N, et al. Chlorogenic acid improves NAFLD by regulating gut microbiota and GLP-1. *Front Pharmacol* (2021) 12:693048. doi: 10.3389/fphar.2021.693048

18. Yan Y, Zhou X, Guo K, Zhou F, Yang H. Chlorogenic acid protects against indomethacin-induced inflammation and mucosa damage by decreasing bacteroides-derived LPS. *Front Immunol* (2020) 11:1125. doi: 10.3389/fimmu.2020.01125

19. Zhou X, He L, Wu C, Zhang Y, Wu X, Yin Y. Serine alleviates oxidative stress *via* supporting glutathione synthesis and methionine cycle in mice. *Mol Nutr Food Res* (2017) 61(11):1700262. doi: 10.1002/mnfr.201700262

20. Zhou X, Liu Y, Xiong X, Chen J, Tang W, He L, et al. Intestinal accumulation of microbiota-produced succinate caused by loss of micrornas leads to diarrhea in weanling piglets. *Gut Microbes* (2022) 14(1):2091369. doi: 10.1080/19490976.2022.2091369

21. Zhou X, Liu Y, Zhang L, Kong X, Li F. Serine-to-Glycine ratios in low-protein diets regulate intramuscular fat by affecting lipid metabolism and myofiber type transition in the skeletal muscle of growing-finishing pigs. *Anim Nutr* (2021) 7 (2):384–92. doi: 10.1016/j.aninu.2020.08.011

22. Chen L, Teng H, Cao H. Chlorogenic acid and caffeic acid from sonchus oleraceus Linn synergistically attenuate insulin resistance and modulate glucose uptake in Hepg2 cells. *Food Chem Toxicol* (2019) 127:182–7. doi: 10.1016/j.fct.2019.03.038

23. Zuñiga LY, Aceves-de la Mora MCA, González-Ortiz M, Ramos-Núñez JL, Martínez-Abundis E. Effect of chlorogenic acid administration on glycemic control, insulin secretion, and insulin sensitivity in patients with impaired glucose tolerance. *J Med Food* (2018) 21(5):469–73. doi: 10.1089/jmf.2017.0110

24. Chen L, Lin X, Fan X, Qian Y, Lv Q, Teng H. Sonchus oleraceus Linn extract enhanced glucose homeostasis through the AMPK/Akt/ GSK-3β signaling pathway in diabetic liver and Hepg2 cell culture. *Food Chem Toxicol* (2020) 136:111072. doi: 10.1016/j.fct.2019

25. Tajik N, Tajik M, Mack I, Enck P. The potential effects of chlorogenic acid, the main phenolic components in coffee, on health: A comprehensive review of the literature. *Eur J Nutr* (2017) 56(7):2215–44. doi: 10.1007/s00394-017-1379-1

26. Cejas JP, Rosa AS, Nazareno MA, Disalvo EA, Frias MA. Interaction of chlorogenic acid with model lipid membranes and its influence on antiradical activity. *Biochim Biophys Acta Biomembr* (2021) 1863(1):183484. doi: 10.1016/j.bbamem.2020.183484

27. Xu M, Yang L, Zhu Y, Liao M, Chu L, Li X, et al. Collaborative effects of chlorogenic acid and caffeine on lipid metabolism *via* the ampkalpha-Lxralpha/SREBP-1c pathway in high-fat diet-induced obese mice. *Food Funct* (2019) 10 (11):7489–97. doi: 10.1039/c9fo00502a

28. Asrih M, Jornayvaz FR. Inflammation as a potential link between nonalcoholic fatty liver disease and insulin resistance. *J Endocrinol* (2013) 218 (3):R25–36. doi: 10.1530/JOE-13-0201

29. Le YJ, He LY, Li S, Xiong CJ, Lu CH, Yang XY. Chlorogenic acid exerts antibacterial effects by affecting lipid metabolism and scavenging ROS in streptococcus pyogenes. *FEMS Microbiol Lett* (2022) 369(1):fnac061. doi: 10.1093/femsle/fnac061

30. Xu W, Luo T, Chai J, Jing P, Xiong L. Chlorogenic acid alleviates the inflammatory stress of LPS-induced BV2 cell *via* interacting with TLR4-mediated downstream pathway. *Comput Math Methods Med* (2022) 2022:6282167. doi: 10.1155/2022/6282167

31. Zamani-Garmsiri F, Ghasempour G, Aliabadi M, Hashemnia SMR, Emamgholipour S, Meshkani R. Combination of metformin and chlorogenic acid attenuates hepatic steatosis and inflammation in high-fat diet fed mice. *IUBMB Life* (2021) 73(1):252–63. doi: 10.1002/iub.2424

32. Budryn G, Zaczynska D, Zyzelewicz D, Grzelczyk J, Zdunczyk Z, Juskiewicz J. Influence of the form of administration of chlorogenic acids on oxidative stress induced by high fat diet in rats. *Plant Foods Hum Nutr* (2017) 72(2):184–91. doi: 10.1007/s11130-017-0608-3

33. Hermawati E, Arfian N, Mustofa M, Partadiredja G. Chlorogenic acid ameliorates memory loss and hippocampal cell death after transient global ischemia. *Eur J Neurosci* (2020) 51(2):651–69. doi: 10.1111/ejn.14556

34. Demidova TY, Lobanova KG, Oinotkinova OS. Gut microbiota is a factor of risk for obesity and type 2 diabetes. *Ter Arkh* (2020) 92(10):97–104. doi: 10.26442/00403660.2020.10.000778

35. Zhang C, Shao H, Li D, Xiao N, Tan Z. Role of tryptophan-metabolizing microbiota in mice diarrhea caused by folium sennae extracts. *BMC Microbiol* (2020) 20(1):185. doi: 10.1186/s12866-020-01864-x

36. Li X, Peng X, Guo K, Tan Z. Bacterial diversity in intestinal mucosa of mice fed with dendrobium officinale and high-fat diet. *Biotech* (2021) 11(1):22. doi: 10.1007/s13205-020-02558-x

37. Jiao A, Yu B, He J, Yu J, Zheng P, Luo Y, et al. Short chain fatty acids could prevent fat deposition in pigs *via* regulating related hormones and genes. *Food Funct* (2020) 11(2):1845–55. doi: 10.1039/c9fo02585e

38. Song J, Zhou N, Ma W, Gu X, Chen B, Zeng Y, et al. Modulation of gut microbiota by chlorogenic acid pretreatment on rats with adrenocorticotropic hormone induced depression-like behavior. *Food Funct* (2019) 10(5):2947–57. doi: 10.1039/c8fo02599a

39. Parkar SG, Trower TM, Stevenson DE. Fecal microbial metabolism of polyphenols and its effects on human gut microbiota. *Anaerobe* (2013) 23:12–9. doi: 10.1016/j.anaerobe.2013.07.009

40. He X, Zheng S, Sheng Y, Miao T, Xu J, Xu W, et al. Chlorogenic acid ameliorates obesity by preventing energy balance shift in high-fat diet induced obese mice. *J Sci Food Agric* (2021) 101(2):631–7. doi: 10.1002/jsfa.10675

41. Bambha K, Wilson LA, Unalp A, Loomba R, Neuschwander-Tetri BA, Brunt EM, et al. Coffee consumption in NAFLD patients with lower insulin resistance is associated with lower risk of severe fibrosis. *Liver Int* (2014) 34 (8):1250–8. doi: 10.1111/liv.12379

42. Wijarnpreecha K, Thongprayoon C, Ungprasert P. Coffee consumption and risk of nonalcoholic fatty liver disease: A systematic review and meta-analysis. *Eur J Gastroenterol Hepatol* (2017) 29(2):e8–e12. doi: 10.1097/MEG.0000000000000776

43. Sewter R, Heaney S, Patterson A. Coffee consumption and the progression of NAFLD: A systematic review. *Nutrients* (2021) 13(7):2381. doi: 10.3390/nu13072381

44. Wu Y, Liu W, Li Q, Li Y, Yan Y, Huang F, et al. Dietary chlorogenic acid regulates gut microbiota, serum-free amino acids and colonic serotonin levels in growing pigs. *Int J Food Sci Nutr* (2018) 69(5):566–73. doi: 10.1080/09637486.2017.1394449

45. Bhandarkar NS, Brown L, Panchal SK. Chlorogenic acid attenuates high-carbohydrate, high-fat diet-induced cardiovascular, liver, and metabolic changes in rats. *Nutr Res* (2019) 62:78–88. doi: 10.1016/j.nutres.2018.11.002

46. Yu F, Han W, Zhan G, Li S, Jiang X, Wang L, et al. Abnormal gut microbiota composition contributes to the development of type 2 diabetes mellitus in Db/Db mice. *Aging (Albany NY)* (2019) 11(22):10454–67. doi: 10.18632/aging.102469

47. Goldstein EJ, Tyrrell KL, Citron DM. Lactobacillus species: Taxonomic complexity and controversial susceptibilities. *Clin Infect Dis* (2015) 60 Suppl 2:S98–107. doi: 10.1093/cid/civ072

48. He L, Zhou X, Liu Y, Zhou L, Li F. Fecal mir-142a-3p from dextran sulfate sodium-challenge recovered mice prevents colitis by promoting the growth of lactobacillus reuteri. *Mol Ther* (2022) 30(1):388–99. doi: 10.1016/j.ymthe.2021.08.02

49. Liu X, Mao B, Gu J, Wu J, Cui S, Wang G, et al. Blautia-a new functional genus with potential probiotic properties? *Gut Microbes* (2021) 13(1):1–21. doi: 10.1080/19490976.2021.1875796

50. Raman M, Ahmed I, Gillevet PM, Probert CS, Ratcliffe NM, Smith S, et al. Fecal microbiome and volatile organic compound metabolome in obese humans with nonalcoholic fatty liver disease. *Clin Gastroenterol Hepatol* (2013) 11(7):868–75.e1-3. doi: 10.1016/j.cgh.2013.02.015

51. Wohlgemuth S, Keller S, Kertscher R, Stadion M, Haller D, Kisling S, et al. Intestinal steroid profiles and microbiota composition in colitic mice. *Gut Microbes* (2011) 2(3):159–66. doi: 10.4161/gmic.2.3.16104

frontiers | Frontiers in Endocrinology

TYPE Review
PUBLISHED 18 November 2022
DOI 10.3389/fendo.2022.1074348



OPEN ACCESS

EDITED BY
Zhoujin Tan,
Hunan University of Chinese Medicine, China

REVIEWED BY
Xiangyang Xie,
Tianjin Medical University, China
Liang Qiu,
Jiangxi University of Traditional Chinese Medicine, China

*CORRESPONDENCE
Fuer Lu
felutjh88@163.com
Dingkun Wang
wdkung@163.com

SPECIALTY SECTION
This article was submitted to Gut Endocrinology, a section of the journal Frontiers in Endocrinology

RECEIVED 19 October 2022
ACCEPTED 07 November 2022
PUBLISHED 18 November 2022

CITATION
He Q, Dong H, Guo Y, Gong M, Xia Q, Lu F and Wang D (2022) Multi-target regulation of intestinal microbiota by berberine to improve type 2 diabetes mellitus.
*Front. Endocrinol.* 13:1074348.
doi: 10.3389/fendo.2022.1074348



# Multi-target regulation of intestinal microbiota by berberine to improve type 2 diabetes mellitus

Qiongyao He[1], Hui Dong[1], Yujin Guo[1], Minmin Gong[1], Qingsong Xia[1], Fuer Lu[2]* and Dingkun Wang[2]*

[1]Institute of Integrated Traditional Chinese and Western Medicine, Tongji Hospital, Tongji Medical College, Huazhong University of Science and Technology, Wuhan, Hubei, China, [2]Department of Integrated Traditional Chinese and Western Medicine, Tongji Medical College, Tongji Hospital, Huazhong University of Science and Technology, Wuhan, Hubei, China

Type 2 diabetes mellitus (T2DM) and its complications are major public health problems that seriously affect the quality of human life. The modification of intestinal microbiota has been widely recognized for the management of diabetes. The relationship between T2DM, intestinal microbiota, and active ingredient berberine (BBR) in intestinal microbiota was reviewed in this paper. First of all, the richness and functional changes of intestinal microbiota disrupt the intestinal environment through the destruction of the intestinal barrier and fermentation/degradation of pathogenic/protective metabolites, targeting the liver, pancreas, visceral adipose tissue (VAT), etc., to affect intestinal health, blood glucose, and lipids, insulin resistance and inflammation. Then, we focus on BBR, which protects the composition of intestinal microbiota, the changes of intestinal metabolites, and immune regulation disorder of the intestinal environment as the therapeutic mechanism as well as its current clinical trials. Further research can analyze the mechanism network of BBR to exert its therapeutic effect according to its multi-target compound action, to provide a theoretical basis for the use of different phytochemical components alone or in combination to prevent and treat T2DM or other metabolic diseases by regulating intestinal microbiota.

KEYWORDS

**BBR, T2DM, intestinal microbiota, microbial metabolites, metabolic diseases**

10.3389/fendo.2022.1074348

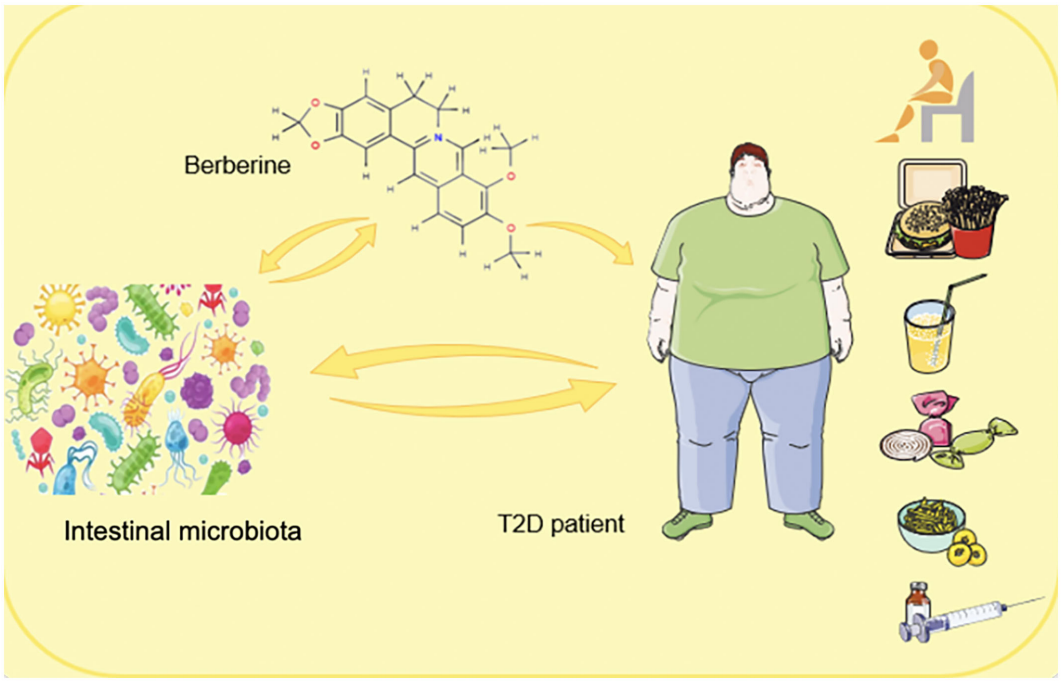


GRAPHICAL ABSTRACT

# 1 Introduction

Diabetes mellitus (DM) is a group of metabolic diseases characterized by hyperglycemia, caused by deficiencies in insulin secretion and/or insulin action (1). In the past few decades, great changes have taken place in human lifestyles around the world. Reducing the level of physical activity and increasing animal food consumption and dietary fat intake make the incidence of T2DM more favorable (2–4). There were about 537 million adults with DM worldwide in 2021 and it is expected to reach 784 million by 2045 (5). DM has brought profound psychological and physical troubles to patients and is related to several serious complications, which have aroused great concern all over the world (6, 7).

The human intestinal tract is a bioreactor with microbiota, containing hundreds or thousands of bacterial groups (8). Most bacteria belong to six well-known bacteria/phyla: Phaeophyta, Bacteroides, Proteus, Actinomycetes, Clostridium, and Verruca, of which Phaeophyta and Bacteroides account for 60-90% of the alliance (8). It is an organism that coevolved with its human host and has more than 500 times as many genes (9). Evidence shows that intestinal microbiota is associated with obesity and obesity-related complications such as T2DM and non-alcoholic fatty liver disease (NAFLD) (10). Many early classic fecal transplantation experiments have shown that intestinal microbiota plays an important role in energy acquisition, VAT accumulation, and insulin resistance (11, 12).

Current treatment of T2DM includes lifestyle intervention, a balanced diet, proper exercise, and medication (13). In recent years, great progress has been made in the use of biguanides and sulfonylureas, but these hypoglycemic drugs still have some limitations due to adverse reactions (14–16). Therefore, attempts to find the treatment of metabolic diseases from natural products have been carried out one after another. Many studies have reported that BBR has obvious effects of reducing blood glucose and lipids, simultaneously anti-obesity and inflammation (17–19). Therefore, it is considered to be one of the most promising natural drugs for the treatment of T2DM. The purpose of this review is to clarify the relationship between T2DM, intestinal microbiota, and BBR, and to deepen the understanding of the mechanism by which BBR plays a role in the treatment of metabolic diseases. It may be helpful for future clinical use of BBR monomers or related formulations to manage T2DM and its complications by regulating intestinal microbiota.

# 2 Effect of Intestinal environment changes on T2DM

## 2.1 Changes in the richness of intestinal microbiota

The composition of intestinal microbiota is determined by the complex interaction of host heredity, diet, (congenital)

immune factors, intestinal environment, and interspecific competition (20). The composition of intestinal microbiota is unique to everyone (21). Due to the high acidity and oxygen content of the stomach and duodenum, the microbial composition changes along the gastrointestinal tract (21). The stomach and small intestine are rich in *Firmicutes* (*Lactobacillaceae*) and *Proteobacteria* (*Enterobacteriaceae*), whereas the large intestine shows a higher portion of *Bacteroidetes* (*Bacteroidaceae*, Prevotellaceae, and *Rikenellaceae*) and *Firmicutes* (*Lachnospiraceae* and *Ruminococcaceae*) (21). The proximal intestinal microbiota produces metabolites such as short-chain fatty acids (SCFAs) and succinic acid by fermenting dietary fiber, which can prevent obesity by increasing energy consumption, promoting anorexia hormone production, slowing gastrointestinal movement, and improving appetite regulation. The distal intestinal microbiota mainly degrades peptides and proteins to produce ammonia, phenols, and branched chain fatty acids by hydrolysis and fermentation, which are harmful to the intestinal and metabolic health of the host (22). In healthy individuals, the composition of intestinal microbiota is abundant, while the diversity of obese and T2DM patients is reduced (23). Two large meta-genomes in China and Europe were used to study the structural characteristics of intestinal microbiota in T2DM patients and healthy people (24–26). It was found that the bacteria rich in T2DM patients were mainly conditional pathogenic bacteria, such as *Escherichia coli*, *Clostridium*, and *Carbella*, etc., while the richness of SCFAs-producing bacteria such as *Enterobacter*, *Clostridium, SS3/4*, *Pseudomonas* and *Rosmarinus* decreased (25).

### 2.1.1 *Akkermansia muciniphila*

Among many bacteria, *Akkermansia muciniphila* (*A.muciniphila*) has been proposed as a new marker of intestinal health because it is a key bacteria at the mucosal interface between the lumen and host cells and plays a very important role in the regulation of a series of metabolic diseases. *A.muciniphila* is a kind of mucus-degrading bacteria, which exists in the mucus layer and can stimulate the production of mucin in the host, thus strengthening the integrity of the epithelial layer. Studies have shown that *A.muciniphila* abundance decreases in obese and T2DM mice, while feeding normalizes *A.muciniphila* can reverse metabolic disorders caused by a high-fat diet (27). In a randomized, double-blind, placebo-controlled, single-center prospective clinical study, daily oral administration of $10^{10}$ A.*muciniphila*, both alive and pasteurized for three months, was safe and well tolerated. Compared with placebo, pasteurization *A.muciniphila* increased insulin sensitivity, and reduced insulinemia and plasma total cholesterol (28). Amuc1100 is a specific protein isolated from the outer membrane of *A.muciniphila*, which interacts with Toll-like receptor (TLR)2 to play an immunomodulatory role *in vivo* and *in vitro*, and improves the intestinal barrier function (29). Reduced *A.muciniphila* can be considered as a biomarker of individuals with prediabetes (30) and can be used for early diagnosis of T2DM before the clinical attack, which will help to promote microbial-mediated early intervention (31).

## 2.2 The changes of metabolites derived from intestinal microbiota

### 2.2.1 SCFAs

*Butyrivibrio, Bifidobacterium bifidum, Megasphaera*, and *Prevotella* can produce SCFAs through the digestion of fibrous polysaccharides, including acetate, propionate, butyrate, etc. (32). SCFAs are an important energy source of colon cells and are related to the improvement of heat production and calorie intake (32). SCFAs play a key role in the homeostasis of glucose metabolism by reducing the oxidative stress of β-cell, increasing insulin release, and reducing the expression of proinflammatory cytokines and anti-lipolysis (33–36). In addition, SCFAs play another potential role in the treatment of T2DM through intestinal gluconeogenesis (IGN). Compared with hepatic gluconeogenesis, IGN accounts for only about 20-25% of total endogenous glucose production during fasting (37), and it may be related to the improvement of glucose homeostasis and the reduction of T2DM risk (38). The glucose produced by the intestine is sent to the portal vein, and the peripheral nervous system in the wall of the portal vein can sense glucose and send signals to the brain to regulate energy and glucose metabolism (37). Propionate and butyrate are typical representatives of SCFAs. Propionate can be used as the substrate of IGN to activate the expression of the IGN gene (free fatty acid receptor FFAR3) through the intracerebral neural circuit, and butyrate can directly stimulate the expression of the IGN gene in intestinal epithelial mucosa through the increase of intracellular cAMP (39). Importantly, SCFAs can also bind to FFAR2 and induce the release of cytoplasmic $Ca^{2+}$ from intestinal epithelial L cells, which in turn promotes the synthesis and secretion of peptide (P)YY and glucagon-like peptide (GLP-1) (40). The release of (P)YY and GLP-1 is essential for pancreatic function, insulin secretion, and appetite regulation (35, 41, 42). The change in the production of SCFAs is also capable of modifying skeletal muscle metabolism and function. SCFAs have been shown to influence lipid, carbohydrate, and protein metabolism in skeletal muscle tissues both *in vitro* and *in vivo*. Furthermore, SCFAs have the potential to increase skeletal muscle mass retention, blood flow, and insulin sensitivity, and to preserve an oxidative phenotype. The activation of adenosine monophosphate-activated protein kinase (AMPK), peroxisome proliferator-activated receptor-δ (PPAR-δ), peroxisome proliferator-activated receptor-1α coactivator (PGC-1α), and the inhibition of histone deacetylases (HDACs) are likely key

mechanisms through which SCFAs induce these changes to skeletal muscle (43, 44). In addition, SCFAs stimulate oxidative metabolism in the liver and VAT *via* activating AMPK to induce a reduction in body weight (45). SCFAs-producing bacteria (*Butyrivibrio, Bifidobacterium bifidum, Megasphaera*, and *Prevotella*) decreased significantly during T2DM, so the protective effect of SCFAs decreased accordingly (27).

### 2.2.2 TMAO

*Clostridium XIVa strains, Eubacterium* sp. *strain AB3007*, and *Escherichia coli* can produce trimethylamine (TMA) by decomposing phosphatidyl, L-carnitine and choline in food, which can be converted into trimethylamine oxide (TMAO) in the liver through liver enzyme Flavinemonooxygenase3 (FMO3) (46). TMAO induces atherosclerosis in mice, which is related to the incidence of human cardiovascular disease (47). However, in recent years, the relationship between TMAO and T2DM has also received widespread attention. A study based on 2694 participants showed that there was a positive correlation between plasma TMAO concentration and T2DM in the Chinese population (48). The protein kinase RNA-like ER kinase (PERK) is a receptor for TMAO. TMAO binds to PERK at physiologically relevant concentrations, selectively activates the PERK branch of the unfolded protein response, and induces the transcription factor Forkhead Box O1 (FoxO1) in the liver, which is a key driver of metabolic disease (49). FOXO1 function is required for the robust activation of gluconeogenic gene expression in hepatic cells to promote hyperglycemia (50).

### 2.2.3 Bile acids

In addition to producing new metabolites, intestinal microbiota may also change the physical and chemical properties of endogenous metabolites. Bile acids (Bas) are the main degradation product of cholesterol, which are used to dissolve lipids and fat-soluble vitamins and play an important role in regulating host energy metabolism. Primary Bas are susceptible to being modified by intestinal microbiota all along the intestinal tract (such as specific strains of Clostridium from the large intestine) (51, 52). These modifications include deconjugation (the removal of amino acid residues) *via* bile salt hydrolase (BSH) activity and further metabolization *via* the removal of hydroxyl groups (ihydroxylation), oxidation (dehydrogenation), or epimerization (51, 52). This results in the formation of secondary Bas such as deoxycholic acid, lithocholic acid, and ursodeoxycholic acid (a secondary BA in humans, although a primary BA in rodents). This bacterial metabolism changes the bioavailability and bioactivities of Bas, and consequently their impact on the metabolic responses they are involved in (53). Secondary Bas can better bind to Takeda G protein-coupled receptor 5 (TGR5) and farnesoid X receptor (FXR). TGR5 is one of the most important receptors of Bas. It is expressed in the intestine and pancreas. Bas activating TGR5 can promote the secretion of GLP-1 by intestinal L cells (54). FXR is another key receptor of Bas, which is highly expressed in the liver, intestine, and kidney. Many studies have shown that activating FXR can improve hyperglycemia and hyperlipidemia by both suppressing hepatic gluconeogenesis *via* FXR/miR-22-3p/PI3K/AKT/FoxO1 pathway and promoting glycogen synthesis through FXR/miR-22-3p/PI3K/AKT/GSK3β pathway (55–59).

### 2.2.4 BCAAs and AAAs

Circulating branched-chain amino acids (BCAAs) and aromatic amino acids (AAAs) are related to insulin resistance and T2DM in prospective cohorts recently (60, 61). For example, Isoleucine, leucine, valine, phenylalanine, and tyrosine are markers of the development of insulin resistance in young, normoglycemic adults, with the most pronounced associations for men (62). The serum metabolome of insulin-resistant individuals is characterized by increased levels of BCAAs and AAAs, which correlate with intestinal microbiota that has an enriched biosynthetic potential for these amino acids (63). *Prevotella copri* and *Bacteroides vulgatus* are identified as the main species driving the association between the biosynthesis of these amino acids and insulin resistance, which can aggravate glucose intolerance and augment circulating levels of these amino acids (64). BCAAs and AAAs are vital to glucose and protein metabolism, and the increase of these amino acid levels may indicate the onset of T2DM (60, 65).

## 2.3 The immune regulation of intestinal microbiota in T2DM

In addition to metabolic interaction, changes in innate immune levels may also be important in the crosstalk between intestinal microbiota and host metabolism. The decrease of *Bifidobacterium species* and the destruction of the intestinal barrier promote the development of metabolic endotoxemia and increase the level of bacterial lipopolysaccharide (LPS) in plasma, which is a component released from the cell wall of Gram-negative bacteria (66). LPS is one of the pathogen-associated molecular patterns (PAMPs), which is recognized by pattern recognition receptors (PRRs), including Toll-like receptors (TLRs) and Nod-like receptors (NLRs) (67, 68). The interaction between PRRs and PAMPs induces the production of cytokines and interferon (IL-1β, IL-18, IL-6, TNF-α, and MCP-1), thus triggering the cascade of pro-inflammatory signals in the body's peripheral tissue (VAT, liver, and muscle) (69). The inflammasome is the core component of innate immune response and is related to a variety of metabolic diseases (70).

LPS can bind to TLR to activate the first signal of the inflammasome and damage-associated molecular patterns (DAMPs) can respond to activate the second signal (67). The inflammasome can promote the production of mature caspase-1, cut Pro-IL-1β and Pro-IL-18 to form mature IL-1β and IL-18, and then release them into extracellular tissue (71). T2DM is associated with increased levels of pro-inflammatory cytokines, chemokines, and inflammatory proteins (72, 73). Therefore, immune dysfunction is also nonnegligible in the pathogenesis of T2DM mediated by intestinal microbiota (74) (Figure 1).

In T2DM patients, the richness and quantity of bacteria changed, accompanied by intestinal mucosal epithelial injury and barrier dysfunction. The decrease of SCFAs secreted by *Butyrivibrio, Bifidobacterium bifidum, Megasphaera* and *Prevotella* leads to the increase of oxidative pressure of β cells and the secretion of proinflammatory cytokines, the downregulation of AMPK signal in the muscle, liver, and VAT, the decrease of P(YY), GLP-1 secretion and IGN proportion of intestinal epithelial L cells. Worsening blood glucose levels by targeting the nervous system, pancreatic β cells, liver, muscle, and VAT. At the same time, *Clostridium XIVa strains, Eubacterium* sp. *strain AB3007*, and *Escherichia coli* metabolize to produce TMAO, induce the expression of transcription factor Foxo1, and then promote hyperglycemia. Specific strains of Clostridium also reduce the dehydroxylation and hydrophobicity of BAs, which decreases the binding of BAs to TGR5 and FXR3 and increases the levels of blood glucose and lipids. In addition, the decrease of *Bifidobacterium species* and the destruction of the intestinal barrier promote the blood concentration of LPS, which induces the expression of cytokines IL-1β, IL-18, TNF-α, IL-6, MCP-1 and chronic inflammation of the body's peripheral tissue.

## 3 Effects of BBR on intestinal microbiota and T2DM

Traditional Chinese medicine (TCM), also known as botanical medicine or phytomedicine, is a scientific and technological resource with treatment or other health benefits. BBR is an isoquinoline alkaloid derived from the stems and roots of Berberis species, including *B. Aristata, B. Darwinii, B. Petiolaris*, and *B. Vulgaris* (75–77). BBR or herbs containing BBR have been used to treat intestinal infections, especially bacterial diarrhea in China for thousands of years (78). In recent years, its curative effect on T2DM patients has also been effectively proven (79–81) and it is widely believed to be an antidiabetic drug that regulates insulin signal transduction (82). Although BBR is a cationic alkaloid, its structure is not optimized for rapid intestinal absorption. The absolute bioavailability of BBR is much less than 1%, and the trace BBR absorbed from the intestine can be excreted from the ileal cavity through the action of P-glycoprotein (83). Due to the significant contradiction between low bioavailability and strong therapeutic effects, it is assumed that the regulation of intestinal microbiota may be one of the mechanisms of its anti-diabetic effect. Other studies have shown that intestinal microbiota may affect the absorptive activity of individual BBR. It is reported that intestinal microbiota can transform BBR to the absorbable form of dihydroberberine (dhBBR) in animals, and its intestinal absorption rate is 5 times higher than that of BBR. The absorbed dhBBR can then be oxidized back to BBR to enter the bloodstream (84). The above evidence suggests that the anti-T2DM mechanism of BBR is at least partly mediated by the regulation of the intestinal environment.

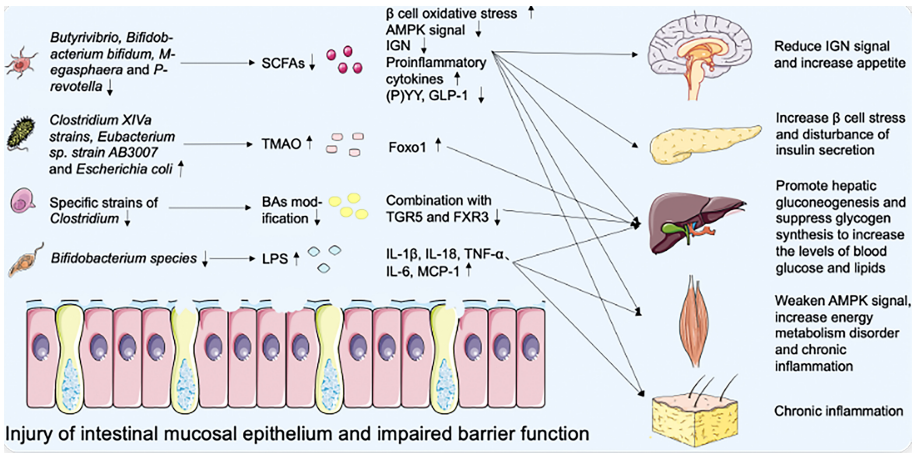


FIGURE 1
Effect of intestinal microbiota disorder on metabolic dysfunction of multiple organs.

## 3.1 BBR changes the richness and quantity of intestinal microbiota

One of the most important functions of BBR is that it can change the composition of intestinal microbiota. A significant decrease in the total bacterial population was observed in rats treated with BBR. BBR has a broad antibacterial spectrum including opportunistic pathogens (*Staphylococcus, Streptococcus, Salmonella, Klebsiella*, and *Pseudomonas*), inducing death of harmful intestinal microbiota (*Escherichia coli*), enhancing the composition of beneficial bacteria (*Bifidobacterium adolescence, Lactobacillus acidophilus, and A.muciniphila*) (85–89), and increasing the ratio of Phaeophyta to Bacteroides, etc. (90). All of these bacteria have a profound effect on blood glucose and lipids levels (91).

## 3.2 BBR improves SCFAs content and the intestinal barrier function

BBR can also increase the number of SCFAs-producing bacteria (*Blautia* and *Allobaculum*) in the intestinal tract (92). Meanwhile, levels of SCFAs are also significantly elevated after treatment with BBR (93). SCFAs work as a mediator between intestinal microbiota, they have the potential to improve glucose homeostasis and insulin sensitivity in patients with T2DM. In the setting of pancreatic dysfunction, they can regulate pancreatic insulin and glucagon secretion through GLP1 augmentation, meanwhile improving blood glucose levels by targeting the nervous system, pancreatic β cells, liver, muscle, and VAT (33). Apart from SCFAs-producing bacteria (93), the abundance of *A.muciniphila* in B6 mice induced by a high-fat diet was 19.1 times higher than that in the control group after BBR intervention, thus regulating tight junction protein and protecting the integrity of the intestinal barrier (94). BBR can increase the goblet cell number and villi length, and reverse the suppressed expressions of mucin, occludin, and zonula occludens-1 (ZO-1) to protect the intestinal barrier function (95).

## 3.3 BBR improves BAs and amino acids metabolism

Moreover, BBR can increase some beneficial bacteria with benzene sulfonyl hydrazine activity, for instance, *Bacteroides*, *Bifidobacterium, Lactobacillus*, and *Clostridium*, promote the decomposition of conjugated bile acids (CBA) and strengthen their excretion through the intestine. *Lactobacillus* converts primary BAs into secondary BAs through decarboxylation (96), and BBR can enhance the expression of FXR and TGR5, which is considered to be an agonist (97). The Phylum Firmicutes have higher BSH activity than the Phylum Bacteroidetes in the intestinal microbiota, and the latter is only active against taurine-conjugated BAs. BBR remarkably increased the *Firmicutes/Bacteroidetes* ratio and it is one of the mechanisms of its induced serum-free BAs increase and lipid-lowering effect (98). Overall, the mechanisms by which BBR alters the intestinal microbiota and improves metabolism are related to its choleretic effects.

In addition, the metabonomic analysis of colonic contents identified 55 different intestinal metabolites and showed that tyrosine, tryptophan, and phenylalanine in the BBR group decreased not only in the colonic contents but also in the serum, indicating that BBR can alleviate the symptoms of T2DM by reducing the contents of BCAAs and AAAs (99, 100).

## 3.4 BBR regulates intestinal immunity

BBR can significantly reduce the abundance of *Proteobacteria*, (such as *Desulfovibrio, and Enterobacter cloacae)*, and inhibit LPS production, as well as prevent serum LPS elevation, regulating intestinal permeability, attenuating insulin resistance and improving metabolic endotoxemia effectively (101). In diet-induced obese (DIO) mice, BBR decreased the levels of LPS and inflammatory mediators (IL-1, IL-6, TNF-α, and MCP-1), blocked the biosynthesis of TLR and NF-κB, improved intestinal and VAT inflammation, and promoted insulin signal transduction and glucose metabolism (102). By activating AMPK activity, BBR inhibited the production of IFN- γ, and Il-17A by lamina propria CD4+T cells *in vivo* and vitro (102, 103). At the same time, the expression of immune-related genes (including *Nfkb1, Stat1*, and *Ifnrg1*) in islets of the BBR group decreased significantly (93). These suggested that the anti-diabetes/obesity potential of BBR is related to its anti-inflammatory effect to some extent.

## 3.5 BBR promotes intestinal GLP-1 secretion

Studies have shown that BBR decreases the variousness of intestinal microbiota, increases the proportion of *Bacteroidetes* and *Firmicutes*, further increases the number of L-cells in the proximal colon, and the expression of serum GLP-1, GLP-2 (95, 104, 105). BBR treatment can elevate plasma GLP-1 and orexin-a, and upregulate hypothalamic GLP-1 receptor expression, which has beneficial effects on various metabolic disorders such as insulin resistance and obesity, thereby inducing regulation of the gut-brain axis of the microbiota (106). It was observed that the decrease of GLP-1 was accompanied by the increase of mitochondrial stress response in the colonic cells of

DIO mice. BBR administration not only restored GLP-1, but also relieved mitochondrial stress pressure, down-regulated intestinal transport speed and appetite, and improved energy metabolism in DIO mice (90) (Figure 2).

BBR can increase the number of SCFAs-producing bacteria and the production of SCFAs in T2DM patients. Its action on FFAR2 can release intracellular $Ca^{2+}$ from intestinal epithelial L cells, activate the synthesis and secretion of GLP-1 and peptide (P)YY, and reduce the level of oxidative stress in L cell mitochondria and ROS production. LPS can bind to TLR to activate the first signal of the inflammasome and DAMP can respond to activate the second signal. The inflammasome can promote the production of mature caspase-1, cut Pro-IL-1β and Pro-IL-18 to form mature IL-1β and IL-18, and then release them into extracellular cells. BBR inhibits the production of bacterial LPS, blocks the biosynthesis of TLR and NF-κB, and reduces the secretion of IL-1β and IL-18 pro-inflammatory cytokines, thus slowing down the level of inflammation in the body's peripheral organs and tissues.

## 3.6 Synergistic effect of BBR and other drugs

Early studies have shown that BBR can increase the oral bioavailability of other drugs. When combined with metformin, it can reduce the degradation of metformin by human and rat intestinal microbiota (107). Compared with anti-T2DM single drug/monomer therapy, the compound prescription of TCM accords with the newly proposed principle of "multi-drug and multi-target". The synergistic effect of TCM includes synergism and toxicity reduction (108, 109), and the mixed bioactive components in the compound can enhance the curative effect of each other (110–112). For example, BBR combined with stachyose can improve glucose metabolism and intestinal microbiota disorder by regulating microRNA and gene expression in the colon of diabetic rats (113). The compatibility of *Rhizoma Coptidis* with *Cinnamon* improves T2DM and diabetic nephropathy more effectively by affecting the pharmacokinetics of BBR (114, 115). In short, these results show that BBR can further play a variety of health promotion effects through synergism.

## 3.7 Clinical trials of BBR in the treatment of hypometabolic disorders

We searched for registered clinical trials investigating the efficacy of BBR in the treatment of hypometabolic disorders. There were numerous and most of the published results reported a positive efficacy of BBR. (Table 1). However, mild diarrhea caused by BBR under clinical conditions can also happen and it is associated with intestinal microbiota disorder, such as the increase in the abundance of *Porphyromonas* and *Prevodiaceae*, as well as *Parasitobacteria*, *Prevodiaceae UCG-001* and *NK3B31* groups (116). But overall, the gastrointestinal reaction of BBR is mild and transient. Compared with its overwhelming health benefits, the side effects of BBR are sporadic. Further long-term toxicity studies on the low toxicity and side effects of BBR are still needed to prove BBR's safety (80).

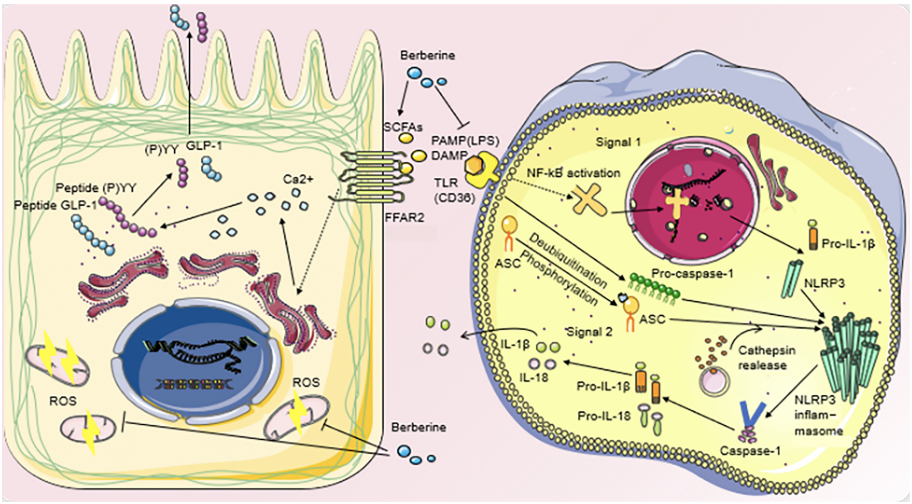


FIGURE 2
Regulatory mechanisms of BBR on metabolic disturbance.

TABLE 1 Clinical trials of BBR registered at ClinicalTrials.gov in the treatment of glucose metabolic disorder.

| Disease | Status | Phase I/II/III/IV | Number of Patients | Intervention measures | Dose | Duration | Start date | Identifier |
|---|---|---|---|---|---|---|---|---|
| Prediabetes | Completed | III | 300 | BBR/bifidobacterium/BBR, bifidobacterium/placebo | 0.5 g, bid | 16 weeks | October 2015 | NCT03330184 |
| Prediabetes | Active, not recruiting | IV | 28 | BBR/metformin | 0.5 g, tid | 14 weeks | March 2016 | NCT03029390 |
| Hyperglycemia | Unknown | IV | 200 | BBR, Insulin/Insulin | 0.5 g, bid | 8 days | July 2016 | NCT02806999 |
| Glucose Metabolism Disorders | Recruiting | – | 50 | BBR/placebo | 0.55 g, bid | 8 weeks | March 2020 | NCT05031715 |
| DM | Completed | IV | 800 | BBR/placebo | – | 2 days | July 2016 | NCT02808351 |
| DM | Completed | I | – | BBR/placebo | – | – | October 2019 | NCT03972215 |
| T2DM | Completed | I, II | 70 | BBR/metformin | – | 13 weeks | January 2004 | NCT00425009 |
| T2DM | – | III | 400 | BBR, probiotics/placebo, probiotics/ BBR, placebo/placebo | 0.6 g, bid | 3 months | August 2016 | NCT02861261 |
| T2DM with Dyslipidemia | Completed | III | 116 | BBR/placebo | 1.0 g/ day | 3 months | April 2005 | NCT00462046 |
| Metabolic Syndrome | Recruiting | – | 40 | BBR/placebo | 1.5 g/ day | – | August 2019 | NCT03976336 |
| Metabolic Syndrome | Not yet recruiting | IV | 5200 | BBR/Healthy lifestyle intervention | 0.5 g, bid | 3 years | December 2021 | NCT05105321 |
| Metabolic Syndrome | Not yet recruiting | III | 40 | BBR/placebo | 0.5 g, tid | 6 months | April 2021 | NCT04860063 |

# 4. BBR efficacy in improving other metabolic diseases

## 4.1 Obesity

Compared with the model group, BBR can restore the relative level of *Bifidobacterium*, the ratio of Bacteroides to Phaeophyta (117), and the abundance of *A.muciniphila* (118). It can also increase the number of SCFAs-producing bacteria (*Isobacteria, Bacteroides, Brucella, Casein*, and *Bacillus)* in obese rats, and the concentration of total SCFAs (acetic acids and propionic acids) (119). In addition, oral BBR increases the secretion of GLP-1 in intestinal L cells, upregulates the levels of GLP-1 receptor, neuropeptide Y, and orexin An in the brain, improves the ultrastructure of the hypothalamus (106) and increases the expression of fasting-induced adipose factors in VAT (120). It can effectively reduce body weight and plasma lipid levels by regulating the microbiota-gut-brain axis.

## 4.2 Hyperlipidemia

A 3-month clinical study has shown that the effective cholesterol-lowering effect of BBR was closely related to the baseline levels of *Alistipes* and *Blautia* bacteria (121). BBR treatment led to the enrichment of beneficial bacteria (*Bacteroides and Blautia*) and the reduction of *Escherichia coli* (122), correcting the composition of intestinal microbiota and fungi to play a role of anti-hyperlipidemia (123). At the same time, the effect of BBR as a lipid reducer has been also proven to be related to Bas conversion and ileal FXR signal pathway. Animal metabonomic analysis showed that BBR treatment increased the levels of pyruvate, 5-hydroxytryptamine, ketogenic, and glycogen amino acids in serum, pyridoxine, and 4-pyridoxic acids in urine. Meanwhile, decreasing taurine and methionine in the liver, and deoxycholate and lithocholic in feces. Indicating that the changes in intestinal microbial metabolites can also affect the level of blood lipids (124, 125).

## 4.3 NAFLD

The level of hepatic BAs transporter is down-regulated due to liver inflammation, which slows down the enterohepatic circulation and promotes the increase of CBA in the serum and liver of patients with NAFLD. High levels of CBA activate sphingosine 1-phosphate receptor 2 (S1PR2) to activate pro-inflammatory and fibrosis pathways, which promotes the progression of non-alcoholic steatohepatitis (NASH). BBR as an anti-inflammatory compound combined with BAs receptor agonist can delay the progression of NASH and improve BAs metabolism by inhibiting microorganisms related to BSH

activity, such as *Clostridium XIVa* and *IV* (124, 126, 127). A study explored the potential mechanism of BBR involved in the intestinal microbiota-immune system axis against NAFLD. It is worth noting that BBR activated an immunosuppressive population in the liver of mice to reduce alcoholic liver injury, which is defined as a granulocytic myeloid-derived suppressor cell (G-MDSC)-like population, and correspondingly reduced cytotoxic T cells and activated IL6/STAT3 signal transduction. These protective effects were eliminated after the consumption of intestinal microbiota, indicating that intestinal microbiota may be involved in mediating the expansion of the G-MDSC population (126, 128). In addition, BBR significantly restored the relative abundance of *Bifidobacterium*, *A.muciniphila*, and the ratio of Bacteroides to Phaeophyta, decreased the levels of serum LPS and several inflammatory cytokines (IL-1, IL-6, and TNF-α), improved the intestinal barrier dysfunction and prevented intestinal toxic substances from entering the liver through the hepatic portal system (117, 129).

## 5 Summary and prospect

BBR has multiple systemic activities on metabolism-related chronic diseases, including antioxidant/anti-inflammatory effects and changes in intestinal microbiota composition and metabolism. BBR works through the drug cloud (dCloud) mechanism. Unlike drug target effects, dCloud is defined as a set of terminal molecular events induced by drugs or related metabolites and the network connections between them. The therapeutic effect of BBR is the result of its dCloud effect on symptoms/signs and the root causes of the disease, which can explain why BBR plays a role in a variety of metabolism-related diseases.

After oral administration, BBR interacts with the intestinal microbiota. BBR can regulate the composition of intestinal microbiota and its metabolites, and intestinal microbiota can also transform BBR into dhBBR. In this process, two types of metabolites can be produced, including intestinal microbiota metabolites (from food and host) and secondary compounds of BBR. Understanding the two-way interaction between BBR and intestinal microbiota is helpful for us to apply BBR in pre-clinical and clinical interventions. However, due to the low bioavailability and natural yield of BBR, the future potential of bioactive natural products for the treatment of diabetes will be based on a structural modification to obtain safer, higher bioavailability and patentable compound molecules. And alternative replenishment methods that rely on biotechnology production and chemical synthesis should be developed to deal with the problem that natural product replenishment is difficult to meet the huge commercial market demand.

This paper introduces the pathogenesis of T2DM caused by intestinal microbiota disorder, meanwhile, focusing on the effective and important active ingredient BBR to treat T2DM by targeting intestinal microbiota. It may be a promising way to control T2DM because it can relieve T2DM through different mechanisms and ways of action, including antimicrobial and anti-inflammatory, protecting the intestinal barrier function, improving microbial metabolism, stabilizing intestinal hormones, and so on. In addition, the clinical trials of registered BBR for the treatment of glucose metabolism disorders are summarized, which is helpful for us to understand the current research and development of BBR and provide a basis for its clinical application in the future. The mechanism of BBR in treating other metabolic diseases (including obesity, hyperlipidemia, and NAFLD) through intestinal microbiota is also brought to notice. However, there is still a long way to go to explain the mechanism of BBR against metabolic diseases and its potential side effects, especially in the context of wide differences in the composition of intestinal microbiota among individuals. We should continue to strengthen the understanding of the common signal transduction mechanism in different bacteria to achieve standardized treatment by targeting common molecules or signaling pathways, and bear in mind the ultimate goal of translating knowledge into practice.

## Author contributions

QH and DW conceived the paper. QH, DW, and FL wrote the article. DW, HD, MG, YG, and QX revised the figures and reviewed the article. All authors reviewed and approved the final version of the manuscript.

## Funding

This study was supported by the National Natural Science Foundation of China, (Grant NO.82274470 and NO.81974567).

## Conflict of interest

The authors declare that the research was conducted in the absence of any commercial or financial relationships that could be construed as a potential conflict of interest.

## Publisher's note

# References


1. Gavin JR III, Alberti KGMM, Davidson MB, DeFronzo RA, Drash A, Gabbe SG., et al. Report of the expert committee on the diagnosis and classification of diabetes mellitus. *Diabetes Care* (2003) 26 Suppl 1:S5–20. doi: 10.2337/diacare.26.2007.s5

2. Choi YJ, Cho YM, Park CK, Jang HC, Park KS, Kim SY, et al. Rapidly increasing diabetes-related mortality with socio-environmental changes in south Korea during the last two decades. *Diabetes Res Clin Pract* (2006) 74(3):295–300. doi: 10.1016/j.diabres.2006.03.029

3. Franks PW, Poveda A. Lifestyle and precision diabetes medicine: Will genomics help optimise the prediction, prevention and treatment of type 2 diabetes through lifestyle therapy? *Diabetologia* (2017) 60(5):784–92. doi: 10.1007/s00125-017-4207-5

4. Imamura F, Micha R, Khatibzadeh S, Fahimi S, Shi P, Powles J, et al. Dietary quality among men and women in 187 countries in 1990 and 2010: A systematic assessment. *Lancet Glob Health* (2015) 3(3):e132–42. doi: 10.1016/s2214-109x(14)70381-x

5. Sun H, Saeedi P, Karuranga S, Pinkepank M, Ogurtsova K, Duncan BB, et al. Idf diabetes atlas: Global, regional and country-level diabetes prevalence estimates for 2021 and projections for 2045. *Diabetes Res Clin Pract* (2022) 183:109119. doi: 10.1016/j.diabres.2021.109119

6. Nanditha A, Ma RC, Ramachandran A, Snehalatha C, Chan JC, Chia KS, et al. Diabetes in Asia and the pacific: Implications for the global epidemic. *Diabetes Care* (2016) 39(3):472–85. doi: 10.2337/dc15-1536

7. Zimmet PZ, Magliano DJ, Herman WH, Shaw JE. Diabetes: A 21st century challenge. *Lancet Diabetes Endocrinol* (2014) 2(1):56–64. doi: 10.1016/s2213-8587(13)70112-8

8. Qin J, Li R, Raes J, Arumugam M, Burgdorf KS, Manichanh C, et al. A human gut microbial gene catalogue established by metagenomic sequencing. *Nature* (2010) 464(7285):59–65. doi: 10.1038/nature08821

9. Li J, Jia H, Cai X, Zhong H, Feng Q, Sunagawa S, et al. An integrated catalog of reference genes in the human gut microbiome. *Nat Biotechnol* (2014) 32(8):834–41. doi: 10.1038/nbt.2942

10. Ley RE, Turnbaugh PJ, Klein S, Gordon JI. Microbial ecology: Human gut microbes associated with obesity. *Nature* (2006) 444(7122):1022–3. doi: 10.1038/4441022a

11. Bäckhed F, Ding H, Wang T, Hooper LV, Koh GY, Nagy A, et al. The gut microbiota as an environmental factor that regulates fat storage. *Proc Natl Acad Sci U S A* (2004) 101(44):15718–23. doi: 10.1073/pnas.0407076101

12. Ridaura VK, Faith JJ, Rey FE, Cheng J, Duncan AE, Kau AL, et al. Gut microbiota from twins discordant for obesity modulate metabolism in mice. *Science* (2013) 341(6150):1241214. doi: 10.1126/science.1241214

13. Khunti K, Davies M. Metabolic syndrome. *BMJ* (2005) 331(7526):1153–4. doi: 10.1136/bmj.331.7526.1153

14. Wang GS, Hoyte C. Review of biguanide (Metformin) toxicity. *J Intensive Care Med* (2019) 34(11-12):863–76. doi: 10.1177/0885066618793385

15. Ramkumar S, Raghunath A, Raghunath S. Statin therapy: Review of safety and potential side effects. *Acta Cardiol Sin* (2016) 32(6):631–9. doi: 10.6515/acs20160611a

16. Hanefeld M, Ganz X, Nolte C. [Hypoglycemia and cardiac arrhythmia in patients with diabetes mellitus type 2]. *Herz* (2014) 39(3):312–9. doi: 10.1007/s00059-014-4086-1

17. Tillhon M, Guamán Ortiz LM, Lombardi P, Scovassi AI. Berberine: New perspectives for old remedies. *Biochem Pharmacol* (2012) 84(10):1260–7. doi: 10.1016/j.bcp.2012.07.018

18. Hunter PM, Hegele RA. Functional foods and dietary supplements for the management of dyslipidaemia. *Nat Rev Endocrinol* (2017) 13(5):278–88. doi: 10.1038/nrendo.2016.210

19. Kong WJ, Vernieri C, Foiani M, Jiang JD. Berberine in the treatment of metabolism-related chronic diseases: A drug cloud (Dcloud) effect to target multifactorial disorders. *Pharmacol Ther* (2020) 209:107496. doi: 10.1016/j.pharmthera.2020.107496

20. Yang G, Wei J, Liu P, Zhang Q, Tian Y, Hou G, et al. Role of the gut microbiota in type 2 diabetes and related diseases. *Metabolism* (2021) 117:154712. doi: 10.1016/j.metabol.2021.154712

21. Scheithauer TP, Dallinga-Thie GM, de Vos WM, Nieuwdorp M, van Raalte DH. Causality of small and Large intestinal microbiota in weight regulation and insulin resistance. *Mol Metab* (2016) 5(9):759–70. doi: 10.1016/j.molmet.2016.06.002

22. Canfora EE, Meex RCR, Venema K, Blaak EE. Gut microbial metabolites in obesity, nafld and T2dm. *Nat Rev Endocrinol* (2019) 15(5):261–73. doi: 10.1038/s41574-019-0156-z

23. Turnbaugh PJ, Hamady M, Yatsunenko T, Cantarel BL, Duncan A, Ley RE, et al. A core gut microbiome in obese and lean twins. *Nature* (2009) 457(7228):480–4. doi: 10.1038/nature07540

24. Gurung M, Li Z, You H, Rodrigues R, Jump DB, Morgun A, et al. Role of gut microbiota in type 2 diabetes pathophysiology. *EBioMedicine* (2020) 51:102590. doi: 10.1016/j.ebiom.2019.11.051

25. Qin J, Li Y, Cai Z, Li S, Zhu J, Zhang F, et al. A metagenome-wide association study of gut microbiota in type 2 diabetes. *Nature* (2012) 490(7418):55–60. doi: 10.1038/nature11450

26. Karlsson FH, Tremaroli V, Nookaew I, Bergström G, Behre CJ, Fagerberg B, et al. Gut metagenome in European women with normal, impaired and diabetic glucose control. *Nature* (2013) 498(7452):99–103. doi: 10.1038/nature12198

27. de la Cuesta-Zuluaga J, Mueller NT, Corrales-Agudelo V, Velásquez-Mejía EP, Carmona JA, Abad JM, et al. Metformin is associated with higher relative abundance of mucin-degrading akkermansia muciniphila and several short-chain fatty acid-producing microbiota in the gut. *Diabetes Care* (2017) 40(1):54–62. doi: 10.2337/dc16-1324

28. Depommier C, Everard A, Druart C, Plovier H, Van Hul M, Vieira-Silva S, et al. Supplementation with akkermansia muciniphila in overweight and obese human volunteers: A proof-of-Concept exploratory study. *Nat Med* (2019) 25(7):1096–103. doi: 10.1038/s41591-019-0495-2

29. Plovier H, Everard A, Druart C, Depommier C, Van Hul M, Geurts L, et al. A purified membrane protein from akkermansia muciniphila or the pasteurized bacterium improves metabolism in obese and diabetic mice. *Nat Med* (2017) 23(1):107–13. doi: 10.1038/nm.4236

30. Yassour M, Lim MY, Yun HS, Tickle TL, Sung J, Song YM, et al. Sub-Clinical detection of gut microbial biomarkers of obesity and type 2 diabetes. *Genome Med* (2016) 8(1):17. doi: 10.1186/s13073-016-0271-6

31. Allin KH, Tremaroli V, Caesar R, Jensen BAH, Damgaard MTF, Bahl MI, et al. Aberrant intestinal microbiota in individuals with prediabetes. *Diabetologia* (2018) 61(4):810–20. doi: 10.1007/s00125-018-4550-1

32. Canfora EE, Jocken JW, Blaak EE. Short-chain fatty acids in control of body weight and insulin sensitivity. *Nat Rev Endocrinol* (2015) 11(10):577–91. doi: 10.1038/nrendo.2015.128

33. Mandaliya DK, Seshadri S. Short chain fatty acids, pancreatic dysfunction and type 2 diabetes. *Pancreatology* (2019) 19(2):280–4. doi: 10.1016/j.pan.2019.01.021

34. Everard A, Cani PD. Gut microbiota and glp-1. *Rev Endocr Metab Disord* (2014) 15(3):189–96. doi: 10.1007/s11154-014-9288-6

35. Fava S. Glucagon-like peptide 1 and the cardiovascular system. *Curr Diabetes Rev* (2014) 10(5):302–10. doi: 10.2174/1573399810666141030125830

36. Koh A, De Vadder F, Kovatcheva-Datchary P, Bäckhed F. From dietary fiber to host physiology: Short-chain fatty acids as key bacterial metabolites. *Cell* (2016) 165(6):1332–45. doi: 10.1016/j.cell.2016.05.041

37. Mithieux G. Nutrient control of energy homeostasis via gut-brain neural circuits. *Neuroendocrinology* (2014) 100(2-3):89–94. doi: 10.1159/000369070

38. Kim YA, Keogh JB, Clifton PM. Probiotics, prebiotics, synbiotics and insulin sensitivity. *Nutr Res Rev* (2018) 31(1):35–51. doi: 10.1017/s095442241700018x

39. De Vadder F, Kovatcheva-Datchary P, Goncalves D, Vinera J, Zitoun C, Duchampt A, et al. Microbiota-generated metabolites promote metabolic benefits via gut-brain neural circuits. *Cell* (2014) 156(1-2):84–96. doi: 10.1016/j.cell.2013.12.016

40. Tolhurst G, Heffron H, Lam YS, Parker HE, Habib AM, Diakogiannaki E, et al. Short-chain fatty acids stimulate glucagon-like peptide-1 secretion *Via* the G-Protein-Coupled receptor Ffar2. *Diabetes* (2012) 61(2):364–71. doi: 10.2337/db11-1019

41. Bindels LB, Dewulf EM, Delzenne NM. Gpr43/Ffa2: Physiopathological relevance and therapeutic prospects. *Trends Pharmacol Sci* (2013) 34(4):226–32. doi: 10.1016/j.tips.2013.02.002

42. Schroeder BO, Bäckhed F. Signals from the gut microbiota to distant organs in physiology and disease. *Nat Med* (2016) 22(10):1079–89. doi: 10.1038/nm.4185

43. den Besten G, Lange K, Havinga R, van Dijk TH, Gerding A, van Eunen K, et al. Gut-derived short-chain fatty acids are vividly assimilated into host carbohydrates and lipids. *Am J Physiol Gastrointest Liver Physiol* (2013) 305(12):G900–10. doi: 10.1152/ajpgi.00265.2013

44. Frampton J, Murphy KG, Frost G, Chambers ES. Short-chain fatty acids as potential regulators of skeletal muscle metabolism and function. *Nat Metab* (2020) 2(9):840–8. doi: 10.1038/s42255-020-0188-7

45. den Besten G, Bleeker A, Gerding A, van Eunen K, Havinga R, van Dijk TH, et al. Short-chain fatty acids protect against high-fat diet-induced obesity *Via* a pparγ-dependent switch from lipogenesis to fat oxidation. *Diabetes* (2015) 64 (7):2398–408. doi: 10.2337/db14-1213

46. Rath S, Heidrich B, Pieper DH, Vital M. Uncovering the trimethylamine-producing bacteria of the human gut microbiota. *Microbiome* (2017) 5(1):54. doi: 10.1186/s40168-017-0271-9

47. Tang WH, Hazen SL. Microbiome, trimethylamine n-oxide, and cardiometabolic disease. *Transl Res* (2017) 179:108–15. doi: 10.1016/j.trsl.2016.07.007

48. Shan Z, Sun T, Huang H, Chen S, Chen L, Luo C, et al. Association between microbiota-dependent metabolite trimethylamine-N-Oxide and type 2 diabetes. *Am J Clin Nutr* (2017) 106(3):888–94. doi: 10.3945/ajcn.117.157107

49. Chen S, Henderson A, Petriello MC, Romano KA, Gearing M, Miao J, et al. Trimethylamine n-oxide binds and activates perk to promote metabolic dysfunction. *Cell Metab* (2019) 30(6):1141–51.e5. doi: 10.1016/j.cmet.2019.08.021

50. Puigserver P, Rhee J, Donovan J, Walkey CJ, Yoon JC, Oriente F, et al. Insulin-regulated hepatic gluconeogenesis through Foxo1-Pgc-1alpha interaction. *Nature* (2003) 423(6939):550–5. doi: 10.1038/nature01667

51. Ridlon JM, Kang DJ, Hylemon PB. Bile salt biotransformations by human intestinal bacteria. *J Lipid Res* (2006) 47(2):241–59. doi: 10.1194/jlr.R500013-JLR200

52. Ridlon JM, Harris SC, Bhowmik S, Kang DJ, Hylemon PB. Consequences of bile salt biotransformations by intestinal bacteria. *Gut Microbes* (2016) 7(1):22–39. doi: 10.1080/19490976.2015.1127483

53. de Aguiar Vallim TQ, Tarling EJ, Edwards PA. Pleiotropic roles of bile acids in metabolism. *Cell Metab* (2013) 17(5):657–69. doi: 10.1016/j.cmet.2013.03.013

54. Shapiro H, Kolodziejczyk AA, Halstuch D, Elinav E. Bile acids in glucose metabolism in health and disease. *J Exp Med* (2018) 215(2):383–96. doi: 10.1084/jem.20171965

55. Chávez-Talavera O, Tailleux A, Lefebvre P, Staels B. Bile acid control of metabolism and inflammation in obesity, type 2 diabetes, dyslipidemia, and nonalcoholic fatty liver disease. *Gastroenterology* (2017) 152(7):1679–94.e3. doi: 10.1053/j.gastro.2017.01.055

56. Kuipers F, Bloks VW, Groen AK. Beyond intestinal soap–bile acids in metabolic control. *Nat Rev Endocrinol* (2014) 10(8):488–98. doi: 10.1038/nrendo.2014.60

57. Ahmad TR, Haeusler RA. Bile acids in glucose metabolism and insulin signalling - mechanisms and research needs. *Nat Rev Endocrinol* (2019) 15 (12):701–12. doi: 10.1038/s41574-019-0266-7

58. Zhang Y, Lee FY, Barrera G, Lee H, Vales C, Gonzalez FJ, et al. Activation of the nuclear receptor fxr improves hyperglycemia and hyperlipidemia in diabetic mice. *Proc Natl Acad Sci U S A* (2006) 103(4):1006–11. doi: 10.1073/pnas.0506982103

59. Zhao T, Wang J, He A, Wang S, Chen Y, Lu J, et al. Mebhydrolin ameliorates glucose homeostasis in type 2 diabetic mice by functioning as a selective fxr antagonist. *Metabolism* (2021) 119:154771. doi: 10.1016/j.metabol.2021.154771

60. Xu M, Qi Q, Liang J, Bray GA, Hu FB, Sacks FM, et al. Genetic determinant for amino acid metabolites and changes in body weight and insulin resistance in response to weight-loss diets: The preventing overweight using novel dietary strategies (Pounds lost) trial. *Circulation* (2013) 127(12):1283–9. doi: 10.1161/circulationaha.112.000586

61. Wang TJ, Larson MG, Vasan RS, Cheng S, Rhee EP, McCabe E, et al. Metabolite profiles and the risk of developing diabetes. *Nat Med* (2011) 17(4):448–53. doi: 10.1038/nm.2307

62. Würtz P, Soininen P, Kangas AJ, Rönnemaa T, Lehtimäki T, Kähönen M, et al. Branched-chain and aromatic amino acids are predictors of insulin resistance in young adults. *Diabetes Care* (2013) 36(3):648–55. doi: 10.2337/dc12-0895

63. Ruiz-Canela M, Guasch-Ferré M, Toledo E, Clish CB, Razquin C, Liang L, et al. Plasma branched Chain/Aromatic amino acids, enriched Mediterranean diet and risk of type 2 diabetes: Case-cohort study within the predimed trial. *Diabetologia* (2018) 61(7):1560–71. doi: 10.1007/s00125-018-4611-5

64. Pedersen HK, Gudmundsdottir V, Nielsen HB, Hyotylainen T, Nielsen T, Jensen BA, et al. Human gut microbes impact host serum metabolome and insulin sensitivity. *Nature* (2016) 535(7612):376–81. doi: 10.1038/nature18646

65. Felig P, Marliss E, Cahill GF Jr. Plasma amino acid levels and insulin secretion in obesity. *New Engl J Med* (1969) 281(15):811–6. doi: 10.1056/nejm196910092811503

66. Amar J, Burcelin R, Ruidavets JB, Cani PD, Fauvel J, Alessi MC, et al. Energy intake is associated with endotoxemia in apparently healthy men. *Am J Clin Nutr* (2008) 87(5):1219–23. doi: 10.1093/ajcn/87.5.1219

67. Sharma BR, Kanneganti TD. Nlrp3 inflammasome in cancer and metabolic diseases. *Nat Immunol* (2021) 22(5):550–9. doi: 10.1038/s41590-021-00886-5

68. Nagashima H, Yamaoka Y. Importance of toll-like receptors in pro-inflammatory and anti-inflammatory responses by helicobacter pylori infection. *Curr Top Microbiol Immunol* (2019) 421:139–58. doi: 10.1007/978-3-030-15138-6_6

69. Rathinam VAK, Zhao Y, Shao F. Innate immunity to intracellular lps. *Nat Immunol* (2019) 20(5):527–33. doi: 10.1038/s41590-019-0368-3

70. Sharma D, Kanneganti TD. The cell biology of inflammasomes: Mechanisms of inflammasome activation and regulation. *J Cell Biol* (2016) 213 (6):617–29. doi: 10.1083/jcb.201602089

71. Man SM. Inflammasomes in the gastrointestinal tract: Infection, cancer and gut microbiota homeostasis. *Nat Rev Gastroenterol Hepatol* (2018) 15(12):721–37. doi: 10.1038/s41575-018-0054-1

72. Hotamisligil GS, Shargill NS, Spiegelman BM. Adipose expression of tumor necrosis factor-alpha: Direct role in obesity-linked insulin resistance. *Science* (1993) 259(5091):87–91. doi: 10.1126/science.7678183

73. Cani PD, Amar J, Iglesias MA, Poggi M, Knauf C, Bastelica D, et al. Metabolic endotoxemia initiates obesity and insulin resistance. *Diabetes* (2007) 56 (7):1761–72. doi: 10.2337/db06-1491

74. Ngo VL, Abo H, Maxim E, Harusato A, Geem D, Medina-Contreras O, et al. A cytokine network involving il-36γ, il-23, and il-22 promotes antimicrobial defense and recovery from intestinal barrier damage. *Proc Natl Acad Sci U S A* (2018) 115(22):E5076–e85. doi: 10.1073/pnas.1718902115

75. Potdar D, Hirwani RR, Dhulap S. Phyto-chemical and pharmacological applications of berberis aristata. *Fitoterapia* (2012) 83(5):817–30. doi: 10.1016/j.fitote.2012.04.012

76. Habtemariam S. The therapeutic potential of berberis darwinii stem-bark: Quantification of berberine and in vitro evidence for alzheimer's disease therapy. *Nat Prod Commun* (2011) 6(8):1089–90. doi: 10.1177/1934578X1100600809

77. Singh A, Bajpai V, Srivastava M, Arya KR, Kumar B. Rapid screening and distribution of bioactive compounds in different parts of berberis petiolaris using direct analysis in real time mass spectrometry. *J Pharm Anal* (2015) 5(5):332–5. doi: 10.1016/j.jpha.2015.05.002

78. Tang J, Feng Y, Tsao S, Wang N, Curtain R, Wang Y. Berberine and coptidis rhizoma as novel antineoplastic agents: A review of traditional use and biomedical investigations. *J Ethnopharmacol* (2009) 126(1):5–17. doi: 10.1016/j.jep.2009.08.009

79. Lan J, Zhao Y, Dong F, Yan Z, Zheng W, Fan J, et al. Meta-analysis of the effect and safety of berberine in the treatment of type 2 diabetes mellitus, hyperlipemia and hypertension. *J Ethnopharmacol* (2015) 161:69–81. doi: 10.1016/j.jep.2014.09.049

80. Yin J, Xing H, Ye J. Efficacy of berberine in patients with type 2 diabetes mellitus. *Metabolism* (2008) 57(5):712–7. doi: 10.1016/j.metabol.2008.01.013

81. Zhang Y, Li X, Zou D, Liu W, Yang J, Zhu N, et al. Treatment of type 2 diabetes and dyslipidemia with the natural plant alkaloid berberine. *J Clin Endocrinol Metab* (2008) 93(7):2559–65. doi: 10.1210/jc.2007-2404

82. Liu LZ, Cheung SC, Lan LL, Ho SK, Xu HX, Chan JC, et al. Berberine modulates insulin signaling transduction in insulin-resistant cells. *Mol Cell Endocrinol* (2010) 317(1-2):148–53. doi: 10.1016/j.mce.2009.12.027

83. Chen W, Miao YQ, Fan DJ, Yang SS, Lin X, Meng LK, et al. Bioavailability study of berberine and the enhancing effects of tpgs on intestinal absorption in rats. *AAPS PharmSciTech* (2011) 12(2):705–11. doi: 10.1208/s12249-011-9632-z

84. Feng R, Shou JW, Zhao ZX, He CY, Ma C, Huang M, et al. Transforming berberine into its intestine-absorbable form by the gut microbiota. *Sci Rep* (2015) 5:12155. doi: 10.1038/srep12155

85. Cernáková M, Kostálová D. Antimicrobial activity of berberine–a constituent of mahonia aquifolium. *Folia Microbiol* (2002) 47(4):375–8. doi: 10.1007/bf02818693

86. Chae SH, Jeong IH, Choi DH, Oh JW, Ahn YJ. Growth-inhibiting effects of coptis japonica root-derived isoquinoline alkaloids on human intestinal bacteria. *J Agric Food Chem* (1999) 47(3):934–8. doi: 10.1021/jf980991o

87. Zhang HY, Piao XS, Zhang Q, Li P, Yi JQ, Liu JD, et al. The effects of forsythia suspensa extract and berberine on growth performance, immunity, antioxidant activities, and intestinal microbiota in broilers under high stocking density. *Poult Sci* (2013) 92(8):1981–8. doi: 10.3382/ps.2013-03081

88. Zhang W, Xu JH, Yu T, Chen QK. Effects of berberine and metformin on intestinal inflammation and gut microbiome composition in Db/Db mice. *BioMed Pharmacother* (2019) 118:109131. doi: 10.1016/j.biopha.2019.109131

89. Dong C, Yu J, Yang Y, Zhang F, Su W, Fan Q, et al. Berberine, a potential prebiotic to indirectly promote akkermansia growth through stimulating gut mucin secretion. *BioMed Pharmacother* (2021) 139:111595. doi: 10.1016/j.biopha.2021.111595

90. Sun Y, Jin C, Zhang X, Jia W, Le J, Ye J. Restoration of glp-1 secretion by berberine is associated with protection of colon enterocytes from mitochondrial overheating in diet-induced obese mice. *Nutr Diabetes* (2018) 8(1):53. doi: 10.1038/s41387-018-0061-x

91. Wang Y, Shou JW, Li XY, Zhao ZX, Fu J, He CY, et al. Berberine-induced bioactive metabolites of the gut microbiota improve energy metabolism. *Metabolism* (2017) 70:72–84. doi: 10.1016/j.metabol.2017.02.003

92. Gao Z, Yin J, Zhang J, Ward RE, Martin RJ, Lefevre M, et al. Butyrate improves insulin sensitivity and increases energy expenditure in mice. *Diabetes* (2009) 58(7):1509–17. doi: 10.2337/db08-1637

93. Xu X, Gao Z, Yang F, Yang Y, Chen L, Han L, et al. Antidiabetic effects of gegen qinlian decoction *Via* the gut microbiota are attributable to its key ingredient berberine. *Genomics Proteomics Bioinf* (2020) 18(6):721–36. doi: 10.1016/j.gpb.2019.09.007

94. He K, Hu Y, Ma H, Zou Z, Xiao Y, Yang Y, et al. Rhizoma coptidis alkaloids alleviate hyperlipidemia in B6 mice by modulating gut microbiota and bile acid pathways. *Biochim Biophys Acta* (2016) 1862(9):1696–709. doi: 10.1016/j.bbadis.2016.06.006

95. Wang Y, Liu H, Zheng M, Yang Y, Ren H, Kong Y, et al. Berberine slows the progression of prediabetes to diabetes in zucker diabetic fatty rats by enhancing intestinal secretion of glucagon-like peptide-2 and improving the gut microbiota. *Front Endocrinol (Lausanne)* (2021) 12:609134. doi: 10.3389/fendo.2021.609134

96. Vincent RP, Omar S, Ghozlan S, Taylor DR, Cross G, Sherwood RA, et al. Higher circulating bile acid concentrations in obese patients with type 2 diabetes. *Ann Clin Biochem* (2013) 50(Pt 4):360–4. doi: 10.1177/0004563212473450

97. Han K, Bose S, Wang JH, Lim SK, Chin YW, Kim YM, et al. *In vivo* therapeutic effect of combination treatment with metformin and scutellaria baicalensis on maintaining bile acid homeostasis. *PLoS One* (2017) 12(9):e0182467. doi: 10.1371/journal.pone.0182467

98. Gu S, Cao B, Sun R, Tang Y, Paletta JL, Wu X, et al. A metabolomic and pharmacokinetic study on the mechanism underlying the lipid-lowering effect of orally administered berberine. *Mol Biosyst* (2015) 11(2):463–74. doi: 10.1039/c4mb00500g

99. Yao Y, Chen H, Yan L, Wang W, Wang D. Berberine alleviates type 2 diabetic symptoms by altering gut microbiota and reducing aromatic amino acids. *BioMed Pharmacother* (2020) 131:110669. doi: 10.1016/j.biopha.2020.110669

100. Yue SJ, Liu J, Wang AT, Meng XT, Yang ZR, Peng C, et al. Berberine alleviates insulin resistance by reducing peripheral branched-chain amino acids. *Am J Physiol Endocrinol Metab* (2019) 316(1):E73–e85. doi: 10.1152/ajpendo.00256.2018

101. Wang H, Zhang H, Gao Z, Zhang Q, Gu C. The mechanism of berberine alleviating metabolic disorder based on gut microbiome. *Front Cell Infect Microbiol* (2022) 12:854885. doi: 10.3389/fcimb.2022.854885

102. Cui HX, Hu YN, Li JW, Yuan K. Hypoglycemic mechanism of the berberine organic acid salt under the synergistic effect of intestinal flora and oxidative stress. *Oxid Med Cell Longev* (2018) 2018:8930374. doi: 10.1155/2018/8930374

103. Takahara M, Takaki A, Hiraoka S, Adachi T, Shimomura Y, Matsushita H, et al. Berberine improved experimental chronic colitis by regulating interferon-Γ- and il-17a-Producing lamina propria Cd4(+) T cells through ampk activation. *Sci Rep* (2019) 9(1):11934. doi: 10.1038/s41598-019-48331-w

104. Wang S, Xu Z, Cai B, Chen Q. Berberine as a potential multi-target agent for metabolic diseases: A review of investigations for berberine. *Endocr Metab Immune Disord Drug Targets* (2021) 21(6):971–9. doi: 10.2174/1871530320666200910105612

105. Yu Y, Liu L, Wang X, Liu X, Liu X, Xie L, et al. Modulation of glucagon-like peptide-1 release by berberine: *In vivo* and in vitro studies. *Biochem Pharmacol* (2010) 79(7):1000–6. doi: 10.1016/j.bcp.2009.11.017

106. Sun H, Wang N, Cang Z, Zhu C, Zhao L, Nie X, et al. Modulation of microbiota-Gut-Brain axis by berberine resulting in improved metabolic status in high-fat diet-fed rats. *Obes Facts* (2016) 9(6):365–78. doi: 10.1159/000449507

107. Alolga RN, Fan Y, Chen Z, Liu LW, Zhao YJ, Li J, et al. Significant pharmacokinetic differences of berberine are attributable to variations in gut microbiota between africans and Chinese. *Sci Rep* (2016) 6:27671. doi: 10.1038/srep27671

108. Wang L, Zhou GB, Liu P, Song JH, Liang Y, Yan XJ, et al. Dissection of mechanisms of Chinese medicinal formula realgar-indigo naturalis as an effective treatment for promyelocytic leukemia. *Proc Natl Acad Sci U S A* (2008) 105(12):4826–31. doi: 10.1073/pnas.0712365105

109. Xu J, Chen HB, Li SL. Understanding the molecular mechanisms of the interplay between herbal medicines and gut microbiota. *Med Res Rev* (2017) 37(5):1140–85. doi: 10.1002/med.21431

110. Cossiga V, Lembo V, Nigro C, Mirra P, Miele C, D'Argenio V, et al. The combination of berberine, tocotrienols and coffee extracts improves metabolic profile and liver steatosis by the modulation of gut microbiota and hepatic mir-122 and mir-34a expression in mice. *Nutrients* (2021) 13(4):1281. doi: 10.3390/nu13041281

111. Neyrinck AM, Sánchez CR, Rodriguez J, Cani PD, Bindels LB, Delzenne NM. Prebiotic effect of berberine and curcumin is associated with the improvement of obesity in mice. *Nutrients* (2021) 13(5):1436. doi: 10.3390/nu13051436

112. Li H, Liu NN, Li JR, Dong B, Wang MX, Tan JL, et al. Combined use of bicyclol and berberine alleviates mouse nonalcoholic fatty liver disease. *Front Pharmacol* (2022) 13:843872. doi: 10.3389/fphar.2022.843872

113. Li C, Cao H, Huan Y, Ji W, Liu S, Sun S, et al. Berberine combined with stachyose improves glycometabolism and gut microbiota through regulating colonic microrna and gene expression in diabetic rats. *Life Sci* (2021) 284:119928. doi: 10.1016/j.lfs.2021.119928

114. Chen G, Yang X, Yang X, Li L, Luo J, Dong H, et al. Jia-Wei-Jiao-Tai-Wan ameliorates type 2 diabetes by improving B cell function and reducing insulin resistance in diabetic rats. *BMC Complement Altern Med* (2017) 17(1):507. doi: 10.1186/s12906-017-2016-5

115. Chen G, Lu F, Xu L, Dong H, Yi P, Wang F, et al. The anti-diabetic effects and pharmacokinetic profiles of berberine in mice treated with jiao-Tai-Wan and its compatibility. *Phytomedicine* (2013) 20(10):780–6. doi: 10.1016/j.phymed.2013.03.004

116. Yue SJ, Liu J, Wang WX, Wang AT, Yang XY, Guan HS, et al. Berberine treatment-emergent mild diarrhea associated with gut microbiota dysbiosis. *BioMed Pharmacother* (2019) 116:109002. doi: 10.1016/j.biopha.2019.109002

117. Cao Y, Pan Q, Cai W, Shen F, Chen GY, Xu LM, et al. Modulation of gut microbiota by berberine improves steatohepatitis in high-fat diet-fed Balb/C mice. *Arch Iran Med* (2016) 19(3):197–203. doi: 10.1126/scitranslmed.aaf4823

118. Zhu L, Zhang D, Zhu H, Zhu J, Weng S, Dong L, et al. Berberine treatment increases akkermansia in the gut and improves high-fat diet-induced atherosclerosis in apoe(-/-) mice. *Atherosclerosis* (2018) 268:117–26. doi: 10.1016/j.atherosclerosis.2017.11.023

119. Zhang X, Zhao Y, Zhang M, Pang X, Xu J, Kang C, et al. Structural changes of gut microbiota during berberine-mediated prevention of obesity and insulin resistance in high-fat diet-fed rats. *PLoS One* (2012) 7(8):e42529. doi: 10.1371/journal.pone.0042529

120. Xie W, Gu D, Li J, Cui K, Zhang Y. Effects and action mechanisms of berberine and rhizoma coptidis on gut microbes and obesity in high-fat diet-fed C57bl/6j mice. *PLoS One* (2011) 6(9):e24520. doi: 10.1371/journal.pone.0024520

121. Wu C, Zhao Y, Zhang Y, Yang Y, Su W, Yang Y, et al. Gut microbiota specifically mediates the anti-hypercholesterolemic effect of berberine (Bbr) and facilitates to predict bbr's cholesterol-decreasing efficacy in patients. *J Adv Res* (2022) 37:197–208. doi: 10.1016/j.jare.2021.07.011

122. Li M, Shu X, Xu H, Zhang C, Yang L, Zhang L, et al. Integrative analysis of metabolome and gut microbiota in diet-induced hyperlipidemic rats treated with berberine compounds. *J Transl Med* (2016) 14(1):237. doi: 10.1186/s12967-016-0987-5

123. Yang Y, Cao S, Xu W, Zang C, Zhang F, Xie Y, et al. Dual modulation of gut bacteria and fungi manifests the gut-based anti-hyperlipidemic effect of coptidis rhizoma. *BioMed Pharmacother* (2022) 153:113542. doi: 10.1016/j.biopha.2022.113542

124. Sun R, Yang N, Kong B, Cao B, Feng D, Yu X, et al. Orally administered berberine modulates hepatic lipid metabolism by altering microbial bile acid metabolism and the intestinal fxr signaling pathway. *Mol Pharmacol* (2017) 91(2):110–22. doi: 10.1124/mol.116.106617

125. Li F, Jiang C, Krausz KW, Li Y, Albert I, Hao H, et al. Microbiome remodelling leads to inhibition of intestinal farnesoid X receptor signalling and decreased obesity. *Nat Commun* (2013) 4:2384. doi: 10.1038/ncomms3384

126. Hylemon PB, Su L, Zheng PC, Bajaj JS, Zhou H. Bile acids, gut microbiome and the road to fatty liver disease. *Compr Physiol* (2021) 12(1):2719–30. doi: 10.1002/cphy.c210024

127. Tian Y, Cai J, Gui W, Nichols RG, Koo I, Zhang J, et al. Berberine directly affects the gut microbiota to promote intestinal farnesoid X receptor activation. *Drug Metab Dispos* (2019) 47(2):86–93. doi: 10.1124/dmd.118.083691

128. Li S, Wang N, Tan HY, Chueng F, Zhang ZJ, Yuen MF, et al. Modulation of gut microbiota mediates berberine-induced expansion of immuno-suppressive cells to against alcoholic liver disease. *Clin Transl Med* (2020) 10(4):e112. doi: 10.1002/ctm2.112

129. Li D, Zheng J, Hu Y, Hou H, Hao S, Liu N, et al. Amelioration of intestinal barrier dysfunction by berberine in the treatment of nonalcoholic fatty liver disease in rats. *Pharmacogn Mag* (2017) 13(52):677–82. doi: 10.4103/pm.pm_584_16

frontiers | Frontiers in Endocrinology

TYPE Review
PUBLISHED 30 November 2022
DOI 10.3389/fendo.2022.1050709



OPEN ACCESS

EDITED BY
Xinhua Shu,
Glasgow Caledonian University,
United Kingdom

REVIEWED BY
Dr Uma Shanker Navik,
Central University of Punjab, India
Bo Qiao,
Hunan University of Chinese Medicine,
China

*CORRESPONDENCE
Zhaofeng Zeng
13874853548@sohu.com

SPECIALTY SECTION
This article was submitted to
Gut Endocrinology,
a section of the journal
Frontiers in Endocrinology

RECEIVED 22 September 2022
ACCEPTED 28 October 2022
PUBLISHED 30 November 2022

CITATION
Guo K, Xu S and Zeng Z (2022)
"Liver–gut" axis: A target of traditional
Chinese medicine for the treatment of
non-alcoholic fatty liver disease.
*Front. Endocrinol.* 13:1050709.
doi: 10.3389/fendo.2022.1050709



# "Liver–gut" axis: A target of traditional Chinese medicine for the treatment of non-alcoholic fatty liver disease

Kangxiao Guo, Sisheng Xu and Zhaofeng Zeng*

Changsha Health Vocational College, Changsha, Hunan, China

Non-alcoholic fatty liver disease (NAFLD) occurs when fat accumulates in the liver even without excessive alcohol intake. Among the current therapeutic approaches for NAFLD, lifestyle modification with dietary changes and regular exercise is the mainstay treatment. With the rise of intestinal microecology, regulation of the "liver–gut" axis can be an effective treatment for NAFLD. This review aimed to assess the modulation of the liver–gut microbiota axis with traditional Chinese medicine (TCM) as a therapeutic approach to NAFLD and further explored its application in the newly discovered therapeutic avenues beyond NAFLD treatment.

KEYWORDS

**"liver–gut" axis, intestinal microorganisms, traditional Chinese medicine, NAFLD, target**

## Introduction

Non-alcoholic fatty liver disease (NAFLD) is a clinicopathological syndrome with liver histological changes similar to alcoholic liver disease, but without a history of excessive alcohol consumption, including non-alcoholic steatosis (non-alcoholic fatty liver, NAFL) without inflammation and non-alcoholic steatohepatitis (NASH), which is associated with hepatocyte death, inflammation, and fibrosis. NAFL causes NASH, which can further evolve into liver cirrhosis; however, NASH can also sometimes lead to other outcomes. Thirty percent of patients with NASH will develop liver cirrhosis within 5–10 years. Clinical studies have shown that NAFLD is related to diabetes, hypertension, insulin resistance, abnormal liver lipid metabolism, and other factors (1). At present, NAFLD is a global epidemic trend and is one of the reasons for the increase of liver cirrhosis and liver cancer, becoming the world's largest chronic liver disease. In Western countries, especially the United States, NAFLD has become the second leading cause of liver transplantation. However, NAFLD is not endemic to Western countries. With the increasing industrialization in Asian countries, as well as changes in lifestyle and diet, the

prevalence of NAFLD in Asia has continued to increase. Li et al. (2) found that the overall prevalence of NAFLD in Asia was 29.62%. Japan had the lowest prevalence (22.28%), while Indonesia had the highest prevalence (51.04%); the general population of Mainland China had a prevalence of 29.81%. It is worth noting that the prevalence of NAFLD in Asia has been increasing year by year (25.28% in 1999–2005, 28.46% in 2006–2011, and 33.90% in 2012–2017). However, in Asia, there was no significant difference in the prevalence of NAFLD in countries with different income levels (high, upper-middle, and low), and there was no difference in the prevalence of NAFLD between rural and urban populations. Therefore, attention should also be paid to the harm caused by NAFLD in non-affluent areas, the low- and middle-income groups in Asia. In addition to its high prevalence, the harm caused by NAFLD is manifested in the fact that it can lead to liver lesions, including cirrhosis and liver cancer. At present, it is believed that NAFLD may have become another important cause of primary liver cancer after hepatitis B (HBV) and hepatitis C (HCV) virus. The annual incidence of primary liver cancer in the Asian population with NAFLD is 1.8‰, and the all-cause mortality rate is 5.3‰. The all-cause mortality of NAFLD patients can be as high as 7.3‰ (2).

Among the current treatment approaches for NAFLD, lifestyle modification with dietary changes and regular exercise is the mainstay (3), but the treatment effect is often not good and more adverse reactions are reported (4). Although promising therapeutic options targeting mechanisms for patients with NAFLD are available (5), particularly for NASH, none has been approved by the international medical community. Presently, a lot of studies have shown that Chinese medicine, relative to Western medicine, has multi-level and multi-target features, integrity, complex chemical composition, fewer adverse reactions, and a long history; therefore, a lot of scholars believe that the treatment of NAFLD using TCM has certain advantages, as long as clinical syndrome differentiation is correct, which often achieves good effects (6).

The human gut microbiota is a complex ecosystem that comprises a wide variety of bacteria, which total to approximately 1–2 kg in mass (7, 8). The gut microbiota maintains a close relationship with the host, with important roles in vitamin production, the mucosal immune system, and bacterial translocation (9). However, an overall understanding of the gut microbiota, including differences in their composition according to geographical regions, gender, and age, is yet to be established (10, 11). Theoretically, the modulation of the gut microbiota through the administration of antibiotics, probiotics, prebiotics, and symbiotics or through fecal microbiota transplantation (FMT) can be an effective approach to the treatment of NAFLD. Recent studies have released results that support this theory (12, 13).

This review aimed to assess the modulation of the liver–gut microbiota axis with traditional Chinese medicine (TCM) as a therapeutic approach for NAFLD and further explored its application in the newly discovered therapeutic avenues beyond NAFLD treatment.

## The pathogenesis of NAFLD

NAFLD is a clinicopathological syndrome characterized by fatty degeneration of liver parenchymal cells caused by alcohol consumption and other liver damage factors (e.g., drug damage, viral infection, and autoimmunity, among others) (14). Comprehensive diagnosis is mainly made through laboratory and ultrasonic examinations. The specific pathogenesis of NAFLD is presently still unclear. The "second hit" theory originated over the past decade has been widely recognized. The "first hit" is hepatic steatosis caused by insulin resistance (IR). IR refers to the decrease in the sensitivity of insulin-acting target organs to insulin; that is, a normal dose of insulin produces a fraction of the normal biological effect. This state leads to the accumulation of triacylglycerols in the liver and the decline of liver tolerance to internal and external injury factors, such as ischemia and hypoxia. In the second hit, under oxidative stress, inflammatory factors, and endotoxins, among other factors, the liver tissue shows inflammation, fibrosis, and other pathological changes, causing NASH (15). Evidence from the latest medical research has shown that the occurrence of NAFLD may also be related to poor dietary habits. A high-fat diet or large amounts of dietary fructose in the diet can cause IR and hyperleptinemia, which are accompanied by NAFLD (16). Inter-microecological imbalance is also one of the important causes of NAFLD (17). Imbalance in the intestinal flora causes damage to the intestinal mucosal barrier, increases the intestinal mucosal permeability, and induces overgrowth of some intestinal flora, including lipopolysaccharides (LPS), short-chain fatty acids (SCFAs), acetic acid, inflammatory inducers, and other harmful substances, through the intestinal barrier into the blood circulation and to the liver, thus activating the host immune system of cytokines and inflammatory mediators, forming an inflammatory response and affecting the liver (18).

## Effect of the "liver–gut" axis on NAFLD

### "Liver–gut" axis

In 1998, Marshall proposed the concept of the "liver–gut" axis. Since then, the relationship between the gut and the liver has been receiving more attention. Studies have confirmed that the liver–gut axis is an important part of the pathogenesis of NAFLD (5). Their common embryonic origin makes the liver and the intestine closely related in terms of anatomy and biological function, and they communicate through the bile duct, portal vein, systemic circulation, and tight bidirectional

10.3389/fendo.2022.1050709

connection. When the permeability of the intestinal mucosa increases, the barrier function is impaired. A lot of bacteria and endotoxins in the intestinal tract enter the portal vein system. Kupffer cells and hepatic stellate cells in the liver are activated by LPS, the main lipid components of the cell wall of Gram-negative bacteria, and the released inflammatory factors participate in the process of liver disease. These inflammatory factors can cause continuous damage to the liver, such as tumor necrosis factor alpha (TNF-α). Enterohepatic circulation is the communication system between the liver and the gut. Bile acids in the gut are recovered by the liver, secreted into the bile ducts, and then reabsorbed in the gut. Therefore, the balance of bile acids in the body determines the homeostasis of the liver–gut axis (19, 20). As important components in the gut, bile acids can inhibit the overgrowth of intestinal bacteria and affect the composition and quantity of the intestinal flora (21, 22).

## "Liver–gut" axis in non-alcoholic fatty liver disease

The intestinal barrier mainly comprises an immune barrier, mechanical barrier, chemical barrier, and biological barrier (as shown in Figure 1). The biological barrier is mainly composed of intestinal microorganisms, and these intestinal microorganisms continuously form a complex and stable microecology with the growth and development of the human body (23). The gut microbial ecosystem includes bacteria, fungi, and viruses, among others, which, together, play a role in food digestion, nutrient absorption, immune regulation, and tumor suppression, which are of great significance to maintaining the intestinal epithelial barrier function. Under the condition of stable balance, the intestinal microecology maintains the coordinated operation of the body's organ functions. When the composition, quantity, metabolic activity, and the distribution of intestinal microbes change under different nutritional, immune, and environmental conditions, this will trigger the body's chronic inflammatory response and even lead to a series of diseases (24).

In terms of anatomical structure and physiological function, the relationship between the liver and the intestine is inseparable. The nutrients absorbed in the intestine can be transported into the liver from the portal system through the blood, and the bile acids and other biologically active substances synthesized in the liver can also be secreted into the intestine for metabolism, thereby inhibiting the overgrowth of intestinal bacteria. When there is imbalance in the intestinal flora, the intestinal mucosal barrier is damaged and the permeability is increased. Bacteria, endotoxins, and metabolites enter the liver through the portal vein, resulting in impaired liver function; the liver then releases a series of inflammatory factors, which in turn cause intestinal damage (Figure 2). Yuan et al. (25) established a mouse model by strain colonization and FMT and found that *Klebsiella pneumoniae*, which produces a large amount of alcohol, can induce mitochondrial damage, impair the intestinal mucosal function, aggravate liver inflammation, and lead to the development of NAFLD. Another study compared the fecal flora of healthy groups and patients with NAFLD and observed changes in the diversity and composition of the flora, with increased proportion of Bacteroidetes and a decreased abundance of Firmicutes (26). In a study of the intestinal microbiota of 37 patients with NAFLD, Jasirwan et al. (27) found that Firmicutes, Bacteroidetes, and Proteobacteria were

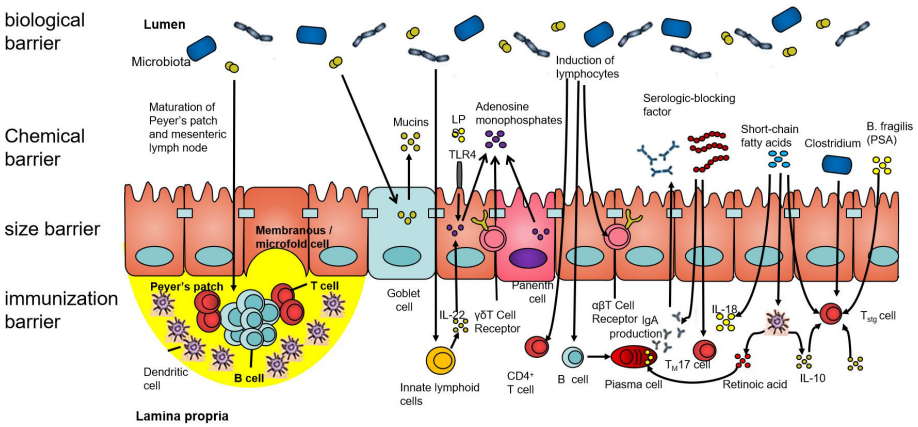


FIGURE 1
The intestinal barrier. The human intestinal tract is an important organ for the digestion and absorption of the nutrients in food. It is also a congenital barrier that maintains the balance of the intestinal environment and effectively prevents pathogenic microorganisms, their metabolites, and sensitizing substances. The intestinal barrier is composed of the biological barrier, chemical barrier, size barrier, and immunization barrier. All four barriers have different characteristics, among which, the structure of the intestinal flora forms an interdependent microbial system and interacts with other microorganisms. Its ecological balance forms the biological barrier of the human gut.

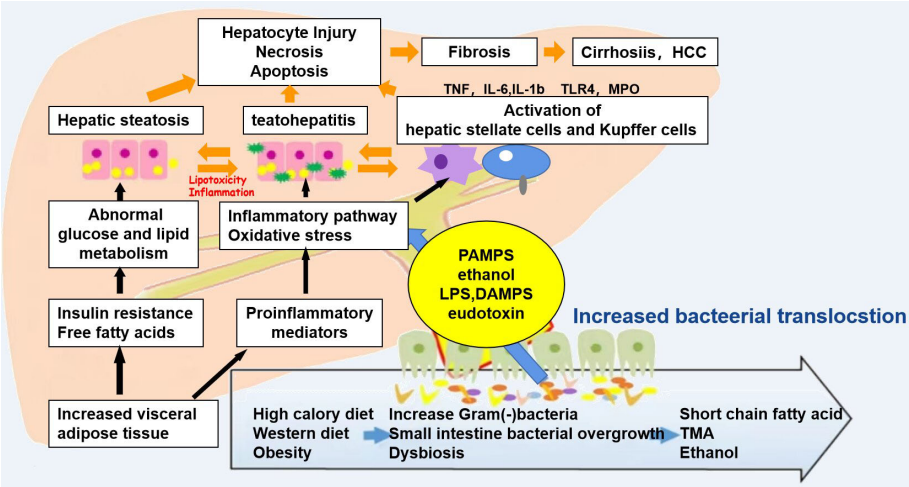


FIGURE 2
Mechanisms associated with the pathophysiology of non-alcoholic fatty liver disease (NAFLD). Diet and obesity lead to prominent changes in the microbiota, which induce intestinal bacterial overgrowth, dysbiosis, intestinal permeability, bacterial translocation, and endotoxemia, resulting in the development of NALFD.

the predominant phyla. *Bacteroides* was more dominant than *Prevotella*, contrary to the results of previous studies on healthy populations in Indonesia. Microbiota dysbiosis was observed in most of the samples. The diversity of the gastrointestinal microbiota was significantly decreased in patients with NAFLD, high triglyceride levels, and central obesity. The Firmicutes/Bacteroidetes ratio was correlated with steatosis and obesity, whereas some of the other species in the lower taxonomy levels were mostly associated with steatosis and obesity without fibrosis. Proteobacteria was the only phylum strongly correlated with fibrosis in patients with an average body mass index. Certain gut microbes were correlated with fibrosis and steatosis. Philips et al. (28) found that the gut microbiota has a significant impact on NAFLD. Their study performed fecal transplantation in eight patients with steroid-resistant alcoholic hepatitis. It was found that the overall survival of patients who received a fecal transplant was 87.5%, while that of patients who did not receive a fecal transplant was 33.3%. One year after transplantation, bowel deformation was observed. A decrease in *Bacillus* and an increase in Firmicutes were found. Studies have shown that *Bifidobacterium* and *Lactobacillus* strains may have different effects on NAFLD and that some *Bifidobacterium* species may have protective effects in the development of NAFLD, NASH, and obesity (29). The genus *Bifidobacterium* can be considered as one of the targets for NAFLD treatment using intestinal microecology. Huang et al. fed Sprague–Dawley (SD) rats with a high-fat diet for 12 weeks to establish an NAFLD model. The study found that the liver tissue of NAFLD model rats was grayish yellow, with obvious fatty lesions, and increased cholesterol/low-density lipoprotein (LDL) cholesterol ratio and alanine (30). The activity of alanine aminotransferase (ALT) in the NAFLD group was significantly higher than that in the normal group ($p < 0.01$). The DNA of the cecal mucosa was extracted, and 16S rDNA high-throughput Illumina sequencing was used to analyze the intestinal flora of NAFLD rats. The results showed that the alpha diversity indices $S_{obs}$ (observed species index), Chao, Ace and Shannon of the normal group flora were all significantly higher than those of the NAFLD model group. In the comparisons at the bacterial phylum level, the ratio of Firmicutes/Bacteroidetes in the normal group was shown to be significantly higher than that in the NAFLD model group ($p < 0.05$), while the proportion of Verrucomicrobia in the NAFLD model group was significantly increased. Comparisons at the bacterial genus level revealed that the intestinal lactobacilli in the NAFLD model group were significantly lower than those in the normal group. This study showed that NAFLD rats developed dysbacteriosis and had a decreased number of beneficial intestinal bacteria. Some studies have also found that lipid metabolism disorders can induce an imbalance in the intestinal flora, which in turn can exacerbate lipid metabolism disorders, both of which are closely related to the occurrence and development of fatty liver (31). Ley et al. (32) found that two different diets resulted in intestinal microbiological changes related to obesity and IR. IR is an important feature of NAFLD, which can be improved by antibiotic treatment (33). However, intestinal symbiotic bacteria are also very important. The study found that the severity of experimental liver fibrosis in sterile mice worsened (34). After the mice were administered small doses of antibiotics, their intestinal microbiota changed and the contents of intestinal SCFAs and cholesterol significantly increased, thus changing the fatty acid and cholesterol

metabolism of the liver (35). Intestinal flora disorder can also directly affect the levels of fat factors, pro- and anti-inflammatory factors, and fat oxidation factors, thereby affecting liver metabolism and promoting liver damage (36).

# Progress in TCM treatment of NAFLD based on the regulation of the "liver–gut" axis

## Association between traditional Chinese medicine "liver and spleen theory" and "liver–gut" axis function

TCM believes that the liver belongs to wood and the spleen belongs to earth. The qi of the spleen can fill the qi and blood metaplasia and nourish the liver. Diseases of the liver transmit diseases to the spleen through the meridians, and damage in the spleen will affect the function of the liver (37). Emotional insufficiency blocks the qi movement, affecting the operation of the body's qi, blood, and body fluids, and the liver qi stagnation accumulates for a long time. Liver stagnation and spleen deficiency are each other's cause and effect. The transportation and transformation of the spleen depends on the normal function of the liver to disperse and relieve the spleen. Therefore, many doctors have advocated the treatment of NAFLD from the perspective of the liver and spleen, with regulation of the liver and spleen as the basic treatment method. Regulation of the liver also includes soothing it, promoting blood circulation, and promoting qi, while regulation of the spleen includes strengthening it, resolving phlegm and damp. The "Consensus on the diagnosis and treatment of non-alcoholic fatty liver diseases" pointed out that NAFLD is located in the liver and involves the spleen, stomach, and other organs. The main clinical symptoms of NAFLD include liver depression and spleen deficiency, damp-turbid internal stop, damp-heat accumulation, and phlegm and blood stasis syndrome, among others. During the development of the disease, spleen deficiency is the basic pathogenesis, as well as liver stagnation and spleen deficiency, phlegm turbidity, and internal accumulation of damp-heat, finally leading to a phlegm–damp–blood stasis inter-association. NAFLD is caused by fat deposits in the liver. Liver stagnation leads to spleen deficiency, and in the etiology and the pathological products of these syndromes, phlegm and dampness are produced by the lack of water dampness. In the final analysis, it is still a dysfunction of the spleen (38). The spleen transports and transforms water dampness. Deficiency of the spleen can lead to the lack of internal water dampness, which then leads to dampness accumulation into phlegm, and water dampness and phlegm-drinking block the normal operation of the blood. If there is luck on the side, with qi and blood circulation, this accumulation will disappear. This shows the importance of strengthening the spleen in the treatment of NAFLD.

From the perspective of modern medicine, the "spleen" in TCM theory performs the "gastrointestinal" function in the narrow sense of modern anatomy. In terms of function, the spleen, the small intestine, and the large intestine are related. The spleen is responsible for promoting clearness and transporting and transforming water and moisture, while the small intestine receives water and grains from the five internal organs and is also responsible for the secretion of clear turbidity. The large intestine, on the other hand, is responsible for conducting dregs and further absorbing body fluids. Research on the internal relationship between the "spleen and stomach–turbid poison" and the "intestinal bacteria–metabolic syndrome" has put forward the theory that, although the intestinal microecology is anatomically located in the intestine, its function belongs to the spleen (39). The liver–gut axis is proposed in modern medicine. It is believed that the intestinal barrier function is damaged, the intestinal bacteria are translocated, endotoxins enter the portal system, the immune mechanism in the liver is activated, and a large number of inflammatory factors are released, thereby causing injury in the intestinal mucosa and other organs. It can be seen through the liver–gut axis that the gut and the liver are closely related in anatomy and function, that they influence each other, and they affect the process of liver disease.

## Modern research on traditional Chinese medicine in the treatment of NAFLD based on the "liver–gut" axis

A large number of studies (12, 40, 41) have confirmed that TCM has a positive effect on the regulation of the intestinal flora, and the destruction of the intestinal microecosystem will lead to digestive disorders, poor digestion, and damage to the microecology, further leading to digestive disorders, indigestion, anorexia, and other symptoms, consistent with the liver and kidney syndrome. The use of TCMs for strengthening the spleen and dispelling dampness, such as Chinese yam, *Poria*, *Codonopsis*, and *Coix* seed, improves the spleen and stomach deficiency syndrome. Certain components of TCM can play a role in the prevention and treatment of NAFLD by improving the intestinal barrier function. Wang et al. (42) found that the *Ophiopogon japonicus* polysaccharide MDG-1 improved NAFLD in mice fed a high-fat diet by regulating the gut microbiota and hepatic lipid metabolism. Zhang et al. (43) showed that berberine can reduce liver inflammation and lipid deposition in NAFLD mice, which may be related to its role in

regulating the intestinal flora. Qi et al. (44) also discovered that berberine hydrochloride can repair the intestinal mechanical barrier function of NAFLD rats and alleviate the steatosis of the liver caused by NAFLD. With the deepening of research on TCM compounds, many of these compounds based on the "liver and spleen theory" have been proven to be able to treat NAFLD by regulating the intestinal barrier. Fang (45) found that Dahuang Zexie Decoction reduced the level of pathogenic bacteria in the intestine of NAFLD rats, thereby reducing the production of LPS, regulating the function of the intestinal mechanical barrier, and improving the inflammation and lipid deposition of the liver. Cui et al. (46) believed that Xiaozhi Yigan Decoction may reduce the liver damage caused by the LPS/TLR4 pathway by improving the intestinal microbial barrier in NAFLD rats. Liver fibrosis is a serious stage in the progression of NAFLD. Chen et al. (47) found that Xiaoyao powder can improve liver fibrosis and restore part of the intestinal flora structure. Removing the spleen-invigorating drugs in the prescription weakens the effect of Xiaoyao powder on the spleen. For liver protection, Shenling Jianpiwei granules have the effect of strengthening the spleen and soothing the liver; moreover, it can reduce the expression of UCP-2 and Cytb in the liver of NAFLD mice, improve the inflammatory response and function of the liver, and protect the liver (48, 49).

In clinical practice, TCM and compound prescriptions are usually boiled in water, and the liquid formulation enters the human gastrointestinal tract after oral administration. Most of the effective ingredients are absorbed in the intestinal tract and react with intestinal microorganisms. The mechanisms of TCM compounds in NAFLD are summarized in Table 1. Yang et al. (50) believed that the intestinal flora including *Bifidobacterium*, *Eubacterium*, *Enterococcus*, and *Escherichia* are involved in the metabolism of saponins, a class of important active ingredients contained in TCMs such as ginseng and *Panax notoginseng*, and

TABLE 1 Mechanisms of Chinese medicine compounds in non-alcoholic fatty liver disease (NAFLD).

| Chinese medicine compound | Drug composition | Related findings |
|---|---|---|
| Liver fat-soluble particles | Astragalus, pueraria, cassia, rhubarb, orange shade, *Salvia miltiorrhiza*, seaweed, Ze diarrhea | Enhanced hepatic PPAR-α mRNA expression and decreased hepatic TNF-α expression |
| Eliminate turbidity and protect the liver | *Bupleurum*, red peony, white peony root, *Fructus aurantii*, xiong, licorice, *Salvia miltiorrhiza*, hawthorn, Ze diarrhea, peach kernel, safflower, gold, tylo, *Angelica*, green calyx plum | Reduced the levels of TNF-α, TNF-$\beta_1$, and CYP2E1 in liver tissues |
| Add flavor to Ze diarrhea soup | Add flavor to Ze diarrhea soup | Inhibited the expression of the TLR4/NF-κB and MAPK pathway and MyD88, NF-κB p65, phospho-p65, p38 MAPK, and phospho-p38 proteins |
| Mercy mushroom fat oil | Mountain Ci mushroom, *Pinellia*, *Poria cocos*, *Bupleurum*, *Salvia miltiorrhiza*, *Coix* seed, *Scutellaria baicalensis*, Ze diarrhea, Chinese wolfberry, hawthorn | Regulated the JNK signaling pathway and downregulated caspase-8, FasL, and phospho-c-Jun mRNA and protein expressions |
| Small trapped chest soup cutting | Yellow tis, *Pinellia*, *Trichosanthes*, wood, turmeric | Downregulated GRP78 and caspase-12 protein expression |
| Tonifying kidney and reducing turbidity | Barbary wolfberry, virgin, *Polygonum multiflorum*, *Poria cocos*, Ze diarrhea, *Coix* seed, reed root, yam, yellow essence, Yin Chen, defeated sauce grass, licorice | Inhibited the JNK signaling pathway and decreased the JNK1, p-JNK, and p-IRS-1 protein expression |
| Taste water and water two elixir | Golden cherry, Gordon euryale, chinensis, astragalus | Increased the IRS-1 mRNA expression |
| Ginseng Ling spleen and stomach particles | North sand ginseng, *Poria cocos*, *Atractylodes*, Chinese yam, lentils, lotus seed, amomum of sand, tangerine peel, *Coix* seed, licorice | Regulated serum and hepatic TNF-α levels and decreased $UCP_2$ and Cytb expression |
| Attached son rational soup | Ginseng, *Atractylodes*, licorice, dried ginger, aconite | The expression of TNF-α and IL-6 in SREBP-1c and FASN was down regulated |
| Liver corning | White snake grass, potted grass, knotweed, chinensis chinensis, *Bupleurum*, ginseng, tylo, *Salvia miltiorrhiza*, yu gold, notoginseng, green wood fragrance, licorice | Reduced the MDA and increased SOD activity |
| Add linglingshu soup | *Poria cocos*, cassia branch, *Atractylodes*, Dangshen, pinellia, hawthorn, herb grass, safflower, chuanxiong, *Polygonum multiflorum*, licorice | Upregulated the expression of AdipoR2 and PPAR-α |
| Protection of liver fat tablets | Ze diarrhea, hawthorn, lotus leaf, puhuang, notoginseng, tangerine peel | Reduced the Firmicutes/Bacteroidetes ratio and promoted the expression of claudin-1 and ZO-1 proteins |
| Lipid-lowering liver soup | Jersey diarrhea, cassia seed, *Salvia miltiorrhiza*, yu gold, seaweed, lotus leaves | decreased APN, TNF-α and regulated occludin and ZO- 1 protein levels |

FASN, fatty acid synthase; MDA, malondialdehyde; SOD, superoxide dismutase; APN, adiponectin.

these substances, after the glycosylation of saponins, showed high bioavailability and biological activity. Luo et al. (51) found that rhubarb granules increased the abundance of *Bifidobacterium*, decreased *Enterobacterium* and *Enterococcus*, regulated the intestinal microecological balance, increased the expression of tight junction proteins and blocking proteins in the intestinal mucosa, and reduced enterogenous toxins such as indophenol sulfate. Xu et al. (52) collected cases of NAFLD with damp-heat accumulation. After treatment with modified Yinchen Wuling powder, the authors detected changes in the intestinal flora. The abundance of enterobacteria and *Staphylococcus* decreased, while *Bacteroides*, *Bifidobacterium*, and *Lactobacillus* increased. Yuan et al. (53) revealed that intervention with Guizhi Decoction improved high-fat diet guidance. The intestinal flora of apolipoprotein E (ApoE) knockout mice was unbalanced. After 4 weeks of treatment, the structure of the intestinal flora changed; *Bacteroides* and *Micrococcus verrucosus* increased, while the proportion of *Firmicum* decreased. Kang et al. (54) found that, in rats fed ginseng polysaccharide for a long time, butyric acid-producing bacteria such as chlamydia significantly increased, and the content of SCFAs generated in the colon of rats also significantly increased.

SCFAs are a class of important metabolites produced by specific colonic anaerobes in the intestine after fermenting dietary fiber and resistant starch, mainly including acetic acid, propionic acid, and butyric acid. As important energy sources and signal molecules, SCFAs primarily transmit signals by inhibiting histone deacetylase and G-protein-coupled receptors (55). After the TCM enters the intestine, intestinal microorganisms will decompose and are utilized to generate a large number of SCFAs (Figure 3). On the one hand, SCFAs can be absorbed into the blood through monocarboxylate transporters (MCTs) on intestinal epithelial cells to reach the fat, liver, and other tissues and combine with receptors on target tissues to promote fat decomposition. On the other hand, SCFAs can also stimulate intestinal endocrine cells to secrete intestinal hormone glucagon peptide 1 and casein to reach the brain, pancreas, and other tissues, inhibiting appetite and energy intake (56). SCFAs can also play an anti-inflammatory role by regulating the chemotaxis of immune cells, the release of reactive oxygen species, and the number and function of intestinal regulatory T cells (Tregs) (57). Moreover, as the main energy source of intestinal epithelial cells, SCFAs can promote the proliferation and differentiation of epithelial cells, reduce cell apoptosis, promote mucin secretion, increase intestinal cross-epithelial resistance and tight connection, and reduce the intestinal mucosal permeability, thereby enhancing the intestinal epithelial barrier function, inhibiting intestinal pathogenic bacteria and intestinal endotoxin LPS from entering the body, and reducing the inflammatory response of body tissues (58). Guo et al. (59) found that the plasma LPS level was significantly negatively correlated with the content of intestinal SCFAs and that Dengzhan Shengmai could improve the intestinal barrier function by increasing SCFAs, which inhibit the entry of intestinal endotoxin LPS into the body, thereby inhibiting the activation of the liver TLR4/NF-κB inflammatory signaling pathway caused by the increase of LPS in mice fed a high-fat diet. Wang et al. (60) confirmed that *Polygonum multiflorum* could regulate the content of SCFAs in the intestine, promote the suitability of SCFAs entering the liver through portal circulation, reduce the accumulation of lipids in

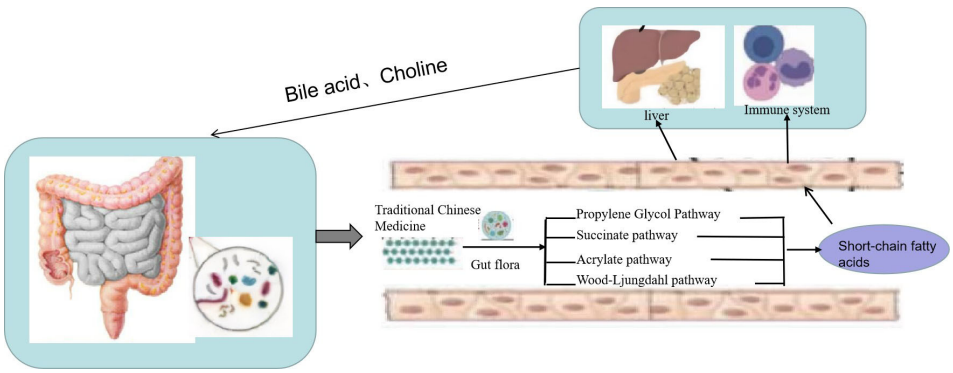


FIGURE 3
Traditional Chinese medicine (TCM) prevents non-alcoholic fatty liver disease (NAFLD) through the "liver–gut" axis. TCM enters the intestine, and intestinal microorganisms will decompose and are utilized to generate a large number of short-chain fatty acids (SCFAs). On the one hand, SCFAs can be absorbed into the blood through monocarboxylate transporters (MCTs) on intestinal epithelial cells to reach the fat, liver, and other tissues and combine with receptors on target tissues to promote fat decomposition. On the other hand, SCFAs can also stimulate intestinal endocrine cells to secrete intestinal hormone glucagon peptide 1 and casein to reach the brain, pancreas, and other tissues to inhibit appetite and energy intake.

liver cells, organize intestinal endotoxin translocation, and effectively protect against NAFLD.

## Future perspectives

The homeostasis of the intestinal flora plays a crucial role in the maintenance of human health (61), and disturbance in the intestinal flora is closely associated with many diseases (62). At present, more and more studies have been performed on the effects of TCM on the liver–gut axis, but current research is still limited. The relationship between TCM syndromes of fatty liver and the liver–gut axis, elucidating the effect and mechanism of TCM on the intestinal flora and intestinal homeostasis, can provide a new research direction for elucidating the mechanism of TCM to provide a new research direction for clarifying the mechanism of action of traditional Chinese medicine. In addition, because the latest biotechnology can be used to detect the intestinal flora, this can improve the level of research on TCM, promote its modernization (63), and provide new ideas for the prevention and treatment of NAFLD.

## Author contributions

KG drafted the manuscript. SX researched a lot of information. ZZ critically revised the initial manuscript. All authors contributed to manuscript revision and read and approved the submitted version

## Funding

This study was supported by grants from the Natural Science Foundation of Changsha (kq2202061) and funding from Changsha Science and Technology Bureau.

## Conflict of interest

The authors declare that the research was conducted in the absence of any commercial or financial relationships that could be construed as a potential conflict of interest.

## Publisher's note



## References

1. Luis CB, Leon AA. The natural course of non-alcoholic fatty liver disease. *Int J Mol Sci* (2016) 17(5):774. doi: 10.3390/ijms17050774

2. Li J, Zou BY, Hui YY. Prevalence, incidence, and outcome of non-alcoholic fatty liver disease in Asia 1999-2019: a systematic review and meta-analysis. *Lancet Gastroenterol &Hepatology* (2019) 4(5):389–98. doi: 10.1016/S2468-1253(19)30039-1

3. Sanyal AJ, Chalasani N, Kowdley KV, McCullough A, Diehl AM, et al. Pioglitazone, vitamin e, or placebo for nonalcoholic steatohepatitis. *N Engl J Med* (2010) 362(18):1675–85. doi: 10.1056/NEJMc1006581

4. Guo HY, Yang HR, Cui GT, Fang NY, Deng LN, Qiao F. Clinical observation of non-alcoholic fatty liver disease (liver depression and spleen deficiency syndrome). *Bright traditional Chin Med* (2019) 34(10):1520–2. doi: 10.13935/j.cnki.sjzx.210829

5. Chassaing B, Etienne-Mesmin L, Gewirtz AT. Microbiota-liver axis in hepatic disease. *Hepatology* (2014) 59(1):328–39. doi: 10.1002/hep.26494

6. Wang J. Progress in TCM treatment of non-alcoholic fatty liver disease. *Med Theory Pract* (2017) 30(12):1747–9.

7. Brandl K, Kumar V, Eckmann L. Gut-liver axis at the frontier of host-microbial interactions. *Am J Physiol Gastrointest Liver Physiol* (2017) 312(5):G413–9. doi: 10.1152/ajpgi.00361.2016

8. Turnbaugh PJ, Hamady M, Yatsunenko T, Cantarel BL, Duncan A, Ley RE, et al. A core gut microbiome in obese and lean twins. *Nature* (2009) 457 (7228):480–4. doi: 10.1038/nature07540

9. Vrieze A, Van Nood E, Holleman F, Salojärvi J, Kootte RS, Bartelsman JF, et al. Transfer of intestinal microbiota from lean donors increases insulin sensitivity in individuals with metabolic syndrome. *Gastroenterology* (2012) 143(4):913–916 e917. doi: 10.1053/j.gastro.2012.06.031

10. Larsen N, Vogensen FK, Berg FW, Nielsen DS, Andreasen AS, Pedersen BK, et al. Gut microbiota in human adults with type 2 diabetes differs from non-diabetic adults. *PloS One* (2010) 5(2):e9085. doi: 10.1371/journal.pone.0009085

11. Boursier J, Diehl AM. Implication of gut microbiota in nonalcoholic fatty liver disease. *PloS Pathog* (2015) 11(1):e1004559. doi: 10.1152/ajpgi.00118.2019

12. He L, Liu YW, Guo YF, Hui HY, Tan ZJ. Diversity of intestinal bacterial lactases gene in antibiotics-induced diarrhea mice treated with Chinese herbs compound qi wei bai Zhu San. *3 Biotech* (2018) 8(1):4. doi: 10.1007/s13205-017-1024-y

13. Hui HY, Wu Y, Zheng T, Zhou SN, Tan ZJ. Bacterial characteristics in intestinal contents of antibiotic-associated diarrhea mice treated with qiweibaizhu powder. *Med Sci Monit* (2020) 13(26):e921771. doi: 10.12659/MSM.921771

14. Suk KT, Kim MY, Baik SK, Gao B, Gual A, Lackner C, et al. Alcoholic liver disease: treatment. *World J Gastroenterol* (2014) 20(36):12934–44. doi: 10.1038/s41572-018-0014-7

15. Huang ZX, Yang MF, Yang Z, Yang YR, Wang FY. Correlation between intestinal inflammation and intestinal flora imbalance in patients with nonalcoholic fatty liver disease. *J Med Postgraduates* (2021) 34(05):482–5. doi: 10.16571/j.cnki.1008-8199.2021.05.007

16. Guo L, Tang LQ. Progress in the pathogenesis and treatment of non-alcoholic fatty liver disease. *Life Sci* (2018) 30(11):1165–72. doi: 10.16286/j.1003-5052.2022.04.028

17. Albillos A, de Gottardi A, Rescigno M. The gut-liver axis in liver disease: Pathophysiological basis for therapy. *J Hepatol* (2020) 72(3):558–77. doi: 10.1016/j.jhep

18. Herbert T, Timon EA, Alexander RM. Multiple parallel hits hypothesis in nonalcoholic fatty liver Disease:Revisited after a decade. *Hepatology* (2021) 73 (2):833–42. doi: 10.1002/hep.31518

19. Miura K, Ohnishi H. Role of gut microbiota and toll-like receptors in nonalcoholic fatty liver diseas. *World J Gastroenterol* (2014) 20(23):7381–91. doi: 10.3748/wjg.v20.i23.7381

20. Yang YH, Qin LM, Zhu XP, Yang XF. Mechanism of bile acid receptor mediated regulation of intestinal barrier function by bile acid. *Guangdong Animal Husbandry Veterinary Sci Technol* (2022) 47(04):47–54. doi: 10.19978/j.cnki.xmsy.2022.04.09

21. Li X, Peng XX, Guo KX, Tan ZJ. Bacterial diversity in intestinal mucosa of mice fed with dendrobium officinale and high-fat diet. *3 Biotech* (2021) 11(1):22. doi: 10.1007/s13205-020-02558-x

22. Guo KX, Xu SS, Zhang QL, et al. Bacterial diversity in the intestinal mucosa of mice fed with asparagus extract under high-fat diet condition. *3 Biotech* (2020) 10(5):228. doi: 10.1007/s13205-020-02225-1

23. He YS, Tang Y, Peng MJ, Peng MJ, Yang ZY, Li WG, et al. Influence of debaryomyces hansenii on bacterial lactase gene diversity in intestinal mucosa of mice with antibiotic-associated diarrhea. *PloS One* (2019) 14(12):e022580. doi: 10.1371/journal.pone.022580

24. Long CX, Liu YW, He L, Yu R, Li DD, Tan ZJ, et al. Bacterial lactase genes diversity in intestinal mucosa of dysbacterial diarrhea mice treated with qiweibaizhu powder. *3 Biotech* (2018) 8(10):423. doi: 10.1007/s13205-018-1460-3

25. Yuan J, Chen C, Cui J, Lu J, Yan C, Wei X, et al. Fatty liver disease caused by high-alcohol-producing klebsiella pneumoniae. *Cell Metab* (2019) 30(6):1172. doi: 10.1016/j.cmet.2019.08.018

26. Wang B, Jiang X, Cao M, Ge JP, Bao QL, Tang LL, et al. Altered fecal microbiota correlates with liver biochemistry in nonobese patients with non-alcoholic fatty liver disease. *Sci Rep* (2016) 6:32002. doi: 10.1038/srep32002

27. Jasirwan COM, Murad A, Hasan I, Simadibrata M, Rinaldi I. Correlation of gut Firmicutes/Bacteroidetes ratio with fibrosis and steatosis stratified by body mass index in patients with non-alcoholic fatty liver disease. *Biosci Microbiota Food Health* (2021) 40(1):50–8. doi: 10.12938/bmfh.2020-046

28. Philips CA, Pande A, Shasthry SM, Jamwal KD, Khillan V, Chandel SS, et al. Healthy donor fecal microbiota transplantation in steroid-ineligible severe alcoholic hepatitis: A pilot study. *Clin Gastroenterol Hepatol* (2017) 15(4):600–2. doi: 10.1016/j.cgh.2016.10.029

29. Nobili V, Putignani L, Mosca A, Chierico FD, Vernocchi P, Alisi A, et al. Bifidobacteria and lactobacilli in the gut microbiome of children with non-alcoholic fatty liver disease: Which strains act as health players. *Arch Med Sci* (2018) 14(1):81–7. doi: 10.5114/aoms.2016.62150

30. Huang HL, Zhou YJ, Zheng CY, Nie YQ, Du JL. Changes and significance of intestinal microbiota in rats with non-alcoholic fatty liver disease [J]. *Guangdong Medicine,37* (2016) 9):1283–6. doi: 10.13820/j.cnki.gdyx.20160503.005

31. Ma CL. Effect of Lactobacillus casei on intestinal flora and lipid metabolism in high-fat diet hamsters and its mechanism. *Chinese Acad Agricultural Sci* (2021) 1 (04):114. doi: 10.27630/d.cnki.gznky.2020.000149

32. Ley RE, Turnbaugh PJ, Klein S, Gordon JI. Microbial ecology:human gut microbes associated with obesity. *Nature* (2006) 444(7122):1022–3. doi: 10.1038/4441022a

33. Janssen AWF, Houben T, Katiraei S, Dijk W, Boutens L, Bolt N, et al. Modulation of the gut microbiota impacts nonalcoholic fatty liver disease: a potential role for bile acids. *J Lipid Res* (2017) 58(7):1399–416. doi: 10.1194/jlr.M075713

34. Mazagova M, Wang L, Anfora AT, Wissmueller M, Lesley S A, Miyamoto Y, et al. Commensal microbiota is hepatoprotective and prevents liver fibrosis in mic. *FASEB J* (2015) 29(3):1043–55. doi: 10.1096/fj.14-259515

35. Cho I, Yamanishi S, Cox L, Methé B A, Zavadil J, Li K, et al. Antibiotics in early life alter the murine colonic microbiome and adiposity. *Nature* (2012) 488 (7413):621–6. doi: 10.1038/nature11400

36. Torres S, Fabersani E, Marquez A, Gauffin-Cano P. Adipose tissue inflammation and metabolic syndrome.The proactive role of probiotics. *Eur J Nutr* (2019) 58(1):27–43. doi: 10.1007/s00394-018-1790-2

37. Zhang CY, Liu TH, Wang W. On intestinal microenvironment is an important biological basis for treating liver disease from the spleen. *Chin J Traditional Chin Med* (2019) 34(7):2877–80.

38. Ma Q, Shi AH, Zhao Q, Chen WL. Research progress in the prevention and treatment of nonalcoholic fatty liver disease by regulating mitochondrial function with traditional Chinese medicine. *Chinese Journal of Traditional Chinese Medicine* (2022) 47(19):5113–20. doi: 10.19540/j.cnki.cjcmm.20220704.601

39. Wu YN, Zhang L, Chen T, Li X, Liu GX. Research progress in the relationship between human intestinal microecology and liver immunity. *Chinese Journal of Microbiology* (2019) 33(02):227–30. doi: 10.13381/j.cnki.cjm.202102021

40. Li C, Zhou K, Xiao N, Peng MJ, Tan ZJ. The effect of qiweibaizhu powder crude polysaccharide on antibiotic-associated diarrhea mice is associated with restoring intestinal mucosal bacteria. *Front Nutr* (2022) 9:952647. doi: 10.3389/fnut.2022.952647

41. Long CX, He L, Guo YF, Liu YW, Xiao NQ, Tan ZJ. Diversity of bacterial lactase genes in intestinal contents of mice with antibiotics-induced diarrhea. *World J Gastroenterol* (2017) 23(42):7584–93. doi: 10.3748/wjg.v23.i42.7584

42. Wang X, Shi LL, Wang XP, Feng Y, Wang Y. MDG-1, an ophiopogon polysaccharide, restrains processof non-alcoholic fatty liver disease *via* modulating the gut-liver axis. *Int J Biol Macromol* (2019) 141:1013–21. doi: 10.1016/j.ijbiomac.2019.09.007

43. Yu ZH, Biao YN, Zhang MQ, Liu CX, Liu ZX, Han YL, et al. Study on the correlation between the effect of Danggui Shaoyao Powder on the prevention and treatment of nonalcoholic fatty liver and intestinal microecology. *Hebei Journal of Traditional Chinese Medicine* (2021) 36(04):1–5. doi: 10.16370/j.cnki.13-1214/r.2021.04.001

44. Qi SF. *Effect of berberine hydrochloride on intestinal flora in rats with nonalcoholic fatty liver disease*. (Shijiazhuang: Hebei Medical University) (2017).

45. Fang J. *Research on the mechanism of treating NAFLD treatment based on the influence of intestinal flora on the mechanical barrier of intestinal mucosa*. (Nanjing: Nanjing University of Traditional Chinese Medicine) (2018).

46. Cui X. *The mechanism of lipid-beneficial liver prescription prevention and treatment of high-fat diet-induced nonalcoholic fatty liver disease in rats*. (Wuhan: Hubei University of Traditional Chinese Medicine) (2017).

47. Miao J, Cui HT, Wang L, Guo LYWang J, Li P. Effects of evodiamine on carbon tetrachloride-induced liver fibrosis mice based on modulating gut microbiota. *Chinese Journal of Labor Hygiene and Occupational Diseases* (2021) 39(6):401–6. doi: 10.3760/CMA.J.CN121094-20201204-00666

48. Wang CH, Tao QM, Wang XH, Wang XR, Zhang XY. Impact of high-fat diet on liver genes expression profiles in mice model of nonalcoholic fatty liver disease. *Environmental Toxicology and Pharmacology* (2016) 45:52–62. doi: 10.1016/j.etap.2016.05.014

49. Yang HY, Ge S. Effects of dietary fiber on obesity related intestinal microecology. *Chinese food and nutrition* (2020) 26(9):12–6. doi: 10.19870/j.cnki.11-3716/ts.20200713.002

50. Yang C, Liu ZD, Song Y, Li JB. Research progress of TCM intervention in gut microflora for prevention and control of diabetes. *Chin J Exp Prescription Med* (2021) 27(7):219–27. doi: 10.19763/j.cnki.2096-7403.2021.04.15

51. Prasath LA, Mohammed AZ, Badreldin HA Annalisa T. The influence of the prebiotic gum acacia on the intestinal microbiome composition in rats with experimental chronic kidney disease. *Biomedicine & Pharmacotherapy* (2020) 133:110992. doi: 10.1016/j.biopha.2020.110992

52. Xu SJ, Xu JD, Yang SZ, Zhang GJ. Clinical effect of Yun Pi Hua Zhuo Granule on nonalcoholic fatty liver and its influence on intestinal flora of patients. *Clinical medical research and practice* (2022) 10:115–7. doi: 10.19347/j.cnki.2096-1413.202210032

53. Yuan XW, Jiang N, Bai D. The regulation of immunity and intestinal flora. *Chin J Exp Prescription Med* (2021) 27(4):24–9. doi: 10.13422/j.cnki.syfjx.20202402

54. Kang A, Zheng X, Wang GJ. Progress in the interactive regulation of active components and intestinal flora in ginseng [J]. *J Nanjing Univ Traditional Chin Med* (2019) 35(5):496–502. doi: 10.14148/j.issn.1672-0482.2019.0496

55. Dalile B, Van Oudenhove L, Vervliet B, Verbeke K. The role of short-chain fatty acids in microbiota-gut-brain communication. *Nat Rev Gastroenterol Hepatol* (2019) 16:461–78. doi: 10.1038/s41575-019-0157-3

56. Canfora EE, Meex RCR, Venema K, Blaak EE. Gut microbial metabolites in obesity, NAFLD and T2DM. *Nat Rev Endocrinol* (2019) 15:261–73. doi: 10.1038/s41574-019-0156-z

57. Ohira H, Tsutsui W, Fujioka Y. Are short chain fatty acids in gut microbiota defensive players for inflammation and atherosclerosis? *J Atheroscler Thromb* (2017) 24:660–72. doi: 10.5551/jat.RV17006

58. Feng Y, Wang Y, Wang P, Huang YL, Wang FJ. Short-chain fatty acids manifest stimulative and protective effects on intestinal barrier function through the inhibition of NLRP3 inflammasome and autophagy. *Cell Physiol Biochem* (2018) 49:190–205. doi: 10.1159/000492853

59. Guo HH, Shen HR, Zhang HJ. Dengzhan shen gmai infants nonalcoholic fatty liver disease *via* regulating endogenous microenvironment. *Acta Pharm Sin* (2022) 9(01):1–23. doi: 10.16438/j.0513-4870.22-0908

60. Wang YF, Lin P, Lu JM, Zhang M, Li . Effect of radix polygoni multiflori and TSG on short-chain fatty acids in intestinal tract of NAFLD Rats. *Mod Chin Med* (2017) 19(9):1254–61. doi: 10.13313/j.issn.1673-4890.2017.9.009

61. Anastasopoulos NT, Lianos GD, Tatsi V, Karampa A, Goussia A, Glantzounis GK, et al. Clinical heterogeneity in patients with non-alcoholic fatty liver disease-associated hepatocellular carcinoma. *Expert Rev Gastroenterol Hepatol* (2020) 14(11):1025–33. doi: 10.1080/17474124.2020.1802244

62. Virović-Jukić L, Stojsavljević-Shapeski S, Forgač J, Kukla M, Mikolašević I. Non-alcoholic fatty liver disease - a procoagulant condition? *Croat Med J* (2021) 62 (1):25–33. doi: 10.3325/cmj.2021.62.25

63. Wang Z, Klipfell E, Bennett BJ, Koeth R, Levison BS, Dugar B, et al. Gut flora metabolism of phosphatidylcholine promotes cardiovascular disease. *Nature* (2011) 472(7341):57–63. doi: 10.1038/nature09922

frontiers | Frontiers in Endocrinology

TYPE Review
PUBLISHED 15 December 2022
DOI 10.3389/fendo.2022.1083707



OPEN ACCESS

EDITED BY
Guang Chen,
Huazhong University of Science and Technology, China

REVIEWED BY
Yi Wu,
Hunan University of Chinese Medicine, China
Kangxiao Guo,
Central South University Forestry and Technology, China

*CORRESPONDENCE
Haijing Xing
xh-jing@163.com
Yueying Wu
misswyy@sina.cn

†These authors have contributed equally to this work and share the first authorship

SPECIALTY SECTION
This article was submitted to Gut Endocrinology, a section of the journal Frontiers in Endocrinology

RECEIVED 29 October 2022
ACCEPTED 24 November 2022
PUBLISHED 15 December 2022

CITATION
Zhou X, Peng X, Pei H, Chen Y, Meng H, Yuan J, Xing H and Wu Y (2022) An overview of walnuts application as a plant-based. *Front. Endocrinol.* 13:1083707. doi: 10.3389/fendo.2022.1083707



# An overview of walnuts application as a plant-based

Xingjian Zhou[1,2†], Xingyu Peng[1,2†], Huan Pei[1,2†], Yuhan Chen[1,2], Hui Meng[1,2], Jiali Yuan[1,2], Haijing Xing[1,2*] and Yueying Wu[1,2*]

[1]Yunnan Provincial Key Laboratory of Molecular Biology for Sinomedicine, Yunnan University of Chinese Medicine, Kunming, Yunnan, China, [2]College of Basic Medicine, Yunnan University of Chinese Medicine, Kunming, Yunnan, China

The plant-based refers to plant-based raw materials or products that are available as the source of protein and fat. Utilization and development of walnuts as a plant-based, resulting in a high-quality protein-rich walnut plant-based product: walnut protein powder and walnut peptides. Progress in research on the application of walnuts as a plant-based has been advanced, solving the problem of wasted resources and environmental pollution caused by the fact that walnut residue, a product of walnuts after oil extraction, is often thrown away as waste, or becomes animal feed or compost. This paper reviews and summarizes the research and reports on walnut plant-based at home and abroad, focusing on the application of walnut plant-based in the preparation process (enzymatic and fermentation methods) and the biological activity of the walnut protein and walnut peptide, to provide a theoretical basis for the further processing of walnuts as a walnut plant-based. It can make full use of walnut resources and play its nutritional and health care value, develop and build a series of walnut plant-based products, improve the competitiveness of walnut peptide products, turn them into treasure, and provide more powerful guidance for the development of food and medicine health industry in Yunnan.

KEYWORDS

**walnut plant base, walnut protein, walnut peptide, bioactivity, gut microbiota**

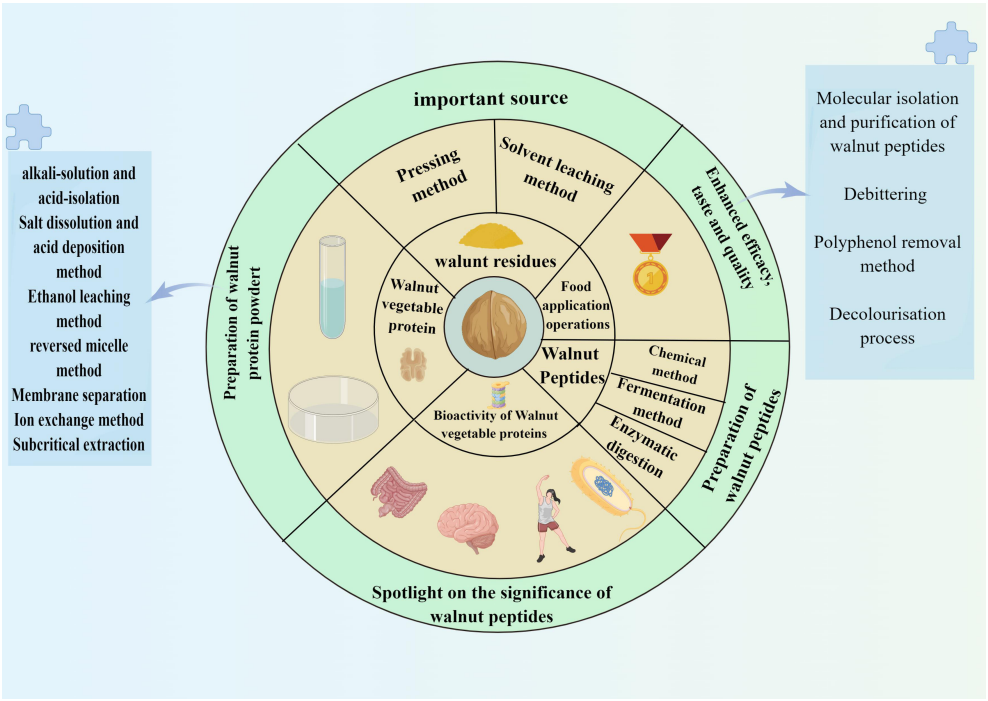


GRAPHICAL ABSTRACT
The walnuts as a Plant-Based.

## 1 Introduction

Walnut (*Juglans regia L.*), as the medicinal and food biological resource in China, belongs to the genus Walnut in the Walnut family, rich in oleic acid, linoleic acid, α-linolenic acid, and other unsaturated fatty acids, vitamins, and proteins. It has a high nutritional value (1, 2), is known as the "longevity fruit" and the "educational fruit," and is an important economic forest tree in China. Yunnan province is the largest walnut-producing area in China (accounting for 27.17% of the national walnut production), and Fengqing County is the main walnut-producing area in Yunnan province (3). By 2020, Fengqing County's walnut cultivation area reaches 1,718,000 mu (mu is a municipal unit of land area in China, about 666.667 square meters), with an annual output of about 103,500 tons and an annual output value of up to 2 billion yuan, ranking first in the country for many years in terms of cultivation area and annual output (4). Walnuts are commonly used to make walnut oil because they contain 65% to 70% oil (5). However, the large number of by-products produced after their oil extraction, walnut residues, are often abandoned and even pollute the environment (6). Recently, plenty of researches have shown that walnut residues can still improve learning and memory as well as antioxidant function (7, 8), therefore, the secondary development and utilization of walnut residues need to be addressed urgently.

In recent years, there has been a boom in "plant-based products" at home and abroad. The term "plant-based products" is derived from the American Plant-Based Foods Association's concept of "finished food products consisting of ingredients obtained from plants such as vegetables, fruits, grains, nuts, seeds and/or legumes (9)"T/CIFST 002-2021, proposed by China's Chinese Society of Food Science and Technology in 2021, means "foods made from plant materials (including algae and fungi) or their products as a source of protein and fat, with or without the addition of other ingredients, and made by a certain process with similar texture, flavor, morphology, and other quality characteristics to those of certain foods of animal origin.".Thus, this paper is intended to review the "walnut plant-based+" series of products using walnuts as the main raw material for plant-based food products, to provide a basis and support for increasing the added value of walnut residues and contributing to Yunnan's biomedical industry.

## 2 Walnut residue is an important source of walnut plant-based

According to the definition of "plant-based food" by the American Plant-Based Food Association and the Chinese Society of Food Science and Technology, we consider that "walnut plant-based" can be understood as: the raw material of the walnut plant or its products that serve as a source of

protein and fat, including walnut kernels and their Walnuts and their by-products after oil extraction (walnut residue). One of them, walnut kernels, is commonly used in the preparation of walnut oil and nuts and is widely used, while walnut residues are often abandoned as a by-product of walnut oil extraction, and even pollute the environment. Hence, the secondary use and exploitation of walnut residues as the main raw material for "walnut plant-based+" products is promising.

## 2.1 Walnut residue is one of the most potential "walnut plant-based+"

It's confirmed that walnut residues contain a variety of nutrients such as protein, fat, inorganic salts, vitamins, and fiber (10). The crude fat, crude fiber, and crude fiber in walnut residues are higher than those of similar nut residues, and of these, 143.4% and 334.8% are higher respectively compared to soybean residue (Figure 1A). The vitamin D3 content is up to 139,000 IU/kg, much higher than most nut residue (11). Besides, walnut residues have 18 amino acids, glutamic acid (21.30%~21.70%), arginine (13.60%~15.20%), and aspartic acid (10.20%~10.50%) are the main amino acids (12) (Figure 1B), which shows that walnut residues have high nutritional value and is a more promising "walnut plant-based +". It can be applied in the development of walnut plant-based foods.

## 2.2 Walnut residue is often obtained by the means of pressing and solvent leaching

At present, the major methods of walnut oil extraction in China include pressing and solvent leaching (13). The pressing method (14) uses mechanical pressing to squeeze the oil out of the walnut kernels. The pressing methods are divided into cold pressing and hot pressing, the cold pressing method is carried out at a low temperature, without the use of chemical materials to refine the oil and meet the edible standard (13, 15). It is currently the most used method in China (16), and the obtained walnut residues can better maintain the physical properties and nutrients of walnut residues, and also has a higher protein extraction rate (6), and the protein extracted from walnut cake dross has better solubility, emulsification, and water absorption, and yet requires higher cost and lower oil output than the hot pressing method, and is prone to oxidative rancidity. The oil output of the hot pressing method is higher, and the oil absorption and emulsion stability of the protein extracted from the walnut residues are better, while the oil extraction temperature is higher, and 30% of the walnut shells are also present during the extraction process, making the composition of the obtained walnut residues complex in composition and serious protein denaturation. The organic solvent leaching method (17) is a way to extract the oil in walnut kernels with organic solvents using the extraction principle. The extraction effect is better and suitable for large-scale production, but the equipment is complicated and the solvent residue leads to protein denaturation and the loss of unsaturated fatty acids. In summary, pressing is the most commonly used method for extracting walnut oil. The properties of the walnut residues obtained from different extraction methods vary, and the researcher selects the extraction method according to the purpose of the study and the actual needs of the product development (Figure 2).

# 3 Walnut plant-based food

## 3.1 Walnut protein powder

As a plant-derived protein powder, walnut protein powder is now widely used in the food sector. Walnut protein powder is mainly a high-protein product obtained by drying and micronizing

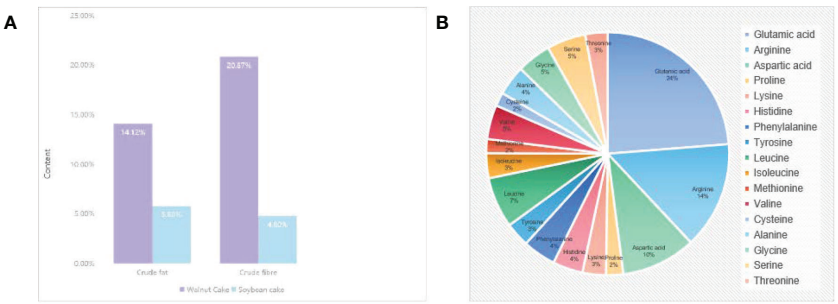


FIGURE 1
The main component of walnut residue. **(A)** Comparison of crude fat and crude fiber in walnut residue and soya residue. **(B)** Composition and content of amino acids in walnut residue.

the by-products produced after the extraction of oils and fats. Walnut powder is mainly divided into two types, which include full-fat and low-fat. The low-fat walnut powder contains less oil and therefore has a longer shelf life, while the full-fat walnut powder has a high oil content and therefore has a shorter shelf life. Therefore, low-fat walnut powder is popular in the market (18). There are two main ways of preparing low-fat walnut protein powder, such as using the cold-pressed walnut residue and Xinjiang high-quality walnut defatted residue as raw material (Figure 3) (19). Walnut phycobilisome is weakly soluble (5) and its emulsification is positively correlated with solubility and is also influenced by the concentration of walnut phycobilisome, temperature, pH, and salt ion levels (10). Yi's study showed (20) that the solubility, emulsification, and emulsion stability of Walnut

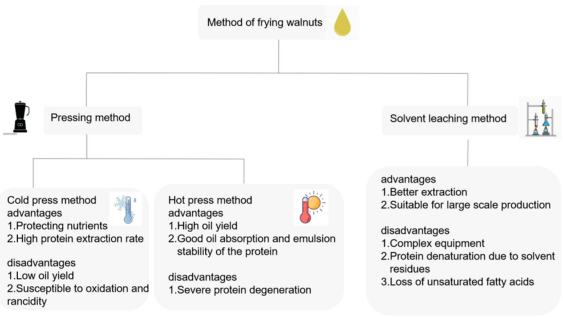


FIGURE 2
Advantages and disadvantages of the press and solvent leaching methods.

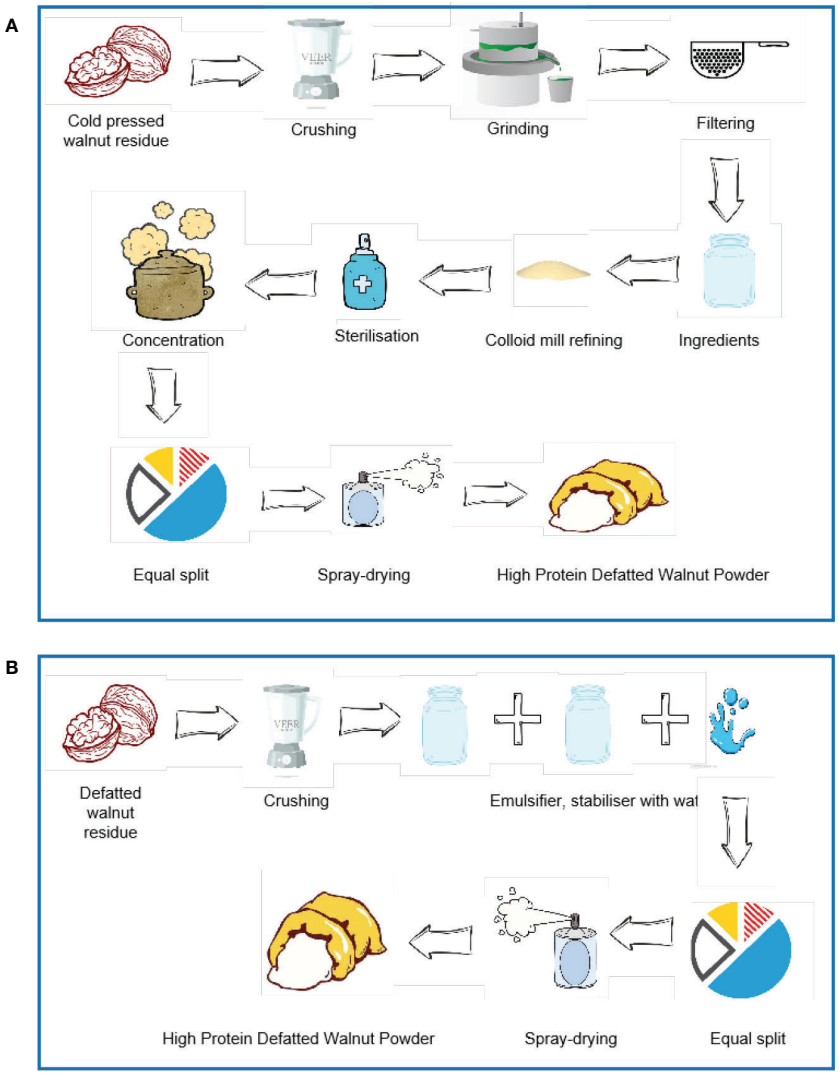


FIGURE 3
There are two main ways of preparing low-fat walnut protein powder. **(A)** The method of using the cold-pressed walnut residue as raw material. **(B)** The method of using Xinjiang high-quality walnut defatted residue as raw material.

vegetable proteins were lower at around pH 5.0. Gao's study (21) confirmed that Walnut vegetable proteins have low emulsification near the isoelectric point and rise in emulsification away from the isoelectric point. Based on the different properties, Walnut protein powders are divided into different categories (Table 1).

### 3.1.1 Walnut protein is often prepared by alkali solution and acid-isolation

Walnut protein powder is mainly prepared using walnut residues. Commonly used methods for the preparation of Walnut protein powder include salt-soluble acid precipitation, dilute acid precipitation, alkali-soluble acid precipitation, enzymatic digestion, reverse micellar method, membrane separation, ion exchange, and physically assisted methods (24) (Table 2). Among all these methods, the alkali-solution and acid-isolation method has the advantages of high purity of the isolated protein and good quality of the product and is the main and commonly used preparation method, which has been widely used in the preparation and practical production of walnut isolated protein at domestic and overseas (Figure 4). However, the effect of acid and alkali made the prepared Walnut protein poor in organoleptic properties, showing a brownish color and requiring further decolorization (5, 24). Yang (28) investigated the effects of four factors on the protein extraction rate, NaOH solution concentration, material-to-liquid ratio, extraction temperature, and extraction time using the alkali-solution and acid-isolation methods. The optimum extraction conditions for alkali-soluble pecan kernel protein were determined as "NaOH concentration 0.02 mol/L, material-to-liquid ratio 1:30 (g/mL), extraction temperature 50°C, extraction time 1.5 h, and an isoelectric point 4.5".To improve the yield of Walnut vegetable proteins, auxiliary extraction techniques such as ultrasonic technology and subcritical water can be used, with mild reaction conditions and easy operation (27, 29, 30). As can be seen, each of the methods for preparing Walnut protein powder has its

TABLE 1 Classification of Walnut protein powders.

| Basis of classification | Category | | | Reference |
|---|---|---|---|---|
| Protein content | Walnut protein powder (protein content < 60%) | Walnut protein concentrate (protein content > 70%) | Walnut isolate (protein content > 90%) | (10) |
| Oil and fat content | Full fat powder | Semi-skimmed powder | Degreasing powder | (22) |
| Solubility | Gluten (more than 70%), clear protein, globulin, alcoholic soluble protein | | | (23) |

TABLE 2 Walnut protein preparation methods and their advantages and disadvantages.

| Preparation methods | Principle | Advantages | Disadvantages | Reference |
|---|---|---|---|---|
| alkali-solution and acid isolation | Separation using the difference in acidity and alkalinity of the components in the raw material mixture | The purity of the isolated protein is up to 90% or more, the quality of the product is good and it is the most widely used in practice. | The removal of soluble components is not complete and the acid solution consumed is high. | (24) |
| Salt dissolution and acid deposition method | Adjust the pH of the raw material mixture to precipitate the walnut protein near the isoelectric point. | High extraction rate, simple operation, and low cost. | The protein obtained has more impurities. | (24) |
| Ethanol leaching method | A certain concentration of ethanol is used to wash the walnut residues to denature the walnut protein, which loses its solubility and precipitates the walnut protein. | It has some feasibility. | Reduces the solubility of the protein by denaturation, which is not conducive to subsequent processing. | (25) |
| reversed micelle method | The solubilization properties of the inverse micelles (oil-in-water microemulsions) are used to dissolve the walnut proteins in the polar nuclei. | The spatial structure of plant proteins is preserved to a greater extent. | In the extraction of large molecular mass proteins, different degrees of physical changes occur and the extraction conditions have a strong influence on the shape of the protein | (26) |
| Membrane separation | Separation of low molecular proteins using RO (Reverse Osmosis) membranes | Low energy consumption, simple operation, no pollution | However, ultrafiltration membranes are susceptible to contamination, which can affect changes in protein properties | (24) |
| Ion exchange method | Modulation of solution pH values by ion exchange, resulting in protein leaching and precipitation | High protein purity | Long production cycles | (27) |
| Subcritical extraction | Separation of proteins by the principle of similar solubility using subcritical water as an extractant | Improved extraction efficiency and greatly reduced extraction times | Protein degradation due to high temperature | (27) |

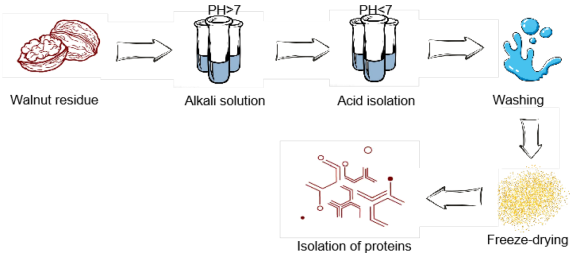


FIGURE 4
Process flow diagram for the preparation of Walnut vegetable protein.

advantages and disadvantages, so the characteristics of the raw material and the actual production requirements should be taken into account when selecting a method for preparing the protein.

### 3.1.2 Bioactivity of walnut vegetable proteins

Walnut protein has biological activities such as antioxidant and anti-inflammatory. Han Haitao et al. showed that the main components of Walnut protein had good antioxidant activity, and the DPPH radical scavenging ability of the clear protein, alcoholic protein, and gluten-2 in walnut protein could reach 97.15%, 93.35%, and 90.58%, respectively (24). Meanwhile, Walnut protein delayed the onset of acute colitis induced by sodium dextran sulfate, slowed down the weight loss in mice caused by colitis, and had significant anti-inflammatory activity due to the hydrolysis of walnut protein into small molecule peptides with anti-colitis activity by the action of intestinal digestive enzymes, which exerted anti-inflammatory effects, which inspired us to focus our research on the biological activity of walnut peptides (12).

## 3.2 Walnut peptides

### 3.2.1 Functional properties of walnut peptides

Numerous studies have confirmed that walnut peptides have a strong antioxidant capacity both *in vitro* and *in vivo*, which is closely related to the amino acid sequence and composition of the peptides (31, 32). Walnut peptides are mostly composed of two to several dozen amino acids through peptide bonds and their relative molecular mass is generally less than 6000 Da (30). As a natural active peptide, the walnut peptide has good characteristics such as high concentration, low viscosity, good solubility, and relative stability to pH changes, and it is better than Walnut protein in terms of foaming, emulsification, and oil absorption, with high safety and excellent application prospects (Figure 5).

### 3.2.2 Walnut peptides are mainly prepared by enzymatic digestion

Walnut peptides have a variety of biological activities, however, whether the peptides can perform normally or maximize their biological activity requires the selection of a suitable preparation and extraction method according to the characteristics of the raw material, the actual production needs, and the available conditions. The preparation of walnut peptides refers to the process of hydrolysis of walnut vegetable proteins into small molecular peptides with molecular weights between amino acids and proteins using biological or chemical methods. Bioactive peptides are prepared from plants by enzymatic, fermentation, and chemical methods (33). Enzymatic and fermentation methods are more commonly used (34, 35) (Table 3), while enzymatic digestion is the most dominant method of preparation (39).

#### 3.2.2.1 Enzymatic preparation of walnut peptides

Walnut residue has 15% to 20% residual oil, which leads to protein denaturation unfavorable to storage, and how to degrease it is an urgent technical problem to be solved (40). Leaching is the main method used to degrease walnut residues; however, this method has solvent residues and is complex to operate. In recent years, subcritical extraction techniques have been increasingly used in the extraction of oil and fats, and are available on a large scale for industrial production (41).

In the preparation of walnut peptides, the choice of enzymes is crucial. The commonly used enzymes and their enzymatic effects are alkaline proteases> papain > trypsin > neutral protease > flavor protease > pepsin (34, 42, 43). Wang Duan (44) et al. used neutral protease to hydrolyze defatted walnut residue powder to prepare peptides and optimized the extraction process of walnut peptides, and the peptide yield was 0.45 g/g under the optimal process conditions. Lu Xiaodan (45) showed that microwave and ultrasonic treatment resulted in significantly higher yields of walnut peptides. Chen Shujun (46) et al. used a complex protease enzyme to optimize the complex protease enzymatic digestion process, and the peptide mass concentration was 10.01 mg/mL and the degree of hydrolysis was 11.45% under the optimal enzymatic conditions.

The above studies illustrate that when preparing walnut peptides by enzymatic digestion, the preparation efficiency and biological activity are influenced by the conditions of enzymatic digestion, the type of complex enzyme, and the sequence of

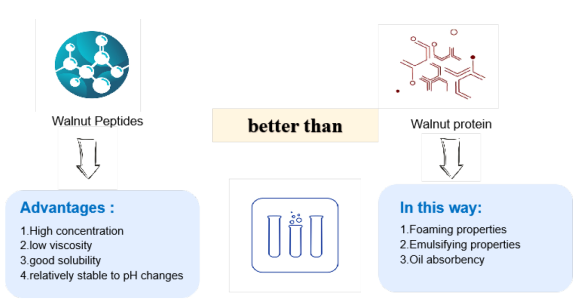


FIGURE 5
Benefits of Walnut Peptides.

TABLE 3 Comparison of walnut peptide preparation methods.

| Preparation methods | Enzymatic digestion | Fermentation method | Chemical method | Reference |
|---|---|---|---|---|
| Definition | Proteolytic preparation of bioactive peptides is a process that uses proteases to hydrolyze proteins to obtain an enzymatic solution, which is then separated and purified to obtain bioactive peptides. | Microbial fermentation for the preparation of active peptides is a method for the orderly degradation of macromolecular proteins through the extracellular enzyme system produced by the beneficial strains themselves to produce various peptides. | Chemical hydrolysis is a method of producing active peptides by breaking the peptide bonds of proteins by bathing them in an acid or base solution at the appropriate concentration for some time and at the appropriate temperature. | (36) |
| Advantages | Mild reaction conditions, safe operation, mature research, directional enzyme catalytic position, and no stereoisomerization or racemization, suitable for mass production | Simple handling, no solvent residues, low processing costs, and a de-bittering effect. | Easy to operate and inexpensive. | (37, 38) |
| Disadvantages | However, there are ionic introductions in the preparation process and the peptides are inevitably colored by the Merad reaction during fermentation, and the hydrophobic peptides produced during hydrolysis can also give the peptides an undesirable flavor (bitterness, and odor), limiting their practical application. | The method requires strain screening, cultivation, longer fermentation cycles, more complex enzyme systems produced by metabolism, and more hydrolysis by-products, and is limited by the safety of the strain used, so microbial fermentation methods are difficult to expand. | However, the extraction rate is low, the reaction process is not easily controlled, the product quality is unstable, the environmental pollution is more serious and the economic efficiency is low, which is not suitable for modern industrial production of walnut peptides. | (34) |

enzymatic digestion and pretreatment. Enzymatic digestion is still the most important method for the preparation of walnut peptides now. To obtain good biologically active walnut peptides efficiently, suitable proteases should be selected according to the actual production needs, providing a favorable guide for the industrial production of walnut peptides.

The exposure of hydrophobic amino acids of the protein after enzymatic digestion causes bitterness limiting its application in food (47). Choosing the right method of de-bittering can improve the taste and flavor of the product and increase its usefulness in processing and production. Three methods are currently commonly used to remove the bitterness of proteinaceous peptides (41) (Table 4).

### 3.2.2.2 Preparation of walnut peptides by fermentation

Fermentation methods are divided into solid and liquid fermentation, with solid fermentation being a microbial fermentation process that takes place on a solid substrate feedstock with little to no free-flowing water in the fermentation substrate (48). Compared to liquid fermentation, solid-state fermentation is less costly, has a wider source of substrates, is less polluting to the environment, is less technically and environmentally demanding, and is more operational (49). Liquid fermentation, with its high level of free water, is a relatively new fermentation technology that began in 1995 (50). Liquid fermentation makes full use of raw materials, and has a short fermentation cycle and a stable product quality, but requires advanced and well-controlled production equipment and a large investment in equipment.

Walnut peptides were mostly prepared by solid-state fermentation of walnut residues. He Ying (51) et al. used lactic acid fermentation of walnut meal to prepare walnut peptides, and the yield of walnut peptides reached 12.84 mg/g and had a powerful free radical scavenging rate and reducing ability. Liu Xiao (52) et al. used Bacillus subtilis and Aspergillus niger for solid-state fermentation of walnut residues, and the result was that Bacillus subtilis fermentation produced a significantly higher content of walnut peptides than Aspergillus niger at 243.97 mg/g. Wu Wanxing (53) used fungal and bacterial microorganisms for solid-state fermentation of walnut residues and concluded that the bacterial peptide yield was significantly

TABLE 4 Comparison of the advantages and disadvantages of the three methods of debittering.

| Methods | Advantages | Disadvantages | Reference |
|---|---|---|---|
| Selective adsorption | Environmentally friendly, safe, and cost-effective | Loss of some amino acids, reducing nutritional value | (41) |
| Enzymatic method | No loss of nutrients | Further alteration of the molecular structure of the short peptide chain affects its functional properties and is costly and unsuitable for industrial production | (41) |
| Cover-up method | No nutrient loss, low cost | A sufficient amount of masking agent needs to be added, which may cause odors. | (41) |

higher than the fungal at 30.20% at the respective optimum fermentation temperatures.

Liquid fermentation has the advantage of a shorter fermentation cycle than solid fermentation, faster cell appreciation, more uniform cell development, and so on. Liang Heng (54) et al. screened Bacillus subtilis, Bacillus natto, and Bacillus licheniformis from Bacillus subtilis for liquid fermentation of walnut meal, The fermentation process was also optimized to verify the inhibitory effect of the polyphenolic substances in walnut residues on the growth of Bacillus subtilis and showed a concentration dependence. Using liquid fermentation technology, Xu Dian (55) investigated the optimal process parameters for the fermentation of Aspergillus niger and determined the antioxidant capacity of four constituents of walnut peptides with different molecular weights. The experimental results showed that the highest peptide content of 7.20 mg/mL was achieved at the optimum process parameters, and the antioxidant capacity of the fermentation liquid was significant, with walnut peptides with a molecular weight of <5 KDa having the strongest antioxidant capacity.

#### 3.2.2.3 Isolation and purification of walnut peptide molecules

Studies have shown that the antioxidant activity of peptides is closely related to their molecular weight (56, 57), and the smaller the molecular weight, the stronger the antioxidant activity of short peptides (32, 46). Therefore, increasing the degree of hydrolysis when carrying out hydrolysis, adding small molecular weight peptides, and separating and purifying the enzymatic digest maximize the biological activity of walnut peptides.Common active peptide isolation methods (Table 5) (33, 58).

Several methods are available for the isolation of bioactive peptides, each with its advantages and disadvantages, and often a single isolation method does not meet the requirements. Thus, to obtain highly active, high-purity target peptides, multiple isolation methods are often used in combination.

#### 3.2.2.4 Others

Walnut seed coat is rich in polyphenols, which can be reacted with browning under the action of polyphenol oxidase, forming brown compounds that seriously affect the quality of walnut further processed products. Cheng Jing (59) used 2% citric acid for pretreatment in the preparation of walnut peptides from walnut residues, which reduced the browning reaction. Decolourisation also plays a crucial role in the preparation of walnut peptides. Wang Wei (60) et al. explored the optimal conditions for the decolorization of enzymatic hydrolysate of walnut protein by activated carbon, and the decolorization rate was 78.05% under these conditions. According to the actual needs of the selection of suitable methods of polyphenol removal and decolorization, the process can improve the quality and market competitiveness of the product and broaden the development of walnut peptides.

### 3.2.3 Walnut peptide bioactivity

The conventional concept is that proteins are ingested and absorbed by the body after being hydrolyzed into amino acids by various proteases, however, the discovery of peptides and peptide absorption channels in the small intestine suggest that proteins are not necessarily absorbed as free amino acids after digestion and degradation, rather they are mainly in the form of oligopeptides (61), that is, small molecules of peptides are more easily absorbed than proteins or amino acids (42). The biological activities and mechanisms of action of walnut peptides in gut microbiota regulation, antioxidants (8, 34, 42), anti-fatigue, memory improvement, anti-epilepsy, and improvement of metabolic diseases have been investigated by domestic and foreign researchers.

#### 3.2.3.1 Gut microbiota regulation

It's shown that the walnut-derived peptide leucine-proline-phenylalanine (LPF) has a protective and restorative effect on dextran sodium sulfate-induced colitis in mice. Besides, the walnut peptide regulated the gut microbiota disorders in mice by increasing the relative abundance of beneficial genera and decreasing the relative abundance of potentially harmful genera (62). Wang et al. showed the effect of walnut-derived peptide PW 5 on Beta-amyloid protein and intestinal microbiota (63). The above studies have verified the role of walnut peptides in gut microbiota regulation.

#### 3.2.3.2 Antioxidant activity

Qian Du (64) et al. proposed the hypothesis that walnut peptides may have functions such as promoting brain development and improving learning and memory by significantly increasing the antioxidant properties of tissues and enhancing the ability for free radical scavenging. The mechanisms of protective effects of three novel nucleotides, LVRL, LRYL, and VLLALVLLR, on high glucose-induced insulin resistance (IR) and oxidative stress in HepG 2 cells were elucidated by Wang et al (65). Walnut-derived peptides significantly reduce reactive oxygen species (ROS). Walnut-derived peptides LVRL and LRYL increase antioxidant enzyme activity pathways by activating Nrf2/HO-1 signaling, thereby inhibiting high glucose-induced ROS production and MAPK activation and improving glucose uptake and IR in HepG 2 cells, resulting in alleviating effects on hepatic IR, probably due to the reduced oxidative stress characteristics of walnut residues.

#### 3.2.3.3 Memory improvement

Alzheimer's disease(AD) is one of the major neurodegenerative diseases in the elderly, with Aβ-induced oxidative stress and

TABLE 5 Classification and characteristics of peptide isolation and purification methods.

| Isolation and purification methods | | Advantages | Disadvantages | Effect | Applied | Reference |
|---|---|---|---|---|---|---|
| Membrane Separation Technology | Ultrafiltration | Easy to operate, low cost, energy saving, and environmental protection, conducted at normal temperature, avoiding the destruction of active peptides by high temperature, effectively retaining the activity of active peptides | Not suitable for the isolation of a specific peptide | Better | Suitable for primary separation, separation of medium to large mixtures | (33) |
| | Nanofiltration | Separation process without adding any chemical reagents, no heating, no phase change, good desalination effect | Research on the design of nanofiltration membrane materials, membrane performance, and structure is not mature enough | Good | Widely used in industrial production | (33) |
| Chromatography | Reversed-phase high-performance liquid chromatography | High resolution, high sensitivity, good separation, simple operation, automatic analysis of target peptides in large batches | Expensive instrumentation and insufficient retention of hydrophilic small molecule peptides | Good | Wide applicability, especially for peptides with small molecular masses | (33) |
| | Gel filtration chromatography | Easy handling, mild operating conditions, no organic solvents required, no effect on the activity of the active peptides | The separation operation is generally slow and difficult to achieve good separation of active peptides with similar molecular weights | Good | Wide applicability for the separation of active peptides | (33) |
| | Ion-exchange chromatography | High sensitivity, good selectivity, and fast analysis | The ionic strength of the eluent, salt concentration, and other influences, and the elution may introduce impurity ions and need to be desalted again | Good | Wider applicability | (33) |
| | Affinity chromatography | High selectivity and good separation | More expensive carriers, adsorption of neuropeptides | Good | The small range of applications and high specificity for the isolation and purification of glycopeptides | (33) |
| salting-out method | | Easy and convenient, low cost | The pure concentration is not high and introduces a lot of salt, which needs to be desalted | Better | Suitable for initial purification only | (58) |
| Electrophoresis | | Low sample volume, high sensitivity, fast analysis, and high separation efficiency | Low feed volume makes mass production difficult | Good | Widely used in active peptide isolation | (58) |
| the aqueous two-phase extraction technique | | The isolated peptides have fewer impurities, do not change the activity and conformation of the peptides, and are less toxic and biocompatible | Water-soluble polymers are difficult to recover, non-volatile, and easily emulsified | Good | Wide applicability for the separation of active peptides | (58) |

neuroinflammation in the brain attributing to the pathogenesis of AD. Zhao et al. showed (66) that the walnut peptide YVLLPSPK improved learning and memory in scopolamine-induced cognitive impairment in mice through a mechanism related to the NF2/KEAP1/HO-1 pathway, providing a deeper theoretical basis for the research on the mechanisms by which walnut peptides improve learning memory and cognitive impairment. Zou et al. (67) demonstrated that the addition of walnut peptides was effective in improving cognitive impairment and memory disorder in mice and that supplementation with walnut peptides was effective in restoring the levels of antioxidant enzymes and inflammatory mediators, thereby reducing the inflammatory response and regulating the antioxidant systems et al. (67) demonstrated that the addition of walnut peptides was effective in improving cognitive impairment and memory deficits in mice, and that supplementation with walnut peptides was effective in restoring levels of antioxidant enzymes and inflammatory mediators, thereby reducing inflammatory responses and modulating the antioxidant system which has a protective effect on AD.

#### 3.2.3.4 Anti-fatigue

It's proved that walnut peptide alleviates fatigue by promoting the synthesis of red blood cells in the animal body so that it could reduce the production of lactic acid and urea ammonia during strenuous exercise and delay fatigue. At the

TABLE 6 Other activities of walnut peptides.

| Active | Research Progress | Reference |
|---|---|---|
| Antiepileptic activity | Jahanbani et al. evaluated the antiepileptic properties of walnut peptide extracts in three different mouse seizure models (pentylenetetrazol-induced clonic seizures, chemical ignition, and maximal electroshock). The experimental results showed that intraperitoneal administration of walnut peptides significantly increased the seizure threshold; walnut peptides exert their antiepileptic properties through the modulation of benzodiazepine receptors. | (62, 70) |
| Improves hyperlipidemia and hepatic lipid metabolism | Rats fed walnut peptide powder counteracted the high-fat-induced increase in body, liver, and epididymal fat weight and could lower total serum cholesterol, triglycerides, and total low-density cholesterol, raise high-density lipoprotein cholesterol and lower the atherosclerotic index. In terms of body weight, the total energy intake of rats in the walnut peptide group was close to that of rats on a high-fat diet, but the body weight of rats in the walnut peptide-treated group was significantly lower than that of rats on a high-fat diet, so that intake of walnut peptides was effective in improving hyperlipidemia and liver lipid metabolism disorders. | (63, 71–73) |
| Anti-cancer activity | Ma et al. used papain to hydrolyze walnut meal to obtain a novel biopeptide with the amino acid sequence CTLEW and investigated the anti-cancer mechanism, showing that the CTLEW peptide could induce apoptosis and autophagy in MCF-7 cells and exhibited selective inhibition and immunomodulatory activity against cancer cell growth. | (64, 74) |
| Laxative for bowel movement | Zhang Ting et al. explored and verified the effect of walnut peptides in improving constipation and laxative effect, and explored the mechanism by which the effect occurred. The researchers inferred that the mechanism of the action of walnut peptides in conjunction with the experimental results may be related to the fact that walnut oligopeptides promote the expression of gastrointestinal hormone endotoxin and gastrin in the serum of mice and inhibit the expression of growth inhibitors. | (65, 75) |

same time, it can rapidly decompose lactic acid and urea ammonia and expel them out of the body after exercise, thus speeding up fatigue recovery (68, 69). Liu et al. showed (8) that walnut oligopeptide significantly inhibited fatigue-induced oxidative stress, improved pyruvate kinase, and succinate dehydrogenation activities in mouse skeletal muscle increased mitochondrial biogenesis factor mRNA expression and mitochondrial content and exerted anti-fatigue effects in mice. Uran et al. (47) measured the time to exhaustion of weighted swimming, serum urea nitrogen and lactate dehydrogenase activity in each group of mice, the blood lactate level in each group of mice, and the liver and muscle glycogen content in each group of mice. The results showed that walnut peptides increased lactate dehydrogenase activity, reduced blood lactate and serum urea nitrogen levels, increased muscle glycogen reserves, and significantly prolonged weight-bearing swimming time, thus having a better anti-fatigue effect. It's shown that, as a plant-derived active peptide, walnut relieve fatigue to some extent.

#### 3.2.3.5 Other activities

Walnut peptides still have other functions, such as antiepileptic activity, improving hyperlipidemia as well as hepatic lipid metabolism, and so on (Table 6).

## 4 Conclusion

The two applications of walnut plant-based are considered in terms of economic benefits, nutritional value, and environmental impact, each with its focus. Walnut plant protein powder is cheaper to produce but has less nutritional and food applications than walnut peptides, while walnut peptides, although slightly more costly than walnut plant protein, have a variety of biological activities and are widely used in food and pharmaceuticals, and researchers have focused on walnut peptides. In recent years, the rich walnut resources of Yunnan have received a great deal of attention from researchers. The application of plant-based products in food has also created a boom in international and domestic markets. Plant-based dairy products, plant-based meat, and other plant-based products are entering the market. Research on walnut plant protein powder and walnut peptides has also focused on their active functions such as antioxidant, anti-fatigue, and memory improvement, and the subsequent development of healthy food and functional food with various functions by combining walnut plant protein powder and walnut peptides with herbs in Yunnan. For example, walnut peptides can be compounded with herbs in Yunnan such as *Gastrodia elata Bl.*, *Polygonati Rhizoma*, and *Radix Puerariae* (76–78) (Table 7) to develop healthy foods and functional foods with anti-fatigue, immunity enhancement, and unique flavors. However, due to Yunnan's backward economic and technological level, the walnut resources are mostly in primary processing products, the walnut plant-based resources are discarded and wasted, and the visibility is low. Consequently, it is not only necessary to combine walnut plant-based products with Yunnan's authentic medicinal herbs to improve their innovation, but also to actively improve the production methods to open up the visibility of Yunnan's walnut plant-based products by joining forces with the government, the public and the media, so that Yunnan's walnut resources and walnut plant-based products go out of Yunnan and out of China and that the walnut plant-based

TABLE 7 Chinese and Latin names of Chinese medicines.

| Chinese name | Chinese Pinyin name | Latin name |
|---|---|---|
| 天麻 | Tianma | *Gastrodia elata Bl* |
| 黄精 | Huangjing | *Polygonati Rhizoma* |
| 葛根 | Gegen | *Radix Puerariae* |

products of Yunnan have a place in the plant-based market at home and abroad.

## Author contributions

Author contributions were as follows: study design YW and HX, data collection XZ, XP and HP, data interpretation YC, HM and JY, manuscript preparation XZ, XP and HP, and funds collection JY. All authors contributed to the article and approved the submitted version.

## Funding

This work was funded in part by a grant from the Yunnan Provincial Science and Technology Department (202102AE090031), Yunnan Science and technology planning project-joint major project of traditional Chinese medicine(2019FF002(-002)), the Provincial Innovation Team of Yunnan University of Chinese Medicine for Traditional Chinese Medicine to Regulate Human Microecology (No. 2018HC011).

## Acknowledgments

We thank all the scholars who provided relevant guidance for the study.

## Conflict of interest

The authors declare that the research was conducted in the absence of any commercial or financial relationships that could be construed as a potential conflict of interest.

## Publisher's note



## References

1. Zhong L, Bornman JF, Wu G, Hornoff A, Dovi KAP, Al-Ali H, et al. The nutritional and phytochemical composition of the indigenous Australian pindan walnut (Terminalia cunninghamii) kernels. *Plant Foods Hum Nutr* (2018) 73 (1):40–6. doi: 10.1007/s11130-017-0647-9

2. Zhang Y, Ma J, Tang Y, Liu Y, Lan H, Zhang H. Research overview and development analysis of walnut shelling equipment in China. *J Chinese Agricultural Mechanization* (2020) 43(09):95–101. doi: 10.13733/j.jcam.issn.2095-5553.2022.09.013

3. Hao Y. *Research on germplasm resources and breeding of walnut*. (Beijing: Beijing Forestry University) (2008).

4. Yang X. *Fengqing county, China: Building the hometown of walnuts* . (Yunnan: World of Wealth) (2020) 9, p. 46–7.

5. Martinez ML, Labuckas DO, Lamarque AL, Maestri DM. Walnut (Juglans regia l.): genetic resources, chemistry, by-products. *J Sci Food Agric* (2010) 90 (12):1959–67. doi: 10.1002/jsfa.4059

6. Burbano JJ, Correa MJ. Composition and physicochemical characterization of walnut flour, a by-product of oil extraction. *Plant Foods Hum Nutr* (2021) 76 (2):233–9. doi: 10.1007/s11130-021-00898-4

7. Gao P, Liu R, Jin Q, Wang X. Comparative study of chemical compositions and antioxidant capacities of oils obtained from two species of walnut: Juglans regia and juglans sigillata. *Food Chem* (2019) 279:279–87. doi: 10.1016/j.foodchem.2018.12.016

8. Chauhan A, Chauhan V. Beneficial effects of walnuts on cognition and brain health. *Nutrients* (2020) 12(2):550. doi: 10.3390/nu12020550

9. McClements DJ, Grossmann L. The science of plant-based foods: Constructing next-generation meat, fish, milk, and egg analogs. *Compr Rev Food Sci Food Saf* (2021) 20(4):4049–100. doi: 10.1111/1541-4337.12771

10. Li X, Guo M, Chi J, Ma J. Bioactive peptides from walnut residue protein. *Molecules* (2020) 25(6):1285. doi: 10.3390/molecules25061285

11. Sun F, Li Xi, Mo F, Li Y, Liu R, Zheng C, et al. Analysis of the nutritional composition of walnut cake for forage. *Feed Res* (2010) 10):37–8+41. doi: 10.13557/j.cnki.issn1002-2813.2010.10.010

12. Mao X, Hua Y, Chen G. Amino acid composition, molecular weight distribution and gel electrophoresis of walnut (Juglans regia l.) proteins and protein fractionations. *Int J Mol Sci* (2014) 15(2):2003–14. doi: 10.3390/ijms15022003

13. Ghafoor K, Juhaimi FA, Geçgel Ü, Babiker EE, Özcan MM. Influence of roasting on oil content, bioactive components of different walnut kernel. *J Oleo Sci* (2020) 69(5):423–8. doi: 10.5650/jos.ess19205

14. Subra-Paternault P, Garcia-Mendoza MDP, Savoire R, Harscoat-Schiavo C. Impact of hydro-alcoholic solvents on the oil and phenolics extraction from walnut (Juglans regia l.) press-cake and the self-emulsification of extracts. *Foods* (2022) 11 (2):186. doi: 10.3390/foods11020186

15. Ahmed IAM, Al-Juhaimi FY, Özcan MM, Osman MA, Gassem MA, Salih HAA. Effects of cold-press and soxhlet extraction systems on antioxidant activity, total phenol contents, fatty acids, and tocopherol contents of walnut kernel oils. *J Oleo Sci* (2019) 68(2):167–73. doi: 10.5650/jos.ess18141

16. Gao P, Ding Y, Chen Z, Zhou Z, Zhong W, Hu C, et al. Characteristics and antioxidant activity of walnut oil using various pretreatment and processing technologies. *Foods* (2022) 11(12):1698. doi: 10.3390/foods11121698

17. Xu Y, Bi S, Xiong C, Dai Y, Zhou Q, Liu Y. Identification of aroma active compounds in walnut oil by monolithic material adsorption extraction of RSC18 combined with gas chromatography-olfactory-mass spectrometry. *Food Chem* (2022) :402:134303. doi: 10.1016/j.foodchem.2022.134303

18. Huo YQ, Liu CJ, Nie RZ, Zhou R, Bao HH, Tang SW. Research progress on the composition, preparation and properties of walnut protein. *J Chin Cereals Oils* (2020) 35(12):191–7. doi: 10.3969/j.issn.1003-0174.2020.12.030

19. Jin ZC, Zhang RG, Han JQ, Ma L, Yang X, Wang XL, et al. Walnut protein and its development and utilization. *Food Ferment Ind* (2016) 42(06):265–70. doi: 10.13995/j.cnki.11-1802/ts.201606046

20. Yi J, Cao C, Zhu Z. Study on factors influencing solubility and emulsification of walnut isolated protein. *J Shaanxi Univ Sci Technol* (2017) 35(05):128–32+38. doi: 10.19481/j.cnki.issn2096-398x.2017.05.023

21. Gao P, Li H, Chen Z, Yang X, Hu C, He D, et al. Optimization of the preparation process and functional properties of walnut isolated protein. *China Oils Fats* (2022) 47(08):34–9. doi: 10.19902/j.cnki.zgyz.1003-7969.210795

22. Sze-Tao KWC, Sathe SK. Walnuts (Juglans regia l): proximate composition, protein solubility, protein amino acid composition and protein *in vitro* digestibility. *J Sci Food Agric* (2000) 80(9):1393–401. doi: 10.1002/1097-0010(200007)80:9<1393::aid-jsfa653>3.0.co;2-f

23. Li M, Zhang Y, You X, Zhou K, Wang Y, Wei P, et al. Processing Technology Optimization of Walnut Beverage. *Storage and Process* (2020) 20 (04):158–164. doi: 10.3969/j.issn.1009-6221.2020.04.025

24. Liu MC, Yang SJ, Hong D, Yang JP, Liu M, Lin Y, et al. A simple and convenient method for the preparation of antioxidant peptides from walnut (Juglans regia l.) protein hydrolysates. *Chem Cent J* (2016) 10:39. doi: 10.1186/s13065-016-0184-x

25. Lei Y, Gao S, Xiang X, Li X, Yu X, Li S. Physicochemical, structural and adhesion properties of walnut protein isolate-xanthan gum composite adhesives using walnut protein modified by ethanol. *Int J Biol Macromol* (2021) 192:644–53. doi: 10.1016/j.ijbiomac.2021.10.022

26. Zhao X, Liu H, Zhang X, Zhu H. Comparison of structures of walnut protein fractions obtained through reverse micelles and alkaline extraction with isoelectric precipitation. *Int J Biol Macromol* (2019) 125:1214–20. doi: 10.1016/j.ijbiomac.2018.09.095

27. Zhao J, Zhang R, Ma YWang X, Feng B, Zhang Y. Optimization of Protein Extraction from Walnut Dregs. *Food Sci* (2014) 35(18):40–6. doi: 10.7506/spkx1002-6630-201418008

28. Yu Y, Bao Y. Extraction and SDS-PAGE Analysis of Alkali-Soluble Proteins from Juglans mandshurica Maxim Kernels. *Food Science* (2012) 33(18):10–3. doi: 1002-6630(2012)18-0010-04

29. Lv S, Taha A, Hu H, Lu Q, Pan S. Effects of ultrasonic-assisted extraction on the physicochemical properties of different walnut proteins. *Molecules* (2019) 24 (23):4260. doi: 10.3390/molecules24234260

30. Li X, Guo M, Chi J, Ma J. Bioactive peptides from walnut residue protein. *Molecules* (2020) 25(6):1285. doi: 10.3390/molecules25061285

31. Wang J, Liu J, John A, Jiang Y, Zhu H, Yang B, et al. Structure identification of walnut peptides and evaluation of cellular antioxidant activity. *Food Chem* (2022) 388:132943. doi: 10.1016/j.foodchem.2022.132943

32. Chen N, Yang H, Sun Y, Niu J, Liu S. Purification and identification of antioxidant peptides from walnut (Juglans regia l.) protein hydrolysates. *Peptides* (2012) 38(2):344–9. doi: 10.1016/j.peptides.2012.09.017

33. Li X, Du MX, FuL W, MY S, JH X, Xie MY. Research progress in the preparation and separation and purification of bioactive peptides. *Sci Technol Food Ind* (2017) 38(20):336–40+46. doi: 10.13386/j.issn1002-0306.2017.20.061

34. Li J, Ye L, Rong R. Research Advances on Enzymatic Preparation and Separation Identification of Bioactive Peptides. *Food Research and Development* (2012) 33(02):195–9. doi: 10.3969/j.issn.1005-6521.2012.02.058

35. Wu WX, Chen CY, Zhao SL, Ge F, Liu DQ, Liu BQ, et al. Study on the preparation of active peptides and their antioxidative activity from solid-state fermented walnut meal. *Sci Technol Food Ind* (2013) 34(16):266–71. doi: 10.13386/j.issn1002-0306.2013.16.044

36. Liu D, Guo Y, Ma H. Production, bioactivities and bioavailability of bioactive peptides derived from walnut origin by-products: a review. *Crit Rev Food Sci Nutr* (2022) 1:1–16. doi: 10.1080/10408398.2022.2054933

37. Li T, Wu C, Liao J, Jiang T, Xu H, Lei H. Application of protein hydrolysates from defatted walnut meal in high-gravity brewing to improve fermentation performance of lager yeast. *Appl Biochem Biotechnol* (2020) 190(2):360–72. doi: 10.1007/s12010-019-03109-8

38. Wang X, Yu H, Xing R, Li P. Characterization, preparation, and purification of marine bioactive peptides. *BioMed Res Int* (2017) 2017:9746720. doi: 10.1155/2017/9746720

39. Lv M, Shi X, Zhang L, Meng J, Wang N, Wang F, et al. Functional properties of walnut peptides and progress of preparation process. *China Oils Fats* (2013) 38 (05):34–8. doi: 10.3969/j.issn.1003-7969.2013.05.009

40. Hao J, Zhang W, Yang H, Zhao J, Zhang R, Zhang Y, et al. Study on the preparation process of microcapsule instant walnut powder by walnut meal. *Journal of Shaanxi Normal University (Natural Science Edition)* (2019) 425 (5):103–8. doi: 10.15983/j.cnki.jsnu.2014.05.044

41. Uğurlu S, Okumuş E, Bakkalbaşı E. Reduction of bitterness in green walnuts by conventional and ultrasound-assisted maceration. *Ultrason Sonochem* (2020) 66:105094. doi: 10.1016/j.ultsonch.2020.105094

42. Liu MC, SJ Y, Hong D, JP Y, Liu M, Lin Y, et al. A simple and convenient method for the preparation of antioxidant peptides from walnut (Juglans regia l.) protein hydrolysates. *Chem Cent J* (2016) 10:39. doi: 10.1186/s13065-016-0184-x

43. Miao FJ, Ning DL. Research progress on biological activity of walnut peptides. *China Oils Fats* (2021) 46(03):48–51. doi: 10.19902/j.cnki.zgyz.1003-7969.2021.03.010

44. Wang D, Zhou H, Wang X, Qiu S, Tian Y. Optimization of enzymatic extraction of walnut peptides by response surface methodology. *Food Res Dev* (2015) 36(15):19–22. doi: 10.13386/j.issn1002-0306.2017.16.027

45. Lu X, Hua Y, Chen Y, Zhang C, Kong X. Effect of processing conditions on the dissolution rate of walnut protein. *J Anhui Agric. Sci* (2018) 46(13):155–9. doi: 10.13989/j.cnki.0517-6611.2018.13.047

46. Chen S, Li L, Shi Y, Hu J, Xu X, Li J, et al. Optimization of enzymatic preparation of walnut peptides by response surface methodology. *Sci Technol Food Ind* (2017) 38(16):142–9+58. doi: 10.13386/j.issn1002-0306.2017.16.027

47. Idowu AT, Benjakul S. Bitterness of fish protein hydrolysate and its debittering prospects. *J Food Biochem* (2019) 43(9):e12978. doi: 10.1111/jfbc.12978

48. Behera SS, Ray RC. Solid state fermentation for production of microbial cellulases: Recent advances and improvement strategies. *Int J Biol Macromol* (2016) 86:656–69. doi: 10.1016/j.ijbiomac.2015.10.090

49. Sun S, Song JM, Zhang CS. Current status of research and application of solid-state fermentation technology. *China Food Addit* (2007) 04):54–8. doi: 10.19902/j.cnki.zgyz.1003-7969.2021.03.010

50. Li L, Wang L, Fan W, Jiang Y, Zhang C, Li J, et al. The application of fermentation technology in traditional Chinese medicine: A review. *Am J Chin Med* (2020) 48(4):899–921. doi: 10.1142/S0192415X20500433

51. He Y, Chen J. Peptides prepared by lactic acid bacteria from walnut meal and their in vitro antioxidant activity. preparation of peptides from fermented walnut meal by lactic acid bacteria and their *in vitro* antioxidant activity. *Food Res Dev* (2022) 43(10):117–23+46. doi: 10.12161/j.issn.1005-6521.2022.10.016

52. Liu X, Guo L, Ma H, Wang K, Wu P, Hong C, et al. Optimization of process conditions for the preparation of walnut peptides by solid-state fermentation of bacillus subtilis and aspergillus niger. *Mod Food Sci Technol* (2018) 34(08):130–7. doi: 10.13982/j.mfst.1673-9078.2018.8.020

53. Wu W, Chen Z, Zhao S, Ge F, Liu D, Liu B, et al. Study on the preparation of active peptides from solid fermented walnut meal and their antioxidant activity. *Sci Technol Food Ind* (2013) 34(16):266–71. doi: 10.13386/j.issn1002-0306.2013.16.044

54. Liang X, Zhao S, Cao G, Cai X, Cheng X, He X, et al. Preliminary study of liquid fermented walnut cake meal. *China Brew* (2013) 32(12):66–9. doi: 10.3969/j.issn.0245-5071.2013.12.016

55. Xu Dian. *Preparation and biological activity of walnut peptides by aspergillus niger fermentation*. (Beijing: Beijing Forestry University) (2014).

56. Jahanbani R, Ghaffari SM, Salami M, Vahdati K, Sepehri H, Sarvestani NN, et al. Antioxidant and anticancer activities of walnut (Juglans regia l.) protein hydrolysates using different proteases. *Plant Foods Hum Nutr* (2016) 71(4):402–9. doi: 10.1007/s11130-016-0576-z

57. Tang X, He Z, Dai Y, Xiong YL, Xie M, Chen J. Peptide fractionation and free radical scavenging activity of zein hydrolysate. *J Agric Food Chem* (2010) 58 (1):587–93. doi: 10.1021/jf9028656

58. Xie B, Fu H, Yang F. Research progress on preparation, purification, identification and structure-activity relationship of bioactive peptides. *Sci Technol Food Ind* (2021) 42(05):383–91. doi: 10.13386/j.issn1002-0306.2020050012

59. Cheng J, Chen D, Qu M, Yu L, Mo Z. Optimization of the preparation process of walnut peptide and its memory improvement function. *Sci Technol Food Ind* (2021) 42(11):135–41. doi: 10.13386/j.issn1002-0306.2021040288

60. Wang W, Li Y, Jiang Y, Shen M. Optimization of enzymatic digestion and decolorization process of walnut protein. *Sci Technol Cereals Oils Foods* (2022) 30 (03):105–12. doi: 10.16210/j.cnki.1007-7561.2022.03.012

61. Bi D, Zhao Y, Jiang R, Wang Y, Tian Y, Chen X, et al. Phytochemistry, bioactivity and potential impact on health of juglans: the original plant of walnut. *Nat Prod Commun* (2016) 11(6):869–80. doi: 10.1177/1934578X1601100643

62. Zhi T, Hong D, Zhang Z, Li S, Xia J, Wang C, et al. Anti-inflammatory and gut microbiota regulatory effects of walnut protein derived peptide LPF in vivo. *Food Res Int* (2022) 152:110875. doi: 10.1016/j.foodres.2021.110875

63. Wang M, Amakye WK, Guo L, Gong C, Zhao Y, Yao M, et al. Walnut-derived peptide PW5 ameliorates cognitive impairments and alters gut microbiota in APP/PS1 transgenic mice. *Mol Nutr Food Res* (2019) 63(18):e1900326. doi: 10.1002/mnfr.201900326

64. Wu L, Liu R, Du Q, Chen Q, Ren J, Fan R, et al. Anti-fatigue effects of walnut peptides in mice. *Food Nutr China* (2018) 24(12):50–4. doi: 10.3969/j.issn .1006-9577.2018.12.012

65. Wang J, Wu T, Fang L, Liu C, Liu X, Li H, et al. Peptides from walnut (Juglans mandshurica maxim.) protect hepatic HepG2 cells from high glucose-induced insulin resistance and oxidative stress. *Food Funct* (2020) 11(9):8112–21. doi: 10.1039/d0fo01753a

66. Zhao F, Liu C, Fang L, Lu H, Wang J, Gao Y, et al. Walnut-derived peptide activates PINK1 *via* the NRF2/KEAP1/HO-1 pathway, promotes mitophagy, and alleviates learning and memory impairments in a mice model. *J Agric Food Chem* (2021) 69(9):2758–72. doi: 10.1021/acs.jafc.0c07546

67. Zou J, Cai PS, Xiong CM, Ruan JL. Neuroprotective effect of peptides extracted from walnut (Juglans sigilata dode) proteins on Aβ25-35-induced memory impairment in mice. *J Huazhong Univ Sci Technol Med Sci* (2016) 36 (1):21–30. doi: 10.1007/s11596-016-1536-4

68. Liu R, Wu L, Du Q, Ren JW, Chen QH, Li D, et al. Small molecule oligopeptides isolated from walnut (Juglans regia l.) and their anti-fatigue effects in mice. *Molecules* (2018) 24(1):45. doi: 10.3390/molecules24010045

69. Kim DI, Kim KS. Walnut extract exhibits anti-fatigue action *via* improvement of exercise tolerance in mice. *Lab Anim Res* (2013) 29(4):190–5. doi: 10.5625/lar.2013.29.4.190

70. Jahanbani R, Bahramnejad E, Rahimi N, Shafaroodi H, Sheibani N, Moosavi-Movahedi AA, et al. Anti-seizure effects of walnut peptides in mouse models of induced seizure: The involvement of GABA and nitric oxide pathways. *Epilepsy Res* (2021) 176:106727. doi: 10.1016/j.eplepsyres.2021.106727

71. Li X, Peng X, Guo K, Tan Z. Bacterial diversity in intestinal mucosa of mice fed with dendrobium officinale and high-fat diet. *3 Biotech* (2021) 11(1):22. doi: 10.1007/s13205-020-02558-x

72. Guo K, Xu S, Zhang Q, Peng M, Yang Z, Li W, et al. Bacterial diversity in the intestinal mucosa of mice fed with asparagus extract under high-fat diet condition. *3 Biotech* (2020) 10(5):228. doi: 10.1007/s13205-020-02225-1

73. Yang XY, Zhong DY, Wang GL, Zhang RG, Zhang YL. Effect of walnut meal peptides on hyperlipidemia and hepatic lipid metabolism in rats fed a high-fat diet. *Nutrients* (2021) 13(5):1410. doi: 10.3390/nu13051410

74. Ma S, Huang D, Zhai M, Yang L, Peng S, Chen C, et al. Isolation of a novel bio-peptide from walnut residual protein inducing apoptosis and autophagy on cancer cells. *BMC Complement Altern Med* (2015) 15:413. doi: 10.1186/s12906-015-0940-9

75. Zhang T, Zhu N, Liu R, Du Q, Wulan, Wang T, et al. Functional effects of walnut oligopeptides on laxative function. *Chin J Public Health* (2019) 35 (09):1225–8. doi: 10.11847/zgggws1119521

76. He L, Liu Y, Guo Y, Shen K, Hui H, Tan Z. Diversity of intestinal bacterial lactase gene in antibiotics-induced diarrhea mice treated with Chinese herbs compound qi wei bai Zhu San. *3 Biotech* (2018) 8(1):4. doi: 10.1007/s13205-017-1024-y

77. Hui H, Wu Y, Zheng T, Zhou S, Tan Z. Bacterial characteristics in intestinal contents of antibiotic-associated diarrhea mice treated with qiweibaizhu powder. *Med Sci Monit* (2020) 26:e921771. doi: 10.12659/MSM.921771

78. Li C, Zhou K, Xiao N, Peng M, Tan Z. The effect of qiweibaizhu powder crude polysaccharide on antibiotic-associated diarrhea mice is associated with restoring intestinal mucosal bacteria. *Front Nutr* (2022) 9:952647. doi: 10.3389/fnut.2022.952647

frontiers | Frontiers in Endocrinology

TYPE Original Research
PUBLISHED 06 January 2023
DOI 10.3389/fendo.2022.1103972



OPEN ACCESS

EDITED BY
Zhoujin Tan,
Hunan University of Chinese Medicine, China

REVIEWED BY
Juntao Kan,
Nutrilite Health Institute, China
Shuai Wang,
Guangzhou University of Chinese Medicine, China
Junhu Cheng,
South China University of Technology, China

*CORRESPONDENCE
Wei Liu
biolwei@sina.com

†These authors have contributed equally to this work

SPECIALTY SECTION
This article was submitted to Gut Endocrinology, a section of the journal Frontiers in Endocrinology

RECEIVED 21 November 2022
ACCEPTED 19 December 2022
PUBLISHED 06 January 2023

CITATION
Ye X, Wu K, Xu L, Cen Y, Ni J, Chen J, Zheng W and Liu W (2023) Methanol extract of *Inonotus obliquus* improves type 2 diabetes mellitus through modifying intestinal flora. *Front. Endocrinol.* 13:1103972. doi: 10.3389/fendo.2022.1103972



# Methanol extract of *Inonotus obliquus* improves type 2 diabetes mellitus through modifying intestinal flora

Xuewei Ye[1†], Kefei Wu[1†], Langyu Xu[1], Yingxin Cen[1], Jiahui Ni[1], Junyao Chen[1], Wenxin Zheng[1] and Wei Liu[2*]

[1]Key Laboratory of Pollution Exposure and Health Intervention of Zhejiang Province, Department of Basic Medical Sciences, Shulan International Medical College, Zhejiang Shuren University, Hangzhou, China, [2]Institute of Plant Protection and Microbiology, Zhejiang Academy of Agricultural Sciences, Hangzhou, China

Type 2 diabetes mellitus (T2DM) poses a significant risk to human health. Previous research demonstrated that *Inonotus obliquus* possesses good hypolipidemic, anti-inflammatory, and anti-tumor properties. In this research, we aim to investigate the potential treatment outcomes of *Inonotus obliquus* for T2DM and discuss its favourable influences on the intestinal flora. The chemical composition of *Inonotus obliquus* methanol extracts (IO) was analyzed by ultra-high-performance liquid chromatography-Q extractive-mass spectrometry. IO significantly improved the blood glucose level, blood lipid level, and inflammatory factor level in T2DM mice, and effectively alleviated the morphological changes of colon, liver and renal. Acetic acid, propionic acid, and butyric acid levels in the feces of the IO group were restored. 16S rRNA gene sequencing revealed that the intestinal flora composition of mice in the IO group was significantly modulated. *Inonotus obliquus* showed significant hypoglycemic and hypolipidemic effects with evident anti-inflammatory activity and improved the morphological structure of various organs and cells. *Inonotus obliquus* increased the levels of short-chain fatty acids in the environment by increasing the population of certain bacteria that produce acid, such as *Alistipes* and *Akkermansia*, which are beneficial to improve intestinal flora disorders and maintain intestinal flora homeostasis. Meanwhile, *Inonotus obliquus* further alleviated T2DM symptoms in db/db mice by down-regulating the high number of microorganisms that are dangerous, such as *Proteobacteria* and *Rikenellaceae_RC9_gut_group* and up-regulating the abundance of beneficial bacteria such as *Odoribacter* and *Rikenella*. Therefore, this study provides a new perspective for the treatment of T2DM by demonstrating that drug and food homologous active substances could relieve inflammation *via* regulating intestinal flora.

KEYWORDS

***Inonotus obliquus*, T2DM, db/db mice, intestinal flora, SCFAs**

# 1 Introduction

Type 2 diabetes mellitus (T2DM), a chronic metabolic condition, is characterized by hyperglycemia, dyslipidemia, and impaired glucose tolerance, which can lead to a variety of chronic complications including diabetic nephropathy, cardiovascular disease, retinopathy, neuropathy, significantly lower patients' quality of life and so on (1–3). With unhealthy lifestyles and dietary habits, the prevalence of diabetes has increased remarkably and become a public health problem that seriously threatens human health (4). A strong correlation between intestinal flora and diabetes began to reveal. Recent studies have shown that the intestinal flora plays an important role in maintaining gut homeostasis, especially in the regulation of inflammation (5). Through the interaction with dietary components, it affects intestinal permeability, glucose homeostasis, insulin sensitivity, glucose lipid metabolism and so on (6–8). Therefore, it is of great clinical significance and prospect to explore safer and more effective natural anti-diabetic drugs to regulate the intestinal flora of diabetic patients (9–11).

*Inonotus obliquus*, an edible fungus belongs to the genus *Fusarium* of the family Polyporaceae, is a valuable medicinal fungus with anti-aging, hypolipidemic, antitumor, anti-inflammatory, and anti-bacterial activities (12). *Inonotus obliquus* polysaccharide enhanced glucose tolerance and insulin sensitivity in T2DM mice, and had a significant hypoglycemic effect on T2DM mice. In addition, *Inonotus obliquus* shows a protective effect on the kidney of mice (13, 14). Previously, *Inonotus obliquus* has been shown to enhance glucose tolerance and insulin sensitivity in T2DM mice and improve hyperglycemic symptoms in type 2 diabetes patients (15). In addition, it can alleviate and protect kidney damage in patients with diabetic end-stage renal disease (16, 17). A recent study showed that a polysaccharide from *Inonotus obliquus* improved intestinal barrier dysfunction in mice with type 2 diabetes by upregating firmicutes abundance, inhibiting bacteroides levels and production of pro-inflammatory factors (18). However, the mechanism and efficacy of *Inonotus obliquus* to improve other symptoms of type 2 diabetes mice by altering intestinal microbiome remain unclear. Thus, this study investigated the beneficial therapeutic effects of *Inonotus obliquus* on intestinal flora dysbiosis in db/db mice. We found that *Inonotus obliquus* displayed consistent hypoglycemic effects, reduced body weight, improved lipid metabolism disorders, alleviated inflammation and the degree of lesions in different organs, and regulated the makeup and metabolism of the intestinal flora in db/db mice.

# 2 Materials and methods

## 2.1 Extraction and principal component analysis of *Inonotus obliquus*

*Inonotus obliquus* was provided by Ji 'an Tianhe Ginseng Antler Products Co., LTD (222894S-2019).

The air-dried *Inonotus obliquus* were pulverized for extraction. The ground powder of *Inonotus obliquus* (1 *kg*) was extracted with 1500 mL of methanol by sonication for 90 min, repeating 3 times. After filtration, all extracts were combined and distilled under reduced pressure. The *Inonotus obliquus* methanol extracts (IO) was concentrated to dryness *in vacuo* to provide samples for biological testing (19).

ACQUITY UPLC® HSS T3 column (2.1 × 150 mm, 1.8 μm) was used for ultra-high-performance liquid chromatography-Q extractive-mass spectrometry (UHPLC-QE-MS) analysis. Positive ions (0.1% formic acid water (C) - 0.1% formic acid acetonitrile (D)); negative ions (5 mM ammonium formate water (A) - acetonitrile (B)) were used as mobile phases. The gradient elution program was set as follows: 0~1 min, 2% B/D; 1~9 min, 2~50% B/D; 9~12 min, 50~98% B/D; 12~13.5 min, 98% B/D; 13.5~14 min, 98%~2% B/D; 14~20 min, 2% D - positive mode (14~17 min, 2% B - negative mode). The Electrospray Ionization Mass Spectrometry (ESI-MS) source conditions were set as sheath gas 30 arb, auxiliary gas 10 arb, capillary temperature 325°C, resolution 60,000 positive and negative ionization mode, spray voltage 3.50 kV (positive), spray voltage 2.50 kV (negative).

## 2.2 Animal experiments

A total of 24 C57BKS-db mice (db/db, male, eight-week-old, 45 ± 5 g) and eight C57/BKS mice (wild type, male, eight-week-old, 25 ± 5 g) were used. Animals (SPF grade) were provided by the Jiangsu GemPharmatech Co., LTD and were kept on adaptive feeding for a week. The protocol was approved by the Committee on the Ethics of Animal Experiments of the Zhejiang Academy of Agricultural Sciences. All mice were kept in an SPF-class animal house of the Zhejiang Academy of Agricultural Sciences, fed with conventional feed ad libitum, and a 16-hour artificial LED light cycle is maintained indoors at a constant temperature of 20 °C and relative humidity of 55%. Mice with random Blood sugar level more than 11.1 mmol/L on various days were chosen at random for the experimental group after blood was drawn from the tail vein over the course of three days. According to blood glucose and body weight, the DB group was created by randomly selecting db/db mice (model, saline), the DM group (metformin hydrochloride 200 mg/kg, positive control), and the IO group (IO intervention, 600 mg/kg) (12, 20, 21). The solvent used for intragastric administration was 0.9% normal saline.There were eight mice in each group. Eight C57/BKS (Wild Type) mice were set as the K group (blank control, saline). The administration was fixed at the same time, once every day, for eight weeks of continuous intervention. Fasting blood glucose, OGTT test, and mice feces were collected weekly. After blood sampling, animals were sacrificed by cervical dislocation at the end of the fourth and eighth weeks. The tissues from the kidney, pancreas, and liver were promptly separated, removed, wiped on filter paper, and weighed on an

electronic balance.The organ weight coefficients were calculated according to the formula: Organ weight coefficient = organ weight (g)/body weight (g) (22). The colon, liver, and kidney tissues were taken and fixed in 4% paraformaldehyde for histopathological examination. The feces, blood samples, and remaining tissues were frozen at -80 °C.

## 2.3 Biochemical testing

### 2.3.1 Analysis of fasting blood glucose and oral glucose tolerance test

The OGTT test was performed after weekly administration. All mice fasted without water the night before the experiment. After 12 h, FBG was determined as 0 min blood glucose. After weighing them, mice were given a glucose solution at a rate of 2 mg/kg *via* gavage. Following glucose loading, blood glucose was taken at 30, 60, 90, and 120 min. The area under the curve (AUC) was then computed (23).

### 2.3.2 The detection of inflammatory factors and blood lipid levels

Blood was extracted from the ocular vein of mice and rested for 2 h. After that, it spent 20 min in a water bath at 37°C. After centrifuging the blood at a temperature of 4 degrees Celsius for 10 min at a rate of 3000 revolutions per min, the serum was collected (24).

ELISA kit was used to test inflammatory factors purchased from Boster Biological Technology Co., LTD. Serum tumor necrosis factor-α (TNF-α, EK0527), interleukin-1β (IL-1β, PROTP10749), interleukin-6 (IL-6, EK0411), and interleukin-10 (IL-10, EK0417) assays were performed according to Boster manufacturer's instructions. Add 100 μL of samples and standards to each well, and react at 37°C for 90 min. Add 100 μL of biotin-labeled antibody to each well, react at 37°C for 60 min, and wash with 0.01M TBS three times after the reaction. Add 100 μL ABC to each well, react at 37°C for 30 min, and wash 5 times with 0.01M TBS again. TMB was reacted at 37°C in the dark for 30 min, and finally TMB stop solution was added for reading.

The blood lipid levels were detected according to the kits purchased from Purebio Biotechnology Co., LTD. Serum Total Cholesterol (TC, CH01, 20210622), Triacylglycerol (TG,TG01, 20210618), High-density lipoprotein cholesterol (HDL-C, HL01, 20210522)and Low-Density Lipoprotein Cholesterol(LDL-C, LDL01, 20210428) concentrations were measured according to the manufacturer's instructions of GPO-PAP method, CHOD-PAP method, direct method-selective inhibition method, direct method-surfactant scavenging method were used for detection.

## 2.4 Histopathological analysis and pathological histology score

After embedding, sectioning, and H&E staining, the histomorphology of the liver, colon, and kidney tissues was observed under the microscope. The pathological tissue score for each organ was based on the relevant literature (6, 25–27) and the scoring criteria are showed in Tables S1-S4. The kidney pathological score was calculated as the sum of the glomerular and tubular scores.

## 2.5 Analysis of intestinal flora and metabolism

### 2.5.1 Short-chain fatty acids (SCFAs) analysis

We determined four major SCFAs: acetic acid, propionic acid, butyric acid, and isobutyric acid. Feces were placed in a centrifuge tube with PBS buffer (pH 7.4) at a ratio of 1:10 to dissolve the samples, and the mixture was vortexed and mixed thoroughly. Filter the supernatant (4°C, 10 000 r/min, 5 min) through 0.45 μm filter paper into a clean centrifuge tube. The filtrate was acidified with crotonic acid at 5:1 for 24 h, and then the SCFAs were determined by gas chromatography (GC) (28). GC (Shimadzu, Japan) with DB-FFAP column (0.32 mm × 30 m × 0.5 μm, Agilent Technologies, USA) was used to quantify the SCFAs. The operation condition was as follows: the flow rate of nitrogen carrier gas: 19.0 mL/min; split ratio: 1:10, the temperature of both detector and injection port: 250 °C. Crotonic acid was used as internal standard.

### 2.5.2 DNA extraction and 16S rRNA gene sequencing

Genomic DNA was extracted from fecal samples with TruSeq Nano DNA LT Sample Preparation Kit (Illumina, USA) following the kit protocol. The bacterial 16S rRNA gene was amplified using a 343F/798R primer set (343 F: TACGGRAGGCAGCAG; 798 R: AGGGTATCTAATCCT) targeting the V3-V4 region. PCR products are detected using electrophoresis and purified using magnetic beads. The DNA concentration was detected using agarose gel electrophoresis and NanoDrop2000, and the 16S rRNA gene targeting the V3-V4 region was amplified by PCR with Tks Gflex DNA polymerase (Tks Gflex DNA Polymerase, Takara, China). Then the PCR product was detected by electrophoresis, purified by magnetic beads and then used as a template for the second round of PCR to perform PCR amplification, electrophoresis detection and magnetic bead purification again. The PCR product was tested for Qubit concentration immediately after purification. According to the concentration of the same amount of polyculture, it was sequenced on the machine. The arduous sequencing and data analysis of 16S rRNA was carried out in Shanghai Ouyi Biological Co., Ltd. Using the Vsearch (29) software, and according to the sequence similarity, the sequences were classified into multiple OUTs, and the sequence similarity of the OUTs of a unit was greater than or equal to 97%. Quantitative Insights Into Microbial Ecology (QIIME) software was used to select sample sequences from generated and deduplicated sequences for each Optical Transformation Unit (OTU) and annotated against the Silva (version 138) database with confidence intervals greater than 0.7 Annotations result. Alpha

diversity analysis (Chao1, Shannon, Simpson and Good's Coverage) and Beta diversity analysis (PCoA, NMDS) were analyzed using QIIME software. In addition, correlation analysis, LDA Effect Size (LEfSe) analysis, and linear discriminant analysis (LDA) were used to calculate and determine difference groups using correlation analysis tools and LEfSe tools, respectively. The flora prediction was analyzed using STAMP software.

## 2.6 Statistical analysis

The mean SD is used to express all experimental data. For normally distributed data, paired t test was performed between two groups, and one-wayANOVA followed by LSD test was performed between multiple groups. $P < 0.05$ was regarded as statistically significant. All data were statistically analyzed using SPSS 22.0 software. 16S rRNA analysis uses Silva (version138) database alignment, whereas species alignment annotation uses an RDP classifier (30) (confidence threshold was 70%).

# 3 Results

## 3.1 Identification of the chemical composition of *Inonotus obliquus*

The components of *Inonotus obliquus* were analyzed and identified using UHPLC-QE-MS. The Traditional Chinese Medicine Systems Pharmacology (TCMSP) and Analysis Platform databases were accessed to screen the bioactive compounds based on oral bioavailability % (OB%) and drug-likeness (DL) content (OB% > 30 and DL > 0.18). Fourteen active compounds were identified after the screening, including six flavonoids, one coumarin, one organic acid, and six other compounds (Anthracenes, beta-Carotene, Endogenous Metabolites, Steroids and steroid derivatives, Fatty Acyls, Carboxylic acids and derivatives). Table 1 shows the mass-to-charge ratios, types and identified compounds of the active compounds.

## 3.2 Effects of *Inonotus obliquus* on FBG and OGTT in db/db mice

Prior to pharmacological intervention, the mice in the DB, DM, and IO groups had substantially lower fasting blood glucose levels than the mice in the K group ($p < 0.001$) (Figure 1A). After three-week drug interventions, the DM and IO groups had much less fasting blood glucose than DB groups. ($p < 0.001$). Blood glucose levels in the IO group leveled off after six weeks and were substantially different from those in the DB group ($p < 0.001$). The mice in each group had elevated glucose levels following oral glucose injection, which persisted for 0 to 30 min. After 30–60 min, the glucose level of mice in each group gradually decreased. In contrast to the K group, the blood glucose and AUC of the DB group at each time point from 0–120 min were notably higher than those in the K group ($p < 0.01$). Compared with the DB group, the mice in the IO group showed a decreasing trend in blood glucose and AUC at each time point, including an evident decrease in blood

TABLE 1 Characterization of chemical constituents of *Inonotus obliquus*.

| No. | RT (min) | m/z | Type | Formula | OB (%) | DL | Identification | Class |
|---|---|---|---|---|---|---|---|---|
| 1 | 5.56 | 303.104 | $[M+H]^+$ | $C_{16}H_{14}O_6$ | 70.31 | 0.27 | Hesperetin | Flavonoids |
| 2 | 5.94 | 301.001 | $[M-H]^-$ | $C_{14}H_6O_8$ | 43.06 | 0.43 | Ellagic acid | Tannins |
| 3 | 6.71 | 291.084 | $[M+H]^+$ | $C_{15}H_{14}O_6$ | 48.96 | 0.24 | Epicatechin | Flavonoids |
| 4 | 7.87 | 269.046 | $[M-H]^-$ | $C_{15}H_{10}O_5$ | 33.52 | 0.21 | Baicalein | Flavonoids |
| 5 | 8.29 | 301.035 | $[M-H]^-$ | $C_{15}H10O_7$ | 46.23 | 0.27 | Morin | Flavonoids |
| 6 | 9.68 | 447.089 | $[M+H]^+$ | $C_{21}H_{18}O_{11}$ | 40.12 | 0.75 | Baicalin | Flavonoids |
| 7 | 9.95 | 283.022 | $[M-H]^-$ | $C_{15}H_8O_6$ | 47.07 | 0.28 | Rhein | Anthracenes |
| 8 | 10.64 | 301.037 | $[M-H]^-$ | $C_{15}H_{10}O_7$ | 46.43 | 0.28 | Quercetin | Flavonoids |
| 9 | 11.18 | 536.183 | $[M]^+$ | $C_{40}H5_6$ | 37.18 | 0.58 | beta-Carotene | Terpenoids and Glycosides |
| 10 | 11.27 | 271.094 | $[M+H]^+$ | $C_{16}H_{14}O_4$ | 34.55 | 0.22 | Imperatorin | Coumarins and derivatives |
| 11 | 11.38 | 272.062 | $[M+H]^+$ | $C_{15}H_{11}O_5$ | 37.99 | 0.21 | Pelargonidin | Endogenous Metabolites |
| 12 | 13.28 | 393.301 | $[M+H]^+$ | $C_{24}H_{40}O_4$ | 40.72 | 0.68 | Deoxycholic acid | Steroids and steroid derivatives |
| 13 | 13.7 | 305.249 | $[M+H]^+$ | $C_{20}H_{32}O_2$ | 45.57 | 0.2 | Arachidonic acid | Fatty Acyls |
| 14 | 13.71 | 439.361 | $[M+H-H_2O]^+$ | $C_{30}H_{48}O_3$ | 55.38 | 0.78 | Betulinic acid | Carboxylic acids and derivatives |

glucose level at 30 min ($p < 0.01$), a remarkable decrease at 120 min ($p < 0.05$) and restored basal level (Figures 1B, C).

## 3.3 Effects of *Inonotus obliquus* on the changes of body weight and organ coefficients in db/db mice

The body weights of the DB, DM, and IO groups were comparable at the start of the trial and were noticeably greater than those of the K group ($p$ <0.01). By the conclusion of the eighth week, the IO group of mice were much lighter than the DB group of mice in terms of body weight ($p < 0.05$) (Figure 1D). The liver organ coefficients of mice in the DB group rose considerably ($p < 0.01$) as compared to the K group ($p < 0.01$). However, the renal and pancreatic organ coefficients, substantially decreased ($p < 0.01$). Mice in the DM group had higher pancreatic organ coefficients than mice in the DB group ($p < 0.05$), and the ratio of liver weight to total weight reduced in mice in the IO group, while the renal and pancreatic weights tended to increase, all of which were closer to those in the K group (Figures 1E–G).

## 3.4 Effects of *Inonotus obliquus* on blood lipid levels

As shown in Figures 2A–D, the mice in the DB group exhibited hyperlipidemia with decreased HDL-C levels ($p < 0.001$) and increased LDL-C, TC, and TG levels. Compared with the mice in the DB group, the mice in the IO group showed a higher HDL-C ($p < 0.01$) and lower LDL-C, TC, and TG levels.

## 3.5 Effects of *Inonotus obliquus* on inflammatory factor

The inflammatory factors TNF-α ($p < 0.001$), IL-1β ($p < 0.001$), and IL-6 ($p < 0.01$) were increased in the DB group mice compared with the K group, although IL-10 was severely diminished ($p < 0.001$). Compared with the DB group, the expression levels of TNF-α and IL-1β were considerably decreased in the IO group ($p < 0.01$) and IL-6 was considerably decreased ($p < 0.05$) which compare to DB group. IL-10 expressed at a considerably greater level ($p < 0.001$). These data are illustrated in Figures 2E–H.

## 3.6 Effects of *Inonotus obliquus* on histomorphological changes in organs

Histopathological damage of the colon, liver, and renal was assessed by HE staining (Figures 3A, D). In K group, the mucosal epithelium of colonic tissues was intact, liver tissues were free of fibrosis, glomeruli were free of hypertrophy, and all tissues were free of inflammatory cell infiltrations. In the DB group of mice, colonic submucosa edema was seen, with a large number of cup cells disappearing, liver tissue steatosis, edema and fibrosis were severe, glomerular hypertrophy and capillary basement membrane thickening were seen, and all tissues were infiltrated with a large number of inflammatory cells. The organ morphology of the T2DM mice and the healthy normal mice were very dissimilar. All histopathological scores were greatly increased in the T2DM mice compared with the healthy normal mice ($p < 0.01$). Compared with the T2DM mice, no loss of cup cells was seen in the colonic tissues of mice

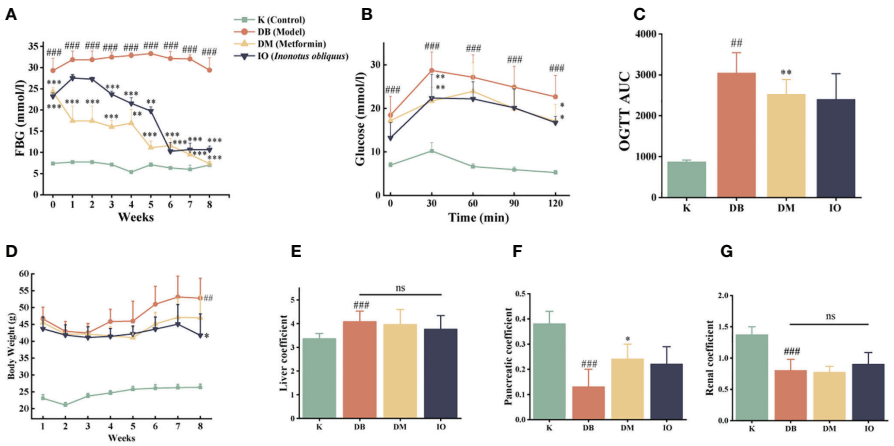


FIGURE 1
Influence of blood glucose utilization and organ coefficient *Inonotus obliquus* and metformin reduced blood glucose in db/db mice during the intervention period. FBG **(A)** and OGTT **(B, C)**. *Inonotus obliquus* and metformin exerted a weight loss effect **(D)**. *Inonotus obliquus* and metformin on liver coefficient **(E)**, pancreatic coefficient **(F)** and renal coefficient **(G)** in db/db mice. Data were expressed as the mean ± SD. $^{\#\#}p < 0.01$ vs. K, $^{\#\#\#}p < 0.001$ vs. K, $^{*}p < 0.05$ vs.DB, $^{**}p < 0.01$vs. DB, $^{***}p < 0.001$vs. DB.

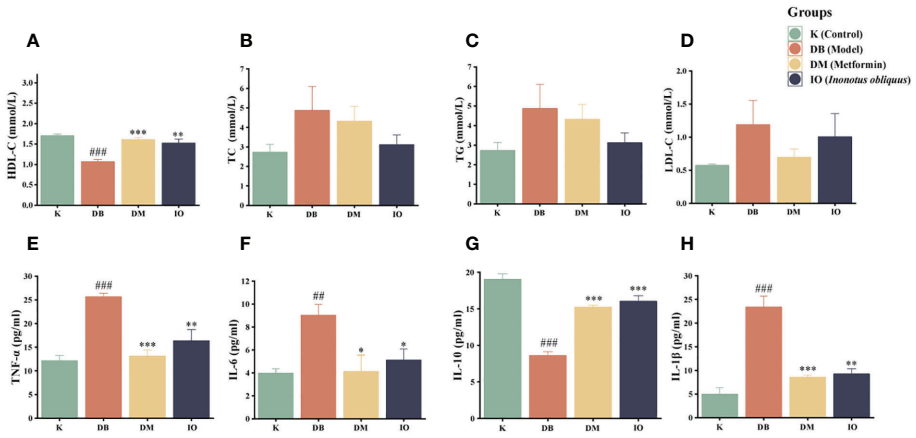


FIGURE 2
Effects of lipid metabolism and inflammatory cytokines. HDL-C **(A)**, TC **(B)**, TG **(C)** and LDL-C **(D)**. TNF-α **(E)**, IL-6 **(F)**, IL-10 **(G)** and IL-1β **(H)** inflammatory cytokines in the plasma of db/db mice. Data were expressed as the mean ± SD. $^{###}p < 0.001$ vs. K, $^{*}p < 0.05$ vs. DB, $^{**}p < 0.01$vs. DB, $^{***}p < 0.001$ vs. DB.

in the *Inonotus obliquus* and metformin-gavaged mice, the degree of crypt damage was reduced, and the colonic histopathological score was extremely significantly lower ($p < 0.001$) (Figures 3A-D). The liver fat degeneration and fibrosis were reduced. In the IO group, the liver tissue score was considerably lower ($p < 0.01$) (Figures 3B, E); There was a more typical glomerular shape, no cystic stenosis, and little inflammatory cell infiltration across all tissues; substantially less renal tissue was scored in the IO group ($p < 0.05$) (Figures 3C, F).

## 3.7 Effects of *Inonotus obliquus* on intestinal flora

### 3.7.1 Alpha and beta diversity analysis

Alpha diversity analysis indicates the degree of species diversity within a single biological environment, which is usually measured using two indices: species richness and species evenness. Species richness is more responsive to the Shannon index, but species evenness is more sensitive to the Simpson index.The chao1 index reflects the community species

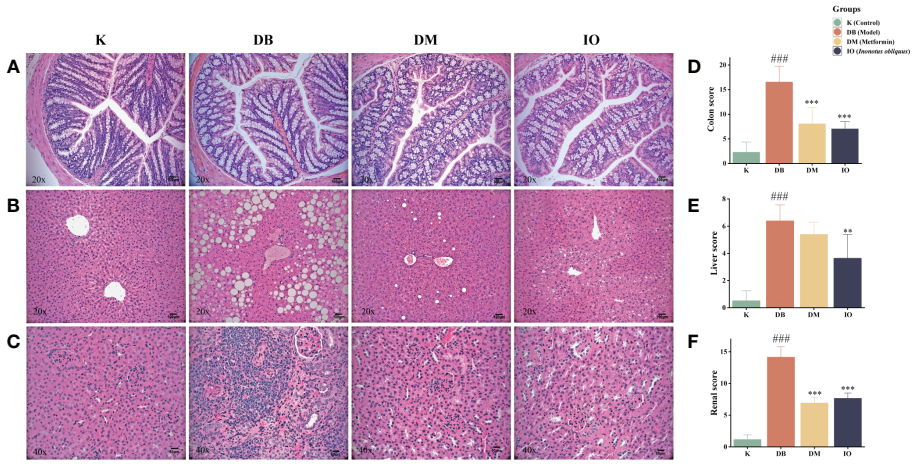


FIGURE 3
Histopathologic changes after 8 weeks of drug intervention. **(A)** Representative images of morphological changes in colon tissue. **(B)** Representative images of morphological changes in liver tissue. **(C)** Representative images of morphological changes in kidney tissue. **(D)** Histogram of colon tissue score. **(E)** Histogram of liver tissue score. **(F)** Histogram of renal tissue score. Data were expressed as the mean ± SD. ###p < 0.001 vs. K, **p < 0.01 vs. DB, ***p < 0.001 vs. DB.

richness; the higher the value, the higher the species richness. Good's Coverage reflects the OTU coverage of the sample (31). As shown in Figures 4A–D, the Good's Coverage values of the samples were above 97%, indicating that the sequences present in the samples were detected. In this study, we found that the intestinal flora richness and homogeneity of mice in the DB, DM and IO groups were reduced compared to the K group. In contrast to the DB group, the DM and IO groups' intestinal flora was more diverse and homogeneous. The differences in non-metric multi-dimensional scaling (NMDS) and principal co-ordinates analysis (PCoA) matrix scores (Figures 4E-F) indicated that all four groups of mice had different intestinal microbiota. The intergroup distance between the mice in groups K and DB was farther, showing that the mice in group DB significantly changed intestinal microbiota composition. The mice in groups IO and DM showed closer intergroup distance and were separated from those in group DB.

### 3.7.2 Changes in flora composition at the phylum and genus levels

The relative abundance values of microorganisms in each group of mice fecal samples were calculated by analyzing the structural distribution of microbial colonies in the samples based on the biotaxonomic level. At the level of the phylum (Figure 5A), the abundance of the same species in different groups was indicated, visually reflecting the variation in colony abundance. The groups were mainly composed of *Bacteroidetes*, *Firmicutes*, *Campilobacterota*, *Actinobacteriota*, and *Desulfobacterota*. Among them, *Firmicutes* and *Bacteroidetes* comprised a more significant proportion. The abundance of *Proteobacteria* (Figure 5B) and *Actinobacteriota* (Figure 5C) was significantly higher in the DB group than in the K group. The abundance of *Proteobacteria* and *Actinobacteria* was decreased in the DM and IO groups compared to the DB group. Compared with the K group at the genus level (Figure 5D), the DB group had a higher relative abundance of the *Rikenellaceae_RC9_gut_group* (Figure 5E) than the K group. *Alistipes* (Figure 5F), *Odoribacter* (Figure 5G), *Rikenella* (Figure 5H), and *Akkermansia* (Figure 5I) decreased in relative abundance.

### 3.7.3 LEfSe analysis

LDA discriminant bar graphs (LDA score > 3) and evolutionary branching graphs (Figures 6A, B) were done at the genus level. According to the findings, in the DB group, Providencia and Proteus were the dominant flora; in the DM group, *Firmicutes*, *Oscillospiraceae*, *Ruminococcaceae*, and *Odoribacter* were the dominant, and *Enterobacteriaceae*, *Escherichia*, and *Shigella* were dominant in IO group.

### 3.7.4 Effect of *Inonotus obliquus* on SCFAs

Butyric acid, acetic acid, and propionic acid are the three most common SCFAs, and they are the major end products of dietary fiber fermentation by gut bacteria. Figures 6C–F showed that the acetic acid, propionic acid, butyric acid, and isobutyric

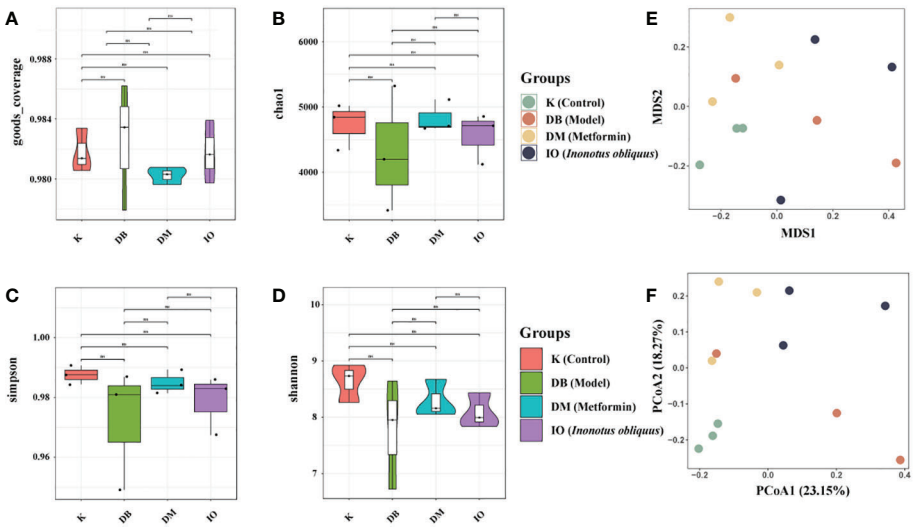


FIGURE 4
Alpha and Beta diversity analysis. Alpha diversity analysis indicates the degree of species diversity within a single biological environment. Beta diversity analysis clearly shows a clear separation between DB groups and IO groups. **(A)** Goods coverage; **(B)** Chao1; **(C)** Simpson; **(D)** Shannon. **(E)** NMDS1 and NMDS2 are two sorting axes, each point in the figure represents a sample, the same color is the same group, the IO group is separated from the module DB group; **(F)** Weighted UniFrac PCoA map based on OTU abundance. NS, non-significant, p>0.05. The first two principal coordinates (PC1 and PC2) of PCoA from weighted UniFrac were plotted for each sample to assess similarity between samples and groups.

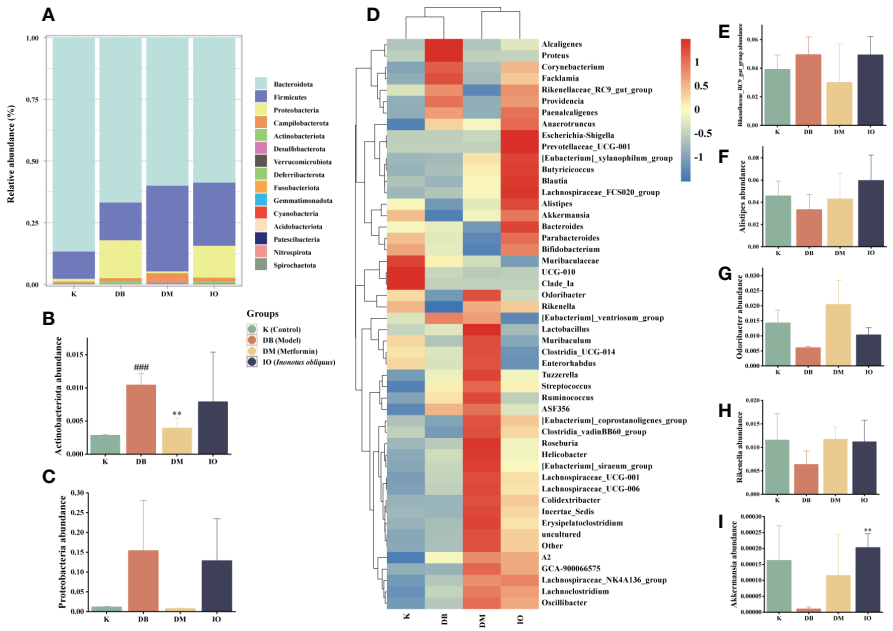


FIGURE 5
Structural changes of intestinal flora. Intestinal flora species abundance at the phylum and genus levels. **(A)** The relative abundance of microbial species at the phylum level in the feces of mice, **(B)** *Actinobacteriota*, **(C)** *Proteobacteria*. **(D)** The relative abundance of microbial species at the genus level in the feces of mice. **(E)** *Rikenellaceae_RC9_gut_group*, **(F)** *Alistipes*, **(G)** *Odoribacter*, **(H)** *Rikenella*, **(I)** *Akkermansia*. Data were expressed as the mean ± SD. $^{###}p < 0.001$ vs. K, $^{**}p < 0.01$ vs. DB.

acid concentrations in the DB group were lower than those in the K group. However, the concentration of acetic acid, propionic acid, butyric acid, and isobutyric acid was increased in the DM and IO groups compared with that of the DB group.

### 3.7.5 Correlation analysis with environmental factors

Figure 6G of the correlation study revealed that *Odoribacter* was inversely connected with OGTT, TNF-α, IL-6, IL-1β, and other physiological and biochemical markers of T2DM ($p < 0.05$), while *Proteus* was favorably correlated with IL-1β, IL-6, and TNF-α ($p < 0.01$) and strongly correlated with TNF ($p < 0.001$).

### 3.7.6 Colony function prediction

As shown in Figure 7, the protein function clusters predicted in this experiment were divided into 23 major groups according to the metabolic functions of the proteins. The annotation information of each functional level of mouse intestinal flora cluster of orthologous group (COG) was the same for each group, while the abundance information of each function differed between groups. In contrast to the mice in the K group, mice in the DB group had highly significant differences in COG function in J: Translation, ribosomal structure and biogenesis, M: Cell wall/membrane/envelope biogenesis, F: Nucleotide transport and metabolism and N: Cell motility ($p < 0.01$). Significant discrepancies were found between the IO and DB groups ($p < 0.05$): B: Chromatin structure and dynamics, K: Transcription, I: Lipid transport and metabolism and H: Coenzyme transport and metabolism.

## 4 Discussion

In this study, we found that *Inonotus obliquus* effectively reduced blood glucose, body weight, and lipids in db/db diabetic mice. It also had significant anti-inflammatory effects and inhibited the progression of lesions in various organs, indicating that the diabetic symptoms in mice were effectively improved. In addition, 16S rRNA gene sequencing of intestinal flora showed that *Inonotus obliquus* treatment could result in alterations in the overall composition and metabolism of intestinal flora in mice, which in turn improve the symptoms of T2DM.

### 4.1 Active substances in IO and its effect on improving diabetes

Using the UHPLC-QE-MS method, we studied the chemical composition of *Inonotus obliquus* and elucidated the major compounds. We identified 14 compounds, including steroids,

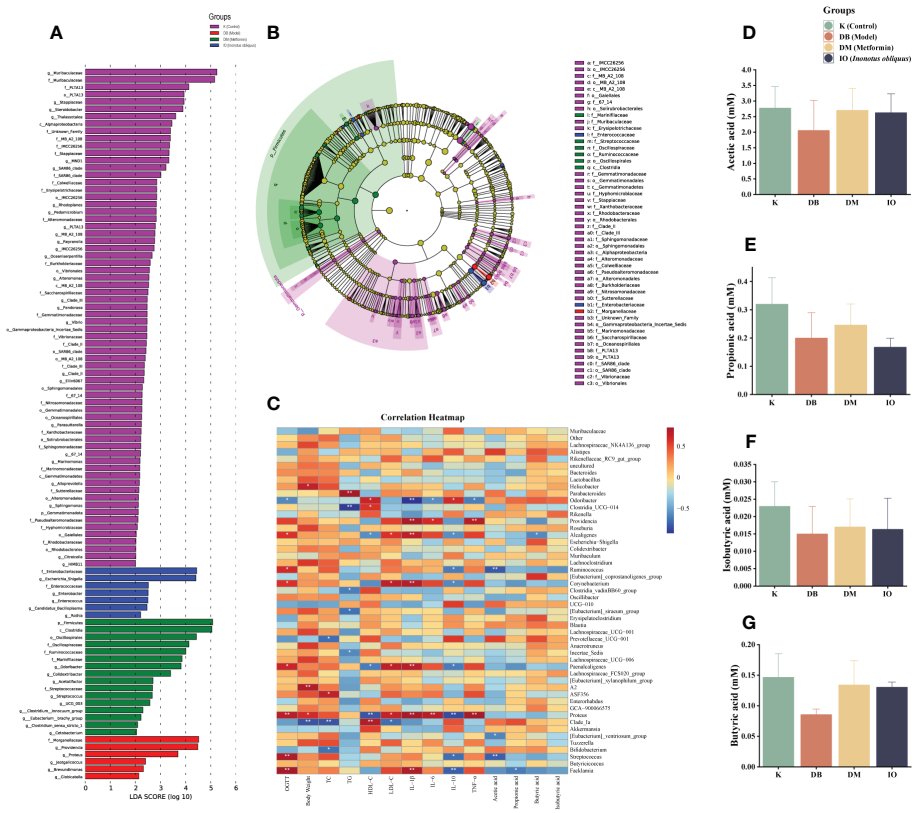


FIGURE 6
LEfSe, SCFAs leves, and correlation analysis. **(A)** Levels LEfSe analyzed gut microbiota that differed significantly among groups. Histogram of LDA scores of fecal 16S rRNA sequences from phylum level to genus level with LDA score >3; **(B)** The inner-to-outer radiating circle represents the evolutionary cladogram from phylum to genus; **(C)** Heat map of the relationship between intestinal microbiota at species level and diabetes-related indexes (The blue and red represent negative and positive correlation, respectively. *$p < 0.05$; **$p < 0.01$); *Inonotus obliquus* and metformin can change the composition of short chain fatty acids (SCFAs) in the stool of mice. *Inonotus obliquus* and metformin could restore fecal short-chain fatty acid content in db/db mice. *Inonotus obliquus* alters fecal short-chain fatty acids (SCFAs) levels of **(D)** acetate acid, **(E)** propionate acid, **(F)** butyrate acid and **(G)** isobutyrate acid.

flavonoids, coumarins, and organic acids. Epicatechin added to the mice diet had higher sensitivity to insulin than controls. Also, epicatechin inhibited gluconeogenesis in the liver, enhanced glycolysis, and promoted muscle glucose uptake by activating 5'AMP-activated protein kinase (AMPK) (32). Thus, by reducing blood glucose, epicatechin may have antidiabetic benefits. An important key characteristics of diabetes is obesity, and it has been demonstrated that β-carotene plays a crucial role in adipogenesis, lipolysis, insulin resistance, and other factors associated with T2DM (33). Thus, beta-carotene plays a role in mature adiposity, helps control lipid metabolism, regulates oxidative stress, and alleviates inflammation. Arachidonic acid is a potent inducer of insulin secretion, while its metabolites contribute differently to insulin resistance and play a crucial part in the onset and progression of prevalent disorders including diabetes and obesity (34). The anti-inflammatory activities of baicalein, baicalin, ellagic acid, and pelargonidin have all been reported (35–38). Additionally, morin might have effects that were anti-inflammatory, antidiabetic, and anticancer by modifying the activity of various enzymes (39). Hesperetin can exert anti-inflammatory activity by reducing pro-inflammatory cytokines and has antioxidant, hypolipidemic, and insulin-sensitizing properties that are therapeutic for various diseases and disorders (40). Quercetin exhibits sufficient anti-inflammatory activity to alleviate T2DM-induced inflammation, and it has been reported that quercetin ameliorates inflammation by downregulating nitric oxide synthase (NOS) expression and reducing TNF-α and nitric oxide production in visceral adipose tissue of obese rats (41, 42).

Imperatorin exerts its anti-inflammatory effect in macrophages at varying doses by inhibiting catalase, superoxide dismutase, and TNF-α (43, 44). In addition, some antitumor drugs also have anti-inflammatory activity (45), which might allow imperatorin to

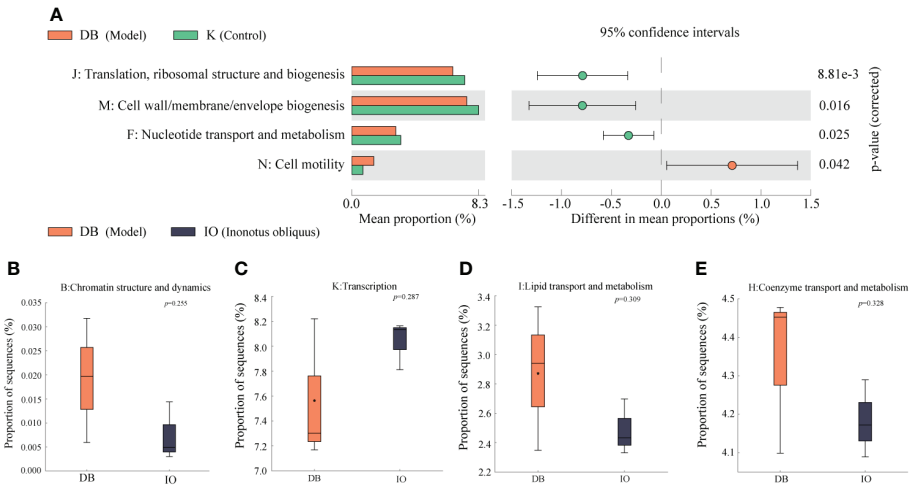


FIGURE 7
Function prediction. **(A)** Analysis of the differences in the prediction of intestinal flora function based on COG pathway between DB group and K group. Analysis of the differences between the DB group and the IO group in the functions of **(B)** Chromatin structure and dynamics, **(C)** Transcription, **(D)** Lipid transport and metabolism, and **(E)** Coenzyme transport and metabolism.

achieve antitumor effects by inhibiting macrophage inflammation. Rhein lowers inflammation by inhibiting the production of adhesion molecules on endothelial cells (ECAM) (46, 47). Thus, it is suggested that rhein has anti-inflammatory activity and improves the symptoms of T2DM. intestinal flora can convert deoxycholic acid to ursodeoxycholic acid (UDCA). UDCA has been found to reduce FBG and insulin concentrations (48). Furthermore, it has antioxidant, anti-inflammatory and cytoprotective effects and plays a significant function in lipid metabolism and intestinal barrier integrity (49). This suggests that deoxycholic acid can be modified to UDCA through intestinal flora metabolism and is able to lower blood glucose and have a positive effect on glucose tolerance while acting in the intestine to alleviate inflammation, protect the intestinal barrier and maintain intestinal microecological balance. In addition, it also has some anticancer potential (50), and because of its large content in *Inonotus obliquus*, it may have antitumor potential that warrants further research in the future (51). The above studies showed that *Inonotus obliquus* contains compounds with good hypoglycemic, lipid metabolism regulation, obesity improvement, and anti-inflammatory activities and has great antitumor potential, which needs further study (52).

## 4.2 The relationship between the improvement of diabetes and intestinal flora

Based on the ameliorative effect on diabetes, we performed 16S rRNA gene sequencing on feces samples and found that the effect of *Inonotus obliquus* on intestinal microbiota was on both the flora composition and the metabolism. Analyses of alpha diversity revealed that after treatment with *Inonotus obliquus*, the diversity and richness of the intestinal flora of mice in the IO group increased relative to the K group, which was similar to the results observed in the DM group. This suggested that *Inonotus obliquus* and metformin administration can significantly affect intestinal microbiota's abundance and improve intestinal flora's dysbiosis in db/db mice. PCoA and NMDS data revealed that IO affected the makeup of the intestinal flora. Compared to the K group, DB group had more *Proteobacteria* at the phylum level than IO group. It has been shown that *Proteobacteria* and TC levels exhibited a substantial positive link, as demonstrated by the present study results, which revealed an increase in TC levels among mice in the DB group and a decrease among mice in the IO group. It also demonstrated that blood glucose is positively correlated with *Proteobacteria*. In the current research, the OGTT level in the DB group rose, whereas the TC level in the IO group declined. The decrease of *Proteobacteria* and *Actinobacteria* in the IO group mice suggested that IO had some improvement effect on mice intestinal flora. IO may regulate glycolipid metabolism and improve glycolipid levels in db/db mice by regulating the abundance of *Proteobacteria* and *Actinobacteriota* flora. When compared to the K group, the relative abundance of the *Rikenellaceae_RC9_gut_group* gene was more abundant in the DB group whereas it was less abundant in the IO group. Another study showed that HFD might enhance the *Rikenellaceae_RC9_gut_group* (53). This suggested that IO may regulate abnormal lipid metabolism by regulating intestinal flora disorders and reducing the abundance of

*Rikenellaceae_RC9_gut_group*, thereby improving the hyperlipidemia level in db/db mice.

## 4.3 Interconnections between microbiota and metabolites

Mice in the DB group had lower levels of *Alistipes*, *Odoribacter*, and *Rikenella* than mice in the K group, whereas mice in the IO group exhibited levels that were greater than those in the DB group. *Alistipes* metabolism could produce some acetic acid and propionic acid. The SCFAs findings revealed that acetic and propionic acid concentrations were higher in the DM and IO groups than in the DB group. By preventing neutrophil and macrophage production of pro-inflammatory cytokines, acetic acid and propionic acid salts can successfully reduce inflammation. It is suggested that intestinal flora metabolize *Inonotus obliquus* to produce acetic acid and propionic acid, which can reduce inflammation in db/db mice.

In addition, it has been demonstrated that *Alistipes* might have a preventive impact against certain diseases, including colitis, liver fibrosis, cancer immunotherapy, and cardiovascular disease. A decrease in its abundance has been associated with an increased recurrence of hepatic encephalopathy, which is consecutively associated with the progression of cirrhosis to a decompensated state (54). Our study found that the liver HE sections showed reduced liver fibrosis in the IO group of mice. It is suggested that *Inonotus obliquus* might improve the severity of liver lesions in db/db mice by increasing the abundance of *Alistipes* in the intestine. The environmental factor correlation analysis results showed that *Odoribacter* and OGTT, TNF-α, IL-6, IL-1β, and other physiological and biochemical correlates of T2DM were negatively correlated ($p < 0.05$). The above-mentioned study showed that abundant *Rikenella* and *Odoribacter* could simultaneously up-regulate OGTT, TNF-α, IL-6, and IL-1β and alleviate the symptoms of T2DM. We found that the relative abundance of *Akkermansia* was reduced in DB mice and elevated in the DM and IO groups compared to the K group, which is consistent with the previous studies (55, 56).

*Akkermansia*, a butyric acid-producing bacterium, decreased in numbers leading to mild inflammation in the intestine of diabetic mice. SCFAs outcomes showned that the mice in the DB group had lower butyric acid levels than those in the K group, whereas the mice in the IO group had higher butyric acid levels than those in the DB group. Butyric acid is essential in maintaining colonic epithelial homeostasis, mainly as an anti-inflammatory agent. Additionally, research has shown that the oral glucose insulin sensitivity (OGIS) model's assessment of postprandial insulin sensitivity was directly connected with butyrate levels (57, 58). This suggests that *Inonotus obliquus* can improve the content of butyrate in db/db mice by increasing the abundance of *Akkermansia*. In this way, it exerts its anti-inflammatory and insulin sensitivity-enhancing effects. The predicted results of flora function suggested that differential flora may improve glucose homeostasis and insulin sensitivity in db/db mice by affecting functions such as E (amino acid transport and metabolism) and G (carbohydrate transport and metabolism). Furthermore, *Akkermansia* is essential for preserving the integrity of the mucin layer (59). The above findings suggested that IO can maintain the integrity of the mucin layer and reduce inflammation by regulating the butyrate content in the SCFAs and the abundance of *Akkermansia* in the intestinal flora to maintain glucose homeostasis. Meanwhile, the hepatic portal vein allows butyrate to get through the epithelial barrier and reach the liver. As an important organ for metabolizing lipids and maintaining cholesterol homeostasis, the liver can regulate lipid metabolism disorders in db/db mice and improve adipose tissue metabolism to regulate lipid levels. The results of LEfse analysis showed that *Proteus*, an opportunistic pathogen, was the dominant flora in the DB group. Additionally, *proteus* was shown to have a correlation with a number of different factors, including body weight, LDL-C, OGTT, IL-1β, IL-6, and TNF-α. Among them, Positive correlations were found with OGTT, IL-1β, and IL-6 ($p < 0.01$), while substantial correlations were seen with TNF-α ($p < 0.001$). *Enterobacteriaceae* was the dominant flora in the IO group of mice, and the evolutionary branching diagram showed that *Enterococcaceae* was similar to DM group. It has been found that *Enterococcaceae* have anti-inflammatory activity, hypocholesterolemic effects, and the capacity to avoid or treat specific illnesses (60). The above study suggested that IO can alleviate inflammation in db/db mice by regulating Proteus and *Enterococcaceae* abundance.

# Conclusions

These studies showed that *Inonotus obliquus* could effectively reduce body weight and fasting blood glucose and alleviate the extent of lesions in the intestine, liver, renal, and pancreatic organs of diabetic mice (Figure 8). Compared with the DB group, treatment with *Inonotus obliquus* effectively changed the intestinal flora composition of db/db mice and improved the intestinal microecological disorders. The mice in the IO group had higher and regulated SCFAs content and alleviated T2DM symptoms by regulating the population density of some bacteria that produce acid such as *Alistipes* and *Akkermansia*.

Meanwhile, *Inonotus obliquus* down-regulated the amount of potentially dangerous bacteria such as *Proteobacteria* and *Rikenellaceae_RC9_gut_group*, and increased the prevalence of good bacteria like *Rikenella* and *Odoribacter*. The glucose homeostasis, blood lipid and inflammation levels, and the degree of organ lesions were further improved in db/db mice (Figure 8). Thus, there is a reciprocal relationship of action, *Inonotus obliquus* can keep the intestinal flora in homeostasis by regulating the abundance of intestinal flora, which in turn can control inflammation and alleviate T2DM-related symptoms. In addition, the controlled symptoms of T2DM lead to maintaining the

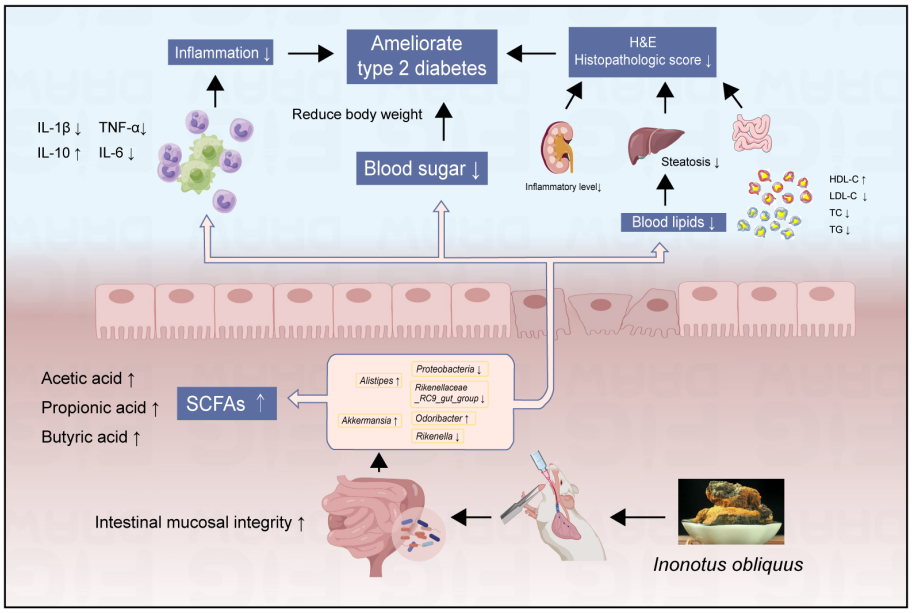


FIGURE 8
The effects of *Inonotus obliquus* on db/db mice.

intestinal flora to keep the gut microbes healthy. This offers the possibility to alleviate T2DM symptoms and a series of characteristic complications caused by T2DM by pharmacological regulation of the intestinal flora.

## Data availability statement

The datasets presented in this study can be found in online repositories. The names of the repository/repositories and accession number(s) can be found below: https://www.ncbi.nlm.nih.gov/, No. PRJNA902960.

## Ethics statement

The animal study was reviewed and approved by ethics committee of Zhejiang Academy of Agricultural Sciences (No. 2021ZAASLA83).

## Author contributions

XY and WL contributed to the study design. XY, KW, LX, YC, JN and WZ conducted animal experiments. KW and LX analyzed the samples and data. All authors contributed to the article and approved the submitted version.

## Funding

This work was supported by the National Key Research and Development Program of China (2018YFC2000500); Scientific Research Project of Zhejiang Education Department (Y202250254); start-up funds from Zhejiang Shuren University (2018R006); National Innovation and Entrepreneurship Program for College Students (202211842020&202211842052); Zhejiang Public welfare project (LGN22C030008), and Hangzhou Agricultural and Society Development Project (202004A20).

## Conflict of interest

The authors declare that the research was conducted in the absence of any commercial or financial relationships that could be construed as a potential conflict of interest.

## Publisher's note

All claims expressed in this article are solely those of the authors and do not necessarily represent those of their affiliated organizations, or those of the publisher, the editors and the reviewers. Any product that may be evaluated in this article, or claim that may be made by its manufacturer, is not guaranteed or endorsed by the publisher.

## Supplementary material

The Supplementary Material for this article can be found online at: https://www.frontiersin.org/articles/10.3389/fendo.2022.1103972/full#supplementary-material

## References

1. Taylor SI, Yazdi ZS, Beitelshees AL. Pharmacological treatment of hyperglycemia in type 2 diabetes. *J Clin Invest* (2021) 131(2):e142243. doi: 10.1172/JCI142243

2. Cole JB, Florez JC. Genetics of diabetes mellitus and diabetes complications. *Nat Rev Nephrol* (2020) 16(7):377–90. doi: 10.1038/s41581-020-0278-5

3. Demir S, Nawroth PP, Herzig S, Ekim Üstünel B. Emerging targets in type 2 diabetes and diabetic complications. *Adv Sci (Weinheim Baden-Wurttemberg Germany)* (2021) 8(18):e2100275. doi: 10.1002/advs.202100275

4. Hemmingsen B, Gimenez-Perez G, Mauricio D, Roqué I Figuls M, Metzendorf M-I, Richter B. Diet, physical activity or both for prevention or delay of type 2 diabetes mellitus and its associated complications in people at increased risk of developing type 2 diabetes mellitus. *Cochrane Database Syst Rev* (2017) 12:CD003054. doi: 10.1002/14651858.CD003054.pub4

5. Pan H, Jian Y, Wang F, Yu S, Guo J, Kan J, et al. NLRP3 and gut microbiota homeostasis: Progress in research. *Cells* (2022) 11(23):3758. doi: 10.3390/cells11233758

6. Larkin BP, Nguyen LT, Hou M, Glastras SJ, Chen H, Faiz A, et al. Low-dose hydralazine reduces albuminuria and glomerulosclerosis in a mouse model of obesity-related chronic kidney disease. *Diabetes Obes Metab* (2022) 24(10):1939–49. doi: 10.1111/dom.14778

7. Zhang Y, Gu Y, Ren H, Wang S, Zhong H, Zhao X, et al. Gut microbiome-related effects of berberine and probiotics on type 2 diabetes (the PREMOTE study). *Nat Commun* (2020) 11(1):5015. doi: 10.1038/s41467-020-18414-8

8. Li X, Peng X, Guo K, Tan Z. Bacterial diversity in intestinal mucosa of mice fed with and high-fat diet. *3 Biotech* (2021) 11(1):22. doi: 10.1007/s13205-020-02558-x

9. Kan J, Wu F, Wang F, Zheng J, Cheng J, Li Y, et al. Phytonutrients: Sources, bioavailability, interaction with gut microbiota, and their impacts on human health. *Front In Nutr* (2022) 9:960309. doi: 10.3389/fnut.2022.960309

10. Guo Y, Chen X, Gong P. Classification, structure and mechanism of antiviral polysaccharides derived from edible and medicinal fungus. *Int J Biol Macromol* (2021) 183:1753–73. doi: 10.1016/j.ijbiomac.2021.05.139

11. Ma Q, Tan D, Gong X, Ji H, Wang K, Lei Q, et al. An extract of leaves rich in organic acids and flavonoids promotes growth in BALB/c mice by regulating intestinal flora. *Animals* (2022) 12(12):1519. doi: 10.3390/ani12121519

12. Lu Y, Jia Y, Xue Z, Li N, Liu J, Chen H. Recent developments in (Chaga mushroom) polysaccharides: Isolation, structural characteristics, biological activities and application. *Polymers* (2021) 13(9):1441. doi: 10.3390/polym13091441

13. Arunachalam K, Sreeja PS, Yang X. The antioxidant properties of mushroom polysaccharides can potentially mitigate oxidative stress, beta-cell dysfunction and insulin resistance. *Front In Pharmacol* (2022) 13:874474. doi: 10.3389/fphar.2022.874474

14. Wang J, Wang C, Li S, Li W, Yuan G, Pan Y, et al. Anti-diabetic effects of inonotus obliquus polysaccharides in streptozotocin-induced type 2 diabetic mice and potential mechanism *via* PI3K-akt signal pathway. *Biomed Pharmacother = Biomed Pharmacother* (2017) 95:1669–77. doi: 10.1016/j.biopha.2017.09.104

15. Xu T, Li G, Wang X, Lv C, Tian Y. Inonotus obliquus polysaccharide ameliorates serum profiling in STZ-induced diabetic mice model. *BMC Chem* (2021) 15(1):64. doi: 10.1186/s13065-021-00789-4

16. Zhang Y, Liao H, Shen D, Zhang X, Wang J, Zhang X, et al. Renal protective effects of on high-fat Diet/Streptozotocin-induced diabetic kidney disease rats: Biochemical, color Doppler ultrasound and histopathological evidence. *Front In Pharmacol* (2021) 12:743931. doi: 10.3389/fphar.2021.743931

17. Chou Y-J, Kan W-C, Chang C-M, Peng Y-J, Wang H-Y, Yu W-C, et al. Renal protective effects of low molecular weight of inonotus obliquus polysaccharide (LIOP) on HFD/STZ-induced nephropathy in mice. *Int J Mol Sci* (2016) 17(9):1535. doi: 10.3390/ijms17091535

18. Su L, Xin C, Yang J, Dong L, Mei H, Dai X, et al. A polysaccharide from inonotus obliquus ameliorates intestinal barrier dysfunction in mice with type 2 diabetes mellitus. *Int J Biol Macromol* (2022) 214:312–23. doi: 10.1016/j.ijbiomac.2022.06.071

19. Garádi Z, Dékány M, Móricz ÁM, Gaál A, Papp V, Béni S, et al. Antimicrobial, antioxidant and antiproliferative secondary metabolites from inonotus nidus-pici. *Mol (Basel Switzerland)* (2021) 26(18):5453. doi: 10.3390/molecules26185453

20. Foretz M, Guigas B, Bertrand L, Pollak M, Viollet B. Metformin: from mechanisms of action to therapies. *Cell Metab* (2014) 20(6):953–66. doi: 10.1016/j.cmet.2014.09.018

21. Foretz M, Guigas B, Viollet B. Understanding the glucoregulatory mechanisms of metformin in type 2 diabetes mellitus. *Nat Rev Endocrinol* (2019) 15(10):569–89. doi: 10.1038/s41574-019-0242-2

22. Zhao X, Wang H, Yang Y, Gou Y, Wang Z, Yang D, et al. Protective effects of silymarin against d-Gal/LPS-Induced organ damage and inflammation in mice. *Drug Design Dev Ther* (2021) 15:1903–14. doi: 10.2147/DDDT.S305033

23. Xue M, Liu Y, Xu H, Zhou Z, Ma Y, Sun T, et al. Propolis modulates the gut microbiota and improves the intestinal mucosal barrier function in diabetic rats. *Biomed Pharmacother = Biomed Pharmacother* (2019) 118:109393. doi: 10.1016/j.biopha.2019.109393

24. Li K, Zhang L, Xue J, Yang X, Dong X, Sha L, et al. Dietary inulin alleviates diverse stages of type 2 diabetes mellitus *via* anti-inflammation and modulating gut microbiota in db/db mice. *Food Funct* (2019) 10(4):1915–27. doi: 10.1039/c8fo02265h

25. Anders H-J, Saxena R, Zhao M-H, Parodis I, Salmon JE, Mohan C. Lupus nephritis. *Nat Rev Dis Primers* (2020) 6(1):7. doi: 10.1038/s41572-019-0141-9

26. Brown GT, Kleiner DE. Histopathology of nonalcoholic fatty liver disease and nonalcoholic steatohepatitis. *Metabol: Clin Exp* (2016) 65(8):1080–6. doi: 10.1016/j.metabol.2015.11.008

27. Li D, Feng Y, Tian M, Ji J, Hu X, Chen F. Gut microbiota-derived inosine from dietary barley leaf supplementation attenuates colitis through PPARγ signaling activation. *Microbiome* (2021) 9(1):83. doi: 10.1186/s40168-021-01028-7

28. Zhang W, Xu J-H, Yu T, Chen Q-K. Effects of berberine and metformin on intestinal inflammation and gut microbiome composition in db/db mice. *Biomed Pharmacother = Biomed Pharmacother* (2019) 118:109131. doi: 10.1016/j.biopha.2019.109131

29. Caporaso JG, Kuczynski J, Stombaugh J, Bittinger K, Bushman FD, Costello EK, et al. QIIME allows analysis of high-throughput community sequencing data. *Nat Methods* (2010) 7(5):335–6. doi: 10.1038/nmeth.f.303

30. Wang Q, Garrity GM, Tiedje JM, Cole JR. Naive Bayesian classifier for rapid assignment of rRNA sequences into the new bacterial taxonomy. *Appl Environ Microbiol* (2007) 73(16):5261–7. doi: 10.1128/AEM.00062-07

31. Ye X, Pi X, Zheng W, Cen Y, Ni J, Xu L, et al. The methanol extract of ameliorates colitis by improving intestinal short-chain fatty acids and gas

production to regulate microbiota dysbiosis in mice. *Front In Nutr* (2022) 9:899421. doi: 10.3389/fnut.2022.899421

32. Herzig S, Shaw RJ. AMPK: guardian of metabolism and mitochondrial homeostasis. *Nat Rev Mol Cell Biol* (2018) 19(2):121–35. doi: 10.1038/nrm.2017.95

33. Beydoun MA, Chen X, Jha K, Beydoun HA, Zonderman AB, Canas JA. Carotenoids, vitamin a, and their association with the metabolic syndrome: A systematic review and meta-analysis. *Nutr Rev* (2019) 77(1):32–45. doi: 10.1093/nutrit/nuy044

34. Sonnweber T, Pizzini A, Nairz M, Weiss G, Tancevski I. Arachidonic acid metabolites in cardiovascular and metabolic diseases. *Int J Mol Sci* (2018) 19 (11):3285. doi: 10.3390/ijms19113285

35. Amor AJ, Gómez-Guerrero C, Ortega E, Sala-Vila A, Lázaro I. Ellagic acid as a tool to limit the diabetes burden: Updated evidence. *Antioxid (Basel Switzerland)* (2020) 9(12):1226. doi: 10.3390/antiox9121226

36. Dinda B, Dinda S, DasSharma S, Banik R, Chakraborty A, Dinda M. Therapeutic potentials of baicalin and its aglycone, baicalein against inflammatory disorders. *Eur J Med Chem* (2017) 131:68–80. doi: 10.1016/j.ejmech.2017.03.004

37. Putta S, Yarla NS, Kumar KE, Lakkappa DB, Kamal MA, Scotti L, et al. Preventive and therapeutic potentials of anthocyanins in diabetes and associated complications. *Curr Med Chem* (2018) 25(39):5347–71. doi: 10.2174/0929867325666171206101945

38. Yu M, Qi B, Xiaoxiang W, Xu J, Liu X. Baicalein increases cisplatin sensitivity of A549 lung adenocarcinoma cells *via* PI3K/Akt/NF-κB pathway. *Biomed Pharmacother = Biomed Pharmacother* (2017) 90:677–85. doi: 10.1016/j.biopha.2017.04.001

39. Caselli A, Cirri P, Santi A, Paoli P. Morin: A promising natural drug. *Curr Med Chem* (2016) 23(8):774–91. doi: 10.2174/0929867323666160106150821

40. Li C, Schluesener H. Health-promoting effects of the citrus flavanone hesperidin. *Crit Rev In Food Sci Nutr* (2017) 57(3):613–31. doi: 10.1080/10408398.2014.906382

41. Pérez-Torres I, Castrejón-Téllez V, Soto ME, Rubio-Ruiz ME, Manzano-Pech L, Guarner-Lans V. Oxidative stress, plant natural antioxidants, and obesity. *Int J Mol Sci* (2021) 22(4):1786. doi: 10.3390/ijms22041786

42. Shabbir U, Rubab M, Daliri EB-M, Chelliah R, Javed A, Oh D-H. Curcumin, quercetin, catechins and metabolic diseases: The role of gut microbiota. *Nutrients* (2021) 13(1):206. doi: 10.3390/nu13010206

43. Deng M, Xie L, Zhong L, Liao Y, Liu L, Li X. Imperatorin: A review of its pharmacology, toxicity and pharmacokinetics. *Eur J Pharmacol* (2020) 879:173124. doi: 10.1016/j.ejphar.2020.173124

44. Kozioł E, Skalicka-Woźniak K. Imperatorin-pharmacological meaning and analytical clues: Profound investigation. *Phytochem Rev: Proc Phytochem Soc Europe* (2016) 15:627–49. doi: 10.1007/s11101-016-9456-2

45. Nasser MI, Zhu S, Hu H, Huang H, Guo M, Zhu P. Effects of imperatorin in the cardiovascular system and cancer. *Biomed Pharmacother = Biomed Pharmacother* (2019) 120:109401. doi: 10.1016/j.biopha.2019.109401

46. Chen Q, Guo H, Hu J, Zhao X. Rhein inhibits NF-b signaling pathway to alleviate inflammatory response and oxidative stress of rats with chronic glomerulonephritis. *Appl Bionics Biomechanics* (2022) 2022:9671759. doi: 10.1155/2022/9671759

47. Zhou Y-X, Xia W, Yue W, Peng C, Rahman K, Zhang H. Rhein: A review of pharmacological activities. *Evidence-Based Complement Altern Med: ECAM* (2015) 2015:578107. doi: 10.1155/2015/578107

48. Ridlon JM, Harris SC, Bhowmik S, Kang D-J, Hylemon PB. Consequences of bile salt biotransformations by intestinal bacteria. *Gut Microbes* (2016) 7(1):22–39. doi: 10.1080/19490976.2015.1127483

49. Sánchez-García A, Sahebkar A, Simental-Mendía M, Simental-Mendía LE. Effect of ursodeoxycholic acid on glycemic markers: A systematic review and meta-analysis of clinical trials. *Pharmacol Res* (2018) 135:144–9. doi: 10.1016/j.phrs.2018.08.008

50. Goossens J-F, Bailly C. Ursodeoxycholic acid and cancer: From chemoprevention to chemotherapy. *Pharmacol Ther* (2019) 203:107396. doi: 10.1016/j.pharmthera.2019.107396

51. Lee SH, Hwang HS, Yun JW. Antitumor activity of water extract of a mushroom, inonotus obliquus, against HT-29 human colon cancer cells. *Phytother Res: PTR* (2009) 23(12):1784–9. doi: 10.1002/ptr.2836

52. Zhao Y, Zheng W. Deciphering the antitumoral potential of the bioactive metabolites from medicinal mushroom inonotus obliquus. *J Ethnopharmacol* (2021) 265:113321. doi: 10.1016/j.jep.2020.113321

53. Wang B, Kong Q, Li X, Zhao J, Zhang H, Chen W, et al. A high-fat diet increases gut microbiota biodiversity and energy expenditure due to nutrient difference. *Nutrients* (2020) 12(10):3197. doi: 10.3390/nu12103197

54. Parker BJ, Wearsch PA, Veloo ACM, Rodriguez-Palacios A. The genus: Gut bacteria with emerging implications to inflammation, cancer, and mental health. *Front In Immunol* (2020) 11:906. doi: 10.3389/fimmu.2020.00906

55. Forslund K, Hildebrand F, Nielsen T, Falony G, Le Chatelier E, Sunagawa S, et al. Disentangling type 2 diabetes and metformin treatment signatures in the human gut microbiota. *Nature* (2015) 528(7581):262–6. doi: 10.1038/nature15766

56. Zhao L, Lou H, Peng Y, Chen S, Zhang Y, Li X. Comprehensive relationships between gut microbiome and faecal metabolome in individuals with type 2 diabetes and its complications. *Endocrine* (2019) 66(3):526–37. doi: 10.1007/s12020-019-02103-8

57. Gérard C, Vidal H. Impact of gut microbiota on host glycemic control. *Front In Endocrinol* (2019) 10:29. doi: 10.3389/fendo.2019.00029

58. Huda MN, Kim M, Bennett BJ. Modulating the microbiota as a therapeutic intervention for type 2 diabetes. *Front In Endocrinol* (2021) 12:632335. doi: 10.3389/fendo.2021.632335

59. Everard A, Belzer C, Geurts L, Ouwerkerk JP, Druart C, Bindels LB, et al. Cross-talk between akkermansia muciniphila and intestinal epithelium controls diet-induced obesity. *Proc Natl Acad Sci United States America* (2013) 110 (22):9066–71. doi: 10.1073/pnas.1219451110

60. Ben Braïek O, Smaoui S. Enterococci: Between emerging pathogens and potential probiotics. *BioMed Res Int* (2019) 2019:5938210. doi: 10.1155/2019/5938210

frontiers | Frontiers in Endocrinology

TYPE Original Research
PUBLISHED 17 January 2023
DOI 10.3389/fendo.2022.1105073



OPEN ACCESS

EDITED BY
Xinhua Shu,
Glasgow Caledonian University,
United Kingdom

REVIEWED BY
Yueying Wu,
Yunnan University, China
Shao Liu,
Hunan Agricultural University, China
Baoming Shen,
Hunan Academy of Forestry, China
Su Min,
Changsha Medical University, China

*CORRESPONDENCE
Ruxiao Hu
173463778@qq.com

SPECIALTY SECTION
This article was submitted to Gut Endocrinology, a section of the journal Frontiers in Endocrinology

RECEIVED 22 November 2022
ACCEPTED 29 December 2022
PUBLISHED 17 January 2023

CITATION
Hu R (2023) *Grifola frondosa* may play an anti-obesity role by affecting intestinal microbiota to increase the production of short-chain fatty acids.
*Front. Endocrinol.* 13:1105073.
doi: 10.3389/fendo.2022.1105073



# *Grifola frondosa* may play an anti-obesity role by affecting intestinal microbiota to increase the production of short-chain fatty acids

Ruxiao Hu*

Edible Fungus Institute of Hunan Province, Changsha, China

**Background:** *Grifola frondosa* (*G. frondosa*) is a fungus with good economic exploitation prospects of food and medicine homologation. This study aims to investigate the effects of *G. frondosa* powder suspension (GFPS) on the intestinal contents microbiota and the indexes related to oxidative stress and energy metabolism in mice, to provide new ideas for developing *G. frondosa* weight loss products.

**Methods:** Twenty Kunming mice were randomly divided into control (CC), low-dose GFPS (CL), medium-dose GFPS (CM), and high-dose GFPS (CH) groups. The mice in CL, CM, and CH groups were intragastrically administered with 1.425 g/(kg·d), 2.85 g/(kg·d), and 5.735 g/(kg·d) GFPS, respectively. The mice in CC group were given the same dose of sterile water. After 8 weeks, liver and muscle related oxidative stress and energy metabolism indicators were detected, and the intestinal content microbiota of the mice was detected by 16S rRNA high-throughput sequencing.

**Results:** After eight weeks of GFPS intervention, all mice lost weight. Compared with the CC group, lactate dehydrogenase (LDH) and malondialdehyde (MDA) contents in CL, CM, and CH groups were increased, while Succinate dehydrogenase (SDH) and Superoxide Dismutase (SOD) contents in the liver were decreased. The change trends of LDH and SDH in muscle were consistent with those in the liver. Among the above indexes, the change in CH is the most significant. The Chao1, ACE, Shannon, and Simpson index in CL, CM, and CH groups were increased. In the taxonomic composition, after the intervention with GFPS, the short-chain fatty acid (SCFA)-producing bacteria such as unclassified Muribaculaceae, *Alloprevotella*, and unclassified Lachnospiraceae increased. In linear discriminant analysis effect size (LEfSe) analysis, the characteristic bacteria in CC, CL, CM, and CH groups showed significant differences. In addition, some characteristic bacteria significantly correlated with related energy metabolism indicators.

**Conclusion:** The preventive effect of *G. frondosa* on obesity is related to changing the structure of intestinal content microbiota and promoting the growth of SCFAs. While excessive intake of *G. frondosa* may not be conducive to the antioxidant capacity and energy metabolism.

KEYWORDS

***Grifola frondosa*, intestinal contents, microbial diversity, short-chain fatty acid, anti-obesity**

# Introduction

*G. frondosa* [*Grifola frondosa* (Dicks.) Gray], also known as maitake, belongs to Basidiomycota, Hymenomycetes, Polyporales, Meruliaceae, and Ramalina. *G. frondosa* is a rare edible and medicinal fungus with effects of anti-obesity, anti-tumor, and regulating immune function, at the same time, it is rich in various bioactive components including polysaccharides, steroids and polyphenols (1). It has a long history of medicinal use in Oriental medicine in China, Japan, and India (2). In addition, *G. frondosa* has a delicious taste and is a good source of dietary fiber, protein, and carbohydrates (3).

The intestinal microbiota is a dynamic flora composed of 100 trillion microorganisms that inhabit the host's intestinal tract (4). They play an irreplaceable role in various physiological activities, such as maintaining immune function, resisting colonization by pathogenic microorganisms, and assisting in nutrient absorption (5, 6). By secreting rich differential enzymes, some pharmaceutical components that do not have pharmacological activity can also be converted by the intestinal microbiota to form new active metabolites, which in turn have different biological effects on the body (7–9). More and more reports also indicated that intestinal microbiota might play a good intermediary role in the beneficial mechanism of *G. frondosa* (10). For example, Li et al. (11) reported that *G. frondosa* heteropolysaccharide could prevent non-alcoholic fatty liver disease by increasing the number of beneficial bacteria *Allobaculum*, *Bacteroides*, and *Bifidobacterium*. Chen et al. (12) reported that a new polysaccharide (GFP-N) extracted from *G. frondosa* could improve the intestinal microbiota of diabetic mice by increasing the abundance of *Akkermansia*, *Lactobacillus*, and *Turicibacter*. In addition, plant dietary fiber can be utilized and decomposed by the intestinal microbiota, partially absorbed by the microbiota itself, and partially converted into beneficial substances such as SCFAs (13). It has been reported that SCFAs can alleviate obesity, regulate intestinal pH, promote intestinal mucus production, and provide energy for epithelial cells (14–16). Among them, acetate, propionate, and butyrate are the intestines' major SCFAs (14). Pan et al. (17) reported that the ethanol extract of *G. frondosa* can reduce the weight of rats fed with high-fat diet and increase the number of beneficial bacteria *Intestinimonas* and *Butyricimonas*, which are important producers of butyrate.

In daily life, people usually eat *G. frondosa* after simple decocting, or grind the *G. frondosa* into powder and use it as a flavoring agent (3). At the same time, the components of glycoprotein, ergosterol and pyrrolefronine in *G. frondosa* also have pharmacological effects of anti-obesity, anti-tumor or anti-diabetes (18–20). However, at present, most studies are on the polysaccharide components and their functions in *G. frondosa*, and there is little research on the effect of direct intervention of *G. frondosa* on intestinal microbiota. SOD and MDA are usually one of the important indicators to measure the body's ability to remove oxygen free radicals and the level of oxidative damage (21). Some reports have shown that *G. frondosa* polysaccharides and polyphenols have the effect of anti-oxidative stress (22–24). LDH is a regulatory enzyme produced by glycolysis of sugars in the body in the absence of oxygen, which converts pyruvic acid into lactic acid, with reversibility (25, 26). SDH is a marker enzyme reflecting mitochondrial function, which can provide electrons for cell mitochondria and the aerobic and productive respiratory chain (27). In his master's degree thesis, Li BG (28) reported the good potential role of *G. frondosa* fermentation broth in anti-fatigue and promoting energy cycle. Therefore, this study intervened the mice with different doses of GFPS to explore its effects on intestinal content microbiota, body weight, energy metabolism or oxidative stress-related indicators of liver and muscle in mice. Aiming to provide new ideas for the development of *G. frondosa* weight loss products and suggestions for people's daily consumption.

# Material and methods

## Animals and feeding environment

In order to eliminate the gender influence (29), this study selected 20 SPF-grade male Kunming mice (20 ± 2 g), purchased from Hunan Slaccas Jingda Laboratory Animal Company (Hunan, China). The animals were raised at a temperature 23-25°C and humidity of 47-53% in the Experimental Animal Center of the Hunan University of Chinese Medicine.

## Medicine

*G. frondosa* is produced in Qingyun County, Lishui City, Zhejiang Province, and is the first fruiting mushroom product of *G. frondosa* stick cultivation (30). Take a certain amount of *G. frondosa*, dry it in an oven at 105-110°C to constant weight, grind it into powder, and pass it through a 60-mesh sieve to obtain *G. frondosa* powder. A proper amount of *G. frondosa* powder was heated with distilled water, and boiled for 5 min. Then, concentrated into low, medium and high dose GFPS of 0.053 g/ml, 0.106 g/ml and 0.215 g/ml, respectively. The solutions were cooled and stored in a refrigerator at 4 °C for standby.

## Animal grouping and feeding

After 3 days of adaptive feeding, the mices were randomly divided into control group (CC), low-dose GFPS group (CL), medium-dose GFPS group (CM) and high-dose GFPS group (CH). The LD, MD and HD groups were given 0.4 mL low, medium and high dose GFPS by gavage, and CC Group was given the same frequency of sterile water by gavage, twice a day for 8 weeks. During this period, each mouse was weighed and recorded every week. The experimental procedures are shown in Figure 1. All animal experimental procedures were in the animal experimental protocol approved by the Institutional Animal Care and Use Committee of the Hunan University of Chinese Medicine.

## Biochemical indicators detection

At the end of the 8 weeks intervention, the mice were sacrificed on a sterile operating platform using cervical dislocation, and then the liver and muscles were taken out. According to the instructions of ELISA kits, the levels of SOD, MDA, LDH and SDH in the liver, and the levels of LDH and SDH in the muscle were detected using Rayto RT-6100 enzyme labeling analyzer. The kits were provided by Quanzhou kenuodi Biotechnology Co., LTD.

## Intestinal content sample collection

Under sterile conditions, the intestinal tissues from jejunum to ileum were longitudinally cut, and the intestinal contents were collected with forceps and stored at -80 °C for subsequent use (31).

## Extraction of total DNA, PCR amplification and high-throughput sequencing

The total microbial genomic DNA of the samples was extracted using a DNA extraction kit (MN NucleoSpin 96 So) through the steps of sample lysis, impurity removal by precipitation, inhibitor removal by filtration, DNA binding, membrane washing, drying, elution, etc. Using the extracted DNA as a template, the V3+V4 variable region of bacterial 16S rDNA was amplified with primers 338F (5'-ACTCCTACGGGAGGCAGCA-3') and 806R (5'-GGACTACHVGGGTWTCTAAT-3'). The amplification reaction system consisted of 50 ng genomic DNA, 0.3 μL Vn F, 0.3 μL Vn R, 5 μL KOD FX Neo Buffer, 2 μL dNTP (2 mM each), and 0.2 μL KOD FX Neo, which were finally supplemented to 10 μl with $ddH_2O$. Amplification conditions: denaturation at 95 °C for 5 min, rapid cooling to 50 °C, heating to 72 °C for 30 s, reacting for 40 s, then reacting at 72 °C for 7 min, and storing at 4 °C for 25 cycles. The amplified PCR products were purified, quantified, and homogenized. After the samples were mixed, they were subjected to column purification using OMEGA DNA purification column, and detected by 1.8% agarose gel electrophoresis. Use Monarch DNA glue recovery kit to cut glue and recover PCR products. The PCR products were sequenced by the Illumina Novaseq 6000 sequencing platform. All samples were processed by Beijing Biomarker Technologies Co, LTD.

## Bioinformatics

The obtained data were filtered by Trimmom (V0.33) (32), spliced by Usearch (v10.0) (33), and chimerism was removed by dada2 method (34) in QIIME2 (v2020.6) (35). Then effective sequences with similarity above 97% are clustered into an operational taxonomic unit (OTU), and the representative sequences of OTU are defined by classification. This study assessed the Alpha diversity of sample communities using ACE, Chao1, Simpson, and Shannon indices. The Beta diversity of sample communities was assessed using non-metric multidimensional scaling (NMDS) based on the unweighted unifrac distance. At the same time, the marked difference species in each group were screened by LEfSe, and the above visualization was completed with R v3.6.3.

## Correlation analysis

The correlation between the two variables can be expressed by the correlation coefficient. The closer the correlation coefficient is to 1, the greater the correlation between two elements, and the closer the correlation coefficient is to 0, indicating that the two elements are more independent. R version 3.6.3 is used to calculate Spearman rank correlation coefficient and draw heat map, network map, and scatter map.

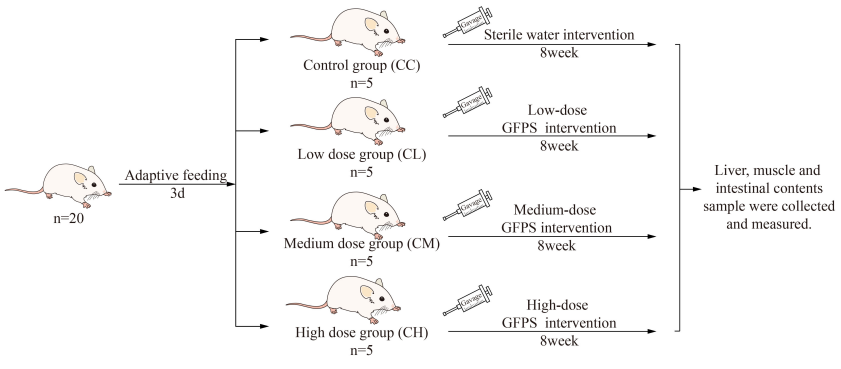


FIGURE 1
Experimental design and general conditions of the animals.

## Statistical analysis

Experimental data were expressed as mean ± standard deviation. All the data were statistically analyzed by SPSS 21.0 statistical software. For comparison among multiple groups, the one-way analysis of variance was used to analyze the data that conformed to the normal distribution and homogeneity of variance, otherwise, the Kruskal-Wallis rank sum test was used. Pairwise comparison among multiple groups was performed using the LSD test. $p < 0.05$ indicated that the difference had statistical significance.

# Results

## Effects of GFPS on body weight

As shown in Figure 2, the body weight gain of mice after GFPS intervention was lower than that of CC group, and the CH and CM groups were significantly lower than CC group ($p_{CH} < 0.01$, $p_{CM} < 0.05$). Meanwhile, the trend of body weight gain in the CH group was the lowest among all GFPS intervention groups and significantly lower than that in the CL group ($p < 0.05$). This indicated that low, medium, and high doses of GFPS intervention had the effects of weight loss and lipid reduction, and the effect of high-dose of GFPS was the most significant.

## Effects of GFPS on LDH, SDH, SOD and MDA content in liver

LDH represented the anaerobic metabolism to some extent, while the up-regulation of SDH activity represented the acceleration of the tricarboxylic acid cycle and increase of Adenosine Triphosphate (25, 26). As shown in Figure 3A, LDH content in liver of different doses of GFPS intervention was significantly higher than that in CC group ($p < 0.01$). Meanwhile, LDH content in liver of CH group was significantly higher compared with the CL and CM groups. In terms of liver SDH content (Figure 3B), the SDH content after different doses of GFPS intervention was lower than that in the CC group, and the SDH content in the liver of the CM and CH groups was significantly lower than that in the CC group ($p < 0.05$). This indicated that the intervention of GFPS had an inhibitory effect on the energy metabolism level of liver cells in mice, and the intervention of high-dose of GFPS was the most effective. MDA is the final metabolite of lipid peroxidation, reflecting the body's ability to be damaged by oxidation, while SOD indirectly reflects the body's ability to remove oxygen free radicals (21). By comparing the levels of MDA and SOD activities, we could assess the effect of GFPS intervention on the antioxidant capacity of the liver in mice. As shown in Figures 3C, D, the MDA content in the CH group was significantly higher than that in other groups ($p_{CC} < 0.01$, $p_{CL} < 0.01$, $p_{CM} < 0.01$), and SOD content was significantly lower than that in the CC group ($p < 0.01$). It indicated that a high-dose of GFPS intervention might not have a beneficial effect on the antioxidant capacity of the liver in mice.

## Effects of GFPS on LDH and SDH content in muscle

Figure 4 shows that SDH content in the muscle of mice decreases with the increase of GFPS dose. At the same time, the LDH content in different mouse groups ranked CC < CL < CM < CH. Among them, the CC group had significant differences with CM and CH groups ($p_{CL} < 0.05$, $p_{CH} < 0.01$), and CH group had significant differences with CL and CM groups ($p_{CL} < 0.01$, $p_{CM} < 0.05$). This is consistent with the changing trend of LDH and SDH in mouse liver after different doses of GFPS. It indicated that the intervention of GFPS inhibited the energy metabolism of muscle cells in mice, and the inhibition was enhanced with the increase of dose.

## Effects of GFPS on intestinal content microbiota of mice

### Effects of different concentrations of GFPS on the OTUs number of intestinal microbiota in mice

As shown in Figure 5A, the numbers of OTUs obtained in CC, CL, CM, and CH groups were 821, 913, 862, and 898, respectively. The unique OTU numbers of CC, CL, CM and CH groups are 58, 61,

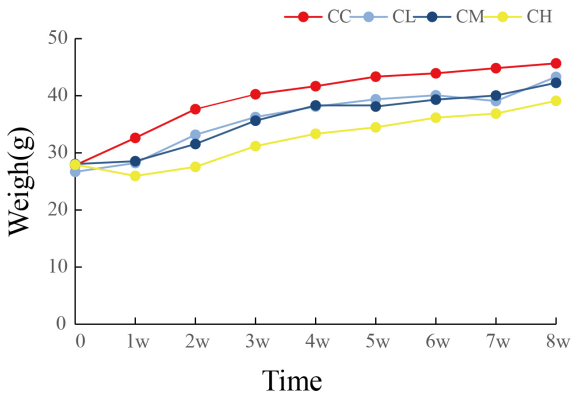


FIGURE 2
Weight changes of mice. CC: control group, CL: low-dose GFPS group, CM: medium-dose GFPS group, CH: high-dose GFPS group.

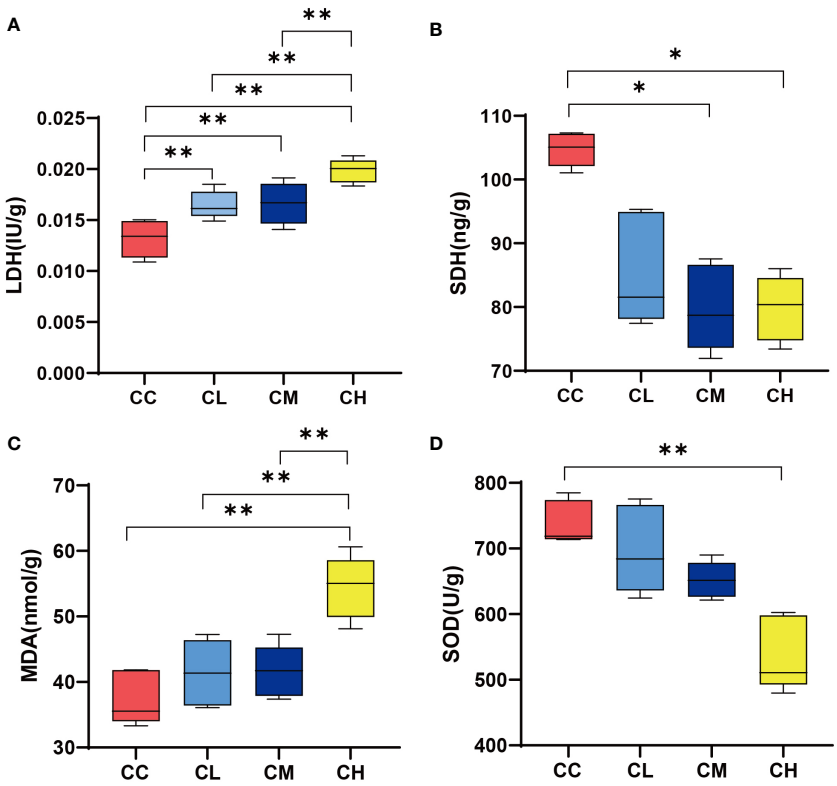


FIGURE 3
LDH, SDH, SOD, and MDA content in liver. **(A)** LDH content. **(B)** SDH content. **(C)** MDA content. **(D)** SOD content. CC: control group, CL: low-dose GFPS group, CM: medium-dose GFPS group, CH: high-dose GFPS group. (*$p < 0.05$, **$p < 0.01$).

54 and 57 respectively. The dilution curve was used to assess whether sequencing was sufficient to cover all taxa and indirectly reflect the abundance of species in the sample. When the curve flattens out, it can be considered that the sequencing depth has covered almost all the species in the sample (36). As can be seen from Figure 5B, the dilution curve sequences of the four groups of samples tended to be gentle when the number was 10000. It shows that the amount of sequencing data is enough for the next analysis.

## Effect of GFPS on the structure of intestinal microbiota in mice

In Alpha diversity analysis, Chao 1, ACE, Simpson, and Shannon are often used to evaluate richness and diversity (37). It can be seen from Table 1 that the ACE, Chao 1, Simpson, and Shannon indexes of GFPS treated mice are slightly higher than CC group mice. The ACE and Chao 1 indexes of the CL group are higher than the CC, CM and CH groups, but there is no statistical significance. This result was

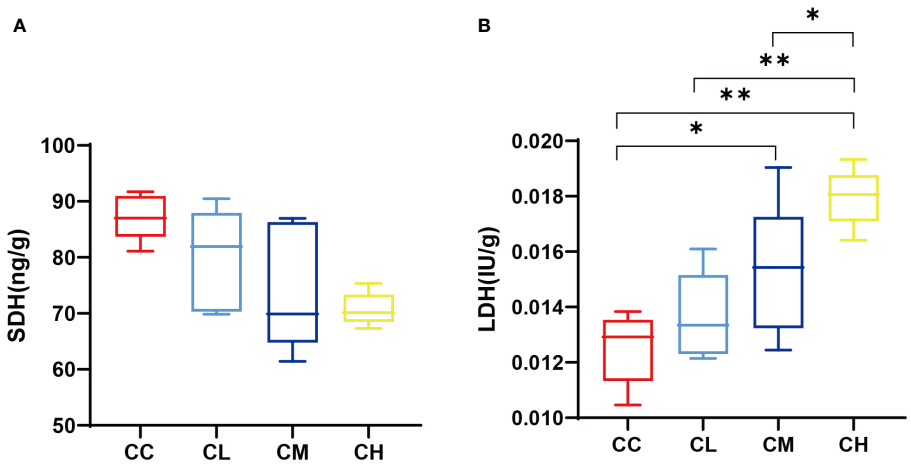


FIGURE 4
muscle SDH and LDH content. **(A)** SDH content. **(B)** LDH content. CC: control group, CL: low-dose GFPS group, CM: medium-dose GFPS group, CH: high-dose GFPS group. (*$p < 0.05$, **$p < 0.01$).

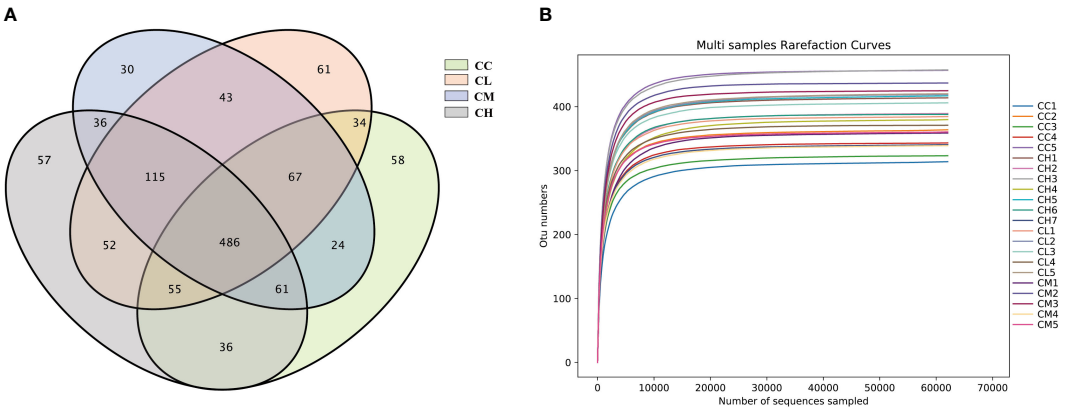


FIGURE 5
OTUs number and dilution curve of intestinal microbiota of mice. **(A)** OTUs number. **(B)** dilution curve. CC: control group, CL: low-dose GFPS group, CM: medium-dose GFPS group, CH: high-dose GFPS group.

consistent with the quantitative result of OTU, suggesting that the intervention of GFPS played a role in promoting the diversity and richness of intestinal content microbiota.

In Beta diversity analysis, the nonlinear NMDS model can better reflect the nonlinear structure of ecological data (38). As shown in Figure 6, the distribution of samples in the CC and CH groups was relatively centralized, while that in CL and CM groups was relatively discrete. At the same time, the samples of the CC group are relatively separated from those of other groups, which indicated that the intervention of GFPS changed the community structure of the bacteria in the intestinal contents of mice.

## Effect of GFPS on the structure and composition of intestinal contents microbiota in mice

At the phylum level (Figure 7A), the intestinal microbiota in the CC group consisted mainly of Bacteroidota (53.94%), Firmicutes (44.11%), Actinobacteriota (0.48%), Desulfobacterota (0.55%), and other low abundance proportion taxa. The abundance of Firmicutes (44.11% *vs* 51.99%, 60.68%, 50.17%) and Actinobacteriota (0.48% *vs* 2.23%, 1.41%, 3.86%) was higher in the CL, CM, and CH groups compared with the CC group. The abundance of Firmicutes (44.11% *vs* 51.99%, 60.68%, 50.17%) and Actinobacteriota (0.48% *vs* 2.23%, 1.41%, 3.86%) was higher in the CL, CM, and CH groups compared with the CC group. Meanwhile, the abundance of Bacteroidota (53.94% *vs* 42.73%, 35.60%, 44.45%) is lower.

At the genus level (Figure 7B), the dominant bacteria in CC, CL, CM, and CH groups were unclassified Muribaculaceae, accounting for 20.51%, 14.70%, 22.17%, and 22.27%, respectively. *Alloprevotella* was the second most common type, accounting for 10.84%, 11.00%, 10.92% and 6.68% respectively, while unclassified *Lachnospiraceae* accounted for 6.18%, 12.33%, 7.84% and 8.39% respectively.

## Effect of GFPS on characteristic bacteria of intestinal contents in mice

In order to further identify the characteristic microbiota of GFPS intervention, LEfSe analysis was performed on the community composition at each taxonomic level in different treatment groups. Figure 8A shows the characteristic bacteria when the logarithmic LDA threshold is 2, and the characteristic bacteria in CC group include *Frisingicoccus*, *Dorea*, unclassified Butyricicoccaceae, *Bacillus*, *Fusicatenibacter*, *Sellimonas*. The characteristic bacterium in the CL group was *Lachnospira*. The characteristic bacteria in the CM group were unclassified UCG 010 and *Caldicoprobacter*. The characteristic bacterium in the CH group was *Faecalibaculum*. The above results could explain that different doses of GFPS could change the intestinal content microbiota. In different classification systems (Figure 8B), the characteristic bacteria among the four groups showed significant differences.

# Correlation analysis of intestinal contents microbiota with liver and muscle index

This study selected characteristic bacteria with logarithmic LDA threshold of 3 for correlation analysis between indicators. Figure 9A shows the correlation heat map between characteristic bacteria and

TABLE 1 Effect of GFPS on Alpha diversity index of intestinal content microbiota in mice.

| Group | ACE | Chao 1 | Simpson | Shannon |
|---|---|---|---|---|
| CC | 361.078 ± 51.137 | 361.400 ± 51.247 | 0.976 ± 0.008 | 6.809 ± 0.411 |
| CL | 400.523 ± 19.347 | 400.700 ± 19245 | 0.981 ± 0.009 | 7.121 ± 0.214 |
| CM | 384.229 ± 39.146 | 384.200 ± 39.163 | 0.983 ± 0.004 | 7.103 ± 0.181 |
| CH | 382.732 ± 23.644 | 382.800 ± 23.760 | 0.981 ± 0.009 | 7.043 ± 0.336 |

All data are expressed as mean ± standard deviation. CC: control group, CL: low-dose GFPS group, CM: medium-dose GFPS group, CH: high-dose GFPS group.

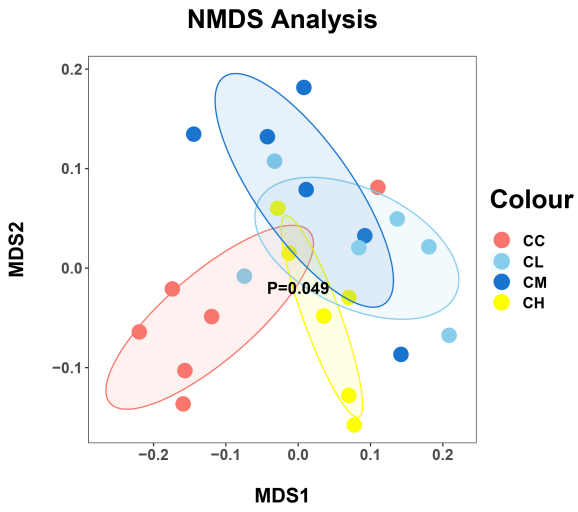


FIGURE 6
The beta diversity of mice intestinal mucosal bacteria. Each point represents a sample, and samples of different groups are represented by different colors. The closer the distance between two points is, the higher the similarity is between two samples, and the smaller the difference is. CC: control group, CL: low-dose GFPS group, CM: medium-dose GFPS group, CH: high-dose GFPS group.

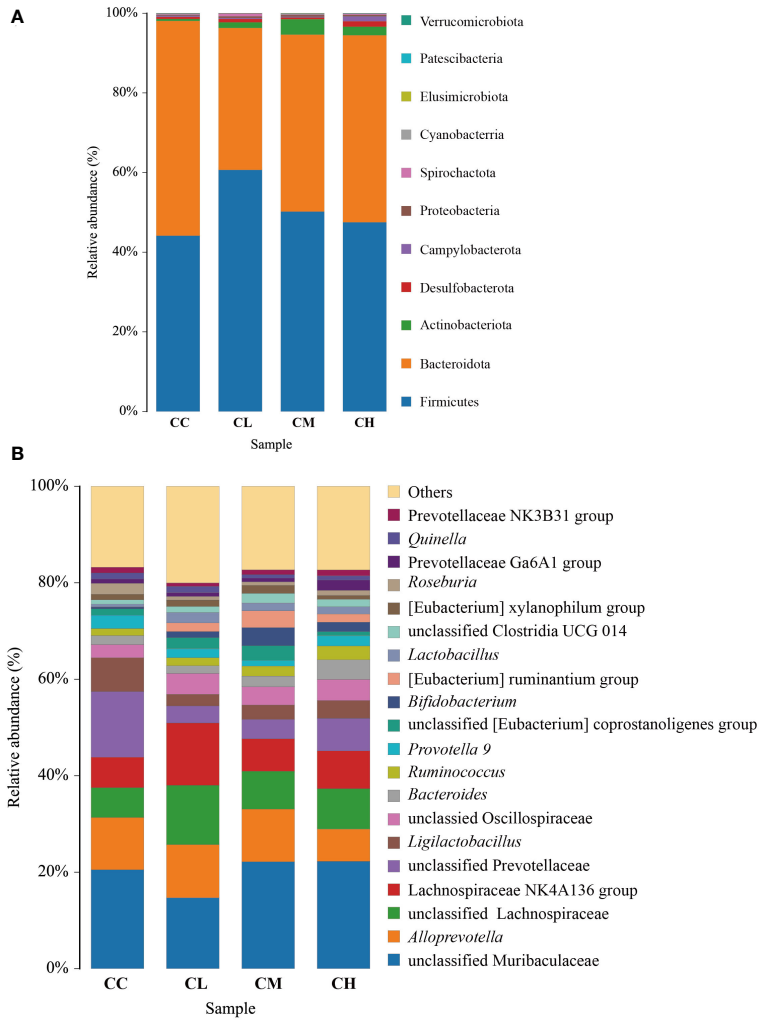


FIGURE 7
Relative abundance of bacteria in intestinal contents of mice after intervention with GFPS. **(A)** Level of phylum. **(B)** Level of genus. CC: control group, CL: low-dose GFPS group, CM: medium-dose GFPS group, CH: high-dose GFPS group.

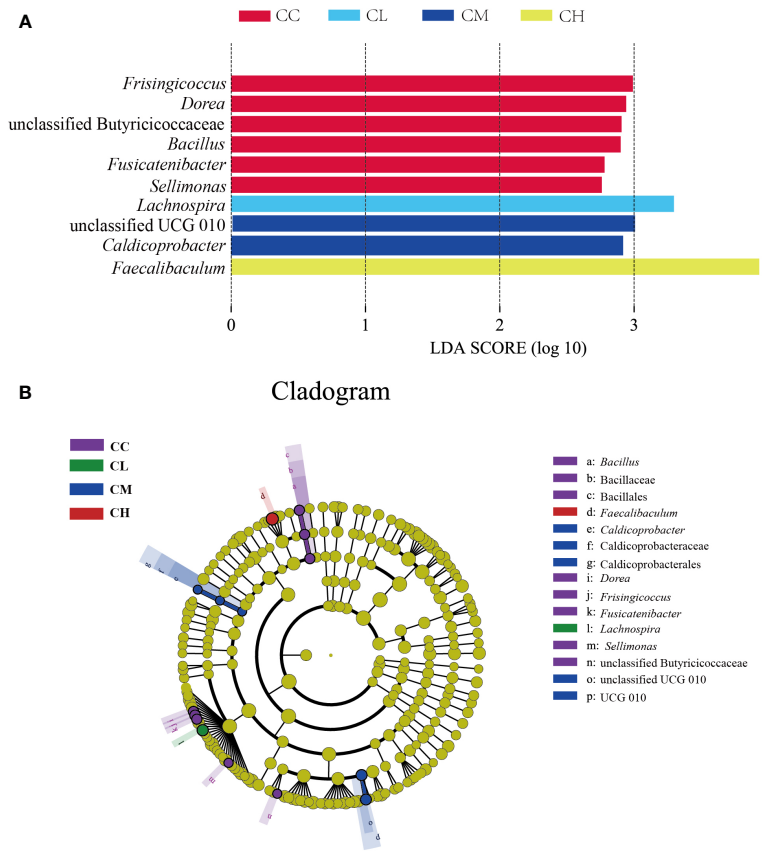


FIGURE 8
Characteristic bacteria of mice with GFPS intervention. **(A)** LDA score plots. **(B)** LEfSe analysis.

liver indexes. LDH had a significant positive correlation with *Faecalibaculum* ($p < 0.05$) and a significant negative correlation with unclassified Butyricicoccaceae ($p < 0.05$). SDH was significantly positively correlated with *Frisingicoccus*, unclassified Butyricicoccaceae, *Fusicatenibacter*, *Sellimonas*, *Dorea* ($p < 0.05$). MDA was significantly negatively correlated with *Sellimonas* ($p < 0.05$). SOD had a significant positive correlation with unclassified Butyricicoccaceae ($p < 0.05$), and a significant negative correlation with *Faecalibaculum* and unclassified UCG 010 ($p < 0.05$). It could be seen from Figures 9B–F that LDH in muscle had a significant positive correlation with *Faecalibaculum* and *Caldicoprobacter* ($p < 0.05$). Muscle SDH significantly negatively correlated with *Caldicoprobacter* and *Faecalibaculum* ($p < 0.05$).

## Discussion

With the improvement of living standards and the strengthening of the concept of a healthy diet, people's demand for healthy and functional foods is growing. Considering the side effects of some synthetic chemicals, multi-target and multi-channel natural plant products have broad application prospects in the development of functional foods and auxiliary drugs (39). Here, this study discussed the effects of GFPS intervention on oxidative stress, energy metabolism indicators, and intestinal microbiota in mice.

In the results of the liver oxidative stress index, the SOD contents decreased and MDA contents increased after the intervention with GFPS. Among them, the intervention of high-dose GFPS showed the most obvious change. This indicates that GFPS can inhibit the antioxidation of mouse liver. Notably, this differs from previous studies on the antioxidant effect of *G. frondosa*. For example, Men et al. (22) intervened the mice with acute liver injury with the polysaccharide extracted from the fruiting body of *G. frondosa*. They found that these *G. frondosa* polysaccharides not only had a protective effect on liver injury, but also decreased MDA content and increased SOD content in the liver. Another study (23) also found that *G. frondosa* polysaccharide intervention could significantly increase the liver antioxidant level of rats with hepatic fibrosis. We speculate that multiple complex components in *G. frondosa* may be the reason for this difference. It has been reported that *Faecalibaculum* has a negative correlation with SOD content, and can be used as a marker bacterium for intestinal oxidative stress (40). Oxidative stress improves cell permeability and causes LDH efflux from cells, thus leading to increased LDH activity (41). In experimental results, this was confirmed by increased LDH content in muscle and liver, which is also consistent with the significant positive correlation between *Faecalibaculum* and LDH in correlation analysis. and the contents of these enzymes in liver and muscle tissues have the LDH and SDH are representative enzymes of anaerobic respiration and aerobic respiration, respectively (42), same trend. This means that GFPS intervention reduced the energy metabolism of

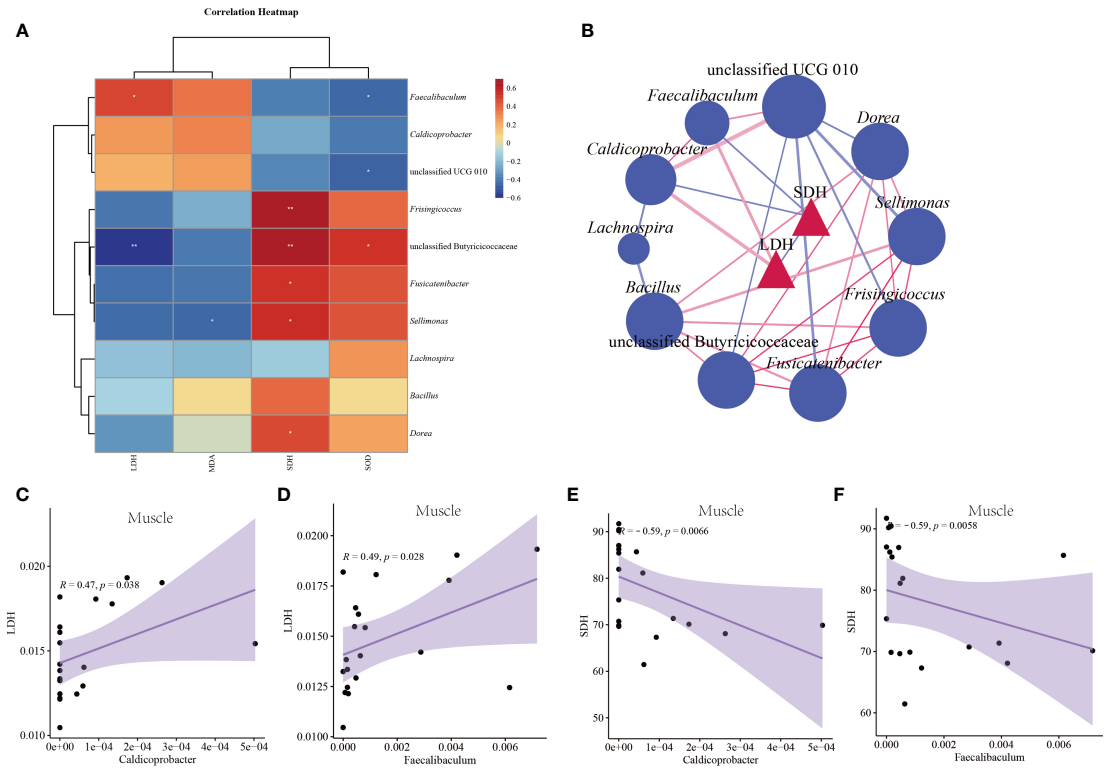


FIGURE 9
Correlation between characteristic bacteria of intestinal contents and indexes in mice. **(A)** Correlation heat map between characteristic bacteria and liver indexes. **(B)** Association network diagram of pathogenic bacteria and muscle indexes. **(C)** Scatter diagram of muscle LDH and *Caldicoprobacter*. **(D)** Scatter diagram of muscle LDH and *Faecalibaculum*. **(E)** Scatter diagram of muscle SDH and *Caldicoprobacter*. **(F)** Scatter diagram of muscle SHD and *Faecalibaculum*. CC: control group, CL: low-dose GFPS group, CM: medium-dose GFPS group, CH: high-dose GFPS group.

muscle and liver in mice to varying degrees, promoted anaerobic respiration, and had a certain dose dependence.

The diversity of intestinal microbiota is generally positively correlated with the quality of diet (43). The Alpha index and OTU results in this experiment showed that GFPS intervention promoted the diversity and richness of the intestinal content microbiota in mice. Meanwhile, the Beta analysis also showed that GFPS intervention changed the structure of intestinal microbiota. By further comparing the changes in the bacterial abundance of the intestinal contents among the four experimental groups, we could understand how GFPS affects the intestinal microbial environment. As the two largest taxonomic phylum in the intestinal microbiota, the increase in the ratio of Firmicutes to Bacteroidetes (F/B) is generally considered to be related to obesity (44). Two recent reports have shown that either *G. frondosa* polysaccharide or direct feeding *G. frondosa* can regulate lipid metabolism, reduce body weight, and is related to the TLR4/NF-κB signaling pathway (45, 46). In this research, the weight growth trend of mice after low, middle, and high doses of GFPS intervention decreased, which also proved this point. But interestingly, compared with the CC group, the F/B value of mouse microbiota in CL, CM, and CH groups increased.

From the perspective of taxonomic composition, the weight loss and intestinal health improvement effects of *G. frondosa* may be related to the promotion of the growth of SCFAs-producing bacteria, which can convert dietary fibers not absorbed by the body into metabolites SCFAs (47). SCFAs have been proved to stimulate energy consumption by promoting lipid oxidation, and the increase in SCFAs production can stimulate a large number of hormones and neural signals in different organs and tissue sites, thereby cumulatively inhibiting short-term appetite and energy intake (48, 49). In addition, SCFAs can also prevent diet-induced obesity by inhibiting the activity of Histone Deacetylase 3 in intestinal epithelial cells (15). Studies have shown that unclassified Muribaculaceae (50), unclassified lachnospiraceae (51), and *Alloprevotella* (52) are all intestinal SCFAs-producing bacteria. At the same time, compared to the CC group, the abundance of unclassified Muribaculaceae was increased in the CM and CH groups, and that of *Alloprevotella* was increased in the CL and CM groups. The abundance of unclassified Lachnospiraceae was increased after GFPS intervention. On the contrary, after high-dose intervention with GFPS, the abundance of *Alloprevotella* was decreased, but the characteristic bacterium *Faecalibaculum* in the CH group was also the producer of SCFAs (53). Studies have shown that *Faecalibaculum* has the effect of inhibiting the development of metabolic diseases (54). Combined with the results of oxidative stress, the MDA content of the CH group was significantly increased ($p < 0.01$), while the increased MDA content might damage the intestinal barrier (55), reduce the absorption of nutrients, and thus reduce body weight. This was also demonstrated by the lowest body weight in the CH group among the four groups (Figure 2). Furthermore, *Lachnospira* was a characteristic bacterium in the CL group, while *Lachnospira* could produce lactic acid and acetate, and lactic acid could become a metabolic substrate for bacteria to produce butyrate or propionate (56). The characteristic bacteria in LM group are *Caldicoprobacter* and unclassified UCG 010. *Caldicoprobacter* is a kind of bacteria that can degrade complex

carbohydrates and ferment hemicellulose into lactic acid, ethanol, and hydrogen. Meanwhile, these products can be transformed into butyrate for colon cells to supply energy (57, 58).

In addition, there were some limitations in this study, such as the small sample size and the emphasis on the integrity and naturalness of *G. frondosa* in the experiment, and no specific discussion on the role of a component in *G. frondosa*. The intestinal microbiota is closely related to our health. In the future, metagenomic functional gene analysis will be used to further explore the relationship between *G. frondosa* and intestinal microbiota.

## Conclusion

In summary, *G. frondosa* can promote health and prevent obesity by changing the structure of intestinal content microbiota, promoting microbiota diversity and richness, and increasing the beneficial bacteria producing SCFAs. However, excessive intake of *G. frondosa* may promote oxidative stress response in mice and inhibit energy metabolism in muscle and liver tissue. Therefore, low-dose (1.425 g/kg·d) of *G. frondosa* may be a good choice for further experiment or product development.

## Data availability statement

The datasets presented in this study can be found in online repositories. The names of the repository/repositories and accession number(s) can be found below: https://www.ncbi.nlm.nih.gov/, PRJNA903652.

## Ethics statement

The animal study was reviewed and approved by the Institutional Animal Care and Use Committee of the Hunan University of Chinese Medicine.

## Author contributions

Experimental design, animal operation, data analysis, and paper writing were all performed by RH. The author confirms being the sole contributor of this work and has approved it for publication.

## Funding

This research was financially supported by the Natural Science Foundation of Hunan Province (No. 2019JJ40166).

## Acknowledgments

I thank the Natural Science Foundation of Hunan Province (No. 2019JJ40166) for the financial support of this study.

## Conflict of interest

The author declares that the research was conducted in the absence of any commercial or financial relationships that could be construed as a potential conflict of interest.

## Publisher's note



## References

1. Xiong WY, He JQ, Dai WZ, Wu YY, Liu B. Research progress on the functional components of grifola frondosa and their biological activities. *Food Machinery* (2022) 38:234–40. doi: 10.13652/j.spjx.1003.5788.2022.90086

2. Alonso EN, Ferronato MJ, Fermento ME, Gandini NA, Romero AL, Guevara JA, et al. Antitumoral and antimetastatic activity of maitake d-fraction in triple-negative breast cancer cells. *Oncotarget* (2018) 9:23396–412. doi: 10.18632/oncotarget.25174

3. He YL, Li XL, Hao C, Zeng PJ, Zhang M, Liu Y, et al. Grifola frondosa polysaccharide: A review of antitumor and other biological activity studies in China. *Discovery Med* (2018) 25:159–76.

4. Lepage P, Leclerc MC, Joossens M, Mondot S, Blottière HM, Raes J, et al. A metagenomic insight into our gut's microbiome. *Gut* (2013) 62:146–58. doi: 10.1136/gutjnl-01805

5. Vicentini FA, Keenan CM, Wallace LE, Woods C, Cavin JB, Flockton AR, et al. Intestinal microbiota shapes gut physiology and regulates enteric neurons and glia. *Microbiome* (2021) 9:210. doi: 10.1186/s40168-021-01165-z

6. Li XY, Peng XX, Guo KX, Tan ZJ. Bacterial diversity in intestinal mucosa of mice fed with dendrobium officinale and high-fat diet. *3 Biotech* (2021) 11:22. doi: 10.1007/s13205-020-02558-x

7. Park EK, Shin J, Bae EA, Lee YC, Kim DH. Intestinal bacteria activate estrogenic effect of main constituents puerarin and daidzin of pueraria thunbergiana. *Biol Pharm Bull* (2006) 29:2432–5. doi: 10.1248/bpb.29.2432

8. Xie Y, Hu FD, Xiang DW, Lu H, Li WB, Zhao AP, et al. The metabolic effect of gut microbiota on drugs *Drug Metab Rev*. (2020) 52:139–56. doi: 10.1080/03602532.2020.1718691

9. Zhou K, Deng N, Yi X, Cai Y, Peng MJ, Xiao NQ. Baohe pill decoction for diarrhea induced by high-fat and high-protein diet is associated with the structure of lactase-producing bacterial community. *Front Cell Infect Microbiol* (2022) 12:1004845. doi: 10.3389/fcimb.2022.1004845

10. Wu JY, Siu KC, Geng P. Bioactive ingredients and medicinal values of grifola frondosa (Maitake). *Foods* (2021) 10:95. doi: 10.3390/foods10010095

11. Li X, Zeng F, Huang YF, Liu B. The positive effects of grifola frondosa heteropolysaccharide on NAFLD and regulation of the gut microbiota. *Int J Mol Sci* (2019) 20:5302. doi: 10.3390/ijms20215302

12. Chen YQ, Liu D, Wang DY, Lai SS, Zhong RT, Liu YY, et al. Hypoglycemic activity and gut microbiota regulation of a novel polysaccharide from grifola frondosa in type 2 diabetic mice. *Food Chem Toxicol* (2019) 126:295–302. doi: 10.1016/j.fct.2019.02.034

13. Holscher HD. Dietary fiber and prebiotics and the gastrointestinal microbiota. *Gut bes* (2017) 8:172–84. doi: 10.1080/19490976.2017.1290756

14. Martin-Gallausiaux C, Marinelli L, Blottière HM, Larraufie P, Lapaque N. SCFA: mechanisms and functional importance in the gut. *Proc Nutr Soc* (2021) 80:37–49. doi: 10.1017/S0029665120006916

15. You HM, Tan Y, Yu DW, Qiu ST, Bai Y, He JC, et al. The therapeutic effect of SCFA-mediated regulation of the intestinal environment on obesity. *Front Nutr* (2022) 9:886902. doi: 10.3389/fnut.2022.886902

16. Barrea L, Muscogiuri G, Annunziata G, Laudisio D, Pugliese G, Salzano C, et al. From gut obiota dysfunction to obesity: could short-chain fatty acids stop this dangerous course? *Hormones (Athens)* (2019) 18:245–50. doi: 10.1007/s42000-019-00100-0

17. Pan YY, Zeng F, Guo WL, Li TT, Jia RB, Huang ZR, et al. Effect of grifola frondosa 95% ethanol extract on lipid metabolism and gut microbiota composition in high-fat diet-fed rats. *Food Funct* (2018) 9:6268–78. doi: 10.1039/c8fo01116h

18. Cui F, Zan X, Li YF, Liu B. Purification and partial characterization of a novel anti-tumor glycoprotein from cultured mycelia of grifola frondosa. *Int J Biol Macromol* (2013) 62:684–90. doi: 10.1016/j.ijbiomac.2013.10.025

19. Chen SD, Yong TQ, Xiao C, Su JY, Zhang YF, Jiao CW, et al. Pyrrole alkaloids and ergosterols from grifola frondosa exert anti-α-glucosidase and anti-proliferative activities. *J Funct Foods* (2018) 43:196–205. doi: 10.1016/j.jff.2018.02.007

20. Zhuang C, Kawagishi H, Preuss HG. Glycoprotein with antidiabetic, antihypertensive, antiobesity and antihyperlipidemic effects from grifola frondosa, and a method for preparing same. *United States patent* (2005).

21. Jiang X, Chu QB, Li LZ, Qin LY, Hao J, Kou L, et al. The anti-fatigue activities of tuber melanosporum in a mouse model. *Exp Ther Med* (2018) 15:3066–73. doi: 10.3892/etm.2018.5793

22. Meng M, Zhang R, Han R, Kong Y, Wang RH, Hou LH. The polysaccharides from the grifola frondosa fruiting body prevent lipopolysaccharide/D-galactosamine-induced acute liver injury *via* the miR-122-Nrf2/ARE pathways. *Food Funct* (2021) 12:1973–82. doi: 10.1039/d0fo03327h

23. Li C, Meng M, Guo MZ, Wang MY, Ju AN, Wang CL. The polysaccharides from grifola frondosa attenuate CCl4-induced hepatic fibrosis in rats *via* the TGF-β/Smad signaling pathway. *RSC Adv* (2019) 9:33684–92. doi: 10.1039/c9ra04679h

24. Yeh JY, Hsieh LH, Wu KT, Tsai CF. Antioxidant properties and antioxidant compounds of various extracts from the edible basidiomycete grifola frondosa (Maitake). *Molecules* (2011) 16:3197–211. doi: 10.3390/molecules16043197

25. Valvona CJ, Fillmore HL, Nunn PB, Pilkington GJ. The regulation and function of lactate dehydrogenase a: Therapeutic potential in brain tumor. *Brain Pathol* (2016) 26:3–17. doi: 10.1111/bpa.12299

26. Wang J, Xue Z, Hua C, Lin J, Shen Z, Song Y, et al. Metabolomic analysis of the ameliorative effect of enhanced proline metabolism on hypoxia-induced injury in cardiomyocytes. *Oxid Med Cell Longev* (2020) 2020:8866946. doi: 10.1155/2020/8866946

27. Xu X, Dou D. The ginseng's fireness is associated with the lowering activity of liver na(+)-K(+)-ATPase. *J Ethnopharmacol* (2016) 190:241–50. doi: 10.1016/j.jep.2016.06.024

28. Li BG. Study on liquid fermentation culture and anti-fatigue activity of grifola frondosa. [Tianjin]: Tianjin University of Science & Technology (2018).

29. Wu Y, Peng XX, Li XY, Li DD, Tan ZJ, Yu R. Sex hormones influence the intestinal microbiota composition in mice. *Front Microbiol* (2022) 13:964847. doi: 10.3389/fmicb.2022.964847

30. Zhou ZQ, Ye CW, Mao KR, Lian CX. Stick cultivation of grifola frondosa and secondary fruiting technology with soil cover. *Edible Fungi* (2007) 3:43–7. doi: 10.3969/j.issn.1000-8357.2007.03.028

31. Shao HQ, Zhang CY, Xiao NQ, Tan ZJ. Gut microbiota characteristics in mice with antibiotic-associated diarrhea. *BMC Microbiol* (2020) 20:313. doi: 10.1186/s12866-020-01999-x

32. Bolger AM, Lohse M, Usadel B. Trimmomatic: a flexible trimmer for illumina sequence data. *Bioinformatics* (2014) 30:2114–20. doi: 10.1093/bioinformatics/btu170

33. Edgar RC. UPARSE: Highly accurate OTU sequences from microbial amplicon reads. *Nat Methods* (2013) 10:996–8. doi: 10.1038/nmeth.2604

34. Callahan BJ, McMurdie PJ, Rosen MJ, Han AW, Johnson AJ, Holmes SP. DADA2: High-resolution sample inference from illumina amplicon data. *Nat Methods* (2016) 13:581–3. doi: 10.1038/nmeth.3869

35. Bolyen E, Rideout JR, Dillon MR, Bokulich NA, Abnet CC, Al-Ghalith GA, et al. Reproducible, interactive, scalable and extensible microbiome data science using QIIME 2. *Nat Biotechnol* (2019) 37:852–7. doi: 10.1038/s41587-019-0209-9

36. Li XY, Deng N, Zheng T, Qiao B, Peng MJ, Xiao NQ, et al. Importance of dendrobium officinale in improving the adverse effects of high-fat diet on mice associated with intestinal contents microbiota. *Front Nutr* (2022) 9:957334. doi: 10.3389/fnut.2022.957334

37. Zhang CY, Shao HQ, Peng XX, Liu TH, Tan ZJ. Microbiotal characteristics colonized in intestinal mucosa of mice with diarrhoea and repeated stress. *3 Biotech* (2020) 10:372. doi: 10.1007/s13205-020-02368-1

38. Yuan XL, Cao M, Liu XM, Du YM, Shen GM, Zhang ZF, et al. Composition and genetic diversity of the nicotiana tabacum microbiome in different topographic areas and growth periods. *Int J Mol Sci* (2018) 19:3421. doi: 10.3390/ijms19113421

39. Guo KX, Xu SS, Zhang QL, Peng MJ, Yang ZY, Li WG, et al. Bacterial diversity in the intestinal mucosa of mice fed with asparagus extract under high-fat diet condition. *3 Biotech* (2020) 10:228. doi: 10.1007/s13205-020-02225-1

40. Ma H, Zhang B, Hu Y, Wang J, Liu J, Qin R, et al. Correlation analysis of intestinal redox state with the gut microbiota reveals the positive intervention of tea polyphenols on hyperlipidemia in high fat diet fed mice. *J Agric Food Chem* (2019) 67:7325–35. doi: 10.1021/acs.jafc.9b02211

41. Jovanovic P, Zoric L, Stefanovic I, Dzunic B, Djordjevic-Jocic J, Radenkovic M, et al. Lactate dehydrogenase and oxidative stress activity in primary open-angle glaucoma aqueous humour. *Bosn J Basic Med Sci* (2010) 10:83–8. doi: 10.17305/bjbms.2010.2743

42. Bao J, Li X, Xing Y, Feng C, Jiang H. Respiratory metabolism and antioxidant response in Chinese mitten crab eriocheir sinensis during air exposure and subsequent reimmersion. *Front Physiol* (2019) 10:907. doi: 10.3389/fphys.2019.00907

43. Laitinen K, Mokkala K. Overall dietary quality relates to gut microbiota diversity and abundance. *Int J Mol Sci* (2019) 20:1835. doi: 10.3390/ijms20081835

44. Stojanov S, Berlec A, Štrukelj B. The influence of probiotics on the Firmicutes/Bacteroidetes ratio in the treatment of obesity and inflammatory bowel disease. *Microorganisms* (2020) 8:1715. doi: 10.3390/microorganisms8111715

45. Jiang X, Hao J, Zhu Y, Liu Z, Li L, Zhou Y, et al. The anti-obesity effects of a water-soluble glucan from grifola frondosa *via* the modulation of chronic inflammation. *Front Immunol* (2022) 13:962341. doi: 10.3389/fimmu.2022.962341

46. Jiang X, Hao J, Liu Z, Ma X, Feng Y, Teng L, et al. Anti-obesity effects of grifola frondosa through the modulation of lipid metabolism *via* ceramide in mice fed a high-fat diet. *Food Funct* (2021) 12:6725–39. doi: 10.1039/d1fo00666e

47. Chambers ES, Preston T, Frost G, Morrison DJ. Role of gut microbiota-generated short-chain fatty acids in metabolic and cardiovascular health. *Curr Nutr Rep* (2018) 7:198–206. doi: 10.1007/s13668-018-0248-8

48. Blaak EE, Canfora EE, Theis S, Frost G, Groen AK, Mithieux G, et al. Short chain fatty acids in human gut and metabolic health. *Benef Microbes* (2020) 11:411–55. doi: 10.3920/BM2020.0057

49. Chambers ES, Morrison DJ, Frost G. Control of appetite and energy intake by SCFA: what are the potential underlying mechanisms? *Proc Nutr Soc* (2015) 74:328–36. doi: 10.1017/S0029665114001657

50. Al-Bulish MSM, Cao WX, Yang RL, Wang YM, Xue CH, Tang QJ. Docosahexaenoic acid-rich fish oil alleviates hepatic steatosis in association with regulation of gut microbiome in ob/ob mice. *Food Res Int* (2022) 157:111373. doi: 10.1016/j.foodres.2022.111373

51. Yu GH, Ji XG, Huang JH, Liao AM, Pan L, Hou YC, et al. Immunity improvement and gut microbiota remodeling of mice by wheat germ globulin. *World J Microbiol Biotechnol* (2021) 37:64. doi: 10.1007/s11274-021-03034-1

52. Chen H, Zhang F, Zhang J, Zhang X, Guo Y, Yao Q. A holistic view of berberine inhibiting intestinal carcinogenesis in conventional mice based on microbiome-metabolomics analysis. *Front Immunol* (2020) 11:588079. doi: 10.3389/fimmu.2020.588079

53. Ye X, Liu Y, Hu J, Gao Y, Ma Y, Wen D. Chlorogenic acid-induced gut microbiota improves metabolic endotoxemia. *Front Endocrinol (Lausanne)* (2021) 12:762691. doi: 10.3389/fendo.2021.762691

54. Wang BT, Kong QM, Li X, Zhao JX, Zhang H, Chen W, et al. A high-fat diet increases gut microbiota biodiversity and energy expenditure due to nutrient difference. *Nutrients* (2020) 12:3197. doi: 10.3390/nu12103197

55. Zhang XY, Li S, Zhou YF, Su W, Ruan XZ, Wang B, et al. Ablation of cytochrome P450 omega-hydroxylase 4A14 gene attenuates hepatic steatosis and fibrosis. *Proc Natl Acad Sci U.S.A.* (2017) 114:3181–5. doi: 10.1073/pnas.1700172114

56. Jalanka J, Major G, Murray K, Singh G, Nowak A, Kurtz C, et al. The effect of psyllium husk on intestinal microbiota in constipated patients and healthy controls. *Int J Mol Sci* (2019) 20:433. doi: 10.3390/ijms20020433

57. Che J, Bai Y, Li X, Ye J, Liao H, Cui P, et al. Linking microbial community structure with molecular composition of dissolved organic matter during an industrial-scale composting. *J Hazard Mater* (2021) 405:124281. doi: 10.1016/j.jhazmat.2020.124281

58. Detman A, Laubitz D, Chojnacka A, Kiela PR, Salamon A, Barberán A, et al. Dynamics of dark fermentation microbial communities in the light of lactate and butyrate production. *Microbiome* (2021) 9:158. doi: 10.1186/s40168-021-01105-x

frontiers | Frontiers in Endocrinology

TYPE Original Research
PUBLISHED 18 January 2023
DOI 10.3389/fendo.2023.1120221



OPEN ACCESS

EDITED BY
Zhoujin Tan,
Hunan University of Chinese Medicine, China

REVIEWED BY
Wuwen Feng,
Chengdu University of Traditional Chinese Medicine, China
Yang Ping,
Jiamusi University, China

*CORRESPONDENCE
Huibo Xu
xhb_6505@163.com
Yufeng Zhao
yfzhao21@sjtu.edu.cn
Chenhong Zhang
zhangchenhong@sjtu.edu.cn

SPECIALTY SECTION
This article was submitted to Gut Endocrinology, a section of the journal Frontiers in Endocrinology

RECEIVED 09 December 2022
ACCEPTED 03 January 2023
PUBLISHED 18 January 2023

CITATION
Li D, Feng G, Li Y, Pan H, Luo P, Liu B, Ding T, Wang X, Xu H, Zhao Y and Zhang C (2023) Benefits of Huang Lian mediated by gut microbiota on HFD/STZ-induced type 2 diabetes mellitus in mice.
*Front. Endocrinol.* 14:1120221.
doi: 10.3389/fendo.2023.1120221



# Benefits of Huang Lian mediated by gut microbiota on HFD/STZ-induced type 2 diabetes mellitus in mice

Dan Li[1], Guangli Feng[1], Yue Li[1], Han Pan[1], Pei Luo[1], Bo Liu[2], Tao Ding[2], Xin Wang[2], Huibo Xu[2]*, Yufeng Zhao[1]* and Chenhong Zhang[1]*

[1]State Key Laboratory of Microbial Metabolism, School of Life Sciences and Biotechnology, Shanghai Jiao Tong University, Shanghai, China, [2]Pharmacodynamics and Toxicology Evaluation Center, Jilin Provincial Academy of Traditional Chinese Medicine, Jilin, China

**Background:** Huang Lian (HL), one of the traditional Chinese medicines (TCMs) that contains multiple active components including berberine (BBR), has been used to treat symptoms associated with diabetes for thousands of years. Compared to the monomer of BBR, HL exerts a better glucose-lowering activity and plays different roles in regulating gut microbiota. However, it remains unclear what role the gut microbiota plays in the anti-diabetic activity of HL.

**Methods:** In this study, a type 2 diabetes mellitus (T2DM) mouse model was induced with a six-week high-fat diet (HFD) and a one-time injection of streptozotocin (STZ, 75 mg/kg). One group of these mice was administrated HL (50 mg/kg) through oral gavage two weeks after HFD feeding commenced and continued for four weeks; the other mice were given distilled water as disease control. Comprehensive analyses of physiological indices related to glycolipid metabolism, gut microbiota, untargeted metabolome, and hepatic genes expression, function prediction by PICRUSt2 were performed to identify potential mechanism.

**Results:** We found that HL, in addition to decreasing body fat accumulation, effectively improved insulin resistance by stimulating the hepatic insulin-mediated signaling pathway. In comparison with the control group, HL treatment constructed a distinct gut microbiota and bile acid (BA) profile. The HL-treated microbiota was dominated by bacteria belonging to Bacteroides and the Clostridium innocuum group, which were associated with BA metabolism. Based on the correlation analysis, the altered BAs were closely correlated with the improvement of T2DM-related markers.

**Conclusion:** These results indicated that the anti-diabetic activity of HL was achieved, at least partly, by regulating the structure of the gut microbiota and the composition of BAs.

KEYWORDS

**Huang Lian, type 2 diabetes mellitus, gut microbiota, bile acids, microbial BA metabolism**

# Introduction

Type 2 diabetes mellitus (T2DM) was the predominant form of diabetes in about 426 million people worldwide in 2017, thereby becoming a major public health problem (1). The prevalence of T2DM may be related to multiple risk factors, such as genetics, and environmental factors (e.g., eating pattern, physical inactivity) (2, 3). Because of the complex pathogenesis, the underlying mechanism of T2DM is still inconclusive. Emerging evidence shows that gut microbiota is an important factor in the development of T2DM (4). Several mechanisms of gut microbiota acting on the glycolipid metabolism of the host have been revealed, for example, bile acids (BAs) that are modified by the gut microbiota, serving as signaling molecules to target farnesoid X receptor (FXR) and G protein-coupled bile acid receptor-1 (TGR5), were found to promote the secretion of glucagon-like peptide-1 (GLP-1) to maintain glucose homeostasis (5), induce thermogenic genes and inhibit lipogenic genes to inhibit obesity (6). Notably, the metabolic benefits of some oral antidiabetic medications were found to be partly mediated by gut microbiota (7–10). For example, metformin, the first-line drug of T2DM, effectively improved glucose homeostasis in T2DM patients partially by regulating the *Bacteroides fragilis*-glycoursodeoxycholic acid (GUDCA)-intestinal FXR axis (11).

In China, Traditional Chinese Medicine (TCM) also serves as an important therapy for managing T2DM, and the efficacy of TCM might be closely related to the gut microbiota. Previously, several mechanisms of TCM in glycolipid metabolism have been reported *in vitro*, such as the up-regulation of the hepatic low-density lipoprotein receptor (12), promotion of intestinal GLP-1 secretion (13), and stimulation of AMPK activity in both myotubes and adipocytes (14). Due to the low bioavailability after oral administration, the maximum concentration ($C_{max}$) of TCM in plasma is too low to reach the effective concentration for targeted regulation *in vitro* studies (15, 16). Therefore, the efficacy of TCM cannot be elucidated solely from the perspective of oral absorption, which might be mediated by gut microbiota. The active ingredients in TCM were shown to be able to regulate the structure and function of the gut microbiota. TCM, however, can be metabolized by gut microbiota to allow easy absorption (17, 18). Berberine (BBR), a monomer from TCM, is used as an effective drug for managing T2DM, which was found to regulate the gut microbiota (19–21). Growing evidence has reported that the anti-diabetic effect might be involved in the modulation of microbial short-chain fatty acids and BA metabolism by BBR (19, 22). A study reported that BBR could effectively alleviate the level of hemoglobin A1c in T2DM patients, which was associated with the inhibition of *Ruminococcus bromii* and its deoxycholic acid (DCA) conversion (23). Thus, investigations on the participation of the gut microbiota in T2DM may reveal new insights for a better understanding of the mechanisms of TCM in treating diabetes.

Compared to BBR, Huang Lian (HL, known as *Coptidis Rhizoma*) which is a TCM containing BBR, exerts a better glucose-lowering effect in mice and shows lower cytotoxicity in HepG2 cells (24–26). This might reflect that multiple ingredients within HL could regulate different pathways/targets to enhance pharmacological potency of HL. Previously, a study found that the modulation effects of HL and BBR on the gut microbiota were different, suggesting that other ingredients, except BBR, also played a significant role in modulating the gut microbiota (27). However, the role of the altered gut microbiota by HL in treating diabetes is still unclear.

In this study, a T2DM mouse model induced by HFD/STZ and an ethanol extraction of HL (28) were used to explore the mechanisms underlying the effect of HL on T2DM. The HL extract contains a total of 69.4% alkaloids. We found that HL treatment markedly improved insulin sensitivity and blunted fat accumulation in mice, which were closely associated with the modulation of microbial BA metabolism and the increase in BA synthesis. Our findings provide fundamental knowledge regarding the benefits of HL for T2DM and suggest that the gut microbiota is a potential target for HL to mitigate T2DM.

# Material and methods

## Extraction of HL extract

The herbal of Huang Lian (origin: Coptis chinensis Franch,; source: Mianyang, Sichuan) was purchased from Anhui Wugeng Traditional Chinese Medicine Pieces Co., Ltd. (Bozhou, China) and identified by Jilin Provincial Academy of Traditional Chinese Medicine according to the Chinese Pharmacopeia method. HL was stored in a ventilated and dry place. And HL extract was prepared as follows. The small pieces of HL were refluxed with 5-fold of 70% ethanol (1:5, w/v) twice for 2 h. Two batches of filtrates were combined, and pH value was adjusted to 1.5-2.0 with hydrochloric acid. The mixture was subsequently dissolved using NaCl. After being refrigerated for 48 h, precipitation was dried by vacuum concentration to obtain HL extract. Then extract was grinded into powder and stored in seal at 4°C. The freeze-dried powder was supplied by Jilin Provincial Academy of Traditional Chinses Medicine and was dissolved in distill water when used in the experiment.

## Quantitative analysis of marker components of HL extract

The contents of marker components within HL extract were analyzed with high performance liquid chromatography (HPLC) method. 25 mL solution (methanol: hydrochlori acid = 100: 1) was added to 40 mg extract powder and the mixture was ultrasound for 20 min. Then mixture was diluted 10 times with solution (methanol: hydrochlori acid = 100: 1) and well vortexed. After centrifugation, the supernatant was analyzed using HPLC system to evaluate the content of epiberberine, coptidis, palmatine, and berberine. HPLC was performed on LC-Q10 AT system, consisting of a binary solvent delivery manager, an auto-sampler, and a UDV detector. Chromatographic separations were performed on an Agilent C18 column (4.6 × 250 mm,5 μm). Flow rate and column temperature were set at 1 ml/min and 25°C, respectively. The injection volume was 10 μL, and the solvent was filtered through 0.45 μm Millipore filter and degassed prior to use. Briefly, acetonitrile (A) and 0.05% potassium dihydrogen phosphate mixed with 0.4% sodium dodecyl sulfate (pH was regulated to 4.0 by phosphoric acid) (B) (50:50) were used as mobile phase. Ultraviolet detection with the wavelength at 345 nm and was used for the determination of epiberberine, coptidis, palmatine, and berberine.

## Animal experiments

Male C57BL/6 mice (5 weeks old) were purchased from Slake experimental Animal Co., Ltd. (Shanghai, China). All mice were housed in a temperature-controlled room (22 ± 3°C) under specific pathogen-free (SPF) conditions with a standard 12 h light/dark cycle. All animal experimental procedures were approved by the Institutional Animal Care and Use Committee (IACUC) of Shanghai Jiao Tong University (No. A2020030). Because there is a certain risk of death in STZ injection, we used additional three and two mice to DM group and DM-HL group, respectively. When we performed the randomly grouping of the mice, the mice were weighted and sorted in order and divided into multiple groups according to body weight. During the experiment, none of mice died with STZ or HL treatment. Eventually, mice were divided into the NC group (n = 8), DM group (n = 11), and DM-HL group (n = 10). The mice in the NC group were fed a normal chow diet (NC, 12450J, 10% calories from fat, 70% calories from carbohydrate, 20% calories from protein, 3.85 kcal/g; produced by Fanbo Biotechnology Co., Ltd., Shanghai, China); other mice were fed a high-fat diet (HFD, D12492, 60% calories from fat, 20% calories from carbohydrate, 20% calories from protein, 5.24 kcal/g; produced by Fanbo Biotechnology Co., Ltd., Shanghai, China). Two weeks after dietary intervention commenced, the mice in the DM-HL group were orally gavaged daily with a dosage of 50 mg/kg HL extract, which continued until the end of the experiment. The mice in the NC and DM groups were gavaged daily with an equivalent volume of distilled water as a control. After the 4-week diet intervention commenced, the mice in the DM and DM-HL groups were injected intraperitoneally with a single dose of streptozotocin (STZ, 75 mg/kg) (S0130, Sigma-Aldrich, Germany) to construct the T2DM model. At the same time, the mice in the NC group received the equivalent volume of citric buffer to eliminate the effects of the injection procedure. All mice were allowed ad libitum access to water and food during the trial. The trial lasted for 6 weeks in total. Body weight was monitored weekly. Fecal samples were collected in week 6 and stored at −80°C for gut microbiota analysis.

All mice were fasted for 6 h before sampling. Blood samples were collected from the orbital vascular plexus. Serum samples were isolated from blood samples after centrifugation for 15 min at 4°C at 3000 g and then stored at −80°C. Liver, adipose tissues (epididymal, retroperitoneal, perirenal), and colon contents were weighed and collected immediately and stored at −80°C or in 4% paraformaldehyde for further analyses.

## Oral glucose tolerance test (OGTT)

After 6 h of fasting, all mice were administered a glucose solution (2 g·kg$^{-1}$ body weight) through oral gavage. The glucose levels at 0 min (which is fasting glucose) and 15, 30, 60, 90, and 120 min after the glucose challenge were measured using a blood glucometer (ACCU-CHEK Performa, Roche, USA). Blood samples at 0 min, 15 min, and 60 min after the glucose challenge were collected from the tip of the tail vein. Serum samples were isolated for insulin detection after centrifugation at 4°C at 3000 rpm for 15 min. The insulin concentration was measured using an ultrasensitive mouse insulin ELISA kit (90080, Crystal Chem, USA).

## Histological analysis of epididymal fat and liver

Fresh epididymal fat and liver were fixed with 4% paraformaldehyde and embedded in paraffin. Then, 4-μm sections were stained with hematoxylin and eosin (H&E) (G1003, Wuhan Servicebio Technology Ltd., China). The adipocyte area and nonalcoholic fatty liver disease (NAFLD) activity score were analyzed using Image Pro Plus v6.0 software (Media Cybernetics Inc., Silver Springs, USA). For epididymal fat, at least 300 adipocytes of each mouse were required to assess the mean area of adipocytes under ×100 magnification. For the liver, three discontinuous scans of each mouse were used to assess the NAFLD activity score under ×100 magnification as previously described (29).

Epididymal fats were fixed overnight with 4% paraformaldehyde. In accordance with the standard process, the tissue was sectioned and stained with Oil Red O. The slices were imaged under microscope.

## Analysis of protein expression by Western Blot

Frozen livers were homogenized using a tissue homogenizer in pro-cooled 1× RIPA buffer (ab156034, Abcam, Cambridge), containing protease and phosphatase inhibitors (P1045, Beyotime, China) (30). Then, homogenates were lysed for 5 min at 25 Hz/s using a TissueLyser (Qiagen, Germany). Protein was isolated from homogenates after centrifugation at 4°C at 12000 rpm for 10 min. A BCA protein Assay Kit (P001P, Beyotime, China) was used to quantify the protein concentration according to the manufacturer's instructions. The protein was boiled at 100°C for 10 min after an equal volume of 2× SDS loading buffer (P0015B, Beyotime, China) was added. An equal amount of protein across all samples was separated on 10% SDS-PAGE gels (180-9117HA, Tanon, China) and diverted immediately to PVDF membranes (G6044-0.45, Servicebio, China). After 2 h of blocking in 8% skimmed milk at room temperature, the membranes were incubated with the primary antibodies overnight at 4°C. After washing 3 times with 0.1% TBST solution, the membranes were incubated with secondary antibodies for 2 h at room temperature. Eventually, the bands were visualized using the ECL stain kit (180-501, Tanon, China), and the intensity of the bands was determined by Image Pro Plus v6.0 software. Primary antibodies were as follows: IRS1 (1:2000, ab131487, Abcam), p-IRS1 (1:3000, 2386, cell signaling), Akt (1:2000, 9272, cell signaling), p-Akt (1:1000, 9271, cell signaling), Glut4 (1:2000, ab33780, Abcam), and GAPDH (1:3000, ab9485, Abcam).

## Quantification of mRNA expression by RT-qPCR

Total RNA was extracted from liver tissues using a RNeasy minikit (74804, Qiagen, Germany). Then, reverse transcription was performed to synthesize cDNA using a SuperScript kit (18080-051, Invitrogen, USA). According to the manufacturer's instructions, cDNA was then amplified using real-time PCR (qPCR) to determine the expression of *Cyp27a1*, *Cyp7b1*, *Cyp7a1*, and *Cyp8b1* in a 20-μL reaction system containing cDNA template, forward

primer, reverse primer, $ddH_2O$, and SYBR Green I PCR Supermix (Bio-Rad). The reaction conditions of forty cycles were as follows: 95°C for 20 s, 56°C for 30 s, and 72°C for 30 s, followed by plate reads for 5 s. Gene expression levels were calculated using the $\Delta\Delta C_T$ method and normalized to *β-actin*. The forward and reverse primer sequences of target genes and *β-actin* were listed as follows (31, 32). *Cyp27a1* gene, F: 5'-CCAGGCACAGGAGAGTACG-3'; R: 5'-GGGCAAG TGCAGCACATAG-3'. *Cyp7b1* gene, F: 5'-GGAGCCACGACCC TAGATG-3'; R: 5'-TGCCAAGATAAGGAAGCCAAC-3'. *Cyp7a1* gene, F: 5'-AGCTCTGGAGGGAATGCCAT-3'; R: 5'-GAGCCGC AGAGCCTCCTT-3'. *Cyp8b1* gene, F: 5'-CCTCTGGACAAGGG TTTTGTG-3'; R: 5'-GCCATCAAGGACGTCAGCA-3'. *β-actin* gene, F: 5'-GGCTGTATTCCCCTCCATCG-3'; R: 5'-CCAGTTG GTAACAATGCCATGT-3'.

## Isolation of fecal DNA

Total DNA was extracted from week 6 fecal samples according to a procedure published previously (33). DNA concentration was determined by a NanoPhotometer and expressed in micrograms (μg). The DNA concentration across all samples was diluted to 10 ng/μL for subsequent analysis.

## Total bacterial loads assessed by qPCR

A plasmid containing the 16S full-length *Roseburia inulinivorans* strain was diluted successively to $10^9$,$10^8$, $10^7$, $10^6$, $10^5$, $10^4$, $10^3$, and $10^2$ copies/μL. According to the manufacturer's instructions, qPCR was performed in a 20-μL reaction system containing a DNA template, Uni331F primer (5'-TCCTACGGGAGGCAGCAGT-3'), Uni797R primer (5'-GGACTACCAGGGTATCTAATCCTGTT-3') (34), $ddH_2O$, and SYBR Green I PCR Supermix (Bio-Rad). The reaction conditions of forty cycles were as follows: 95°C for 10 s, 65°C for 60 s, and 80°C for 5 s, followed by plate reads for 5 s. A standard curve was constructed according to the linearity between the copy number of plasmids and the $C_T$value. The copy number of DNA samples was calculated according to the standard curve.

## Analysis of 16S rRNA gene V3-V4 sequencing

An amplicon library was prepared by amplifying the V3-V4 region of the 16S rRNA gene according to previously published procedures (35). To profile the composition of microbial communities, high-throughput sequencing of the prepared amplicon library was performed on an Illumina Miseq platform (Illumina, Inc., USA).

Raw paired-end reads were analyzed with Quantitative Insights into Microbial Ecology2 software (QIIME2, v2021.4). After the removal of the adapters and primers with the "Cutadapt" plugin, DADA2 was used to obtain amplicon sequence variants (ASVs) through denoising, merging, and filtering. Then, a rooted phylogenetic tree was constructed with the "FastTree" plugin based on representative sequences of ASVs. Subsequently, the taxonomy of ASVs was identified based on the Silva138 16S rRNA database. In combination with the quantified total bacterial load, the relative abundance of ASVs was converted into absolute abundance for subsequent analysis (36, 37).

Redundancy analysis (RDA) was performed using Canoco 5 software (Microcomputer Power, USA) to identify key variations of ASVs responding to the T2DM model and HL treatment, which drive the segregation of the gut microbiota among groups. A heatmap representing the abundance variations of the key ASVs generated from the RDA model was constructed using the "Complexheatmap" R package. Pairwise comparisons (DM *vs.* NC, DM-HL *vs.* DM, DM-HL *vs.* NC) of ASVs were assessed using a Mann-Whitney U test. Microbial functional genes were predicted using PICRUSt2 based on the Greengenes database of 16S rRNA sequences (38) and the Kyoto Encyclopaedia of Genes and Genomes (KEGG) database.

## Untargeted metabolomics analysis of the colon content

The colon content was homogenized in 600 μL 2-chlorophenylalanine (4 ppm) methanol and vortexed for 30 s. Then, homogenates were sonicated at room temperature for 10 min. The supernatants were collected after centrifugation (4°C, 12000 rpm, 10 min) and filtration with a 0.22-μm membrane for high-performance liquid chromatography-mass spectrometry analysis (HPLC-MS/MS). Quality control (QC) samples were prepared with the same procedures. HPLC-MS/MS was performed by Suzhou PANOMIX Biomedical Tech Co., Ltd. (Suzhou, China). Chromatographic separation was performed with an ACQUITY UPLC® HSS T3 (150 × 2.1 mm, 1.8 μm, water) column maintained at 40°C. Data-dependent acquisition in the MS/MS experiment was operated with an HCD scan. The raw data of metabolites were converted into mzXML format with Proteowizard software. Then, perk identification, filtration, and alignment were performed using the "XCMS" R package. The output metabolites were identified based on the Metlin metabolites database (metlin.scripps.edu), MoNA metabolite database (mona.fiehnlab.ucdavis.edu), and in-house MS2 database.

Variable importance in projection (VIP) scores calculated by the orthogonal projection to latent structure-discriminant analysis (OPLS-DA) model were used to estimate the importance of each variable to drive the segregation of the metabolome among the two groups. Through pairwise comparison between groups (DM *vs.* NC, DM-HL *vs.* DM, DM-HL *vs.* NC), differential metabolites were selected based on the following criteria: 1) VIP > 1.5 in the OPLS-DA model, 2) fold-change > 2, and 3) $p < 0.05$ (including methods used for testing and $p$ value correction). MetaboAnalyst was used for the analysis of pathway enrichment (MetaboAnalyst).

## Statistical analysis

Statistical analysis was performed using GraphPad Prism version 8.0 (GraphPad Software, Inc., USA). Gut microbiota data were exhibited by a box plot, and significance was analyzed using one-way analysis of variance (ANOVA) followed by Tukey's multiple comparisons. Physiological data, metabolites, and functional genes were expressed as the mean ± SEM, and significant differences were evaluated by one-way ANOVA or an unpaired $t$ test with Welch's correction. Spearman correlations were constructed with R software (v4.0.5). $P < 0.05$ is considered to be statically significant.

10.3389/fendo.2023.1120221

# Results

## HPLC analysis of HL extract

The chromatographic peaks of the main chemical constituents within HL extract were shown in Supplementary Figure S1. The contents of epiberberine, coptidis, palmatine, and berberine were determined to be 1.18%, 6.71%, 5.34%, and 44.34%, respectively. In short, the content of total alkaloids within HL extract was determined to be 69.43% using spectrophotometry.

## HL treatment blunted insulin resistance and fat accumulation

We used HFD with one streptozotocin (STZ, 75 mg/kg) injection to induce T2DM in C57BL/6 mice. One group of these mice was administered HL (50 mg/kg·day) by oral gavage after 2 weeks of feeding with HFD, which continued for an additional 4 weeks (DM-HL group), and the others were given distilled water as a disease control (DM group). At the end of the trial, fasting glucose and glucose levels during the oral glucose tolerance test (OGTT) were significantly higher in the DM group compared to that in the healthy mice (NC group) (Figures 1A, B). Fasting insulin, the area under the curve (AUC) of insulin during OGTT, HOMA-IR, and the insulin resistance index were also significantly higher in the DM group than in the NC group (Figures 1C–F). It was indicated that the mice in the DM group suffered glucose tolerance impairment and insulin resistance. Notably, although HL treatment had no effect on fasting glucose, fasting insulin, HOMA-IR, and insulin levels during OGTT, the mice in the DM-HL group had significantly reduced insulin resistance index and blood glucose levels (from the 30$^{th}$ min during OGTT) compared to the DM group (Figures 1A–F), suggesting that HL treatment may increase insulin sensitivity but not insulin secretion. In the insulin signaling pathway, binding of insulin to the insulin receptor would induce the phosphorylation of insulin receptor substrates (p-IRS1), phosphorylate the downstream signaling substance Akt (p-Akt), and then increase the level of glucose transporter (Glut4), leading to glucose uptake (39). Thus, we measured the levels of p-IRS1, p-Akt, and Glut4 in the liver to

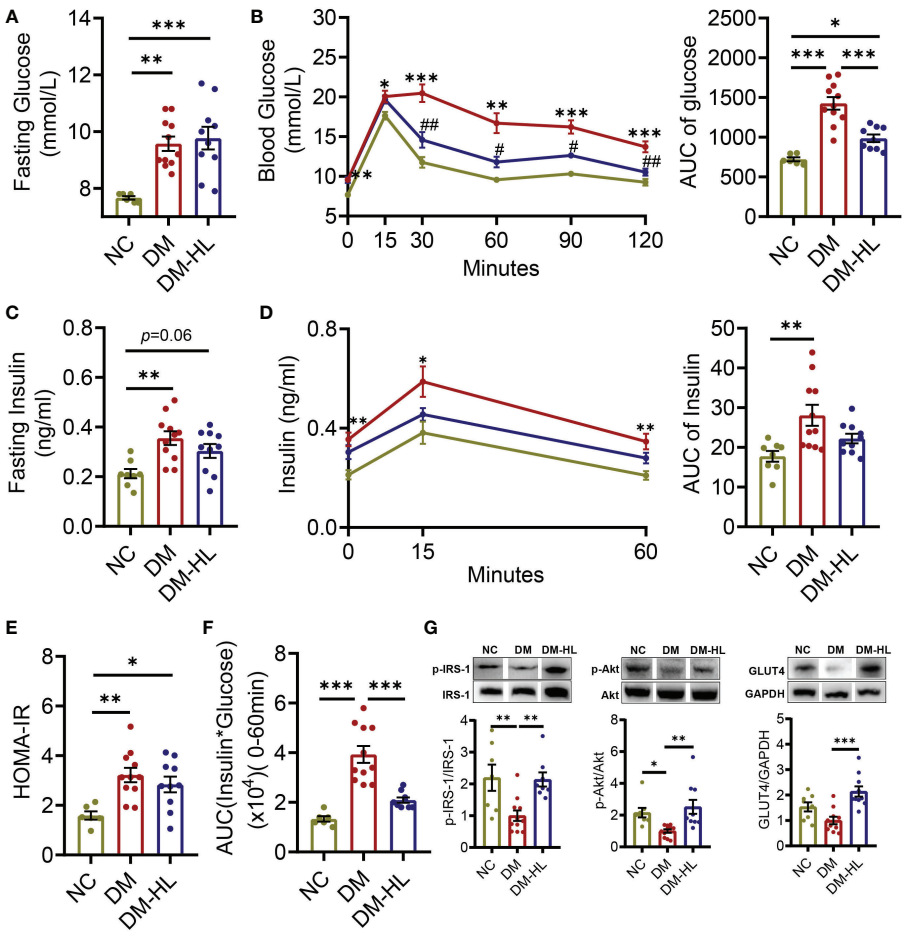


FIGURE 1
HL treatment improved glucose homeostasis and insulin sensitivity. **(A)** Fasting blood glucose. **(B)** Blood glucose levels and the AUC of blood glucose during OGTT. **(C)** Fasting serum insulin. **(D)** Serum insulin levels and the AUC of serum insulin during OGTT. **(E)** Homeostasis model assessment of insulin resistance (HOMA-IR). **(F)** Insulin resistance index (the product of the AUC of blood glucose multiplied by the AUC of serum insulin). **(G)** The phosphorylation of IRS1 and Akt, as well the expression of Glut4 in the liver. The relative abundances of p-IRS1, p-Akt, and Glut4 were normalized by IRS1, Akt, and GADPH, respectively. Data are presented as the mean ± SEM. Significance was evaluated using one-way ANOVA followed by Tukey's *post-hoc* test. *$p$ < 0.05, ** $p$ < 0.01, ***$p$ < 0.001. For the curve of graph **(B, D)**, *$p$ < 0.05, **$p$ < 0.01, ***$p$ < 0.001 *vs.* NC group; # $p$ < 0.05, ## $p$ < 0.01 *vs.* DM group.

evaluate the impact of HL on insulin sensitivity. We found that HL treatment reversed the down-regulation of the phosphorylation of IRS1 and Akt induced by HFD/STZ, and the level of Glut4 was dramatically higher in the DM-HL group than in the DM group (Figure 1G). These results suggested that HL intervention alleviated glucose tolerance by stimulating insulin sensitivity and glucose uptake.

In addition to impaired glucose tolerance, we also observed that the mice in the DM group had significantly higher body weight gain and over-accumulation of fat (Figure 2, Supplementary Figure S2). Across the experiment, HL treatment effectively inhibited excess body weight gain and successfully blunted lipid accumulation, as reflected by significantly lower body weight gain from week 3 during the experiment, as well as reduced adipocyte size and lipid droplets in epididymal fat and the NAFLD activity score in the DM-HL group than in the DM group (Figure 2, Supplementary Figure S2). These results suggest that HL treatment effectively inhibited obesity and fat accumulation induced by HFD/STZ.

## HL treatment shifted the structure of the gut microbiota

To determine the effects of HL treatment on the gut microbiota in T2DM mice, we collected fecal samples from all mice at the end of the trial for gut microbiota analyses. First, the total bacterial loads were determined by qPCR of the 16S rRNA gene. We found that the total bacterial loads of mice in the DM group and DM-HL group decreased by 3.8 times and 3.3 times, respectively, compared to the NC group, indicating significantly lower total bacterial loads in all HFD/STZ-treated mice (Supplementary Figure S3). Next, we sequenced the V3-V4 region of the 16S rRNA gene to analyze the structure and composition of the gut microbiota. Due to significant differences in the total bacterial loads among the three groups, the relative abundance of ASVs could not accurately reflect the alteration of the gut microbial structure (37). Therefore, for further analyses, we converted the relative abundance to the absolute abundance of ASVs based on the total bacterial loads of each sample. The richness and diversity of the gut microbiota, represented by the number of species and Shannon index, were similar between the DM group and NC group, while the mice in the DM-HL group had markedly reduced richness and diversity of gut microbiota, suggesting that HL may have antimicrobial activity against specific bacteria (Figure 3A). Principal coordinate analysis (PCoA) based on the Bray-Curtis distance at the ASV level showed obvious discriminations of the gut microbial structure among the three groups (Figure 3B). The structure of the gut microbiota in the DM group significantly separated from that in the NC group along PC1 (explained 34.78% of the total variance) and PC2 (explained 27.14% of the total variance). Specifically, compared to the DM group, the samples in the DM-HL group were more distinct from those in the NC group along PC1, while the samples in the DM-HL group were closer to those in the NC group along PC2. Notably, the Bray-Curtis distance of the gut microbiota in the mice between the DM-HL group and NC group was significantly higher than that between the DM group and NC group (Figure 3C). In short, HL did not reverse the gut microbiota disrupted by HFD/STZ treatment but constructed a strikingly distinct gut microbiota.

Redundancy analysis (RDA) based on the Monte Carlo permutation procedure (MCPP, $p = 0.0001$) also showed a

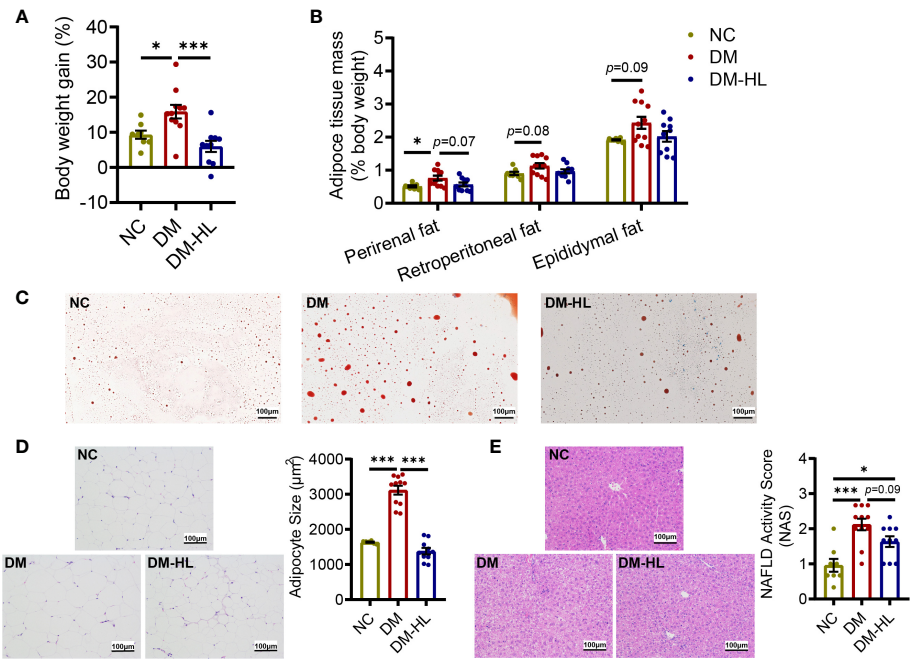


FIGURE 2
HL treatment blunted obesity and fat accumulation. **(A)** The body weight gain (% 1st day body weight). **(B)** Perirenal, Retroperitoneal, and Epididymal mass (% body weight), respectively. **(C)** Red oil staining sections of epididymal fat (scale bar = 100 μm). **(D)** Representative H&E staining sections of epididymal fat (scale bar = 100 μm) and the mean adipocyte area. **(E)** Representative H&E staining sections of the liver (scale bar = 100 μm) and NAFLD activity score. Data are presented as the mean ± SEM. Significance was evaluated using one-way ANOVA followed by Tukey's *post-hoc* test. *p < 0.05, ***p < 0.001.

10.3389/fendo.2023.1120221

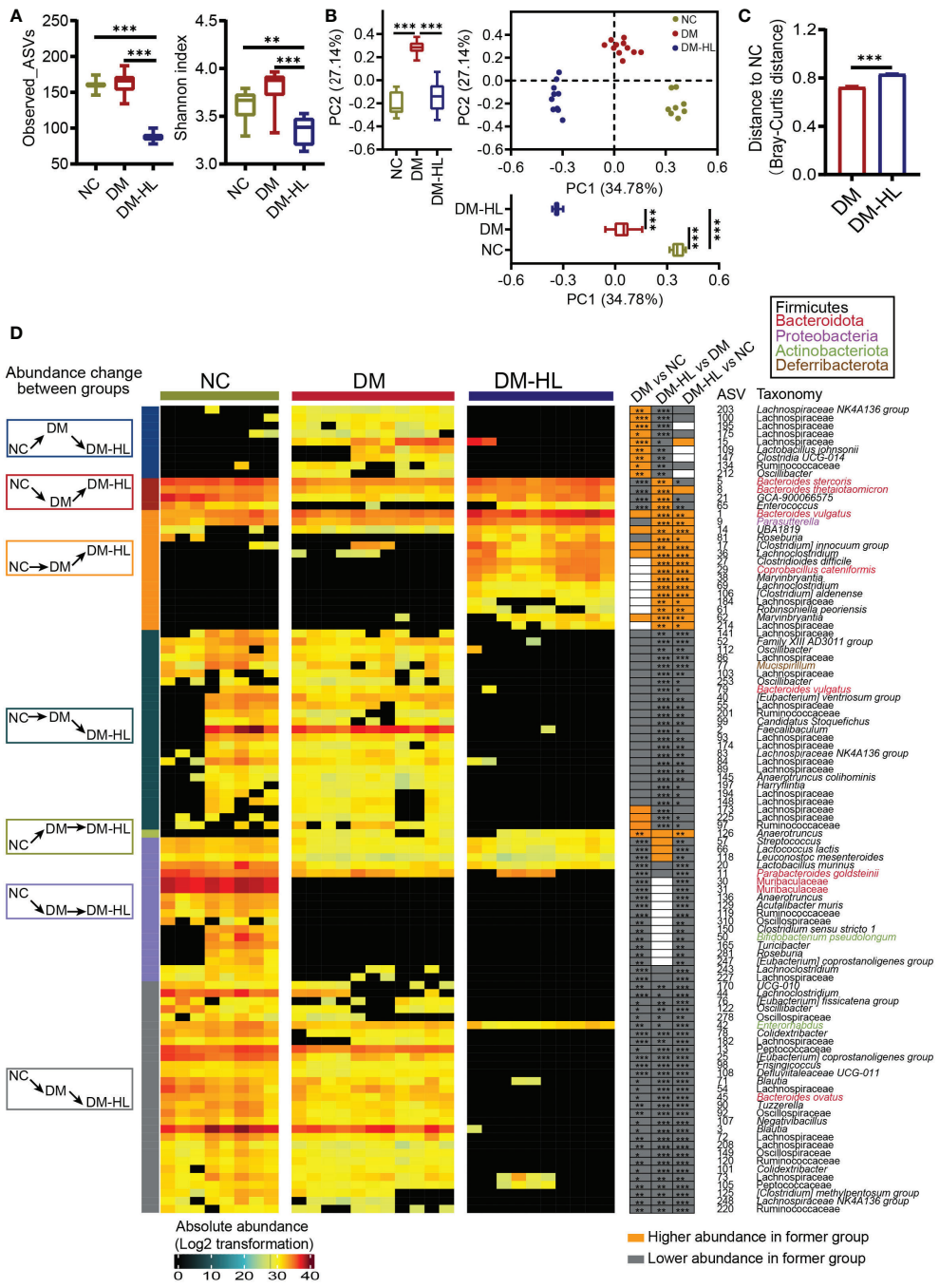


FIGURE 3
HL treatment significantly shaped a unique structure of the gut microbiota. **(A)** α-diversity of the gut microbiota represented as Observed_ASVs and the Shannon index. Data was shown in box plot. And the line in the middle of box is plotted at the median, the inferior and superior limits of the box correspond to the 25$^{th}$ and 75$^{th}$ percentiles, the whiskers correspond to maximum and minimum. Significance was analyzed using one-way ANOVA followed by Tukey's *post-hoc* test. **(B)** Principal coordinate analysis (PCoA) of the gut microbiota based on the Bray-Curtis distance. The box plots showed the changes of gut microbiota among three groups on PC1 or PC2 (the line in the middle of box is plotted at the median, the inferior and superior limits of the box correspond to the 25$^{th}$ and 75$^{th}$ percentiles, the whiskers correspond to maximum and minimum). Significance was analyzed using one-way ANOVA followed by Tukey's *post-hoc* test. **(C)** Bray-Curtis distance from the DM group and DM-HL group to the NC group. Data are presented as the mean ± SEM. Significance was analyzed using a two-tailed Mann-Whitney test. $^{**}p < 0.01$, $^{***}p < 0.001$. **(D)** Heatmap of 101 ASVs across all samples. The color of the block corresponds to the $\log_2$-transformed value based on the absolute abundance of each sample. Left, several classifications of the change in ASV abundance among groups; frame colors indicate specific situations of change. Right, the changing direction of 101 ASVs through pairwise comparison of groups analyzed by the two-tailed Mann-Whitney test. Orange indicates that ASV abundance was higher in the latter group, and the grey indicates that ASV abundance was lower in the former group.

significant effect of the T2DM model and HL treatment on the gut microbiota, which was consistent with the PCoA results. Then, we applied RDA to identify gut microbes responding to the T2DM model and/or HL treatment. Eventually, we selected 101 ASVs as key variations that accounted for at least 46.8% of the variability explained by both axes (Supplementary Figure S4). Compared to the NC group, the DM group significantly altered 61 ASVs (10 ASVs increased and 51 ASVs decreased). Among these 61 ASVs altered by the DM group, HL treatment changed 42 ASVs (4 ASVs increased and 38 ASVs decreased) and about one-third of them (13 out of 42 ASVs) were reversed to the same direction as the ASVs observed in the NC group. Of the 13 reversed ASVs, four were enriched (belonging to *Bacteroides*, *Enterococcus*, *Lachnospiraceae GCA-900066575*) and nine were reduced (belonging to Lachnospiraceae, Ruminococcaceae, *Lactobacillus*, *Clostridia UCG-014*, *Oscillibacter*) in the DM-HL group. The rest of the HL-changed ASVs (29 out of 42 ASVs) were significantly inhibited by HL treatment and most of them were eliminated in the DM-HL group except for ASV42 (belonging to *Enterornabdus*). In addition, the abundance of 40 ASVs belonging to various taxa were affected only by HL treatment, including the enrichment of 15 ASVs and the elimination of 25 ASVs in the DM-HL group. Overall, 76 out of 101 identified key ASVs were almost undetectable in the DM-HL group, including 34 ASVs belonging to the Lachnospiraceae family. Only 25 out of 101 identified key ASVs were predominant in the DM-HL group that accounted for about 48.6% of the total bacterial loads (12.1% in the NC group; 12.9% in the DM group), of which the top five abundant ASVs belonged to the *Bacteroides* (ASV1, ASV5, ASV8), *Parasutterella* (ASV9), and *Clostridium innocuum* (ASV17) groups. Moreover, we noticed that some ASVs in the same family or genus showed different behaviors. For example, among the 44 ASVs in the Lachnospiraceae family, 13 ASVs were increased while 31 ASVs were decreased in the DM-HL group compared with the DM group. Similar results were also found in the genera *Bacteroides* and *Roseburia*, indicating that the response of bacteria is species or even strain-specific (Figure 3D). These results showed a significantly distinct gut microbiota with lower total bacterial loads and diversity that developed in the DM-HL group.

## HL treatment changed the metabolites in the colon

To determine how the T2DM model and HL treatment impact the metabolites of the gut microbiota in mice, the untargeted metabolites of the colon of all mice were tested by HPLC-MS/MS. In total, we identified 541 metabolites under polar ionic mode. The principal-component analysis (PCA) and orthogonal projection to latent structure-discriminant analysis (OPLS-DA) exhibited obvious discriminations of metabolites among the three groups (Figure 4A, Figure S5A). Subsequently, we determined a total of 119 differential metabolites through pairwise comparisons between groups (VIP > 1.5 in the OPLS-DA model, fold-change > 2, and $p < 0.05$) (Supplementary Figure S5B; Supplementary Table S1). The number of differential metabolites in the mice between the DM-HL group and NC group was much higher than that between the DM group and NC group (71 vs. 37).

Among 119 differential metabolites, we recognized multiple herbal ingredients based on the TCMID database (http://www.megabionet.org/tcmid/), including BBR, tyrosol, yamogenin, 26-hydroxyecdysone, and 2,4-dihydroxyacetophenone, which may be present in the HL extract that was significantly enriched in the DM-HL group compared with the DM group (Supplementary Figure S6). Pathway enrichment analysis revealed that the differential metabolites between the DM and NC groups were mainly associated with nutrient and energy metabolisms, such as carbohydrate, lipid, amino acid, nucleotide, and cofactor and vitamin metabolisms. Notably, taurine and hypotaurine metabolism, and primary BA biosynthesis, which were highly related to microbial BA metabolism, were among the top 5 pathways enriched in the DM-HL group compared to the DM and NC groups (Figures 4B, C; Supplementary Figure S7). It has been reported that members of the gut microbiota can deconjugate the conjugated primary BAs to release free primary BAs and amino acids (taurine or glycine) and subsequently modify the free primary BAs to produce a broad range of secondary BAs (40). To assess the impact of HL on BA metabolism, we identified 12 metabolites in the gut that were involved in microbial BA metabolism (Figure 4D; Supplementary Figures S8C, D). For the conjugated primary BAs, the levels of GCA and GCDCA were similar between the DM group and DM-HL group, while the HL treatment resulted in significantly higher levels of TCA and TCDCA compared to the DM group. As a result of microbial deconjugation, the mice in the DM-HL group had higher levels of taurine and UDCA compared with the DM group, in combination with a significantly decreased level of CDCA. For the secondary BAs, the levels of THCA, DCA, and ACA were significantly enriched in the DM-HL group compared to the DM group. No significant difference was observed in LCA between groups, but the downstream metabolite of iso-LCA was reduced after HL treatment. These results showed that HL treatment dramatically changed the composition of the BA pool, leading to increased BA-related metabolites except for CDCA, LCA, and iso-LCA, which were the downstream metabolites of TCDCA.

To investigate the potential contribution of BA-related metabolites to the benefits of HL, we analyzed the correlations between BA-related metabolites and T2DM-related parameters using Spearman's correlation (Figure 4E). We found that 11 out of 12 BA-related metabolites were significantly correlated with at least one parameter. Among these 11 metabolites, five metabolites enriched in the DM-HL group, including ACA, UDCA, TCDCA, taurine, and TCA, were negatively correlated with both body weight gain and adipocyte size. Moreover, ACA was also negatively correlated with the AUC of glucose during OGTT and insulin resistance. Two metabolites that markedly decreased in the DM-HL group, i.e., CDCA and iso-LCA, were positively correlated with body weight gain and adipocyte size. These correlations suggested that BA-related metabolites may be key mediators of the microbiota-host interaction during HL treatment, leading to the protective effect of HL on HFD/STZ-induced T2DM.

## The alteration of BAs was related to the gut microbiota

To further determine the role of the altered gut microbiota in mediating the composition of BAs that are potentially protective against T2DM, we investigated the absolute abundance of putative

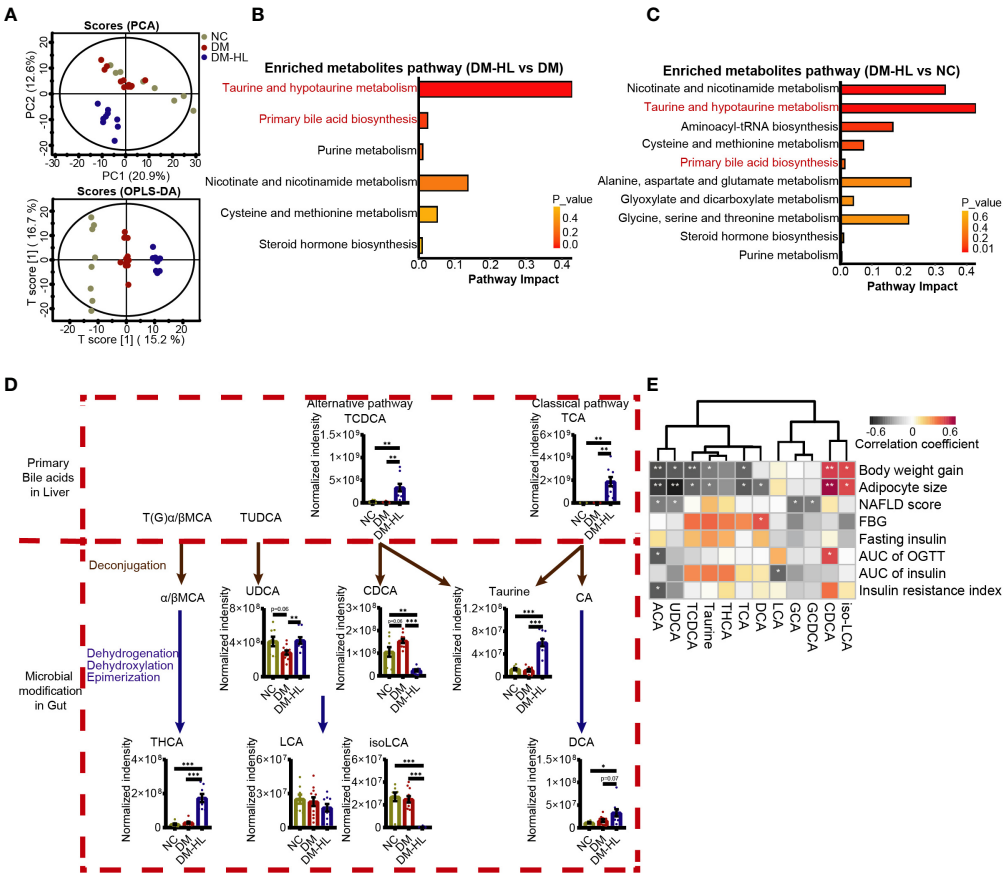


FIGURE 4
HL treatment altered the bile acid profile in the colon. **(A)** Principal component analysis (PCA) and orthogonal projection to latent structure-discriminant analysis (OPLS-DA) plot of the metabolome across all samples. **(B)** Enriched metabolite pathway in the DM-HL group compared to the DM group based on metabolic enrichment pathway analysis. **(C)** Enriched metabolite pathway in the DM-HL group compared to the NC group. **(D)** Metabolites involved in

functional genes of gut microbiota involved in BA metabolism using Phylogenetic Investigation of Communities by Reconstruction of Unobserved States (PICRUSt2) analysis. We observed that the abundance of the *cbh* gene, which is responsible for the deconjugation of BAs, increased markedly following HL treatment, and the abundance of *bai* operons (*bai*B, *bai*CD, *bai*H) that encoded several essential proteins for BA dehydroxylation was also higher in the DM-HL group than in the DM group (Figures 5A, B). It is suggested that HL treatment might improve the capability of microbial BA metabolism. Then, Spearman's correlation analysis was performed to identify the potential relationships between key microbes and BA-related metabolites (Figure 5C). In total, 11 out of 12 metabolites were correlated with at least one ASV. Among these 11 metabolites, metabolites of ACA, taurine, THCA, TCA, and TCDCA, showed a significantly positive correlation with ASVs that were enriched in the DM-HL group (mainly belonging to *Marvinbryantia*, *Clostridium*, *Coprobacillus*, *Roseburia*, *Parasutterella*, *Bacteroides*) and negative correlations with ASVs that were suppressed by HL treatment (mainly belonging to unclassified Lachnospiraceae, *Oscillibacter*). On the contrary, CDCA and iso-LCA showed the opposite trends of correlations with the gut microbiota than the above-mentioned five metabolites. Altogether, the results indicated that the enriched gut microbes in the DM-HL group might be essential for the alteration of BA composition, possibly through the improvement of microbial BA metabolism.

## Discussion

The hypoglycemic effect of HL has been well-documented (41). However, the underlying mechanisms of the effect of HL on T2DM remain to be clarified in detail. Here, we demonstrated that an ethanol extract of HL effectively prevented HFD/STZ-induced T2DM in mice. The study revealed how HL modulated gut microbiota to alter the composition of the BA pool, which might be associated with the improvement of metabolic outcomes.

We observed that several enriched chemical compounds in the DM-HL group (BBR, tyrosol, yamogenin, 26-hydroxyecdysone, 2,4-dihydroxyacetophenone) might be derived from HL extract, contributing to the efficiency of HL in treating diabetes. It is well known that BBR exerts excellent anti-inflammatory and anti-diabetic activity (19, 20). In addition, tyrosol is also well-known for its antioxidant property and was reported to decrease the glucose level, as well as promote adipose thermogenesis to inhibit obesity in mice (42, 43). Moreover, yamogenin can inhibit TG accumulation and the expression of fatty acid synthesis-related genes (*FAS*, *SREBP1c*) in HepG2 hepatocytes (44). Thus, thepharmacological potency of HL against T2DM might be related to the fact that multiple compounds regulate targets in multiple pathways, which provides a reasonable explanation as to the better hypoglycemic efficiency of HL compared to BBR.

10.3389/fendo.2023.1120221

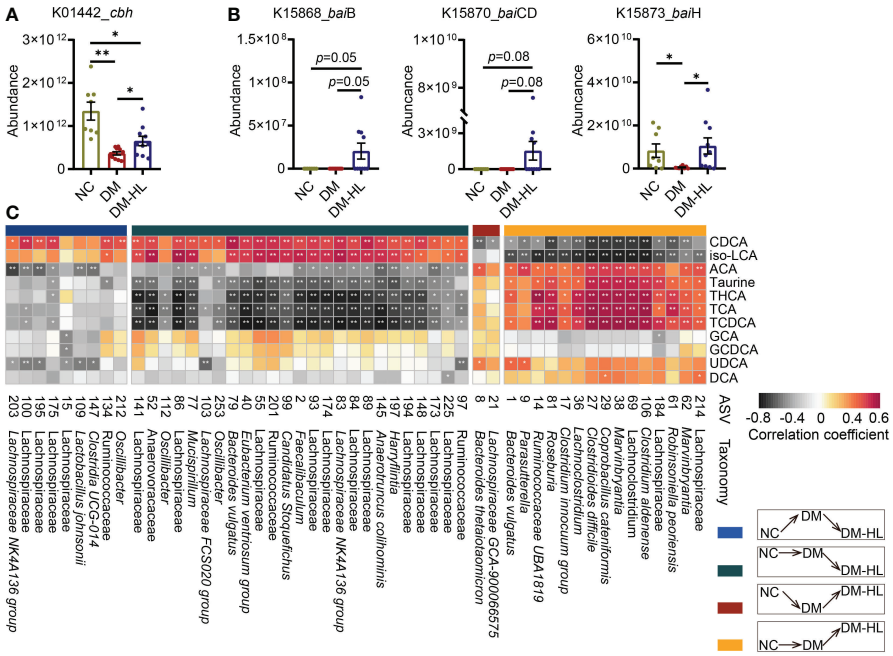


FIGURE 5
Alteration of BA composition was related to that in the gut microbiota. **(A)** The absolute abundance of the *cbh* gene predicted by PICRUSt2. **(B)** The absolute abundance of the *bai*B, *bai*CD, and *bai*H genes predicted by PICRUSt2. **(C)** The Spearman correlation between metabolites and microbes. ASVs belong to different classifications based on their inconsistent responses to HFD/STZ treatment and HL administration. The metabolites were involved in microbial bile acid metabolism in the gut. The color of the block indicates the correlation (red = positive, black = negative). The corrected *p* value was adjusted by FDR. $*p < 0.05$; $**p < 0.01$. For graph **(A, B)**, data are presented as the mean ± SEM, and significance was evaluated by an unpaired *t* test with Welch's correction. $*p < 0.05$, $**p < 0.01$.

In the current study, we showed the reduced richness and diversity of gut microbiota in the DM-HL group compared to the DM group, and most ASVs of the gut microbiota belonging to various taxa were almost eliminated by HL, which reflected the antibacterial activity of HL. A study that used HL (Huanglian Decoction) as an agent in stressed mice with ulcers reported similar results (45). Previously, HL exhibited a good therapeutic effect on bacterial infectious diseases in the clinic and exerted a broad spectrum of antibacterial activities, especially against opportunistic pathogens, such as *Pseudomonas*, *Staphylococcus*, and *Salmonella* (41, 46–48) These findings suggest that the reduced diversity of the gut microbiota after HL treatment might be associated with its broad anti-bacterial effect. However, the underlying antibacterial role of HL still needs further investigation.

The BAs (including UDCA, THCA, and DCA) generated by the gut microbiota through various pathways (deconjugation, dihydroxylation, oxidation, and epimerization) (40) increased in the DM-HL group compared to the DM group, which indicated the alteration of microbial BA metabolism. In the current study, a gut microbiota predominated by *Bacteroides* and the *Clostridium innocuum* group was constructed in our DM-HL group, with increases in genes (*cbh*, *bai*) associated with microbial BA metabolism Previously, *Bacteroides* and *Clostridium* spp. were recognized as bile salt hydrolase (BSH)-producing bacteria, contributing to BA metabolism in the gut (49–51). These findings indicated that, in our study, HL treatment altered the composition of secondary BAs, possibly by expanding the capacity of microbial BA metabolism. However, we also noticed that the downstream metabolites of TCDCA, CDCA, and iso-LCA were markedly decreased by HL treatment, which might be explained by the substrate-specific characteristics of BSH (52). Additionally, our data suggested the promotion of hepatic BA synthesis by HL. Specifically, the up-regulation of hepatic BA synthesis genes (*Cyp7a1*, *Cyp27a1*) and the enrichment of conjugated primary BAs (TCA, TCDCA) in the gut were observed in the DM-HL group (Supplementary Figures S8A, B). It has been reported that hepatic BA synthesis can be partially controlled by secondary BAs by regulating FXR (53–55), and the reduction of ileal FXR signal induced by BAs accelerated BA synthesis in mice (56). In addition, CDCA is the most effective ligand for FXR, while UDCA and THCA are characterized as FXR antagonists (5, 57, 58). These findings suggest that secondary BAs in the DM-HL group might promote hepatic BA synthesis by inhibiting FXR. Collectively, our findings indicate that HL treatment affects the composition of the BA pool by modulating gut microbiota.

Close associations were observed between BAs and T2DM-related parameters, suggesting that the altered BA pool in the DM-HL group affected host health. Specifically, UDCA and DCA, which were negatively correlated with obesity, were enriched in the DM-HL group. In previous studies, UDCA and DCA were reported to reduce the uptake of long-chain fatty acids in HFD-fed mice by inhibiting the liver-specific fatty acid transport protein 5 (59). UDCA has also been reported to promote hepatic lipid excretion in feces (60). These mechanisms might explain the improved lipid accumulation in the current study. Moreover, the enrichment of THCA was also observed in the DM-HL group. The reduction of THCA has been identified in the plasma of diabetic patients,

and THCA can stimulate GLP-1 secretion and maintain glucose homeostasis *in vivo* (5, 61). Thereby, our findings suggest that the modified BA pool with increased protective BAs in the DM-HL group might play an important role in T2DM treatment.

In conclusion, HL extracts that are high in various active components can effectively improve impaired glucose tolerance and lipid accumulation in T2DM mice, possibly by altering the structure of the gut microbiota and BA pool. We propose that the beneficial effects of HL on T2DM, at least partly, depend on the gut microbiota. Our study highlights the key role of the HL extract in alleviating T2DM and provides a theoretical basis for the clinical study of using HL in T2DM patients.

## Data availability statement

The datasets presented in this study can be found in online repositories. The names of the repository/repositories and accession number(s) can be found below: https://www.ncbi.nlm.nih.gov/, PRJNA859559.

## Ethics statement

All animal experimental procedures were approved by the Institutional Animal Care and Use Committee (IACUC) of Shanghai Jiao Tong University (No. A2020030).

## Author contributions

BL, TD, and XW prepared the HL extract. YZ and HX conceived the original idea. DL designed the study, conducted experiments and data analysis, and wrote the manuscript. GF performed the animal trial and sample collections and revised the manuscript. YL, HP, and PL participated in the bioinformatics analysis of the gut microbiota and metabolites; CZ designed and supervised the study, and revised the manuscript. All authors contributed to the article and approved the submitted version.

## Funding

This work was supported by the 'Significant New Drug Creation' of China, National Science and Technology Major Project (2017ZX09301031).

## Conflict of interest

The authors declare that the research was conducted in the absence of any commercial or financial relationships that could be construed as a potential conflict of interest.

## Publisher's note



## Supplementary material

The Supplementary Material for this article can be found online at: https://www.frontiersin.org/articles/10.3389/fendo.2023.1120221/full#supplementary-material

## References

1. Khan M, Hashim MJ, King JK, Govender RD, Mustafa H, Al Kaabi J. Epidemiology of type 2 diabetes - global burden of disease and forecasted trends. *J Epidemiol Glob Health* (2020) 10:107–11. doi: 10.2991/jegh.k.191028.001

2. Wu Y, Ding Y, Tanaka Y, Zhang W. Risk factors contributing to type 2 diabetes and recent advances in the treatment and prevention. *Int J Med Sci* (2014) 11:1185–200. doi: 10.7150/ijms.10001

3. Kolb H, Martin S. Environmental/lifestyle factors in the pathogenesis and prevention of type 2 diabetes. *BMC Med* (2017) 15:131. doi: 10.1186/s12916-017-0901-x

4. Ma QT, Li YQ, Li PF, Wang M, Wang JK, Tang ZY, et al. Research progress in the relationship between type 2 diabetes mellitus and intestinal flora. *Biomedicine Pharmacotherapy* (2019) 117:109138. doi: 10.1016/j.biopha.2019.109138

5. Zheng X, Chen T, Jiang R, Zhao A, Wu Q, Kuang J, et al. Hyocholic acid species improve glucose homeostasis through a distinct TGR5 and FXR signaling mechanism. *Cell Metab* (2021) 33 791-803:e797. doi: 10.1016/j.cmet.2020.11.017

6. Jadhav K, Xu Y, Xu Y, Li Y, Xu J, Zhu Y, et al. Reversal of metabolic disorders by pharmacological activation of bile acid receptors TGR5 and FXR. *Mol Metab* (2018) 9:131–40. doi: 10.1016/j.molmet.2018.01.005

7. Wu H, Esteve E, Tremaroli V, Khan MT, Caesar R, Manneras-Holm L, et al. Metformin alters the gut microbiome of individuals with treatment-naive type 2 diabetes, contributing to the therapeutic effects of the drug. *Nat Med* (2017) 23:850–8. doi: 10.1038/nm.4345

8. Zhang X, Fang Z, Zhang C, Xia H, Jie Z, Han X, et al. Effects of acarbose on the gut microbiota of prediabetic patients: A randomized, double-blind, controlled crossover trial. *Diabetes Ther* (2017) 8:293–307. doi: 10.1007/s13300-017-0226-y

9. Zhang F, Wang M, Yang J, Xu Q, Liang C, Chen B, et al. Response of gut microbiota in type 2 diabetes to hypoglycemic agents. *Endocrine* (2019) 66:485–93. doi: 10.1007/s12020-019-02041-5

10. Zhang C, Ma S, Wu J, Luo L, Qiao S, Li R, et al. A specific gut microbiota and metabolomic profiles shifts related to antidiabetic action: The similar and complementary antidiabetic properties of type 3 resistant starch from canna edulis and metformin. *Pharmacol Res* (2020) 159:104985. doi: 10.1016/j.phrs.2020.104985

11. Sun L, Xie C, Wang G, Wu Y, Wu Q, Wang X, et al. Gut microbiota and intestinal FXR mediate the clinical benefits of metformin. *Nat Med* (2018) 24:1919–29. doi: 10.1038/s41591-018-0222-4

12. Li Z, Jiang JD, Kong WJ. Berberine up-regulates hepatic low-density lipoprotein receptor through ras-independent but AMP-activated protein kinase-dependent raf-1 activation. *Biol Pharm Bull* (2014) 37:1766–75. doi: 10.1248/bpb.b14-00412

13. Yu Y, Liu L, Wang X, Liu X, Liu X, Xie L, et al. Modulation of glucagon-like peptide-1 release by berberine: *in vivo* and *in vitro* studies. *Biochem Pharmacol* (2010) 79:1000–6. doi: 10.1016/j.bcp.2009.11.017

14. Lee YS, Kim WS, Kim KH, Yoon MJ, Cho HJ, Shen Y, et al. Berberine, a natural plant product, activates AMP-activated protein kinase with beneficial metabolic effects in diabetic and insulin-resistant states. *Diabetes* (2006) 55:2256–64. doi: 10.2337/db06-0006

15. Hua W, Ding L, Chen Y, Gong B, He J, Xu G. Determination of berberine in human plasma by liquid chromatography-electrospray ionization-mass spectrometry. *J Pharm BioMed Anal* (2007) 44:931–7. doi: 10.1016/j.jpba.2007.03.022

16. Jiang S, Xu J, Qian DW, Shang EX, Liu P, Su SL, et al. Comparative metabolites in plasma and urine of normal and type 2 diabetic rats after oral administration of the traditional Chinese scutellaria-coptis herb couple by ultra performance liquid

chromatography-tandem mass spectrometry. *J Chromatogr B Analyt Technol BioMed Life Sci* (2014) 965:27–32. doi: 10.1016/j.jchromb.2014.05.028

17. Cheng H, Liu J, Tan Y, Feng W, Peng C. Interactions between gut microbiota and berberine, a necessary procedure to understand the mechanisms of berberine. *J Pharm Anal* (2022) 12:541–55. doi: 10.1016/j.jpha.2021.10.003

18. Liu J, Tan Y, Cheng H, Zhang D, Feng W, Peng C. Functions of gut microbiota metabolites, current status and future perspectives. *Aging Dis* (2022) 13:1106–26. doi: 10.14336/AD.2022.0104

19. Habtemariam S. Berberine pharmacology and the gut microbiota: A hidden therapeutic link. *Pharmacol Res* (2020) 155:104722. doi: 10.1016/j.phrs.2020.104722

20. Xu X, Gao Z, Yang F, Yang Y, Chen L, Han L, et al. Antidiabetic effects of gegen qinlian decoction *via* the gut microbiota are attributable to its key ingredient berberine. *Genomics Proteomics Bioinf* (2020) 18:721–36. doi: 10.1016/j.gpb.2019.09.007

21. Fang X, Wu H, Wang X, Lian F, Li M, Miao R, et al. Modulation of gut microbiota and metabolites by berberine in treating mice with disturbances in glucose and lipid metabolism. *Front Pharmacol* (2022) 13:870407. doi: 10.3389/fphar.2022.870407

22. Wang Y, Shou JW, Li XY, Zhao ZX, Fu J, He CY, et al. Berberine-induced bioactive metabolites of the gut microbiota improve energy metabolism. *Metabolism* (2017) 70:72–84. doi: 10.1016/j.metabol.2017.02.003

23. Zhang Y, Gu Y, Ren H, Wang S, Zhong H, Zhao X, et al. Gut microbiome-related effects of berberine and probiotics on type 2 diabetes (the PREMOTE study). *Nat Commun* (2020) 11(1):5015. doi: 10.1038/s41467-020-18414-8

24. Fu Y, Hu BR, Tang Q, Fu Q, Zhang QY, Xiang JZ. Effect of jatrorrhizine, berberine, Huanglian decoction and compound-mimic prescription on blood glucose in mice. *Chin Traditional Herbal Drugs* (2005) 36(4):548-51.

25. Xie W, Gu D, Li J, Cui K, Zhang Y. Effects and action mechanisms of berberine and rhizoma coptidis on gut microbes and obesity in high-fat diet-fed C57BL/6J mice. *PloS One* (2011) 6:e24520. doi: 10.1371/journal.pone.0024520

26. Chen HY, Ye XL, Cui XL, He K, Jin YN, Chen Z, et al. Cytotoxicity and antihyperglycemic effect of minor constituents from rhizoma coptis in HepG2 cells. *Fitoterapia* (2012) 83:67–73. doi: 10.1016/j.fitote.2011.09.014

27. He K, Hu Y, Ma H, Zou Z, Xiao Y, Yang Y, et al. Rhizoma coptidis alkaloids alleviate hyperlipidemia in B6 mice by modulating gut microbiota and bile acid pathways. *Biochim Biophys Acta* (2016) 1862:1696–709. doi: 10.1016/j.bbadis.2016.06.006

28. Wang X, Qu XB, Liu B, Wang X, Song LL, Xu HB. Screening and verification of compatibility proportion of effective components from traditional Chinese medicine of diabetes. *Chin J Exp Traditional Med Formulae.* (2019) 25(21):45-52. doi: 10.13422/j.cnki.syfjx.20192136

29. Kleiner DE, Brunt EM, Van Natta M, Behling C, Contos MJ, Cummings OW, et al. Design and validation of a histological scoring system for nonalcoholic fatty liver disease. *Hepatology* (2005) 41:1313–21. doi: 10.1002/hep.20701

30. Zhang Y, Wan J, Liu S, Hua T, Sun Q. Exercise induced improvements in insulin sensitivity are concurrent with reduced NFE2/miR-432-5p and increased FAM3A. *Life Sci* (2018) 207:23–9. doi: 10.1016/j.lfs.2018.05.040

31. Al-Aqil FA, Monte MJ, Peleteiro-Vigil A, Briz O, Rosales R, Gonzalez R, et al. Interaction of glucocorticoids with FXR/FGF19/FGF21-mediated ileum-liver crosstalk. *Biochim Biophys Acta Mol Basis Dis* (2018) 1864:2927–37. doi: 10.1016/j.bbadis.2018.06.003

32. Ding LL, Yang QL, Zhang EY, Wang YM, Sun SM, Yang YB, et al. Notoginsenoside Ft1 acts as a TGR5 agonist but FXR antagonist to alleviate high fat diet-induced obesity and insulin resistance in mice. *Acta Pharm Sin B* (2021) 11:1541–54. doi: 10.1016/j.apsb.2021.03.038

33. Godon JJ, Zumstein E, Dabert P, Habouzit F, Moletta R. Molecular microbial diversity of an anaerobic digestor as determined by small-subunit rDNA sequence analysis. *Appl Environ Microbiol* (1997) 63:2802–13. doi: 10.1128/Aem.63.7.2802-2813.1997

34. Nadkarni MA, Martin FE, Jacques NA, Hunter N. Determination of bacterial load by real-time PCR using a broad-range (universal) probe and primers set. *Microbiol (Reading)* (2002) 148:257–66. doi: 10.1099/00221287-148-1-257

35. Zhang Q, Wu Y, Wang J, Wu G, Long W, Xue Z, et al. Accelerated dysbiosis of gut microbiota during aggravation of DSS-induced colitis by a butyrate-producing bacterium. *Sci Rep* (2016) 6:27572. doi: 10.1038/srep27572

36. Tettamanti Boshier FA, Srinivasan S, Lopez A, Hoffman NG, Proll S, Fredricks DN, et al. Complementing 16S rRNA gene amplicon sequencing with total bacterial load to infer absolute species concentrations in the vaginal microbiome. *mSystems* (2020) 5(2): e00777-19. doi: 10.1128/mSystems.00777-19

37. Llorens-Rico V, Vieira-Silva S, Goncalves PJ, Falony G, Raes J. Benchmarking microbiome transformations favors experimental quantitative approaches to address compositionality and sampling depth biases. *Nat Commun* (2021) 12(1):3562. doi: 10.1038/s41467-021-23821-6

38. Langille MG, Zaneveld J, Caporaso JG, Mcdonald D, Knights D, Reyes JA, et al. Predictive functional profiling of microbial communities using 16S rRNA marker gene sequences. *Nat Biotechnol* (2013) 31:814–21. doi: 10.1038/nbt.2676

39. Lizcano JM, Alessi DR. The insulin signalling pathway. *Curr Biol* (2002) 12:R236–238. doi: 10.1016/s0960-9822(02)00777-7

40. Guzior DV, Quinn RA. Review: microbial transformations of human bile acids. *Microbiome* (2021) 9:140. doi: 10.1186/s40168-021-01101-1

41. Yan D, Wei L, Xiao XH, Zhou DL, Han YM. Microcalorimetric investigation of effect of berberine alkaloids from coptis chinensis franch on intestinal diagnostic flora growth. *Chin Sci Bull* (2009) 54:369–73. doi: 10.1007/s11434-009-0001-1

42. Chandramohan R, Pari L, Rathinam A, Sheikh BA. Tyrosol, a phenolic compound, ameliorates hyperglycemia by regulating key enzymes of carbohydrate metabolism in streptozotocin induced diabetic rats. *Chem Biol Interact* (2015) 229:44–54. doi: 10.1016/j.cbi.2015.01.026

43. Li X, Wei T, Li J, Yuan Y, Wu M, Chen F, et al. Tyrosol ameliorates the symptoms of obesity, promotes adipose thermogenesis, and modulates the composition of gut microbiota in HFD fed mice. *Mol Nutr Food Res* (2022) 66:e2101015. doi: 10.1002/mnfr.202101015

44. Moriwaki S, Murakami H, Takahashi N, Uemura T, Taketani K, Hoshino S, et al. Yamogenin in fenugreek inhibits lipid accumulation through the suppression of gene expression in fatty acid synthesis in hepatocytes. *Bioscience Biotechnol Biochem* (2014) 78:1231–6. doi: 10.1080/09168451.2014.915736

45. Zhang Q, Guo JJ, Yau YM, Wang YJ, Cheng YB, Tuo X, et al. Effect of huanglian decoction on the intestinal microbiome in stress ulcer (SU) mice. *Evid Based Complement Alternat Med* (2021) 2021:3087270. doi: 10.1155/2021/3087270

46. Feng X, Yan D, Zhao KJ, Luo JY, Ren YS, Kong WJ, et al. Applications of microcalorimetry in the antibacterial activity evaluation of various rhizoma coptidis. *Pharm Biol* (2011) 49:348–53. doi: 10.3109/13880209.2010.523428

47. Jiang ZY, Deng HY, Yu ZJ, Ni JY, Kang SH. The effect of ultrafine process on the dissolution, antibacterial activity, and cytotoxicity of coptidis rhizoma. *Pharmacognosy Res* (2016) 8:71–7. doi: 10.4103/0974-8490.171097

48. Aswathanarayan JB, Vittal RR. Inhibition of biofilm formation and quorum sensing mediated phenotypes by berberine in pseudomonas aeruginosa and salmonella typhimurium. *RSC Adv* (2018) 8:36133–41. doi: 10.1039/c8ra06413j

49. Kawamoto K, Horibe I, Uchida K. Purification and characterization of a new hydrolase for conjugated bile acids, chenodeoxycholyltaurine hydrolase, from bacteroides vulgatus. *J Biochem* (1989) 106:1049–53. doi: 10.1093/oxfordjournals.jbchem.a122962

50. Coleman JP, Hudson LL. Cloning and characterization of a conjugated bile acid hydrolase gene from clostridium perfringens. *Appl Environ Microbiol* (1995) 61:2514–20. doi: 10.1128/aem.61.7.2514-2520.1995

51. Wolf PG, Devendran S, Doden HL, Ly LK, Moore T, Takei H, et al. Berberine alters gut microbial function through modulation of bile acids. *BMC Microbiol* (2021) 21(1):24. doi: 10.1186/s12866-020-02020-1

52. Kim GB, Yi SH, Lee BH. Purification and characterization of three different types of bile salt hydrolases from bifidobacterium strains. *J Dairy Sci* (2004) 87:258–66. doi: 10.3168/jds.S0022-0302(04)73164-1

53. Inagaki T, Choi M, Moschetta A, Peng L, Cummins CL, Mcdonald JG, et al. Fibroblast growth factor 15 functions as an enterohepatic signal to regulate bile acid homeostasis. *Cell Metab* (2005) 2:217–25. doi: 10.1016/j.cmet.2005.09.001

54. Wahlstrom A, Sayin SI, Marschall HU, Backhed F. Intestinal crosstalk between bile acids and microbiota and its impact on host metabolism. *Cell Metab* (2016) 24:41–50. doi: 10.1016/j.cmet.2016.05.005

55. Schneider KM, Albers S, Trautwein C. Role of bile acids in the gut-liver axis. *J Hepatol* (2018) 68:1083–5. doi: 10.1016/j.jhep.2017.11.025

56. Li Y, Tian Y, Cai W, Wang Q, Chang Y, Sun Y, et al. Novel iota-carrageenan tetrasaccharide alleviates liver lipid accumulation *via* the bile acid-FXR-SHP/PXR pathway to regulate cholesterol conversion and fatty acid metabolism in insulin-resistant mice. *J Agric Food Chem* (2021) 69:9813–21. doi: 10.1021/acs.jafc.1c04035

57. Makishima M, Okamoto AY, Repa JJ, Tu H, Learned RM, Luk A, et al. Identification of a nuclear receptor for bile acids. *Science* (1999) 284:1362–5. doi: 10.1126/science.284.5418.1362

58. Mueller M, Thorell A, Claudel T, Jha P, Koefeler H, Lackner C, et al. Ursodeoxycholic acid exerts farnesoid X receptor-antagonistic effects on bile acid and lipid metabolism in morbid obesity. *J Hepatol* (2015) 62:1398–404. doi: 10.1016/j.jhep.2014.12.034

59. Nie B, Park HM, Kazantzis M, Lin M, Henkin A, Ng S, et al. Specific bile acids inhibit hepatic fatty acid uptake in mice. *Hepatology* (2012) 56:1300–10. doi: 10.1002/hep.25797

60. Tsuchida T, Shiraishi M, Ohta T, Sakai K, Ishii S. Ursodeoxycholic acid improves insulin sensitivity and hepatic steatosis by inducing the excretion of hepatic lipids in high-fat diet-fed KK-ay mice. *Metabolism* (2012) 61:944–53. doi: 10.1016/j.metabol.2011.10.023

61. Zheng XJ, Chen TL, Zhao AH, Ning ZC, Kuang JL, Wang SL, et al. Hyocholic acid species as novel biomarkers for metabolic disorders. *Nat Commun* (2021) 12(1):1487. doi: 10.1038/s41467-021-21744-w

frontiers | Frontiers in Endocrinology

TYPE Clinical Trial
PUBLISHED 19 January 2023
DOI 10.3389/fendo.2022.1107071



OPEN ACCESS

EDITED BY
Xinhua Shu,
Glasgow Caledonian University,
United Kingdom

REVIEWED BY
Tianhao Liu,
Affiliated Hospital of Jiangnan University,
China
Kangxiao Guo,
Central South University Forestry and
Technology, China
Haoqing Shao,
Hunan University of Medicine, China

*CORRESPONDENCE
Mingyu Sun
mysun248@hotmail.com

†These authors have contributed equally to this work

SPECIALTY SECTION
This article was submitted to
Gut Endocrinology,
a section of the journal
Frontiers in Endocrinology

RECEIVED 24 November 2022
ACCEPTED 29 December 2022
PUBLISHED 19 January 2023

CITATION
Hui D, Liu L, Azami NLB, Song J, Huang Y, Xu W, Wu C, Xie D, Jiang Y, Bian Y and Sun M (2023) The spleen-strengthening and liver-draining herbal formula treatment of non-alcoholic fatty liver disease by regulation of intestinal flora in clinical trial. *Front. Endocrinol.* 13:1107071. doi: 10.3389/fendo.2022.1107071



# The spleen-strengthening and liver-draining herbal formula treatment of non-alcoholic fatty liver disease by regulation of intestinal flora in clinical trial

Dengcheng Hui[1,2,3†], Lu Liu[1,2,3†], Nisma Lena Bahaji Azami[1,2,3], Jingru Song[4], Yanping Huang[5], Wan Xu[1], Chao Wu[1,2,3], Dong Xie[2], Yulang Jiang[1,2,3], Yanqin Bian[6] and Mingyu Sun[1,2,3*]

[1]Shuguang Hospital Affiliated to Shanghai University of Traditional Chinese Medicine, Shanghai, China, [2]Shanghai University of Traditional Chinese Medicine, Shanghai, China, [3]Institute of Liver Diseases, Key Laboratory of Liver and Kidney Diseases, Shuguang Hospital Affiliated to Shanghai University of Traditional Chinese Medicine, Shanghai, China, [4]Department of Gastroenterology, Hangzhou TCM Hospital Affiliated to Zhejiang Chinese Medical University, Hangzhou, Zhejiang, China, [5]Department of Good Clinical Practice Office, Tongren Hospital, Shanghai Jiao Tong University School of Medicine, Shanghai, China, [6]Arthritis Institute of Guanghua Hospital, Shanghai University of Traditional Chinese Medicine, Shanghai, China

**Objective:** As a metabolic disease, one important feature of non-alcoholic fatty liver disease (NAFLD) is the disturbance of the intestinal flora. Spleen-strengthening and liver-draining formula (SLF) is a formula formed according to the theory of "One Qi Circulation" (Qing Dynasty, 1749) of Traditional Chinese Medicine (TCM), which has shown significant therapeutic effect in patients with NAFLD in a preliminary clinical observation. In this study, we aim to explore the mechanism of SLF against NAFLD, especially its effect on glucolipid metabolism, from the perspective of intestinal flora.

**Methods:** A prospective, randomized, controlled clinical study was designed to observe the efficacy and safety of SLF in the treatment of NAFLD. The study participants were randomly and evenly divided into control group and treatment group (SLF group). The control group made lifestyle adjustments, while the SLF group was treated with SLF on top of the control group. Both groups were participated in the study for 12 consecutive weeks. Furthermore, the feces of the two groups were collected before and after treatment. The intestinal flora of each group and healthy control (HC) were detected utilizing 16S rRNA gene sequencing.

**Results:** Compared with the control group, the SLF group showed significant improvements in liver function, controlled attenuation parameter (CAP), and liver stiffness measurement (LSM), meanwhile, patients had significantly lower lipid and homeostasis model assessment of insulin resistance (HOMA-IR) with better security. Intestinal flora 16S rRNA gene sequencing results indicated reduced flora diversity and altered species abundance in patients with NAFLD. At the phylum level, *Desulfobacterota* levels were reduced. Although *Firmicutes* and *Bacteroidetes* did not differ significantly between HC and NAFLD, when grouped by alanine transaminase (ALT) and aspartate transaminase (AST) levels in NAFLD, *Firmicutes* levels were significantly higher in patients with ALT or AST

abnormalities, while *Bacteroidetes* was significantly lower. Clinical correlation analysis showed that *Firmicutes* positively correlated with gender, age, ALT, AST, LSM, and Fibroscan-AST (FAST) score, while the opposite was true for *Bacteroidetes*. At the genus level, the levels of *Alistipes*, *Bilophila*, *Butyricimonas*, *Coprococcus*, *Lachnospiraceae_NK4A136* group *Phascolarctobacterium*, *Ruminococcus*, *UCG-002*, and *UCG-003* were reduced, whereas abundance of *Tyzzerella* increased. There was no statistically significant difference in *Firmicutes* and *Bacteroidota* levels in the SLF group before and after treatment, but both bacteria tended to retrace. At the genus level, *Coprococcus* (*Lachnospiraceae* family), *Lachnospiraceae_NK4A136 group* (*Lachnospiraceae* family), and *Ruminococcus* (*Ruminococcaceae* family) were significantly higher in the SLF group after treatment, and there was also a tendency for *Bilophila* (*Desulfovibrionaceae* family) to be back-regulated toward HC.

**Conclusions:** SLF can improve liver function and glucolipid metabolism in patients with NAFLD and lower down liver fat content to some extent. SLF could be carried out by regulating the disturbance of intestinal flora, especially *Coprococcus*, *Lachnospiraceae_NK4A136* group, and *Ruminococcus* genus.

KEYWORDS

**non-alcoholic fatty liver disease, traditional Chinese medicine, spleen-strengthening and liver-draining formula, intestinal flora, glucolipid metabolism**

# Introduction

Non-alcoholic fatty liver disease (NAFLD), is common disease characterized by steatosis in more than 5% of hepatocytes with no excessive alcohol consumption, and is a form of liver reaction to a metabolic syndrome (1). The incidence of NAFLD in adults ranges from 20 to 30% (2), which is expected to continue to rise because of the ongoing obesity epidemic that begins in childhood, the increase in diabetes, as well as other factors in recent years (3). Non-alcoholic steatohepatitis (NASH) is the further stage of non-alcoholic fatty liver, accompanied by liver inflammation and hepatocellular ballooning, which may further develop into liver cirrhosis and hepatocellular carcinoma with a high probability (4). There are no specific therapeutic drugs for NAFLD approved by the Food and Drug Administration at present, so the investigation of effective therapeutics is warranted.

In recent years, Traditional Chinese Medicine (TCM) has been favored by a growing number of patients because of its good efficacy with few side effects. There is a promising development and application prospect in the prevention and treatment of NAFLD with TCM, and definite curative clinical efficacy has been achieved. Spleen-strengthening and liver-draining formula (SLF) is a formula formed according to the theory of "One Qi Circulation" of TCM, which originated in the Qing Dynasty (in 1749). SLF is composed of Radix Bupleuri (Chaihu) 9g, Paeoniae Radix Alba (Baishao) 10g, Radix glehniae (Beishashen) 15g, Atractylodis Macrocephalae Rhizoma (Baizhu) 10g, Poria cocos (Fuling) 10g, Citrus Reticulata (Chenpi) 9g, Radix Glycyrrhizae preparate (Gancao) 6g, Sedum sarmentosum (Chuipencao) 15g, Carbonized hawthorn (Shanzhatan) 9g, Salvia miltiorrhiza (Danshen) 15g. In a preliminary clinical observation, SLF showed significant therapeutic effects in patients with NAFLD, including their levels of liver function, blood glucose, and lipids, as well as TCM symptoms.

Recent studies have shown that the imbalance of intestinal flora was closely related to metabolic diseases such as NAFLD, diabetes, and obesity (4). Dysregulation of the intestinal flora is a characteristic of NAFLD, and the signatures of intestinal flora correlate with the severity of the disease by changing bacterial metabolites (4). Furthermore, accumulating evidence suggests that the gut-liver axis is pivotal in NAFLD, especially its the progression to more advanced diseases (5). Consequently, it has been extensively studied for the treatment of this disease by regulating intestinal flora, which has become one of the research focuses in this field.

In this study, we observed the clinical therapeutic result of SLF based on a prospective, randomized, controlled clinical study, and the effect of SLF on intestinal flora of NAFLD was analyzed by 16S rRNA gene sequencing, to further clarify the mechanism of SLF in the treatment of NAFLD.

# Material and methods

## Ethical approval

The study was conducted in conformity with the guidelines set out in the declaration of Helsinki. The study protocol and informed consent were approved by the Institutional Review Board of Shuguang Hospital Affiliated to Shanghai University of Traditional

Chinese Medicine (Ethics No. 2020-863-72-01). All the patients who agreed to participate in the trial signed informed consent forms before the trial, and the participants could withdraw from the study at any time freely.

## Study design and participants

This study was designed as a randomized, controlled trial. Participants were recruited from Shuguang Hospital Affiliated to the Shanghai University of Traditional Chinese Medicine from September 2020 to September 2021 who meet the diagnostic of NAFLD. The diagnostic criteria are as follows: (1) No history of alcohol consumption or consumption of less than 30 g of alcohol per day in men (less than 20 g per day in women). (2) Except for certain diseases that can lead to NAFLD including Hepatitis B and C virus, autoimmune liver disease, drug-induced liver disease, genetic metabolic disease, etc. (3) Imaging features of the liver conform with the diagnostic criteria for diffuse fatty liver disease (6).

Eligible patients were between 18 and 70 years old, consistent with the diagnosis of NAFLD; ALT, AST and GGT<5×upper limit of normal (ULN); BMI ≤ 30kg/$m^2$; Disease duration≥6 months; Agreed to participate in the trial and sign the informed consent form. Patients excluded if (1) they had liver cirrhosis and other specific diseases which can lead to the fatty liver such as alcoholic liver disease, viral hepatitis, drug-induced liver disease, Wilson's disease and autoimmune liver disease, etc.; (2) suffered from other serious diseases including malignant tumors, cardiopulmonary diseases, kidney failure and so on; (3) had a history of neurological disease or mental illness; had taken or were required to continuously take lipid-lowering and hepatoprotective drugs within 30 days before enrollment in the trial; (4) were pregnant or nursing, or were planning to get pregnant during the study period; (5) were allergic to the relevant drugs used in the clinic study; (6) or were participating in other clinical trials.

## Interventions description

A screening test had to be conducted for all patients who meet the inclusion criteria during the screening period in clinic. It included the general status of patients, symptoms, and signs associated with the disease, and laboratory detection, including the following: liver function, HOMA-IR, hemorrheologic, FibroTouch, and other examinations. The control group was treated by lifestyle modifications, including diet and exercise. Here, brisk walking was recommended to the patients in this group, and the exercise time had to be ≥150 min per week (7). At the same time, patients had to manage their dietby following a calorie-restricted diet. Patients were to consume, 25kcal/kg/day and reduce their intake of foods and drinks containing fructose (8). On the other hand, the SLF group received SLF formula (use water to decoct twice, filtered liquid after together, simmer to 200mL), twice a day (100mL each time). Besides, diet and exercise which were taken as basic treatment were the same as control group. The intervention was to last for 12 weeks, and we conducted outpatient follow-up visits every 2 weeks during this period.

## Outcomes evaluation

The outcomes included liver function, hepatic fat, blood glucose and lipids, and HOMA-IR. In addition, we recorded the compliance and adverse events of participants, and monitored participants' health status through blood and urine tests, including kidney function checks and electrocardiogram.

## Stool sample collection

Stool samples were collected from all patients who were recruited with genetic testing sample collectors before and after treatment. Samples were collected only once from HC. All patients were required not to take antibiotics or probiotic preparations in the two weeks preceding the study, and they had to stop eating after 8 PM, before the collection of specimens. They then kept specimens until the next morning in a designated area in the hospital. After collection, specimens were stored at -80°C immediately until further processing. And the stool samples of 11 patients in the SLF group and the control group were randomly selected for subsequent intestinal flora sequencing.

## 16S rRNA gene sequencing analysis

When the raw sequencing data were completed, FastQC was used to check the length and quality of sequencing data control, and errors and low-quality sequences was removed simultaneously. After that, DADA2 (9) was used to generate a variable error model trained on sequencing data for this problem to correct errors and incorporate sequences into amplified sequence variants (ASVs). After quality control and denoising, the feature table and representative sequence were obtained. In this study, QIIME2 (10), which is most widely used in the microbiome, were used to process data as in 16S rRNA gene sequencing analysis. And PICRUSt2 (11) was used to predict functional abundance based on the marker gene sequences. The 16S rRNA gene sequencing was completed with the assistance of Liebing Biotechnology Co., LTD. (Shanghai, China).

## Statistical analysis

All data were statistically analyzed using Graphpad Prism 9.4.0 and R 4.2.1. Measurement data followed a normal distribution, with mean ± standard deviation ($\bar{x} \pm s$), and don't follow adopted median (top and bottom quartile). Two independent samples t-test (obeying normal distribution) or Mann-Whitney test were used for comparison among groups; paired t-test (following a normal distribution) or Wilcoxon rank sum test was used for intra-group comparison. Frequency and chi-square test were used for enumeration data. Hierarchical data were expressed by frequency, and comparison between groups was performed through the Mann-Whitney test. The abundance of intestinal flora was expressed by total-sum normalization (TSS). Results were statistically significant when $P<0.05$.

# Results

## Baseline comparison

After strict inclusion and exclusion criteria, a total of 88 patients were enrolled in this study, with 44 in each group, which made up the intent-to-treat population. In the control group 4 patients were lost to follow up and 2 patients in the treatment group. The final 82 patients (40 in the control group and 42 in the SLF group) were included in the efficacy and safety evaluation, which constituted the per-protocol population (Figure 1). There were no statistical differences between the two groups in terms of gender ($P$=0.58), age ($P$=0.09), Classification of fatty liver ($P$=0.92), body mass index (BMI) ($P$=0.54), and onset time ($P$=0.75), which indicated that follow-up comparisons could be conducted (Table 1).

## SLF had a clinical efficacy on improving the liver function and FibroTouch, as well as relieving symptoms of fatigue

Liver function was tested for normality in both groups, and ALT, AST, and gamma glutamyl transpeptidase (GGT) did not conform to a normal distribution ($P$<0.05). The differences in ALT, AST, and GGT between the two groups before treatment were not statistically significant and could be compared. According to the results after treatment, differences in the group were performed first, ALT ($P$=0.004) and GGT ($P$<0.001) in the control group were statistically different than before receiving treatment, but not in AST ($P$=0.233). ALT ($P$<0.001), AST ($P$=0.020), and GGT ($P$<0.001) in the SLF group also decreased significantly. Next, when comparing between groups, there was a statistical difference in AST ($P$=0.034), but not in ALT ($P$=0.663) and GGT ($P$=0.136) in the SLF group compared with the control group. (Figure 2A-C).

We also compared FibroTouch before and after treatment in both groups. There was no statistical difference in CAP between the two groups pre-treatment ($P$=0.911), but a statistical difference was shown in both groups after treatment when compared to pre-treatment ($P$=0.027 in the control group and $P$<0.001 in the SLF group). However, when the control group and SLF group were compared, there was a statistically significant difference in CAP after treatment ($P$=0.002). Similarly, SLF could improve LSM to a certain extent statistically ($P$=0.001) (Figure 2D-E).

In our clinical practice, we found that patients with NAFLD are often accompanied with fatigue symptoms. Therefore, we use the fatigue scale-14 (FS-14) to assess the fatigue symptoms of patients, which includes physical fatigue and mental fatigue (12). We eventually found that SLF improved the physical fatigue ($P$<0.001) as well as the total score ($P$<0.001) of the patients. Although no significant change was found in mental fatigue in the SLF group ($P$=0.059), there was a significant difference compared with the control group after treatment ($P$=0.009) (Figure 2F).

## SLF could improve glycolipid metabolism with a good security

In order to investigate the effects of SLF on blood lipids, we conducted a statistical analysis of total cholesterol (TC) and

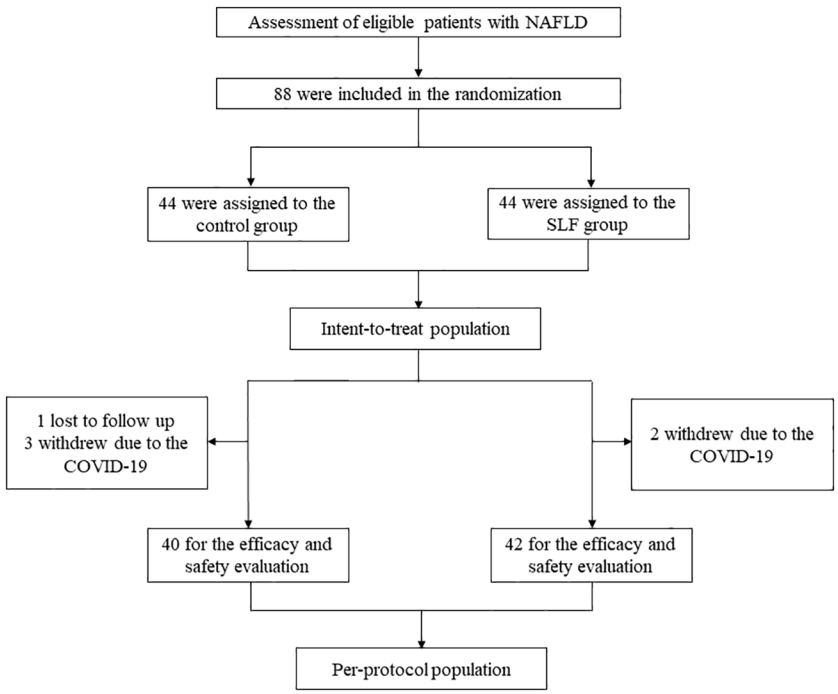


FIGURE 1
Flow chart of the study. A total of 88 NAFLD patients who were assessed to be eligible were made up of the intent-to-treat population. These patients were randomly divided into the control group and the SLF group, and 1 patient was lost to follow up and 3 patients withdrew due to COVID-19 in the control group, whereas 2 patients in the SLF group. The remaining 82 patients made up the per-protocol population.

TABLE 1 Baseline of the NAFLD in the control group and SLF group.

| Index | Group | Control n=40 | SLF n=42 | $\chi 2/Z$ | *P* |
|---|---|---|---|---|---|
| Sex | Male | 28 | 27 | 0.30 | 0.58 |
| | Female | 12 | 15 | | |
| Age | 18-39 | 22 | 15 | -1.71 | 0.09 |
| | 40-59 | 15 | 22 | | |
| | ≥60 | 3 | 5 | | |
| Classification of Fatty liver | Mild | 13 | 12 | -0.11 | 0.92 |
| | Moderate | 16 | 21 | | |
| | Severe | 11 | 9 | | |
| BMI(kg/m$^2$) | ≤23.9 | 10 | 11 | -0.61 | 0.54 |
| | 24-27.9 | 19 | 23 | | |
| | ≥28 | 11 | 8 | | |
| Onset time(Years) | ≤1 | 7 | 9 | -0.32 | 0.75 |
| | 1-5 | 19 | 16 | | |
| | 5-10 | 11 | 11 | | |
| | >10 | 3 | 6 | | |

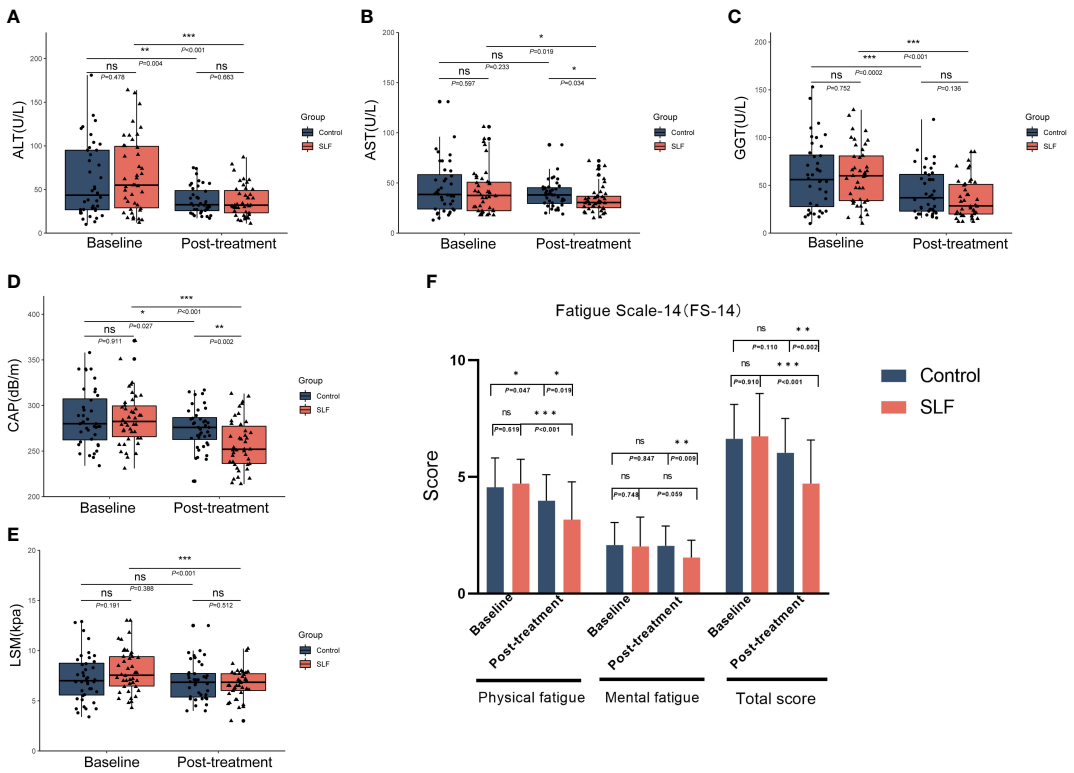


FIGURE 2
SLF had a clinical efficacy on improving the liver function and FibroTouch, as well as relieving symptoms of fatigue. ALT, AST, GGT, CAP, LSM and FS-14 was compared in the two groups to evaluate the efficacy of SLF in liver function and FibroTouch, as well as the symptoms of fatigue. **(A)** Comparison of ALT in the control group and SLF group. **(B)** Comparison of AST in the control group and SLF group. **(C)** Comparison of GGT in the control group and SLF group. **(D)** Comparison of CAP in the control group and SLF group. **(E)** Comparison of LSM in the control group and SLF group. **(F)** Comparison of FS-14 in the control group and SLF group. ALT, Alanine transaminase; AST, Aspartate aminotransferase; GGT, Gamma glutamyl transpeptidase; CAP, Controlled attenuation parameter; LSM, Liver stiffness measurement; FS-14, Fatigue scale-14. ns, no significance. **P* < 0.05, ***P* < 0.01 and ****P* < 0.001.

triglyceride (TG) of the two groups. After treatment in the control group, TC ($P$=0.418) and TG ($P$=0.877) were not statistically different than baseline. While in the SLF group, TC ($P$=0.006) and TG ($P$=0.011) were significantly lowered (Figure 3B, C), but low-density lipoprotein (LDL) ($P$=0.147), high density lipoprotein (HDL) ($P$=0.320), and free fatty acids (FFA) ($P$=0.060) were not statistically different than before treatment.

IR is closely related to the development of NAFLD, and we compared the correlation between HOMA-IR and CAP and found that they had a positive correlation (r=0.46 in the control group and r=0.32 in the SLF group) (Figure 3A). Patients' fasting plasma glucose (FPG) and fasting insulin (FINS), which were used to calculate HOMA-IR, were measured before and after enrollment in the group. The FPG was not statistically different between the two groups before treatment. When comparing within groups, there was no statistical difference in FPG ($P$=0.753) in the control group compared to baseline, whereas a statistical difference was shown in the SLF group ($P$=0.002) (Figure 3D). The patients' HOMA-IR was calculated by using FPG and FINS, and the ability of SLF to improve IR was evaluated by comparing HOMA-IR between the two groups. Surprisingly, HOMA-IR had improved in the SLF group ($P$= 0.004) (Figure 3E). We also compared the body mass index (BMI) of patients in the two groups, and a statistically significant difference was observed in the SLF group ($P$=0.004) (Figure 3F).

We compared the safety indicators between the control group and SLF group, and found that the white blood cell (WBC), red blood cell (RBC), platelet (PLT), neutrophil granulocyte (GRA), hemoglobin (Hb), urea nitrogen (BUN), creatinine (Cr) and glomerular filtration rate (GFR) within groups had no statistically significant difference ($P$>0.05), which indicated that the SLF has a good security (Table 2).

## Reduced species diversity and altered intestinal flora abundance were observed in NAFLD

We randomly selected 11 patients, each from the control group and SLF group, and stool specimens were collected from these patients before and after treatment and sent for examination. A total of 53 stool samples (44 NAFLD and 9 HC) were detected utilizing 16S rRNA gene sequencing to analyze the changes of intestinal flora for the mechanism of the potential therapeutic effect of NAFLD by SLF. Alpha diversity was used to observe the diversity of the flora between the HC and NAFLD. We found that there were significant differences in chao1 ($P$=0.0085), Shannon entropy ($P$=0.02), observed features ($P$=0.0065) and faith_pd ($P$=0.009), which indicated reduced species diversity in NAFLD (Figures 4A-D). Unfortunately, differences in beta diversity between the HC and NAFLD were not observed (Figure S1A).

We then compared the abundance percentages of HC and NAFLD groups at the phylum to genus levels, and found that there were varying degrees of alterations in each level (Figure 4E, 5A, Figure S1B-D). Differentially abundant taxa were observed in Figure S2, which were analyzed by linear discriminant analysis effect size (LEfSe). At the phylum level, *Firmicutes*, *Bacteroidetes*, *Actinobacteriota*, *Desulfobacterota*, and *Proteobacteria* were compared to observe the difference between the two groups. The results showed that *Desulfobacterota* was significantly lower in NAFLD patients when compared with HC ($P$=0.044) (Figure 4F). In contrast, there were no significant differences in the other phyla for the time being (Figure 4G).

At the genus level, the levels of *Alistipes*, *Bilophila*, *Butyricimonas*, *Coprococcus*, *Erysipelotrichaceae_UCG-003*, *Lachnospiraceae*

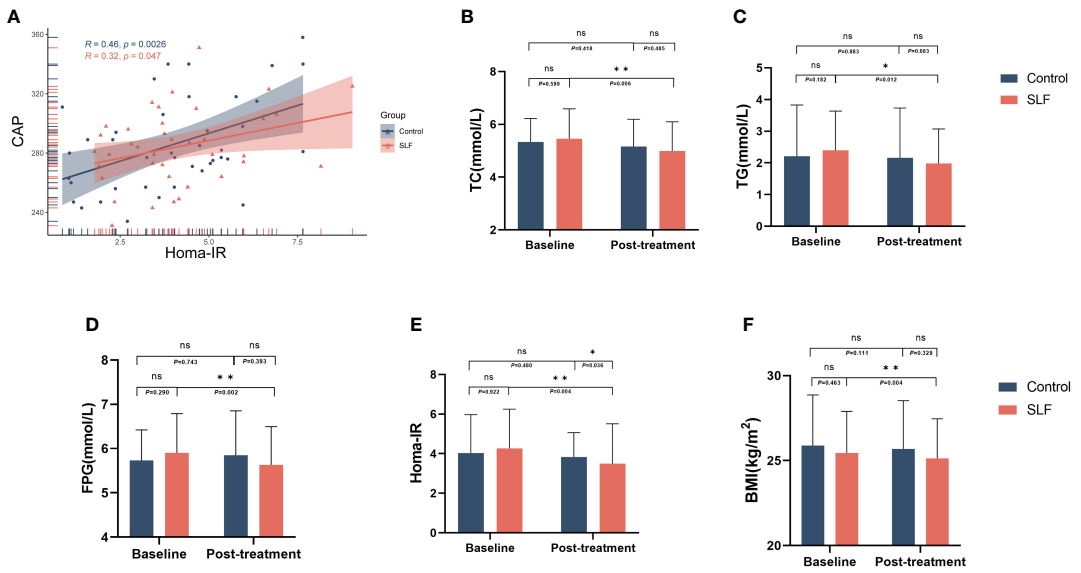


FIGURE 3
SLF could improve glycolipid metabolism. TC, TG, FPG, HOMA-IR, and BMI were compared to evaluate the efficacy of SLF on metabolism, especially glycolipid metabolism. **(A)** Correlation of HOMA-IR and CAP. **(B)** Comparison of TC in the control group and SLF group. **(C)** Comparison of TG in the control group and SLF group. **(D)** Comparison of FPG in the control group and SLF group. **(E)** Comparison of HOMA-IR in the control group and SLF group. **(F)** Comparison of BMI in the control group and SLF group. TC, Total cholesterol; TG, Triglyceride; FPG, Fasting blood glucose; HOMA-IR, Homeostasis model assessment of insulin resistance; BMI, Body mass index. ns, no significance. *$P$ < 0.05 and **$P$ < 0.01.

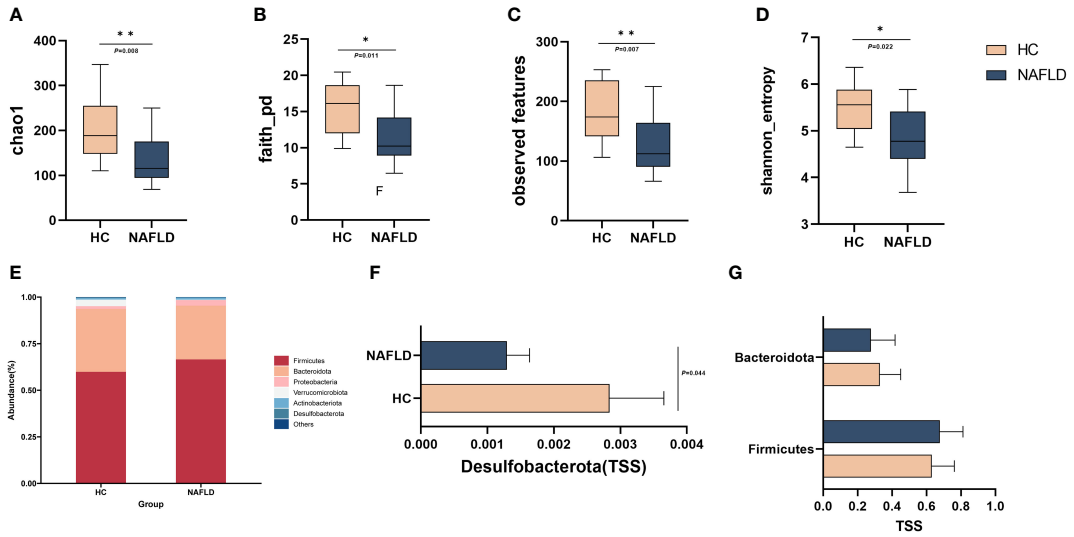


FIGURE 4
Reduced species diversity and altered intestinal flora abundance were observed in NAFLD. **(A-D)** Comparison of intestinal flora alpha diversity in HC and NAFLD. **(E)**The abundance percentages of HC and NAFLD groups at the phylum level. **(F)** Comparison of the abundance of *Desulfobacterota* in the phylum level. **(G)** Comparison of the abundance of *Firmicutes* and *Bacteroidetes* in the phylum level. TSS, Total-sum normalization. *$P < 0.05$ and **$P < 0.01$.

*NK4A136* group, *Phascolarctobacterium*, *Ruminococcus* and *UCG-002* were reduced, whereas the abundance of *Tyzzerella* increased (Figure 5C-L). The heatmap showed the difference in the genus level between the two groups, indicating that NAFLD may be associated with changes in the abundance of these intestinal flora (Figure 5B).

## Intestinal flora correlated with clinical indicators of NAFLD, and SLF might play a role in regulating *Firmicutes* and *Bacteroidetes*

To further investigate whether intestinal flora affected the severity of NAFLD, we investigated the correlation between *Firmicutes*, *Bacteroidetes*, *Actinobacteriota*, *Desulfobacterota* and *Proteobacteria* bacteria and FibroTouch, lipids, glucose, gender, age, liver function and Fibroscan-AST (FAST) score(a novel diagnostic signature in NAFLD) (13). Clinical correlation analysis indicated that *Firmicutes* positively correlated with gender, age, ALT, AST, LSM, and FAST score, while the opposite was true for *Bacteroidetes* (Figure 6A). When grouped by ALT and AST levels, we found that patients with abnormal ALT or AST had higher level of *Firmicutes* phylum and lower level of *Bacteroidetes* (Figures 6B, C), suggesting that the abundance of *Firmicutes* and *Bacteroidetes* may be related to the severity of the disease.

Our clinical trial results showed that SLF ameliorated the condition of NAFLD patients. Whether SLF played a therapeutic role of altering the disturbance of the intestinal flora was still unclear. Consequently, we observed the changes in intestinal flora before and after treatment. Surprisingly, we found that SLF may regulate *Firmicutes* and *Bacteroidetes* levels. Although compared with pre-treatment, *Firmicutes* and *Bacteroidetes* levels in the SLF group were not a statistically significant difference, but they both tended to retrace (Figures 6D, E), and the ratio of *Firmicutes* and *Bacteroidetes* was significantly reduced in the SLF group ($P$=0.004) (Figure 6F).

## SLF exerted its effect by regulating the disturbance of specific intestinal flora genera

At the genus level, some of the intestinal flora abundances altered. In our study, we found *Coprococcus* (*Lachnospiraceae* family), *Lachnospiraceae_NK4A136 group* (*Lachnospiraceae* family), and *Ruminococcus* (*Ruminococcaceae* family) were significantly higher in the SLF group after treatment, and there was also a tendency for *Bilophila* (*Desulfovibrionaceae* family) to be back-regulated toward HC (Figures 7A-D). In addition, at the genus level, SLF could also enhance the level of *Butyricicoccus* and *Blautia*, implying that SLF relieved the symptoms of patients with NAFLD by regulating the disturbance of intestinal flora.

We applied PICRUSt2 to predict the metabolic function of intestinal flora. Metacyc pathway enrichment analysis showed enhanced super pathway of polyamine biosynthesis II ($P$=0.021), peptidoglycan recycling I ($P$=0.035), polyisoprenoid biosynthesis ($P$=0.037), D-fructuronate degradation ($P$=0.041), 4-deoxy-L-threo-hex-4-enopyranuronate degradation ($P$=0.045), L-rhamnose degradation I ($P$=0.048) and β-(1,4)-mannan degradation ($P$=0.049) after treatment, whereas chorismate biosynthesis I ($P$=0.040) and super pathway of aromatic amino acid biosynthesis ($P$=0.040) decreased (Figure 7E).

# Discussion

NAFLD is often accompanied with disorders of glucolipid metabolism (14–16), which may be the most common initial

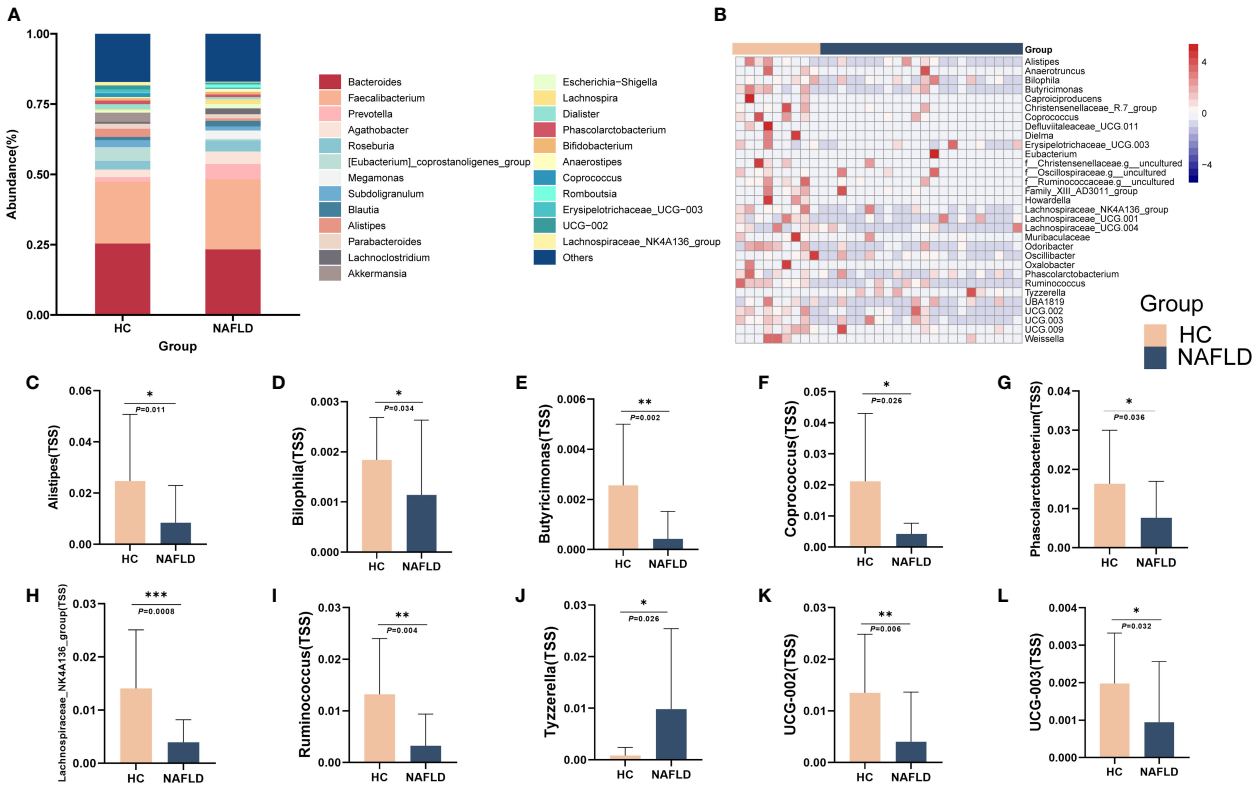


FIGURE 5
Altered intestinal flora abundance at genus level was observed in NAFLD. **(A)** The abundance percentages of HC and NAFLD groups at the genus level. **(B)** The heatmap of some of the intestinal flora genera with differences between HC and NAFLD. **(C-L)** Comparison of *Alistipes*, *Bilophila*, *Butyricimonas*, *Coprococcus*, *Erysipelotrichaceae_UCG-003*, *Lachnospiraceae NK4A136 group*, *Phascolarctobacterium*, *Ruminococcus*, *Tyzzerell* and *UCG-002* in genus level. TSS, Total-sum normalization. *$P < 0.05$, **$P < 0.01$ and ***$P < 0.001$.

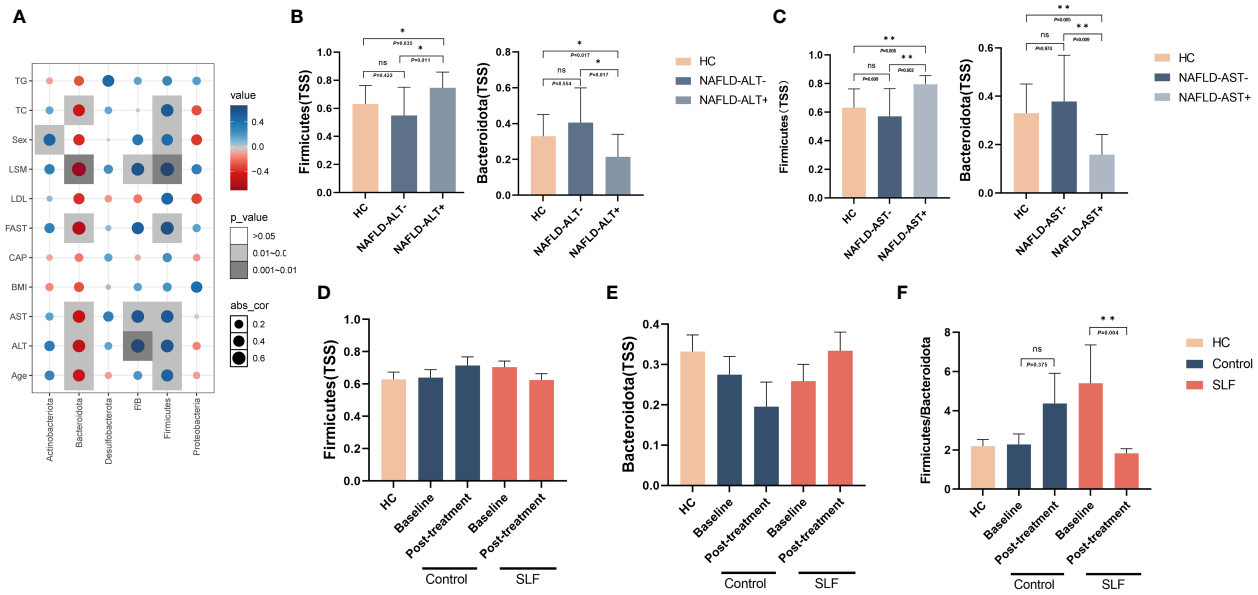


FIGURE 6
Intestinal flora were correlated with clinical indicators of NAFLD, and SLF might play a role in regulating *Firmicutes* and *Bacteroidetes*. **(A)** Correlation analysis between *Firmicutes*, *Bacteroidetes*, *Actinobacteriota*, *Desulfobacterota*, *Proteobacteria* and F/B with FibroTouch, lipids, glucose, gender, age, liver function and FAST score. **(B)** Comparison of *Firmicutes* and *Bacteroidetes* levels by ALT subgroup. **(C)** Comparison of *Firmicutes* and *Bacteroidetes* levels by AST subgroup. **(D)** Changes in *Firmicutes* levels in the two groups before and after treatment. **(E)** Changes in *Bacteroidetes* levels in the two groups before and after treatment. **(F)** Changes in F/B in the two groups before and after treatment. F/B: The ratio of *Firmicutes* and *Bacteroidetes*. TSS, Total-sum normalization. ns, no significance. *$P < 0.05$ and **$P < 0.01$.

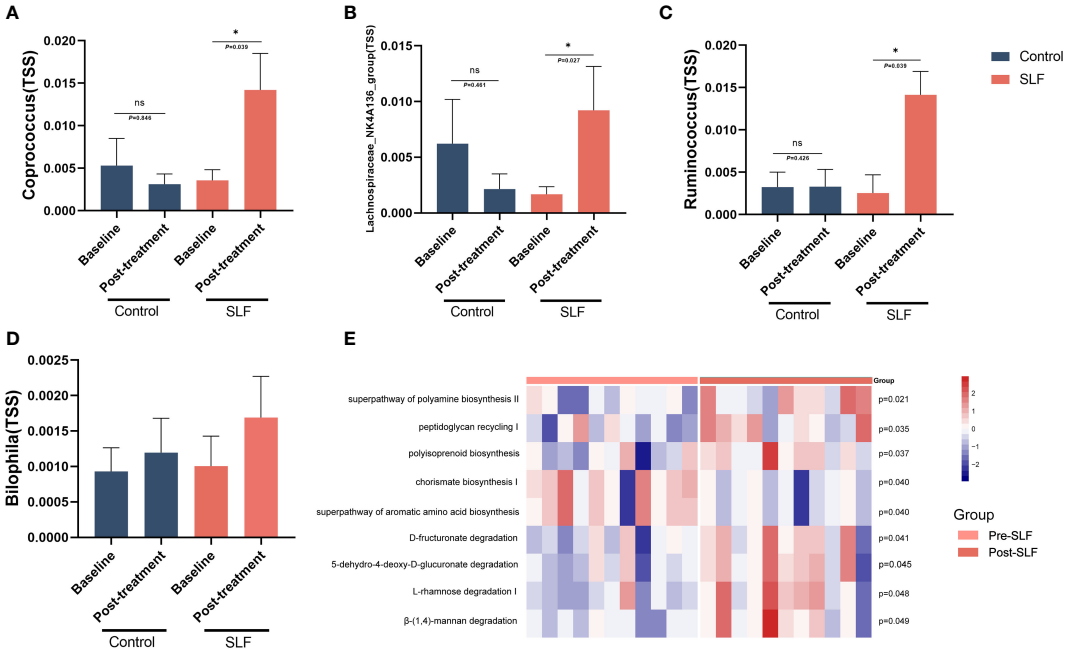


FIGURE 7
SLF exerted its effect by regulating the disturbance of specific intestinal flora genera. **(A)** Comparison of the level of *Coprococcus* genus in control and SLF group. **(B)** Comparison of the level of *Lachnospiraceae_NK4A136 group* genus in control and SLF group. **(C)** Comparison of the level of *Ruminococcus* genus in control and SLF group. **(D)** Comparison of the level of *Bilophila* genus in control and SLF group. **(E)** The heatmap of differential metabolic pathways of intestinal flora between pre-SLF and post-SLF. TSS: Total-sum normalization. *$P < 0.05$.

predisposing factors for the development of NAFLD (16). IR, an important feature of NAFLD, is present in all stages of NAFLD development. Circulating insulin and glucose promotes *de novo* lipogenesis (DNL) through activation of sterol regulating element binding protein 1c (SREBP1c) and the carbohydrate response element binding protein (ChREBP) (17, 18). It can promote the prevention and treatment of NAFLD through regulating hepatocyte glucolipid metabolism (19). In the early stages of NAFLD, restoration of metabolic disorders through herbal discriminatory treatment may inhibit the development of NAFLD. TCM, as a major part of comprehensive treatment, plays a key role in the treatment of NAFLD. SLF is a formula formed based on the traditional theory of "One Qi Circulation", which has the function of strengthening the spleen, resolving dampness and draining the liver to relieve depression. In our study, SLF has a definitive efficacy in improving liver function and glucolipid metabolism of NAFLD, as well as relieving the symptoms of fatigue, which may become an adjuvant therapy in the clinical treatment of NAFLD patients.

The study of intestinal flora has become a hot spot in the study of metabolic diseases and microorganisms has grown rapidly in the past few decades. The intestinal flora participates in the absorption and metabolism of nutrients (including the metabolism of carbohydrates, lipids, and amino acids) in the human body, which plays a strong part in maintaining fitness (20). It has been proved that intestinal flora could influence the microbiota-gut-liver axis to regulate intestinal metabolism (20). Increasing evidence indicates that there are multiple links between intestinal flora and hepatic steatosis: (1) Appetite signal of the host is influenced by it; (2) It can also increase energy extraction from the intestine; (3) Changes in the metabolism of bile acids, which affect the fat and lipid vitamins obtained in the intestine; (4) Modulation of choline metabolism; (5) Promotion of inflammation in host organisms; (6) Bowel bacterial overgrowth and increased intestinal permeability will contribute to bacteria translate into the systemic circulation and endotoxemia (21–24). Furthermore, study found that alterations in the dominant intestinal flora and the abundance and diversity of microbial composition decreased in NAFLD patients (25). Compared with healthy people, the levels of *Firmicutes* and *Proteobacteria* in the gut of NAFLD patients were significantly increased (25, 26).In addition, research shows that intestinal flora plays a vital role in disorders of glucolipid metabolism. The individuals with glucolipid metabolic disorders are always accompanied by intestinal flora disorders and decreased diversity compared to normal individuals (27). In recent years, it has been found that the disorder of intestinal flora may be one of the main causes of the disorder of glucolipid metabolic (28). Therefore, it is considered as a potential therapeutic target for the prevention and treatment of NAFLD and disorders of glycolipid metabolism by regulating the intestinal flora.

As a consequence, we speculate there is a link between abnormal intestinal flora and NAFLD. With the increased understanding of the "gut-liver axis" and the popularity of fecal amplicon sequencing, the gut microbiome seems to occupy an undisputed position in the pathogenesis of NAFLD. Similar to our study, the diversity and abundance of intestinal flora in NAFLD have been shown to change to varying degrees in both animal and human studies (29–31). Therefore, it may be helpful for the prevention and treatment of NAFLD by means of adjusting the intestinal microecology, restoring the normal interaction between "intestinal flora and host", alleviating

TABLE 2 Comparison of safety indicators between the control group and SLF group.

| Index | Group | Baseline | Post-treatment | *P* |
|---|---|---|---|---|
| WBC($\times10^9$/L) | Control | 5.98 ± 1.08 | 5.86 ± 1.44 | 0.643 |
| | SLF | 6.12 ± 1.23 | 6.20 ± 1.46 | 0.792 |
| RBC($\times10^{12}$/L) | Control | 4.98 ± 0.48 | 5.12 ± 0.56 | 0.202 |
| | SLF | 4.99 ± 0.50 | 5.00 ± 0.67 | 0.884 |
| PLT($\times10^9$/L) | Control | 227.68 ± 53.22 | 247.34 ± 53.05 | 0.089 |
| | SLF | 227.90 ± 50.62 | 242.93 ± 62.91 | 0.231 |
| GRA(%) | Control | 55.84 ± 8.90 | 53.62 ± 7.61 | 0.164 |
| | SLF | 55.71 ± 7.12 | 54.12 ± 6.66 | 0.246 |
| Hb(g/L) | Control | 149.12 ± 15.63 | 152.67 ± 13.07 | 0.247 |
| | SLF | 152.63 ± 17.08 | 153.41 ± 16.11 | 0.820 |
| BUN(mmol/L) | Control | 5.04 ± 1.05 | 5.30 ± 1.23 | 0.260 |
| | SLF | 5.04 ± 1.00 | 5.48 ± 1.36 | 0.069 |
| Cr(umol/L) | Control | 72.75 ± 15.91 | 68.78 ± 14.07 | 0.179 |
| | SLF | 71.22 ± 18.41 | 70.62 ± 13.44 | 0.840 |
| GFR | Control | 102.52 ± 14.00 | 98.08 ± 14.47 | 0.081 |
| (ml/(min×1.73m$^2$)) | SLF | 99.60 ± 15.47 | 98.97 ± 16.55 | 0.810 |

IR, and promoting glucose and lipid metabolism.

The clinical investigations and animal experiments have showed that TCM could reverse the dysregulation of intestinal flora and maintain the balance of intestinal micro-ecological system (32).This clinical efficacy may be the result of SLF regulation of intestinal flora and there are some pieces of evidence that herbs in SLF may regulate the intestinal flora. Studies have shown that radix bupleuri could increase intestinal flora diversity and decrease the level of *Prevotella* and *Ochrobactrum* (33). Aqueous extract of Paeoniae Radix Alba could regulate the intestinal mucosal barrier and increase the level of *norank_f_Muribaculaceae*, *Lactobacillus*, *Akkermansia*, etc. (34). Poria cocos oligosaccharides could improve disorders of glucolipid metabolism by regulating intestinal flora (35). Salvia miltiorrhiza Polysaccharide combined with probiotics can improve insulin resistance and NAFLD *via* modulating intestinal flora (36). In addition, Atractylodes macrocephala Koidz and Citrus also have the function of regulating intestinal flora (37, 38). Glycyrrhizic acid could stabilize intestinal flora in chronic liver injury through increased probiotics and decreased pernicious bacteria (39). Procyanidins from hawthorn supplementation significantly relieved lipid accumulation in the serum and liver, and protected the structure of liver in lipid metabolism disorder (LMD) rats. Procyanidins from hawthorn (HPC) especially increased the abundances of *Akkermansia*, *Bacteroides* and *Adlercreutzia*, and decreased *Lactobacillus*, *Bifidobacterium*, *Blautia*, *Lachnospiraceae* and *Subdoligranulum*, which could also regulated the structure of intestinal flora (40).

We collected the stool samples of patients who were diagnosed with NAFLD and HC to examine the composition and abundance of the intestinal flora *via* 16S rRNA high-throughput gene sequencing technology to further validate our view based on the hypothesis that NAFLD is related to the abnormal intestinal flora. Intestinal flora may be affected by different living habit; hence, we ensured the same lifestyle intervention of SLF and control groups. Although there were no differences observed in *Proteobacteria* and *Fusobacteria* phyla, the phylum *Desulfobacterota* was significantly lower in NAFLD. As the two major phyla of the intestinal flora, *Firmicutes* and *Bacteroidetes* may be altered in patients with NAFLD and affect the development of NAFLD. A trial comparing the human intestinal flora of NAFLD (n=25) and HC (n=22) found that NAFLD patients had a lower abundance of the *Bacteroidetes* (31). In other experiments, the ratio of *Firmicutes* and *Bacteroidetes* was significantly higher in NAFLD patients (41, 42). Although opposite results have also been found (43, 44), our study identified clinically relevant alterations in the *Firmicutes* and *Bacteroidetes* phyla, which may play a critical role in the development of NAFLD. In particular, we found a positive correlation between the Firmicutes phylum and the FAST score (13), a potential signature for non-invasive diagnosis of NASH, while the opposite for the *Bacteroidetes* phylum.

In our study, significant changes occurred in *Coprococcus*, *Lachnospiraceae _NK4A136* group and *Ruminococcus* after SLF treatment. *Coprococcus* is capable of actively fermenting carbohydrates and is one of the important producers of butyric acid. *Lachnospiraceae_NK4A136* group belongs to the family *Lachnospiraceae* and is a potentially beneficial bacterium associated with obesity. It is also related to the production of butyric acid (45, 46). *Ruminococcus* play a crucial role in metabolism. It has been shown that the level of *Ruminococcus* is reduced in patients with NAFLD (41), which is similar to our results. Whereas SLF could call back the level of *Ruminococcus*. These results suggest that SLF may treat NAFLD by modulating certain specific enterobacterial genera.

Nonetheless, our study has some shortcomings. The treatment course of NAFLD patients is relatively short, and the sample size is

not enough, which leads to not obvious differences and incomplete recovery of the disorder flora after SLF treatment. In subsequent studies, we will expand the sample size to further confirm the effect of SLF on intestinal flora in NAFLD patients. In addition, we only observed the effect of SLF on different classification levels of intestinal flora in patients. In future research, we will further study the potential mechanisms of different strains of SLF.

## Conclusion

Our study suggested that NAFLD had relations with disturbances in the intestinal flora, which manifested as the levels of *Tyzzerella* increased and *Alistipes*, *Bilophila*, *Butyricimonas*, *Coprococcus*, *Erysipelotrichaceae UCG-003*, *Lachnospiraceae NK4A136* group, *Phascolarctobacterium*, *Ruminococcus* and *UCG-002* decreased. SLF could improve liver function and glucolipid metabolism in patients who were diagnosed with NAFLD and lower liver fat content to some extent. The effect of SLF may be carried out by regulating the disturbance of intestinal flora, especially *Coprococcus*, *Lachnospiraceae_NK4A136* group, and *Ruminococcus* genus.

## Data availability statement

The data presented in the study are deposited in the NCBI repository, accession number PRJNA921570.

## Ethics statement

The studies involving human participants were reviewed and approved by the Institutional Review Board of Shuguang Hospital Affiliated to Shanghai University of Traditional Chinese Medicine (Ethics No. 2020-863-72-01). The patients/participants provided their written informed consent to participate in this study.

## Author contributions

DH: Project management, Methodology, Writing manuscript. LL: Conceptualization, Investigation, Methodology. NA: Conceptualization, Revision. JS, YH and WX: Visualization. CW, DX and YJ: Revision. YB: Supervision, Methodology. MS: Funding acquisition, Writing – review and editing. All authors contributed to the article and approved the submitted version.

## Funding

This work was supported by the major project of Shanghai Municipal S and T Commission (no.19401972300), Shandong Province Key R&D Program (Major Science and Technology Innovation Project, 2021CXGC010509), Shanghai Key Laboratory of Traditional Chinese Clinical Medicine, Key Disciplines of Liver and Gall Bladder Diseases, and Key Laboratory of Chronic Deficienc Liver Disease of the State Administration of Traditional Chinese Medicine of the People's Republic of China (20DZ2272200), Shanghai Key Specialty of Traditional Chinese Clinical Medicine (shslczdzk01201), Outstanding TCM reserve talents of Shanghai University of Traditional Chinese Medicine (2020).

## Conflict of interest

The authors declare that the research was conducted in the absence of any commercial or financial relationships that could be construed as a potential conflict of interest.

## Publisher's note



## Supplementary material

The Supplementary Material for this article can be found online at: https://www.frontiersin.org/articles/10.3389/fendo.2022.1107071/full#supplementary-material

SUPPLEMENTARY FIGURE 1
**(A)** Comparison of intestinal flora beta diversity in HC and NAFLD, including unweighted and weighted Unifrac PCoA. **(B)** The abundance percentages of HC and NAFLD groups at the class level. **(C)** The abundance percentages of HC and NAFLD groups at the order level. **(D)** The abundance percentages of HC and NAFLD groups at the family level.

SUPPLEMENTARY FIGURE 2
Differentially abundant taxa between HC and NAFLD samples analyzed by linear discriminant analysis effect size (LEfSe).

## References

1. Buzzetti E, Pinzani M, Tsochatzis EA. The multiple-hit pathogenesis of non-alcoholic fatty liver disease (NAFLD). *Metabolism: Clin Exp* (2016) 65(8):1038–48. doi: 10.1016/j.metabol.2015.12.012

2. Angulo P. Nonalcoholic fatty liver disease. *New Engl J Med* (2002) 346(16):1221–31. doi: 10.1056/NEJMra011775

3. Cotter TG, Rinella M. Nonalcoholic fatty liver disease 2020: The state of the disease. *Gastroenterology* (2020) 158(7):1851–64. doi: 10.1053/j.gastro.2020.01.052

4. Chen J, Vitetta L. Gut microbiota metabolites in NAFLD pathogenesis and therapeutic implications. *Int J Mol Sci* (2020) 21(15):5214. doi: 10.3390/ijms21155214

5. Sharpton SR, Schnabl B, Knight R, Loomba R. Current concepts, opportunities, and challenges of gut microbiome-based personalized medicine in nonalcoholic fatty liver disease. *Cell Metab* (2021) 33(1):21–32. doi: 10.1016/j.cmet.2020.11.010

6. National Workshop on Fatty Liver and Alcoholic Liver Disease, Chinese Society of Hepatology, Chinese Medical Association, Fatty Liver Expert Committee and Chinese Medical Doctor Association[Guidelines of prevention and treatment for nonalcoholic fatty liver disease: a 2018 update]. *Zhonghua Gan Zang Bing Za Zhi* (2018) 26(3):195–203. doi: 10.3760/cma.j.issn.1007-3418.2018.03.008

7. Zhang H-J, He J, Pan L-L, Ma Z-M, Han C-K, Chen C-S, et al. Effects of moderate

and vigorous exercise on nonalcoholic fatty liver disease: A randomized clinical trial. *JAMA Intern Med* (2016) 176(8):1074–82. doi: 10.1001/jamainternmed.2016.3202

8. Schugar RC, Crawford PA. Low-carbohydrate ketogenic diets, glucose homeostasis, and nonalcoholic fatty liver disease. *Curr Opin Clin Nutr Metab Care* (2012) 15(4):374–80. doi: 10.1097/MCO.0b013e3283547157

9. Callahan BJ, McMurdie PJ, Rosen MJ, Han AW, Johnson AJ, Holmes SP, et al. DADA2: High-resolution sample inference from illumina amplicon data. *Nat Methods* (2016) 13(7):581–3. doi: 10.1038/nmeth.3869

10. Bolyen E, Rideout JR, Dillon MR, Bokulich NA, Abnet CC, Al-Ghalith GA, et al. Author correction: Reproducible, interactive, scalable and extensible microbiome data science using QIIME 2. *Nat Biotechnol* (2019) 37(9):1091. doi: 10.1038/s41587-019-0252-6

11. Douglas GM, Maffei VJ, Zaneveld JR, Yurgel SN, Brown JR, Taylor CM, et al. PICRUSt2 for prediction of metagenome functions. *Nat Biotechnol* (2020) 38(6):685–8. doi: 10.1038/s41587-020-0548-6

12. Taylor-East R, Grech A, Gatt C. The mental health of newly graduated doctors in Malta. *Psychiatr Danub* (2013) 25 Suppl 2:S250–S5.

13. Newsome PN, Sasso M, Deeks JJ, Paredes A, Boursier J, Chan WK, et al. FibroScan-AST (FAST) score for the non-invasive identification of patients with non-alcoholic steatohepatitis with significant activity and fibrosis: a prospective derivation and global validation study. *Lancet Gastroenterol Hepatol* (2020) 5(4):362–73. doi: 10.1016/S2468-1253(19)30383-8

14. Hassan K, Bhalla V, El Regal ME, A-Kader HH. Nonalcoholic fatty liver disease: A comprehensive review of a growing epidemic. *World J Gastroenterol* (2014) 20 (34):12082–101. doi: 10.3748/wjg.v20.i34.12082

15. Tsochatzis E, Papatheodoridis GV, Manesis EK, Kafiri G, Tiniakos DG, Archimandritis AJ. Metabolic syndrome is associated with severe fibrosis in chronic viral hepatitis and non-alcoholic steatohepatitis. *Alimentary Pharmacol Ther* (2008) 27 (1):80–9. doi: 10.1111/j.1365-2036.2007.03538.x

16. Chen S, Zhao X, Wan J, Ran L, Qin Y, Wang X, et al. Dihydromyricetin improves glucose and lipid metabolism and exerts anti-inflammatory effects in nonalcoholic fatty liver disease: A randomized controlled trial. *Pharmacol Res* (2015) 99:74–81. doi: 10.1016/j.phrs.2015.05.009

17. Ipsen DH, Lykkesfeldt J, Tveden-Nyborg P. Molecular mechanisms of hepatic lipid accumulation in non-alcoholic fatty liver disease. *Cell Mol Life Sci* (2018) 75(18):3313–27. doi: 10.1007/s00018-018-2860-6

18. Smith GI, Shankaran M, Yoshino M, Schweitzer GG, Chondronikola M, Beals JW, et al. Insulin resistance drives hepatic *de novo* lipogenesis in nonalcoholic fatty liver disease. *J Clin Invest* (2020) 130(3):1453–60. doi: 10.1172/JCI134165

19. Jazayeri-Tehrani SA, Rezayat SM, Mansouri S, Qorbani M, Alavian SM, Daneshi-Maskooni M, et al. Nano-curcumin improves glucose indices, lipids, inflammation, and nesfatin in overweight and obese patients with non-alcoholic fatty liver disease (NAFLD): a double-blind randomized placebo-controlled clinical trial. *Nutr Metab (Lond)* (2019) 16:8. doi: 10.1186/s12986-019-0331-1

20. Wang S-Z, Yu Y-J, Adeli K. Role of gut microbiota in neuroendocrine regulation of carbohydrate and lipid metabolism *via* the microbiota-Gut-Brain-Liver axis. *Microorganisms* (2020) 8(4):527. doi: 10.3390/microorganisms8040527

21. Machado MV, Cortez-Pinto H. Diet, microbiota, obesity, and NAFLD: A dangerous quartet. *Int J Mol Sci* (2016) 17(4):481. doi: 10.3390/ijms17040481

22. Paolella G, Mandato C, Pierri L, Poeta M, Di Stasi M, Vajro P. Gut-liver axis and probiotics: their role in non-alcoholic fatty liver disease. *World J Gastroenterol* (2014) 20 (42):15518–31. doi: 10.3748/wjg.v20.i42.15518

23. Mouzaki M, Comelli EM, Arendt BM, Bonengel J, Fung SK, Fischer SE, et al. Intestinal microbiota in patients with nonalcoholic fatty liver disease. *Hepatol (Baltimore Md)* (2013) 58(1):120–7. doi: 10.1002/hep.26319

24. Zhao Y, Zhou J, Liu J, Wang Z, Chen M, Zhou S. Metagenome of gut microbiota of children with nonalcoholic fatty liver disease. *Front Pediatr* (2019) 7:518. doi: 10.3389/fped.2019.00518

25. Loomba R, Seguritan V, Li W, Long T, Klitgord N, Bhatt A, et al. Gut microbiome-based metagenomic signature for non-invasive detection of advanced fibrosis in human nonalcoholic fatty liver disease. *Cell Metab* (2019) 30(3):607. doi: 10.1016/j.cmet.2019.08.002

26. Lelouvier B, Servant F, Païssé S, Brunet AC, Benyahya S, Serino M, et al. Changes in blood microbiota profiles associated with liver fibrosis in obese patients: A pilot analysis. *Hepatol (Baltimore Md)* (2016) 64(6):2015–27. doi: 10.1002/hep.28829

27. Gérard P. Gut microbiota and obesity. *Cell Mol Life Sci* (2016) 73(1):147–62. doi: 10.1007/s00018-015-2061-5

28. Karlsson FH, Tremaroli V, Nookaew I, Bergström G, Behre CJ, Fagerberg B , et al. Gut metagenome in European women with normal, impaired and diabetic glucose control. *Nature* (2013) 498(7452):99–103. doi: 10.1038/nature12198

29. Grabherr F, Grander C, Effenberger M, Adolph TE, Tilg H. Gut dysfunction and non-alcoholic fatty liver disease. *Front Endocrinol* (2019) 10:611. doi: 10.3389/fendo.2019.00611

30. Zhu L, Baker S, Gill C, Liu W, Alkhouri R, Baker RD, et al. Characterization of gut microbiomes in nonalcoholic steatohepatitis (NASH) patients: a connection between endogenous alcohol and NASH. *Hepatol (Baltimore Md)* (2013) 57(2):601–9. doi: 10.1002/hep.26093

31. Shen F, Zheng R-D, Sun X-Q, Ding WJ, Wang XY, Fan JG. Gut microbiota dysbiosis in patients with non-alcoholic fatty liver disease. *Hepatobil Pancreat Dis Int* (2017) 16(4):375–81. doi: 10.1016/S1499-3872(17)60019-5

32. Yu L, Xing ZK, Mi SL, Wu X. [Regulatory effect of traditional Chinese medicine on intestinal microbiota]. *Zhongguo Zhong yao za zhi = Zhongguo zhongyao zazhi = China J Chin materia Med* (2019) 44(1):34–9. doi: 10.19540/j.cnki.cjcmm.20181101.013

33. Feng Y, Gao X, Meng M, Xue H, Qin X. Multi-omics reveals the mechanisms of antidepressant-like effects of the low polarity fraction of bupleuri radix. *J Ethnopharmacol* (2020) 256:112806. doi: 10.1016/j.jep.2020.112806

34. Yan B-F, Chen X, Chen Y-F, Liu S-J, Xu C-X, Chen L, et al. Aqueous extract of paeoniae radix alba (Paeonia lactiflora pall.) ameliorates DSS-induced colitis in mice by tunning the intestinal physical barrier, immune responses, and microbiota. *J Ethnopharmacol* (2022) 294:115365. doi: 10.1016/j.jep.2022.115365

35. Zhu L, Ye C, Hu B, Xia H, Bian Q, Liu Y, et al. Regulation of gut microbiota and intestinal metabolites by poria cocos oligosaccharides improves glycolipid metabolism disturbance in high-fat diet-fed mice. *J Nutr Biochem* (2022) 107:109019. doi: 10.1016/j.jnutbio.2022.109019

36. Wang W, Xu AL, Li ZC, Li Y, Xu SF, Sang HC, et al. Combination of probiotics and polysaccharide alleviates hepatic steatosis *via* gut microbiota modulation and insulin resistance improvement in high fat-induced NAFLD mice. *Diabetes Metab J* (2020) 44 (2):336–48. doi: 10.4093/dmj.2019.0042

37. Wang R, Zhou G, Wang M, Peng Y, Li X. The metabolism of polysaccharide from atractylodes macrocephala koidz and its effect on intestinal microflora. *Evid Based Complement Alternat Med* (2014) 2014:926381. doi: 10.1155/2014/926381

38. Zeng S-L, Li S-Z, Xiao P-T, Cai Y-Y, Chu C, Chen B-Z, et al. Citrus polymethoxyflavones attenuate metabolic syndrome by regulating gut microbiome and amino acid metabolism. *Sci Adv* (2020) 6(1):eaax6208. doi: 10.1126/sciadv.aax6208

39. Wang S, Li XY, Ji HF, Shen L. Modulation of gut microbiota by glycyrrhizic acid may contribute to its anti-NAFLD effect in rats fed a high-fat diet. *Life Sci* (2022) 310:121110. doi: 10.1016/j.lfs.2022.121110

40. Han X, Zhao W, Zhou Q, Chen H, Yuan J, Zhang XF, et al. Procyanidins from hawthorn alleviate lipid metabolism disorder inhibiting insulin resistance and oxidative stress, normalizing the gut microbiota structure and intestinal barrier, and further suppressing hepatic inflammation and lipid accumulation. *Food Funct* (2022) 13 (14):7901–17. doi: 10.1039/D2FO00836J

41. Yu JS, Youn GS, Choi J, Kim CH, Kim BY, Yang SJ, et al. Lactobacillus lactis and pediococcus pentosaceus-driven reprogramming of gut microbiome and metabolome ameliorates the progression of non-alcoholic fatty liver disease. *Clin Transl Med* (2021) 11 (12):e634. doi: 10.1002/ctm2.634

42. Xie K, He X, Chen K, Sakao K, Hou DX. Ameliorative effects and molecular mechanisms of vine tea on western diet-induced NAFLD. *Food Funct* (2020) 11(7):5976–91. doi: 10.1039/D0FO00795A

43. Zhu C, Guan Q, Song C, Zhong L, Ding X, Zeng H, et al. Regulatory effects of lactobacillus fermented black barley on intestinal microbiota of NAFLD rats. *Food Res Int* (2021) 147:110467. doi: 10.1016/j.foodres.2021.110467

44. Da Silva HE, Teterina A, Comelli EM, Taibi A, Arendt BM, Fischer SE, et al. Nonalcoholic fatty liver disease is associated with dysbiosis independent of body mass index and insulin resistance. *Sci Rep* (2018) 8(1):1466. doi: 10.1038/s41598-018-19753-9

45. Wang B, Yu H, He Y, Wen L, Gu J, Wang X, et al. Effect of soybean insoluble dietary fiber on prevention of obesity in high-fat diet fed mice *via* regulation of the gut microbiota. *Food Funct* (2021) 12(17):7923–37. doi: 10.1039/D1FO00078K

46. He X-Q, Liu D, Liu H-Y, Wu D-T, Li H-B, Zhang X-S, et al. Prevention of ulcerative colitis in mice by sweet tea *via* the regulation of gut microbiota and butyric-Acid-Mediated anti-inflammatory signaling. *Nutrients* (2022) 14(11):2208. doi: 10.3390/nu14112208

frontiers | Frontiers in Endocrinology

TYPE Original Research
PUBLISHED 19 January 2023
DOI 10.3389/fendo.2022.1106875



OPEN ACCESS

EDITED BY
Zhoujin Tan,
Hunan University of Chinese Medicine, China

REVIEWED BY
Yang Ping,
Jiamusi University, China
Su Min,
Changsha Medical University, China

*CORRESPONDENCE
Yuansong Wang
2426104415@qq.com

†These authors have contributed equally to this work

SPECIALTY SECTION
This article was submitted to Gut Endocrinology, a section of the journal Frontiers in Endocrinology

RECEIVED 24 November 2022
ACCEPTED 29 December 2022
PUBLISHED 19 January 2023

CITATION
Lv S, Zhang Z, Su X, Li W, Wang X, Pan B, Li H, Zhang H and Wang Y (2023) Qingrequzhuo capsule alleviated methionine and choline deficient diet-induced nonalcoholic steatohepatitis in mice through regulating gut microbiota, enhancing gut tight junction and inhibiting the activation of TLR4/NF-κB signaling pathway. *Front. Endocrinol.* 13:1106875. doi: 10.3389/fendo.2022.1106875



# Qingrequzhuo capsule alleviated methionine and choline deficient diet-induced nonalcoholic steatohepatitis in mice through regulating gut microbiota, enhancing gut tight junction and inhibiting the activation of TLR4/NF-κB signaling pathway

Shuquan Lv[1†], Zhongyong Zhang[1†], Xiuhai Su[1], Wendong Li[1], Xiaoyun Wang[1], Baochao Pan[2], Hanzhou Li[3], Hui Zhang[2] and Yuansong Wang[1*]

[1]Department of Endocrinology, Cangzhou Hospital of Integrated Traditional Chinese Medicine and Western Medicine of Hebei Province Affiliated to Hebei University of Chinese Medicine, Cangzhou, China, [2]Graduate School, Hebei University of Chinese Medicine, Shijiazhuang, China, [3]Graduate School, Chengde Medical University, Chengde, China

Qingrequzhuo capsule (QRQZ), composed of Morus alba L., Coptis chinensis Franch., Anemarrhena asphodeloides Bunge, Alisma plantago-aquatica subsp. orientale (Sam.) Sam., Citrus × aurantium L., Carthamus tinctorius L., Rheum palmatum L., Smilax glabra Roxb., Dioscorea oppositifolia L., Cyathula officinalis K.C.Kuan, has been used to treat nonalcoholic steatohepatitis (NASH) in clinic. However, the mechanism of QRQZ on NASH remains unclear. Recent studies have found that the dysfunction of gut microbiota could impair the gut barrier and induce the activation of TLR4/NF-kB signaling pathway, and further contribute to the inflammatory response in NASH. Modulating the gut microbiota to reduce inflammation could prevent the progression of NASH. In this study, a mouse model of NASH was generated by methionine and choline deficient diet (MCD) and treated with QRQZ. First, we evaluated the therapeutic effects of QRQZ on liver injury and inflammation in the NASH mice. Second, the changes in the gut microbiota diversity and abundance in each group of mice were measured through 16S rRNA sequencing. Finally, the effects of QRQZ on gut mucosal permeability, endotoxemia, and liver TLR4/NF-kB signaling pathway levels were examined. Our results showed that QRQZ significantly reduced the lipid accumulation in liver and the liver injury in NASH mice. In addition, QRQZ treatment decreased the levels of inflammatory cytokines in liver. 16S rRNA sequencing showed that QRQZ affected the diversity of gut microbiota and affected the relative abundances of Dubosiella, Lachnospiraceae_NK4A136_group, and Blautiain NASH mice. Besides, QRQZ could increase the expression of tight junction proteins (zonula occludens-1 and occludin) in gut and decrease the lipopolysaccharide (LPS) level in serum. Western blot results also showed that QRQZ treatment decreased the protein expression ofTLR4, MyD88 and the phosphorylation of IkB and NF-kBp65 and

qPCR results showed that QRQZ treatment down-regulated the gene expression of interleukin (IL)-1b, IL-6, and tumor necrosis factor (TNF)-a in liver. In conclusion, our study demonstrated that QRQZ could reduce the lipid accumulation and inflammatory response in NASH model mice. The mechanisms of QRQZ on NASH were associated with modulating gut microbiota, thereby inducing the tight junction of gut barrier, reducing the endotoxemia and inhibiting the activation of TLR4/NFkB signaling pathway in liver.

KEYWORDS

**nonalcoholic steatohepatitis, Qingrequzhuo capsule, methionine and choline deficient diet, gut microbiota, TLR4/NF-κB signaling pathway**

## Introduction

Non-alcoholic fatty liver disease (NAFLD) is one of the most common chronic liver diseases. The incidence of NAFLD has increased in recent years with the changing lifestyle and diet structure in China, thereby making NAFLD the second major liver disease after viral hepatitis. NAFLD may progress to liver fibrosis, cirrhosis, and even malignant transformation in the long term (1). During NAFLD development, nonalcoholic steatohepatitis (NASH) progresses to liver fibrosis and cirrhosis, and the interventions for NASH become a break point for NAFLD treatment. Currently, no specific treatment exists, and the disease is clinically managed through diet modification and increased exercise as the basic treatment of weight control and fat loss; however, a combined administration of drugs is needed to achieve comprehensive treatment (2). Therefore, the development of safe and effective drugs to delay disease progression has garnered considerable attention as a hot topic of research in this field.

Many studies have shown that traditional Chinese medicine (TCM) has a favorable therapeutic effect on NAFLD and NASH (3). A clinical randomized multicenter controlled study showed that Lingguizhugan decoction significantly improved dyslipidemia and insulin resistance in patients with NAFLD (4). In addition, a propensity score-matched cohort study confirmed that TCM intervention was effective in preventing the progression to cirrhosis in patients with NAFLD and NASH (5). A meta-analysis also confirmed the significant advantages of TCM in improving abnormal liver function and dyslipidemia in NASH patients (6). Elucidating the mechanism of action of TCM in the treatment of NAFLD and NASH can greatly facilitate the modernization of TCM and is becoming a hot spot in for researchers.

Gut microbiota are a group of microorganisms that colonize in the gut and have a symbiotic relationship with the host. They are large in number, with a total of 10–100 trillion in number, and dominated by bacteria while including archaea, fungi, protozoa, and viruses (7). The number and types of bacterial strains are in dynamic balance, which is a part of the body's internal homeostasis. Bacterial abundance and compositional complexity increase from the stomach to the colon, showing increasing diversity, and are influenced by genetics, age, lifestyle, medications, and diet (8). These microbes have a symbiotic relationship with the human body, and play an important role in food digestion and nutrient absorption, such as decomposing complex polysaccharides, synthesizing multiple vitamins, and participating in the enterohepatic circulation of bile acids (9). A large number of studies have reported that patients with NAFLD have altered gut microbiota or dysbiosis, and significantly higher amounts of γ-proteobacteria and *Prevotella* have been identified in stool samples from children with NAFLD (10). In the NAFLD group, the *Firmicutes*/*Bacteroides* (*F/B*) ratio was lower than that in the healthy population, whereas the proportion of *Lactobacillus* spp. was higher in the healthy population, suggesting a disproportionate ratio between the species (11). An increase in fecal *Bacteroides*, *Escherichia coli*, and *Ruminococcus* and a decrease in beneficial bacteria such as *Lactobacillus* and *Bifidobacterium* is observed in patients with NASH (12). Regulation of gut microbiota has facilitated in opening new avenues of research for the treatment of NASH. Modulation of gut microbiota by butyrate alleviated high-fat diet (HFD)-induced NASH by improving gut mucosal permeability (13). Modulation of gut microbiota by indole-3-propionic acid promoted gut mucosal tight junctions, which consequently inhibited the liver inflammatory response in NASH mice (14) Soyasaponin $A_2$ alleviated methionine and choline-deficient diet (MCD)-induced abnormalities in lipid metabolism in NASH mice by regulating gut microbiota and bile acid metabolism (15). Further investigation revealed that the imbalance of gut microbiota may lead to changes in the permeability of the gut mucosa, which subsequently leads to the entry of bacterial metabolites including lipopolysaccharide (LPS) from the intestine into the liver through the peripheral blood. This activates the toll-like receptor 4 (TLR4)/nuclear factor kappa B (NF-κB) signaling pathway and causes an inflammatory response in the liver, and inhibition of the inflammatory response by regulating the bacterial groups effectively improved NAFLD and NASH (16). Many studies have also demonstrated the regulatory effects of TCM on gut microbiota. Jianganxiaozhi formula improved the liver inflammatory response in NAFLD rats by regulating the abundance of *Alloprevotella*, *Lactobacillus*, and *Turicibacter* in the gastrointestinal tract to reduce the gut mucosal permeability in rats (17). Qiwei Baizhu Powder can treat diarrhea\ through promoting the proliferation of *Lactobacillus* and downregulating the abundances of *Proteus*, *Clostridium*,

*Eubacterium*, *Facklamia*, and *Escherichia* (18–20). The combination of *Scutellaria baicalensis* Georgi and *Coptis chinensis* Franch could increase the abundance of short-chain fatty acids (SCFAs)-producing bacteria such as *Bacteroidales S24-7 group_norank*, *Parasutterella*, *Prevotellaceae UCG-001*, *Ruminiclostridium*, and *Ruminiclostridium* in type 2 diabetes mellitus (T2DM) rats (21).

Qingrequzhuo capsule (QRQZ), composed of *Morus alba* L., *Picrorhiza kurroa* Royle ex Benth., *Anemarrhena asphodeloides* Bunge, *Alisma plantago-aquatica subsp. orientale* (Sam.) Sam., *Citrus* × *aurantium* L., *Carthamus tinctorius* L., *Rheum officinale* Baill., *Smilax glabra* Roxb., *Dioscorea oppositifolia* L., and *Cyathula officinalis* K.C.Kuan, has shown in clinical studies to improve glucose metabolism measures, reduce the level of inflammatory cytokines and improve vascular endothelial function in patients with T2DM and NAFLD, with a good safety profile in treatment (22) However, the underlying mechanism of action remains unclear. In this study, a mouse model of NASH was generated by MCD and treated with QRQZ. First, we evaluated the therapeutic effects of QRQZ on liver injury and inflammatory response in the NASH mice. Second, the changes in the gut microbiota diversity and abundance in each group of mice were measured through 16S rRNA sequencing. Finally, the effects of QRQZ on gut mucosal permeability, endotoxemia, and liver TLR4/NF-κB signaling pathway levels were examined. This study was aimed to explore the effects of QRQZ on improving gut mucosal permeability by regulating gut microbiota, and its mechanism in the inhibition of the TLR4/NF-κB signaling pathway activation to alleviate NASH.

# Materials and methods

## Reagents

MCD was purchased from Sibeifu Bioscience Co., Ltd. (Beijing, China). Polyene phosphatidylcholine (PPC) was purchased from Sanofi. (Beijing, China). QRQZ was purchased from Cangzhou Hospital of Integrated Traditional Chinese Medicine and Western Medicine of Hebei Province. Triglyceride (TG, cat: A110-1-1), total cholesterol (TC, cat: A111-1-1), alanine aminotransferase (ALT, cat: C009-1-1), aspartate aminotransferase (AST, cat: C0101-2-1), superoxide dismutase (SOD, cat: A001-3-2), methane dicarboxylic aldehyde (MDA, cat: A003-1-2), and glutathione peroxidase (GSH-Px, cat: A006-2-1) biochemical test kits were obtained from Jiancheng Biological Engineering Institute (Nanjing, China). Enzyme-linked immunosorbent assay (ELISA) kits of mouse tumor necrosis factor alpha (TNF-α, cat: ml002095), interleukin (IL)-1β (cat: ml301814), IL-6 (cat: ml063159), LPS (cat: ml037221-2) were purchased from Enzyme-linked Biotechnology Co., Ltd. (Shanghai, China). Antibodies for zonula occludens-1 (ZO-1, cat:61-7300) and occludin (cat: 71-1500) were purchased from Thermo Fisher Scientific. Antibodies for TLR4 (cat: 19811-1-AP) and myeloid differentiation primary response 88 (MyD88, cat: 67969-1-Ig) were purchased from Proteintech Group, Inc. Antibodies for nuclear factor of kappa light polypeptide gene enhancer in B-cells inhibitor (IκB, cat: ab32518), phospho-IκB (p-IκB, cat: ab133462) were purchased from Abcam. Antibodies for nuclear factor kappa-light-chain-enhancer of activated B cells p65 subunit (NF-κBp65, cat: #8242), and phospho-NF-κBp65(p-NF-κBp65, cat: #3033) were purchased from Cell Signaling Technology.

## Animals

Sixty male C57BL/6 mice, weighing 20 ± 2g, were purchased from Beijing HFK Bioscience Co., Ltd. (SCXK 2021-0006). The feeding conditions of animals can be found in the Supplementary Material. The animal study was approved by Ethics Committee of Hebei University of Chinese Medicine (Approval no. CZX2021-KY-026).

## Preparations of QRQZ

QRQZ was prepared by the pharmacy department of Cangzhou Hospital of Integrated Traditional Chinese and Western Medicine. Briefly, 15 g of *Morus alba* L., 9 g of *Coptis chinensis* Franch., 12 g of *Anemarrhena asphodeloides* Bunge, 12 g of *Alisma plantago-aquatica subsp. orientale* (Sam.) Sam., 15 g of *Citrus* × *aurantium* L., 9 g of *Carthamus tinctorius* L., 6g of *Rheum palmatum* L., 15 g of *Smilax glabra* Roxb., 12 g of *Dioscorea oppositifolia* L., 12 g of *Cyathula officinalis* K.C.Kuan were weighed, mixed, decocted and evaporated to obtain the extract powder of QRQZ. Then, the powders were made into capsule (0.5g per capsule) based on the medical institution preparation standard in Hebei (approval number: Z20050795).

## Animal grouping

After 1 week of acclimatization feeding, all mice were randomly divided into the control, model, PPC, QRQZ low-dose (LD-QRQZ), QRQZ middle-dose (MD-QRQZ), and QRQZ high-dose (HD-QRQZ) groups (n = 10 per group). The control group received normal diet and the remaining 5 experimental groups were administered the MCD (Sucrose 45.53%, Sodium Bicarbonate 0.75%, Corn Starch 15%, Maltodextrin 5%, Cellulose 3%, Corn Oil 10%, Multi Mineral S10001 3.5%, Multi Vitamin V10001 1%, Methionine 0%, Choline 0%, Alanine 0.35%, Arginine 1.21%, Asparagine 0.6%, Winterine 0.35%, Cystine 0.35%, glutamic acid 0.4%, glycine 2.33%, histidine 0.45%, isoleucine 0.82%, leucine 1.11%, lysine 1.8%, phenylalanine 0.75%, proline 0.35%, serine 0.35%, threonine 0.82%, tryptophan 0.18%, tyrosine 0.5%, valine 0.82%). The PPC group was administered 88 mg/kg of PPC through oral gavage. The contents of QRQZ were collected and dissolved in saline to prepare QRQZ mixture. The mixture was treated to mice through the gavage. The LD-QRQZ group, MD-QRQZ group and HD-QRQZ group received orally treatment of 0.48,

0.96, and 1.92 g/kg of QRZS respectively; and the control and model groups received an equal volume of saline as vehicle in parallel. All mice were gavaged once per day for 42 days. The mice were weighed and the weights were recorded every 7 days.

## Preparation of tissue samples

After 42 days of treatment, the mice were anesthetized with sodium pentobarbital. Blood was extracted from the heart, then the mice were sacrificed, and the serum was separated and stored at −80° C. The livers were quickly removed and weighed, and the liver tissues used for pathological sections in each group were isolated from the same location of the liver lobe and placed in 4% paraformaldehyde solution for fixation or quick-freezing storage. The remaining samples were quick-frozen and stored at −80°C. After careful extrusion of the cecum contents for collection, the colon was cut off and placed in 4% paraformaldehyde solution for fixation.

## Pathological staining

Paraffin sections were prepared from the 4% paraformaldehyde-fixed liver and colon tissues, and were observed under a light microscope after hematoxylin and eosin (HE) staining or sirius red staining. The NASH activity score (NAS) of liver was calculated as described previously (23, 24). The intestinal injury was evaluated by a 0–4 grading scale as previously reported (25). Besides, frozen liver tissues were sectioned and stained with oil red O. The positive area for oil red O and sirius red staining was quantified using Image Pro Plus 6.0 software based on the average optical density (AOD) (26).

## Biochemical testing

The liver was mixed with normal saline in the ratio of 1:9 (weight: volume), then ultrasonicated in an ice-water bath to completely lyse the homogenate, and centrifuged (2500 rpm, 10 min) to obtain the supernatant, which was 10% liver tissue homogenate. The concentrations of TG, TC, SOD, MDA, GSH-Px, and total protein were measured using commercial kits. Levels of HYP in liver tissue was tested to evaluate the fibrosis of liver. Serum concentrations of ALT and AST were measured using a commercial kit.

## ELISA

The concentrations of IL-1β, IL-6, and TNF-α in the liver tissue homogenate and the serum LPS level were measured using a double-antibody one-step sandwich ELISA. Briefly, the test sample, the standard and the detection antibody were added to the microplate wells coated with the capture antibody, and the plate was placed in a warm bath followed by thorough washing of the wells, after which the reaction substrate was added for color development. Absorbance was measured using a plate reader. The standard curve was plotted using the results of the standards, and the concentrations of the analytes in each sample were calculated.

## 16S rRNA sequencing

### Fecal genomic DNA extraction

The total genomic DNA from the cecal contents of the mice was extracted with the cetyltrimethylammonium bromide (CTAB)/ sodium dodecyl sulfate (SDS) method, and the DNA concentration and purity were measured with 1% agarose gel. DNA was diluted to 1 ng/μL with sterile water based on the concentration.

### Polymerase chain reaction amplification and sequencing of 16S rRNA

The primers 338F (5′-ACTCCTACGGGAGGCAGCAG-3′) and 806R (5′-GGACTACHVGGGTWTCTAAT-3′) were used to amplify the V3 to V4 regions of the 16S rRNA gene. The PCR amplification system included 10 ng of template DNA, 0.2 μM of forward and reverse primers, and 15 μL Phusion® High-Fidelity PCR Master Mix (New England Biolabs). The reaction conditions were as follows: pre-denaturation at 98°C for 1 minute, denaturation at 95°C for 10 seconds, annealing at 50°C for 30 seconds, and extension at 72°C for 30 seconds, for a total of 15 cycles; with a final holding at 72°C for 5 minutes. The mixture was then stored at 4°C. The mixed PCR products were purified with the Qiagen Gel Extraction Kit (Qiagen, Germany), and tested with 2% agarose gel electrophoresis. The sequencing library was generated using TruSeq® DNA PCR-Free Sample Preparation Kit (Illumina, USA), and the library quality was assessed by Qubit@ 2.0 Fluorometer (Thermo Scientific) and Agilent Bioanalyzer 2100 system. Finally, the library was sequenced on the Illumina NovaSeq platform to obtain 250 bp of end-to-end sequences.

## Sequencing data analysis

The raw sequencing data were assembled and quality-controlled with FLASH (V1.2.7, http://ccb.jhu.edu/software/FLASH/) to obtain the final effective tags. The tags were clustered with Uparse (Uparse v7.0.1001, http://drive5.com/uparse/) at the 97% similarity level to obtain the operational taxonomic units (OTUs). The OTUs were annotated with taxonomic information against the Mothur algorithm-based Silva database (http://www.arb-silva.de/). The MUSCLE software (Version 3.8.31, http://www.drive5.com/muscle/) was used for multiple sequence alignment. The OTUs abundance information was normalized by the sequence number corresponding to the sample with the shortest sequence. Alpha diversity index and beta diversity analysis were subsequently performed. The Wilcoxon rank-sum test was used to test for inter-group differences in the diversity indices, the Kruskal–Wallis rank-sum test (Games–Howell was chosen as the *post-hoc* test) combined with the multiple testing method FDR were used to screen for differential bacteria, and a difference with $P < 0.05$ indicated statistical significance.

## Immunohistochemistry

Paraffin sections were made from the 4% paraformaldehyde-fixed colon tissues and placed in an incubator at 60°C overnight, with the endogenous peroxidase treated with methanol-hydrogen peroxide, followed by clearing with PBS and distilled water. After

antigen recovery and blocking, the sections were stained immunohistochemically, with rabbit anti-ZO-1 (1:50) or rabbit anti-occludin (1:125) added dropwise to the sections, and incubated at 4°C overnight. After washing, the secondary antibody (1:10000) was added dropwise. The sections were then washed, mounted after color development and hematoxylin re-staining, and observed under a light microscope for expression of ZO-1 and occludin in the colon tissues. The expression in the positive regions was quantitatively analyzed using the Image Pro Plus 6.0 software based on the AOD (27).

## Reverse transcriptase quantitative PCR

The mRNA of *IL-1β*, *IL-6*, and *TNF-α* was determined for their hepatic expression with reverse transcriptase quantitative PCR (qPCR) after extraction of the total RNA from the liver tissues. The primer sequences were included in Supplementary Material. The mRNA expression was relative to that of *β-actin*. The relative expression was calculated with the $2^{-\Delta\Delta CT}$ method.

## Western blot

20 mg of liver tissues were weighed and added with 150 μL of RIPA lysis buffer, the homogenate was centrifuged, and the proteins were retained. The total protein concentration was determined with the bicinchoninic acid (BCA) assay. An equal amount of 10 μg of protein was collected from each sample for separation with sodium dodecyl sulfate–polyacrylamide gel electrophoresis (SDS-PAGE) under the following conditions: 90 V for 20 minutes and 130 V for 1 hour. The separated proteins after electrophoresis were then transferred to the PVDF membrane at 130 V and 300 mA for 2 hours, blocked with 5% skim milk powder at room temperature for 2 hours, and added with the rabbit anti-mouse primary antibodies of TLR4, MyD88, IκB, p-IκB, NF-κBp65, p-NF-κBp65 and β-actin at dilutions of 1:1000, 1: 1000, 1:1000, 1:1000, 1:1000, 1:1000, 1:1000, and 1:2000, respectively. The membranes were incubated overnight at 4°C. After the membranes were washed, the secondary antibody (goat anti-rabbit IgG diluted at 1:9000) was added, followed by incubation at room temperature for 2 hours. After the membranes were washed with tris-buffered saline with 0.1% tween 20 (TBST), enhanced chemiluminescence (ECL) reagents were added for development and detection, and the grayscale values of the bands were quantitatively analyzed with Image Pro Plus 6.0.

## Statistical analysis

Statistical analysis was performed with the statistical software SPSS 20.0, and data are expressed as mean ± standard deviation (SD). One-way analysis of variance (ANOVA) with Tukey's HSD (honest significant difference) *post-hoc* test was used for intergroup comparisons. Spearman's correlation analysis was used to evaluate the correlation of therapeutic indicators and changed gut microbiota. A difference with $P < 0.05$ indicated statistical significance.

# Results

## QRQZ treatment improved the liver injury and inflammation in NASH mice

Mice treated with MCD for 42 days showed a significant decrease in body weight and liver index compared to the control group, whereas treatment with both PPC and HD-QRQZ increased body weight and liver index (Figures 1A, B). HYP test result showed that the HYP levels were higher in model group compared with the control. PPC and HD-QRQZ treatment lowered the concentration of HYP in liver (Figure 1C). HE staining showed that the model group had disorganized hepatic plate arrangement, inflammatory cell infiltration, and a large amount of vacuolar-like degeneration; Oil red O staining revealed that the liver in the model group had extremely severe steatosis, with huge fat droplets occupying most of the area; Sirius red staining showed increased collagen deposition in liver as expected. (Figure 2A); and PPC and QRQZ interventions alleviated the above pathological changes in different degrees. (Figures 2B–D).

In addition, several biochemical parameters were measured for a more comprehensive assessment on the liver injury. In terms of fat metabolism, TC and TG appeared to be significantly increased in the liver tissues of the model group compared to those in the control group; in terms of liver function, the serum ALT and AST activities were also significantly increased in the model group compared to those in the control group; and in terms of oxidative stress indicators, the SOD and GSH-Px activities decreased and the MDA levels increased in the model group compared to those in the control group. In contrast, these indicators were significantly improved in the PPC and HD-QRQZ groups (Table 1). The ELISA results showed that the inflammatory cytokines IL-1β, IL-6, and TNF-α were significantly increased in the liver tissues of the model group compared to those in the control group, and PPC significantly reduced the levels of these inflammatory cytokines. Besides, at different dosages, QRQZ reduced the levels of these inflammatory cytokines in a dose-dependent manner to varying degrees, and the effect was most significant in the HD-QRQZ group (Figure 1D).

The above results showed that NASH was well induced through the administration of MCD to mice for 6 weeks, and that QRQZ had a therapeutic effect on NASH, which was most significant at the high dose. Therefore, the HD-QRQZ group was selected for the subsequent gut microbiota study.

## QRQZ treatment affected the gut microbiota in NASH mice

The 16S rRNA sequencing results were used to construct a clustering table for subsequent analysis of different groups of mouse gut microbiota. The diversity of the gut microbial community was assessed by calculating the Shannon and Simpson indices. The results showed that the Shannon index and Simpson index were decreased in the model group compared to those in the control group, indicating that NASH reduced the diversity of gut microbiota in the mice (Figures 3A, B). Then, we calculated the magnitude of differences in the microbial communities between different groups with the principal coordinate analysis (PCoA). The PCoA results showed

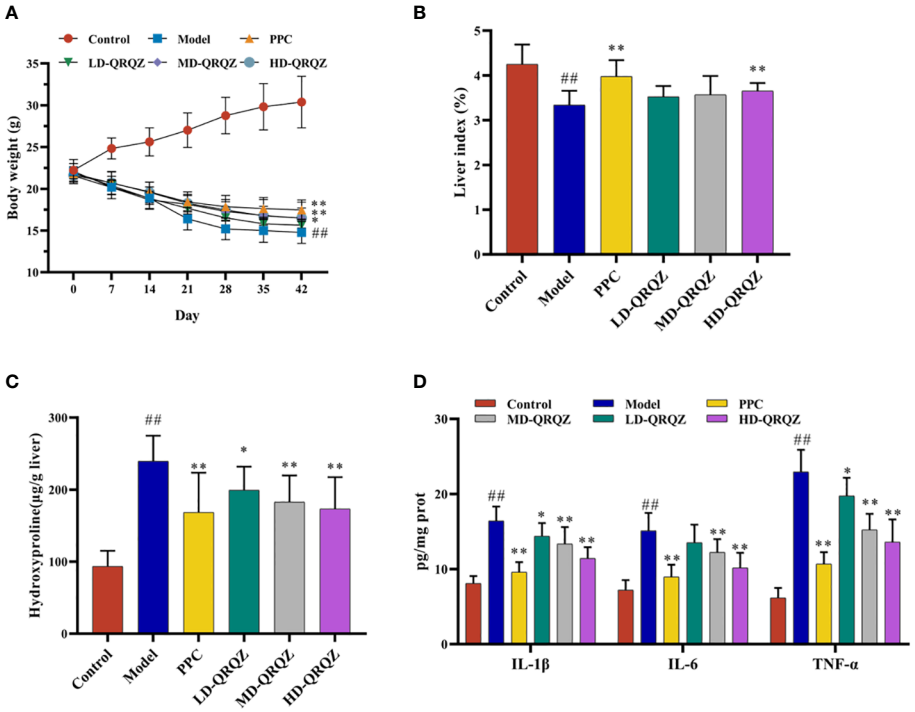


FIGURE 1
QRQZ alleviated liver injury and inflammation in MCD induced NASH mice. **(A)** Body weight change curves of each group. **(B)** The liver/body weight indexes of each group. **(C)** Hydroxyproline levels in liver of each group. **(D)** Serum pro-inflammatory cytokines of each group. Data are presented as the mean ± standard deviation. ##$P < 0.01$ as compared to the Control group; *$P < 0.05$ as compared to the Model group; **$P < 0.01$ as compared to the Model group.

that the sample points of the model group were significantly separated and distant from those of the control group, whereas the sample points of the HD-QRQZ group were well separated from those of the model group (Figure 3C).

As shown in Figure 3D, *Firmicutes* and *Bacteroidetes* were the dominant taxa in gut microbiota at the phylum level for each group. The *F/B* ratio was significantly increased in the model group compared to that in the control group, whereas the *F/B* ratio was significantly decreased after HD-QRQZ intervention (Figure 3E). At the genus level, the relative abundance of *Faecalibaculum*, *Lachnospiraceae_NK4A136_group*, and *Colidextribacter* was significantly increased in the model group compared to that in the control group, the relative abundance of *Lactobacillus*, *Muribaculaceae*, *Blautia* was significantly decreased; compared to the model group, the relative abundance of *Dubosiella* and *Blautia* was significantly increased in the HD-QRQZ group, and the relative abundance of *Lachnospiraceae_NK4A136_group* was significantly decreased (Figure 3F).

The correlation analysis showed that *Faecalibaculum* and *Colidextribacter* were positively correlated with the majority of NASH pathological indicators, oxidative stress indicators, and inflammatory cytokines while *Lactobacillus* and *Muribaculaceae* showed negatively correlation with most of the indicators (Figure 3G).

## QRQZ treatment reduced colonic permeability and alleviated endotoxemia in NASH mice

HE staining result showed incomplete arrangement of epithelial cells in colon can be observed in model group while HD-QRQZ alleviated the pathological changes in colon (Figure 4A). Likewise, the intestinal injury score was higher in model group compared with the control and HD-QRQZ treatment reduced the intestinal injury score in colon (Figure 4B). The effect of QRQZ on the intestinal expression levels of the tight junction proteins ZO-1 and occludin in the NASH mice was examined through immunohistochemical assays. The results showed that the areas of positive expression of ZO-1 and occludin were significantly reduced in the colonic tissues of mice in the model group compared to that in the control group. HD-QRQZ treatment elevated the positive areas of ZO-1 and occludin to different degrees in the mouse colonic tissues (Figures 4A, C, D). In addition, we assessed endotoxemia in each group of mice by measuring the LPS level in serum with ELISA, and the serum LPS level was significantly increased in the NASH mice compared to those in the control group, and it was reduced significantly after HD-QRQZ intervention (Figure 4E).

10.3389/fendo.2022.1106875

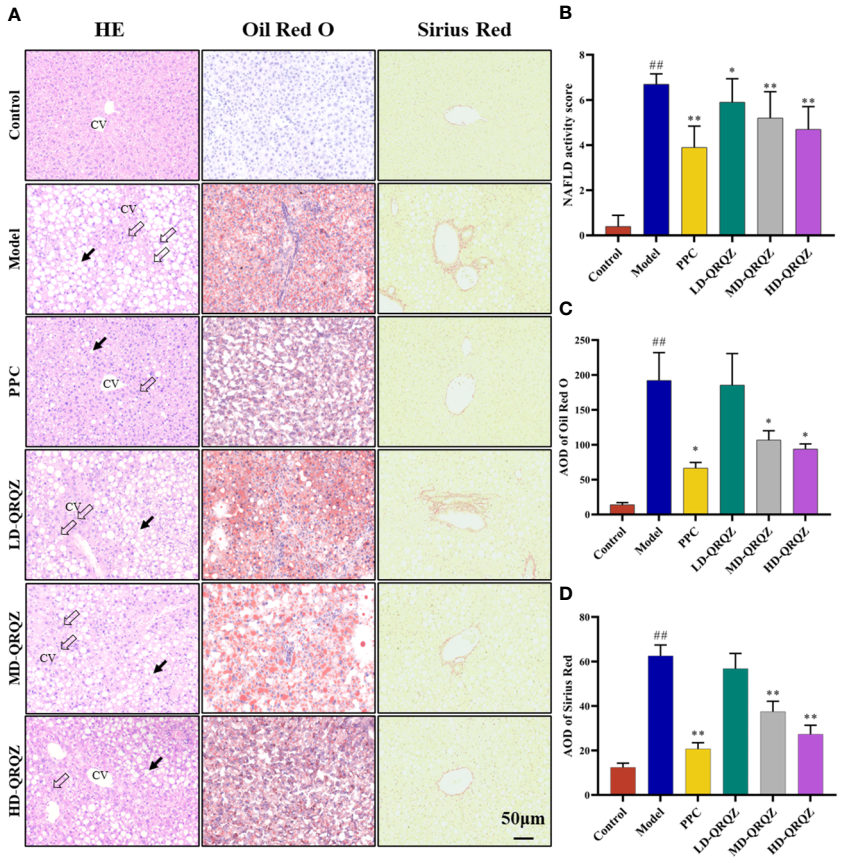


FIGURE 2
QRQZ alleviated hepatic pathological changes in MCD induced NASH mice. **(A)** HE staining, Oil Red O and Sirius Red staining of liver tissue. Black arrow indicated lipid accumulation. Hollow arrow indicated inflammatory foci. CV: Central vein. (200×). **(B-D)** NAS of HE staining of liver **(B)**. AOD of Oil Red O **(C)** and Sirius Red staining **(D)**. Data are presented as the mean ± standard deviation. ##$P$ < 0.01 as compared to the Control group; *$P$ < 0.05 as compared to the Model group; **$P$ < 0.01 as compared to the Model group.

## QRQZ treatment inhibited the activation of TLR4/NF-κB signaling pathway in the liver of NASH mice

The levels of TLR4, MyD88, p-IκB, and p-NF-κBp65, which are important factors of the TLR4/NF-κB signaling pathway, were measured in liver with western blotting. The results showed that the protein levels of TLR4 and MyD88 and the phosphorylation levels of IκB and NF-κBp65 were significantly increased in the liver of the model group compared to those in the control group; however, after high-dose of QRQZ treatment, the TLR4 and MyD88 protein levels and IκB and NF-κBp65 phosphorylation levels were significantly reduced in the mouse liver (Figures 5A, B). In addition, qPCR was used to measure the mRNA expression of *IL-1β*, *IL-6*, and *TNF-α* in the liver, important downstream target genes of TLR4/NF-κB, and the results showed that the mRNA expression of *IL-1β*, *IL-6*, and *TNF-α* was upregulated in the liver tissues of the NASH mice compared to that in the control group. In contrast, high-dose of QRQZ treatment

TABLE 1 Changes in physiological indices, oxidative stress factors after QRQZ treatment.

| | Biochemical Parameters | Control | Model | PPC | LD-QRQZ | MD-QRQZ | HD-QRQZ |
|---|---|---|---|---|---|---|---|
| **Liver lipid profile** | **TC** (μmol/g prot) | 82.8 ± 21.8 | 161.6 ± 41.6$^{\#\#}$ | 93.9 ± 36.9** | 113.7 ± 28.4* | 92.6 ± 32.8** | 91.9 ± 38.8** |
| | **TG** (μmol/g prot) | 120.2 ± 27.4 | 817.0 ± 51.7$^{\#\#}$ | 309.8 ± 40.4** | 721.2 ± 38.6** | 581.0 ± 50.4** | 514.3 ± 53.3** |
| **Liver function** | **ALT** (U/L) | 31.4 ± 14.1 | 207.0 ± 27.8$^{\#\#}$ | 71.4 ± 33.3** | 172.6 ± 45.0 | 143.6 ± 25.1** | 99.7 ± 46.4** |
| | **AST** (U/L) | 79.8 ± 24.6 | 216.7 ± 39.6$^{\#\#}$ | 134.2 ± 57.0** | 178.1 ± 50.9 | 164.2 ± 56.3* | 150.0 ± 42.9** |
| **Oxidative stress** | **SOD** (U/mg prot) | 196.4 ± 19.4 | 101.5 ± 33.0$^{\#\#}$ | 166.0 ± 20.8** | 129.5 ± 21.0* | 146.2 ± 19.6** | 153.6 ± 17.7** |
| | **MDA** (nmol/mg prot) | 5.5 ± 1.0 | 21.0 ± 1.9$^{\#\#}$ | 10.8 ± 2.2** | 16.1 ± 2.6** | 13.7 ± 2.8** | 12.6 ± 1.5** |
| | **GSH-Px** (U/mg prot) | 48.2 ± 4.5 | 25.4 ± 3.1$^{\#\#}$ | 37.5 ± 1.7** | 28.5 ± 2.0* | 30.0 ± 2.9** | 32.0 ± 3.3** |

Control, Model, PPC, LD-QRQZ, MD-QRQZ and HD-QRQZ (n = 10 per group) groups. Data are presented as the mean ± standard deviation. $^{\#\#}$P < 0.01 as compared to the Control group; *P < 0.05 as compared to the Model group; **P < 0.01 as compared to the Model group.

10.3389/fendo.2022.1106875

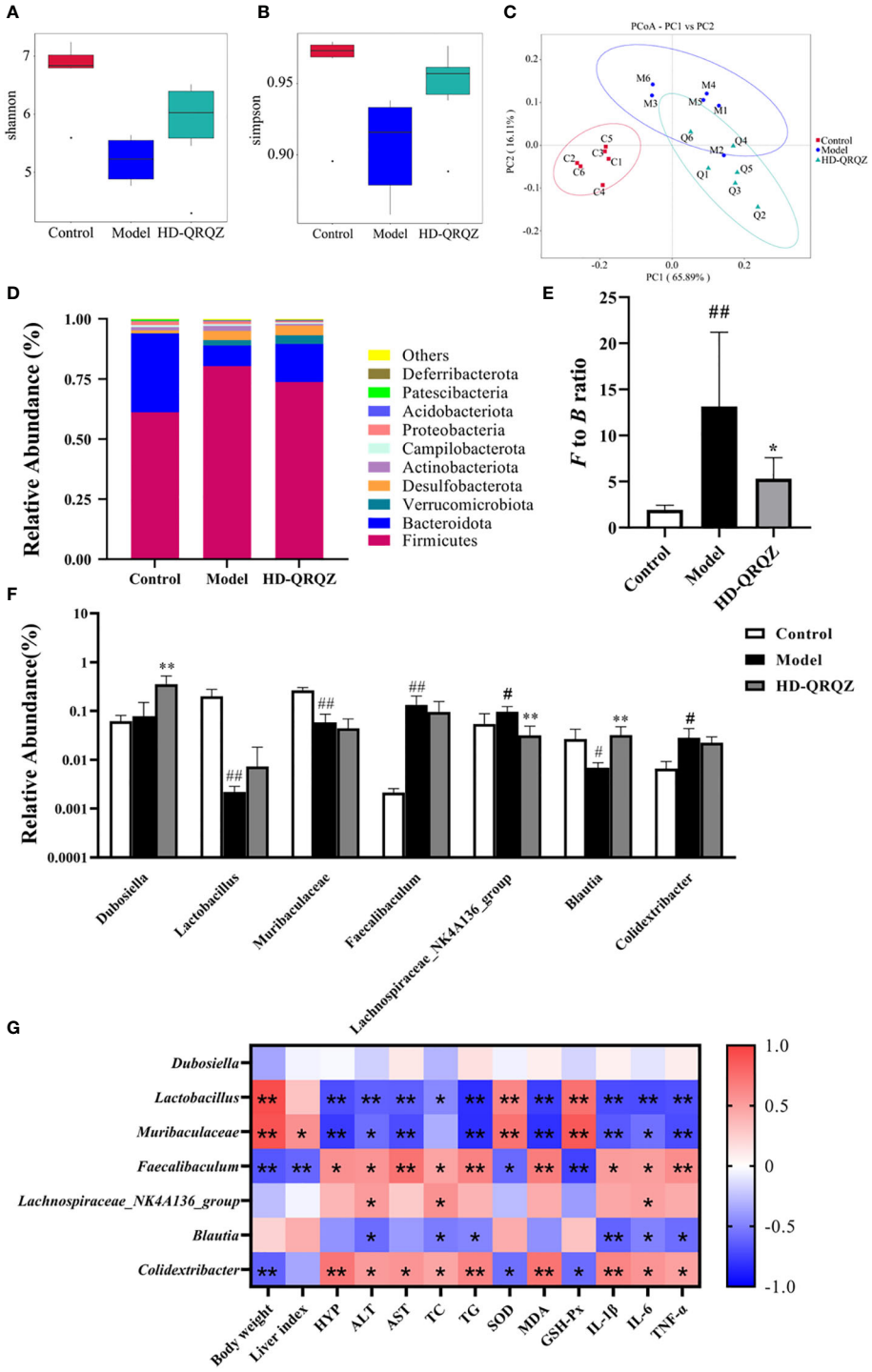


FIGURE 3
QRQZ treatment affected the gut microbiota community in Model mice. **(A, B)** Shannon and Simpson index was higher in HD-QRQZ group than that in the Model group. **(C)** PCoA indicated more similar beta diversity between HD-QRQZ and Control groups than that between the Model and Control groups (C: Control group; M: Model group; Q: HD-QRQZ group). **(D, E)** At the phylum level, QRQZ treatment decreased the *F* to *B* ratio in Model mice. **(F)** At the genus level, QRQZ treatment affected the relative abundances of *Dubosiella, Lachnospiraceae_NK4A136_group, Blautia*, in Model mice. **(G)** Correlation analysis of therapeutic indicators and changed gut microbiota using spearman's analysis (heatmap). Color coding scale indicates the pearson correlation coefficient from heatmap, the deeper red or blue indicates the higher absolute of the value. $^{*}P < 0.05$, $^{**}P < 0.01$. Control, Model and HD-QRQZ (n = 6 per group) groups. Data are presented as the mean ± standard deviation. $^{\#}p < 0.05$ as compared to the control group; $^{\#\#}P < 0.01$ as compared to the Control group; $^{*}P < 0.05$ as compared to the Model group; $^{**}P < 0.01$.

10.3389/fendo.2022.1106875

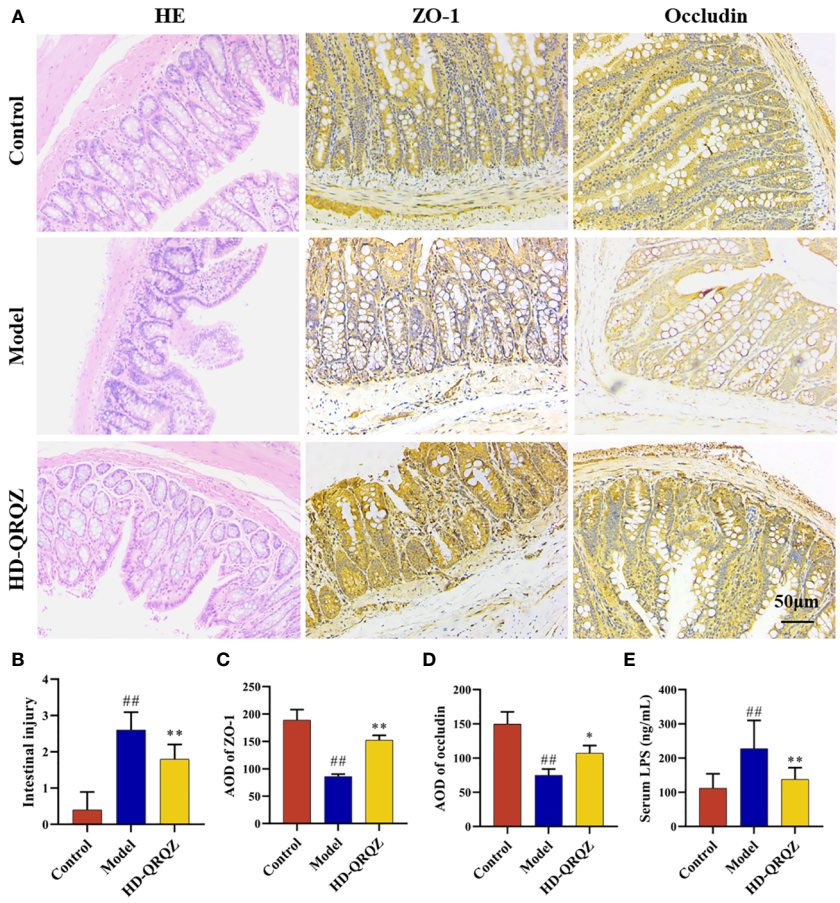


FIGURE 4
QRQZ improved the gut barrier. **(A)** HE staining of colon from each group and immunohistochemistry showed expression of ZO-1 and Occludin in colon. (200×) **(B)** Histological assessment of intestinal injury. **(C, D)** AOD of ZO-1 and Occludin. **(E)** Serum LPS levels of each group. Control, Model and HD-QRQZ (n = 6 per group) groups. Data are presented as the mean ± standard deviation. $^{\#\#}P < 0.01$ as compared to the Control group; $^{*}P < 0.05$ as compared to the Model group; $^{**}P < 0.01$ as compared to the Model group.

significantly downregulated the mRNA level of *IL-1β*, *IL-6*, and *TNF-α* in the liver of the NASH mice (Figure 5C).

## Discussion

In the present study, we generated NASH model mice based on MCD. The MCD is widely used in animal studies of NASH, and MCD-based models have replicated the histological features of steatohepatitis and fibrosis observed in human NASH, including steatosis, intralobular inflammation and hepatocyte ballooning (28). The advantage of choosing MCD for modeling is that it effectively and reproducibly induces liver steatosis and inflammation similar to human NASH histology in a relatively short period of time. Furthermore, male C57BL/6 mice show the most inflammation and necrosis as well as histological features that most similar to NASH (29). Although the MCD model lacks the key metabolic features of NASH, such as insulin resistance and obesity, which would lead to a significant decrease in the body mass of mice (28), it is still recognized as one of the major models of NASH because it manifests similar and equally severe histological features as human NASH (30). The generation mechanism of this model is deficiency of methionine and choline, which are necessary for hepatic β-oxidation and very-low-density lipoprotein (VLDL) production, whereas the lack of choline affects hepatic VLDL secretion, leading to lipid deposition in the liver. In addition, oxidative stress and changes in cytokines and adipocytokines can lead to liver damage (29). Our results also demonstrated a significant increase in the serum transaminase levels, as well as an increase in the liver TG level. Histological staining showed that the model mice had significant steatosis, fibrosis, and a large number of inflammatory cell infiltrates in the liver, which is consistent with the pathological changes of NASH. Liver fibrosis is also an important pathological feature of NASH, we also used Sirius red staining and tested the levels of HYP in liver to evaluate the liver fibrosis in each group. Our results showed that the collagen deposition and the levels of HYP were significantly increased in the NASH model mice. QRQZ significantly improved abnormal liver function in NASH mice while reducing hepatic lipid deposition and improving the liver fibrosis. Furthermore, studies have shown that *Morus alba* L. could inhibit lipogenesis in liver in obese mice (31). Hesperetin and Naringenin in *Citrus* × *aurantium* L could reduce hepatic steatosis NAFLD and NASH models (32, 33). *Rheum palmatum* L. could also ameliorate HFD-induced hepatic steatosis (34). These herbs and components may exert the major regulatory effects on hepatic steatosis. In addition, PPC was chosen as a positive control drug in this study, and PPC is commonly used in clinical

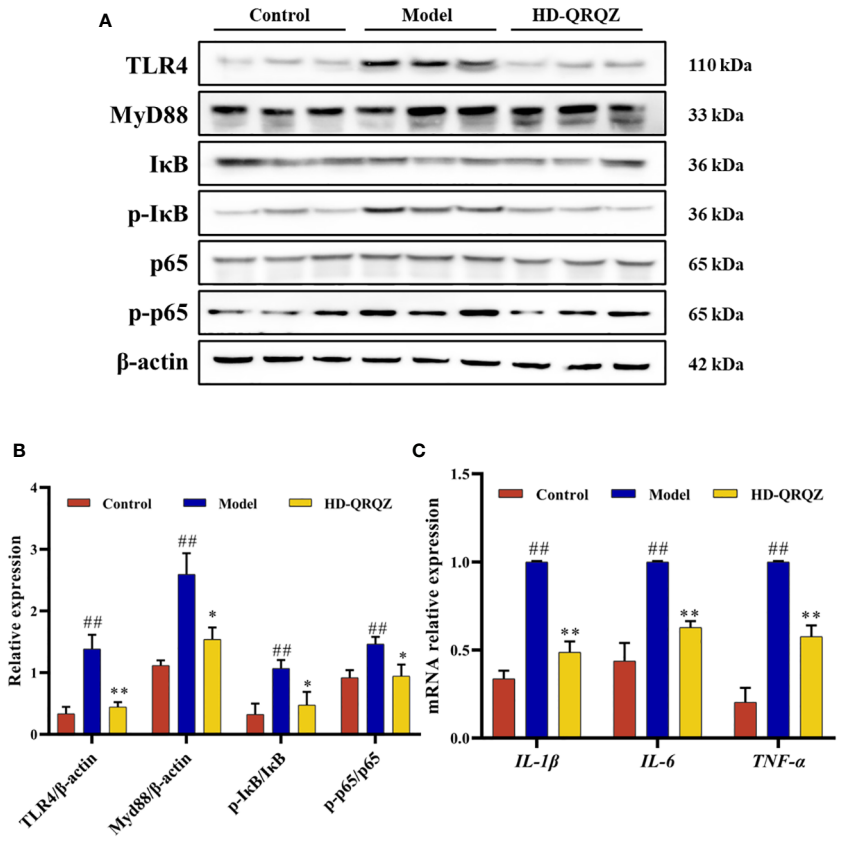


FIGURE 5
Effects of QRQZ on TLR4/NF-κB signaling pathway and mRNA expression of pro-inflammatory cytokines in liver. **(A, B)** The protein expression of TLR4, MyD88, IκB, p- IκB, p65, p- p65 in liver was detected by western blot. **(C)** mRNA expression of pro-inflammatory cytokines (*IL-1β*, *IL-6* and *TNF-α*) in liver was investigated using qPCR. Control, Model and HD-QRQZ (n = 3 per group) groups. Data are presented as the mean ± standard deviation. $^{\#\#}P < 0.01$ as compared to the Control group; $^{*}P < 0.05$ as compared to the Model group; $^{**}P < 0.01$ as compared to the Model group.

practice for the treatment of NASH (35). The outcomes of the present study revealed that there was no significant difference in the improvement of liver function or liver lipid deposition between the MD-QRQZ and HD-QRQZ interventions and PPC, thereby suggesting that QRQZ can be used as an alternative to PPC in the treatment of NASH.

Oxidative stress is an important pathological process in NASH. The results of this study showed that QRQZ increased the SOD and GSH-Px activities and decreased the MDA level in the NASH liver tissues. Cytokines are important inflammatory markers in NASH, and studies have found elevated concentrations of IL-1β, IL-6, and TNF-α in NASH patients, with TNF-α being the most significant (36, 37). This study showed that IL-1β, IL-6, and TNF-α levels were significantly increased in the liver of the model group, and the elevation of TNF-α was the most significant, which are consistent with previous studies. All inflammatory cytokines decreased in varying degrees after QRQZ treatment, with the most significant decreases achieved after administering medium and high doses. Besides, coptisine from *Coptis chinensis* Franchcan has been demonstrated with anti-inflammatory effect through inhibiting the activation of NF-κB (38). *Citrus* × *aurantium* L. and its flavonoids possessed multiple bioactive potentials including anti-oxidative and anti-inflammatory activities (39, 40). Carthamus red from *Carthamus tinctorius* L. exerted anti-oxidative effect in $CCl_4$-induced liver injury model rats (41). Previous studies have also demonstrated that *Smilax glabra* Roxb. and its active ingredients showed a wide range of pharmacological effects, including anti-inflammatory and anti-oxidative potentials (42). These herbs and components may exert the major anti-inflammatory and anti-oxidative effects in QRQZ.

Gut microbiota play an important role in NASH pathogenesis. In recent years, several pathways involving the gut–liver axis, gut barrier function, liver steatosis, and liver inflammation were suggested as the main mechanisms linking gut microbiota to NASH (43). Studies on the regulation of gut microbiota for treatment of NASH by antibiotic therapy and fecal transplantation have been performed in animals with favorable outcomes (44, 45), and clinical trials based on fecal transplantation are being conducted. The combined α- diversity and β-diversity in the 16S rRNA analysis in this study showed that the gut microbiota of the NASH model mice was severely disturbed, and the microbiota diversity and interpopulation differences were significantly changed, whereas the HD-QRQZ group showed higher population diversity, but failed to achieve a similar differential population structure to the control group. Changes in the *F/B* ratio are closely associated with many diseases. Although many studies have concluded that the *F/B* ratio is associated with obesity and NAFLD (46), fewer studies have associated the *F/B* ratio with NASH. This study showed that the *F/B* ratio in the NASH model group was significantly increased than that in the control group, whereas the

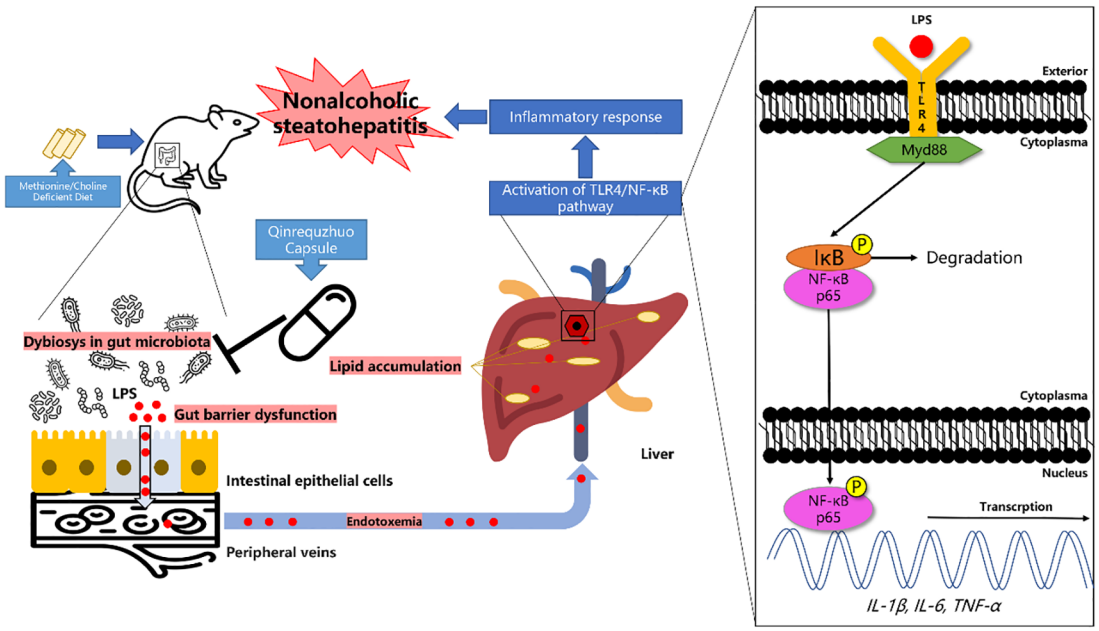


FIGURE 6
Graphical abstract.

ratio showed some improvement after treatment with HD-QRQZ, suggesting the *F/B* ratio as a potential reference for the diagnosis of NASH gut microbiota.

We also selected the top few bacteria with the greatest relative total abundance at the genus level for comparison. The relative abundance of *Faecalibaculum*, *Lachnospiraceae_NK4A136_group*, and *Colidextribacter* was significantly increased while the relative abundance of *Lactobacillus*, *Muribaculaceae*, *Blautia* was significantly decreased in the model group compared to that in the control group. HD-QRQZ could decrease the relative abundance of *Lachnospiraceae_NK4A136_group* and increase the relative abundance of *Dubosiella* and *Blautia*. *Dubosiella* abundance appeared to be negatively correlated with measures related to obesity and colonic inflammation (47–49). Several species under the genus *Lactobacillus* have been shown to improve lipid metabolism and inhibit lipid peroxidation (50, 51), and a clinical trial demonstrated that a mixed supplementation of several bacteria of the genus *Lactobacillus* improved liver fat accumulation and regulated gut microbiota (52). In this study, *Lactobacillus* has shown negative correlations with nearly all pathological indicators, suggesting that it may be a potentially beneficial bacterium. However, the results of this study found that QRQZ, although enhancing the level of *Lactobacillus* genus, failed to elevate its relative abundance to above 1%, so it is unclear whether this enhancement played a strong ameliorative role. *Muribaculaceae* is the producer of SCFAs such as succinic acid, acetic acid, and propionic acid, which have important anti-inflammatory properties as well as effects on glucose and lipid homeostasis (53). Moreover, several studies have confirmed a positive correlation between the increased abundance of *Muribaculaceae* and improvement in NAFLD (54, 55). Similar results were obtained in this study that *Muribaculaceae* had wide and negative correlations with therapeutic indicators. The abundance of *Faecalibaculum* is known to be significantly elevated in NAFLD mice, which was consistent with our results (56, 57). Positive correlations were also found between *Faecalibaculum* and most therapeutic indicators. According to studies, the abundance of family *Lachnospiraceae* is significantly increased in the feces of NAFLD patients (58), some drugs reduce the abundance of *Lachnospiraceae_NK4A136_group* while improving liver injury, and this genus of bacteria is positively correlated with ALT and AST (59). This study found the positive correlations between *Lachnospiraceae_NK4A136_group* and ALT, TC and IL-6 levels. *Blautia* is a controversial genus of bacteria that has been shown to be positively correlated with serum TG levels in patients with obesity and early NAFLD (60, 61). However, as a SCFA producer, the bacteria can produce acetic acid, have a probiotic function, and can influence the colonization of specific bacteria, all of which are supported by studies (62, 63). Our results also showed that the abundance of *Blautia* was negatively correlated with ALT, TC, TG, and cytokines in NASH mice. Taken together, we speculate that *Blautia* bacteria are involved in the regulation of gut microbiota in MCD-induced NASH mice, and that the acetic acid produced by *Blautia* may delay the development of NASH, although the pros and cons of this regulation are not yet known. *Colidextribacter* reportedly showed increased abundance in hyperlipidemic animals, which is positively correlated with serum TC (64, 65). This study showed that *Colidextribacter* had positive correlations with most therapeutic indicators. So we hypothesize that its elevated abundance in NASH mice may be associated with the development of hyperlipidemia. In summary, our results demonstrated that HD-QRQZ could regulate the disordered gut microbiota in NASH mice, and this alteration may have a potential association with improved lipid metabolism. Besides, aqueous extract of *Morus alba* L. could reinforce *Muribaculaceae* while polyphenols and polysaccharides from *Morus alba* L. could increase *Lachnospiraceae_NK4A136_group* and decrease *Faecalibaculum* in mice fed with HFD (66, 67). *Coptis chinensis* Franchcan could

increase the abundance of *Blautia* in ulcerative colitis rats (68). Water extract of *Anemarrhena asphodeloides* Bunge could also increase the abundance of *Blautia* in diabetic rats (69). Hydroxysafflor yellow A extracted from *Carthamus tinctorius* L. could reverse gut microbiota dysbiosis in mice fed with HFD (70). An anthraquinone-glycoside from *Rheum palmatum* L. could increase the abundance of *Lactobacillus* while decrease the abundance of *Lachnospiraceae_NK4A136_group* in T2DM rats (71). *Dioscorea oppositifolia* L. could increase the amount of *Lactobacillus* in mice with diarrhea (72). These herbs and components may exert the major regulatory effects on gut microbiota.

We then examined the effects of QRQZ on the expression of gut tight junction proteins ZO-1 and occludin in the NASH mice *via* immunohistochemistry, and also measured the serum LPS level. The results showed that QRQZ significantly increased the expression of ZO-1 and occludin in the intestine of the NASH mice, and decreased the serum LPS level. Barrier function is a fundamental role of all epithelial cells and is based on the integrity and contribution of many cytoskeletal and membrane proteins that constitute and regulate the tight-junction complexes that exist between cells (73). Studies have shown that the colon is the main site of leakage owing to disruption of the barrier function in NASH patients (74), which leads various microbial products to enter the internal environment, such as inflammation-triggering LPS. Both ZO-1 and occludin are tight junction proteins that play key roles in maintaining the integrity of the gut barrier, and animal experiments have demonstrated that elevated expression of them can reduce gut permeability (75, 76). LPS is an important component of the gut microbiota cell wall. When the gut mucosal barrier is damaged, the gut microbiota LPS can be released into the blood, which consequently aggravates the inflammatory response of the body (77).

Further study showed that QRQZ reduced important factors of the TLR4/NF-κB signaling pathway, TLR4, MyD88, p-IκB and p-NF-κBp65 in the liver of NASH mice, and downregulated the gene expression of pro-inflammatory cytokines IL-1β, IL-6, and TNF-α in the liver. Endotoxins can induce an inflammatory response by activating liver inflammatory cells. TLR4 is an important member of the Toll-like receptor family and is a receptor of LPS. LPS enters the liver and binds to TLR4, thereby promoting massive expression and activation of TLR4. Activated TLR4 then recruits MyD88 in the cells to bind to itself to form a dimer, which in turn causes NF-κB activation. NF-κB is an important nuclear transcription factor that plays an important regulatory role in the inflammatory response. NF-κB is a heterodimer composed of p50 and p65. Under normal conditions, NF-κB binds to its inhibitory protein, IκB, to form an inactive trimer that is present in the cytoplasm. MyD88 phosphorylates IκB, and the phosphorylated IκB dissociates from the NF-κB complex, which in turn leads to phosphorylation of the NF-κBp65 subunit, and the p-NF-κBp65 enters the nucleus and promotes the expression of pro-inflammatory cytokines such as IL-1β, IL-6, and TNF-α, facilitating the inflammatory response (78). A study showed that knockout of myeloid differentiation factor 2 (MD2) and TLR4 genes abrogated liver injury and inflammation in a mouse model of MCD-induced NASH (79).

In conclusion, our study demonstrated that QRQZ could reduce the lipid accumulation and inflammatory response in NASH model mice. The mechanisms of QRQZ on NASH were associated with modulating gut microbiota, thereby inducing the tight junction of gut barrier, reducing the endotoxemia and inhibiting the activation of TLR4/NF-κB signaling pathway in liver (Figure 6).

## Data availability statement

The data presented in the study are deposited in the BioProject repository, accession number PRJNA904915.

## Ethics statement

The animal study was approved by Ethics Committee of Hebei University of Chinese Medicine (Approval no. CZX2021-KY-026).

## Author contributions

SL and XS carried out the experiments and manuscript writing. SL, XW, BP and HL provided experimental help. ZZ, HZ and XS performed data analysis and result interpretation. WL supervised the experiments. YW and XS provided ideas and technical guidance for the whole work. All authors contributed to the article and approved the submitted version.

## Funding

This work was supported by the Scientific Program Project of Administration of Traditional Chinese Medicine in Hebei Province Administration of Traditional Chinese Medicine in Hebei Province.(No. 2021311). The Construction Project of Workshop of Prestigious Chinese Physician Xiuhai Su (2022-75).

## Conflict of interest

The authors declare that the research was conducted in the absence of any commercial or financial relationships that could be construed as a potential conflict of interest.

## Publisher's note



## Supplementary material

The Supplementary Material for this article can be found online at: https://www.frontiersin.org/articles/10.3389/fendo.2022.1106875/full#supplementary-material

# References


1. Kanwal F, Shubrook JH, Younossi Z, Natarajan Y, Bugianesi E, Rinella ME, et al. Preparing for the NASH epidemic: A call to action. *Gastroenterology* (2021) 161:1030–1042.e8. doi: 10.1053/j.gastro.2021.04.074

2. Sheka AC, Adeyi O, Thompson J, Hameed B, Crawford PA, Ikramuddin S. Nonalcoholic steatohepatitis. *JAMA* (2020) 323:1175. doi: 10.1001/jama.2020.2298

3. Luo J, Liao J, Wang Y, Zhao J, Xie X, Qu F, et al. Advances in traditional Chinese medicine for liver disease therapy in 2021. *Traditional Med Res* (2022) 7:58. doi: 10.53388/tmr20220219002

4. Xu J, Wang R, You S, Zhang L, Zheng P, Ji G, et al. Traditional Chinese medicine lingguizhugan decoction treating non-alcoholic fatty liver disease with spleen-yang deficiency pattern: Study protocol for a multicenter randomized controlled trial. *Trials* (2020) 21(1):512. doi: 10.1186/s13063-020-04362-7

5. Huang C-Y, Wu M-Y, Wang H-C, Liao Y-C, Tou S-I, Yen H-R. Chinese Herbal medicine decreases incidence of cirrhosis in patients with non-alcoholic fatty liver disease in Taiwan: A propensity score-matched cohort study. *J Altern Complementary Med* (2021) 27(7):596-605. doi: 10.1089/acm.2020.0494

6. Shi K-Q, Fan Y-C, Liu W-Y, Li L-F, Chen Y-P, Zheng M-H. Traditional Chinese medicines benefit to nonalcoholic fatty liver disease: A systematic review and meta-analysis. *Mol Biol Rep* (2012) 39:9715–22. doi: 10.1007/s11033-012-1836-0

7. Lozupone CA, Stombaugh JI, Gordon JI, Jansson JK, Knight R. Diversity, stability and resilience of the human gut microbiota. *Nature* (2012) 489:220–30. doi: 10.1038/nature11550

8. Meroni M, Longo M, Dongiovanni P. The role of probiotics in nonalcoholic fatty liver disease: A new insight into therapeutic strategies. *Nutrients* (2019) 11:2642. doi: 10.3390/nu11112642

9. Qin J, Li R, Raes J, Arumugam M, Burgdorf KS, Manichanh C, et al. A human gut microbial gene catalogue established by metagenomic sequencing. *Nature* (2010) 464:59–65. doi: 10.1038/nature08821

10. Michail S, Lin M, Frey MR, Fanter R, Paliy O, Hilbush B, et al. Altered gut microbial energy and metabolism in children with non-alcoholic fatty liver disease. *FEMS Microbiol Ecol* (2014) 91:1–9. doi: 10.1093/femsec/fiu002

11. Zahra M, Hossein P, Nazgol M-G, Sareh E, Azita H, Parastoo S, et al. Fecal microbiota in non-alcoholic fatty liver disease and non-alcoholic steatohepatitis: A systematic review. *Arch Iranian Med* (2020) 23:44–52.

12. Arab JP, Arrese M, Shah VH. Gut microbiota in non-alcoholic fatty liver disease and alcohol-related liver disease: Current concepts and perspectives. *Hepatol Res* (2020) 50:407–18. doi: 10.1111/hepr.13473

13. Zhou D, Pan Q, Xin F-Z, Zhang R-N, He C-X, Chen G-Y, et al. Sodium butyrate attenuates high-fat diet-induced steatohepatitis in mice by improving gut microbiota and gastrointestinal barrier. *World J Gastroenterol* (2017) 23:60. doi: 10.3748/wjg.v23.i1.60

14. Zhao Z-H, Xin F-Z, Xue Y, Hu Z, Han Y, Ma F, et al. Indole-3-propionic acid inhibits gut dysbiosis and endotoxin leakage to attenuate steatohepatitis in rats. *Exp Mol Med* (2019) 51:1–14. doi: 10.1038/s12276-019-0304-5

15. Xiong F, Zheng Z, Xiao L, Su C, Chen J, Gu X, et al. Soyasaponin a 2 alleviates steatohepatitis possibly through regulating bile acids and gut microbiota in the methionine and choline-deficient (MCD) diet-induced nonal. *Mol Nutr Food Res* (2021) 65:2100067. doi: 10.1002/mnfr.202100067

16. Brandl K, Schnabl B. Intestinal microbiota and nonalcoholic steatohepatitis. *Curr Opin Gastroenterol* (2017) 33:128–33. doi: 10.1097/mog.0000000000000349

17. Liao J, Xie X, Gao J, Zhang Z, Qu F, Cui H, et al. Jian-Gan-Xiao-Zhi decoction alleviates inflammatory response in nonalcoholic fatty liver disease model rats through modulating gut microbiota. *Evidence-Based Complementary Altern Med* (2021) 2021:1–13. doi: 10.1155/2021/5522755

18. Li C, Zhou K, Xiao N, Peng M, Tan Z. The effect of qiweibaizhu powder crude polysaccharide on antibiotic-associated diarrhea mice is associated with restoring intestinal mucosal bacteria. *Front Nutr* (2022) 9:952647. doi: 10.3389/fnut.2022.952647

19. Long C-X, Shao H-Q, Luo C-Y, Yu R, Tan Z-J. Bacterial diversity in the intestinal mucosa of dysbiosis diarrhea mice treated with qiweibaizhu powder. *Gastroenterol Res Pract* (2020) 2020:1–8. doi: 10.1155/2020/9420129

20. Xie G, Deng N, Zheng T, Peng X, Zhang S, Tan Z. Total glycosides contribute to the anti-diarrheal effects of qiwei baizhu powder *via* regulating gut microbiota and bile acids. *Front Cell Infection Microbiol* (2022) 12:945263. doi: 10.3389/fcimb.2022.945263

21. Xiao S, Liu C, Chen M, Zou J, Zhang Z, Cui X, et al. Scutellariae radix and coptidis rhizoma ameliorate glycolipid metabolism of type 2 diabetic rats by modulating gut microbiota and its metabolites. *Appl Microbiol Biotechnol* (2019) 104:303–17. doi: 10.1007/s00253-019-10174-w

22. Zhang Z, Jia C, Qi Y, Wang X, Su X, Wang Y, et al. Clinical observation on curative effects of Qing-Re-Qu-Zhuo capsule in treatment of type 2 diabetes mellitus and nonalcoholic fatty liver disease. *Acta Chin Med Pharmacol* (2013) 41:3. doi: CNKI:SUN:ZYXB.0.2013-06-025

23. Li H, Xi Y, Xin X, Tian H, Hu Y. Salidroside improves high-fat diet-induced non-alcoholic steatohepatitis by regulating the gut microbiota–bile acid–farnesoid X receptor axis. *Biomed Pharmacother* (2020) 124:109915. doi: 10.1016/j.biopha.2020.109915

24. Kleiner DE, Brunt EM, Natta MV, Behling C, Contos MJ, Cummings OW, et al. Design and validation of a histological scoring system for nonalcoholic fatty liver disease. *Hepatology* (2005) 41:1313–21. doi: 10.1002/hep.20701

25. Oktar BK, Gülpinar MA, Bozkurt A, Ghandour S, Çetinel Ş, Moini H, et al. Endothelin receptor blockers reduce I/R-induced intestinal mucosal injury: Role of blood flow. *Am J Physiology-Gastrointestinal Liver Physiol* (2002) 282:G647–55. doi: 10.1152/ajpgi.2002.282.4.g647

26. Escorcia W, Ruter DL, Nhan J, Curran SP. Quantification of lipid abundance and evaluation of lipid distribution in caenorhabditis elegans by Nile red and oil red O staining. *J Visualized Experiments* (2018) 5;(133):57352. doi: 10.3791/57352

27. Taylor CR, Levenson RM. Quantification of immunohistochemistry? Issues concerning methods, utility and semiquantitative assessment II. *Histopathology* (2006) 49:411–24. doi: 10.1111/j.1365-2559.2006.02513.x

28. Takahashi Y. Animal models of nonalcoholic fatty liver disease/nonalcoholic steatohepatitis. *World J Gastroenterol* (2012) 18:2300. doi: 10.3748/wjg.v18.i19.2300

29. Peng C, Stewart AG, Woodman OL, Ritchie RH, Qin CX. Non-alcoholic steatohepatitis: A review of its mechanism, models and medical treatments. *Front Pharmacol* (2020) 11:603926. doi: 10.3389/fphar.2020.603926

30. Li H, Toth E, Cherrington NJ. Asking the right questions with animal models: Methionine- and choline-deficient model in predicting adverse drug reactions in human NASH. *Toxicol Sci* (2017) 161:23–33. doi: 10.1093/toxsci/kfx253

31. Ann J-Y, Eo H, Lim Y. Mulberry leaves (Morus alba l.) ameliorate obesity-induced hepatic lipogenesis, fibrosis, and oxidative stress in high-fat diet-fed mice. *Genes Nutr* (2015) 10(6):46. doi: 10.1007/s12263-015-0495-x

32. Li J, Wang T, Liu P, Yang F, Wang X, Zheng W, et al. Hesperetin ameliorates hepatic oxidative stress and inflammation *via* the PI3K/AKT-Nrf2-ARE pathway in oleic acid-induced HepG2 cells and a rat model of high-fat diet-induced NAFLD. *Food Funct* (2021) 12:3898–918. doi: 10.1039/d0fo02736g

33. Hua YQ, Zeng Y, Xu J, Xu XL. Naringenin alleviates nonalcoholic steatohepatitis in middle-aged apoe–/–mice: role of SIRT1. *Phytomedicine* (2021) 81:153412. doi: 10.1016/j.phymed.2020.153412

34. Yang M, Li X, Zeng X, Ou Z, Xue M, Gao D, et al. Rheum palmatum l. attenuates high fat diet-induced hepatosteatosis by activating AMP-activated protein kinase. *Am J Chin Med* (2016) 44:551–64. doi: 10.1142/s0192415x16500300

35. Hong-ling S, Yu-xia Z, Zheng-jun G, Xu-yang D, Jiang-yi Z, Wei-rong L, et al. Efficacy comparison between bicyclol and polyene phosphatidylcholine treatments for the patients with nonalcoholic fatty liver disease. *Chin J Hepatol* (2011) 19:552–3. doi: 10.3760/cma.j.issn.1007-3418.2011.07.019

36. Mridha AR, Wree A, Robertson AAB, Yeh MM, Johnson CD, Rooyen DMV, et al. NLRP3 inflammasome blockade reduces liver inflammation and fibrosis in experimental NASH in mice. *J Hepatol* (2017) 66:1037–46. doi: 10.1016/j.jhep.2017.01.022

37. Kugelmas M. Cytokines and NASH: A pilot study of the effects of lifestyle modification and vitamin e. *Hepatology* (2003) 38:413–9. doi: 10.1053/jhep.2003.50316

38. Wu J, Luo Y, Deng D, Su S, Li S, Xiang L, et al. Coptisine from coptis chinensis exerts tderse beneficial properties: A concise review. *J Cell Mol Med* (2019) 23:7946–60. doi: 10.1111/jcmm.14725

39. Suntar I, Khan H, Patel S, Celano R, Rastrelli L. An overview onCitrus aurantiumL.: Its functions as food ingredient and therapeutic agent. *Oxid Med Cell Longevity* (2018) 2018:1–12. doi: 10.1155/2018/7864269

40. He W, Li Y, Liu M, Yu H, Chen Q, Chen Y, et al. Citrus aurantium l. and its flavonoids regulate TNBS-induced inflammatory bowel disease through anti-inflammation and suppressing isolated jejunum contraction. *Int J Mol Sci* (2018) 19:3057. doi: 10.3390/ijms19103057

41. Wu S, Yue Y, Tian H, Li Z, Li X, He W, et al. Carthamus red from carthamus tinctorius l. exerts antioxidant and hepatoprotective effect against CCl4-induced liver damage in rats *via* the Nrf2 pathway. *J Ethnopharmacol* (2013) 148:570–8. doi: 10.1016/j.jep.2013.04.054

42. Wu H, Wang Y, Zhang B, Li Y, Ren Z, Huang J, et al. Smilax glabra roxb.: A review of its traditional usages, phytochemical constituents, pharmacological properties, and clinical applications. *Drug Design Dev Ther* (2022) 16:3621–43. doi: 10.2147/dddt.s374439

43. Kolodziejczyk AA, Zheng D, Shibolet O, Elinav E. The role of the microbiome in NAFLD and NASH. *EMBO Mol Med* (2018) 11(2):e9302. doi: 10.15252/emmm.201809302

44. Zhou D, Pan Q, Shen F, Cao H, Ding W, Chen Y, et al. Total fecal microbiota transplantation alleviates high-fat diet-induced steatohepatitis in mice *via* beneficial regulation of gut microbiota. *Sci Rep* (2017) 7(1):1529. doi: 10.1038/s41598-017-01751-y

45. Ma J, Zhou Q, Li H. Gut microbiota and nonalcoholic fatty liver disease: Insights on mechanisms and therapy. *Nutrients* (2017) 9:1124. doi: 10.3390/nu9101124

46. Gangarapu V, Yildiz K, Ince AT, Baysal B. Role of gut microbiota: Obesity and NAFLD. *Turkish J Gastroenterol* (2014) 25:133–40. doi: 10.5152/tjg.2014.7886

47. Wan F, Han H, Zhong R, Wang M, Tang S, Zhang S, et al. Dihydroquercetin supplement alleviates colonic inflammation potentially through improved gut microbiota community in mice. *Food Funct* (2021) 12:11420–34. doi: 10.1039/d1fo01422f

48. Hu M, Zhang L, Ruan Z, Han P, Yu Y. The regulatory effects of citrus peel powder on liver metabolites and gut flora in mice with non-alcoholic fatty liver disease (NAFLD). *Foods* (2021) 10:3022. doi: 10.3390/foods10123022

49. Guo X, Cao X, Fang X, Guo A, Li E. Inhibitory effects of fermented ougan (Citrus reticulata cv. suavissima) juice on high-fat diet-induced obesity associated with white adipose tissue browning and gut microbiota modulation in mi. *Food Funct* (2021) 12:9300–14. doi: 10.1039/d0fo03423a

50. Li X, Liu Y, Guo X, Ma Y, Zhang H, Liang H. Effect of lactobacillus casei on lipid metabolism and intestinal microflora in patients with alcoholic liver injury. *Eur J Clin Nutr* (2021) 75:1227–36. doi: 10.1038/s41430-020-00852-8

51. Lin M-Y, Yen C-L. Inhibition of lipid peroxidation by lactobacillus acidophilus and bifidobacterium longum. *J Agric Food Chem* (1999) 47:3661–4. doi: 10.1021/jf981235l

52. Wong VW-S, Tse C-H, Lam TT-Y, Wong GL-H, Chim AM-L, Chu WC-W, et al. Molecular characterization of the fecal microbiota in patients with nonalcoholic steatohepatitis – a longitudinal study. *PloS One* (2013) 8:e62885. doi: 10.1371/journal.pone.0062885

53. Francino MP. The gut microbiome and metabolic health. *Curr Nutr Rep* (2017) 6:16–23. doi: 10.1007/s13668-017-0190-1

54. Chen J, Ding X, Wu R, Tong B, Zhao L, Lv H, et al. Novel sesquiterpene glycoside from loquat leaf alleviates type 2 diabetes mellitus combined with nonalcoholic fatty liver disease by improving insulin resistance, oxidative stress, inflammation and G. *J Agric Food Chem* (2021) 69:14176–91. doi: 10.1021/acs.jafc.1c05596

55. Chen H, Sun Y, Zhao H, Qi X, Cui H, Li Q, et al. α-lactalbumin peptide asp-Gln-Trp alleviates hepatic insulin resistance and modulates gut microbiota dysbiosis in high-fat diet-induced NAFLD mice. *Food Funct* (2022) 13(19):9878-92. doi: 10.1039/d2fo01343f

56. Luo X, Zhang B, Pan Y, Gu J, Tan R, Gong P. Phyllanthus emblica aqueous extract retards hepatic steatosis and fibrosis in NAFLD mice in association with the reshaping of intestinal microecology. *Front Pharmacol* (2022) 13:893561. doi: 10.3389/fphar.2022.893561

57. Gu C, Zhou Z, Yu Z, He M, He L, Luo Z, et al. The microbiota and it's correlation with metabolites in the gut of mice with nonalcoholic fatty liver disease. *Front Cell Infection Microbiol* (2022) 12:870785. doi: 10.3389/fcimb.2022.870785

58. Shen F, Zheng R-D, Sun X-Q, Ding W-J, Wang X-Y, Fan J-G. Gut microbiota dysbiosis in patients with non-alcoholic fatty liver disease. *Hepatobiliary Pancreatic Dis Int* (2017) 16:375–81. doi: 10.1016/s1499-3872(17)60019-5

59. Liu Q, Cai B, Zhu L, Xin X, Wang X, An Z, et al. Liraglutide modulates gut microbiome and attenuates nonalcoholic fatty liver in db/db mice. *Life Sci* (2020) 261:118457. doi: 10.1016/j.lfs.2020.118457

60. Goffredo M, Mass K, Parks EJ, Wagner DA, McClure EA, Graf J, et al. Role of gut microbiota and short chain fatty acids in modulating energy harvest and fat partitioning in youth. *J Clin Endocrinol Metab* (2016) 101:4367–76. doi: 10.1210/jc.2016-1797

61. Carbajo-Pescador S, Porras D, García-Mediavilla MV, Martínez-Flórez S, Juarez-Fernández M, Cuevas MJ, et al. Beneficial effects of exercise on gut microbiota functionality and barrier integrity, and gut-liver axis crosstalk in an *in vivo* model of early obesity and NAFLD. *Dis Models Mech* (2019) 12(5):dmm039206. doi: 10.1242/dmm.039206

62. Aoki R, Onuki M, Hattori K, Ito M, Yamada T, Kamikado K, et al. Commensal microbe-derived acetate suppresses NAFLD/NASH development *via* hepatic FFAR2 signalling in mice. *Microbiome* (2021) 9(1):188. doi: 10.1186/s40168-021-01125-7

63. Hosomi K, Saito M, Park J, Murakami H, Shibata N, Ando M, et al. Oral administration of blautia wexlerae ameliorates obesity and type 2 diabetes *via* metabolic remodeling of the gut microbiota. *Nat Commun* (2022) 13(1):4477. doi: 10.1038/s41467-022-32015-7

64. Yan S, Chen J, Zhu L, Guo T, Qin D, Hu Z, et al. Oryzanol alleviates high fat and cholesterol diet-induced hypercholesterolemia associated with the modulation of the gut microbiota in hamsters. *Food Funct* (2022) 13:4486–501. doi: 10.1039/d1fo03464b

65. Duan R, Guan X, Huang K, Zhang Y, Li S, Xia J, et al. Flavonoids from whole-grain oat alleviated high-fat diet-induced hyperlipidemia *via* regulating bile acid metabolism and gut microbiota in mice. *J Agric Food Chem* (2021) 69:7629–40. doi: 10.1021/acs.jafc.1c01813

66. Du Y, Li D, Lu D, Zhang R, Zheng X, Xu B, et al. Morus alba l. water extract changes gut microbiota and fecal metabolome in mice induced by high-fat and high-sucrose diet plus low-dose streptozotocin. *Phytother Res* (2022) 36:1241–57. doi: 10.1002/ptr.7343

67. Wan M, Li Q, Lei Q, Zhou D, Wang S. Polyphenols and polysaccharides from morus alba l. fruit attenuate high-fat diet-induced metabolic syndrome modifying the gut microbiota and metabolite profile. *Foods* (2022) 11:1818. doi: 10.3390/foods11121818

68. Xie Q, Li H, Ma R, Ren M, Li Y, Li J, et al. Effect of coptis chinensis franch and magnolia officinalis on intestinal flora and intestinal barrier in a TNBS-induced ulcerative colitis rats model. *Phytomedicine* (2022) 97:153927. doi: 10.1016/j.phymed.2022.153927

69. Yan D, Fan P, Sun W, Ding Q, Zheng W, Xiao W, et al. Anemarrhena asphodeloides modulates gut microbiota and restores pancreatic function in diabetic rats. *Biomed Pharmacother* (2021) 133:110954. doi: 10.1016/j.biopha.2020.110954

70. Liu J, Yue S, Yang Z, Feng W, Meng X, Wang A, et al. Oral hydroxysafflor yellow a reduces obesity in mice by modulating the gut microbiota and serum metabolism. *Pharmacol Res* (2018) 134:40–50. doi: 10.1016/j.phrs.2018.05.012

71. Cui H-X, Zhang L-S, Luo Y, Yuan K, Huang Z-Y, Guo Y. A purified anthraquinone-glycoside preparation from rhubarb ameliorates type 2 diabetes mellitus by modulating the gut microbiota and reducing inflammation. *Front Microbiol* (2019) 10:1423. doi: 10.3389/fmicb.2019.01423

72. Zhang N, Liang T, Jin Q, Shen C, Zhang Y, Jing P. Chinese Yam (Dioscorea opposita thunb.) alleviates antibiotic-associated diarrhea, modifies intestinal microbiota, and increases the level of short-chain fatty acids in mice. *Food Res Int* (2019) 122:191–8. doi: 10.1016/j.foodres.2019.04.016

73. Hull BE, Staehelin LA. The terminal web. a reevaluation of its structure and function. *J Cell Biol* (1979) 81:67–82. doi: 10.1083/jcb.81.1.67

74. Farhadi A, Gundlapalli S, Shaikh M, Frantzides C, Harrell L, Kwasny MM, et al. Susceptibility to gut leakiness: a possible mechanism for endotoxaemia in non-alcoholic steatohepatitis. *Liver Int* (2008) 28:1026–33. doi: 10.1111/j.1478-3231.2008.01723.x

75. Musch MW, Walsh-Reitz MM, Chang EB. Roles of ZO-1, occludin, and actin in oxidant-induced barrier disruption. *Am J Physiology-Gastrointestinal Liver Physiol* (2006) 290:G222–31. doi: 10.1152/ajpgi.00301.2005

76. Zhang B, Guo Y. Supplemental zinc reduced intestinal permeability by enhancing occludin and zonula occludens protein-1 (ZO-1) expression in weaning piglets. *Br J Nutr* (2009) 102:687–93. doi: 10.1017/s0007114509289033

77. Fuke N, Nagata N, Suganuma H, Ota T. Regulation of gut microbiota and metabolic endotoxemia with dietary factors. *Nutrients* (2019) 11:2277. doi: 10.3390/nu11102277

78. Saha M, Manna K, Saha KD. Melatonin suppresses NLRP3 inflammasome activation *via* TLR4/NF-κB and P2X7R signaling in high-fat diet-induced murine NASH model. *J Inflammation Res* (2022) 15:3235–58. doi: 10.2147/jir.s343236

79. Csak T, Velayudham A, Hritz I, Petrasek J, Levin I, Lippai D, et al. Deficiency in myeloid differentiation factor-2 and toll-like receptor 4 expression attenuates nonalcoholic steatohepatitis and fibrosis in mice. *Am J Physiology-Gastrointestinal Liver Physiol* (2011) 300:G433–41. doi: 10.1152/ajpgi.00163.2009

frontiers | Frontiers in Endocrinology

TYPE Original Research
PUBLISHED 25 January 2023
DOI 10.3389/fendo.2022.1102605



OPEN ACCESS

EDITED BY
Zhoujin Tan,
Hunan University of Chinese Medicine, China

REVIEWED BY
Zipeng Gong,
Guizhou Medical University, China
Bo Hong,
Qiqihar Medical University, China
Yuelei Jin,
Taizhou University, China

*CORRESPONDENCE
Lihong Wang
wlh_6663@163.com
Hong Zhao
zhaohong1981@jmsu.edu.cn

†These authors have contributed equally to this work and share first authorship

SPECIALTY SECTION
This article was submitted to Gut Endocrinology, a section of the journal Frontiers in Endocrinology

RECEIVED 19 November 2022
ACCEPTED 12 December 2022
PUBLISHED 25 January 2023

CITATION
Ping Y, Li C, Wang L and Zhao H (2023) Effects of *Atractylodes Macrocephala Rhizoma* polysaccharide on intestinal microbiota composition in rats with mammary gland hyperplasia. *Front. Endocrinol.* 13:1102605. doi: 10.3389/fendo.2022.1102605



# Effects of *Atractylodes Macrocephala Rhizoma* polysaccharide on intestinal microbiota composition in rats with mammary gland hyperplasia

Yang Ping†, Changxu Li†, Lihong Wang* and Hong Zhao*

College of Pharmacy, Jiamusi University, Jiamusi, Heilongjiang, China

**Background:** In recent years, mammary gland hyperplasia (MGH) has been considered to be one of the diseases caused by endocrine disorders. It has been shown that diseases caused by endocrine disorders can be treated by regulating intestinal microbial. As a commonly used medicine in clinical practice, *Atractylodes Macrocephala Rhizoma* has good functions in regulating intestinal homeostasis. Therefore, this paper studied the effect of *Atractylodes Macrocephala Rhizoma* polysaccharide (AMP) on the intestinal flora of MGH rats, providing a new idea for polysaccharide treatment of MGH.

**Materials and methods:** Eighteen female SD rats were selected and randomly divided into three groups: blank control group (Con), model control group (Mod), and AMP group, six rats in each group. MGH rat models were established by estradiol-progesterone combination and treated with AMP gastric infusion. The levels of $E_2$, P, and PRL in the serum of rats were measured, the intestinal contents were collected, and 16s rRNA high- throughput sequencing technology was analyzed the changes of intestinal flora in the MGH rats.

**Results:** AMP has good therapeutic effects on MGH rats, decreasing estradiol ($E_2$) and prolactin (PRL) levels and increasing progesterone (P) levels; at the same time, it can regulate the abundance and diversity of intestinal flora of MGH rats, improve the disorder of intestinal flora caused by MGH, and change the community structure, increase the abundance of beneficial flora, and decrease the abundance of pathogenic flora.

**Conclusion:** AMP can improve the intestinal microbiological environment of MGH rats, maintain the microecological balance of intestinal microbial, and improve MGH symptoms.

KEYWORDS

***Atractylodes Macrocephala Rhizoma* polysaccharide, mammary gland hyperplasia, intestinal microbial, endocrine disorders, high-throughput sequencing**

# 1 Introduction

The accelerated pace of life and the recent increase in environmental pollution, unreasonable dietary habits, poor living habits, and mental factors often accompany modern women, causing a series of adverse reactions such as Mammary gland hyperplasia (MGH). MGH is a degenerative disease and progressive connective tissue growth caused by hyperplasia of mammary fiber and epithelial tissue (1). Modem medical research has shown that the development of MGH is closely linked to endocrine disorders. An imbalance in the ratio of estradiol to progesterone leads to excessive proliferation and regression of the breast parenchyma (2–4). It was reported that MGH was the disease with the highest incidence among female breast diseases, and its incidence rate is as high as 75%, and the incidence rate is still rising year by year. The age of onset is also getting lower and lower, and even some breast hyperplasia will have canceration, which has become a major health problem for women around the world (5–9). At present, for the examination and treatment of MGH, pathological biopsy or surgical resection of suspicious nodules revealed by some imaging examinations were typically utilized. Oral drugs mainly include oral sex hormone drugs (such as bromocriptine, tamoxifen, danazol, etc.) and non-sex hormone drugs (thyroxine, iodine, evening primrose oil, etc.). However, surgical resection has a large wound surface, which brings irreversible psychological and physiological damage to patients; drugs easily cause multiple toxic side effects such as menstrual blood loss, menstrual disorder, dizziness, nausea, vomiting, etc., and some drugs can also cause certain damage to the human gastrointestinal tract and central nervous system (10–12). Therefore, the search for a noninvasive, efficient treatment of MGH drugs has become a research hotspot at home and abroad.

Studies have demonstrated that endocrine imbalance can affect the composition of the intestinal microbiota and can directly or indirectly alter bacterial physiology and independent gene expression (13–15). MGH is caused by endocrine imbalance, in which the imbalance of estrogen secretion is an important signal of MGH. The abundance of intestinal microbiota is not simply related to the level of estrogen but also can affect the level of estrogen secretion. In endocrine balance, a variety of bacteria in the intestinal microbiota is involved in estrogen metabolism. For example, intestinal bacteria with structures such as β-glucuronidase and β-glucosidase can facilitate the reabsorption of estrogen through the intestine and re-enter the hepatic and intestinal circulation, eventually reaching the target organs it regulates to act (16–18). When there is an endocrine imbalance, the intestinal microbiota is altered and the β-glucuronidase content increases, raising the level of estrogen in the mammary glands. Breast epithelial cells that are chronically exposed to high levels of estrogen and become lesions occur, leading to their excessive proliferation, causing MGH (19, 20). Therefore, it was hypothesized that the treatment of MGH can be obtained by regulating the intestinal microbiota of homeostasis and balancing the level of estrogen secretion.

The earliest understanding of the mammary gland in Chinese medicine can be traced back to the Nei Jing, where it is written that "a woman's breast belongs to the liver, while the nipple belongs to the stomach" and that "Chong and Ren meridians can regulate the Qi and blood of the 12 meridians and they stop at the breast upward and form menstruation downward", which explains the close relationship between the breast and the spleen and stomach in terms of physiological function and meridian affiliation. Chinese herbal medicine has a very beneficial effect on the balance of the intestinal micro-ecology, and the intestinal microbiota coincides with the theory of "spleen and stomach" in Chinese Medicine (21–23). *Atractylodes Macrocephala Rhizoma* is the dry rhizome of the Asteraceae plant *Atractylodes macrocephala Koidz*, which has the effect of strengthening the spleen and stomach, drying and dampening water. Modern research shows that *Atractylodes Macrocephala Rhizoma* contains a variety of volatile components, polysaccharides, and amino acids, which have various pharmacological activities such as improving the function of the gastrointestinal tract and regulating the intestinal microbiota (24, 25).Therefore, this project will use AMP to treat MGH rats and analyze the effect of AMP on the intestinal microbiota of MGH rats through 16S RNA high-throughput sequencing, to provide theoretical support for the treatment of MGH from the perspective of intestinal microecology, as well as to provide an experimental basis for fully exploiting the medicinal value of AMP. The research idea is illustrated in Figure 1.

# 2 Materials and methods

## 2.1 Animals and reagents

Eighteen specific pathogen-free (SPF) grade female non-pregnant SD rats (200 ± 20 g) were purchased from Changchun Yisi Experimental Animal Technology Co., Ltd. (License No.: SCXK (Ji)-2018-0007) and housed in the SPF grade animal room. All animals were raised in the control room with a temperature of 24 ± 2°C and a humidity of 60% ± 5%. The light–dark cycle was 12/12 h. All experimental procedures involving animals were approved by the Animal Ethics Committee of the Animal Experimental Center of Jiamusi University.

Estradiol benzoate and progesterone injection were purchased from Shanghai Quanyu Biotechnology (Zhumadian) Animal Pharmaceutical Co., Ltd. Estradiol ($E_2$), progesterone

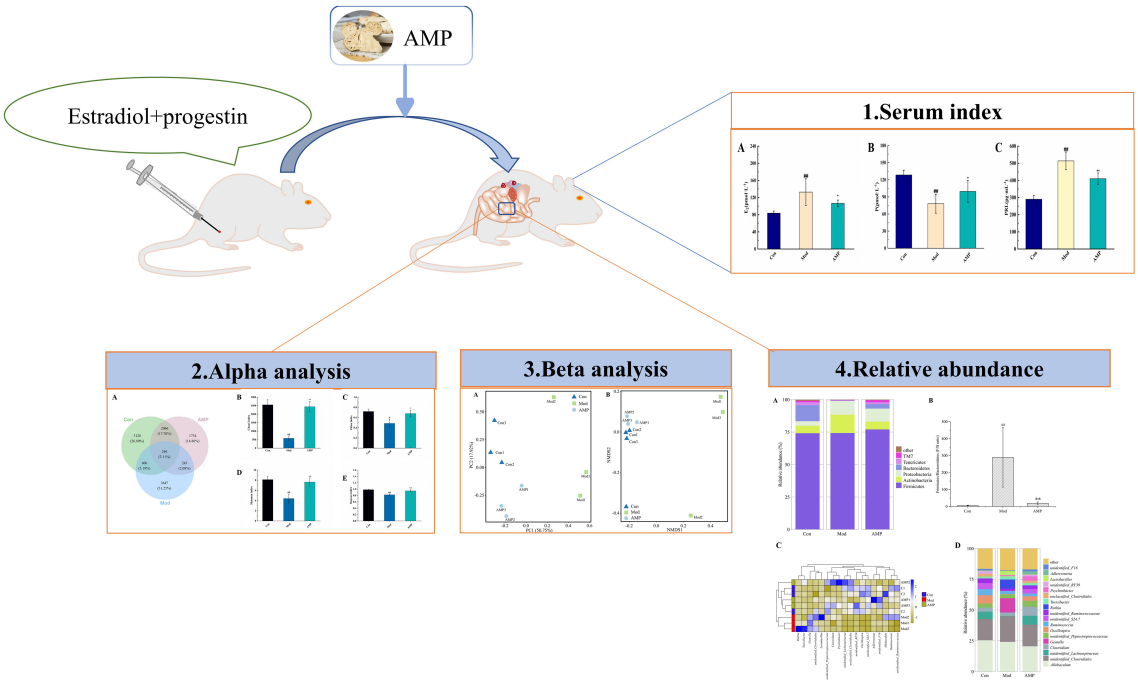


FIGURE 1
Experimental flow graph.

(P), and prolactin (PRL) kits were purchased from Jiangsu Enzyme Immunity Industrial Co., Ltd.

## 2.2 Medicine

*Atractylodes Macrocephala Rhizoma* was purchased from Jiamusi Baicaotang pharmacy.

According to the previous research method to prepare AMP, take degreased *Atractylodes Macrocephala Rhizoma*, add distilled water according to the ratio of the material to liquid of 1:18 g · $ml^{-1}$; reflux at 90°C for extraction for 3 h, three times; combine the filtrates; concentrate under reduced pressure; centrifuge; add absolute ethanol to the filtrate, with supernatant ethanol concentration of 80%; stand at 4°C for 12 h; centrifuge; collect precipitation; redissolve; concentrate; freeze dry; and then obtain the *Atractylodes Macrocephala Rhizoma* crude polysaccharide. AMP with a polysaccharide content of 64.23% was obtained after deproteinization using the Sevage method.

## 2.3 Experimental design

Eighteen female SD rats were chosen and fed adaptively for 7 days. They were randomly divided into the blank control group (Con), model control group (Mod), and AMP group, with six rats in each group. Except for the Con group, which was injected with the same amount of normal saline intramuscularly, rats in the other groups were injected with estradiol benzoate 0.5 $mg{\cdot}kg^{-1}{\cdot}D^{-1}$ intramuscularly for 25 days, followed by progesterone 5 $mg{\cdot}kg^{-1}{\cdot}D^{-1}$ intramuscularly for 5 days. After successful modeling, rats in the AMP group were given a 280 $mg{\cdot}kg^{-1}{\cdot}D^{-1}$ polysaccharide solution, and rats in Con and Mod groups were given the same amount of normal saline for 30 days.

### 2.3.1 Collection and detection of serum samples

After the last administration, rats in each group fasted for 12h. After weighing, rats were anesthetized by intraperitoneal injection of 2% pentobarbital sodium. The rats were done by cervical dislocation. Blood was drawn from the abdominal aorta and placed in the procoagulant tube for 20 min to separate the serum. The serum levels of $E_2$, P, and PRL were identified by ELISA.

### 2.3.2 Collection of intestinal cecal content samples

After taking blood from the abdominal aorta, the rats were quickly executed by cervical dislocation. Under aseptic conditions, the cecal content was taken with sterilized forceps and placed in a 5 ml sterile EP tube, numbered, weighed, and

quickly placed in liquid nitrogen. After the sample is collected, it was moved to -80°C for storage.

### 2.3.3 16S rRNA genes high-throughput sequencing

Take the cecal content. The total DNA in content was extracted in strict accordance with the DNA extraction kit. A nanodrop spectrophotometer was utilized to quantify DNA (DNA quantitative analysis), and the purity and concentration of the extracted genomic DNA were identified by electrophoresis. Amplification was performed using the 16S rDNA V3-V4 variable region, and the Quant-it PicoGreen dsDNA Assay Kit was used for fluorescence quantification. For further fluorescence quantification, samples should be combined in the appropriate proportions. Afterward, Illumina's NovaSeq 6000 sequencer was utilized for double-end sequencing of rat cecal contents.

### 2.3.4 Bioinformatics and statistical analysis

OTU clustering of non-repetitive sequences was made with 97% similarity using QIIME2 DADA2 software. Species classification was annotated using the Greensenes database (release 13.8). alpha-Diversity indices (Chao1, ACE, Simpson, and Shannon indices) were calculated to obtain the species richness and diversity. Meanwhile, the beta-diversity was analyzed in the gut microbiota of different samples; the similarity and difference of community composition between samples (or subpopulations) were obtained by analyzing the beta-diversity of gut microbiota in different samples.

SPSS 26.0 statistical software was used for data analysis. All data in the experiment were expressed as mean ± standard deviation (X ± s). One-way ANOVA was used for comparison between groups. $p < 0.05$ was considered statistically significant. The drawing is expected to be completed by using the R 4.1.3 and GraphPad Prism 8 software.

# 3 Results

## 3.1 General condition of rats and the effect of AMP on the serum indicators

Before modeling, the rats had normal appetite and response, smooth hair, and dry feces. After modeling, Mod group rats had poor appetite, listlessness, and no light hair, and the body weight decreased significantly compared with the Con group. The rat teats were red, swollen, and elevated, and some rats showed thin, soft, and yellow watery stools, which proved that the MGH model was successfully prepared. After the AMP treatment intervention, the AMP group rats returned to their gradually normalized food intake, the body weight increased significantly, and the nipple swelling and diarrhea symptoms of rats were alleviated. Furthermore, it was suggested that AMP had a certain therapeutic effect on MGH model rats, and it can improve the unfavorable symptoms caused by breast hyperplasia. As showed in Figure 2, compared with the Con group, the serum levels of $E_2$ and PRL in the Mod group rats were significantly increased ($p < 0.05$), and P levels were significantly decreased ($p < 0.01$). Compared to the Mod group, serum levels of $E_2$ and PRL levels in the AMP group were significantly increased ($p < 0.01$), and P levels were significantly decreased ($p < 0.05$).

## 3.2 Sequencing data quality assessment of intestinal contents microbiota

According to the statistics of the length of the sequence obtained in this sequencing, the length of the sequence obtained in each sample is concentrated at around 400–500 bp. As shown in Figure 3, the samples continued to increase, the rate of increase in OTU number slowed down, and the curve tended to flatten, demonstrating that with the addition of new samples,

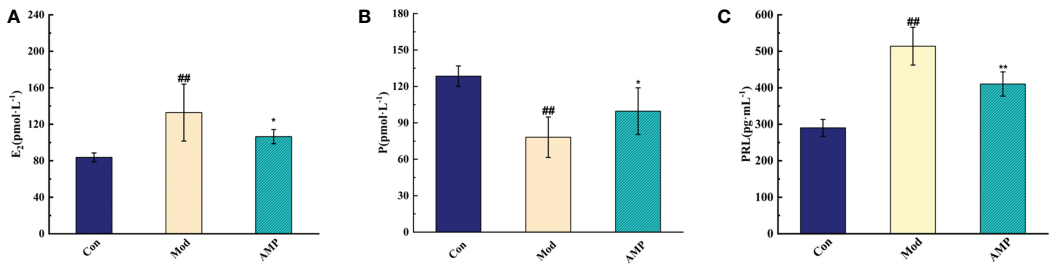


FIGURE 2
Effect of AMP on serum indexes of MGH rats, n = 6 **(A)**, effect of AMP on $E_2$ of MGH rats; **(B)**, effect of AMP on P of MGH rats; **(C)**, effect of AMP on PRL of MGH rats). Compared with Con group, # represents $P < 0.05$, ## represents $P < 0.01$; Compared with Mod group, * represents $P < 0.05$, ** represents $P < 0.01$.

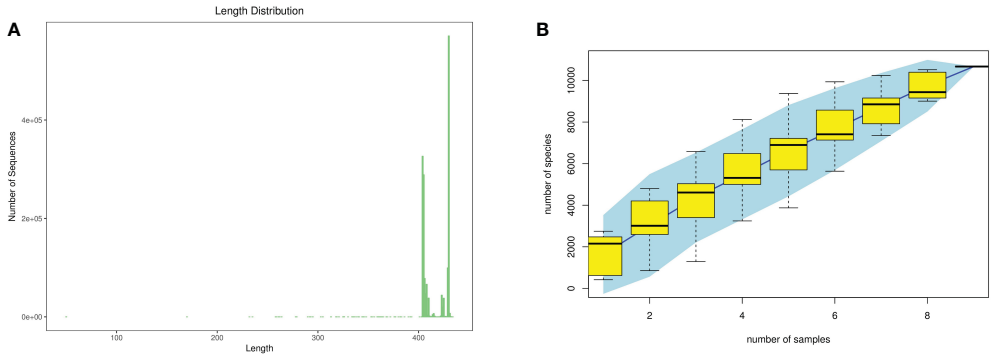


FIGURE 3
Quality evaluations of sequencing data of rat intestinal contents microbiota **(A)**, sequence length distribution diagram; **(B)**, species accumulation curve diagram).

the total number of OTUs almost did not increase, which proved that the sample of this study was sufficient to meet the needs of the study.

## 3.3 Effect of AMP on OTU number and alpha-diversity of intestinal contents in the MGH rats

OUT and Venn diagrams reflected the similarity and overlap of the bacterial community of different samples and visualized the similarity and uniqueness of sample points at the OTU level. As show in Figure 4, The total OTUs in the Con, Mod, and AMP groups were 3128, 3647, and 1734, respectively, and the number of OTUs in the intersection of the three groups was 246. The OTU number in the Mod group was significantly higher than the Con group. MGH disease can lead to the imbalance of intestinal microbiota in rats and increase in the number of harmful microbiota. After treatment with AMP, the OTU number in the rat intestine decreased significantly but was still lower than that in the Con group.

alpha-Diversity describes the biodiversity within a given area or ecosystem, i.e., it assesses the biodiversity of a given sample and is usually characterized by the calculation of diversity indices based on species richness or evenness, e.g., Chao1 and Pielou indices are often used to estimate the total number of species in a community: the larger the index, the greater the total number of community species. Shannon and Simpson indices

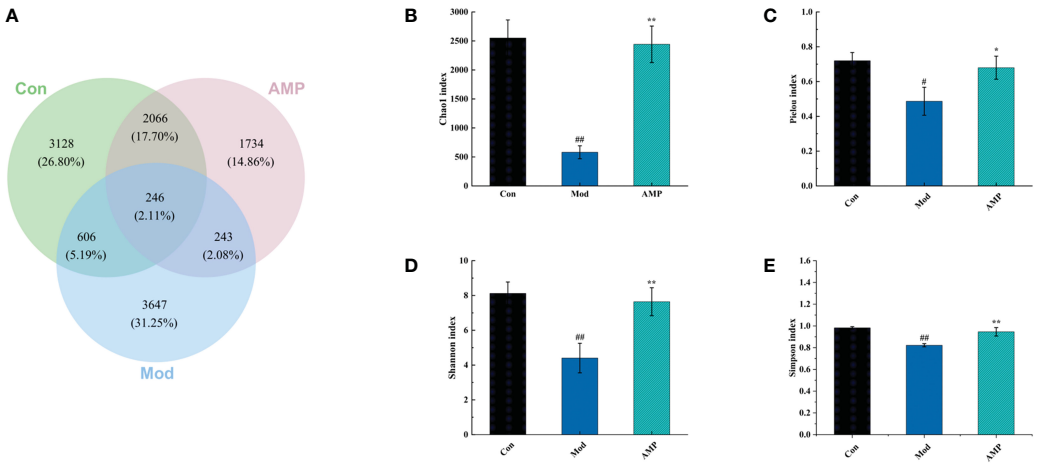


FIGURE 4
Effect of AMP on the number of intestinal OUT and alpha diversity of MGH rats **(A)**, number of intestinal OUT of rats; **(B)**, Chao1 index; **(C)**, Pielou index; **(D)**, Shannon index; **(E)**, Simpson index). Compared with Con group, # represents P < 0.05, ## represents P < 0.01; Compared with Mod group, * represents P < 0.05, ** represents P < 0.01.

can take into account both species richness and evenness, and they provide an objective picture of community species diversity. The larger the value of the Simpson index, or the smaller the value of the Shannon index, the lower the community diversity (26, 27). In the alpha analysis, the Pielou and Chao 1 indices were used to evaluate species richness, and the Simpson and Shannon index were used to evaluate microbial diversity. Compared with the Con group, the Mod group showed a highly significant decrease in Chao 1 index ($p < 0.01$), a significant decrease in Pielou index ($p < 0.05$), and Shannon index and Simpson index both highly significantly decreased ($p < 0.01$), indicating that MGH can reduce the richness and diversity of rat intestinal microbiota. Compared with the Mod group, the AMP group showed a highly significant increase in the Chao 1 index of rat microbiota ($p < 0.01$); Pielou index ($p < 0.05$), Shannon index ($p < 0.01$), and Simpson index ($p < 0.01$) were significantly increased, indicating that AMP could increase the abundance and diversity of intestinal microbiota in MGH rats.

## 3.4 Effect of AMP on intestinal beta-diversity in MGH rats

beta-Diversity describes the differences in species composition between habitat communities, i.e., the differences between samples. Principal component analysis (PCA) is a simplified data analysis technique that can reflect differences and distances between samples by analyzing sample composition at 97% similarity. PCA uses variance decomposition to reflect differences across multiple data sets on a two-dimensional coordinate plot, with the axis distance best reflecting the two eigenvalues of the variance value. The more similar the sample composition, the closer the distances reflected in the PCA plot (28). As showed in Figure 5A, the principal component variable 1 was 50.75% and the principal component variable 2 was 17.92%. The distance between the Con group and Mod group was significantly different, indicating that MGH had a certain effect on the composition of intestinal microbiota in rats. Compared with the Con group, the distance between the AMP group was small and relatively concentrated. The distance between points in non-metric analysis (NMDS) reflects the difference between samples and groups. The more distance, the more different, and vice versa. As shown in Figure 5B, compared with the Con group, the Mod group was relatively dispersed, indicating that the species was very different. Compared with the Mod group, the AMP group was relatively concentrated, which was closer to the Con group, indicating that there was little difference in species composition within the groups. The PCA and NMDs showed that the AMP had a significant restored effect on the species composition of intestinal microbiota in MGH rats.

## 3.5 Effect of AMP on the relative abundance of intestinal microbiota in MGH rats

As shown in the Figure 6A, the relative abundance of intestinal microbiota of MGH rats was shown at the phylum level, in which four taxa, Firmicutes, Actinobacteres, Proteobacteres, and Bacteroidetes, were the dominant phylum,

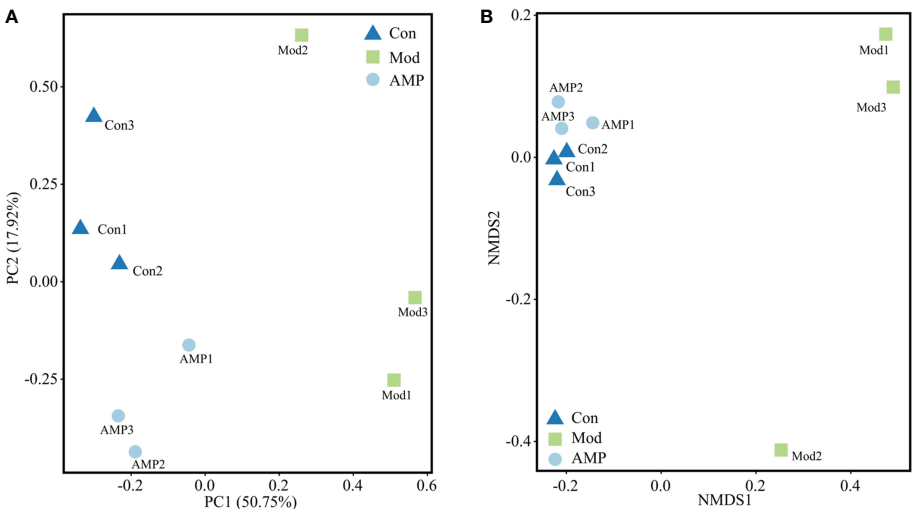


FIGURE 5
Effect of AMP on intestinal beta diversity of MGH rats **(A)**, PCA; **(B)**, NMDS).

10.3389/fendo.2022.1102605

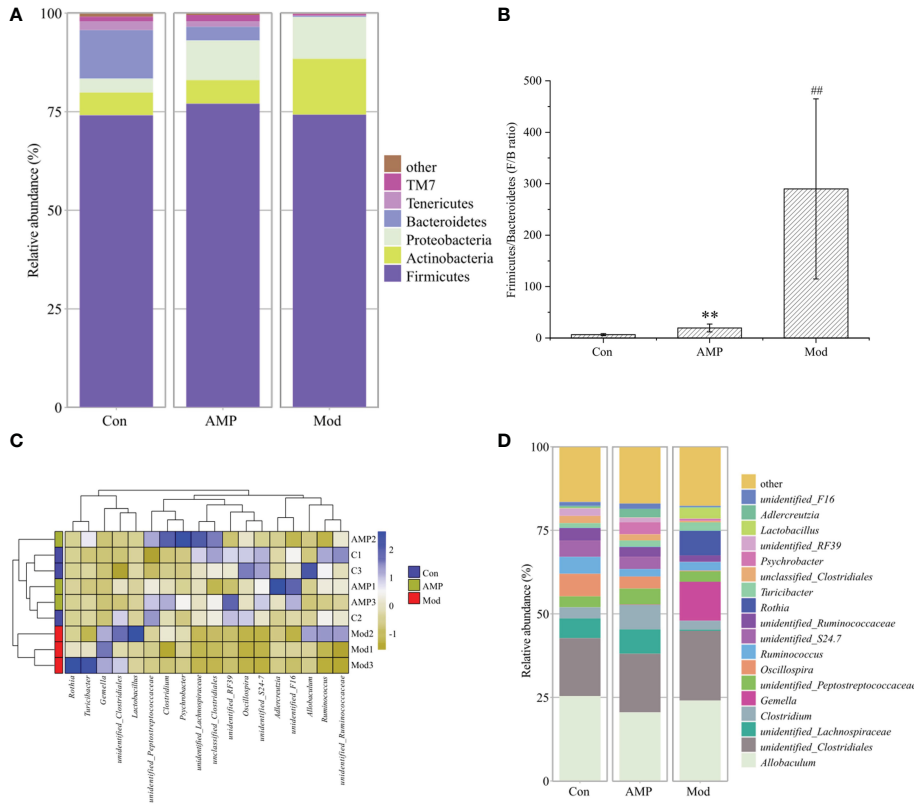


FIGURE 6
Effect of AMP on the relative abundance of intestinal microbiota in MGH rats (relative abundance **(A)**, phyla level; **(B)**, Firmicutes/Bacteroides; thermogram of relative abundance at **(C)**, phyla level; relative abundance at **(D)**, genus level). Compared with Con group, # represents $P < 0.05$, ## represents $P < 0.01$; Compared with Mod group, * represents $P < 0.05$, ** represents $P < 0.01$.

accounting for a larger proportion of the total microbiota, about 95%. Compared with the Con group, in the Mod group the relative abundance of Firmicutes decreased but was not significant; the Bacteroidetes decreased significantly ($p < 0.05$), and the Actinobacteres and Proteobacteres increased but were not significantly different. The AMP group compared with the Mod group, the relative abundance of Firmicutes and Bacteroidetes increased, but there was no significant difference, and the Actinobacteres and Proteobacteres decreased, but there was no significant difference. Figure 6B shows the ratio of Firmicutes and Bacteroidetes (F/B ratio). Compared with the Con group, F/B was higher in the Mod group, and the AMP group was higher too compared to Mod group. The Figure 6C shows that, a heat map can simultaneously provide information on community species composition and abundance and visually reflect the similarities and differences in community composition of different samples or subgroups through color changes. In the changes of detected phyla, Con group and AMP group were clustered into one category, while Mod group was more dispersed due to the influence of MGH. As shown in Figure 6D, at the genus level *Allobaculum*, *Clostridiales*, *Lachnospiraceae*, and *Clostridium* were the dominant genera. Compared with the Con group, the relative abundance of Actinobacteres and Clostridium in the Mod group decreased. Lachnospiraceae decreased significantly ($p < 0.05$) and *Clostridiales* increased. Compared with the Mod group, the AMP group *Lachnospiraceae* was higher, *Clostridium* was highly significant ($p < 0.01$), *Clostridiales* was higher, and *Allobaculum* was lower.

## 4 Discussion

The human intestinal microbiome is a diverse and complex ecosystem and is home to thousands of microorganisms that co-evolve with their hosts and play important roles in health and disease. The important role of intestinal microbial in health and disease has become a research focus (28–31). Intestinal microbial diversity is tightly associated with levels of estrogen and its metabolites (32–34). A reduction in intestinal microbial diversity can reduce the activity of β-glucuronidase that can reduce the circulation form of estrogen in the body and break it down into

active ingredients, resulting in a large estrogen accumulation in the mammary gland, and leading to endocrine disorders (35–37). Modern medicine also believes that the occurrence of MGH is linked to endocrine disorders, in particular, it is related to the imbalance of balance hypothalamic-pituitary-ovarian-mammary gland endocrine axis, in which the secretion of estrogen increases and the secretion of progesterone decreases. The imbalance of female/progesterone ratio is the main cause of mammary gland hyperplasia (38–41). The mammary gland is an important target organ for the effect of estrogen, and when estrogen secretion in the female organism is too high, it will cause the female breast tissue to be in a state of over-stimulation, and the poor physical condition will have an impact on the mammary gland, leading to MGH (42, 43). Metabolic enzymes changed regulated by the intestinal microbiota will affect the estrogen level change, which leads to endocrine dysregulation, eventually causing MGH (36, 44). Thus, estrogen can be participated in the development of MGH through changes in the metabolic levels of intestinal microbiota.

In this experiment, $E_2$, P, and PRL were significant indicators to determine whether the rats had MGH. Compared with the Con group, the Mod group $E_2$ and PRL levels were increased significantly and P levels were decreased significantly, compared with the Mod group; the AMP group $E_2$ and PRL levels were reduced and P levels were increased, indicating that AMP could alleviate the symptoms on rats MGH effectively. By 16S RNA amplified sequencing, in alpha-diversity analysis, the Mod group Chao1, Pielou, Shannon, and Simpson indices were decreased in the intestinal tract of rats, indicating that MGH had an inhibitory effect on the richness and diversity of intestinal microbiota in rats. Compared with the Mod group, the AMP group Chao1, Pielou, Shannon, and Simpson indexes in the intestinal tract of rats were significantly increased, which was similar to that in the Con group, indicating that AMP had a certain improvement effect on the intestinal microbiota of rats with MGH. In the beta-diversity analysis, AMP improved the chances of microbial community structure in intestinal contents of MGH rats and gradually restored it to the normal level. However, there were still discrete individual samples in the Mod group, which may be due to the inter-individual differences.

Under normal conditions, Firmicutes and Bacteroidetes are in dynamic balance in the intestinal tract and the ratio of relative abundance is seen as an important marker of intestinal microbiota disorders, and an increase in F/B value represents an endocrine disorder on the other hand (45–47). In this experiment, MGH changed the structure and composition of the microbiota in the intestinal contents of rats, and through the phylum level analysis on the changes of the microbiota relative abundance, we can further understand how AMP treats the MGH by regulating the intestinal microbiota. In the Mod group, the relative abundance of Proteobacteres and the F/B value also increased, suggesting that MGH can lead to the imbalance of the intestinal micro-ecological environment; after AMP treatment, the relative abundance of Proteobacteres decreased, and the value was similar to the Con group; the F/B value also decreased but was still higher than that of the Con group. Therefore, it can be deduced that AMP is beneficial to restore the major intestinal microbiota. Actinobacteres are a gram-positive bacterium, which can protect the host and nutrient from attack by pathogens in the intestine (48–50). In this experiment, compared with Con group, the relative abundance of Actinobacteres in the Mod group increased, indicating that the MGH caused resistance of intestinal microbiota. Compared with Mod group, the relative abundance of Actinobacteres in the AMP group was reduced, which indicated that the administration of AMP could alleviate the intestinal microbiota disorder. According to the analysis of genus level, Clostridiales is generally considered to be related to body inflammation, *Clostridium* contains 20α-hydroxy steroid dehydrogenase, which converts glucocorticoids into androgens, when *Clostridium* is unbalanced, a large number of androgens will be synthesized, which will cause intestinal microorganisms dysregulation and eventually lead to endocrine disorders and pathological lesions in women (51, 52). Combined with the results of this experiment, compared to the Con group, the relative abundance of *Allobaculum*, Clostridiales, and Lachnospiraceae decreased and the *Clostridium* increased in the Mod group; compared to the Mod group, the relative abundance of Lachnospiraceae, *Clostridium*, Clostridiales increased, and *Allobaculum* decreased in the AMP group. Further studies are needed to investigate this difference. Based on the above experiments, AMP can maintain the endocrine balance by regulating the homeostasis of intestinal microbiota, so as to affect the occurrence and progress of MGH.

In general, MGH caused by endocrine dysregulation breaks the intestinal microbiota balance in rats, and the diversity and richness of intestinal microbiota are destroyed to varying degrees. Through the study of AMP in the treatment of MGH and its effect on intestinal microbiota, this experiment proved that AMP had a certain therapeutic effect on MGH and also had a definite recovery effect on the diversity, richness, and community structure of intestinal microbiota in MGH rats. However, the therapeutic effect of a single polysaccharide component on MGH by regulating intestinal microbiota has not been excellent. Therefore, the therapeutic effect of the AMP of MGH through intestinal microbiota needs further study.

## Data availability statement

The original contributions presented in the study are publicly available. This data can be found here: https://doi.org/10.5061/dryad.gf1vhhmtc.

## Ethics statement

The animal study was reviewed and approved by the Animal Ethics Committee of the Jiamusi University.

## Author contributions

YP prepared the drafting of manuscript and interpretation of data. CL performed the experiment and analyzed in the analyzing of part of the data. LW and HZ designed the study and revised the manuscript. All authors contributed to manuscript revision, read, and approved the submitted version.

## Funding

This study was supported by the Natural Science Foundation of Heilongjiang Province (Grant No. LH2022H093), Science and Technology Innovation Team Construction Plan Fund of the Provincial Education Department (Grant No.2021-KYYEF-0638), Postdoctoral Scientific Research Development Fund of Heilongjiang Province (Grant No. LBH-Q20185), Jiamusi University's Scientific Innovation Team (cxtd202103), and the Jiamusi University Ph.D. Special Foundation (JMSUBZ2020-14).

## Conflict of interest

The authors declare that the research was conducted in the absence of any commercial or financial relationships that could be construed as a potential conflict of interest.

## Publisher's note

All claims expressed in this article are solely those of the authors and do not necessarily represent those of their affiliated organizations, or those of the publisher, the editors and the reviewers. Any product that may be evaluated in this article, or claim that may be made by its manufacturer, is not guaranteed or endorsed by the publisher.

## Supplementary material

The Supplementary Material for this article can be found online at: https://www.frontiersin.org/articles/10.3389/fendo.2022.1102605/full#supplementary-material

## References

1. Zhang H-B, Yan P-H, Lu J, Sun L, Zhao L-J, Du X, et al. Clinical observation of electroacupuncture combined with scraping therapy for mammary hyperplasia. *World Journal of Acupuncture – Moxibustion* (2020) 30(2):146–150. doi: 10.1016/j.wjam.2020.02.011

2. Shi M, Ma Y, Xu P. Evaluation of the mechanism of Rujiling capsules in the treatment of hyperplasia of mammary glands based on network pharmacologyand molecular docking. *Indian J Pharmacol* (2022) 54(2):110–117. doi: 10.4103/ijp.ijp-374-21

3. Li X, Xin P, Wang C, Wang Z, Wang Q, Kuang H. Mechanisms of traditional Chinese medicine in the treatment of mammary gland hyperplasia. *Am J Chin Med* (2017) 45:443–58. doi: 10.1142/S0192415X17500276

4. Tower H, Dall G, Davey A, Stewart M, Lanteri P, Ruppert M, et al. Estrogen-induced immune changes within the normal mammary gland. *Sci Rep* (2022) 12 (1):18986. doi: 10.1038/s41598-022-21871-4

5. Ma D, Liu G, Zhang X, Zhang Q, Gao T, Liu M. Massage treatment of hyperplasia of mammary glands: A protocol for a systematic review and meta-analysis. *Medicine* (2020) 99(52):e23601. doi: 10.1097/MD.0000000000023601

6. Ma M, Zhang L, Wang X. Effect of auricular point pressing therapy on hyperplasia of mammary glands: A protocol for systematic review and meta-analysis. *Med (Baltimore).* (2021) 2:100. doi: 10.1097/MD.0000000000024875

7. Qian LQ, Pei XH, Xu ZY, Wang C. Clinical observation on treatment of hyperplasia of mammary gland by lirukang granule. *Chin J Integr Med* (2007) 13:120–4. doi: 10.1007/s11655-007-0120-y

8. Wang L, Zhao D, Di L, Cheng D, Zhou X, Yang X, et al. The anti-hyperplasia of mammary gland effect of thladiantha dubia root ethanol extract in rats reduced by estrogen and progestogen. *J Ethnopharmacol* (2011) 8:134+136–140. doi: 10.1016/j.jep.2010.11.071

9. Ma W, Jin ZN, Wang X, Fu FM, Guo WH, Xu YY, et al. Clinical practice guideline for diagnosis and treatment of hyperplasia of the mammary glands: Chinese society of breast surgery (CSBrS) practice guideline 2021. *Chin Med J (Engl)* (2021) 134(16):1891–3. doi: 10.1097/CM9.0000000000001521

10. Wibowo E, Pollock PA, Hollis N, Wassersug RJ. Tamoxifen in men: A review of adverse events. *Andrology* (2016) 4:776–88. doi: 10.1111/andr.12197

11. Wang X, Chen YG, Ma L, Li ZH, Li JY, Liu XG, et al. Effect of Chinese medical herbs-huiru yizeng yihao on hyperprolactinemia and hyperplasia of mammary gland in mice. *Afr J Tradit Complement Altern Med* (2013) 10:24–35. doi: 10.4314/ajtcam.v10i4.5

12. Guan HL, Wang Y, Gui YF, Zhang CL. Effect of Chinese herbal medicine compound on breast hyperplasia: A protocol of systematic review. *Med (Baltimore)* (2020) 99(49):e23463. doi: 10.1097/MD.0000000000023463

13. Org E, Mehrabian M, Parks BW, Shipkova P, Liu X, Drake TA, et al. Sex differences and hormonal effects on gut microbiota composition in mice. *Gut Microbes* (2016) 7:313–22. doi: 10.1080/19490976

14. Harada N, Minami Y, Hanada K, Hanaoka R, Kobayashi Y, Izawa T, et al. Relationship between gut environment, feces-to-food ratio, and androgen deficiency-induced metabolic disorders. *Gut Microbes* (2020) 12:1817719. doi: 10.1080/19490976.2020.1817719

15. Liu Q, Sun W, Zhang H. Interaction of gut microbiota with endocrine homeostasis and thyroid cancer. *Cancers (Basel)* (2022) 14(11):2656. doi: 10.3390/cancers14112656

16. Zhu J, Liao M, Yao Z, Liang W, Li Q, Liu J, et al. Breast cancer in postmenopausal women is associated with an altered gut metagenome. *Microbiome* (2018) 6:136. doi: 10.1186/s40168-018-0515-3

17. Plottel C, Blaser M. Microbiome and malignancy. *Cell Host Microbe* (2011) 10:324–35. doi: 10.1016/j.chom.2011.10.003

18. d'Afflitto M, Upadhyaya A, Green A, Peiris M. Association between sex hormone levels and gut microbiota composition and diversity-a systematic review. *J Clin Gastroenterol* (2022) 56(5):384–92. doi: 10.1097/MCG.0000000000001676

19. McIntosh FM, Maison N, Holtrop G, Young P, Stevens VJ, Ince J, et al. Phylogenetic distribution of genes encoding β-glucuronidase activity in human colonic bacteria and the impact of diet on faecal glycosidase activities. *Environ Microbiol* (2012) 14:1876–87. doi: 10.1111/j.1462-2920.2012.02711.x

20. Yoon K, Kim N. Roles of sex hormones and gender in the gut microbiota. *J Neurogastroenterol Motil.* (2021) 27(3):314–25. doi: 10.5056/jnm20208

21. Rooks MG, Garrett WS. Gut microbiota, metabolites and host immunity. *Nat Rev Immunol* (2016) 16:341–52. doi: 10.1038/nri.2016.42

22. Zhou B, Yuan Y, Zhang S, Guo C, Li X, Li G, et al. Intestinal Flora and Disease Mutually Shape the Regional Immune System in the Intestinal Tract. *Front Immunol* (2020) 11:575. doi: 10.3389/fimmu.2020.00575

23. Yang S, Hao S, Wang Q, Lou Y, Jia L, Chen D. The interactions between traditional Chinese medicine and gut microbiota: Global research status and trends. *Front Cell Infect Microbiol* (2022) 12:1005730. doi: 10.3389/fcimb.2022.1005730

24. Zhu B, Zhang Q-L, Hua J-W, Cheng W-L, Qin L-P. The traditional uses, phytochemistry, and pharmacology of atractylodes macrocephala koidz.: A review. *J Ethnopharmacology* (2018) 226:143–67. doi: 10.1016/j.jep.2018.08.023

25. Feng J, Zhang C, Chen H, Chen Z, Chen Y, He D, et al. Shen-Ling-Bai-Zhu-San enhances the antipneumonia effect of cefixime in children by ameliorating gut microflora, inflammation, and immune response. *Evid Based Complement Alternat Med* (2022) 2022::7752426. doi: 10.1155/2022/7752426

26. Li C, Zhou K, Xiao N, Peng M, Tan Z. The effect of qiweibaizhu powder crude polysaccharide on antibiotic-associated diarrhea mice is associated with restoring intestinal mucosal bacteria. *Front Nutr* (2022) 9:952647. doi: 10.3389/fnut.2022.952647

27. Wang H, Zhang H, Gao Z, Zhang Q, Gu C. The mechanism of berberine alleviating metabolic disorder based on gut microbiome. *Front Cell Infect Microbiol* (2022) 12:854885. doi: 10.3389/fcimb.2022.854885

28. Wang Y, Sheng HF, He Y, Wu JY, Jiang YX, Tam NF, et al. Comparison of the levels of bacterial diversity in freshwater, intertidal wetland, and marine sediments by using millions of illumina tags. *Appl Environ Microbiol* (2012) 78:8264–71. doi: 10.1128/AEM.01821-12

29. Li X, Deng N, Zheng T, Qiao B, Peng M, Xiao N, et al. Importance of dendrobium officinale in improving the adverse effects of high-fat diet on mice associated with intestinal contents microbiota. *Front Nutr* (2022) 9:957334. doi: 10.3389/fnut.2022.957334

30. Zhang D, Liu J, Cheng H, Wang H, Tan Y, Feng W, et al. Interactions between polysaccharides and gut microbiota: A metabolomic and microbial review. *Food Res Int* (2022) 160:111653. doi: 10.1016/j.foodres.2022.111653

31. Ou J, Wang Z, Liu X, Song B, Chen J, Li R, et al. Regulatory effects of marine polysaccharides on gut microbiota dysbiosis: A review. *Food Chem X* (2022) 15:100444. doi: 10.1016/j.fochx.2022.100444

32. Baker JM, Al-Nakkash L, Herbst-Kralovetz MM. Estrogen-gut microbiome axis: Physiological and clinical implications. *Maturitas* (2022) 103:45–53. doi: 10.1016/j.maturitas.2017.06.025

33. Xujie Y, Xiaohua P. Value and influencing factors of valid Traditional Chinese Medicine compound prescription patents for mammary gland hyperplasia. *J Tradit Chin Med* (2022) 42(6):1012–8. doi: 10.19852/j.cnki.jtcm.2022.06.010

34. Franasiak JM, Scott RTJr. Introduction: Microbiome in human reproduction *Fertil Steril.* (2015) 104:1341–3. doi: 10.1016/j.fertnstert.2015.10.021

35. Shin NR, Whon TW, Bae JW. Proteobacteria: microbial signature of dysbiosis in gut microbiota. *Trends Biotechnol* (2015) 33:496–503. doi: 10.1016/j.tibtech.2015.06.011

36. Ma Y, Liu T, Li X, Kong A, Xiao R, Xie R, et al. Estrogen receptor β deficiency impairs gut microbiota: a possible mechanism of IBD-induced anxiety-like behavior. *Microbiome* (2022) 10(1):160. doi: 10.1186/s40168-022-01356-2

37. Lin H, Liu Z, Liu Z, Lin Z. Incompatible effects of panax ginseng and veratrum nigrum on estrogen decline in rats using metabolomics and gut microbiota. *J Pharm BioMed Anal* (2022) 208:114442. doi: 10.1016/j.jpba.2021

38. Liu Y, Wu D, Wang K, Chen H, Xu H, Zong W, et al. Dose-dependent effects of royal jelly on estrogen- and progesterone-induced mammary gland hyperplasia in rats. *Mol Nutr Food Res* (2022) 66(5):e2100355. doi: 10.1002/mnfr.202100355

39. Attia MA. Neoplastic and non-neoplastic lesions in the mammary gland, endocrine and genital organs in aging male and female sprague-dawley rats. *Arch Toxicol* (1996) 70(8):461–73. doi: 10.1007/s002040050300

40. Song D, Shi X, Li C, Cao X, Lu Y, Li J. Effect of vitamin D3 on hyperplasia of mammary glands in experimental rats. *Gland Surg* (2022) 11(1):136–146. doi: 10.21037/gs-21-851

41. Harvell DM, Strecker TE, Tochacek M, Xie B, Pennington KL, McComb RD, et al. Rat strain-specific actions of 17beta-estradiol in the mammary gland: correlation between estrogen-induced lobuloalveolar hyperplasia and susceptibility to estrogen-induced mammary cancers. *Proc Natl Acad Sci U S A.* (2000) 97 (6):2779–84. doi: 10.1073/pnas.050569097

42. Yan Z, Yun-Yun L, Zhou T, Li-Rong C, Xiao-Li Y, Yong L. The relationship between using estrogen and/or progesterone and the risk of mammary gland hyperplasia in women: a meta-analysis. *Gynecol Endocrinol* (2022) 38(7):543–7. doi: 10.1080/09513590.2022.2076831

43. Li X, Wang Z, Wang Y, Zhang Y, Lei X, Xin P, et al. Anti-hyperplasia effects of total saponins from phytolaccae radix in rats with mammary gland hyperplasia *via* inhibition of proliferation and induction of apoptosis. *Front Pharmacol* (2018) 9:467. doi: 10.3389/fphar.2018.00467

44. Lin H, Liu Z, Liu Z, Lin Z. Incompatible effects of panax ginseng and veratrum nigrum on estrogen decline in rats using metabolomics and gut microbiota. *J Pharm BioMed Anal* (2021) 208:114442. doi: 10.1016/j.jpba.2021.114442

45. Jose PA, Maharshi A, Jha B. Actinobacteria in natural products research: Progress and prospects. *Microbiol Res* (2021) 246:126708. doi: 10.1016/j.micres.2021.126708

46. Guo Y, Qi Y, Yang X, Zhao L, Wen S, Liu Y, et al. Association between polycystic ovary syndrome and gut microbiota. *PloS One* (2022) 11(4):e0153196. doi: 10.1371/journal.pone.0153196

47. Wang L, Xian YF, Loo SKF, Ip SP, Yang W, Chan WY, et al. Baicalin ameliorates 2,4-dinitrochlorobenzene-induced atopic dermatitis-like skin lesions in mice through modulating skin barrier function, gut microbiota and JAK/STAT pathway. *Bioorg Chem* (2022) 119:105538. doi: 10.1016/j.bioorg.2021.105538

48. Qi X, Yun C, Pang Y, Qiao J. The impact of the gut microbiota on the reproductive and metabolic endocrine system. *Gut Microbes* (2021) 13:1–21. doi: 10.1080/19490976.2021.1894070

49. Dinesh R, Srinivasan V TES, Anandaraj M, Srambikkal H. Endophytic actinobacteria: Diversity, secondary metabolism and mechanisms to unsilence biosynthetic gene clusters. *Crit Rev Microbiol* (2017) 43(5):546–66. doi: 10.1080/1040841X.2016

50. Arnone AA, Cook KL. Gut and breast microbiota as endocrine regulators of hormone receptor-positive breast cancer risk and therapy response. *Endocrinology* (2022) 164(1):bqac177. doi: 10.1210/endocr/bqac177

51. Sandhu BK, McBride SM. Clostridioides difficile. *Trends Microbiol* (2022) 26 (12):1049–50. doi: 10.1016/j.tim.2018.09.004

52. Sun WJ, Wu EY, Zhang GY, Xu BC, Chen XG, Hao KY, et al. Total flavonoids of abrus cantoniensis inhibit CD14/TLR4/NF-κB/MAPK pathway expression and improve gut microbiota disorders to reduce lipopolysaccharide-induced mastitis in mice. *Front Microbiol* (2022) 13:985529. doi: 10.3389/fmicb.2022.985529

frontiers | Frontiers in Endocrinology

TYPE Review
PUBLISHED 25 January 2023
DOI 10.3389/fendo.2022.1085092



OPEN ACCESS

EDITED BY
Zhoujin Tan,
Hunan University of Chinese Medicine, China

REVIEWED BY
Jun Zhang,
Hunan Vocational College of Science and Technology, China
Xiaoliang Li,
Heilongjiang University of Chinese Medicine, China

*CORRESPONDENCE
Chunxia Huang
87816925@qq.com

SPECIALTY SECTION
This article was submitted to Gut Endocrinology, a section of the journal Frontiers in Endocrinology

RECEIVED 31 October 2022
ACCEPTED 06 December 2022
PUBLISHED 25 January 2023

CITATION
Su M, Hu R, Tang T, Tang W and Huang C (2023) Review of the correlation between Chinese medicine and intestinal microbiota on the efficacy of diabetes mellitus. *Front. Endocrinol.* 13:1085092. doi: 10.3389/fendo.2022.1085092



# Review of the correlation between Chinese medicine and intestinal microbiota on the efficacy of diabetes mellitus

Min Su[1,2], Rao Hu[2], Ting Tang[2], Weiwei Tang[2] and Chunxia Huang[1,2]*

[1]Hunan Key Laboratory of The Research and Development of Novel Pharmaceutical Preparation, Changsha Medical University, Changsha, China, [2]Department of Biochemistry and Molecular Biology, School of Basic Medicine, Changsha Medical University, Changsha, China

Diabetes mellitus is a serious metabolic disorder that can lead to a number of life-threatening complications. Studies have shown that intestinal microbiota is closely related to the development of diabetes, making it a potential target for the treatment of diabetes. In recent years, research on the active ingredients of traditional Chinese medicine (TCM), TCM compounds, and prepared Chinese medicines to regulate intestinal microbiota and improve the symptoms of diabetes mellitus is very extensive. We focus on the research progress of TCM active ingredients, herbal compounds, and prepared Chinese medicines in the treatment of diabetes mellitus in this paper. When diabetes occurs, changes in the abundance and function of the intestinal microbiota disrupt the intestinal environment by disrupting the intestinal barrier and fermentation. TCM and its components can increase the abundance of beneficial bacteria while decreasing the abundance of harmful bacteria, regulate the concentration of microbial metabolites, improve insulin sensitivity, regulate lipid metabolism and blood glucose, and reduce inflammation. TCM can be converted into active substances with pharmacological effects by intestinal microbiota, and these active substances can reverse intestinal microecological disorders and improve diabetes symptoms. This can be used as a reference for diabetes prevention and treatment.

KEYWORDS

traditional Chinese medicine, diabetes, metabolism, active ingredients, intestinal microbiota

## 1 Introduction

Diabetes mellitus [Xiaokezheng or Xiaodanzheng in traditional Chinese medicine (TCM)] is a serious disorder of metabolism to islets. Insulin resistance (IR) and impaired islet cell functions are characterized by an increase in glycemia, lipid metabolism disorders, and systemic inflammation that can lead to a variety of serious

complications (1). According to the World Health Organization, diabetes is one of the diseases with the most known complications (2, 3). Long-term increases in blood glucose are accompanied by large blood vessels and microvascular damage, putting the heart, brain, kidneys, peripheral nerves, eyes, feet, and other organs at risk. Type 2 diabetes mellitus (T2DM) is one of the world's most significant public health issues, accounting for 90% of diabetes cases (4). T2DM has been rapidly increasing worldwide in recent years (5).

An important internal environment for human physiological and metabolic activities is a healthy intestinal environment. More and more studies indicate that changes in the gut microbiota are associated with altered glucose homeostasis and play an important role in the onset and progression of obesity and T2DM. The host's intestinal microbiota influences body weight, bile acid metabolism, proinflammatory activity, IR, and gut hormone modulation (6). Reduced microbial diversity has been linked to IR and energy metabolism, particularly as the *Firmicutes/Bacteroidetes* (F/B) ratio rises (7). The variation in fecal microbiome trends between normal and obese T2DM patients was different (8, 9). For example, Liu Shixuan et al. compared the abundance of intestinal microbiota in diabetic patients and controls, finding that *Actinomycetes*, *Clostridium*, *Escherichia*, and *Proteus* were significantly enriched in the T2DM group, while *Rossella*, *Eubacterium*, and *Faecalibacterium* decreased (10). *Roseburia*, *Eubacterium*, and *Faecalibacterium* are all members of the phylum Pachylocycetes and have been shown to promote intestinal barrier repair and inhibit inflammatory factors (11). It is clear that changes in this microbiota will have an impact on the intestinal barrier function. The reason is the change of proteins related to the maintenance of the intestinal barrier.

Diabetes treatment options are numerous at the moment. However, the effect of a drug on the intestinal microbiota is a very important evaluation index for drug safety and efficacy. TCM has shown remarkable efficacy in the treatment of diabetes. In practice, Chinese medicine has summed up many classic prescriptions for the treatment of diabetes (12, 13). At present, there are extensive studies on the active ingredients of TCM, TCM compounds, and prepared Chinese medicines to regulate the structure of the intestinal microbiota and improve the symptoms of diabetes. So many studies have shown that there is an interactive relationship between intestinal microbiota and TCM. On one hand, intestinal microbiota can transform the active ingredients in herbal medicine, and on the other hand, these active ingredients can reverse the imbalance of intestinal microbiota, and the symptoms of diabetes can be improved after the intestinal microbiota imbalance is restored (14–17). Therefore, the gut microbiota can be used as a target for TCM to prevent and treat T2DM (18). This review aims to provide the relationship between T2DM, intestinal microbiota, and TCM, as well as the mechanisms of action of herbal components in metabolic diseases. This could help future clinical trials of TCM for the treatment of diabetes mellitus.

## 2 Correlation of intestinal microbiota with T2DM and its mechanism of action

The composition of intestinal bacteria is more diverse in healthy people, whereas obese or diabetic patients have a reduced diversity of intestinal microbiota, with more conditionally pathogenic bacteria and less beneficial microbiota. The intestinal microbiota and its metabolites travel from multiple pathways involving the body's physiological processes, including immunomodulation, metabolism, and even brain function (19). In the studies of the "microbial-gut-brain-hepatic axis", the intestinal microbiota controls intestinal enteroendocrine cells (EECs); they could secrete cholecystokinin (CCK), leptin, peptide YY (PYY), glucagon-like peptide-1 (GLP-1) and 5-hydroxytryptophan (5-HT). These intestinal peptides could cause the disorders of glucose and lipid metabolism by regulating the central nervous system and associated signaling pathways (20). *Clostridium*, *Bacillus*, *Enterococcus*, *Bifidobacterium*, *Lactobacillus*, and *Bacteroides* could produce bile salt hydrolase (BSH). BSH could act on amino acids that conjugate bile acids, produce free bile acids, and further modify the formation of secondary bile acids. Bile acids combined with the G protein–coupled bile acid receptor (Gpbar1) and farnidol X receptor (FXR) regulates glucose and lipid metabolism, stimulates the release of PYY and GLP-1, increases the body's sensitivity to insulin, and reduce the glycemia levels (21–25). *Vibrio butyrates*, *Rochesella*, *faecochoncilli*, *Bifidobacterium*, *Eubacterium* and *Clostridium flex* can cause fermentation and produce short-chain fatty acids (SCFAs). SCFAs combined with G protein-couple receptor (Gpr41/Gpr43) can also stimulate the release of PYY and GLP-1, improving IR. Dysbacteriosis in T2DM patients leads to an increase in Gram-negative bacteria–producing lipopolysaccharides (LPSs) and a decrease in the microbiota that protect the intestinal mucosal barrier (26). Thus, the expression of intestinal epithelial tight-junction proteins is inhibited, and the permeability of the intestine increases, promoting the absorption of LPSs (27). LPSs activate receptors (CD14/TLR4) on the surface of immune cells; promote interleukin-1 (IL-1), tumor necrosis factor-α (TNF-α), interleukin-6 (IL-6), and other proinflammatory factor secretions; and induce chronic low-grade inflammation, and long-term accumulation weakens the body's responsiveness to insulin and induces IR (28). The mechanism of action of the intestinal microbiota and diabetes is shown in Figure 1.

Probiotics have been reported to modulate the intestinal microbiota to prevent or delay the onset of T2DM by including

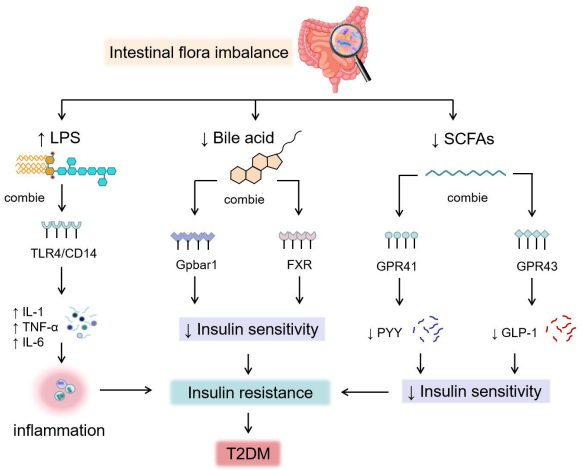


FIGURE 1
The mechanism of action of the intestinal microbiota and diabetes.

improving the gut barrier, improving intestinal integrity, alleviating inflammation, increasing glucagon-like peptide (GLP) 1 and GLP 2, increasing the production of SCFAs, decreasing LPS levels and endoplasmic reticulum stress, improving peripheral insulin sensitivity, and so on (29). The above proves that adjusting the gut microbiota can treat diabetes.

# 3 Effects of Chinese herb ingredients on intestinal microbiota

A review has shown that the abundance of bioactive constituents in Chinese herbs has a protective effect on the balance of the intestinal microecosystem, directly or indirectly regulating the imbalance of the intestinal microbiota (30). The possible mechanisms by which the active ingredient of Chinese herbs intervenes in the intestinal microbiota in the treatment of T2DM are as follows.

## 3.1 Polysaccharides

Polysaccharides are a class of natural polymers made of aldose or ketose connected by glycoside bonds, which are commonly found in botanicals. Chinese herbal polysaccharides improve glycolipid metabolism, inflammation, and intestinal barrier regulation, primarily by regulating intestinal microbiota species. Lycium barbarum polysaccharides (LBPs) have been reported to ameliorate diabetes by enhancing the gut barrier *via* modulating the gut microbiota and activating gut mucosal TLR2+ intraepithelial γδ T cells in rats. LBP could suppress inflammation in T2DM by decreasing the levels of plasma proinflammatory IL-1β, IL-6, IL-17A, and TNF-α in diabetic rats. LBP also could reduce the levels of glycated hemoglobin (GHb), triacylglycerol (TG), and total cholesterol (TC) (31). A polysaccharide isolated from Ganoderma lucidum ameliorates hyperglycemia by repairing islet cells and increasing insulin secretion, promoting the synthesis and storage of glycogen in the liver and improving the activities of antioxidant enzymes and IR (32). Moutan cortex polysaccharides also reconstruct gut microbiota, improve intestinal barrier function, reduce serum proinflammatory mediators, and elevate the SCFA contents. Moutan cortex polysaccharides alleviate diabetic kidney disease (DKD) in rats (33). Cyclocarya paliurus polysaccharides modulate the gut microbiota and SCFAs by stimulating SCFA receptors including GPR41, GPR43, and GPR109a and upregulating the expression of GLP-1 and PYY, thereby treating alleviate T2DM symptoms (34).

## 3.2 Saponins

Saponins are widely found in licorice, bupleurum, ginseng, Panax notoginseng, astragalus, and other Chinese herbs that play an important role in the prevention and treatment of diabetes. Polygonatum sibiricum saponin could decrease the abundance of Firmicutes in T2DM rats and increase the abundance of Bacteroidetes; thereby, it could significantly decrease the levels of insulin secretion and fasting blood glucose (FBG), TG, TC, and low-density lipoprotein cholesterol (LDL-C) and increase the content of high-density lipoprotein cholesterol (HDL-C) (35). Ginsenoside Rg1 treatment improves blood glucose, the blood lipid profile (total cholesterol, triglycerides, and LDL-C levels), the IR index, and liver function (aspartate transaminase and alanine transaminase levels). The levels of inflammatory cytokines (including IL-6, IL-1, and TNF-a) substantially decreased after ginsenoside Rg1 treatment (36). Other studies show that ginsenoside Rg5 improved the symptoms of hyperglycemia, repaired intestinal barrier function, relieved metabolic endotoxemia-related inflammation, and reversed gut microbiota dysbiosis in the colon with significantly decreased F/B ratios. More importantly, the effects of ginsenoside Rg5 were further confirmed by partial changes in the gut microbiota induced by broad-spectrum antibiotics because ginsenoside Rg5 increased the abundance of *Bacteroidetes* and *Proteobacteria* and dramatically decreased the abundance of *Firmicutes* and *Verrucomicrobia* in the gut of diabetic db/db mice (37). Oleuropein can increase the relative abundance of *Verrucomicrobia* and *Deferribacteres* and decreases the relative abundance of *Bacteroides*. Thereby, it has a significant effect on improving glucose tolerance, decreasing FBG levels, lowering the homeostasis model assessment–IR index, and improving diabetes-related metabolic disorders (38). Aloin modulated the bacterial community in the gut by raising the abundance of *Bacteroidota* and reducing the richness of *Firmicutes*, *Proteobacteria*, and *Actinobacteriota*. Thus, aloin ameliorated IR *via* activating the

IRS1/PI3K/Akt signaling pathway and regulating the gut microbiota, Thereby, it diminished weight loss, reduced FBG levels and hemoglobin A1c activity, and promoted glucose tolerance and fasting serum insulin activity in T2DM rats (39).

## 3.3 Polyphenols

Polyphenols are secondary metabolites found abundantly in a wide variety of Chinese herbs. The polyphenols and intestinal microbiota could interact with each other. The polyphenols in Chinese herbs can be further transformed, absorbed, and utilized by the intestinal microbiota. At the same time, polyphenols can regulate the composition of the intestinal microbiota by inhibiting pathogenic bacteria and promoting the growth of beneficial bacteria. There are reports that oral treatment with 200 mg/kg honokiol for 8 weeks significantly decreases the FBG in T2DM rats. The phosphorylation of the phospho-insulin receptor B-subunit (IR) and downstream insulin signaling factors such as AKT and ERK1/2 increased in a dose-dependent manner in the adipose, skeletal muscle, and liver tissue of honokiol-treated rats. Honokiol may also improve insulin-stimulated GLUT4 translocation by increasing the abundance of *Akkermansia* and SCFA-producing *Bacteroides* while decreasing *Oscillospira* (40, 41). Curcumin significantly improved gut integrity, hyperglycemia, IR, and endotoxemia in diabetic rats by reversing intestinal microbiota disturbances in diabetic rats (42). Interestingly, resveratrol also lowered blood glucose levels by modulating the gut microbiota but not when combined with curcumin, which may be related to their differential regulation of the gut microbiota (43).

## 3.4 Alkaloids

Alkaloids are a class of nitrogen-containing organic compounds that are an important part of Chinese herbs and have anti-inflammatory, antidiabetic, anti-obesity, and antihyperlipidemic effects (44). Berberine was found to reduce the Bacteroidetes/Firmicutes ratio in a study. Berberine, through its direct antibacterial action, could regulate glucose metabolism and body weight in Goto–Kakizaki (GK) rats by inhibiting the growth of harmful bacteria. Analysis indicated that FBG was negatively correlated with *Allobaculum* and strongly positively correlated with *Clostridia*. Body weight showed a negative correlation with *Akkermansia* and a positive correlation with *Desulfovibrionaceae* (45). Berberine action with intestinal bacteria reduced serum MCP-1, TNF-, and IL-6 expression, which was accompanied by decreased levels, improving glucose tolerance in diabetic rats (46). Total alkaloids of *Corydalis saxicola* (TACS) action caused the mouse intestinal microbiota to return to a controlled level. TACS could intervene in intestinal microbial disorders through four metabolic pathways (BCAAs), bile acids, arginine and proline, and purine metabolism (47). Mulberry total biotobasine significantly increased the abundance of microbiota that promote SCFA production such as *Erysipelotrichaceae* and *Bacteroides* and reduced the abundance of harmful microbiota such as *Desulfovibrio* and *Rikenellaceae*. Therefore, mulberry total biotobasine promotes insulin secretion and ameliorates the β cells of diabetes rats' dysfunction and mass reduction both *in vivo* and *in vitro* (48).

## 3.5 Licorice extract

High-dose licorice extract could effectively decrease the levels of nuclear factor kappa-B (NF-κB), toll-like receptor 4 (TLR4) through reshaping the gut microbiota structure. At a normal glucose level, licorice extract decreased AMP-activated protein kinase α (AMPKα) phosphorylation, and at high glucose, licorice extract augmented the cytosolic calcium concentration. Therefore, it alleviated hyperglycemia and glucose intolerance in T2DM rats and improved the function and morphology of diabetic islets. More importantly, all the doses of licorice extract regulate intestinal microbiota balance by increasing the contents of *Akkermansia*, *Alloprevotella*, and *Bacteroides* and decreasing the contents of *Lachnospiraceae*, especially for the high dose of licorice extract. Licorice extract could also alleviate serum LPSs and FBG. These results indicated that the antidiabetic effect of licorice extract might be attributed to the regulation of the gut microbiota and the colon TLR4/NF-κB signaling pathway in diabetic rats (49).

## 3.6 Flavonoids

Pueraria, Scutellaria, Gingko leaves, and other medicines contain flavonoids, which have a wide range of biological activities. The gut microbiota play essential roles in the digestion and absorption of flavonoids and affect the occurrence and progression of T2DM. Flavonoids effectively increased insulin levels, decreased FBG content, reduced lipid accumulation in plasma, alleviated oxidative injury and inflammation, and relieved liver and kidney damage in diabetic mice (50). For example, Pueraria extract contains nine flavonoids; they can increase intestinal probiotics to improve metabolic disorders caused by diabetes and decrease *Clostridium celatum* levels to alleviate inflammation. Flavonoids have the potential to be used to control type 2 diabetes by regulating glycolipid metabolism and inflammation levels (50, 51).

## 3.7 Ethanol extract of Sargarsum fusiforme

The ethanol extract of Sargarsum fusiforme could significantly reduce food intake, water intake, and FBG while improving glucose tolerance, blood lipid levels, and hepatic oxidative stress in diabetic rats. The ethanol extract of Sargarsum fusiforme could reduce the abundance of bacteria related to diabetes or other metabolic

diseases (such as *Romboutsia* and *Enterorhabdus*), and increase the abundance of benign bacteria (such as *Lachnoclostridium* and *Intestinimonas*). In the gut contents of diabetes rats, branched-chain amino acid levels were decreased, aromatic amino acid levels were decreased, and 4-hydroxyphenylacetic acid levels were increased, suggesting that EE may alter the ratio of these compounds by modulating the gut microbiota while affecting T2DM (52).

The mechanism of Chinese medicinal ingredients acting on intestinal microbiota in the treatment of diabetes is shown in Table 1.

# 4 Effects of Chinese herbal compounding on intestinal microbiota and diabetes

Chinese herbal compounding has been used to treat diabetes for thousands of years. These traditional remedies mostly contain herbs that benefit Qi. The main effects and their mechanisms are as follows.

## 4.1 Huang-Lian-Jie-Du decoction

It was discovered that Huang-Lian-Jie-Du decoction (HLJDD) could improve metabolic disturbances such as lipids, hyperglycemia, and inflammation; shape the microbiome; and restore dysregulated microbiota function in T2DM rats. HLJDD treatment could not only restore gut dysbiosis in T2DM rats, as evidenced by an increase in SCFA-producing and anti-inflammatory bacteria(e.g., *Akkermansia*, *Blautia*, and *Parabacteroides*), as well as a decrease in conditioned pathogenic bacteria (e.g., *Aerococcus*, *Corynebacterium*, and *Staphylococcus*), but also modulate the dysregulated function of the gut microbiome in T2DM rats (53). The changes in intestinal microbial populations may be due to the action of the active ingredients saponin and berberine in HLJDD.

TABLE 1 Progress on the mechanism of Chinese medicinal ingredients acting on intestinal microbiota in the treatment of diabetes.

| TCM Ingredients | Effects on gut microbiota | | metabolites | | Therapeutic effect | Document |
|---|---|---|---|---|---|---|
| | Promotes | Reduces | Promotes | Reduces | | |
| **Polysaccharide** | *Lactobacillus*<br>*Bacteroides*<br>*Ruminococcaceae*<br>*Bifidobacterium*<br>*Alistipes* | *Blautia*<br>*Desulfovibrio* | SCFAs<br>PYY<br>GLP-1 | GHb<br>TG, TC<br>LPS | Improves diabetes-related biochemical abnormalities and alleviates type 2 diabetes symptoms | 34920067<br>35307460<br>32663709 |
| **Saponins** | *Bacteroides*<br>*Proteobacteria* | *Firmicutes*<br>*Verrucomicrobia*<br>*Proteobacteria*<br>*Actinobacteriota* | HDL-C<br>insulin | FBG<br>TG, TC<br>LDL | Improves insulin resistance and symptoms of hyperglycemia, repairs intestinal barrier function, relieves inflammation, and reverses gut microbiota dysbiosis | 34517283<br>28362999<br>32307991<br>34206641<br>31181236 |
| **Polyphenols** | *Akkermansia*<br>*Bacteroides* | *Oscillospira*<br>*Firmicutes* | SCFAs<br>insulin | FBG | Improves the insulin sensitivity and reduces blood glucose | 26674084<br>31921106<br>34818970<br>31473511 |
| **Alkaloid** | *Erysipelotrichaceae*<br>*Bacteroides* | *Desulfovibrio*<br>*Rikenellaceae* | SCFAs | FBG<br>LPS | Regulates blood glucose, improves blood lipids, and reduces insulin resistance | 30837071<br>33716449<br>27702567<br>31214133<br>35308210 |
| **Licorice extract** | *Akkermansia*<br>*Bacteroides*<br>*Alloprevotella* | *Lachnospiraceae* | – | FBG<br>LPS<br>TG, TC | Improves insulin resistance, serum lipids, and endotoxemia-related colonic inflammation. | 35227470 |
| **Pueraria leaf extract** | *Probiotics* | *Clostridium* | insulin | FBG | Ameliorates oxidative injury and inflammation and relieves liver and kidney damage | 35289350 |
| **Flavonoids** | *Akkermansia* | *Clostridium* | insulin | FBG<br>TG, TC | Alleviates oxidative injury and inflammation and relieves liver and kidney damage | 35289350 |
| **Ethanol extract of Sargarsum fusiforme** | *Lachnoclostridium*<br>*Intestinimonas*<br>*Oscillibacter* | *Romboutsia*<br>*Enterorhabdus*<br>*Lachnospiraceae* | 4-HA | FBG<br>AAA<br>BCAA | Improves the level of inflammation and reduces blood glucose. | 34399527 |

## 4.2 Xie-xin decoction

The Xie-xin decoction (XXD) from Zhang Zhongjing's Medical Treasures of the Golden Chamber is a compound recipe for heat-clearing and detoxication. Since the Tong Dynasty, this classic prescription of Dahuang, Huanglian, and Huangqin has been widely used to treat diabetes with remarkable therapeutic effects (54). According to one study, XXD can significantly improve hyperglycemia, lipid metabolism, and inflammation in T2DM rats by increasing the abundance of the gut microbiota, particularly some SCFA-producing and anti-inflammatory bacteria (e.g., *Alloprevotella*, *Adlercreutzia*, *Blautia*, *Barnesiella*, *Papillibacter*, and *Lachnospiraceae*) (55). The mechanism of action may be related to the various flavonoids, saponins, and polysaccharides in XXD.

## 4.3 Ge-gen-Qin-lian decoction

Ge-gen-Qin-lian decoction (GGQLD), a well-known TCM prescription for diabetes, is made up of Pueraria, Huangqin, Huanglian, and licorice. GGQLD treatment altered the overall gut microbiota structure and enriched many butyrate-producing bacteria (e.g., *Roseburia* and *Faecalibacterium*), lowering glucose and serum proinflammatory cytokine concentrations and attenuating intestinal inflammation. Treatment with GGQLD significantly increased the levels of SCFAs in rat feces. Furthermore, after treatment, the expression of immune-related genes such as Ifnrg1, Stat1, and Nfkb1 in pancreatic islets was significantly reduced. A study found that by interacting with intestinal bacteria, GGQLD significantly reduced FBG, glycosylated hemoglobin, and glycosylated serum protein levels in diabetic rats, as well as fasting serum insulin levels (56).The mechanisms of action of GGQLD might be related to the augmentation of the upregulation of the mRNA expression of adiponectin and adiponectin protein concentration (57). Saponins, flavonoids, and berberine were detected in GGQLD, and the efficacy of GQD might be attributed primarily to its key ingredient, berberine, which is likely to alleviate T2DM *via* the modulation of the intestinal microbiota, thereby reducing systemic and local inflammation.

## 4.4 Pi-Dan-Jian-Qing decoction

Pi-Dan-Jian-Qing decoction (PDJQD), which contains Astragalus, Pseudostellaria heterophylla, Atractylodes, Potentilla discolor Bunge, Scrophularia, Coptidis, Scutellaria, Pueraria, and Salvia miltiorrhiza Bunge, among other ingredients, has been used in clinic to treat T2DM (58). By increasing the relative abundances of *Akkermansia*, *Bacteroides*, *Blautia*, *Desulfovibrio*, and *Lactobacillus* while decreasing the relative abundance of Prevotella, PDJQD could reduce the F/B ratio. The modulatory effects of PDJQD on the TCA cycle, histidine metabolism, and tryptophan metabolism have been linked to changes in the abundance of *Akkermansia*, *Bacteroides*, and *Lactobacillus* (59). Treatment with PDJQD improved hyperglycemia, hyperlipidemia, IR, and pathological changes in the liver, pancreas, kidney, and colon in T2DM rats. The polysaccharide and flavonoid components of PDJQD may have reduced proinflammatory cytokine levels and inhibited oxidative stress by acting on the intestinal microbiota.

The mechanism of Chinese medicine prescription acting on intestinal microbiota in the treatment of diabetes is shown in Table 2.

# 5 Effects of prepared Chinese medicine on intestinal microbiota and diabetes

Prepared Chinese medicine is made from Chinese herbal medicine as raw materials and is processed into specific dosage forms of Chinese medicine products according to the prescribed prescription and preparation process for the purpose of disease prevention and treatment. It has the properties of a stable nature, precise efficacy, and relatively small toxic side effects and is simple to take, carry, store, and keep. The following are the main effects and mechanisms of prepared Chinese medicine, which is commonly used in the treatment of diabetes.

## 5.1 Shen-Ling-Bai-Zhu powder

Shen-Ling-Bai-Zhu powder (SLBZP) is a TCM formulation that has been widely used to improve T2DM. SLBZP is composed of ginseng, schisandra, astragalus, yam, dioscorea, raspberry, maitake, poria, etc. It is rich in saponins, flavonoids and polysaccharides, which are its most important active ingredients. A study showed that, after high-dose SLBZP treatment, the relative abundance of *Roseburia*, *Lactobacillus*, *Staphylococcus*, and *Psychrobacter* significantly decreased, while the relative abundance of *Acinetobacter*, *Ochrobactrum*, *Prevotella*, *Anaerostipes*, *Bilophila*, and *Turicibacter* increased significantly in the 9-week rats (60). Changes in intestinal microbiota are followed by changes in their metabolites, such as SCFA levels. Furthermore, SLBZP significantly reduced insulin, IR, and leptin resistance in rats. SLBZP could alleviate chronic inflammation in rats based on changes in the serum levels of monocyte chemoattractant protein-1 (MCP-1) and interleukin 1 (IL-1) (61). The findings show that SLBZP can lower blood glucose, body weight, glycosylated hemoglobin, and lipid levels, allowing it to control obesity, relieve chronic

TABLE 2 Progress on the prescription of Chinese herbal compounding acting on intestinal microbiota in the treatment of diabetes.

| Chinese medicinesprescription | Effects on gut microbiota | | metabolites | | Therapeutic effect | Document |
|---|---|---|---|---|---|---|
| | Promotes | Reduces | Promotes | Reduces | | |
| **Huang-Lian-Jie-Du Decoction** | *Akkermansia*<br>*Blautia*<br>*Parabacteroides* | *Aerococcus*<br>*Corynebacterium*<br>*Staphylococcus* | SCFAs<br>Bile acid | Glucose<br>TG,TC<br>LDL<br>HDL | Improves the metabolic disturbance of lipids, hyperglycemia, and inflammation and shapes the microbiome | 24368167<br>30349514 |
| **Xie-xin Decoction** | *Alloprevotella*<br>*Adlercreutzia*<br>*Blautia*<br>*Barnesiella*<br>*Papillibacter*<br>*Lachnospiraceae* | *Coriobacteriaceae* | SCFAs | Glucose<br>TG,TC<br>LDL<br>HDL | Significantly ameliorates hyperglycemia, lipid metabolism, and inflammation | 29487347 |
| **Ge-gen-Qin-lian Decoction** | *Faecalibacterium*<br>*Roseburia*<br>*Clostridium*<br>*Ruminococcus*<br>*Dorea*<br>*Butyricicoccus*<br>*Coprococcus* | – | SCFAs | Glucose | Reduces blood glucose levels, regulates intestinal microbiota, induces ileal gene expression, and relieves systemic and local inflammation | 23219338<br>33359679 |
| **Pi-Dan-Jian-Qing Decoction** | *Lactobacillus*<br>*Blautia*<br>*Bacteroides,*<br>*Desulfovibrio*<br>*Akkermansia* | *Prevotella* | SOD<br>GSH-Px<br>HDL | Glucose<br>TG,TC<br>LDL | Improves hyperglycemia; hyperlipidemia; insulin resistance (IR); and pathological changes of liver, pancreas, kidney, and colon | 34938667 |

inflammation, regulate intestinal microbiota and metabolites, and prevent T2DM.

## 5.2 Shen-Qi compound

Shen-Qi compound (SQC), composed of astragalus, ginseng, Lycium, etc., is a kind of TCM formulation that has been widely used to improve T2DM. Studies have demonstrated that SQC can reduce glycemic variability, alleviate the inflammatory response, etc. Astragalus, ginseng, and Lycium can provide polysaccharides and saponins, and the mechanism by which SQC treats diabetes by interacting with intestinal microbiota may be related to these two active ingredients. SQC intervention could regulate the serum levels of insulin and glucagon and improve injury to the intestinal mucosal barrier of GK rats. After SQC intervention, the ratio of Bacteroidetes to Firmicutes could be improved in the gut. Moreover, SQC improves glycolysis, gluconeogenesis, the citrate cycle, lipid metabolism, amino acid metabolism, and SCFA metabolism by regulating the relative abundance of *Blautia, Prevotellaceae, Rothia, Roseburia, Lactobacillus*, *Butyricimonas*, and *Bacteroides* (62).

## 5.3 Liu-Wei-Di-Huang pills

Liu-Wei-Di-Huang (LWDH) pills are a Yin-nourishing and kidney-tonifying prescription in TCM with promising pharmacological characteristics. Its main components are processed Rehmanniae Radix, Moutan Cortex, yam, Poria cocos, and Rhizoma Alismatis (63). LWDH Pills were reported to possibly be used to treat diabetes, that is, new applications of classic herbal formulae. The modulation of the gut microbiota by the flavonoids, saponins, and polysaccharides of LWDH is one possible mechanism for its diabetes treatment. GK rats treated with LWDH altered the microbial structure and promoted the abundance of bacteria in *Firmicutes*, including *Allobaculum*, *Lactobacillus*, and *Ruminococcus*' increased SCFA levels involving butyric acid, propionic acid, and acetic acid. LWDH reduces T2DM and jejunal injury *via* intestinal bacterial action, with the SCFAs-GPR43/41-GLP-1 pathway being one possible mechanism (64).

## 5.4 San-Huang-Yi-Shen capsule

San-Huang-Yi-Shen capsule (SHYS) has been used in the treatment of diabetic nephropathy (DN) in the clinic for many years. SHYS is composed of ginseng, astragalus, angelica, donkey-hide gelatin, rhizoma, and other ingredients. The active ingredients flavonoids, saponins, and polysaccharides of SHYS may regulate the intestinal microbiota. SHYS affected the beta diversity of the gut microbiota community in DN model rats. SHYS could decrease the F/B ratio. SHYX treatment affected the relative abundances of Anaerovibrio, Allobaculum, Bacteroides, Lactobacillus, etc. SHYX regulates

arginine biosynthesis, the TCA cycle, tyrosine metabolism, and arginine and proline metabolism in DN model rats by influencing intestinal microbiota and metabolite levels (65). SHYS treatment alters intestinal microbiota and metabolism, which modulates body weight, hyperglycemia, proteinuria, and renal pathology in DN rats.

## 5.5 Tang-Nai-Kang

Tang-Nai-Kang (TNK) is a kind of TCM that is a mixture of extracts from five herbal plants: Spica Prunellae Vulgaris, Fructus Ligustri Lucidi, Psidium guajava, Radix Ginseng, and Saururus Chinensis. Over the years, TNK has been widely used to treat diabetes mellitus. Studies have shown that TNK ameliorates glucose intolerance and IR in prediabetic SHR/cp rats and obese Zucker rats (66). TNK could alleviate hyperglycemia and improve the composition and abundance of the gut microbiota in diabetic KKAy mice. TNK treatment increased the abundance and diversity of intestinal microbial species, such as *Akkermansia* and *Allobaculum*, while decreasing *Lactobacillus* (67). The high-dose TNK treatment significantly reduced FPG levels while increasing body weight in KKAy mice (67). Other studies have shown that TNK treatment significantly decreased fasting serum insulin (FINS) and FBG; increased the insulin sensitivity index (ISI); improved impaired glucose tolerance; reduced the serum levels of interleukin-6 (IL-6), C-reactive protein (CRP), and tumor necrosis factor-Δ (TNF-Δ); and increased serum adiponectin in SHR rats (68). The underlying hypoglycemic mechanisms of TNK may be due to the high number of saponins it contains.

The mechanism of Chinese medicinal preparations on intestinal microbiota and diabetes mellitus is shown in Table 3.

# 6 Summary and prospect

Beneficial Qi TCM promotes the growth of probiotics, inhibits the colonization of pathogenic bacteria in the intestine, and influences intestinal epithelial cell differentiation and apoptosis, and positive regulation of the gut microbiota is beneficial in the treatment of metabolic syndromes. Several studies have shown that the beneficial role of TCM is related to gut microbiota regulation. Chinese medicine can modulate the composition and activity of the metabolites of intestinal bacteria by affecting their growth. For example, herbal medicine makes the metabolites of the intestinal microbiota increase in SCFAs, which can regulate the composition and activity of their metabolites by influencing growth, regulating the concentration of metabolites, disrupting the intestinal barrier, improving insulin sensitivity, regulating lipid metabolism and blood glucose levels, and improving the level of inflammation, which can explain why TCM plays a role in a variety of metabolic diseases such as diabetes (69).

TCM can regulate the composition of intestinal microbiota and its metabolites, and intestinal microbiota can also transform and promote the absorption of Chinese herbal ingredients. This paper discusses the role of gut microbes in the development of T2DM, as well as how to treat T2DM by targeting the gut microbiota with herbs and their active ingredients (70). The

TABLE 3 Research progress of Chinese medicine preparations acting on intestinal microbiota in the treatment of diabetes mellitus.

| Prepared Chinese medicines | Effects on gut microbiota | | Metabolites | | Therapeutic effect | Document |
|---|---|---|---|---|---|---|
| | Promotes | Reduces | Promotes | Reduces | | |
| **Shen-ling-Bai-zhu Powder** | *Psychrobacter*<br>*Lactobacillus*<br>*Roseburia*<br>*Staphylococcus* | *Anaerostipes*<br>*Turicibacter*<br>*Bilophila*<br>*Ochrobactrum*<br>*Acinetobacter*<br>*Prevotella* | SCFAs<br>insulin | Glucose<br>TG,TC<br>LDL<br>HDL | Regulates intestinal microbiota and metabolites and relieves chronic inflammation to control obesity | 35285199 |
| **Shen-Qi Compound** | *Bacteroidetes* | *Firmicutes* | SCFAs<br>insulin | Glucose<br>TG,TC | Improves gluconeogenesis, glycolysis, amino acid metabolism, lipid metabolism, the citrate cycle, and butanoate metabolism | 35219959 |
| **Liu-Wei-Di-Huang Pills** | *Allobaculum*<br>*Lactobacillus*<br>*Ruminococcus* | – | SCFAs<br>insulin | Glucose | Reduces blood glucose levels and regulates intestinal microbiota | 35857109 |
| **San-Huang-Yi-Shen Capsule** | *Lactobacillus*<br>*Allobaculum*<br>*Anaerovibrio*<br>*Bacteroides* | *Candidatus_Saccharimonas* | L-Glutamine<br>Acetylcholine | L-Phenylalanine<br>L-Tyrosine | Alleviates hyperglycemia and improves renal function, pathological changes in the kidney, oxidative stress, and inflammatory response | 35058786 |
| **Tang-Nai-Kang** | *Akkermansia*<br>*Allobaculum* | *Lactobacillus* | FPG<br>insulin | CRP<br>Glucose | Reduces blood glucose levels and increases the insulin sensitivity index | 34868327<br>31682379 |

active ingredients such as saponins, flavonoids, polysaccharides, and alkaloids contained in TCM can act on intestinal microbiota, which is a possible mechanism to treat diabetes. Changes in the abundance of certain pathological bacteria contribute directly to the development of diabetes. By utilizing intestinal mucin, intestinal probiotics can mediate the metabolism of TCM ingredients and *in vivo* substances, as well as maintain the integrity of the gut barrier, such as *Akkermansia muciniphila*. It may be a promising method of controlling T2DM because it can relieve T2DM through various mechanisms and modes of action, such as improving microbial metabolism and protecting the intestinal barrier function and having an anti-inflammatory effect (71, 72). All of these help us understand current TCM research and development and provides a foundation for future clinical applications (73).

However, there is still a long way to go in explaining the mechanism of TCM against metabolic diseases and its potential side effects, particularly given the wide variations in the composition of intestinal microbiota among individuals. We should continue to improve our understanding of the common signal transduction mechanism in different bacteria in order to achieve standardized treatment by targeting common molecules or signaling pathways, with the ultimate goal of translating knowledge into practice in mind.

## Data availability statement

The original contributions presented in the study are included in the article/supplementary material. Further inquiries can be directed to the corresponding author.

## Author contributions

MS and CH conceived the paper. MS, CH, and RH analyzed the relevance of the literature and wrote the article. TT and WT revised the figures and reviewed the article. All authors reviewed and approved the final version of the manuscript.

## Funding

Hunan Provincial Education Department Scientific Research Project: Hunan Education Bulletin[2019]No.353-19C0196. Students Innovative Training Program of Hunan Province: Hunan Education Bulletin[2018] No.255-1098.

## Conflict of interest

The authors declare that the research was conducted in the absence of any commercial or financial relationships that could be construed as a potential conflict of interest.

## Publisher's note



## References

1. Che QY, Luo TT, Shi JH, He YH, Xu DL Mechanisms by which traditional Chinese medicines influence the intestinal flora and intestinal barrier. *Front Cell Infection Microbiol* (2022) 12:863779. doi: 10.3389/fcimb.2022.863779

2. Mi WS, Xia Y, Bian YH. Meta-analysis of the association between aldose reductase gene (CA)n microsatellite variants and risk of diabetic retinopathy. *Exp Ther Med* (2019) 18:4499–509. doi: 10.3892/etm.2019.8086

3. Chen YH, Tan S, Liu M, Li JM. LncRNA TINCR is downregulated in diabetic cardiomyopathy and relates to cardiomyocyte apoptosis. *Scand Cardiovasc J* (2018) 52:335–9. doi: 10.1080/14017431.2018.1546896

4. Ahmad A, Yang WW, Chen GF, Shafiq M, Javed S, Zaidi ASS, et al. Analysis of gut microbiota of obese individuals with type 2 diabetes and healthy individuals. *PloS One* (2019) 14:e0226372. doi: 10.1371/journal.pone.0226372

5. Han JL, Lin HL. Intestinal microbiota and type 2 diabetes: from mechanism insights to therapeutic perspective. *World J Gastroenterol* (2014) 47:17737–45. doi: 10.3748/wjg.v20.i47.17737

6. Xia F, Wen LP, Ge BC, Li YX, Li FP, Zhou BJ, et al. Gut microbiota as a target for prevention and treatment of type 2 diabetes: Mechanisms and dietary natural products. *World J Diabetes* (2021) 12:1146 –1163. doi: 10.4239/wjd.v12.I8.1146

7. Umirah F, Neoh CF, Ramasamy K, Lim SM. Differential gut microbiota composition between type 2 diabetes mellitus patients and healthy controls: A systematic review. *Diabetes Res Clin Pract* (2021) 173:108689. doi: 10.1016/j.diabres.2021.108689

8. Ma QT, Li YQ, Li PF, Wang M, Wang JK, Tang ZY, et al. Research progress in the relationship between type 2 diabetes mellitus and intestinal flora. *Biomed Pharmacother* (2019) 117:109138. doi: 10.1016/j.biopha.2019.109138

9. Cunningham AL, Stephens JW, Harris DA. Gut microbiota influence in type 2 diabetes mellitus (T2DM). *Gut Pathog* (2021) 13:50–0. doi: 10.1186/S13099-021-00446-0

10. Sun Y, Huang YC, Ye FH, Liu WW, Jin XH, Lin KX, et al. Effects of probiotics on glycemic control and intestinal dominant flora in patients with type 2 diabetes mellitus: A protocol for systematic review and meta-analysis. *Med (Baltimore)* (2020) 99:e23039. doi: 10.1097/md.0000000000023039

11. Doumatey AP, Adeyemo A, Zhou J, Lei L, Adebamowo SN, Adebamowo C, et al. Gut microbiome profiles are associated with type 2 diabetes in urban africans. *Front Cell Infect Microbiol* (2020) 10:63. doi: 10.3389/fcimb.2020.00063

12. He L, Liu YW, Guo YF, Shen KJ, Hui HY, Tan ZJ. Diversity of intestinal bacterial lactase gene in antibiotics-induced diarrhea mice treated with Chinese herbs compound qi wei bai Zhu San. *3 Biotech* (2018) 8:4. doi: 10.1007/s13205-017-1024-y

13. Hui HY, Wu Y, Zheng T, Zhou SN, Tan ZJ. Bacterial characteristics in intestinal contents of antibiotic-associated diarrhea mice treated with qiweibaizhu powder. *Med Sci Monit* (2020) 26:921771. doi: 10.12659/msm.921771

14. Zheng YJ, Ding QY, Wei Y, Gou XW, Tian JX, Li M, et al. Effect of traditional Chinese medicine on gut microbiota in adults with type 2 diabetes: A

systematic review and meta-analysis. *Phytomedicine* (2020) 88:153455. doi: 10.1016/j.phymed.2020.153455

15. Zhang YL, Xu YN, Zhang L, Chen YJ, Wu T, Liu R, et al. Licorice extract ameliorates hyperglycemia through reshaping gut microbiota structure and inhibiting TLR4/NF-κB signaling pathway in type 2 diabetic mice. *Food Res Int* (2022) 153:110945. doi: 10.1016/j.foodres.2022.110945

16. Xie DD, Zhao XT, Chen MW. Prevention and treatment strategies for type 2 diabetes based on regulating intestinal flora. *BioSci Trends* (2021) 5:313–20. doi: 10.5582/bst.2021.01275

17. Li XY, Peng XX, Guo KX, Tan ZJ. Bacterial diversity in intestinal mucosa of mice fed with dendrobium officinale and high-fat diet. *3 Biotech* (2021) 11:22. doi: 10.1007/s13205-020-02558-x

18. Guo KX, Xu SS, Zhang QL, Peng MJ, Yang ZY, Tan ZJ, et al. Bacterial diversity in the intestinal mucosa of mice fed with asparagus extract under high-fat diet condition. *3 Biotech* (2020) 10:228. doi: 10.1007/s13205-020-02225-1

19. Wang FJ, Zhao T, Wang WW, Dai QQ, Ma XH. Will intestinal flora therapy become a new target in type-2 diabetes mellitus? a review based on 13 clinical trials. *Nutricion Hospitalaria* (2021) 39:425–43. doi: 10.20960/nh.03866

20. Wang SZ, Yu YJ, Adeli K. Role of gut microbiota in neuroendocrine regulation of carbohydrate and lipid metabolism via the microbiota-gut-brain-liver axis. *Microorganisms* (2020) 8:527. doi: 10.3390/microorganisms8040527

21. Sun T, Zhang B, Ru QJ, Chen XM, Lv BD. Tocopheryl quinone improves non-alcoholic steatohepatitis (NASH) associated dysmetabolism of glucose and lipids by upregulating the expression of glucagon-like peptide 1 (GLP-1) via restoring the balance of intestinal flora in rats. *Pharm Biol* (2021) 59:723–31. doi: 10.1080/13880209.2021.1916542

22. Herrera CR, Vidal GX. Cardiovascular outcomes, heart failure and mortality in type 2 diabetic patients treated with glucagon-like peptide 1 receptor agonists (GLP-1 RAs):A systematic review and meta-analysis of observational cohort studies. *Int J Clin Pract* (2020) 74:e13553. doi: 10.1111/ijcp.13553

23. Bordoni M, Biagioli M, Giorgio CD, Marchianò S, Roselli R, Bellini R, et al. Tu1111: Regulation of intestinal ACE2 expression by the bile acid receptor GPBAR1 is mediated by a GPBAR1/GLP-1/GLP-1R axis. *Gastroenterology* (2022) 162:S–887. doi: 10.1016/S0016-5085(22)62099-7

24. Priyadarshini M, Kotlo KU, Dudeja PK, Layden BT. Role of short chain fatty acid receptors in intestinal physiology and pathophysiology. *Compr Physiol* (2018) 8:1091–115. doi: 10.1002/cphy.c170050

25. Li XX, Zhang XX, Zhang R, Ni ZJ, Elam E, Thakur K, et al. Gut modulation based anti-diabetic effects of carboxymethylated wheat bran dietary fiber in high-fat diet/streptozotocin-induced diabetic mice and their potential mechanisms. *Food Chem Toxicol* (2021) 152:112235. doi: 10.1016/j.fct.2021.112235

26. Cuesta ZJ, Mueller NT, Corrales AV, Velásquez MEP, Carmona JA, Abad JM, et al. Metformin is associated with higher relative abundance of mucin-degrading akkermansia muciniphila and several short-chain fatty acid-producing microbiota in the gut. *Diabetes Care* (2017) 40:54–62. doi: 10.2337/dc16-1324

27. Olivares M, Neyrinck AM, Pötgens SA, Beaumont M, Salazar N, PD C, et al. The DPP-4 inhibitor vildagliptin impacts the gut microbiota and prevents disruption of intestinal homeostasis induced by a Western diet in mice. *Diabetologia* (2018) 61:1838–48. doi: 10.1007/s00125-018-4647-6

28. Ryu JK, Kim SJ, Rah SH, Kang JI, Jung HE, Lee DS, et al. Reconstruction of LPS transfer cascade reveals structural determinants within LBP,CD14,and TLR4-MD2 for efficient lps recognition and transfer. *Immunity* (2017) 46:38–50. doi: 10.1016/j.immuni.2016.11.007

29. Zhai LX, Wu JY, Lam YY, Kwan HY, Bian ZX, Wong HLX, et al. Gut-microbial metabolites, probiotics and their roles in type 2 diabetes. *Int J Mol Sci* (2021) 22:12846. doi: 10.3390/ijms222312846

30. Li CR, Zhou K, Xiao NQ, Peng MJ, Tan ZJ. The effect of qiweibaizhu powder crude polysaccharide on antibiotic-associated diarrhea mice is associated with restoring intestinal mucosal bacteria. *Front Nutr* (2022) 9:952647. doi: 10.3389/fnut.2022.952647

31. Lu HX, Liu P, Zhang XX, Bao T, Wang T, Guo L, et al. Inulin and lycium barbarum polysaccharides ameliorate diabetes by enhancing gut barrier via modulating gut microbiota and activating gut mucosal TLR2+ intraepithelial γδ T cells in rats. *J Funct Foods* (2021) 79:104407. doi: 10.1016/j.jff.2021.104407

32. Shao WM, Xiao C, Yong TQ, Zhang YF, Hu HP, Xie T, et al. A polysaccharide isolated from ganoderma lucidum ameliorates hyperglycemia through modulating gut microbiota in type 2 diabetic mice. *Int J Biol Macromol* (2021) 197:23–38. doi: 10.1016/j.ijbiomac.2021.12.034

33. Zhang M, Yang LC, Zhu MM, Yang B, Yang YJ, Jia XB, et al. Moutan cortex polysaccharide ameliorates diabetic kidney disease via modulating gut microbiota dynamically in rats. *Int J Biol Macromol* (2022) 206:849–60. doi: 10.1016/j.ijbiomac.2022.03.077

34. Yao Y, Yan LJ, Chen H, Wu N, Wang WB, Wang DS. Cyclocarya paliurus polysaccharides alleviate type 2 diabetic symptoms by modulating gut microbiota and short-chain fatty acids. *Phytomedicine* (2020) 77:153268. doi: 10.1016/j.phymed.2020.153268

35. Chai YY, Luo JY, Bao YH. Effects of polygonatum sibiricum saponin on hyperglycemia, gut microbiota composition and metabolic profiles in type 2 diabetes mice. *Biomed Pharmacother* (2021) 143:112155. doi: 10.1016/j.biopha.2021.112155

36. Tian W, Chen L, Zhang L, Wang B, Li XB, Fan KR, et al. Effects of ginsenoside Rg1 on glucose metabolism and liver injury in streptozotocin-induced type 2 diabetic rats. *Genet Mol Res* (2017) 16:gmr16019463. doi: 10.4238/gmr16019463

37. Wei YG, Yang HX, Zhu CH, Deng JJ, Fan DD. Hypoglycemic effect of ginsenoside Rg5 mediated partly by modulating gut microbiota dysbiosis in diabetic db/db mice. *J Agric Food Chem* (2020) 68:5107–17. doi: 10.1021/acs.jafc.0c00605

38. Zheng SJ, Wang YN, Fang JJ, Geng RX, Li MJ, Zhao YH, et al. Oleuropein ameliorates advanced stage of type 2 diabetes in db/db mice by regulating gut microbiota. *Nutrients* (2021) 13:2131–1. doi: 10.3390/nu13072131

39. Zhong RT, Chen LB, Liu YY, Xie SX, Li SM, Zhao C, et al. Anti-diabetic effect of aloin *via* JNK-IRS1/PI3K pathways and regulation of gut microbiota. *Food Sci Hum Wellness* (2022) 11:189–98. doi: 10.1016/j.fshw.2021.07.019

40. Sun J, Fu XQ, Liu Y, Wang YS, Huo B, Guo YD, et al. Hypoglycemic effect and mechanism of honokiol on type 2 diabetic mice. *Drug Design Dev Ther* (2015) 9:6327–42. doi: 10.2147/DDDT.S92777

41. Ding YN, Song ZH, Li H, Chang L, Pan TL, Gu XL, et al. Honokiol ameliorates high-Fat-Diet-Induced obesity of different sexes of mice by modulating the composition of the gut microbiota. *Front Immunol* (2019) 10:2800. doi: 10.3389/fimmu.2019.02800

42. Huang JZ, Guan BB, Lin LJ, Wang YP. Improvement of intestinal barrier function, gut microbiota, and metabolic endotoxemia in type 2 diabetes rats by curcumin. *Bioengineered* (2021) 12:11947–58. doi: 10.1080/21655979.2021.2009322

43. Sreng N, Champion S, Martin JC, Khelaifia S, Christensen JE, Padmanabhan R, et al. Resveratrol-mediated glycemic regulation is blunted by curcumin and is associated to modulation of gut microbiota. *J Nutr Biochem* (2019) 72:108218. doi: 10.1016/j.jnutbio.2019.108218

44. Osman AG, Haider S, Chittiboyina AG, Khanab IA. Utility of alkaloids as chemical and biomarkers for quality, efficacy, and safety assessment of botanical ingredients. *Phytomedicine* (2018) 54:347–56. doi: 10.1016/j.phymed.2018.03.064

45. Zhao JD, Li Y, Sun M, Yu CJ, Li JY, Wang SH, et al. Effect of berberine on hyperglycaemia and gut microbiota composition in type 2 diabetic goto-kakizaki rats. *World J Gastroenterol* (2021) 27:708–24. doi: 10.3748/wjg.v27.i8.708

46. Ye LF, Liang S, Guo C, Yu XZ, Zhao J, Zhang H, et al. Inhibition of M1 macrophage activation in adipose tissue by berberine improves insulin resistance. *Life Sci* (2016) 166:82–91. doi: 10.1016/j.lfs.2016.09.025

47. Liu X, Zheng H, Lu RG, Huang HM, Zhu HL, Yin CL, et al. Intervening effects of total alkaloids of corydalis saxicola bunting on rats with antibiotic-induced gut microbiota dysbiosis based on 16S rRNA gene sequencing and untargeted metabolomics analyses. *Front Microbiol* (2019) 10:1151. doi: 10.3389/fmicb.2019.01151

48. Lei L, Huan Y, Liu Q, Li CN, Cao H, Ji WM, et al. Morus alba L.(Sangzhi) alkaloids promote insulin secretion, restore diabetic β-cell function by preventing dedifferentiation and apoptosis. *Front Pharmacol* (2022) 13:841981. doi: 10.3389/FPHAR.2022.841981

49. Zhang YL, Xu YN, Zhang L, Chen YJ, Wu T, Liu R, et al. Licorice extract ameliorates hyperglycemia through reshaping gut microbiota structure and inhibiting TLR4/NF-κB aignaling pathway in type 2 diabetic mice. *Food Res Int* (2022) 153:110945. doi: 10.1016/J.FOODRES.2022.110945

50. Zhang SS, Zhang NN, Guo S, Liu SJ, Hou YF, Li SM, et al. Glycosides and flavonoids from the extract of pueraria thomsonii benth leaf alleviate type 2 diabetes in high-fat diet plus streptozotocin-induced mice by modulating the gut microbiota. *Food Funct* (2022) 13:3931–45. doi: 10.1039/d1fo04170c

51. Han S, Luo Y, Hu ZM, Qin DD, Luo FJ. Targeting gut microbiota in type 2 diabetes mellitus: potential roles of dietary flavonoids. *Food Biosci* (2022) 45:101500. doi: 10.1016/j.fbio.2021.101500

52. Wu SY, Zuo JH, Cheng Y, Zhang Y, Zhang ZS, Wu MJ, et al. Ethanol extract of sargarsum fusiforme alleviates HFD/STZ-induced hyperglycemia in association with modulation of gut microbiota and intestinal metabolites in type 2 diabetic mice. *Food Res Int* (2021) 147:110550–0. doi: 10.1016/j.foodres.2021.110550

53. Chen MY, Liao ZQ, Lu BY, Wang MX, Lin L, Zhang SB, et al. Huang-Lian-Jie-Du-Decoction ameliorates hyperglycemia and insulin resistant in association with gut microbiota modulation. *Front Microbiol* (2018) 9:2380. doi: 10.3389/fmicb.2018.02380

54. Du LJ, Pang B, Tan YM, Yang YN, Zhang MZ, Pang Q, et al. Banxia xiexin decoction ameliorates t-BHP-induced apoptosis in pancreatic beta cells by

activating the PI3K/AKT/FOXO1 signaling pathway. *J Diabetes Res* (2020) 2020:3695689. doi: 10.1155/2020/3695689

55. Wei XY, Tao JH, Xiao SW, Jiang S, Shang EX, Zhu ZH, et al. Xiexin tang improves the symptom of type 2 diabetic rats by modulation of the gut microbiota. *Sci Rep* (2018) 8:3685. doi: 10.1038/s41598-018-22094-2

56. Xu XZ, Gao ZZ, Yang FQ, Yang YY, Chen L, Han L, et al. Antidiabetic effects of gegen qinlian decoction via the gut microbiota are attributable to its key ingredient berberine. *Genomics,Proteomics&Bioinformatics* (2020) 18:721736. doi: 10.1016/j.gpb.2019.09.007

57. Zhang CH, Xu GL, Liu YH, Rao Y, Yu RY, Zhang ZW, et al. Anti-diabetic activities of gegen qinlian decoction in high-fat diet combined with streptozotocin-induced diabetic rats and in 3T3-L1 adipocytes. *Phytomedicine* (2013) 20:221–9. doi: 10.1016/j.phymed.2012.11.002

58. Xie XH, Zhao J, Chen YQ, Wen WB. Efficacy of pidan jianqing decoction in treatment of type 2 diabetes with spleen deficiency and damp-heat syndrome. *TMR Pharmacol* (2021) 1:23. doi: 10.53388/tmrpr20211009023

59. Xie XH, Liao JB, Ai YL, Gao JM, Zhao J, Qu F, et al. Pi-Dan-Jian-Qing decoction ameliorates type 2 diabetes mellitus through regulating the gut microbiota and serum metabolism. *Front Cell Infection Microbiol* (2021) 11:748872. doi: 10.3389/fcimb.2021.748872

60. Zhang LJ, Zhan LB, Hang TY, Luo JT, Zhao CY. Shenling baizhu powder alleviates chronic inflammation to prevent type 2 diabetes of ZDF rats via intestinal flora. *Chin J Chin Materia Med* (2022) 47:1988–000. doi: 10.19540/j.cnki.cjcmm.20210907.401

61. Wang AF, Wei SF, Zhang Y, Xu L, Zhang TX, Xing GE, et al. Effects of shenling baizhu powder combined with metformin on miR146a, glucagon-like peptide-1 (GLP-1) and blood lipids in obese patients with type 2 diabetes mellitus (T2DM). *Diabetes New World* (2022) 25:15–8. doi: 10.16658/j.cnki.1672-4062.2022.06.015

62. Zhang XY, Wang HT, Xie CG, Hu ZP, Zhang Y, Peng SH, et al. Shenqi compound ameliorates type-2 diabetes mellitus by modulating the gut microbiota and metabolites. *J Chromatogr B* (2022) 1194:123189–9. doi: 10.1016/j.jchromb.2022.123189

63. Liang XJ, Li HY, Li S. A novel network pharmacology approach to analyse traditional herbal formulae: the liu-Wei-Di-Huang pill as a case study. *Mol Biosyst* (2014) 10:1014–22. doi: 10.1039/c3mb70507b

64. Yi ZY, Chen L, Wang Y, He D, Zhao D, Zhang SH, et al. The potential mechanism of liu-Wei-Di-Huang pills in treatment of type 2 diabetic mellitus: from gut microbiota to short-chain fatty acids metabolism. *Acta Diabetol* (2022) 59:1295–308. doi: 10.1007/S00592-022-01922-Y

65. Su XH, Yu WX, Liu AR, Wang CX, Li XZ, Gao JJ, et al. San-Huang-Yi-Shen capsule ameliorates diabetic nephropathy in rats through modulating the gut microbiota and overall metabolism. *Front Pharmacol* (2022) 12:808867. doi: 10.3389/fphar.2021.808867

66. Li LY, Yoshitomi H, Wei Y, Qin LL, Zhou JX, Xu TH, et al. Tang-Nai-Kang alleviates prediabetes and metabolic disorders and induces a gene expression switch toward fatty acid oxidation in SHR. cg-Leprcp/NDmcr rats. *PloS One* (2015) 10: e0122024. doi: 10.1371/journal.pone.0122024

67. Zhang LP, Wang F, He HL, Jiao TT, Wu LL. Tangnaikang alleviates hyperglycemia and improves gut microbiota in diabetic mice. *Evidence-Based Complementary Altern Med* (2021) 2021:1089176. doi: 10.1155/2021/1089176

68. Li LY, Qin LL, Wu XL, Wang HY, Jiang YY, Wei Y, et al. Tangnaikang improves insulin resistance and β-cell apoptosis by ameliorating metabolic inflammation in SHR.Cg-Leprcp/NDmcr rats. *J Traditional Chin Med* (2017) 37:361–70. doi: 10.1016/S0254-6272(17)30072-9

69. Wu FF, Guo XF, Zhang JC, Zhang M, Ou ZH, Peng YZ. Phascolarctobacterium faecium abundant colonization in human gastrointestinal tract. *Exp Ther Med* (2017) 14:3122–6. doi: 10.3892/etm.2017.4878

70. Yan YW, Li Q, Shen L, Guo KX, Zhou X. Chlorogenic acid improves glucose tolerance, lipid metabolism, inflammation and microbiota composition in diabetic db/db mice. *Front Endocrinol* (2022) 13. doi: 10.3389/fendo.2022.1042044

71. Yang YY, Chen Z, Yang XD, Deng RR, Shi LX, Yao LY, et al. Piperazine ferulate prevents high-glucose-induced filtration barrier injury of glomerular endothelial cells. *Exp Ther Med* (2021) 22:1175. doi: 10.3892/etm.2021.10607

72. Zhang XJ, Deng YX, Shi QZ, He MY, Chen B, Qiu XM. Hypolipidemic effect of the Chinese polyherbal huanglian jiedu decoction in type 2 diabetic rats and its possible mechanism. *Phytomedicine* (2014) 21:615–23. doi: 10.1016/j.phymed.2013.11.004

73. Yang YY, Shi LX, Li JH, Yao LY, Xiang DX. Piperazine ferulate ameliorates the development of diabetic nephropathy by regulating endothelial nitric oxide synthase. *Mol Med Rep* (2019) 19:2245–53. doi: 10.3892/mmr.2019.9875

frontiers | Frontiers in Endocrinology

TYPE Original Research
PUBLISHED 31 January 2023
DOI 10.3389/fendo.2023.1133167



OPEN ACCESS

EDITED BY
Xinhua Shu,
Glasgow Caledonian University,
United Kingdom

REVIEWED BY
Yi Tao,
Zhejiang University of Technology, China
Guojun Yan,
Nanjing University of Chinese Medicine,
China

*CORRESPONDENCE
Guo-shui Tao
taoguoshui@sina.com
Yu-zheng Xue
9862018034@jiangnan.edu.cn

†These authors share first authorship

SPECIALTY SECTION
This article was submitted to
Gut Endocrinology,
a section of the journal
Frontiers in Endocrinology

RECEIVED 28 December 2022
ACCEPTED 09 January 2023
PUBLISHED 31 January 2023

CITATION
Liu T-h, Wang J, Zhang C-y, Zhao L,
Sheng Y-y, Tao G-s and Xue Y-z (2023)
Gut microbial characteristical comparison
reveals potential anti-aging function of
*Dubosiella newyorkensis* in mice.
*Front. Endocrinol.* 14:1133167.
doi: 10.3389/fendo.2023.1133167



# Gut microbial characteristical comparison reveals potential anti-aging function of *Dubosiella newyorkensis* in mice

Tian-hao Liu[1,2†], Juan Wang[1,2†], Chen-yang Zhang[1,2†], Lin Zhao[1,2], Ying-yue Sheng[1,2], Guo-shui Tao[3*] and Yu-zheng Xue[1,2*]

[1]Affiliated Hospital of Jiangnan University, Wuxi, Jiangsu, China, [2]Medical College of Jiangnan University, Wuxi, Jiangsu, China, [3]Wuxi Traditional Chinese Medicine Hospital, Wuxi, Jiangsu, China

**Introduction:** Previous study has indicated *Dubosiella newyorkensis* may act as a potential probiotic in age-related diseases. However, its detailed role in aging has not yet been promulgated. This study aimed to explore the potential anti-aging role of *Dubosiella newyorkensis* by comparing the anti-aging effect of resveratrol in young and old mice.

**Method:** Measurement of intestinal aging-related factors in colon and serum, and vascular endothelial function-related factors in serum were performed by enzyme-linked immunosorbent assay (ELISA). Gut microbial analysis of intestinal contents were identified by 16S rRNA gene sequencing.

**Results:** The effect of *Dubosiella newyorkensis* on reducing malondialdehyde (MDA) and increasing superoxide dismutase (SOD) in aged mice were greater than that of resveratrol. While the effect of *Dubosiella newyorkensis* on nitric oxide (NO) level was less than that of resveratrol, the reduction of vascular endothelial growth factor (VEGF) and pentosidine (PTD) was better than that of resveratrol in young mice. In young mice, *Dubosiella newyorkensis* promoted an increase in the beneficial genus *Lactobacillus, Bifidobacterium* and *Ileibacterium* less effectively as compared with resveratrol treatment. In aged mice, *Dubosiella newyorkensis* promoted the increase of *Bifidobacterium, Ileibacterium* less effectively than resveratrol, and promoted the increase of *Akkermansia, Staphylococcus, Verrucomicrobiota* expression better as compared with resveratrol treatment. Both young and old mice showed the same results for the remaining markers, including changes in gut microbial composition and predictions of function.

**Conclusion:** *Dubosiella newyorkensis* has similar anti-aging functions with resveratrol. *Dubosiella newyorkensis* may even be more effective than resveratrol

in reducing oxidative stress, improving vascular endothelial function, and redistributing gut microbiota. The research provides an innovative strategy of *Dubosiella newyorkensis* to improve aging.

KEYWORDS

aging, gut microbiota, *Dubosiella newyorkensis*, resveratrol, signal transduction

# 1 Introduction

Aging is a gradual and unavoidable step in the metabolic process of the organism, characterized by a degenerative change in the organism's degree of health and capacity to maintain its own internal homeostasis, indicated by a loss of the organism's ability to adapt to its environment. It is a multi-linked biological process that results from the combined action of several causes, and its processes are highly complicated, including changes in the structure and function of various organ systems. These alterations can raise the likelihood of biological death and are frequently followed with illness development (1). As the population ages, the incidence of diseases associated with aging will gradually increase (2, 3) and cardiovascular disease is the current leading worldwide cause of mortality (4). Aging is inevitable, so the search for effective anti-aging techniques and methods to delay the destruction of aging, significantly improve the quality of life of the elderly, and reduce the burden on families, society, and the nation is a top priority for society and scientists. There are more than 300 theories about aging (5), but most of them are not credible, among which the accepted theory of oxidative stress suggests that biological macromolecules damage, including DNA, proteins and lipid peroxidation is a predisposing event for aging (6–8). Oxidative stress can also lead to endothelial nitric oxide synthase (eNOS) dysregulation and vascular endothelial dysfunction, thereby inducing vascular senescence (9). Oxidative stress-related endothelial damage is the initiating factor of cardiovascular disease (10, 11). The gut microbial community and the human body are in a mutually beneficial symbiotic relationship; however, aging alters the composition of the gut microbiota. Compared to healthy young adults, the gut microbial diversity generally decreases in older adults, and the number of pathogenic gut microbiota increases significantly. Alterations in the microbiota lead to damage to the intestinal barrier and increased intestinal permeability, induce the production of inflammatory substances, stimulate the host systemic immune response, and ultimately result in a long-term chronic pro-inflammatory state in the organism, damaging the immune system and leading to mutated and senescent cells that cannot be cleared properly (12). Vascular health and gut microbiota play a key role in human aging. *Dubosiella* is a potential probiotic found in our preliminary research to improve obesity, hypertension and liver disease (13). *Dubosiella newyorkensis* is a stain of *Dubosiella* identified in 2017 (14). The abundances of *Dubosiella newyorkensis* were greatly reduced in $APP^{swe}/PS1^{\Delta E9}$ (PAP) mice with cognitive decline and age (15). But the evidence of correlation between *Dubosiella* with aging is not strong.

Resveratrol is recognized as an anti-aging wonder drug, and there have been numerous studies showing that it can improve oxidative stress and vascular endothelial function and regulate intestinal microbiota thus achieving anti-aging effects (16–19). Therefore, this study was conducted to investigate the anti-aging potential of *Dubosiella newyorkensis* by comparing the intervention of resveratrol and *Dubosiella newyorkensis*, in two animal models of young and aged mice. This study revealed that *Dubosiella newyorkensis* and resveratrol have similar anti-aging functions. Even, *Dubosiella newyorkensis* may be superior to resveratrol in reducing oxidative stress, improving vascular endothelial function and improving gut microbiota distribution. The research provides an innovative strategy to improve aging.

**Abbreviations:** ELISA, enzyme-linked immunosorbent assay; MDA, malondialdehyde; CAT, catalase; GSH-Px or GPx; glutathione peroxidase, SOD, superoxide dismutase; NO, nitric oxide; ET-1, endothelin-1; Ang II, angiotensin II; VEGF, vascular endothelial growth factor; VCAM-1, vascular cell adhesion molecule-1; OTUs, operational taxonomic units; AGEs, advanced glycosylation end products; TMAO, trimethylamine oxide; BA, bile acid.

# 2 Methods

## 2.1 Design and grouping

A total of sixteenth C56BL/6J mice (6-8 weeks old, male, provided by Changzhou cavens experimental animal Co., Ltd.) were randomly divided into resveratrol intervention young group (Resveratrol_young) and *Dubosiella newyorkensis* intervention young group (TSD_64_young). Meanwhile, sixteenth 14-month-old C56BL/6J mice (male, provided by Changzhou cavens experimental animal Co., Ltd.) were randomly designed as older of resveratrol intervention (Resveratrol_aged) and older of *Dubosiella newyorkensis* intervention (TSD_64_aged), with 6 mice in each group for experimental validation. The ethics committee of Jiangnan University approved the animal experiment (NO.20211015c0650220).

## 2.2 Intervention

A normal diet and free drink water for 4 weeks were performed in the all groups. Nantong Troffer Feed Technology Co., Ltd. (Nantong, China) provided the feed (production license (2014): 06092), which was then sterilized by Nantong Michael Irradiation Co., Ltd. (Nantong, China). Resveratrol intervention in young and aged mice were gavaged using resveratrol (44 mg/kg/day), while the mice in young and aged groups for *Dubosiella newyorkensis* intervention were administered by gavage with the same 100 μL *Dubosiella newyorkensis*. *Dubosiella newyorkensis* was NYU-BL-A4 (ATCC:

TSD_64) provided by the International Conservation Center, qualified by Guangdong Institute of Microbiology, and cultured in $10^8$ cfu with Guangdong Institute of Microbiology.

## 2.3 Measurement of intestinal aging-related factors in colon and serum by enzyme-linked immunosorbent assay (ELISA)

To reduce suffering, isoflurane anesthesia was administered to all mice after 4 weeks. After that, blood was extracted from the eyeball and centrifuged after 2-4 h for 5 min at 3000 rpm. The supernatant was then sub packed for storage into 1.5-mL sterilized EP tubes. The colon tissue (1-2 cm) was gathered and stored in the EP tubes. Lastly, the levels of malondialdehyde (MDA), catalase (CAT), glutathione peroxidase (GSH-Px), and superoxide dismutase (SOD) in the colon and serum were assessed in accordance with the kit's instructions, which were bought from Jiangsu Meimian Industrial Co., Ltd (Yancheng, China).

## 2.4 Detection of vascular endothelial function-related factors in serum by ELISA

Then, using kits provided by Jiangsu Meimian Industrial Co., Ltd (Yancheng, China) and following the operating instructions, the levels of nitric oxide (NO), endothelin-1 (ET-1), angiotensin II (AngII), vascular endothelial growth factor (VEGF), vascular cell adhesion molecule-1 (VCAM-1) and pentosidine (PTD) were determined.

## 2.5 16S rRNA gene sequencing, gut microbial analysis of intestinal contents

The intestinal contents of 6 mice in each group were randomly selected for subsequent analysis. The intestinal contents were used to extract microbial DNA through E.Z.N.A.® soil DNA Kit (Omega Bio-Tek, Norcross, GA, U.S.). The final DNA concentration and purification was assessed using NanoDrop 2000 UV-vis spectrophotometer (Thermo Scientific, Wilmington, USA), and DNA quality was estimated using 1% agarose gel electrophoresis. The V3-V4 hypervariable portions of the bacterium 16S rRNA gene were amplified by a thermocycler PCR system (GeneAmp 9700, ABI, USA) with primers 338F (5'-ACTCCTACGGGAGGCAGCAG-3') and 806R (5'-GGACTACHVGGGTWTCTAAT-3'). The PCR products were extracted from a 2% agarose gel, purified with a AxyPrep DNA Gel Extraction Kit (Axygen Biosciences, Union City, CA, USA), and quantified with QuantiFluorTM-ST (Promega, USA) according to the manufacturer's instructions.

The purified amplicons were sequenced on an Illumina MiSeq platform (Illumina, San Diego, USA) at an equimolar ratio (Shanghai, China). The operational taxonomic units (OTUs) were clustered using UPARSE (http://drive5.com/uparse/) with a unique 'greedy' technique that performs chimera filtering and OTU clustering at the same time. Finally, the RDP Classifier algorithm was used to compare the taxonomy of each 16S rRNA gene sequence to the 16S rRNA database (Silva (SSU123)).

## 2.6 Statistical analysis

GraphPad Prism software was used to analyze all data, which were all expressed as mean standard error (SEM). The Kruskal-Wallis test, one-way ANOVA, unpaired T-test were used for all analyzes. $P < 0.05$ means a meaningful difference. The Majorbio I-Sanger Cloud Platform (www.i-sanger.com) was utilized to examine the 16S rRNA gene sequencing data.

A brief operation flow was shown in Figure 1.

# 3 Results

## 3.1 Changes in oxidative stress in mice

As the results shown, in the aged mice experiment, the reduction of MDA in serum was significantly more pronounced in

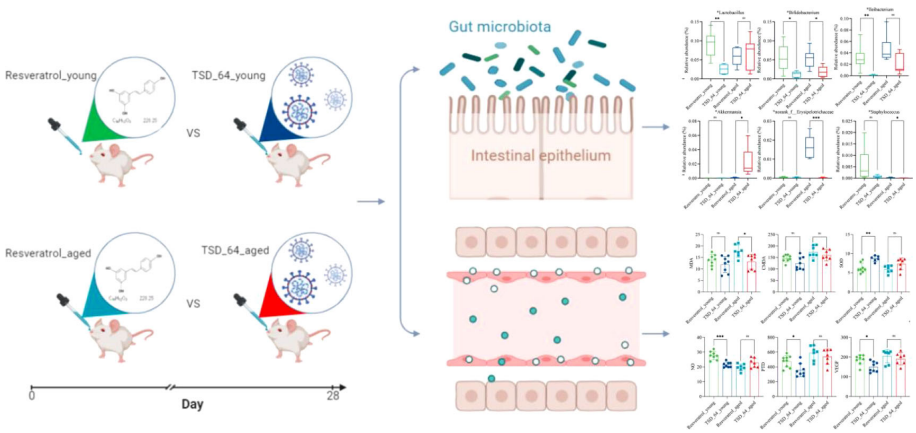


FIGURE 1
Flow chart of the study. Young and aged mice were gavaged using resveratrol and *dubosiella newyorkensis*. Colon and serum samples were collected for testing indexes of oxidative stress, vascular endothelial and gut microbiota, to analyze the similarities and differences of resveratrol and *dubosiella newyorkensis*. The group of young mice gavaged with resveratrol was named Resveratrol_young; The group of young mice gavaged with *dubosiella newyorkensis* was named TSD_64_young; The group of aged mice gavaged with resveratrol was named Resveratrol_aged; The group of young mice gavaged with *dubosiella newyorkensis* was named Resveratrol_aged.

TSD_64_aged group than Resveratrol_aged group (Figure 2A), and in young mice experiment, the effect of elevated SOD in serum was better in TSD_64_young group than Resveratrol_young group, and the difference was statistically significant (Figure 2D). No difference in the effect of changing the level of CAT and GSH-Px in the serum (Figures 2B, C). and also no difference in the effect of changing the level of those indicators in the colon (Figures 2E–H). It indicates that *Dubosiella newyorkensis* may have similar functions to resveratrol in improving oxidative stress and is superior with resveratrol in reducing the oxidative stress indicator MDA and increasing antioxidant enzyme SOD in the serum, and no difference in regulation for intestinal stress.

## 3.2 Changes of vascular endothelial function in mice

The results of the endothelial functional status index showed that NO levels of increasing in the TSD_64_young group was not as great as that in Resveratrol_young group (Figure 3A), but in reducing two indicators, VEGF and PTD, TSD_64_young group was better than Resveratrol_young group (Figures 3B, C). There was no difference in the rest of the indicators (Figures 3D–F). It is thus clear that *Dubosiella newyorkensis* also had similar effects to resveratrol in improving vascular function. Moreover, *Dubosiella newyorkensis* has less vasodilatory capacity than resveratrol, but is stronger than resveratrol in inhibiting the proliferation of vascular endothelial cells and in resisting the synthesis of advanced glycosylation end products (AGEs) pentosidine. In summary, *Dubosiella newyorkensis* has similar effects to resveratrol in improving oxidative stress and vascular endothelial function. Therefore, it was further investigated whether its changes of gut microbiota has similarities.

## 3.3 Overall structure and composition of gut microbiota

### 3.3.1 Changes in OTU count and diversity of gut microbiota in mice

The Venn diagram analyzed the unique or common operational taxonomic units(OTUs) between the different sample groups, visualizing the similarity and uniqueness at the OTU level. Eighty OTUs were common to the four groups. Eighty-six OTUs were unique to the Resveratrol_young group, with a total of 671 OTUs, and forty-three were unique to the TSD_64_young group, with a total of 665 OTUs. This suggests that in the young group, *Dubosiella newyorkensis* reduced the number of gut microbial species compared to resveratrol. Forty-seven OTUs were unique to the Resveratrol_aged group, with a total of 632 OTUs. Seventy were unique to the TSD_64_aged group, with a total of 632 OTUs (Figure 4A). This suggests that in the aged group, *Dubosiella newyorkensis* increased the number of gut microbial species compared to resveratrol. Species richness was determined by ACE and Chao. Shannon and Simpson indices were used to assess the diversity of the community, with an overall assessment of α-diversity (Figures 4B–E). ACE, Chao and Shannon indices were slightly higher in the TSD_64_young group

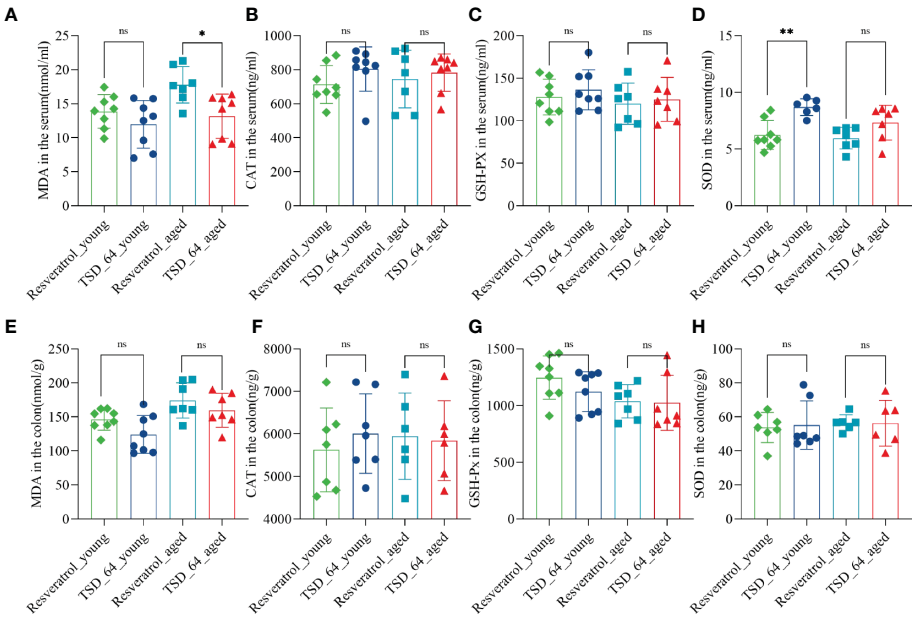


FIGURE 2
Changes in oxidative stress in the colon and serum in mice. **(A)** The level of MDA in serum. **(B)** The level of CAT in serum. **(C)** The level of GSH-PX in serum. **(D)** The level of SOD in serum. **(E)** The level of MDA in colon. **(F)** The level of CAT in colon. **(G)** The level of GSH-PX in colon. **(H)** The level of SOD in colon. Malondialdehyde (MDA), catalase (CAT), glutathione peroxidase (GSH-Px), and superoxide dismutase (SOD) in the colon and serum were assessed. The values are expressed as mean ± standard deviation. "ns" represented no significant difference, **P*<0.05, ***P*<0.01. The group of young mice gavaged with resveratrol was named Resveratrol_young; The group of young mice gavaged with *dubosiella newyorkensis* was named TSD_64_young; The group of aged mice gavaged with resveratrol was named Resveratrol_aged; The group of young mice gavaged with *dubosiella newyorkensis* was named Resveratrol_aged. N=6-8 per group.

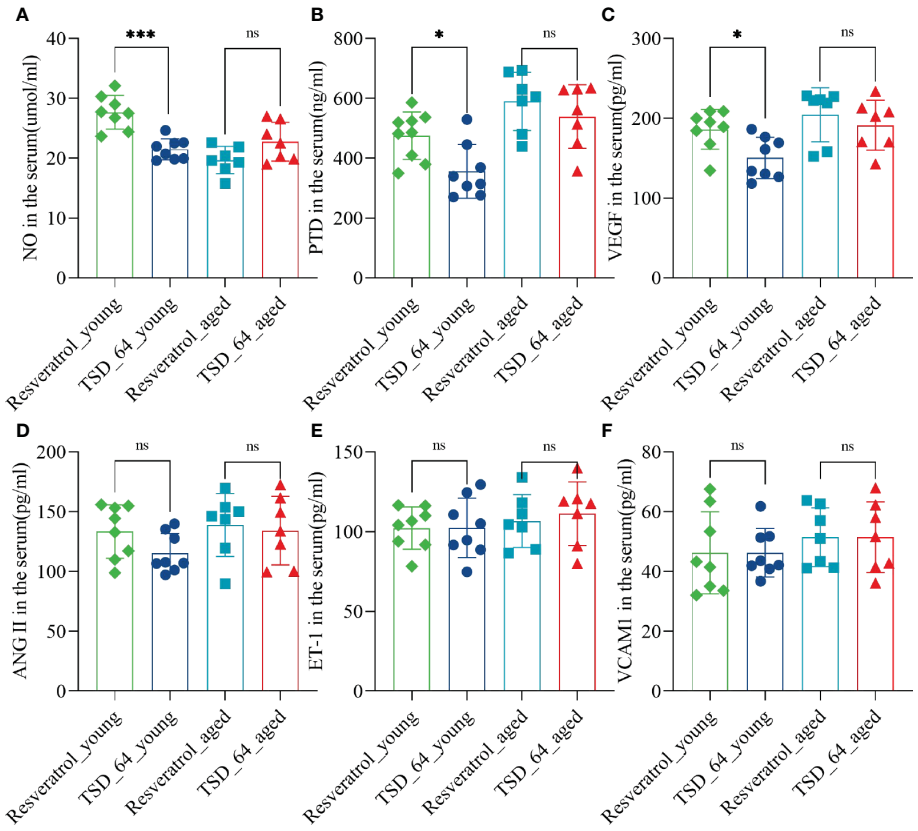


FIGURE 3
Changes of vascular endothelial function in mice. **(A)** The levels of NO. **(B)** The levels of PTD. **(C)** The levels of VEGF. **(D)** The levels of ANG II. **(E)** The levels of ET-1. **(F)** The levels of VCAM1. nitric oxide (NO), endothelin-1 (ET-1), angiotensin II (Ang II), vascular endothelial growth factor (VEGF), vascular cell adhesion molecule-1 (VCAM-1) and Pentosidine (PTD) were assessed. The values are expressed as mean ± standard deviation. "ns" represented no significant difference, **P*<0.05, ****P*<0.001. The group of young mice gavaged with resveratrol was named Resveratrol_young; The group of young mice gavaged with *dubosiella newyorkensis* was named TSD_64_young; The group of aged mice gavaged with resveratrol was named Resveratrol_aged; The group of young mice gavaged with *dubosiella newyorkensis* was named Resveratrol_aged. N=6-8 per group.

than in the Resveratrol_young group ($p > 0.05$, $p > 0.05$, and $p > 0.05$). The Simpson index of the TSD_64_young group has no difference from that of the Resveratrol_young group ($p > 0.05$). ACE, Chao, and Simpson indices were slightly lower in the TSD_64_aged group than in the Resveratrol_aged group ($p > 0.05$, $p > 0.05$, and $p > 0.05$). The Shannon index of the TSD_64_aged group has no difference from that of the Resveratrol_aged group ($p > 0.05$).

Alpha-diversity analysis showed that no significant differences in microbial community were observed between the four groups. β-diversity analysis by PCoA, PCA, NMDS (Figures 5A–C) was used to further understand the effect of *Dubosiella newyorkensis* and resveratrol on the overall structural changes of the intestinal microbial community. Samples from the TSD_64_young group were effectively separated from those from the Resveratrol_aged group, showing a clear grouping phenomenon. However, samples from the TSD_64_aged group showed grouping and aggregation with samples from the Resveratrol_aged group. All these findings suggest that the use of both resveratrol and *Dubosiella newyorkensis* significantly modulates the intestinal microbial structure of mice. The small difference between resveratrol and *Dubosiella newyorkensis* in aging mice better illustrates the similarity between the two in terms of anti-aging.

### 3.3.2 Changes in the composition of the gut microbiota

To further investigate the specific changes in gut microbial composition induced by the two interventions in the young and aged mice, we analyzed the differences in taxonomic composition at both the phylum and genus levels. As shown, at the phylum level, the intestinal microbiota of all experimental groups consisted mainly of *Firmicutes* and *Bacteroidetes* (Figure 6A). The relative abundance of *Actinobacteria* was significantly lower in the TSD_64_young group compared with the Resveratrol_young group (Figure 6C), and in aged mice, the relative abundance of *Verrucomicrobiota* was significantly increased in the TSD_64_aged group compared to the Resveratrol_aged group (Figure 6D). At the genus level, the groups were mainly composed of *norank_f:Muribaculaceae, Dubosiella*, followed by *Lactobacillus, unclassified_f:Lachnospiraceae* (Figure 6B). At the genus level, A significant decrease in the relative abundance of *Lactobacillus, Bifidobacterium* and *Ileibacterium* could be observed in the

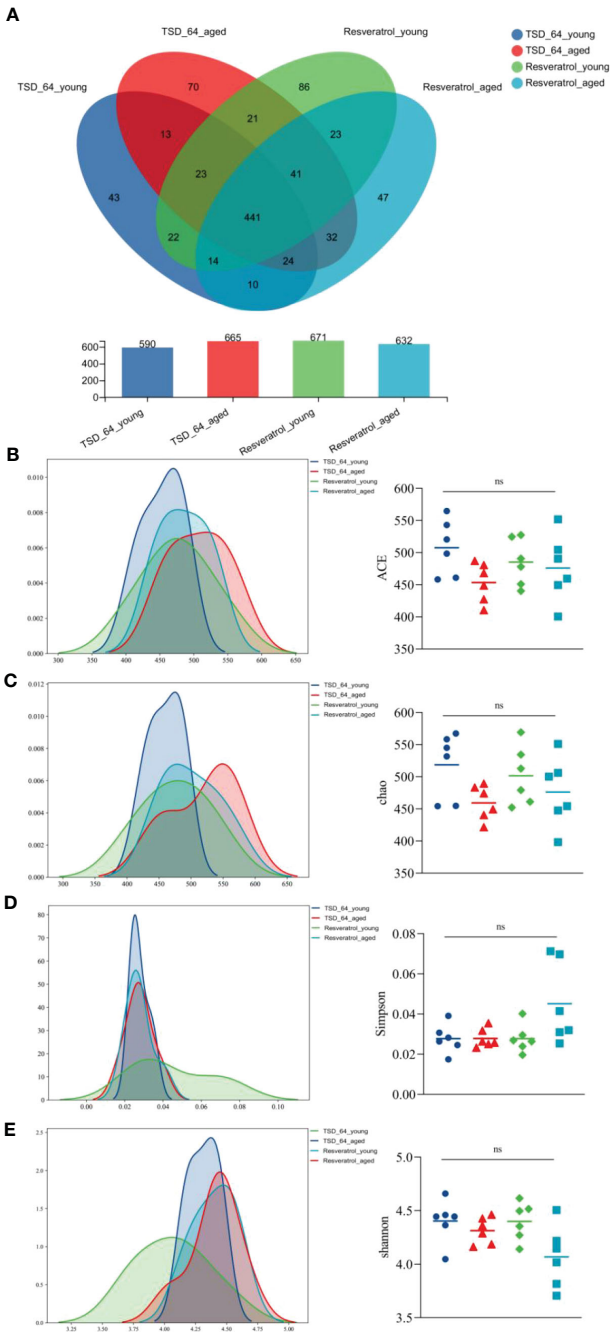


FIGURE 4
Changes in OTU count and alpha diversity of gut microbiota in mice. **(A)** Venn diagram of the OTU counts in the four groups. **(B)** Abundance-based Coverage Estimator (ACE). **(C)** Chao1. **(D)** Simpson index (Simpson). **(E)** Shannon-Wiener index(Shannon). The abundance index (community richness) was assessed using ACE and Chao to reflect the abundance of species within the community. A larger ACE index indicates a larger number of species in the community. The greater the chao index, the greater the number of OTUs, indicating a higher number of species in a community. The species diversity index was assessed using simpson and shannon reflects the combined status of species richness and evenness. Higher Shannon index values indicate higher alpha diversity in the community. Larger Simpson index values indicate lower community diversity. The values are expressed as mean ± standard deviation. "ns" represented no significant difference. The group of young mice gavaged with resveratrol was named Resveratrol_young; The group of young mice gavaged with *dubosiella newyorkensis* was named TSD_64_young; The group of aged mice gavaged with resveratrol was named Resveratrol_aged; The group of young mice gavaged with *dubosiella newyorkensis* was named Resveratrol_aged. N=6 per group.

TSD_64_young group compared to the Resveratrol_young intervention group. the relative abundance of *Bifidobacterium, norank_f:Erysipelotrichaceae* and *Staphylococcus* decreased in the TSD_64_aged group compared to the Resveratrol_aged group, while the relative abundance of *Akkermansiaceae* increased (Figures 6E–J). The differences in the abundance of the other phylum and genus levels were not significant. This suggests that there are similarities in the composition of the gut microbiota affected by *Dubosiella newyorkensis* and resveratrol, with *Dubosiella newyorkensis* being less effective than resveratrol in increasing the relative abundance of beneficial bacteria, but more effective in reducing the relative abundance of harmful bacteria.

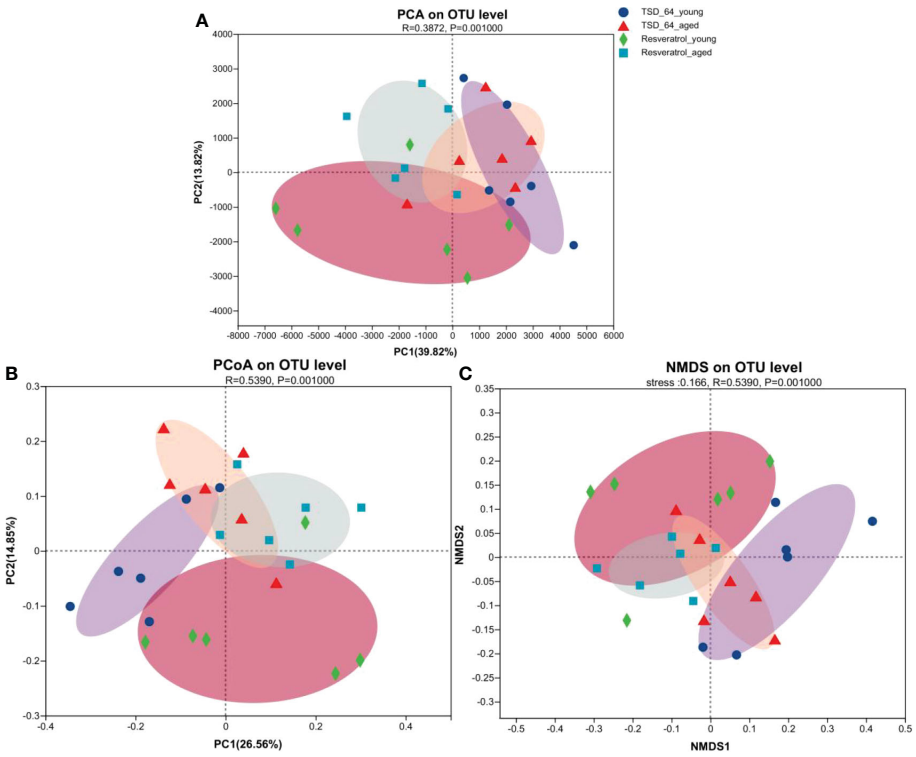


FIGURE 5
Changes in beta diversity of gut microbiota in mice. **(A)** Principal Components Analysis (PCA). **(B)** Principal Co-ordinates Analysis (PCoA). **(C)** Non-metric multidimensional scaling (NMDS). Unconstrained PCoA (for principal coordinates PCo1 and PCo2) and Unconstrained PCA (for principal coordinates PC1 and PC2) with Bray-Curtis distance showing that the gut microbiota of Resveratrol_young and Resveratrol_aged separate from those of TSD_64_young and TSD_64_young in the first axis. NMDS plots are presented based on Bray-Curtis similarity. The 2D stress value for each panel ranges between 0.11-0.18. TSD_64_young communities are presented with round symbols, TSD_64_aged communities with triangle symbols, Resveratrol_young communities with rhombus symbols and Resveratrol_aged communities with square symbols. In each panel, smaller symbols depict individual samples. *P*=0.001, permutational multivariate analysis of variance (PERMANOVA) by Adonis. The group of young mice gavaged with resveratrol was named Resveratrol_young; The group of young mice gavaged with *dubosiella newyorkensis* was named TSD_64_young; The group of aged mice gavaged with resveratrol was named Resveratrol_aged; The group of young mice gavaged with *dubosiella newyorkensis* was named Resveratrol_aged. N=6 per group.

### 3.3.3 Analysis of significantly different gut microbiota

Further, we analyzed the similarities and differences of significantly different microbiota among different groups and different interventions. The results of LDA Effect Size analysis showed that the expression of *Prevotellaceae_UCG-001* was significant in TSD_64_young group, and *Bacilli, Erysipelotrichales, Erysipelotrichaceae, Dubosiella, Lactobacillales, Lactobacillus, Lactobacillaceae, Bifidobacteriaceae, Bifidobacterium, Bifidobacteriales, Actinobacteria* were significantly expressed in Resveratrol_young group. In aged mice, *Odoribacter, Marinifilaceae, Verrucomicrobiales, Akkermansia, Verrucomicrobiae, Akkermansiaceae, Verrucomicrobiota* were significantly expressed in the TSD_64_aged group, and *Ileibacterium* was significantly expressed in the Resveratrol_aged group (Figures 7A, B). Random forest plots showing the order of importance (Figure 7C) were taken to intersect with the significantly expressed groups in the LEFSe analysis to obtain *Odoribacter, Ileibacterium, Dubosiella, Lactobacillus, Bifidobacterium, Verrucomicrobiota, Akkermansia. Akkermansia*. Further Stamp analysis revealed that in young mice, *Dubosiella, Lactobacillus, Bifidobacterium* and *Ileibacterium* were relatively low expressed in the TSD_64_young group compared to the Resveratrol _young group (Figure 7E). *Dubosiella, Bifidobacterium, norank_f: EResveratrol_youngsipelotrichacea* were relatively low expressed in the TSD_64_aged group compared to the Resveratrol_aged group, whereas *Staphylococcus, Akkermansia* and *Verrucomicrobiota* were relatively highly expressed (Figure 7D). The results were shown by ROC curves (Figures 7F, G). Compared with the Resveratrol_young group, *Dubosiella, Lactobacillus, Bifidobacterium, Ileibacterium, Prevotellaceae_UCG-001, Akkermansia, Staphylococcus, Actinobacteriota, Verrucomicrobiota*, AUC > 0.7, especially the significantly expressed genus *Lactobacillus* and *Prevotellaceae_UCG-001*, which is unique to young mice, could serve as a biological annotator for the intervention of *Dubosiella newyorkensis*, but its expression did not differ between the two drug interventions. *Dubosiella, Bifidobacterium, Ileibacterium, Akkermansia, Staphylococcus, Actinobacteriota, Verrucomicrobiota*, AUC > 0.7 in the TSD_64_aged group compared to the Resveratrol_aged group. These gut microbiota served as microbial markers for the *Dubosiella newyorkensis* intervention in aged mice. In conclusion, in young mice, *Dubosiella newyorkensis* promoted an increase in the beneficial genus *Lactobacillus, Bifidobacterium* and *Ileibacterium* less effectively than resveratrol. In aged mice, *Dubosiella newyorkensis* promoted the increase of *Bifidobacterium, Ileibacterium* less effectively than resveratrol, and promoted the increase of *Akkermansia, Staphylococcus, Verrucomicrobiota* expression better than resveratrol. Therefore, *Dubosiella newyorkensis* was similar to the effect of

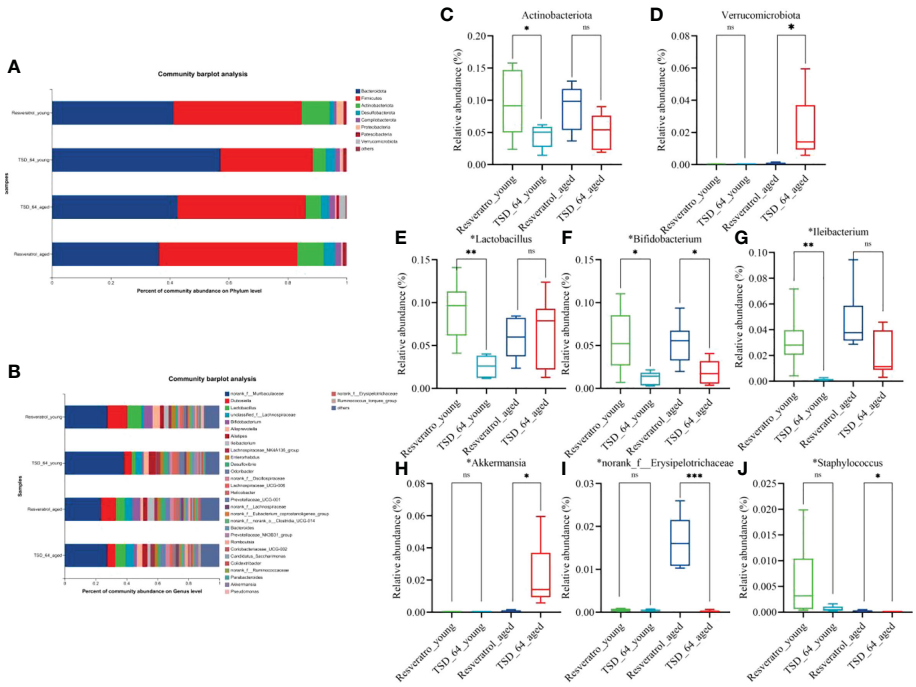


FIGURE 6
Changes in the composition of the gut microbiota. **(A)** Horizontal bar diagram of the phylum level. **(B)** Horizontal bar diagram of the genus level. **(C)** Relative composition abundance of *Actinobacteria*. **(D)** Relative composition abundance of *Verrucomicrobiota*. **(E)** Relative composition abundance of *Lactobacillus*. **(F)** Relative composition abundance of *Bifidobacterium*. **(G)** Relative composition abundance of *Ileibacterium*. **(H)** Relative composition abundance of *Akkermansi*.**(I)** Relative composition abundance of *norank_f:Muribaculaceae*. **(J)** Relative composition abundance of *Staphylococcus*. The values are expressed as mean ± standard deviation. Statistical tests using unpaired t-tests. "ns" represented no significant difference, **P*<0.05, ***P*<0.01, *** *P*<0.001. The group of young mice gavaged with resveratrol was named Resveratrol_young; The group of young mice gavaged with *dubosiella newyorkensis* was named TSD_64_young; The group of aged mice gavaged with resveratrol was named Resveratrol_aged; The group of young mice gavaged with *dubosiella newyorkensis* was named Resveratrol_aged. N=6 per group.

resveratrol on gut microbiota, can remodel the gut microbiota as well as resveratrol. Thus, it can promote the abundance of thick-walled bacterial phylum and increase the beneficial bacteria and thus act.

## 3.4 Predict function

The results of function prediction showed that a total of 356 KEGG pathways were enriched, visualizing the top 20 pathways (Figure 8A), and an unpaired t-test between groups for the top 20 significantly enriched KEGG pathways revealed no difference in enrichment between the two groups of mice for the two interventions (Figure 8B). This suggests that may have the same biological role as resveratrol and be involved in the same regulatory pathways. It may be because *Dubosiella newyorkensis* and the positive drug resveratrol have similar pathways of action so there is no difference in functional pathways. In conclusion, *Dubosiella newyorkensis* may exert the same biological functions as resveratrol.

# 4 Discussion

Some of the more successful pre-anti-aging attempts include calorie restriction (especially the mTORC1 signaling pathway), removal of senescent cells, reversal of stem cell senescence, fecal transplantation (microbiome suppression), guided autophagy, and reduction of inflammation (20). The most mainstream approach is to eliminate senescent cells with the latest discoveries of molecular compounds that remove senescent cells, including metformin, resveratrol, spermidine, rapamycin, NAD + supplements, and senolytics (21). Among them, resveratrol comes from grape skin, grape seed, peanut coat and thuja extract. It is a plant-derived polyphenol with antioxidant, free radical scavenging and anti-aging effects, and is recognized as an anti-aging wonder drug (22, 23). Study shows resveratrol can effectively scavenge ROS accumulation (24, 25) and increases antioxidant defenses (26, 27). Evidence from studies shown that an increase or restoration in the level of CAT, GPx, GR, and GSH was more pronounced when resveratrol was administered in HCC (28). Another study also showed that restoration could enhance SOD, GSH-Px, and CAT activities and HO-1 protein levels and decrease MDA content were detected in the brain tissue of the Res-treated mice (29). Study shows that resveratrol significantly reduces MDA levels (30). So here, the activities of the antioxidant enzymes GPx, SOD and CAT and the levels of the small molecule MDA were used to assess the levels of oxidative stress in tissues and serum. The results showed that *Dubosiella newyorkensis* was superior to resveratrol in lowering the index MDA in aging mice, while elevating the antioxidant enzyme SOD in young mice was superior to the oxidative stress index. This indicates that *Dubosiella newyorkensis* has superior antioxidant potential to resveratrol. *In vitro* cell culture studies revealed that resveratrol promotes eNOS activity, which helps catalyze the production of NO by vascular endothelial cells in order to play a role in maintaining arterial diastole (31). Studies with endothelial cells

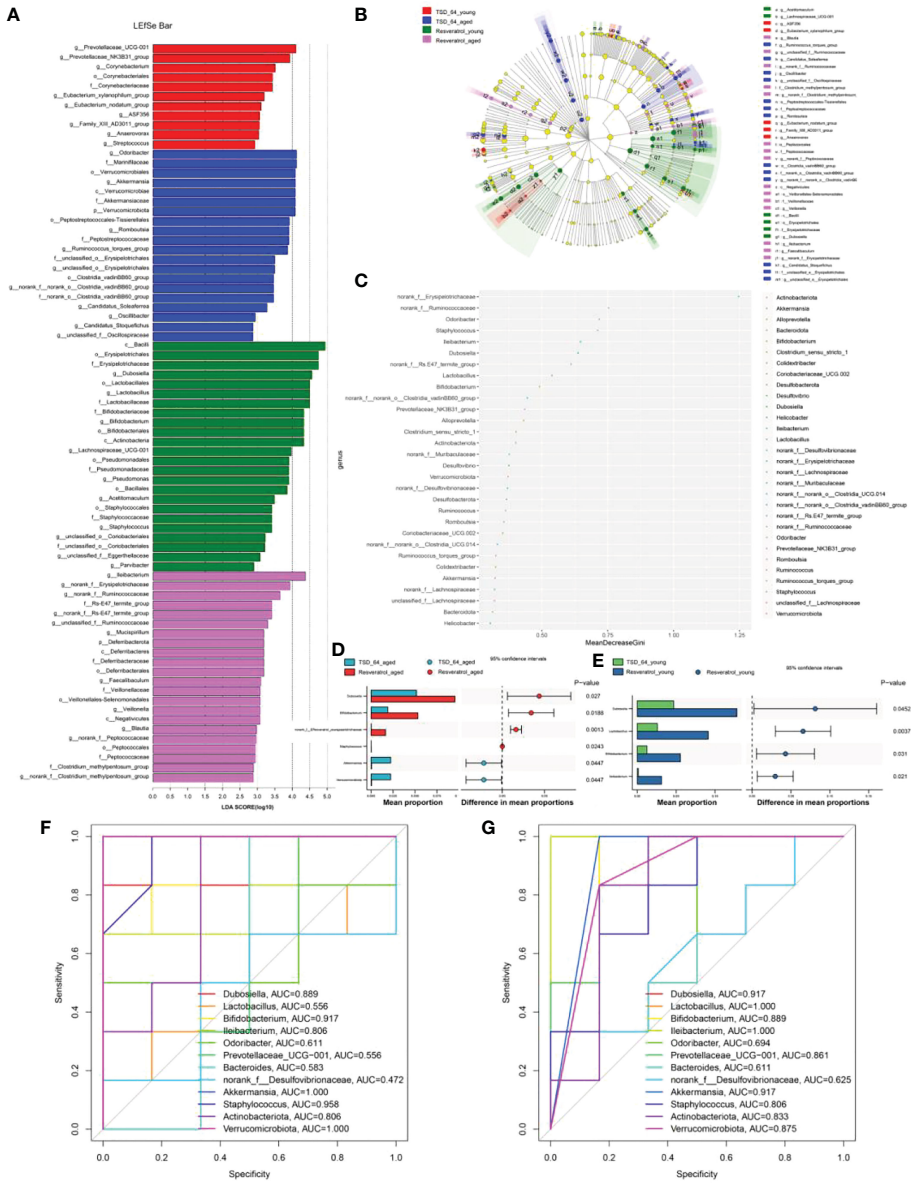


FIGURE 7
Analysis of significantly different gut microbiota in mice. **(A)** LDA Effect Size (LEfSe) analysis. **(B)** Cladogram. **(C)** Random Forest. **(D)** STAMP analysis in young mice. **(E)** STAMP analysis in aged mice. **(F)** ROC curve in young mice. **(G)** ROC curve in aged mice. The LEfSe analysis mainly shows us the significantly different species with LDA scores greater than the preset value, i.e., statistically different Biomaker, with a default preset value of 2.0. Cladogram shows us each small circle at a different taxonomic level represents a taxon at that level, and the diameter of the small circles represents the relative abundance. Species with no significant differences are uniformly colored yellow, species with significant differences Biomarker follows the group coloring, for example, red nodes indicate microbial taxa that play an important role in the red group, and so on. Species names corresponding to Biomarkers not shown in the figure are displayed on the right side, with letter numbers corresponding to those in the figure. Random forest for feature importance ranking and feature selection. STAMP analysis: the bar chart on the left shows the difference in values between the two groups. The dotted bar graph on the right side shows the percentage of species between the two groups for all species in the two sample groups, respectively. As long as the area under the ROC curve is greater than 0.7, it proves that the diagnostic test has some diagnostic value. The group of young mice gavaged with resveratrol was named Resveratrol_young; The group of young mice gavaged with *dubosiella newyorkensis* was named TSD_64_young; The group of aged mice gavaged with resveratrol was named Resveratrol_aged; The group of young mice gavaged with *dubosiella newyorkensis* was named Resveratrol_aged. N=6 per group.

cultured *in vitro* revealed that resveratrol inhibits the expression of adhesion molecules in endothelial cells (32). Resveratrol reverses endothelin-1-induced vascular mitogenic triggering of atherosclerotic signaling (33). High concentrations of resveratrol inhibit angiotensin II-induced ERK1/2 phosphorylation and subsequent proliferation in cardiovascular smooth muscle cells (34). The role of resveratrol in inhibiting VEGF-induced endothelial cell proliferation, migration, invasion and angiogenesis (35). Resveratrol glycosides inhibit the formation of advanced glycosylation end products (AGEs), pentosidine (PTD) and prevent the accumulation of AGEs in the body, thereby treating AGEs-related diseases (36). Therefore, NO, ET-1,Ang II, VCAM-1, VEGF and PTD were used to assess the level of vascular endothelial function (37). The results also confirmed that *Dubosiella newyorkensis* has the same effect as resveratrol in improving

10.3389/fendo.2023.1133167

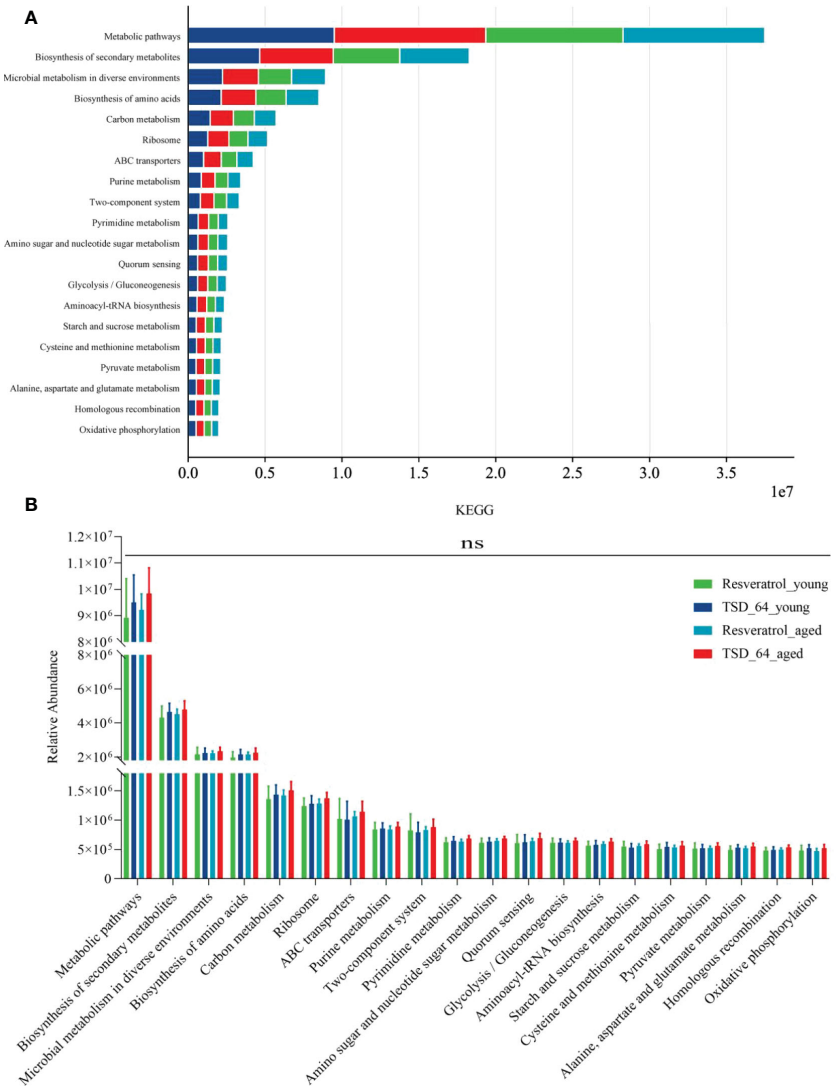


FIGURE 8
Prediction of function. **(A)** Visualization the top 20 KEGG pathways between the four groups of composition. **(B)** Unpaired t-test for the top 20 KEGG pathways between the four groups of composition. The values are expressed as mean ± standard deviation. Statistical tests using unpaired t-tests. "ns" represented no significant difference, *$P$<0.05, **$P$<0.01, ***$P$<0.001. The group of young mice gavaged with resveratrol was named Resveratrol_young; The group of young mice gavaged with *dubosiella newyorkensis* was named TSD_64_young; The group of aged mice gavaged with resveratrol was named Resveratrol_aged; The group of young mice gavaged with *dubosiella newyorkensis* was named Resveratrol_aged. N=6 per group.

vascular endothelial dysfunction. It was even superior to resveratrol in lowering VEGF and PTD in young mice, but there was no difference in aging mice, so *Dubosiella newyorkensis* has anti-primary aging potential. It has been shown that bacterial-derived metabolites can influence host longevity (38)and the gut microbiome releases an excess of small molecules. can bind genomic DNA directly and act as transcriptional co-regulators by recruiting transcription factors. thereby affecting the development of aging-related diseases (39). Resveratrol regulates trimethylamine oxide (TMAO) synthesis and bile acid (BA) metabolism by reshaping gut microbiota, thereby alleviating trimethylamine oxide-induced atherosclerosis (40). Resveratrol reshapes the gut microbiota of mice, including increasing the ratio of Bacillus-thick-walled bacteria, significantly inhibiting the growth of Prevotella, and increasing the relative abundance of *Bacillus*, *Lactobacillus*, *Bifidobacterium* and *Akkermansi* (41). Here we compared the effect of *Dubosiella newyorkensis* on gut microbiota and found that *Dubosiella newyorkensis* could increase beneficial genera such as *Lactobacillus, Bifidobacterium, Ileibacterium, Akkermansia, Staphylococcus, Verrucomicrobiota* and thus improve the gut microbiota. In summary, we believe that *Dubosiella newyorkensis* is an anti-aging drug with similar functions to resveratrol that improves oxidative stress, endothelial dysfunction and gut microbiota. *Dubosiella newyorkensis* could be an alternative or synergistic drug to resveratrol, offering new potential for future development of anti-aging drugs. The absence of differences in the first 20 predictions of gut microbiota function reinforces the similarity between *Dubosiella newyorkensis* and resveratrol.

Of course there are many shortcomings in this study, firstly, in terms of experimental design, the study did not establish a negative control. Only based on the initial study found that *Dubosiella newyorkensis* may have potential anti-aging effects, so the anti-aging wonder drug resveratrol was used as the standard to compare whether *Dubosiella*

*newyorkensis* have similar functions in improving oxidative stress, vascular endothelial function, and regulation of gut microbiota, so as to investigate the positive effect of *Dubosiella newyorkensis* on aging. Secondly, in terms of selected indicators, only oxidative stress, vascular endothelial function, and gut microbiota affecting aging were selected as aging indicators, when in fact there are many indicators about aging. Finally, the experiment was only conducted in animal experiments, without clinical data to support.

## 5 Conclusion

In present study, by comparing the intervention of *Dubosiella newyorkensis* and resveratrol in young and aged mice, it was scientifically verified that *Dubosiella newyorkensis* and resveratrol have similar anti-aging functions. *Dubosiella newyorkensis* may even be superior to resveratrol in reducing oxidative stress, improving vascular endothelial function and improving gut microbiota distribution, which can be used as a novel anti-aging drug. It provides ideas and directions for clinical anti-aging and development of potential drugs.

## Data availability statement

The datasets presented in this study can be found in online repositories. The names of the repository/repositories and accession number(s) can be found below: https://www.ncbi.nlm.nih.gov/, PRJNA885520.

## Ethics statement

The animal study was reviewed and approved by the ethics committee of Jiangnan University approved the animal experiment.

## Author contributions

T-HL, C-YZ, G-ST, and Y-ZX participated in study design. T-HL, LZ, and Y-YS conducted animal experiment operation. JW and T-HL helped to draft and revise the manuscript. T-HL and JW carried out the statistical analysis of data. All authors contributed to the article and approved the submitted version.

## Funding

The study was supported by the National Natural Sciences Foundation of China (82074307, 82174148), Wuxi Municipal Health Commission Scientific Research Fund Youth Project (Q202106), Wuxi Science and Technology Innovation and Entrepreneurship Fund "Light of Taihu Lake" Science and Technology Tackling Project, and Doctoral talent startup fund of Affiliated Hospital of Jiangnan University.

## Conflict of interest

The authors declare that the research was conducted in the absence of any commercial or financial relationships that could be construed as a potential conflict of interest.

## Publisher's note



## References

1. Kirkwood TB. "Understanding the odd science of aging. *Cell* (2005) 120(4):437–47. doi: 10.1016/j.cell.2005.01.027

2. Jaul E, Barron J. Age-related diseases and clinical and public health implications for the 85 Years old and over population. *Front Public Health* (2017) 5:3355. doi: 10.3389/fpubh.2017.00335

3. Beard JR, Officer AM, Cassels AK. The World Report on Ageing and Health. *Gerontologist* (2016) 56(2):S163–6. doi: 10.1093/geront/gnw037

4. Timmis A, Vardas P, Townsend N, Torbica A, Katus H, De Smedt D, et al. European Society of cardiology: Cardiovascular disease statistics 2021. *Eur Heart J* (2022) 43(8):716–99. doi: 10.1093/eurheartj/ehab892

5. da Costa JP, Vitorino R, Silva GM, Vogel C, Duarte AC, Rocha-Santos T. A synopsis on aging-theories, mechanisms and future prospects. *Ageing Res Rev* (2016) 29:90–1125. doi: 10.1016/j.arr.2016.06.005

6. Piedrafita G, Keller MA, Ralser M. The impact of non-enzymatic reactions and enzyme promiscuity on cellular metabolism during (Oxidative) stress conditions. *Biomolecules* (2015) 5(3):2101–22. doi: 10.3390/biom5032101

7. Rinnerthaler M, Bischof J, Streubel MK, Trost A, Richter K. Oxidative stress in aging human skin. *Biomolecules* (2015) 5(2):545–89. doi: 10.3390/biom5020545

8. Thanan R, Oikawa S, Hiraku Y, Ohnishi S, Ma N, Pinlaor S, et al. Oxidative stress and its significant roles in neurodegenerative diseases and cancer. *Int J Mol Sci* (2014) 16 (1):193–217. doi: 10.3390/ijms16010193

9. Kvietys PR, Granger DN. Role of reactive oxygen and nitrogen species in the vascular responses to inflammation. *Free Radic Biol Med* (2012) 52(3):556–92. doi: 10.1016/j.freeradbiomed.2011.11.002

10. Pennathur S, Heinecke JW. Oxidative stress and endothelial dysfunction in vascular disease. *Curr Diabetes Rep* (2007) 7(4):257–64. doi: 10.1007/s11892-007-0041-3

11. Higashi Y. Roles of oxidative stress and inflammation in vascular endothelial dysfunction-related disease. *Antioxidants (Basel)* (2022) 11(10):1958. doi: 10.3390/antiox11101958

12. O'Toole PW, Jeffery IB. Gut microbiota and aging. *Science* (2015) 350(6265):1214–5. doi: 10.1126/science.aac8469

13. Liu TH, Zhao L, Zhang CY, Li XY, Wu TL, Dai YY, et al. Gut microbial evidence chain in high-salt diet exacerbates intestinal aging process. *Front Nutr* (2022) 9:10468335. doi: 10.3389/fnut.2022.1046833

14. Cox LM, Sohn J, Tyrrell KL, Citron DM, Lawson PA, Patel NB, et al. Description of two novel members of the family erysipelotrichaceae: Ileibacterium valens gen. nov., sp. nov. and dubosiella newyorkensis, gen. nov., sp. nov., from the murine intestine, and emendation to the description of faecalibaculum rodentium. *Int J Syst Evol Microbiol* (2017) 67(5):1247–54. doi: 10.1099/ijsem.0.001793

15. Sun P, Zhu H, Li X, Shi W, Guo Y, Du X, et al. Comparative metagenomics and metabolomes reveals abnormal metabolism activity is associated with gut microbiota in alzheimer's disease mice. *Int J Mol Sci* (2022) 23(19):11560. doi: 10.3390/ijms231911560

16. Rauf A, Imran M, Suleria HAR, Ahmad B, Peters DG, Mubarak MS. A comprehensive review of the health perspectives of resveratrol. *Food Funct* (2017) 8 (12):4284–305. doi: 10.1039/C7FO01300K

17. Liu TH, Tu WQ, Tao WC, Liang QE, Xiao Y, Chen LG. Verification of resveratrol inhibits intestinal aging by downregulating Atf4/Chop/Bcl-2/Bax signaling pathway: Based on network pharmacology and animal experiment. *Front Pharmacol* (2020) 11:10645. doi: 10.3389/fphar.2020.01064

18. Gacar G, Gocmez SS, Halbutoğulları ZS, Kılıç KC, Kaya A, Yazir Y, et al. Resveratrol improves vascular endothelial dysfunction in the unpredictable chronic mild stress model of depression in rats by reducing inflammation. *Behav Brain Res* (2023) 438:1141865. doi: 10.1016/j.bbr.2022.114186

19. Zhou DD, Luo M, Huang SY, Saimaiti A, Shang A, Gan RY, et al. Effects and mechanisms of resveratrol on aging and age-related diseases. *Oxid Med Cell Longev* (2021) 2021:9932218. doi: 10.1155/2021/9932218

20. Mullard A. Anti-ageing pipeline starts to mature. *Nat Rev Drug Discovery* (2018) 17(9):609–12. doi: 10.1038/nrd.2018.134

21. Piskovatska V, Strilbytska O, Koliada A, Vaiserman A, Lushchak O. Health benefits of anti-aging drugs. *Subcell Biochem* (2019) 91:339–925. doi: 10.1007/978-981-13-3681-2_13

22. Baur JA, Sinclair DA. Therapeutic potential of resveratrol: The in vivo evidence. *Nat Rev Drug Discovery* (2006) 5(6):493–506. doi: 10.1038/nrd2060

23. Sajish M, Schimmel P. A human trna synthetase is a potent Parp1-activating effector target for resveratrol. *Nature* (2015) 519(7543):370–3. doi: 10.1038/nature14028

24. Mahal HS, Mukherjee T. Scavenging of reactive oxygen radicals by resveratrol: Antioxidant effect. *Res Chem Intermed* (2006) 32(1):59–71. doi: 10.1163/156856706775012941

25. Negre-Salvayre A, Coatrieux C, Ingueneau C, Salvayre R. Advanced lipid peroxidation end products in oxidative damage to proteins. potential role in diseases and therapeutic prospects for the inhibitors. *Br J Pharmacol* (2008) 153(1):6–20. doi: 10.1038/sj.bjp.0707395

26. Bellaver B, Souza DG, Souza DO, Quincozes-Santos A. Resveratrol increases antioxidant defenses and decreases proinflammatory cytokines in hippocampal astrocyte cultures from newborn, adult and aged wistar rats. *Toxicol In Vitro* (2014) 28 (4):479–84. doi: 10.1016/j.tiv.2014.01.006

27. Truong VL, Jun M, Jeong WS. Role of resveratrol in regulation of cellular defense systems against oxidative stress. *Biofactors* (2018) 44(1):36–49. doi: 10.1002/biof.1399

28. Rawat D, Chhonker SK, Naik RA, Koiri RK. Modulation of antioxidant enzymes, Sirt1 and nf-Kb by resveratrol and nicotinamide in alcohol-aflatoxin B1-induced hepatocellular carcinoma. *J Biochem Mol Toxicol* (2021) 35(1):e22625. doi: 10.1002/jbt.22625

29. Kong D, Yan Y, He XY, Yang H, Liang B, Wang J, et al. Effects of resveratrol on the mechanisms of antioxidants and estrogen in alzheimer's disease. *BioMed Res Int* (2019) 2019):8983752. doi: 10.1155/2019/8983752

30. Hoseini A, Namazi G, Farrokhian A, Reiner Ž, Aghadavod E, Bahmani F, et al. The effects of resveratrol on metabolic status in patients with type 2 diabetes mellitus and coronary heart disease. *Food Funct* (2019) 10(9):6042–51. doi: 10.1039/C9FO01075K

31. Duffy SJ, Vita JA. Effects of phenolics on vascular endothelial function. *Curr Opin Lipidol* (2003) 14(1):21–7. doi: 10.1097/00041433-200302000-00005

32. Ferrero ME, Bertelli AE, Fulgenzi A, Pellegatta F, Corsi MM, Bonfrate M, et al. Activity in vitro of resveratrol on granulocyte and monocyte adhesion to endothelium. *Am J Clin Nutr* (1998) 68(6):1208–14. doi: 10.1093/ajcn/68.6.1208

33. El-Mowafy AM, Alkhalaf M, Nassar NN. Resveratrol reverses et-1-Evoked mitogenic effects in human coronary arterial cells by activating the kinase-G to inhibit erk-enzymes. *Int J Cardiol* (2009) 136(3):263–9. doi: 10.1016/j.ijcard.2008.04.094

34. Zhang X, Wang Y, Yang W, Hou X, Zou J, Cao K. Resveratrol inhibits angiotensin ii-induced Erk1/2 activation by downregulating quinone reductase 2 in rat vascular smooth muscle cells. *J BioMed Res* (2012) 26(2):103–9. doi: 10.1016/S1674-8301(12)60019-0

35. Hu WH, Chan GK, Duan R, Wang HY, Kong XP, Dong TT, et al. Synergy of ginkgetin and resveratrol in suppressing vegf-induced angiogenesis: A therapy in treating colorectal cancer. *Cancers (Basel)* (2019) 11(12):1828. doi: 10.3390/cancers11121828

36. Liu M, Tang F, Liu Q, Xiao J, Cao H, Chen X. Inhibition of resveratrol glucosides (Res) on advanced glycation endproducts (Ages) formation: Inhibitory mechanism and structure-activity relationship. *Nat Prod Res* (2020) 34(17):2490–94. doi: 10.1080/14786419.2018.1538224

37. Parsamanesh N, Asghari A, Sardari S, Tasbandi A, Jamialahmadi T, Xu S, et al. Resveratrol and endothelial function: A literature review. *Pharmacol Res* (2021) 170:1057255. doi: 10.1016/j.phrs.2021.105725

38. Dodd D, Spitzer MH, Van Treuren W, Merrill BD, Hryckowian AJ, Higginbottom SK, et al. A gut bacterial pathway metabolizes aromatic amino acids into nine circulating metabolites. *Nature* (2017) 55(7682):648–52. doi: 10.1038/nature24661

39. Teng Y, Mu J, Xu F, Zhang X, Sriwastva MK, Liu QM, et al. Gut bacterial isoamylamine promotes age-related cognitive dysfunction by promoting microglial cell death. *Cell Host Microbe* (2022) 30(7):944–60.e8. doi: 10.1016/j.chom.2022.05.005

40. Ke Y, Li D, Zhao M, Liu C, Liu J, Zeng A, et al. Gut flora-dependent metabolite trimethylamine-N-Oxide accelerates endothelial cell senescence and vascular aging through oxidative stress. *Free Radic Biol Med* (2018) 116:88–1005. doi: 10.1016/j.freeradbiomed.2018.01.007

41. Chaplin A, Carpéné C, Mercader J. Resveratrol, metabolic syndrome, and gut microbiota. *Nutrients* (2018) 10(11):1651. doi: 10.3390/nu10111651

frontiers | Frontiers in Endocrinology

TYPE Original Research
PUBLISHED 09 February 2023
DOI 10.3389/fendo.2023.1106812



OPEN ACCESS

EDITED BY
Guang Chen,
Huazhong University of Science and Technology, China

REVIEWED BY
Chen-yang Zhang,
Affiliated Hospital of Jiangnan University, China
Xin Guo,
Shandong University, China

*CORRESPONDENCE
Rong Yu
yurong8072@qq.com
Yongjun Wu
wuyj@21cn.com

†These authors have contributed equally to this work

SPECIALTY SECTION
This article was submitted to Gut Endocrinology, a section of the journal Frontiers in Endocrinology

RECEIVED 24 November 2022
ACCEPTED 16 January 2023
PUBLISHED 09 February 2023

CITATION
Huang Y-l, Xiang Q, Zou J-j, Wu Y and Yu R (2023) Zuogui Jiangtang Shuxin formula Ameliorates diabetic cardiomyopathy mice *via* modulating gut-heart axis. *Front. Endocrinol.* 14:1106812. doi: 10.3389/fendo.2023.1106812



# Zuogui Jiangtang Shuxin formula Ameliorates diabetic cardiomyopathy mice *via* modulating gut-heart axis

Ya-lan Huang[1,2†], Qin Xiang[3†], Jun-ju Zou[3], Yongjun Wu[4*] and Rong Yu[1*]

[1]The First Hospital of Hunan University of Chinese Medicine, Hunan University of Chinese Medicine, Changsha, China, [2]Graduate School, Hunan University of Chinese Medicine, Changsha, China, [3]School of Traditional Chinese Medicine, Hunan University of Chinese Medicine, Changsha, China, [4]School of Pharmacy, Hunan University of Chinese Medicine, Changsha, China

**Background:** There is growing evidence demonstrating that the gut microbiota plays a crucial role in multiple endocrine disorders, including diabetic cardiomyopathy (DCM). Research shows that the Chinese herb reduces disease occurrence by regulating gut microbiota. Zuogui Jiangtang Shuxin formula (ZGJTSXF), a Chinese medicinal formula, has been clinically used for treatment of DCM for many years. However, there is still no clear understanding of how ZGJTSXF treatment contributes to the prevention and treatment of DCM through its interaction with gut microbiota and metabolism.

**Methods:** In this study, mice models of DCM were established, and ZGJTSXF's therapeutic effects were assessed. Specifically, serum glycolipid, echocardiography, histological staining, myocardial apoptosis rate were assessed. Using 16s rRNA sequencing and high-performance liquid chromatography-tandem mass spectrometry (HPLC-MS/MS), we determined the impact of ZGJTSXF on the structure of gut microbiota and content of its metabolite TMAO. The mechanism of ZGJTSXF action on DCM was analyzed using quantitative real-time PCR and western blots.

**Results:** We found that ZGJTSXF significantly ameliorated DCM mice by modulating gut-heart axis: ZGJTSXF administration improved glycolipid levels, heart function, cardiac morphological changes, inhibited cardiomyocytes apoptosis, and regulate the gut microbiota in DCM mice. Specifically, ZGJTSXF treatment reverse the significant changes in the abundance of certain genera closely related to DCM phenotype, including Lactobacillus, Alloprevotella and Alistipes. Furthermore, ZGJTSXF alleviated DCM in mice by blunting TMAO/PERK/FoxO1 signaling pathway genes and proteins.

**Conclusion:** ZGJTSXF administration could ameliorate DCM mice by remodeling gut microbiota structure, reducing serum TMAO generation and suppressing TMAO/PERK/FoxO1 signaling pathway.

KEYWORDS

**Zuogui Jiangtang Shuxin formula, diabetic cardiomyopathy, gut microbiota, gut - heart axis, TMAO/PERK/FOXO1**

# Introduction

Over the past few decades, type 2 diabetes mellitus (T2DM) and its complications have increased annually (1). As a common cardiovascular complication of diabetes, diabetic cardiomyopathy (DCM) primarily manifests as an abnormal myocardium, independent of coronary artery disease, valvular disease, and cardiovascular risk factors such as hypertension (2, 3). A persistent condition in which glucose and lipid metabolism causes cardiomyocyte death, myocardial fibrosis, ventricular remodeling, and diastolic and systolic dysfunction (4). It is one of the primary causes of death among diabetics (5). In spite of intensive efforts, no definitive therapeutic methods have been developed for treating DCM. Furthermore, there are a limited number of treatment options and no understanding of the underlying pathogenesis of essential DCM. As a result, identifying potential therapeutic targets and discovering novel mechanisms of DCM are essential to preventing and treating the disease.

Maintaining a healthy microbiota in the gut is crucial for maintaining homeostasis. However, when gut microbial homeostasis is disrupted, it can induce the development of different diseases. It has recently been found that dysbiosis of the gut microbiota plays a role in multiple conditions, including obesity, metabolic syndrome, diabetes, and cardiovascular disease, which are closely linked to DCM (6). There are many ways in which gut microbiota communicate with heart, including the production of trimethylamine-N-oxide (TMAO), short-chain fatty acids (SCFAs), bile acids, lipopolysaccharide (LPS), and phenylacetylglutamine (PAGln) (7, 8). This intimate connection defines the term gut-heart axis. Numerous cardiovascular disorders have been linked to the gut-heart axis, and addressing the gut-heart axis may ameliorate DCM (9). TMAO is one of the more extensively studied metabolites formed by the gut microbiota and comes with a potential role in cardiovascular diseases (10–12). Plasma TMAO levels are also associated with a significantly higher risk of type 2 diabetes and metabolic syndrome (13). In the context of pathogenesis, further research is needed to better understand how microbiota gut-derived metabolites TMAO communicate with the heart. Research conducted by Chen et al. indicated that TMAO bound and activated PERK (an endoplasmic reticulum stress sensor), which caused FoxO1 to induce insulin resistance and metabolic dysfunction (14). Furthermore, inhibition of TMAO production can reduce the activation of PERK and inhibit FoxO1, which may prevent hyperglycemia (14, 15). Converging evidences above, we postulated that TMAO/PERK/FoxO1 signaling pathway is possibly a potent target for the treatment of DCM. The above-mentioned ideas are only our reasonable speculation, and the specific mechanism needs to be more thoroughly investigated.

Over 2,000 years of history have been devoted to traditional Chinese medicine (TCM), which is widely used to treat metabolic and cardiovascular disorders. Recently, gut microbiota has emerged as an invaluable field for understanding TCM (16). There is compelling evidence that TCM may influence gut microbiota and metabolic components through interactions with gut microbiota (17). The Zuogui Jiangtang Shuxin formula (ZGJTSXF), a herbal compound based on meridian theory, is a herb that addresses a wide range of health conditions. The ZGJTSXF has been widely used in clinical practice for the treatment of diabetic cardiovascular complications. This is due to its effectiveness in nourishing Yin and benefiting Qi, invigorating blood, and removing toxins. Although studies have shown the efficacy of ZGJTSXF in DCM, the mechanism of action of ZGJTSXF in the treatment of DCM are not fully understood, which limits the further development and clinical application of ZGJTSXF. In light of this, further investigation of ZGJTSXF in terms of the prevention and treatment of DCM upon gut microbiota-mediated insight may contribute to the understanding of its mechanism of action and the potential clinical applications of the compound.

Here, the effects of ZGJTSXF treatment on mice models of DCM were evaluated first. We investigated the shifts in gut microbiota and content of its metabolite TMAO using 16S rRNA gene sequencing and HPLC-MS/MS. To determine the potential therapeutic effects of ZGJTSXF on the gut-heart axis, a holistic correlation analysis uniting gut microbiome and metabolomics was conducted. Throughout the whole process, our results presented substantial evidence about how ZGJTSXF ameliorated DCM by reshaping gut microbiota and modifying metabolites. This provided more theoretical and experimental proof of gut microbiota as an essential factor in diseases.

# Materials and methods

## Preparation and component analysis of ZGJTSXF

Herbs in ZGJTSXF [composed of Panax ginseng C. A. Meyer, Astragalus membranaceus (Fisch.), Bunge, Rehmannia glutinosa (Gaetn.) Libosch. ex Fisch. et Mey., Pueraria lobata (Willd.), Ohwi, Cornus officinalis Sieb. et Zucc., Salvia miltiorrhiza Bunge, Coptis chinensis Franch., Ophiopogon japonicus (Linn. f.) Ker-Gawl. and Crataegus pinnatifida Bge] were provided by herbal pharmacy of First Hospital of Hunan University of Chinese Medicine (Hunan, China) and authenticated by Professor Professor Yong-jun Wu from School of Pharmacy of Hunan University of Chinese Medicine. We weighed each medicinal material accurately and soaked it in distilled water for one hour. The drugs were boiled twice in water, each time for one hour. A water decoction containing the 2 g·mL−1 original medicinal material was prepared from the double-extracted solutions using filtration, concentration, and packaging. The resulting decoction was stored in a refrigerator (4°C) until it was used.

Take 15 ml of herbal decoction, centrifuge at a high speed (12,000 rpm, 15 min), and analyze the supernatants using ultra high performance liquid chromatography - high resolution mass spectrometry (UPLC-Q-Exactive-Orbitrap-MS). UPLC-Q-TOF/MS grade acetonitrile and HPLC grade acetonitrile, methanol, formic acid, were provided by Merck KGaA (Darmstadt, Germany). UPLC-Q-Exactive-Orbitrap-MS analysis was analyzed on a Waters Corporation Xbridge BEH C18 (2.1 mm×100 mm, 2.6 m) system, which was maintained at 40°C. The flow rate was set at 0.3mL/min, and the injection volume was 10 μL. The mobile phase was consisted of 0.1% formic acid water (A) - 0.1% formic acid acetonitrile (B) (0~1.5 min, 2%~2% B; 1.5~20 min, 2%~45% B; 20~27 min, 45%~95% B; 27~32 min, 95%~95% B; 32~32.1 min, 95%~2% B; 32.1~35 min, 2%~2% B). The eluent was detected by a quadrupole orbitrap high resolution mass spectrometer in the ESI positive and negative ion

mode. The raw data were processed using Xcalibur 4.3 and Compound Discoverer 3.2 software (Thermo Fisher Scientific, USA).

## Experimental animals and study design

The MKR mice, which were first established by Fernandez and colleagues and bear a dominant-negative IGF-1R in skeletal muscle (18), were obtained from Dr. Derek LeRoith in National Institutes of Health Diabetes Research Center (Bethesda, MD, USA). MKR mice were housed in a temperature (22 ± 2 °C) controlled room with a 12 h light/dark cycle. MKR mice were used for breeding and their offspring were used for experiments.

Twelve male MKR mice (8 weeks old) were randomly divided into two groups: 1) diabetic cardiomyopathy model group (DCM, n = 6); 2) ZGJTSXF treatment group (ZGJTSXF, n = 6). Both groups were kept on a high-fat diet supplemented with 1% choline for four weeks. After four weeks, MKR mice were injected with 1% streptozotocin (STZ; Sigma Aldrich Co., USA) dissolved in citrate buffer (pH=4.5) at a dose of 40 mg/kg/day for 5 days. Fasting blood glucose (FBG) values and echocardiography were tested to determine the development of diabetes in desired groups. Age-matched and sex-matched nondiabetic normal C57BL/6 mice were used as control group (CON, n = 6). Our previous study explored the efficacy of three doses (16.84 g/kg/d, 33.67 g/kg/d, and 67.34 g/kg/d) of this prescription, and the result demonstrated that ZGJTSXF owns optimal efficacy when it is administered at 33.67 g/kg/d; therefore, a dose of 33.67 g/kg/d was chosen for the experiments in the current study (unpublished observations). The mice in the CON and DCM groups were given equal volumes of distilled water. All groups were gavaged once a day for 4 weeks. The protocols for animal care and handling were approved by the Animal Ethical Committee of the Hunan University of Chinese Medicine.

## Serum glycolipid profile

The mice were fasted for eight hours after the last administration. The tail vein was then accessed for blood collection. Blood glucose levels were measured with a blood glucose monitor (GT-1980. Aikelai Medical Electronics (Pinghu) Co., Ltd., China). An oral glucose tolerance test (OGTT) was conducted on mice after fasting for 8 hours (free access to water). A blood glucometer measured blood glucose levels in tail veins after glucose loading at 0, 30, 60, 90, and 120 minutes. An area under the curve (AUC) for glucose was calculated using the trapezoidal method based on five glucose measurements. Following an eight-hour fast, mice were anesthetized with light isoflurane anesthesia and blood was drawn from the retroorbital plexus. Blood samples were processed immediately, centrifuged and frozen at −80 °C until assayed. Fasting serum insulin (FINS) was determined according to the manufacturer's instructions using an enzyme linked immunosorbent assay (ELISA) kit (Wuhan, China). Insulin resistance index (HOMA-IR) was estimated according to the formula: HOMA-IR=FBG (mmol/L)×FBI (mIU/mL)/22.5. The serum total cholesterol (TC) and serum triglycerides (TG) levels as well as the high density lipoprotein cholesterol (HDL-C) and serum low density lipoprotein cholesterol (LDL-C) levels were determined using commercially available kits (Nanjing Jiancheng Bioengineering Institute, Nanjing, China).

## Echocardiography analysis

We anesthetized the animals with 1.5% isoflurane in 95% oxygen and 5% carbon dioxide, and removed their chest hair with a depilatory cream before examination. We assessed *in vivo* heart function using a high-resolution ultrasound imaging system (VINNO 6, Vinno Corporation, Suzhou, China) and measured chamber dimensions with a 23 MHz frequency transducer. An M-mode recording was obtained from short-axis parasternal views. We measured and recorded the internal dimensions of ejection fraction (EF), fractional shortening (FS), left ventricular end-systolic diameter (LVIDs), left ventricular end-diastolic diameter (LVIDd), left ventricular end-systolic volume (LVEDV), and left ventricular end-diastolic volume (LVEDV). A reading average is calculated based on at least three measurements in echocardiography.

## Histological analysis

Heart tissues were fixed for 24 hours in 0.01 M phosphate-buffered saline and 10% formalin. A slide was prepared by embedding fixed tissues in paraffin and separating them into thin sections of 5 um thickness. The slides were stained with hematoxylin and eosin (H&E), Picrosirius Red Stain Kit (Wellbio, Changsha, China), and Masson's trichrome stain Kit (Wellbio, Changsha, China) for histopathological comparisons and determined by the light microscopy (Motic China Group Co., Ltd.).

## Terminal deoxynucleotidyl transferase dUTP nick end labeling staining

As needed, TdT and dUTP reagents from the TUNEL kit were mixed at a ratio of 1:5 according to the sample size. Sections were incubated in a water bath at 37°C for 60 minutes after being covered and placed in a wet box. A dropwise application of 4', 6-diamidino-2-phenylindole stain was applied to the slides after they had been rinsed three times in PBS for 5 minutes each. New glass slides were used for sealing the cells, as well as anti-fluorescence quenching tablets. Photographs were taken of the slides under a fluorescence microscope (BX53, OLYMPUS, Japan). Apoptotic cells fluoresce red. MicroPublisher imaging system (Q-imaging) was used to calculate AI using five visual fields of each tissue. The AI calculation was based on the following equation: AI = apoptotic nuclei/total cardiac nuclei.

## Gut microbial analysis of cecal contents

Each cecal content sample was extracted using HiPure Stool DNA Kit B (Magen, Shanghai, China) following the manufacturer's instructions and quantified by ultraviolet spectroscopy. The 16S rDNA V3-V4 region was amplified by PCR (94°C for 2 min,

followed by 30 cycles at 98°C for 10 s, 62°C for 30 s and 68°C for 30 s and a final extension at 68°C for 5 min) using universal forward and reverse primers 341F (CCTACGGGNGGCWGCAG) and 806R (GGACTACHVGGGTATCTAAT). AxyPrep DNA Gel Extraction Kit (Axygen Biosciences, Union City, CA, US) was used to purify amplicons from 2% agarose gels. Life Technologies, Foster City, USA) provided the ABI StepOnePlus Real-Time PCR System for quantification. An illumina sequencing platform was used to sequence paired-end amplicons pooled in equimolar concentrations according to Gene Denovo Biotechnology Co. Ltd (Guangzhou, China). Raw reads were further filtered using FASTP (version 0.18.0). Raw tags were merged using FLASH (version 1.2.11) with a minimum overlap of 10 bp and a 2% mismatch error rate. Quality filtering and removal of chimeric sequences were then performed before determining which tags are effective, and then clustering them according to the ≥97% similarity cutoff using UPARSE software (version 9.2.64). An analysis of principal components (PCA) was conducted using Vegan R (version 2.5.3). In order to analyze the effect of the DCM and ZGJTSXF on the overall microbiota structure, we used QIIME software (version 1.9.1, University of Colorado, Denver, CO, USA) to obtain observed species, abundance-based coverage estimator (ACE), Shannon diversity index, and Simpson diversity index. Utilizing the R project, we analyzed bacteria mainly at the phylum and genus level. In the Vegan package (version 2.5.3) of the R project, Welch's t-test was applied to compare species between groups. In addition, the linear discriminant analysis (LDA) effect size measurement (LefSe) analysis based on Kruskal-Wallis rank-sum test and Tukey HSD test was conducted to identify the abundant taxonomy with significant differences among the three groups. In order to calculate the heat map of cluster stacking, we used R and Omicsmart (Gene Denovo Biotechnology Co. Ltd, Guangzhou, China), a dynamic real-time interactive platform for data analysis.

## Serum TMAO detected by HPLC-MS/MS

In this study, serum TMAO was measured by high-performance liquid chromatography-tandem mass spectrometry (HPLC-MS/MS). The sample was prepared by adding 10 uL of TMAO d9 (Toronto Research Chemicals Inc., Toronto, Canada) to 100 uL serum; 300 uL of acetonitrile precipitated the protein, vortexed for 1 min, centrifuged at 1,000 rpm, 4°C for 5 min; and 200 uL of the remaining supernatant was injected into a Waters Atlantis HILIC Silica column for analysis.

## Real-time quantitative PCR analysis

The total RNA of cells and tissues was extracted using the Total RNA Extracting Kit (Foregene Co. Ltd., China). Total RNA was reverse-transcribed to synthesize single strand complementary DNA (cDNA) using RT EasyTM II (with gDNase) (RT-01032) kit (Foregene Co. Ltd., China). Real Time PCR EasyTM-SYBR Green I (QP-01014; Foregene Co. Ltd., China) and LightCycler 96 Instrument (Roche, Mannheim, Germany) were used for real-time quantitative PCR (qPCR). GAPDH was used as the internal reference gene for qPCR, and gene expression levels were calculated with the $2^{-\Delta\Delta}$CT method. The primers of each gene are as follows: Forward-PERK, 5'-CAGTGTTTGGCTTAGGGGCA-3; Reverse-PERK, 5'-TCATTCT CGGCATCCAGTGC-3; Forward-FoxO1, 5'-TTTCGTCCTCG AACCAGCTC-3; Reverse-FoxO1, 5'- TACACCAGGGAATGCA CGTC-3; Forward-Bim, 5'-AAATGGCCAAGCAACCTTCTG-3'; Reverse-Bim, 5'- CTTGCGGTTCTGTCTGTAGGG-3'; Forward-Puma, 5'-TGGGAGATATTGGCGGAAGC-3'; Reverse-Puma,5'-GTATCTTACAGGCTGGGCCG-3'; Forward-TNFSF10, 5'-GGAAGACCTCAGAAAGTGGCA-3'; Reverse-TNFSF10, 5'-CTCGATGACCAGCTCTCCATT-3';

Forward-GAPDH, 5'-ACTCTTCCACCTTCGATGCC-3; Reverse-GAPDH, 5'-TGGGATAGGGCCTCTCTTGC-3'.

## Western blot analysis

A homogenized heart tissue sample was centrifuged at 12,000 rpm at 4°C for 10 minutes in lysis buffer (Biyuntian Biotech Co. Ltd., China). The protein-containing supernatant was collected. The protein concentrations were determined using the BCA (Bicinchoninic Acid) protein assay kit from Biyuntian Company. Proteins were separated by 10% sodium dodecyl-sulfate polyacrylamide gel electrophoresis (SDS-PAGE) and transferred to polyvinylidene difluoride membranes (PVDF). After soaking in TBST buffer supplemented with 5% bovine serum albumin (BSA) for 1 h, these PVDF membranes were incubated with primary antibodies overnight at 4°C. It was then washed three times with TBST and incubated at room temperature for 1 hour with secondary antibodies conjugated to horseradish peroxidase (HRP). Rewashed with TBST, the membranes were imaged on X-ray film by chemiluminescence. The super-sensitive ECL chemiluminescent substrate kit was purchased from Biosharp Life Science Co., Ltd. (China). The band intensity was analyzed using ImageJ software (National Institutes of Health, Maryland, USA). The primary antibodies used in this study were as follows: FOXO1 Antibody (AF301660), FoxO1 (phospho Ser256) Polyclonal Antibody (AF00557), Bim Antibody (AF300342), Bim (phospho Ser59) Polyclonal Antibody (AF00289), PUMA Antibody (AF300458) were provided by AiFang biological (Hunan, China), Phospho-PERK (Thr982) Antibody (DF7576) was purchased from Affinity Biosciences (Jiangsu, China), Anti -TRAIL Rabbit pAb (GB11413) were provided by Sevier Biotechnology Co., Ltd. (Wuhan, China)., Anti-PERK antibody [EPR19876-294] (ab229912) and anti-GAPDH antibody [EPR16891] (ab181602) were supplied by Abcam Biotech (Shanghai, China).).

## Statistical analysis

We express all data as mean ± standard deviation. When the measurement data conformed to normal distribution and the homogeneity of variance test was homogeneous, one-way ANOVA was used to compare groups, whereas paired samples t-tests were used to compare before-and-after data. Otherwise, the Kruskal-Wallis test and the Wilcoxon rank test are used. $P<0.05$ was considered statistically significant. SPSS 22.0 (IBM, USA) was used for all analyses.

# Results

## Major components in ZGJTSXF according to UPLC-Q-exactive-orbitrap-MS analysis

Based on the established UPLC-Q-Exactive-Orbitrap-MS method, 290 Chemical compounds were identified. These components can be divided into ten categories: flavonoids, acids/small peptides, phenylpropanoids, phenols, saponins, organic acids, alkaloids, nucleosides, iridoids and oligoses. In this study, the chromatogram and detailed composition of ZGJTSXF are shown in Supplementary Figure S1 and Table S1.

## ZGJTSXF administration improves glucose and lipid metabolism in DCM mice

First, we evaluated the impacts of ZGJTSXF administration on FBG in mice with DCM. The results showed that the FBG levels of the DCM group were significantly higher than those of the CON group ($P$<0.01). After 4 weeks of intervention, compared with the DCM group, the ZGJTSXF group showed significantly reduced serum FBG levels in DCM mice ($P$<0.01) (Figure 1A). Therefore, we confirmed that ZGJTSXF administration did exhibit significant benefits in terms of lowering FBG.

Next, we evaluated the impacts of ZGJTSXF administration on oral glucose tolerance in mice with DCM. As shown in Figure 1B and Figure 1C, after the intake of glucose, compared with the CON group, the DCM group had significantly increased blood glucose level at each time point ($P$<0.01), while the ZGJTSXF group after treatment significantly alleviated the blood glucose increase in DCM mice ($P$<0.01).

we also evaluated the impacts of ZGJTSXF administration on fasting serum insulin (FINS) in mice with DCM. As shown in Figure 1, The results showed that the FINS levels of the DCM group were significantly higher than those of the CON group ($P$<0.01)(Figure 1D). After 4 weeks of intervention, compared with the DCM group, the ZGJTSXF group showed significantly reduced FINS levels in DCM mice ($P$<0.01). Due to its good correlation to glycemic clamp, HOMA-IR has been widely utilized as insulin resistance index in clinical and epidemiological studies (19, 20). The results showed that the insulin resistance index were increased in the DCM group compared with the CON group ($P$<0.01), whereas lower insulin resistance index were found in the ZGJTSXF group compared with that in the DCM group ($P$<0.01) (Figure 1E).

In addition, the antihyperlipidemic effect of ZGJTSXF in DCM mice has also been emphasized in this experiment. As shown in Figure 1, DCM group showed significant increased serum TG, TC, and LDL-C and decreased serum HDL-C compared with the CON group ($P$<0.01). Administration of ZGJTSXF reduced serum TG (Figure 1F), TC (Figure 1G), LDL-C (Figure 1H) and increased HDL-C in diabetic mice (Figure 1I) ($P$<0.01).

## ZGJTSXF administration promoted myocardial function and myocardial histology in DCM mice

We evaluated the effects of ZGJTSXF on echocardiography in DCM mice. As shown in Figure 2A, echocardiography analysis found that mice in DCM group had significantly reduced left ventricle ejection fraction (LVEF) and left ventricle fractional shortening (LVFS), compared with mice in CON group. Notably, mice ZGJTSXF groups showed significantly increased LVEF and LVFS (Figures 2B–C) ($P$<0.01). The left ventricular internal end-systolic diameter (LVIDs), left ventricular internal end-diastolic diameter (LVIDd), left ventricular end-systolic volume (LVESV) and left ventricular end-diastolic volume (LVEDV) of mice in the DCM group significantly increased compared to those of mice in the CON groups ($P$<0.01). On the contrary, the ZGJTSXF group exhibited significantly reduced left ventricular internal end-systolic diameter (LVIDs), left ventricular internal end-diastolic diameter (LVIDd), left ventricular end-systolic volume (LVESV) and left ventricular end-diastolic volume (LVEDV) compared with the DCM group ($P$<0.01) (Figures 2D–G).

We further checked how ZGJTSXF administration could influence the histological changes in myocardial tissues. As shown in Figure 2H, in the CON group of mice, the ventricular wall and papillary muscle cells were arranged neatly and regularly; the nuclei were of uniform size; the cell gaps were not widened or narrowed; the morphology and structure were good. No pathological changes were detected in the CON group. In the DCM group, there was vacuolar degeneration of cardiomyocytes, coagulative necrosis of the cardiomyocytes, small focal inflammatory cell infiltrates in the interstitial myocardium and myocardial fibrosis. However, coagulative necrosis of the cardiomyocytes, small focal inflammatory cell infiltrates in the interstitial myocardium and myocardial fibrosis were significantly improved in the ZGJTSXF groups, compared to the DCM group.

Cardiovascular fibrosis contributes to the pathogenic remodeling and structural changes of diabetic hearts (21), which further contributes to DCM myocardial dysfunction. We investigated whether ZGJTSXF could inhibit cardiac fibrosis synthesis. As a major method for assessing cardiac fibrosis, Masson staining uses collagen deposition to determine collagen deposition. Figures 2I, J show that collagen was practically absent in the CON group, whereas collagen clumps accumulated in the DCM group ($P$ < 0.01). There was an improvement in cardiac fibrosis in the ZGJTSXF treatment group ($P$ < 0.05). Sirius red staining reacts with collagen fibers to test collagen deposition. As shown in Figure 2K and Figure 2L, no significant collagen was observed in the CON group, but significant increase collagen appeared in DCM group ($P$ <0.01). However, ZGJTSXF administration remarkably decreased collagen content in DCM mice ($P$ <0.01).

## ZGJTSXF administration inhibited apoptosis in DCM mice

We quantitated the apoptosis of mouse cardiomyocytes through TUNEL assay. As shown in Figure 3A and Figure 3B, the apoptosis rate of cardiomyocytes in the DCM group was significantly higher than that in the CON group ($P$ <0.01). Compared with the DCM group, the ZGJTSXF groups demonstrated significantly reduced cardiomyocyte apoptosis ($P$ <0.01).

## ZGJTSXF administration affected the structure of the gut microbiota in DCM mice

Intestinal microbes have been recognized to play an important role in ameliorating DCM. Studies indicated that oral drug

10.3389/fendo.2023.1106812

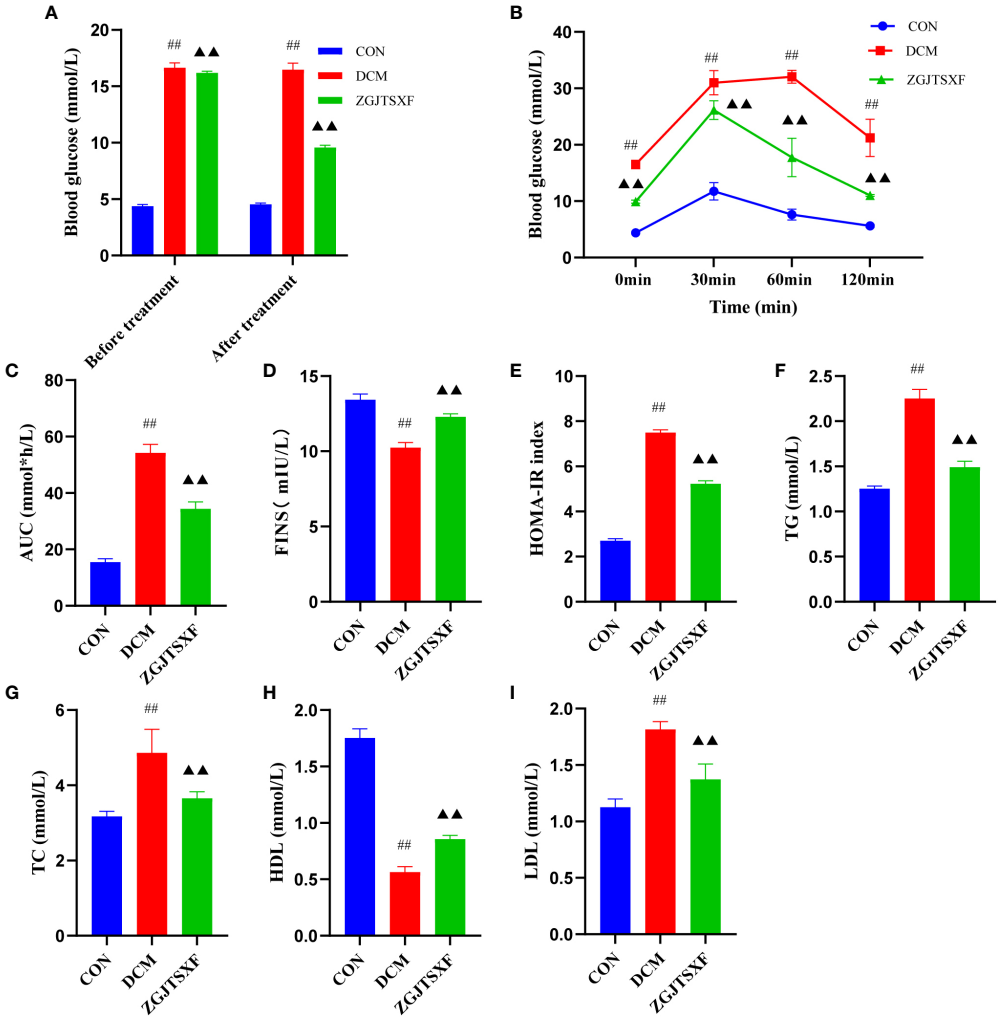


FIGURE 1
ZGJTSXF administration can improve glucose and lipid metabolism. **(A)** Fasting blood glucose levels before and after treatment in all groups of mice. **(B)** Oral glucose tolerance test (OGTT) levels of each group at different time periods. **(C)** The area under the curve (AUC) of plasma glucose during OGTT. **(D)** Fasting serum insulin (FINS). **(E)** Insulin resistance index (homeostasis model assessment of insulin resistance, HOMA-IR). **(F)** Triglycerides(TG). **(G)** Total Cholesterol (TC). **(H)** High-Density lipoprotein Cholesterol (HDL). **(I)** low-Density lipoprotein Cholesterol. $^{\#\#}P<0.01$, compared with the CON group; $^{\blacktriangle\blacktriangle}P<0.01$, compared with the DCM group.

administration may influence disease development *via* modulating composition and metabolites of gut microbiota (22). To this end, gut microbiota were investigated in animals after oral administration with ZGJTSXF.

The gut microbiota diversity and richness were evaluated by Sobs, Chao1, ACE and Shannon indexes. Compared with the control and ZGJTSXF treatment groups (Figures 4A–D), relatively few bacterial species were seen in the DCM groups ($P < 0.05$, $P < 0.001$), indicating that ZGJTSXF is altering bacterial community abundance. β-diversity analysis was used to assess the discrepancies between microbial communities. UPGMA clustering tree and principal coordinates analysis (PCoA) based on Jaccard distance were used to analyze changes in the overall structure of gut microbiota (Figures 4E, F). Using UPGMA and PCoA, it was evident that DCM and CON were aggregated separately. This suggested that the CON group samples and the DCM model group samples had different compositions and structures. In contrast, the distance between the ZGJTSXF treatment group and the CON group was closer than that between the DCM model group and the CON treatment group. These results suggested that ZGJTSXF altered the diversity reduction of intestinal microorganisms and the structure of microbial communities challenged by DCM.

We determined the relative abundance of the phylum (Figure 4G) and found that the DCM mice displayed an increased the relative abundance of Firmicutes (74.21% vs. 57.70%) and decreased abundance of Bacteroidetes (22.50% vs. 36.33%) compared with those in the CON group. In contrast, the microbiota imbalance was ameliorated by ZGJTSXF administration as it decreased the abundance of Firmicutes (68.29% vs. 74.21%) and increased Bacteroidetes (26.09% vs. 22.51%) (Figure 4H). Furthermore, treatment with ZGJTSXF reduced the ratio of Firmicutes to Bacteroidetes in DCM mice, although the difference was not statistically significant (Supplementary Figure S2). A decrease in Bacteroidetes or an increase in Firmicutes or an increase in the ratio of Firmicutes to Bacteroidetes contributes to the risk of diabetes (23). Therefore, this result showed that the ZGJTSXF could reduce the risk of diabetes.

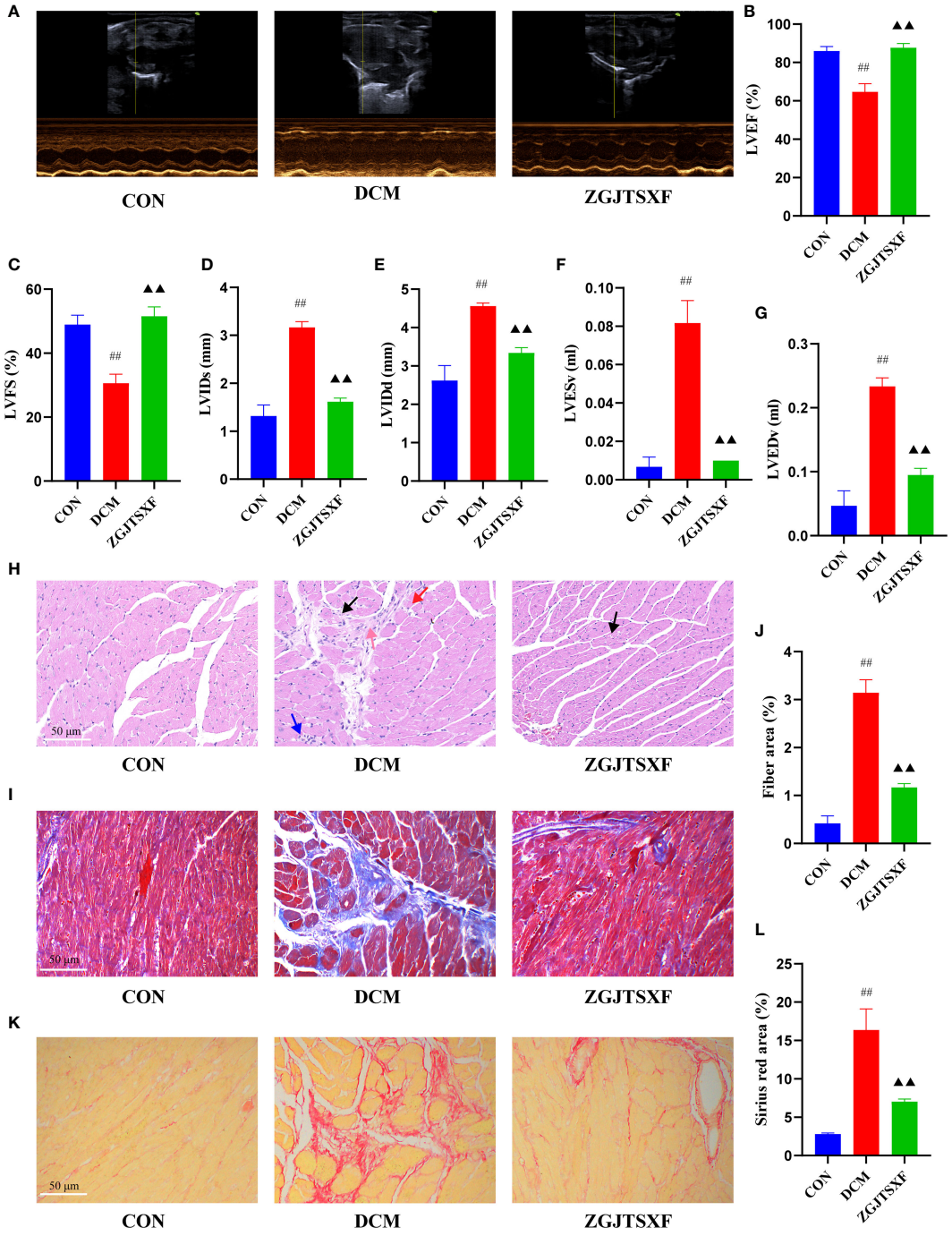


FIGURE 2
ZGJTSXF administration changed myocardial function and myocardial histology in DCM mice. **(A–G)** Echocardiographic observation of changes in cardiac function in various groups of mice. **(A)** Representative M-mode echocardiograms in mice of the indicated groups. **(B)** Summary on the left ventricle fractional shortening (LVFS). **(C)** Summary on the left ventricle ejection fraction (LVEF). **(D)** Summary on left ventricular internal end-systolic diameter (LVIDs). **(E)** Summary on left ventricular internal end-diastolic diameter (LVIDd). **(F)** Summary on left ventricular end-systolic volume (LVESV). **(G)**Summary on left ventricular end-diastolic volume (LVEDV). **(H)** Representative images of a mice myocardial tissues after HE staining (Scale bar, 50 μm). **(I)** Representative images of mice myocardial tissues after masson staining (Scale bar, 50 μm). **(J)** Fiber rate of cardiomyocytes in mice of the indicated group was summarized. **(K)** Representative images of a mice myocardial tissues after sirius red staining (Scale bar, 50 μm). **(L)** Sirius red area of cardiomyocytes in mice of the indicated group was summarized. Black arrow, vacuolar degeneration of cardiomyocytes; red arrow, coagulative necrosis of the cardiomyocytes; blue arrow, small focal inflammatory cell infiltrates in the interstitial myocardium; pink arrow, myocardial fibrosis. $^{\#\#}P<0.01$, compared with the CON group; $^{▲▲}P<0.01$, compared with the DCM group.

At the genus level (Figure 4I), DCM mice had a higher relative abundance of Lactobacillus, Bacteroides, Alloprevotella and Alistipes and had a lower relative abundance Lachnospiraceae_NK4A136_group, Ruminococcaceae_UCG-014, Eubacterium_xylanophilum_group and Desulfovibrio compared with those of CON mice. However, the abundance of these bacteria in the ZGJTSXF group were reversed and returned to CON group compared with the DCM group.

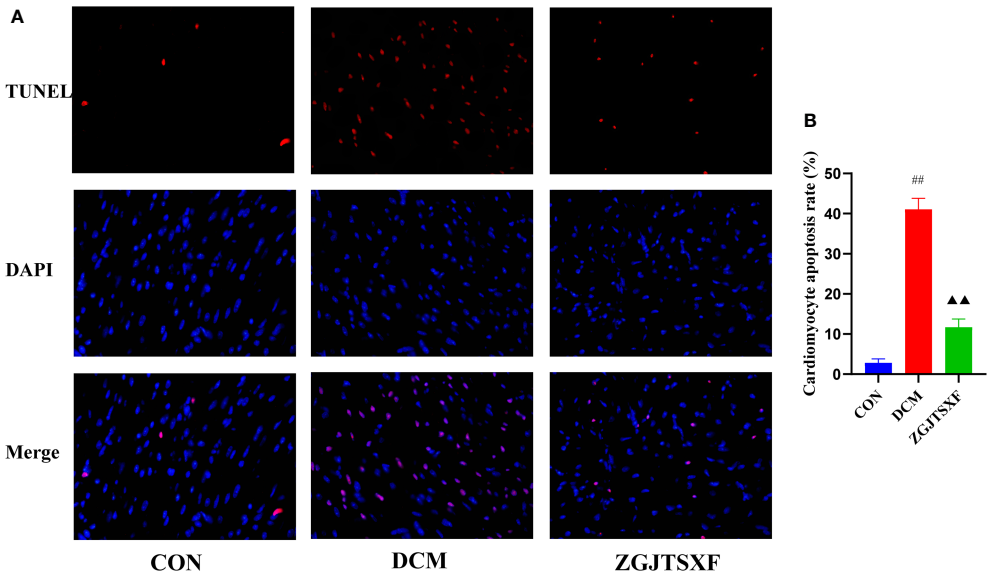


FIGURE 3
Apoptosis of mouse myocardial tissues was evaluated by TUNEL staining. **(A)** Representative images of apoptosis of mice myocardial tissues after TUNEL staining. **(B)** Apoptosis rate of cardiomyocytes in mice of the indicated group was summarized. $^{\#\#}P<0.01$, compared with the CON group; $^{▲▲}P<0.01$, compared with the DCM group.

The LEfSe analysis, which emphasizes the statistical significance and biological correlation, was also performed to search for biomarkers with statistical significance among the CON, DCM and ZGJTSXF groups (Figures 4J, K). In this study, the discriminative features of the bacterial taxa were identified with an LDA score >2.0. According to the ranked bacterial taxa, the DCM group revealed that twenty-eight communities were selectively enriched, which were Lactobacillus, Lactobacillaceae, Lactobacillales, Alistipes, Streptococcus_acidominimus, Alistipes_inops and Acidimicrobiia Microtrichales et al. After treatment, the mice of the ZGJTSXF group were enriched in thirty communities such as Ruminococcaceae_NK4A214_group, Saccharimonadia, Saccharimonadales, Candidatus_Saccharimonas, Saccharimonadaceae and Patescibacteria. Combined with the differential gut microbiota analyzed by Tukey HSD test at the genus level (Figures 4L), it can be concluded that Lactobacillus, Alloprevotella, Alistipes, Rikenellaceae_RC9_gut_group, Lachnospiraceae_UCG-006, Parabacteroides, Eubacterium_ventriosum_group, Odoribacter, Ruminococcaceae_UCG-013, Clostridium_sensu_stricto_1 played the most significant role in ZGJTSXF treatment.

## Diabetic cardiomyopathy-related genera regulated by ZGJTSXF

The correlations between 69 genera that changed significantly among the three groups and 18 DCM-related pathological indices were conducted by Spearman's correlation analysis. The results were presented as a heatmap (Supplementary Figure S3). In general, there were 41 genera closely related to the phenotype of DCM (≥4 pathological indices were closely correlated with certain genus). Among them, Butyricicoccus, Prevotellaceae_UCG-001, Bifidobacterlum, Lachnoclostridium, Lachnospiraceae_FCSo20_group, Marvinbryantia, Blautia, Oscillibacter, UBA1819, Ruminiclostridium_5, Anaerotruncus, A2, Eubacterium_nodatum_group, GCA-900066575, Parvibacter, Ruminococcaceae_UCG-013, Eubacterium_xylanophilum_group, Desulfovibrio, Family_XIIL_UCG-001, Eubacterium_coprostanoligenes_group, Eubacterium_ventriosum_group and Candidatus_Arthromitus showed a positive correlation with FINS, HDL-C, EF%, FS% and a negative correlation with LVESv, TG, LVIDs, TC, LDL-C, blood glucose, LVIDd, LVEDv, fiber area, AUC of OGTT, HOMA-IR, cardiomyocyte apoptosis rate, Sirius red area. Alistipes, Corynebacterium_1, Escherichia-Shigella, Bifidobacterium, Klebsiella, Odoribacter, Lactobacillus, Parabacteroides, Rikenellaceae_RC9_gut_group, Alloprevotella, Clostridium_sensu_stricto_1 showed a negative correlation with FINS, HDL-C, EF%, FS% and positive correlation with with LVESv, TG, LVIDs, TC, LDL-C, blood glucose, LVIDd, LVEDv, fiber area, AUC of OGTT, HOMA-IR, cardiomyocyte apoptosis rate, Sirius red area.

## Correlations between gut microbiota and serum TMAO level

Spearman's correlation analysis was also conducted to analyze the correlations between the 69 significant changed genera and serum TMAO level. As shown in Supplementary Figure S4, Rikenellaçeae_RC9_gut_group, Alloprevotella, Odoribacter, Parabacteroides, Lactobacillus, Bifidobacterium, Klebsiella, Corynebacterium_1, Alistipes and Clostridium_sensu_stricto_1 showed a positive correlation with Serum TMAO level. Eubacterium_brachy_group, Prevotellaceae_UCG-001, Marvinbryantia, Lachnospiraceae_UCG-006, Eubacterium_ventriosum_group, Ruminococcaceae_UCG-013, GCA-900066575, Desulfovibrio, Candidatus_Arthromitus, Eubacterium_coprostanoligenes_group, Lachnospiraceae_FCS020_group, Anaerotruncus, Eubacterium_xylanophilum_group, Family_XIIl_UCG-

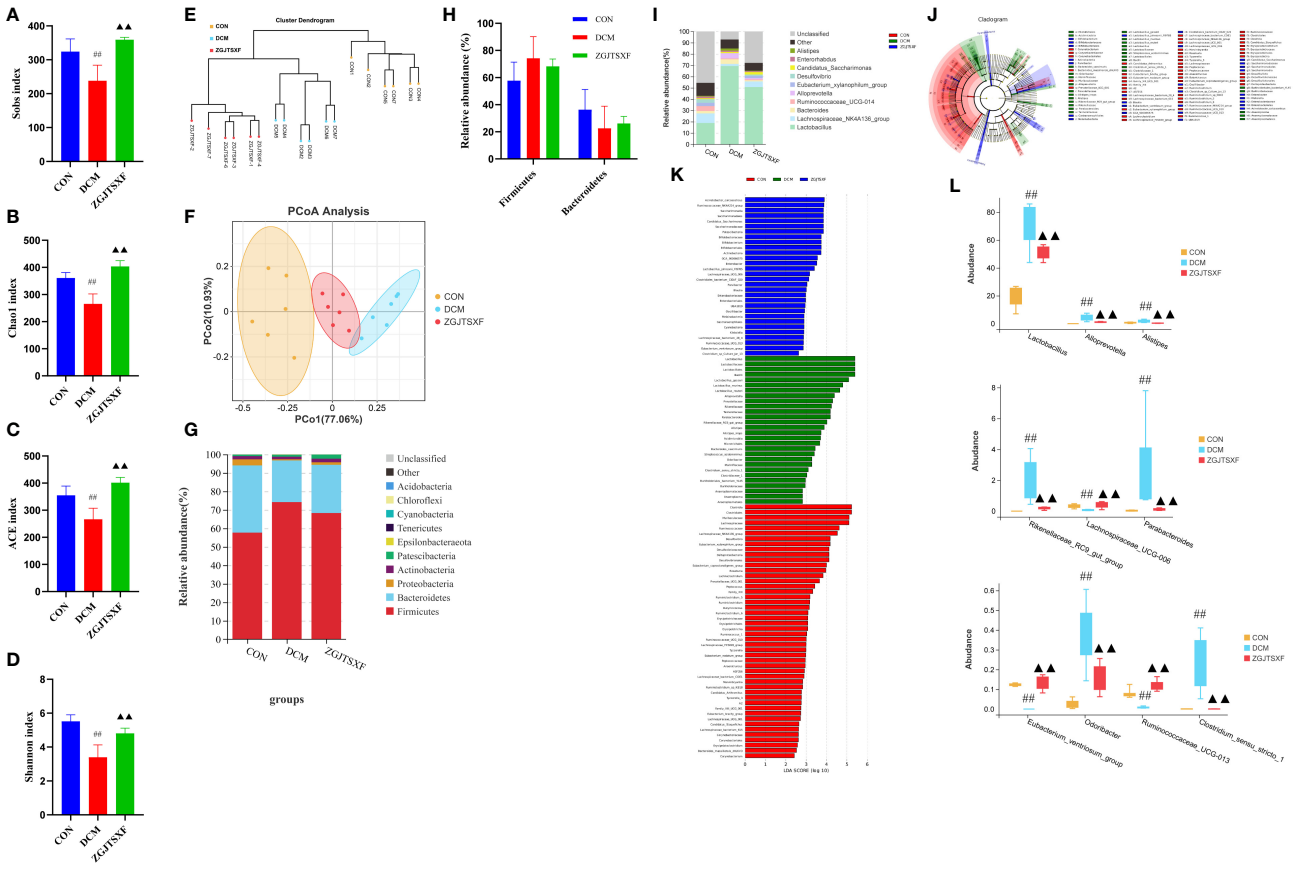


FIGURE 4
ZGJTSXF administration changed the structure of the gut microbiota in DCM mice. **(A–D)** Analysis of α diversity of gut microbiota in mice. **(A)** Sobs 1 index. **(B)** Chao 1 index. **(C)** ACE index. **(D)** Shannon index. **(E, F)** Analysis of β diversity of gut microbiota in mice. **(E)** UPGMA clustering tree and **(F)** principal coordinates analysis (PCoA) based on Jaccard distance. **(G)** The overall composition of the gut microbiota at the phylum level. **(H)** The relative abundance of Firmicutes and Bacteroidetes. **(I)** The overall composition of the gut microbiota at the Genus level. **(J)** Cladogram generated by the LEfSe analysis **(K)** Linear discriminant analysis (LDA) score for taxa differing between three groups. An LDA score greater than 2 indicated a higher relative abundance in the corresponding group than in the three groups. Blue bars represent taxa that are significantly increased in the DCM group. Green bars represent taxa that are significantly increased in the ZGJTSXF group. Red bars represent taxa that are significantly increased in the CON group. **(L)** The relative abundance of Lactobacillus, Alloprevotella, Alistipes, Rikenellaceae_RC9_gut_group, Lachnospiraceae_UCG-006, Parabacteroides, Eubacterium_ventriosum_group, Odoribacter, Ruminococcaceae_UCG-013, Clostridium_sensu_stricto_1. $^{\#\#}P<0.01$, compared with the CON group; ▲▲$P<0.01$, compared with the DCM group.

001, Ruminiclostridium_5, Eubacterium_nodatum_group, Butyricicoccus, Lachnoclostridium, A2, Oscillibacter, Blautia, Ruminococcaceae UCG-004, Roseburia, Ruminococcaceae_UCG-00, Lachnospiraceae_NK4A136_group showed a negative correlation with Serum TMAO level. Of these genera, Lactobacillus, Alloprevotella, Alistipes, Rikenellaceae_RC9_gut_group, Lachnospiraceae_UCG-006, Parabacteroides, Eubacterium_ventriosum_group, Odoribacter, Ruminococcaceae_UCG-013, Clostridium_sensu_stricto_1 could be significantly reversed by ZGJTSXF in DCM mice. Therefore, these genera might be the targets of ZGJTSXF in the treatment of DCM mice.

## ZGJTSXF administration suppressing the TMAO/PERK/FoxO1 pathway in myocardial tissues of DCM mice

In order to explored the underlying mechanism of TMAO mediated DCM. We first quantitated TMAO contents in serum *via* HPLC-MS/MS. We found that TMAO levels were higher in the DCM group than the mice in CON group. However, this was reversed by ZGJTSXF administration ($P<0.01$). Our results suggested that ZGJTSXF reduced TMAO synthesis levels in DCM mice (Figure 5A).

The transcription and protein levels of TMAO/PERK/FoxO1 pathway molecules and apoptosis-associated molecules (Bim, PUMA and TNFSF10) were quantitated by qPCR and western blot assays. Compared with the CON group, the DCM group had significantly increase mRNA levels of PERK, FoxO1, Bim, PUMA and TNFSF10 in the myocardial tissues ($P<0.01$). After the 4-week treatment period, compared with the DCM group, the ZGJTSXF group showed significantly reduced mRNA expression of PERK (Figure 5B), FoxO1 (Figure 5C), Bim (Figure 5D), PUMA (Figure 5E) and TNFSF10 (Figure 5F) in mice with DCM ($P <$ 0.01). The western blot assay (Figure 5G) showed largely consistent expression patterns of these molecules among the groups. The ZGJTSXF treatment could significantly reduce the ratios of p-PERK/PERK (Figure 5H), p-FoxO1/FoxO1 (Figure 5I), p-Bim/Bim (Figure 5J), PUMA/GAPDH (Figure 5K), TNFSF10/GAPDH (Figure 5L) that were upregulated in the DCM group ($P<0.05$,

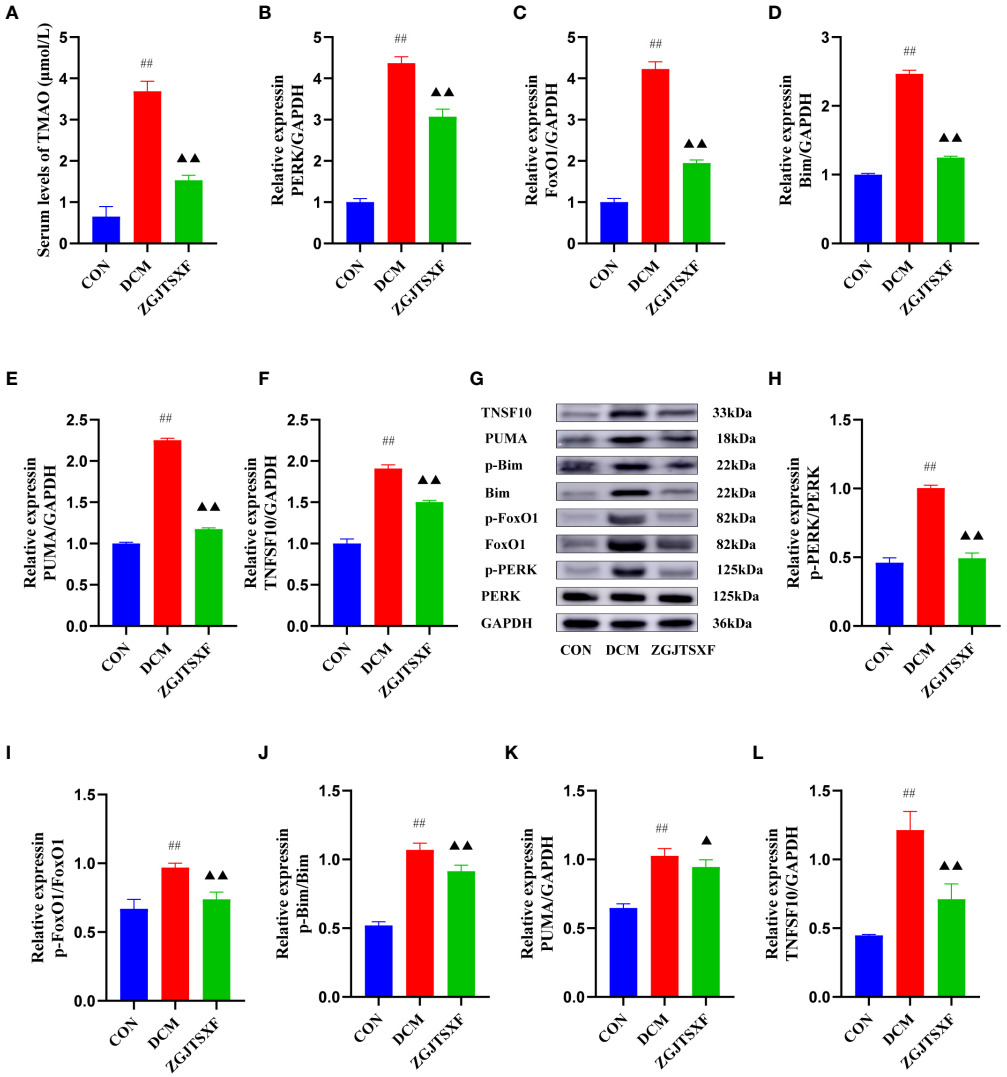


FIGURE 5
ZGJTSXF administration inhibited TMAO/PERK/FoxO1 pathway in DCM mice **(A)** The TMAO contents in serum. The mRNA levels of **(B)** PERK, **(C)** FoxO1, **(D)** Bim**(E)** PUMA**(F)** TNFSF10. **(G)** Representative images of western blot bands are shown. **(H)** The protein levels of phosphorylated PERK (p-PERK), **(I)**The protein levels of phosphorylated FoxO1 (p-FoxO1), **(J)** The protein levels of phosphorylated Bim (p-Bim), **(K)** The protein levels of PUMA, **(L)** The protein levels of TNFSF10. $^{\#\#}P<0.01$, compared with the CON group; $▲▲P<0.01$, $▲P<0.05$, compared with the DCM group.

0.01). Taken together, these results demonstrated that ZGJTSXF administration inhibited apoptosis and blunted the TMAO/PERK/FoxO1 pathway in myocardial tissues of DCM mice.

## Discussion

DCM is a serious complication of diabetes. In spite of much effort, only limited progress has been made. During the present study, we demonstrated that ZGJTSXF can ameliorate the progression of DCM, and that the gut-heart axis may play an instrumental role.

Herbal medicine has been used to treat diabetes and its complications including DCM for thousands of years around the world. Most herbal medicines are taken orally and absorbed through the intestines. Normally, oral drugs go through the gastrointestinal system for metabolism (17). They interact with a large number of microorganisms in the intestine after oral medication (17, 24). It is possible to improve the body's dysfunction and pathological conditions through herbal medicines by regulating the gut microbiota's composition and metabolism. By participating in the metabolic transformation of herbs, the gut microbiota can also improve the bioavailability of herbal compounds (25). According to the UPLC-Q-Exactive-Orbitrap-MS analysis result, ZGJTSXF contain many bioactive compounds, including flavonoids, phenylpropanoids, organic acids, alkaloids. A small fraction of flavonoids (except flavanols) are absorbed through the small intestine as glycosides, which are naturally formed when flavonoids combine with sugar. The colonic microflora absorb glycosylated flavonoids into the body during digestion, converting them into phenolic acid and other metabolites. Microorganisms can catabolize flavonoids, changing their bioavailability and activity, regulating the colonic flora (26–36). Under the action of intestinal bacteria, phenylpropanoids undergo biotransformations such as lactone hydrolysis or demethylation (37, 38). As a prototype, organic acids are absorbed in the stomach and small intestine. Following this, they are digested further by intestinal mucosa and gut microbiota by hydrolysis by esterase. When bacteria metabolize polyphenols or carbohydrates,

they produce organic acids (39, 40). It is related to Clostridium, Escherichia coli, and Lactobacillus that organic acids are produced. The formation of lactic acid regulates intestinal peristalsis and inhibits the reproduction of harmful bacteria. The biological world produces alkaloids, which are nitrogen-containing organic compounds. It is one of the most vital components of Chinese medicine because of its physiological properties. There are some alkaloids that are hydrophilic and soluble in organic solvents as well. As a result of gut microbiota action, alkaloids often consist of small molecules, ether bonds, coordination bonds, etc., which are susceptible to hydrolysis and dehydration (41–44). With all of this in mind, we could speculate that ZGJTSXF might alleviate DCM by regulating the intestinal microbiota. For this aim, we designed this study.

In high-fat and STZ-induced diabetic mice, we found ZGJTSXF administration could improve fasting blood sugar, blood lipid, fasting blood insulin and insulin resistance. Further research on echocardiography and histological analysis, we discovered that the ZGJTSXF groups can improve left ventricular systolic and diastolic functions in DCM mice. We discovered that the ZGJTSXF groups can reduce hypertrophy, vacuolar degeneration of cardiomyocytes, myocardial interstitial infiltration of inflammatory cells, capillary basement membrane thickened, and myocardial fibrosis caused by diabetic cardiomyopathy, thus improving cardiac function. Additionally, the effects of ZGJTSXF on cardiomyocyte apoptosis in DCM mice were also investigated. The results showed the ZGJTSXF groups demonstrated significantly reduced cardiomyocyte apoptosis. Although ZGJTSXF exerts many health benefits. However, it is still unclear whether gut microbiota plays a role in the occurrence of DCM.

Having a healthy gut microbiota plays an important role in maintaining normal heart function and development (8, 45–47). There has been a great deal of interest in recent years regarding the presence of gut microbiota and specific gut microbiota-dependent pathways as well as downstream metabolites in cardiovascular disease and metabolic disorders (8, 45). In the present study, we used 16S gene rRNA sequencing to identify changes in gut microbial diversity and composition following ZGJTSXF treatment. A recent study found that metabolic diseases are associated with decreased gut microbial diversity (48). Our result is consistent with recent studies, we also observed significant decreases in Sobs, Chao1, ACE, and Shannon indexes in DCM model mice. It was, however, reversed by ZGJTSXF. Based on UPGMA and PCoA, there was a clear cluster separation between ZGJTSXF mice and DCM mice. The ZGJTSXF group had a smaller distance from the CON group, indicating that the ZGJTSXF treatment significantly normalized the biological community structure.

The results of LEfSe analysis and environmental factor correlation analysis showed that Lactobacillus, Alloprevotella, Alistipes, Rikenellaceae_RC9_gut_group, Lachnospiraceae_UCG-006, Parabacteroides, Eubacterium_ventriosum_group, Odoribacter, Ruminococcaceae_UCG-013, Clostridium_sensu_stricto_1 played important roles in DCM. Lactobacillus genus represents a common probiotic, but this protective effect may depend on the presence of other intestinal bacteria and work together in a complementary manner (49). Most other studies have reported that Lactobacillus was found in higher abundance in control groups than in diabetic groups (50, 51). But here, the abundance of Lactobacillus being significantly higher in the DCM group than in the CON group. Other studies have produced similar results on the abundance of Lactobacillus in diabetic patients (52, 53). Research has shown that increased Lactobacilli levels were positively correlated with fasting glucose, glycosylated hemoglobin, and a long-term measure of blood glucose control (54). Thus, increased Lactobacillus in the intestines could be a consequence of increased glucose levels in diabetic patients. On the other hand, lactobacilli also have the potential to cause infections, but this is considered rare. Lactobacilli-induced infections are more common in immunocompromised and diabetic patients, but sometimes also in subjects without underlying diseases or risk factors (55). Here, we also found that Alloprevotella genus was significantly increased in DCM group. In addition, we found that Alloprevotella were positively correlated with levels of LVESv, TG, LVIDs, TC, LDL-C, blood glucose, LVIDd, LVEDv, fiber area, AUC of OGTT, HOMA-IR, cardiomyocyte apoptosis rate, blood glucose, Sirius red area but negatively correlated with FINS, HDL-C, EF%, FS%, indicating that Alloprevotella genus may contribute to DCM. The specific function of the Rikenellaceae_RC9_gut_group is currently unknown, but the Rikenellaceae_RC9_gut_group is closely related to members of the genus Alistipes, and Alistipes can produce TMAO (56). It was reported that Lachnospiraceae_UCG-006 were potentially related to obesity and inflammation. Increase the the abundance of Lachnospiraceae_UCG-006 was reported to improve insulin resistance and reduce inflammation (57). Parabacteroides is also known to be associated with diet-induced obesity. Lecomte et a. reported that Parabacteroides is one of the major succinate producers in the gut, and is also associated with obesity (58). Eubacterium_ventriosum_group belongs to Lachnospiraceae. Dang et al. showed that decrease of Eubacterium_ventriosum_group was associated with enhanced systemic inflammation (59). In a previous study, Odoribacter was reported to be highly abundant in hypercholesterolemic subjects and the isobutyric acid proportion was positively associated with Odoribacter abundance (60). In addition, Odoribacter was also reported to exhibit higher abundance in diabetic mice and cause some health problems such as abdominal inflammation (61). Clostridium_sensu_stricto_1, a genus belonging to butyrate-producing Clostridia bacteria, the proliferation of Clostridium species in the colon may produce toxins and lead to intestinal epithelial damage (62).

Furthermore, the correlation analysis between the differential intestinal microbiota and serum TMAO level showed that serum TMAO level were positively associated with Lactobacillus, Alloprevotella, Alistipes, Parabacteroides, Odoribacter and Clostridium_sensu_stricto_1 but negatively with Lachnospiraceae_UCG-006, Eubacterium_ventriosum_group, Ruminococcaceae_UCG-013. Interestingly, we found that ZGJTSXF treatment reduced the abundance of gut bacteria positively correlated with TMAO and increased the abundance of gut bacteria negatively correlated with TMAO. TMAO is an oxidation product of trimethylamine (TMA), which is produced by gut microbiota from dietary choline and phosphatidylcholine. After absorption in the gut, TMA reaches the liver where it is converted to TMAO by hepatic flavin-containing monooxygenases(FMO3) (63, 64). In recent years, TMAO have been extensively studied due to their potential cardiovascular risks (10–12). According to the current evidence, ZGJTSXF is believed to reduce DCM by regulating the intestinal microbiota. But it is still elusive whether ZGJTSXF improve DCM Mice by alleviation gut - heart axis.

There have been several studies demonstrating the link between high circulating TMAO levels and a number of diseases, including metabolic syndrome (65, 66), insulin resistance (66), obesity (67), and nonalcoholic fatty liver disease (68). Interestingly, when we analyzed the gut

microbiota, we found an altered increased abundance in the TMAO-producing gut microbiota. Therefore, we hypothesized that the gut microbiota communicates with the host through the small molecule metabolite-TMAO. Thus, we next examined the metabolites of the gut microbiota, TMAO, and how TMAO communicates with the heart, providing important evidence to support the gut-heart axis. We found that the TMAO concentration in the model group was higher than that in the control group; while the TMAO concentration in the ZGJTSXF group were significantly downregulated. PERK is an endoplasmic reticulum (ER) stress sensor. When TMAO is absorbed at physiologically relevant concentrations, it activates the transcription factor PERK, which in turn induces FoxO1 (14). Studies have shown that excessive activation of cardiac FoxO1 causes DCM and heart failure *via* insulin receptor substrate downregulation (69). Cardiomyocyte apoptosis is a crucial factor leading to myocardial dysfunction (70). The activation of FoxO1 has recently been demonstrated to modulate the expression of genes involved in apoptosis, including Bim, PUMA, TNFSF10. Previous data have suggested that Bim, PUMA, TNFSF10 is a downstream target of FoxO1 transcription factors. Recently, Bim, PUMA, TNFSF10 has been shown to be mediated by FoxO1-induced apoptosis (71–73). Our results are consistent with the above findings. In the DCM state, gut microbiota dysbiosis leads to the increase of TMAO levels in the circulating. TMAO binds and induces phosphorylation of PERK in the cardiomyocytes and then PERK induced FoxO1, which promoted cardiac fibrosis, dysfunction and cardiomyocyte apoptosis. In this research, the high expression levels of PERK, FoxO1 in DCM mice were reversed after ZGJTSXF treatment. The results showed that the preventative effect of ZGJTSXF alleviated DCM were due to blunte the expression of key genes and proteins in the TMAO/PERK/FoxO1 signaling pathway which is associated with its modulation on gut microbiota imbalance.

## Conclusion

In conclusion, the present study showed that ZGJTSXF could ameliorate DCM. The therapeutic effect of ZGJTSXF on DCM mice might be mediated by changes in the gut microbiotaand its metabolite levels. The findings suggested that ZGJTSXF was a promising complementary option for DCM. The efficacy and safety of ZGJTSXF are worth investigating in the clinic in the future.

## Data availability statement

The data presented in the study are deposited in the SRA database, accession number PRJNA924008.

## Ethics statement

The animal study was reviewed and approved by EthicsCommittee of Hunan University of Traditional Chinese Medicine (Hunan, China).

## Author contributions

Y-LH, QX, and RY designed the experiment. Y-LH, and QX performed the experiment. Y-LH and YW analyzed the data and wrote the manuscript. Y-LH, QX, J-JZ, YW and RY revised the manuscript. All authors contributed to the article and approved the submitted version.

## Funding

This work was supported by grants from the National Natural Science Foundation of China (82074400, U21A20411, 82004185), Hunan Provincial Technology Key Research and Development Program (2020SK2101), Postgraduate Research and Innovation Project of Hunan Province (CX20210692), Hunan Provincial Key Laboratory of Translational Medicine for TCM Recipe and Syndrome Research (2018TP1021).

## Conflict of interest

The authors declare that the research was conducted in the absence of any commercial or financial relationships that could be construed as a potential conflict of interest.

## Publisher's note



## Supplementary material

The Supplementary Material for this article can be found online at: https://www.frontiersin.org/articles/10.3389/fendo.2023.1106812/full#supplementary-material

## References

1. Aliyari R, Hajizadeh E, Aminorroaya A, Sharifi F, Kazemi I, Baghestani AR. Multistate models to predict development of late complications of type 2 diabetes in an open cohort study. *Diabetes Metab Syndr Obes* (2020) 13:1863–72. doi: 10.2147/DMSO.S234563

2. Jia G, Whaley-Connell A, Sowers JR. Diabetic cardiomyopathy: a hyperglycaemia- and insulin-resistance-induced heart disease. *Diabetologia* (2018) 61:21–8. doi: 10.1007/s00125-017-4390-4

3. Jia G, Hill MA, Sowers JR. Diabetic cardiomyopathy: An update of mechanisms contributing to this clinical entity. *Circ Res* (2018) 122:624–38. doi: 10.1161/CIRCRESAHA.117.311586

4. Tan Y, Zhang Z, Zheng C, Wintergerst KA, Keller BB, Cai L. Mechanisms of diabetic cardiomyopathy and potential therapeutic strategies: preclinical and clinical evidence. *Nat Rev Cardiol* (2020) 17:585–607. doi: 10.1038/s41569-020-0339-2

5. Liu C, Lu XZ, Shen MZ, Xing CY, Ma J, Duan YY, et al. N-acetyl cysteine improves the diabetic cardiac function: possible role of fibrosis inhibition. *BMC Cardiovasc Disord* (2015) 15:84. doi: 10.1186/s12872-015-0076-3

6. Palmu J, Salosensaari A, Havulinna AS, Cheng S, Inouye M, Jain M, et al. Association between the gut microbiota and blood pressure in a population cohort of 6953 individuals. *J Am Heart Assoc* (2020) 9:e016641. doi: 10.1161/JAHA.120.016641

7. Wang YB, de Lartigue G, Page AJ. Dissecting the role of subtypes of gastrointestinal vagal afferents. *Front Physiol* (2020) 11:643. doi: 10.3389/fphys.2020.00643

8. Witkowski M, Weeks TL, Hazen SL. Gut microbiota and cardiovascular disease. *Circ Res* (2020) 127:553–70. doi: 10.1161/CIRCRESAHA.120.316242

9. Suganya K, Son T, Kim KW, Koo BS. Impact of gut microbiota: How it could play roles beyond the digestive system on development of cardiovascular and renal diseases. *Microb Pathog* (2021) 152:104583. doi: 10.1016/j.micpath.2020.104583

10. Liu X, Xie Z, Sun M, Wang X, Li J, Cui J, et al. Plasma trimethylamine n-oxide is associated with vulnerable plaque characteristics in CAD patients as assessed by optical coherence tomography. *Int J Cardiol* (2018) 265:18–23. doi: 10.1016/j.ijcard.2018.04.126

11. Roncal C, Martínez-Aguilar E, Orbe J, Ravassa S, Fernandez-Montero A, Saenz-Pipaon G, et al. Trimethylamine-N-Oxide (TMAO) predicts cardiovascular mortality in peripheral artery disease. *Sci Rep* (2019) 9:15580. doi: 10.1038/s41598-019-52082-z

12. Senthong V, Wang Z, Fan Y, Wu Y, Hazen SL, Tang WH. Trimethylamine n-oxide and mortality risk in patients with peripheral artery disease. *J Am Heart Assoc* (2016) 5 (10):e004237. doi: 10.1161/JAHA.116.004237

13. DiNicolantonio JJ, McCarty M, OKeefe J. Association of moderately elevated trimethylamine n-oxide with cardiovascular risk: is TMAO serving as a marker for hepatic insulin resistance. *Open Heart.* (2019) 6:e000890. doi: 10.1136/openhrt-2018-000890

14. Chen S, Henderson A, Petriello MC, Romano KA, Gearing M, Miao J, et al. Trimethylamine n-oxide binds and activates PERK to promote metabolic dysfunction. *Cell Metab* (2019) 30:1141–51.e5. doi: 10.1016/j.cmet.2019.08.021

15. Miao J, Ling AV, Manthena PV, Gearing ME, Graham MJ, Crooke RM, et al. Flavin-containing monooxygenase 3 as a potential player in diabetes-associated atherosclerosis. *Nat Commun* (2015) 6:6498. doi: 10.1038/ncomms7498

16. Yue SJ, Wang WX, Yu JG, Chen YY, Shi XQ, Yan D, et al. Gut microbiota modulation with traditional Chinese medicine: A system biology-driven approach. *Pharmacol Res* (2019) 148:104453. doi: 10.1016/j.phrs.2019.104453

17. Feng W, Ao H, Peng C, Yan D. Gut microbiota, a new frontier to understand traditional Chinese medicines. *Pharmacol Res* (2019) 142:176–91. doi: 10.1016/j.phrs.2019.02.024

18. Fernández AM, Kim JK, Yakar S, Dupont J, Hernandez-Sanchez C, Castle AL, et al. Functional inactivation of the IGF-I and insulin receptors in skeletal muscle causes type 2 diabetes. *Genes Dev* (2001) 15:1926–34. doi: 10.1101/gad.908001

19. Wallace TM, Levy JC, Matthews DR. Use and abuse of HOMA modeling. *Diabetes Care* (2004) 27:1487–95. doi: 10.2337/diacare.27.6.1487

20. Hanley AJ, Williams K, Gonzalez C, D'Agostino RBJr, Wagenknecht LE, Stern MP, et al. Prediction of type 2 diabetes using simple measures of insulin resistance: combined results from the San Antonio heart study, the Mexico city diabetes study, and the insulin resistance atherosclerosis study. *Diabetes* (2003) 52:463–9. doi: 10.2337/diabetes.52.2.463

21. Huynh K, McMullen JR, Julius TL, Tan JW, Love JE, Cemerlang N, et al. Cardiac-specific IGF-1 receptor transgenic expression protects against cardiac fibrosis and diastolic dysfunction in a mouse model of diabetic cardiomyopathy. *Diabetes* (2010) 59:1512–20. doi: 10.2337/db09-1456

22. Zhang J, Sun Y, Wang R, Zhang J. Gut microbiota-mediated drug-drug interaction between amoxicillin and aspirin. *Sci Rep* (2019) 9:16194. doi: 10.1038/s41598-019-52632-5

23. Magne F, Gotteland M, Gauthier L, Zazueta A, Pesoa S, Navarrete P, et al. The Firmicutes/Bacteroidetes ratio: A relevant marker of gut dysbiosis in obese patients. *Nutrients* (2020) 12(5):1474. doi: 10.3390/nu12051474

24. Hamasaki N, Ishii E, Tominaga K, Tezuka Y, Nagaoka T, Kadota S, et al. Highly selective antibacterial activity of novel alkyl quinolone alkaloids from a Chinese herbal medicine, gosyuyu (Wu-Chu-Yu), against helicobacter pylori. *vitro. Microbiol Immunol* (2000) 44:9–15. doi: 10.1111/j.1348-0421.2000.tb01240.x

25. Zuo F, Zhou ZM, Yan MZ, Liu ML, Xiong YL, Zhang Q, et al. Metabolism of constituents in huangqin-tang, a prescription in traditional Chinese medicine, by human intestinal flora. *Biol Pharm Bull* (2002) 25:558–63. doi: 10.1248/bpb.25.558

26. Lee NK, Choi SH, Park SH, Park EK, Kim DH. Antiallergic activity of hesperidin is activated by intestinal microflora. *Pharmacology* (2004) 71:174–80. doi: 10.1159/000078083

27. Yang XW, Zhang JY, Xu W, Li J, Zhang WQ. The biotransformation of kaempferitrin by human intestinal flora. *Yao Xue Xue Bao* (2005) 40:717–21. doi: 10.16438/j.0513-4870.2005.08.009

28. Taiming L, Xuehua J, Meijuan Z, Sijian L, Zhuo C. Absorption characteristics of baicalin and baicalein in rat small intestine. *Chin Pharm J* (2006), 1784–7.

29. Knaup B, Kahle K, Erk T, Valotis A, Scheppach W, Schreier P, et al. Human intestinal hydrolysis of phenol glycosides - a study with quercetin and p-nitrophenol glycosides using ileostomy fluid. *Mol Nutr Food Res* (2007) 51:1423–9. doi: 10.1002/mnfr.200700036

30. Shi R, Zhou H, Liu Z, Ma Y, Wang T, Liu Y, et al. Influence of coptis chinensis on pharmacokinetics of flavonoids after oral administration of radix scutellariae in rats. *Biopharm Drug Dispos* (2009) 30:398–410. doi: 10.1002/bdd.674

31. Trinh HT, Joh EH, Kwak HY, Baek NI, Kim DH. Anti-pruritic effect of baicalin and its metabolites, baicalein and oroxylin a, in mice. *Acta Pharmacol Sin* (2010) 31:718–24. doi: 10.1038/aps.2010.42

32. Zhou J, Chen Y, Wang Y, Gao X, Qu D, Liu C. A comparative study on the metabolism of epimedium koreanum nakai-prenylated flavonoids in rats by an intestinal enzyme (lactase phlorizin hydrolase) and intestinal flora. *Molecules* (2013) 19:177–203. doi: 10.3390/molecules19010177

33. Zhou J, Ma YH, Zhou Z, Chen Y, Wang Y, Gao X. Intestinal absorption and metabolism of epimedium flavonoids in osteoporosis rats. *Drug Metab Dispos* (2015) 43:1590–600. doi: 10.1124/dmd.115.064386

34. Xin L, Liu XH, Yang J, Shen HY, Ji G, Shi XF, et al. The intestinal absorption properties of flavonoids in hippophaë rhamnoides extracts by an *in situ* single-pass intestinal perfusion model. *J Asian Nat Prod Res* (2019) 21:62–75. doi: 10.1080/10286020.2017.1396976

35. Jin X, Lu Y, Chen S, Chen D. UPLC-MS identification and anticomplement activity of the metabolites of sophora tonkinensis flavonoids treated with human intestinal bacteria. *J Pharm BioMed Anal* (2020) 184:113176. doi: 10.1016/j.jpba.2020.113176

36. Wang Y, Chen B, Cao J, Huang Y, Wang G, Peng K, et al. Effects of mulberry leaf flavonoids on intestinal mucosal morphology and gut microbiota of litopenaeus vannamei. *Chin J Anim. Nutr* (2020) 32:1817–25. doi: 10.3969/j.issn.1006-267x.2020.04.040

37. Jan KC, Hwang LS, Ho CT. Biotransformation of sesaminol triglucoside to mammalian lignans by intestinal microbiota. *J Agric Food Chem* (2009) 57:6101–6. doi: 10.1021/jf901215j

38. Zhao Y, Song F, Zhao L, Liu S. Studies on the biotransformation of arctigenin using electrospray ionization mass spectrometry. *Acta Chim Sinica.* (2009) 67:1123–6.

39. Weikao C, Wenzheng J, Hengshan T. The *In vivo* process of chlorogenic acid and drug interaction. *Pharmacol Clin Chin Materia Med* (2008), 118–20.

40. Kim BG, Jung WD, Mok H, Ahn JH. Production of hydroxycinnamoyl-shikimates and chlorogenic acid in escherichia coli: production of hydroxycinnamic acid conjugates. *Microb Cell Fact.* (2013) 12:15. doi: 10.1186/1475-2859-12-15

41. Sun Y, Zhang HG, Shi XG, Duan MY, Zhong DF. Study on metabolites on aconitine in rabbit urine. *Yao Xue Xue Bao* (2002) 37:781–3. doi: 10.16438/j.0513-4870.2002.10.007

42. Weiming C. *Study on the chemical constituents of sinomenium chinensis and the metabolism of sinomenine in rats* (2005). Shenyang, China: Shenyang Pharmaceutical University.

43. Huaixia C, Peng D, Fengmei H, Yong C. Study on the metabolism of scopolamine in rat gut microbiota. *J Hubei Univ* (2006), 414–6.

44. Yufeng Z, Fengrui S, Xinhua G, Shuying L. Studies on the biotransformation of aconitine in human intestinal bacteria using soft-ionization mass spectrometry. *Chem J Chin Univ* (2008), 55–9.

45. Tang WH, Kitai T, Hazen SL. Gut microbiota in cardiovascular health and disease. *Circ Res* (2017) 120:1183–96. doi: 10.1161/CIRCRESAHA.117.309715

46. Wang Z, Zhao Y. Gut microbiota derived metabolites in cardiovascular health and disease. *Protein Cell* (2018) 9:416–31. doi: 10.1007/s13238-018-0549-0

47. Xu H, Wang X, Feng W, Liu Q, Zhou S, Liu Q, et al. The gut microbiota and its interactions with cardiovascular disease. *Microb Biotechnol* (2020) 13:637–56. doi: 10.1111/1751-7915.13524

48. Le Chatelier E, Nielsen T, Qin J, Prifti E, Hildebrand F, Falony G, et al. Richness of human gut microbiome correlates with metabolic markers. *Nature* (2013) 500:541–6. doi: 10.1038/nature12506

49. Rivière A, Gagnon M, Weckx S, Roy D, De Vuyst L. Mutual cross-feeding interactions between bifidobacterium longum subsp. longum NCC2705 and eubacterium rectale ATCC 33656 explain the bifidogenic and butyrogenic effects of arabinoxylan oligosaccharides. *Appl Environ Microbiol* (2015) 81:7767–81. doi: 10.1128/AEM.02089-15

50. Halawa MR, El-Salam MA, Mostafa BM, Sallout SS. The gut microbiome, lactobacillus acidophilus; relation with type 2 diabetes mellitus. *Curr Diabetes Rev* (2019) 15:480–5. doi: 10.2174/1573399815666190206162143

51. Aydin S, Ozkul C, Yucel NT, Karaca H. Gut microbiome alteration after reboxetine administration in type-1 diabetic rats. *Microorganisms* (2021) 9(9):1948. doi: 10.3390/microorganisms9091948

52. Leiva-Gea I, Sánchez-Alcoholado L, Martín-Tejedor B, Castellano-Castillo D, Moreno-Indias I, Urda-Cardona A, et al. Gut microbiota differs in composition and functionality between children with type 1 diabetes and MODY2 and healthy control subjects: A case-control study. *Diabetes Care* (2018) 41:2385–95. doi: 10.2337/dc18-0253

53. Alkanani AK, Hara N, Gottlieb PA, Ir D, Robertson CE, Wagner BD, et al. Alterations in intestinal microbiota correlate with susceptibility to type 1 diabetes. *Diabetes* (2015) 64:3510–20. doi: 10.2337/db14-1847

54. Karlsson FH, Tremaroli V, Nookaew I, Bergström G, Behre CJ, Fagerberg B, et al. Gut metagenome in European women with normal, impaired and diabetic glucose control. *Nature* (2013) 498:99–103. doi: 10.1038/nature12198

55. Rossi F, Amadoro C, Colavita G. Members of the lactobacillus genus complex (LGC) as opportunistic pathogens: A review. *Microorganisms* (2019) 7(5):126. doi: 10.3390/microorganisms7050126

56. Yang T, Qu H, Song X, Liu Q, Yang X, Xu J, et al. Luhong granules prevent ventricular remodelling after myocardial infarction by reducing the metabolites TMAO and LPS of the intestinal flora. *Evid Based Complement Alternat Med* (2019) 2019:8937427. doi: 10.1155/2019/8937427

57. Yang S, Cao S, Li C, Zhang J, Liu C, Qiu F, et al. Berberrubine, a main metabolite of berberine, alleviates non-alcoholic fatty liver disease *via* modulating glucose and lipid metabolism and restoring gut microbiota. *Front Pharmacol* (2022) 13:913378. doi: 10.3389/fphar.2022.913378

58. Lecomte V, Kaakoush NO, Maloney CA, Raipuria M, Huinao KD, Mitchell HM, et al. Changes in gut microbiota in rats fed a high fat diet correlate with obesity-associated metabolic parameters. *PloS One* (2015) 10:e0126931. doi: 10.1371/journal.pone.0126931

59. Dang JT, Mocanu V, Park H, Laffin M, Hotte N, Karmali S, et al. Roux-en-Y gastric bypass and sleeve gastrectomy induce substantial and persistent changes in microbial communities and metabolic pathways. *Gut Microbes* (2022) 14:2050636. doi: 10.1080/19490976.2022.2050636

60. Granado-Serrano AB, Martín-Garí M, Sánchez V, Riart Solans M, Berdún R, Ludwig IA, et al. Faecal bacterial and short-chain fatty acids signature in hypercholesterolemia. *Sci Rep* (2019) 9:1772. doi: 10.1038/s41598-019-38874-3

61. Geurts L, Lazarevic V, Derrien M, Everard A, Van Roye M, Knauf C, et al. Altered gut microbiota and endocannabinoid system tone in obese and diabetic leptin-resistant mice: impact on apelin regulation in adipose tissue. *Front Microbiol* (2011) 2:149. doi: 10.3389/fmicb.2011.00149

62. Schönherr-Hellec S, Aires J. Clostridia and necrotizing enterocolitis in preterm neonates. *Anaerobe* (2019) 58:6–12. doi: 10.1016/j.anaerobe.2019.04.005

63. Wang Z, Klipfell E, Bennett BJ, Koeth R, Levison BS, Dugar B, et al. Gut flora metabolism of phosphatidylcholine promotes cardiovascular disease. *Nature* (2011) 472:57–63. doi: 10.1038/nature09922

64. Koeth RA, Wang Z, Levison BS, Buffa JA, Org E, Sheehy BT, et al. Intestinal microbiota metabolism of l-carnitine, a nutrient in red meat, promotes atherosclerosis. *Nat Med* (2013) 19:576–85. doi: 10.1038/nm.3145

65. Papandreou C, Moré M, Bellamine A. Trimethylamine n-oxide in relation to cardiometabolic health-cause or effect. *Nutrients* (2020) 12(5):1330. doi: 10.3390/nu12051330

66. Roy S, Yuzefpolskaya M, Nandakumar R, Colombo PC, Demmer RT. Plasma trimethylamine-n-oxide and impaired glucose regulation: Results from the oral infections, glucose intolerance and insulin resistance study (ORIGINS). *PloS One* (2020) 15:e0227482. doi: 10.1371/journal.pone.0227482

67. Dehghan P, Farhangi MA, Nikniaz L, Nikniaz Z, Asghari-Jafarabadi M. Gut microbiota-derived metabolite trimethylamine n-oxide (TMAO) potentially increases the risk of obesity in adults: An exploratory systematic review and dose-response meta-analysis. *Obes Rev* (2020) 21:e12993. doi: 10.1111/obr.12993

68. León-Mimila P, Villamil-Ramírez H, Li XS, Shih DM, Hui ST, Ocampo-Medina E, et al. Trimethylamine n-oxide levels are associated with NASH in obese subjects with type 2 diabetes. *Diabetes Metab* (2021) 47:101183. doi: 10.1016/j.diabet.2020.07.010

69. Battiprolu PK, Hojayev B, Jiang N, Wang ZV, Luo X, Iglewski M, et al. Metabolic stress-induced activation of FoxO1 triggers diabetic cardiomyopathy in mice. *J Clin Invest.* (2012) 122:1109–18. doi: 10.1172/JCI60329

70. Liu L, Yan M, Yang R, Qin X, Chen L, Li L, et al. Adiponectin attenuates lipopolysaccharide-induced apoptosis by regulating the Cx43/PI3K/AKT pathway. *Front Pharmacol* (2021) 12:644225. doi: 10.3389/fphar.2021.644225

71. Zhang X, Tang N, Hadden TJ, Rishi AK. Akt, FoxO and regulation of apoptosis. *Biochim Biophys Acta* (2011) 1813:1978–86. doi: 10.1016/j.bbamcr.2011.03.010

72. Lee JH, Mellado-Gil JM, Bahn YJ, Pathy SM, Zhang YE, Rane SG. Protection from β-cell apoptosis by inhibition of TGF-β/Smad3 signaling. *Cell Death Dis* (2020) 11:184. doi: 10.1038/s41419-020-2365-8

73. Benz F, Roy S, Trautwein C, Roderburg C, Luedde T. Circulating MicroRNAs as biomarkers for sepsis. *Int J Mol Sci* (2016) 17(1):78. doi: 10.3390/ijms17010078

frontiers | Frontiers in Endocrinology

TYPE Original Research
PUBLISHED 28 February 2023
DOI 10.3389/fendo.2023.1158318



OPEN ACCESS

EDITED BY
Zhoujin Tan,
Hunan University of Chinese Medicine, China

REVIEWED BY
Xue Wang,
Heilongjiang University of Chinese Medicine, China
Cheng Yuan,
Qiqihar Medical University, China
Su Min,
Changsha Medical University, China

*CORRESPONDENCE
Hong Zhao
zhaohong1981@jmsu.edu.cn

†These authors have contributed equally to this work and share the first authorship

SPECIALTY SECTION
This article was submitted to Gut Endocrinology, a section of the journal Frontiers in Endocrinology

RECEIVED 03 February 2023
ACCEPTED 15 February 2023
PUBLISHED 28 February 2023

CITATION
Ping Y, Gao Q, Li C, Wang Y, Wang Y, Li S, Qiu M, Zhang L, Tu A, Tian Y and Zhao H (2023) Construction of microneedle of *Atractylodes macrocephala Rhizoma* aqueous extract and effect on mammary gland hyperplasia based on intestinal flora. *Front. Endocrinol.* 14:1158318. doi: 10.3389/fendo.2023.1158318



# Construction of microneedle of *Atractylodes macrocephala Rhizoma* aqueous extract and effect on mammary gland hyperplasia based on intestinal flora

Yang Ping†, Qi Gao†, Changxu Li, Yan Wang, Yuliang Wang, Shuo Li, Mingjing Qiu, Linqian Zhang, Ailing Tu, Yu Tian and Hong Zhao*

College of Pharmacy, Jiamusi University, Jiamusi, Heilongjiang, China

**Background:** A microneedle patch loaded with *Atractylodes macrocephala Rhizoma* water extract was prepared for the treatment of mammary gland hyperplasia. To explore the relationship between Mammary gland hyperplasia and intestinal flora.

**Materials and methods:** Preparation of the microneedle patch by micromolding method, the prescription of the microneedle was optimized by the Box-Behnken Design response surface test, and the micro-morphology, penetration, toughness, and brittleness were investigated. *In vitro* release of drug-loaded microneedles was measured by diffusion cell method. The rat model of mammary gland hyperplasia was prepared by the combination of estradiol benzoate-progesterone, and the microneedle patch of *Atractylodes macrocephala Rhizoma* aqueous extract was used for intervention treatment. The change of levels in $E_2$, P, and PRL in rat serum was determined. The intestinal contents of rats were collected and the changes in intestinal flora in MGH rats were analyzed by 16s rRNA high-throughput sequencing.

**Results:** The optimized microneedle formula is a PVA concentration of 6.0%, HA concentration of 15.5%, and PVPK30 concentration of 16.0%. The prepared microneedle tip loaded with *Atractylodes macrocephala Rhizoma* aqueous extract has complete, sharp, and no bubbles and the needle rate of the microneedle array is in the range of 95%~100%. The bending rate of the microneedle is about 12.7%, and it has good flexibility, and the microneedle can puncture 4 layers of Parafilm® membrane smoothly, and the puncture rate is more than 96%. The *in vitro* release of the microneedle was characterized by rapid release. The results of animal experiments showed that *Atractylodes macrocephala Rhizoma* aqueous extract microneedle patch could significantly reduce the $E_2$ level, significantly reduce the PRL level, and significantly increase the P level. At the same time, it can regulate the abundance and diversity of

intestinal flora in MGH rats, improve the intestinal flora disorder caused by mammary gland hyperplasia, and balance the community structure.

**Conclusion:** The prepared microneedle containing *Atractylodes macrocephala Rhizoma* aqueous extract has good toughness and brittle strength, can penetrate the skin and enter the dermis, and effectively deliver drugs to play a role in the treatment of mammary gland hyperplasia.

KEYWORDS

aqueous extract, microneedle, mammary gland hyperplasia, intestinal flora, *Atractylodes macrocephala Rhizoma*

# 1 Introduction

Mammary gland hyperplasia (MGH) is a non-inflammatory and non-tumor chronic proliferative disease, mainly characterized by breast lumps and breast pain. At present, hormone inhibition and local resection are commonly used in western medicine. Hormone inhibition can only relieve symptoms and has a large side effect. Local resection is not easy for patients to accept. In recent years, traditional Chinese medicine (TCM) has had the advantages of good compliance and fewer adverse reactions in treating MGH, which can effectively improve the symptoms of patients. The patients were satisfied with the external treatment of TCM. External treatment of percutaneous drug delivery can avoid the "first-pass effect" of the liver and damage to the gastrointestinal tract so that the drug can enter the blood circulation through the skin and play a systemic role. At the same time, it can effectively improve bioavailability, maintain stable and lasting blood drug concentrations, and have other advantages.

Microneedle is a kind of transdermal drug delivery. The extremely delicate micro needle cluster made by micro-manufacturing technology can penetrate the cuticle of the skin, forming temporary aqueous micropores on the skin surface, so that the drug can diffuse into the skin through the micropores, thus exerting the efficacy to achieve microcirculation. Soluble microneedles, also known as dissolving microneedles (DMN) (1, 2), are polymer microneedles that encapsulate drugs in biodegradable polymer materials. When DMN is inserted into the skin, the polymer degrades spontaneously to release drugs. The drug release rate is mainly related to the properties of drugs and dosage forms. Therefore, DMN can achieve local or systemic therapeutic effects in the short or long term. At the same time, the tiny pores left by DMN on the skin surface can heal themselves in a short time, reducing the risk of infection caused by the fracture of the solid tip in the skin, and realizing a safe and painless drug delivery method in a real sense.

Modern medical investigation shows that MGH is caused by endocrine disorders. The mammary gland is a target organ of sexual hormones, it regulates hyperplasia of breast tissue and the cycle through by regulating serum hormones, and hypothalamic-pituitary-gonads (3). As early as 1883, it was proposed that the MGH may be associated with sexual hormones. It was first proposed in 1947 that the disorder of estrogen and progestogen was the cause of the MGH (4). However, the endocrine imbalance can affect the intestinal flora composition and directly or indirectly change bacterial physiology and independent gene expression (5). Estrogen imbalance, as an important sign of endocrine disorder, has also been proven to significantly affect the changes in intestinal microbiota (6). A large number of studies have proved that TCM can regulate the imbalance of intestinal microbiota significantly, Cuiru Li et al. showed that QWBZP crude polysaccharide helped to restore the diversity, relative abundance, and community structure of intestinal mucosal bacteria to a certain extent (7). Xiaoya Li et al. explored the role of intestinal contents microbiota in the regulation of adverse effects caused by high-fat diet by DO from the perspective of intestinal microecology. And demonstrated that the mechanism of DO against a high-fat diet diseases might be attributed to the inhibition of Ruminococcus and Oscillospira, leading to a promotion in the state of host health (8, 9). Moreover, intestinal flora coincides with the "spleen and stomach" theory of TCM. TCM can promote the growth of beneficial bacteria, inhibit the excessive production of harmful bacteria, balance the number of beneficial bacteria and pathogenic bacteria, and maintain a healthy intestinal environment (10). The composition and quantity of intestinal flora are in balance under normal conditions. Once the balance is broken by factors such as intestinal pH value, mental pressure, eating habits, and antibiotic use, it will cause metabolic obstacles, metabolic disorders, and even other related diseases to some extent (11–16). The dried rhizome of the plant *Atractylodes macrocephala* Koidz is useful for drying and moistening water, nourishing the stomach, and strengthening the spleen. *Atractylodes macrocephala Rhizoma* has been reported to include amino acids, polysaccharides, and a range of volatile components. It also has been proven to have pharmacological effects, such as controlling intestinal flora and enhancing digestive function (17). In order to provide theoretical support for the treatment of MGH from the perspective of intestinal microecology and provide an experimental basis for the full exploitation of the medicinal value of Atractylodes macrocephala Rhizoma aqueous extract (AM-ae), this study will prepare a microneedle patch for the treatment of MGH rats using AM-ae. It will also analyze the effect of AM-ae on the intestinal microbiota

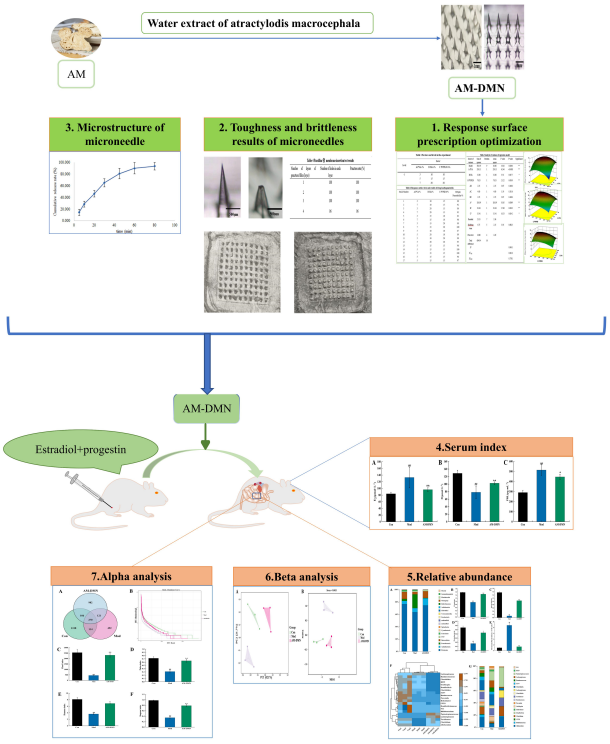


FIGURE 1
Experimental flow graph.

of MGH rats by 16S RNA high-throughput sequencing. Figure 1 depicts the concept for the research.

# 2 Materials and methods

## 2.1 Drugs and materials

Polyvinyl alcohol 224 (purchased from Shanghai McLean Biochemical Technology Co., Ltd., CAS No. 9002-89-5; alcoholysis degree: 87.0-89.0 mol%; viscosity: 40.0-48.0 mPa. s); Hyaluronic acid (purchased from Shanghai McLean Biochemical Technology Co., Ltd., batch number: C12698745; molecular weight: 200000-400000); Polyvinylpyrrolidone K30 (purchased from Shanghai Aladdin Biochemical Technology Co., Ltd., batch number: H2112016; molecular weight: 40000, high purity); Water extract of *Atractylodes macrocephala Rhizoma* (self-made in the laboratory); Absolute ethanol (purchased from Tianjin Kaitong Chemical Reagent Co., Ltd.); Parafilm M ® (Bemis Company, Inc).

Eighteen SPF-grade female non-pregnant SD rats (200 ± 20 g) were purchased from Changchun Lewis Laboratory Animal Technology Co., Ltd (Licence No.: SCXK(Ji)-2018-0007) and housed in SPF-grade animal rooms. The temperature and humidity in the rearing room were controlled, temperature: 24 ± 2°C, humidity: 60 ± 5%. The light and dark cycle was 12/12 h. All experimental procedures involving animals were approved by the Animal Ethics Committee of the Animal Experimentation Centre of Jiamusi University.

Purchases were made from Shanghai Quanyu Biotechnology (Zhumadian) Animal Pharmaceutical Co., Ltd. for estradiol benzoate and progesterone injection. Estradiol ($E_2$), progesterone (P), and prolactin (PRL) kit was purchased from Jiangsu enzyme immunity Industrial Co., Ltd.

## 2.2 Instruments and equipment

FA2004N Electronic Analytical Balance (Shanghai Hengping Scientific Instrument Co., Ltd.); PDMS mold (Micropoint Technologies PTE LTD, Singapore); Xiangyi TDZ5-WS desktop low-speed centrifuge (Hunan Xiangyi Laboratory Instrument Development Co., Ltd.); Air blast dryer (Shanghai Hengping Scientific Instrument Co., Ltd.); Electron Microscope (Shanghai Hengping Scientific Instrument Co., Ltd.).

## 2.3 Preparation method of microneedle

Weigh the appropriate amount of polyvinyl alcohol 224 (PVA), hyaluronic acid (HA), polyvinylpyrrolidone K30 (PVPK30), and add an appropriate amount of double steaming water to dissolve them, and put them in the refrigerator to swell for 30~40 min. The three kinds of drug solutions are proportional to 1:1:1 ~ 1:1: 5 Mix well (solution 1), take the extract of *Atractylodes macrocephala Rhizoma* water with the drug loading capacity of 0.3%~2.5%, dissolve in a certain amount of anhydrous ethanol (solution 2), mix the solutions 1 and 2 evenly, drop them into the PDMS mold, and centrifuge at 2700~3300 r/min for 8~12min. After removal, it was dried for 50~70min in a drying box at 30°, then the backing layer solution was drip-added to the PDMS mold, centrifuged in a centrifuge at 3000r/min for 8~12min, and dried in a drying box at 55~65° for 50~70min. The drug-loaded microneedle array is obtained after demoulding.

## 2.4 Response surface prescription optimization

Based on single factor test, three factors, namely PVA concentration (A), HA concentration (B), and PVPK30 concentration (C), were selected as independent variables with the microneedle penetration rate of 800μm was taken as the response value, and the response surface test is designed according to the principle of Box Behnken Design (BBD). The optimization analysis was carried out according to the test results, and the formulation composition response surface method test design is shown in Table 1.

TABLE 1 Factors and levels in the experiment.

| Levels | Factors | | |
|---|---|---|---|
| | A:PVA c% | B:HA c% | C:PVPK30 c% |
| -1 | 3 | 10 | 10 |
| 0 | 5 | 15 | 15 |
| 1 | 7 | 20 | 20 |

## 2.5 Characterization of AM-DMN

The morphology of microneedle arrays was observed by electron microscope. The toughness of the microneedles was evaluated by the compression performance test: the microneedle tip was placed down on a smooth plane, a plane was added on the back of the microneedle to make it stressed evenly, and then place a certain weight of weight, and gradually increase the weight of the weight. Remove the weight after every 1-2 minutes of action, and the changes in the microneedle tip and height were observed.

The brittleness of the microneedles is characterized by the mechanical strength of the microneedles. The mechanical strength of the prepared microneedles can be evaluated by the Parafilm® membrane insertion experiment. Stack 4 pieces of Parafilm ® film together, with a thickness of about 0.5~1 mm was placed on the foam. The microneedles were inserted into the Parafilm® membrane and pressed for about 30~60 s. After the microneedles were removed, the number of layers of the membrane broken by the microneedles and the number of holes in each membrane was recorded.

The microneedle patch was placed on the dialysis membrane by diffusion cell method, and the receiving cell contained 10 mL PBS. The samples were taken at 37° for 1, 2, 5, 30, 60, and 300 min. The content of the aqueous extract of *Atractylodes macrocephala Rhizoma* in a microneedle patch was determined by the UPLC method, and the drug release performance of the microneedle patch was evaluated.

## 2.6 Experimental approach

A total of 18 female SD rats were chosen, acclimated, and fed for a week. Six rats from each group were randomly assigned to one of three groups: an AM-DMN group, a model control group (Mod), and a blank control group (Con). The rats in each group were injected with estradiol benzoate 0.5 mg-kg$^{-1}$-D$^{-1}$ intramuscularly for 25 days, followed by progesterone 5 mg-kg$^{-1}$-D$^{-1}$ intramuscularly for 5 days, except for the Con group, which received an identical dose of saline. The AM-DMN group received treatment with a medication microneedle patch after successful modeling, whereas the Con and Mod groups received treatment with a blank microneedle patch. These treatments were alternated every two days for a total of 21 days (18).

## 2.7 Collection and analysis of serum samples

Rats in each group fasted for 12 hours after the last dose. The rats were weighed and anesthetized intraperitoneally and injected with 2% sodium pentobarbital. The execution was performed using the cervical dislocation method. To isolate the serum, blood was taken from the abdominal aorta and stored in a procoagulant tube for 20 min. ELISA was used to determine serum $E_2$, P, and PRL levels (18).

## 2.8 Collection of samples of intestinal cecum contents

After the death of the rats, the contents of the cecum were extracted using sterile forceps, placed in 5mL sterile EP tubes, numbered and weighed, then immediately immersed in liquid nitrogen under sterile conditions. After collection, the samples were transferred to -80°C for storage (18).

## 2.9 16S rRNA gene high-throughput sequencing

The cecum's contents were taken. Following the instructions on the DNA extraction kit exactly, the total DNA content was extracted. DNA was measured with a nanodrop spectrophotometer (DNA quantitative analysis), and electrophoresis was used to determine the purity and concentration of the extracted genomic DNA. The 16S rDNA V3–V4 variable region was used for amplification, and the Quantit PicoGreen dsDNA analysis kit was used for fluorescence quantification. Samples were blended in the proper ratios for further fluorescence measurement. The contents of the rat cecum were then double-end sequenced using Illumina's NovaSeq 6000 sequencer (18).

## 2.10 Bioinformatics and statistical analysis

Using the QIME2 DADA2 program, non-repeat sequence OTU clustering was carried out at a 97% similarity. The Greenenes database (version 13.8) was used to annotate the classification of species. To determine species richness and diversity, alpha diversity indices (Chao1, ACE, Simpson, and Shannon indices) were computed. Additionally, the beta diversity of the gut microbiota in various samples was examined, and this can determine the similarities and variations in the community composition of the various samples (or subgroups).

Data were analyzed using SPSS 26.0 statistical software. All data in the experiment are expressed as mean ± standard deviation (X ± s). One-way ANOVA was used for comparison between groups. $p<0.05$ was considered statistically significant. Drawings were expected to be completed using R 4.1.3 and GraphPad Prism 8 software.

# 3 Results

## 3.1 Prescription optimization of microneedles

With the penetration rate of 800μm microneedle as the index, the drug-carrying material test results in Table 2 were analyzed by using Design Expert 8.0.6 software, and the regression equation of the penetration rate of 800μm microneedle was obtained as follows: 800μm=97.80+5.13A+2.00 B+3.13 C-0.75 AB+1.00 AC+0.75 BC-4.90 $A^2$-4.65 $B^2$-2.90 $C^2$.

10.3389/fendo.2023.1158318

TABLE 2 Response surface tests and results of drug-loading materials.

| Serial Number | A:PVA/ % | B:HA/ % | C:PVPK30/ % | Penetrability/ % |
|---|---|---|---|---|
| 1 | 3 | 10 | 15 | 80 |
| 2 | 7 | 10 | 15 | 92 |
| 3 | 3 | 20 | 15 | 86 |
| 4 | 7 | 20 | 15 | 95 |
| 5 | 3 | 15 | 10 | 82 |
| 6 | 7 | 15 | 10 | 90 |
| 7 | 3 | 15 | 20 | 88 |
| 8 | 7 | 15 | 20 | 100 |
| 9 | 5 | 10 | 10 | 87 |
| 10 | 5 | 20 | 10 | 89 |
| 11 | 5 | 10 | 20 | 90 |
| 12 | 5 | 20 | 20 | 95 |
| 13 | 5 | 15 | 15 | 96 |
| 14 | 5 | 15 | 15 | 100 |
| 15 | 5 | 15 | 15 | 100 |
| 16 | 5 | 15 | 15 | 96 |
| 17 | 5 | 15 | 15 | 97 |

The software Design Expert 8.0.6 was used to establish the model, and the multiple quadratic regression response surface model of 800μm microneedle penetration rate was obtained. The multiple linear regression and binomial fitting analysis were conducted on the test results of microneedle prescription materials to verify the significance of the regression model and factors. The results of ANOVA are shown in Table 3.

It can be seen from Table 3 that F=19.20, p=0.0004 in the established regression model, indicating that the difference in the regression model is extremely significant; The p of the misfitting term is 0.6823>0.05, and the model difference is not significant, indicating that the equation is reliable; The regression coefficient $R^2$ = 96.11%>85%, indicating that the equation is well fitted. The regression equation can be used to replace the real point of the test to describe the relationship between each variable and the response value. The correction coefficient $R^2_{Adj}$ = 0.9110 indicates that the model can explain the change in the penetration rate of microneedles of 91.10% 800μm. The data in Table 3 show that the test design is reliable with small errors, which is suitable for the actual situation and can be used to analyze and predict the results of the microneedle preparation test.

It can be seen from the *p*-value in Table 3 that the PVA concentration (A) and PVPK30 concentration (C) in the primary item have a very significant impact on the preparation of microneedles, and the HA concentration (B) has a significant impact; In the quadratic term, $A^2$ and $B^2$ have extremely significant effects on the preparation of microneedles, and $C^2$ has significant effects on the preparation of microneedles. Among the interaction terms, AB, AC, and BC had no

TABLE 3 Analysis of variance of regression model.

| Source of variance | Sum of squares | freedom | mean square | F value | *p* value | Significance |
|---|---|---|---|---|---|---|
| Model | 581.39 | 9 | 64.60 | 19.20 | 0.0004 | ** |
| A-PVA | 210.13 | 1 | 210.13 | 62.46 | <0.0001 | ** |
| B-HA | 32.00 | 1 | 32.00 | 9.51 | 0.0177 | * |
| C-PVPK30 | 78.13 | 1 | 78.13 | 23.22 | 0.0019 | ** |
| AB | 2.25 | 1 | 2.25 | 0.67 | 0.4404 | |
| AC | 4.00 | 1 | 4.00 | 1.19 | 0.3116 | |
| BC | 2.25 | 1 | 2.25 | 0.67 | 0.4404 | |
| $A^2$ | 101.09 | 1 | 101.09 | 30.05 | 0.0009 | ** |
| $B^2$ | 91.04 | 1 | 91.04 | 27.06 | 0.0013 | ** |
| $C^2$ | 35.41 | 1 | 35.41 | 10.53 | 0.0142 | * |
| Residual | 23.55 | 7 | 3.36 | | | |
| Disfitting term | 6.75 | 3 | 2.25 | 0.54 | 0.6823 | |
| Pure error | 16.80 | 4 | 4.20 | | | |
| Total difference | 604.94 | 16 | | | | |
| $R^2$ | | | | | 0.9611 | |
| $R^2_{Adj}$ | | | | | 0.9110 | |
| $R^2_{pred}$ | | | | | 0.7781 | |

p ≤ 0.01 indicates that the factor has a very significant effect on the response value (**), P ≤ 0.05 indicates that the factor has a significant effect on the response value (*).

significant influence on the preparation of microneedles. According to the value of F in Table 3, it can be concluded that the influence of the three factors on the preparation of microneedles is PVA concentration (A)>PVPK30 concentration (C)>HA concentration (B).

As shown in Figure 2 (A1, B1, C1) for the response surface and contour map of interaction effects of microneedle materials PVA, HA, and PVPK30 created by the response surface regression model.

Validation experiment: Solve the regression fitting equation of the microneedle material, and obtain the best preparation conditions: A=6.08, B=15.74, C=16.27. Under this condition, the predicted penetration rate of the microneedle is 100.045%. According to the experimental and practical feasibility, the conditions for preparing microneedles by adjusting the modified drug loading material are as follows: PVA concentration was 6.0%, HA concentration was 15.5%, and PVPK30 concentration was 16.0%. Under these conditions, the penetration rate of microneedles was 97.5%, and the relative error of the predicted value of the model was only 2.54% (< 5%), indicating that the response surface method optimized the conditions for the preparation of microneedles, the preparation scheme parameters obtained were accurate and reliable, and had certain application value.

## 3.2 Characterization of AM-DMN

The morphology of the whole micro-needle array is a pyramid; The needle tip is complete and sharp, without bending, broken needle and bubble; The needle output rate of the microneedle array is in the range of 95%~100%; The micro-needle tip and the backing layer have good compatibility, the tip and the backing layer are not separated, and the backing layer is flat without bubbles. As shown in Figure 3A.

With the weight of 100g, 200g, 300g, 400g, and 500g increasing in turn, the tip of the microneedle will slightly bend. When the weight of the weight is 500g, the height of the microneedle will change from 800 μ M reduced to 696 ± 2.5 μ m. The bending rate of the microneedle is about 12.7% (Figure 3B), which shows that the prepared microneedle has good flexibility.

As shown in Table 4 and Figure 3C, the prepared height is 800μm, the microneedle can puncture 4 layers of Parafilm®membrane smoothly, and the puncture rate is more than 96%. The thickness of the cuticle of skin and active epidermis is about 100 μm. The thickness of the dermis is about 3-5 mm. Therefore, the prepared microneedle has good mechanical strength (brittleness) and can successfully penetrate the dermis to form a microchannel on the skin surface.

The *in vitro* release results of drug-loaded microneedles are shown in Figure 3D. Because the microneedle carrier material is a soluble polymer material, the cumulative release percentage reaches 64.96% within 30 minutes of the release, which is characterized by rapid release.

## 3.3 Effect of AM-ae on serum indexes of MGH rats

As shown in Figure 4, after modeling, compared with the Con group, the serum levels of $E_2$ and PRL in the Mod group rats were highly significantly increased ($p$<0.01), and P levels were highly significantly decreased ($p$<0.01). After treatment with AM-DMN, compared with the Mod group, the $E_2$ content in the serum of rats

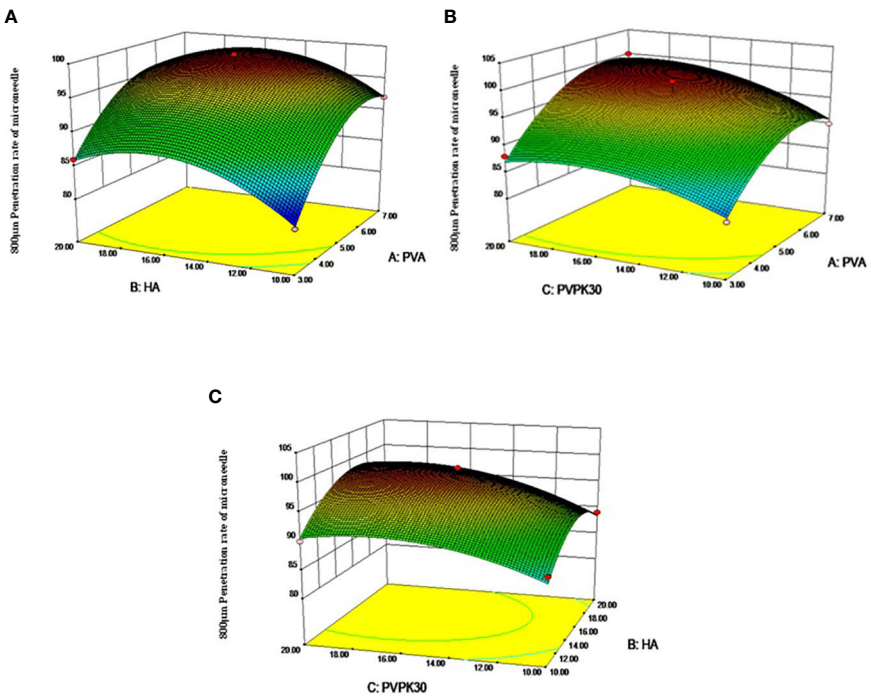


FIGURE 2
Response surface diagram and contour diagram of the interaction of various factors of microneedle prescription on the influence of microneedle preparation. **(A)** PVA and HA interactive response surface, **(B)** PVA and PVPK30 interactive response surface, **(C)** PVPK30 and HA interactive response surface)

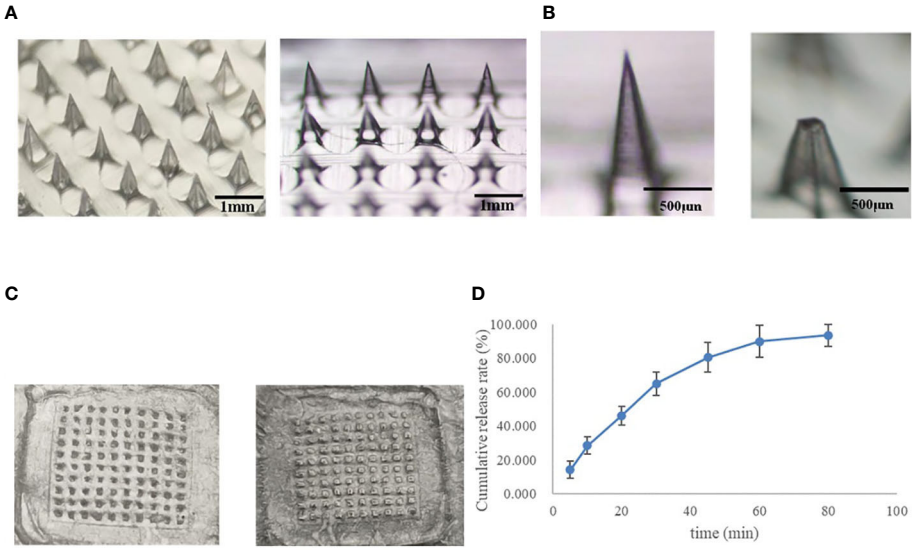


FIGURE 3
Microneedle characterization results **(A)**. Microneedle, **(B)** Appearance of microneedle under microscope (Left: 800 μ m. Right: 696 ± 2.5 μ m), **(C)** Micropuncture into 4 layers Parafilm® membrane (Left: front, right: reverse), **(D)** Microneedle release *in vitro* (n=3)).

TABLE 4 Parafilm ® membrane insertion test results.

| Number of layers of punctured film | Number of holes in each layer | Puncture rate (%) |
|---|---|---|
| 1 | 100 | 100 |
| 2 | 100 | 100 |
| 3 | 100 | 100 |
| 4 | 96 | 96 |

in the AM-DMN group was significantly decreased ($p$<0.01), the PRL content was significantly decreased ($p$<0.05), and the P content was significantly increased ($p$<0.01).

## 3.4 Evaluation of the quality of sequencing data of intestinal contents microbiota

As shown in Figure 5A, according to the sequence length data derived from this sequencing, each sample's sequence length was primarily 400–500 bp. Figure 5B illustrates as sample size rose, the number of OTUs climbed more slowly and then flattened out, showing that the total number of OTUs barely increased when more samples were added. This demonstrated that the samples used in this investigation were adequate to suit the needs of the study.

## 3.5 Effect of AM-ae on intestinal OTU, abundance grade, and alpha diversity in MGH rats

Figure 6A displays the OTU analysis. There was 1318, 492, and 982 OTUs total in the Con, Mod, and AM-DMN groups, respectively. There were 270 OTUs in the junction of the three groups. OTUs were considerably lower in the Mod group compared to the Con group, suggesting that MGH illness can cause rats' gut microbiota to become unbalanced and to become less numerous. following AM-DMN therapy, the OTU count increased, but in the gut remained lower than in the Con group. Based on abundance log2 values, the rank-abundance distribution curve was drawn (Figure 6B). According to our findings, the Con group contained the most OTUs, which is in line with the Venn diagram previously mentioned. Alpha diversity refers to the diversity within a specific area or ecosystem and is a comprehensive indicator reflecting richness and evenness. Chao1 and Pielou indices are used to evaluate richness, and the larger its values, the more abundant the total number of species in the environment. As two other indicators for assessing diversity, the Shannon and Simpson index, the higher the value, the higher the diversity of species in the environment. As can be seen from Figures 6C-F, compared with the Con group, the Chao1, Pielou, Shannon, and Simpson in the intestinal flora of Mod rats were highly significantly decreased ($p$<0.01), it was demonstrated that MGH decreased the rat gut microbiota's diversity and abundance. The Chao 1 index ($p$<0.01), Pielou index ($p$<0.05), Shannon index ($p$<0.01), and Simpson index ($p$ <0.01) in the rat microbiota were considerably greater in the AM-DMN group compared to the Mod group, demonstrating that AM-DMN can increase the quantity and diversity of the intestinal microbiota in MGH rats.

## 3.6 Effect of AM-ae on intestinal Beta diversity in MGH rats

Beta diversity is also known as inter-habitat diversity. It is often used to study the relationship of species diversity between communities or the differences between samples. Its research methods include PCA and NMDS. The PCA diagram (Figure 7A) and NMDS diagram (Figure 7B)

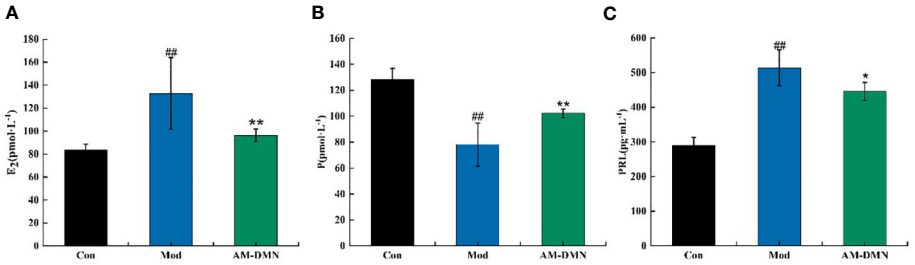


FIGURE 4
Effect of AM-ae on serum indexes of MGH rats **(A)**. Effect of AM-ae on $E_2$ of MGH rats, **(B)** Effect of AM-ae on P of MGH rats, **(C)** Effect of AM-ae on PRL of MGH rats).

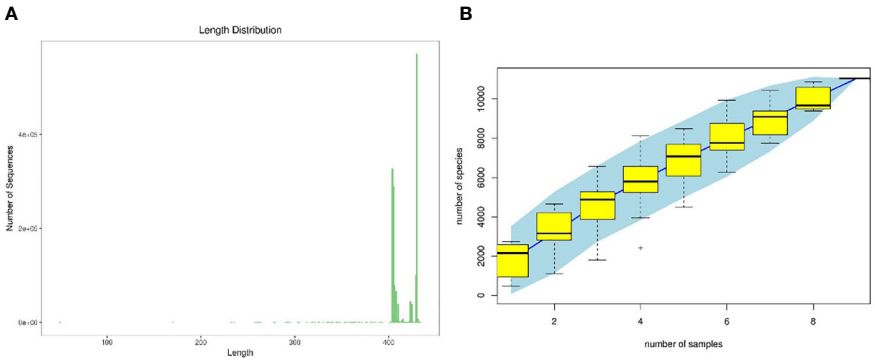


FIGURE 5
Quality evaluations of sequencing data of rat intestinal contents microbiota **(A)**. sequence length distribution diagram, **(B)** species accumulation curve diagram).

show that the distance between the intestinal microflora structure of the Mod group and Con group is significantly different, indicating that MGH can change the intestinal microflora structure of rats.

Compared with the Mod group, after AM-DMN treatment, the community structure similarity between the AM-DMN group and Con group is higher and relatively concentrated. β Diversity analysis showed that AM-ae could repair the bacterial structure of intestinal mucosa and restore it to normal.

## 3.7 Effect of AM-ae on the relative abundance of intestinal microflora in MGH rats

The relative abundance of intestinal mucosal bacteria at the phylum level in rats was shown in Figure 8A, in which four taxa, Firmicutes, Bacteroidetes, Actinobacteria, and Proteobacteria were the dominant phylum, accounting for a larger proportion of the total microbiota, about 95%. As shown in Figure 8B-D, compared with the Con group, in the Mod group the relative abundance of Firmicutes, Bacteroidetes, and Proteobacteria decreased highly significantly ($p<0.01$). In the AM-DMN group compared with the Mod group, the relative abundance of Firmicutes and Bacteroidetes increased highly significantly ($p<0.01$), and the Proteobacteres increased significantly ($p<0.05$).

Figure 8E shows that the F/B ratio of Firmicutes and Bacteroides in the Mod group is significantly higher ($p<0.01$), but the F/B ratio was significantly decreased after AM-DMN treatment ($p<0.01$). The horizontal heat map of rat intestinal flora is shown in Figure 8F. The heat map can simultaneously reflect the information on species composition and abundance of the community, and visually reflect the differences and similarities of the composition of different samples or sub-groups of communities through color changes. At the same time, cluster analysis is carried out according to the similarity of species or samples. Among the tested genera, Con and AM-DMN can be well clustered into one group, while the Mod group is relatively scattered, which may be due to the differences in the changes of intestinal flora in rats caused by MGH. It can be seen from Figure 8G that Allobaculum, Clostridiales, S24-7, and Ruminococcaceae, etc. are the dominant genera at the genus level. Compared with the Con group, the relative abundance of Actinobacteria, Clostridium, S24-7, and Ruminoccaceae in intestinal flora of rats in the Mod group was significantly lower ($p<0.01$); Compared with the Mod group, the relative abundances of Allobaculum, Clostriales, S24-7 and Ruminoccaceae in AM-DMN group were significantly higher ($p<0.01$). It was confirmed that AM-ae could improve the disturbance of intestinal flora caused by MGH.

# 4 Discussion

Skin is the main barrier to transdermal drug delivery, which is composed of the epidermis, dermis, subcutaneous tissue, sebaceous glands, and sweat glands. Among them, the cuticle is the largest drug

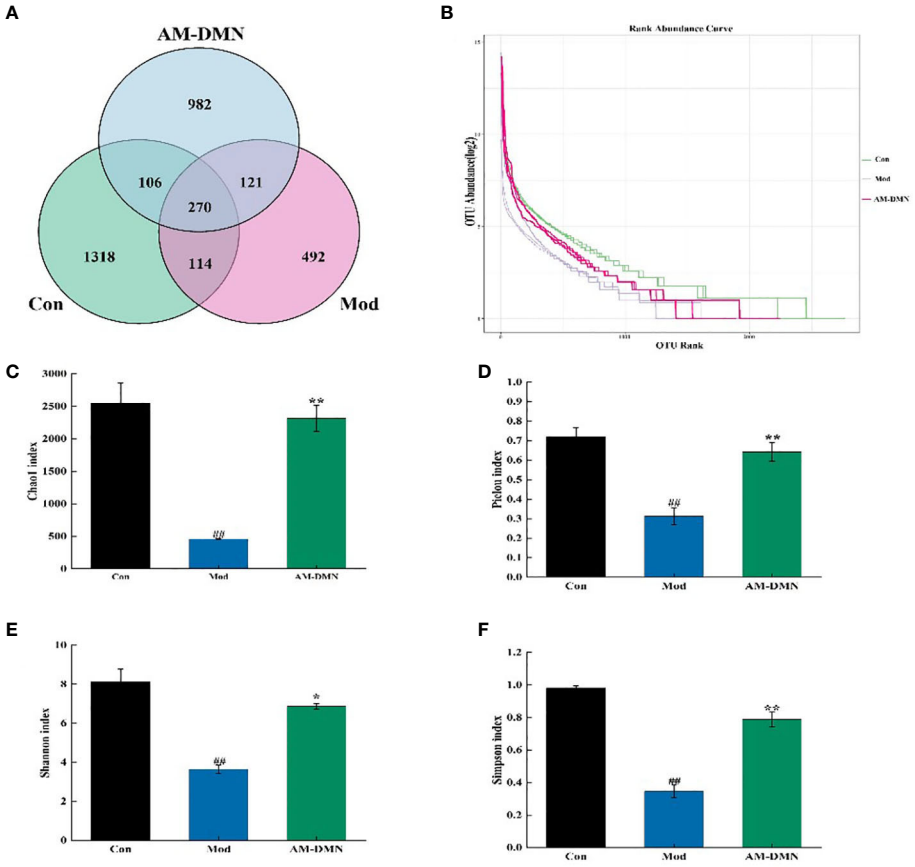


FIGURE 6
Effect of AM-ae on the number of intestinal OUT and alpha diversity of MGH rats **(A)**. number of intestinal OUT of rats, **(B)** Abundance grade curve, **(C)** Chao1 index, **(D)** Pielou index, **(E)** Shannon index, **(F)** Simpson index).

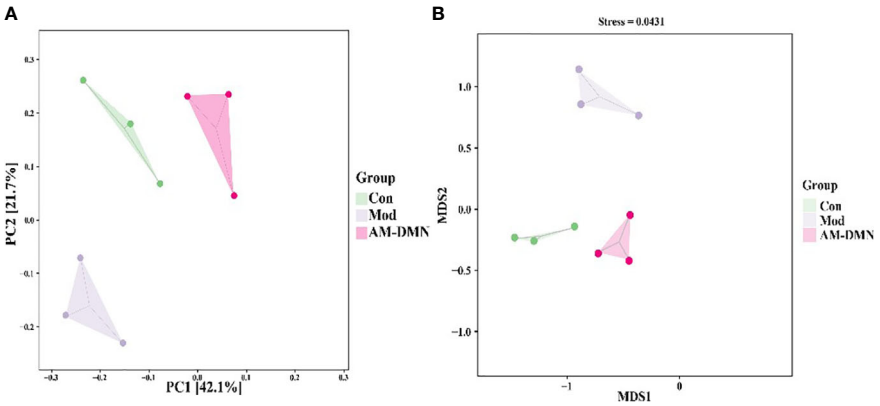


FIGURE 7
Effect of AM-ae on intestinal beta diversity of MGH rats **(A)**. PCA, **(B)** NMDS).

administration barrier. It is a special lipid, which has a strong barrier effect on both hydrophilic and lipophilic compounds, resulting in low drug permeability and unsatisfactory therapeutic effect. Therefore, to improve the barrier effect of cuticles on hydrophilic and lipophilic drugs, chemical and physical methods are usually used to improve the drug's skin permeability (19). The chemical method is to add absorption enhancers into the prescription, which can improve the permeability of drugs on the skin surface. However, excellent absorption enhancers need to meet many conditions, such as non-toxicity, non-irritant and non-allergic and have good compatibility with drugs and other excipients, so it is difficult and limited to select the appropriate absorption enhancers. Microneedles are one of the physical transdermal drug delivery methods, which can puncture the cuticle and deliver drugs to the skin, improving the permeability and

10.3389/fendo.2023.1158318

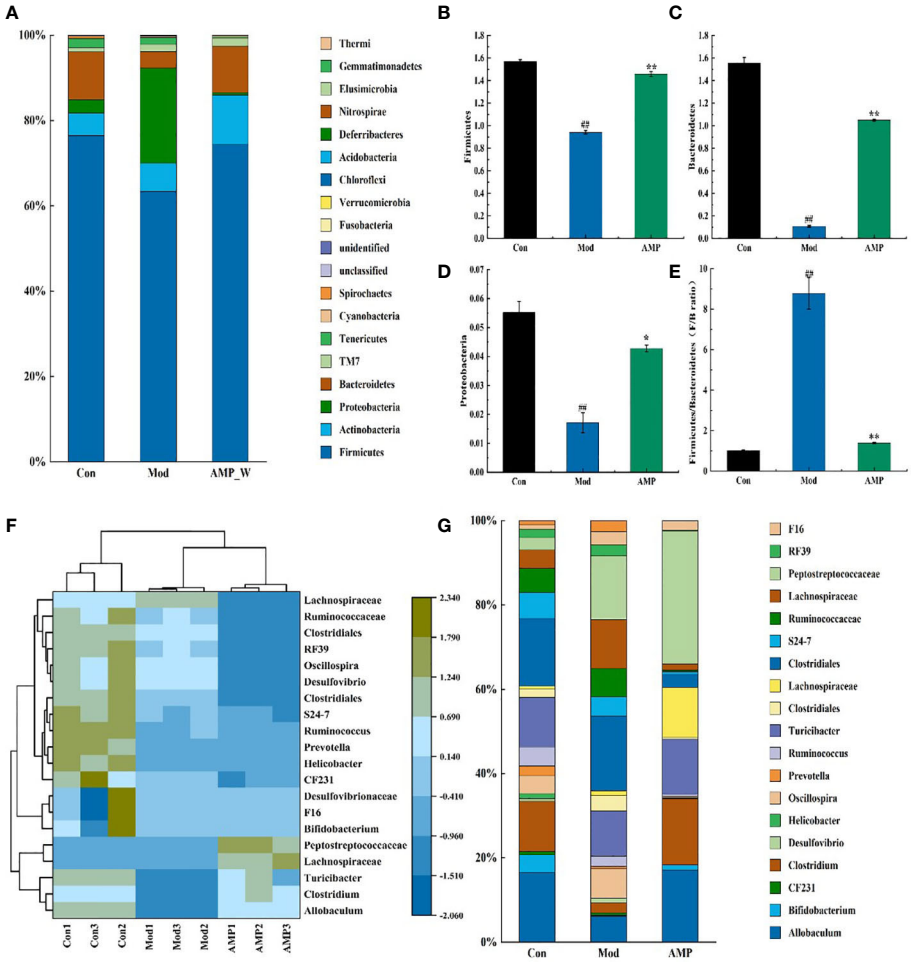


FIGURE 8
Effect of AM-ae on the relative abundance of intestinal microbiota in MGH rats **(A)**. Relative abundance of door level, **(B)** Firmicutes, **(C)** Bacteroidetes, **(D)** Proteobacteres, **(E)** Firmitutes/Bacteroides, **(F)** Horizontal relative abundance heat map, **(G)** Relative abundance at genus level).

bioavailability, Besides, the drug delivery process is safe and non-irritating to the skin, which is a painless and minimal invasive drug delivery method (20, 21). In this study, DMN was prepared from a biodegradable polymer material, which has the characteristics of biological stability, non-immunogenicity, non-toxicity, and no irritation to the human body. According to relevant literature reports, DMN is often used as a carrier for drug delivery such as insulin, 5-aminolevulinic acid, low molecular weight heparin, ovalbumin, adenovirus vector, a variety of vaccine antigens, and biomolecular molecules (22). It has been used in the treatment of skin diseases (23–25), metabolic diseases (26, 27), immune diseases (2, 28), and medical cosmetology (29, 30). The results of this study showed that the construction of soluble microneedles based on AM-ae has a good therapeutic effect on the treatment of breast hyperplasia.

MGH is a pathological hyperplasia of the breast lobule caused by an imbalance between estrogen and progesterone, when the $E_2$ level is excessive or the P level is too low *in vivo*, may lead to incomplete epithelial differentiation of the proliferating glands and non-regeneration of proliferative tissues, leading to MGH (31). In mammals, as a cytokine, PRL can regulate mammary gland development, promote milk secretion, and affect milk protein synthesis, while excessive PRL can cause structure disorder of the mammary gland (32). Sex hormones affect the intestinal microbiota by regulating intestinal barrier permeability and integrity, sex hormone receptors, β-glucuronidase, bile acids, intestinal immunity, etc. At the same time, intestinal flora also affects the secretion of sex hormones. Yi Wu et al. demonstrated that sex hormones may be involved in sexual dimorphism in bile acid metabolism by regulating the abundance of these bacteria (33). *Atractylodis Macrocephalae Rhizoma*, a dried rhizome of Atractylodes macrocephala Koidz., a plant of the composite family, has a long history of medicinal use in China. It is mainly used for deficiency of the spleen, lack of food, abdominal distension and diarrhea, phlegm, dizziness and palpitation, edema, spontaneous sweating, fetal movement, etc. The pharmacological effects of *Atractylodis Macrocephalae Rhizoma* are mainly in the gastrointestinal system, immune system, and urinary system. It has the functions of anti-aging, enhancing immunity, anti-tumor, anti-inflammatory, regulating gastrointestinal function, and regulating water and salt metabolism (34). According to the results of pharmacological experiments, AM-DMN can significantly reduce the content of $E_2$ and PRL, and increase the contents of P, which has the effect of treating MGH. Some studies have shown that intestinal flora

plays an important role in estrogen metabolism because intestinal flora can affect the enterohepatic circulation and reabsorption of estrogen. Estrogen and its metabolites can be excreted from bile glycolaldehyde or sulfonation. According to radioactive element labeling, about 65% of estradiol is excreted through bile, and the estradiol reabsorption process occurs when estrogen is excreted in the bile unclotted by β-glucuronidase in the gut, resulting in its reabsorption into circulation (35, 36). Shimizu K et al. found that adding intestinal flora of normal mice could normalize the estrous cycle of sterile female mice with reproductive impairment (37). The results of 16s rRNA showed that after administration of AM-DMN, the abundance, and diversity of intestinal flora in MGH mice increased, the relative abundance of dominant bacteria Firmicutes and Bacteroidetes increased, the F/B value decreased, and the resorption of estrogen decreased. Based on this, we speculated that the effect of AM-DMN on MGH mice may be related to the regulation of intestinal flora composition and abundance, but the specific mechanism still needs to be further explored. In conclusion, the prepared AM-DMN has a complete microneedle array, and the performance test results meet the requirements, which can improve intestinal flora and hormone disturbance induced by MGH through topical application.

## Data availability statement

The datasets presented in this study can be found here: doi: 10.5061/dryad.79cnp5j0h.

## Ethics statement

All experimental procedures involving animals were approved by the Animal Ethics Committee of the Animal Experimental Center of Jiamusi University.

## Author contributions

YP prepared the drafting of the manuscript and interpretation of data. QG and YLW analyzed in the analyzing of part of the data. CXL, YW, SL, MJQ, LQZ, ALT and YT performed the experiment. HZ designed the study and revised the manuscript. All authors contributed to the manuscript revision, read, and approved the submitted version.

## Funding

This study was supported by the National innovation and entrepreneurship training program (202210222135), Basic Scientific Research Funds for Higher Education Institution in Heilongjiang Province (2022-KYYWF-0611, 2022-KYYWF-0616) 2022-KYYWF-0612, Jiamusi University Ph.D. Special Foundation (JMSUBZ2020-14).

## Conflict of interest

The authors declare that the research was conducted in the absence of any commercial or financial relationships that could be construed as a potential conflict of interest.

## Publisher's note

All claims expressed in this article are solely those of the authors and do not necessarily represent those of their affiliated organizations, or those of the publisher, the editors and the reviewers. Any product that may be evaluated in this article, or claim that may be made by its manufacturer, is not guaranteed or endorsed by the publisher.

## Supplementary material

The Supplementary Material for this article can be found online at: https://www.frontiersin.org/articles/10.3389/fendo.2023.1158318/full#supplementary-material

## References

1. Ghazi RF, Al-Mayahy MH. Levothyroxine sodium loaded dissolving microneedle arrays for transdermal delivery. *J ADMET DMPK* (2022) 10:213–30. doi: 10.5599/admet.1317

2. Liu S, Yang G, Li M, Sun F, Li Y, Wang X, et al. Transcutaneous immunization *via* dissolving microneedles protects mice from lethal influenza H7N9 virus challenge. *J Vaccine* (2022) 40:6767–75. doi: 10.1016/j.vaccine.2022.09.008

3. Arendt LM, Kuperwasser C. Form and function: how estrogen and progesterone regulate the mammary epithelial hierarchy. *J J Mammary Gland Biol Neoplasia* (2015) 20:9–25. doi: 10.1007/s10911-015-9337-0

4. Li X, Xin P, Wang C, Wang Z, Wang Q, Kuang H. Mechanisms of traditional Chinese medicine in the treatment of mammary gland hyperplasia. *J Am J Chin Med* (2017) 45:443–58. doi: 10.1142/S0192415X17500276

5. Qi X, Yun C, Pang Y, Qiao J. The impact of the gut microbiota on the reproductive and metabolic endocrine system. *J Gut Microbes* (2021) 13:1–21. doi: 10.1080/19490976.2021.1894070

6. Org E, Mehrabian M, Parks BW, Shipkova P, Liu X, Drake TA, et al. Sex differences and hormonal effects on gut microbiota composition in mice. *J Gut Microbes* (2016) 7:313–22. doi: 10.1080/19490976.2016.1203502

7. Li C, Zhou K, Xiao N, Peng M, Tan Z. The effect of qiweibaizhu powder crude polysaccharide on antibiotic-associated diarrhea mice is associated with restoring intestinal mucosal bacteria. *Front Nutr* (2022) 9:952647. doi: 10.3389/fnut.2022.952647

8. Li X, Deng N, Zheng T, Qiao B, Peng M, Xiao N, et al. Importance of dendrobium officinale in improving the adverse effects of high-fat diet on mice associated with intestinal contents microbiota. *Front Nutr* (2022) 9:957334. doi: 10.3389/fnut.2022.957334

9. Li X, Peng X, Guo K, Tan Z. Bacterial diversity in intestinal mucosa of mice fed with dendrobium officinale and high-fat diet. *3 Biotech* (2021) 11:22. doi: 10.1007/s13205-020-02558-x

10. El Kaoutari A, Armougom F, Gordon JI, Raoult D, Henrissat B. The abundance and variety of carbohydrate-active enzymes in the human gut microbiota. *J Nat Rev Microbiol* (2013) 11:497–504. doi: 10.1038/nrmicro3050

11. Liu J, Qiao B, Deng N, Wu Y, Li D, Tan Z. The diarrheal mechanism of mice with a high-fat diet in a fatigued state is associated with intestinal mucosa microbiota. *3 Biotech* (2023) 13:77. doi: 10.1007/s13205-023-03491-5

12. Liang H, Jiang F, Cheng R, Luo Y, Wang J, Luo Z, et al. A high-fat diet and high-fat and high-cholesterol diet may affect glucose and lipid metabolism differentially through gut microbiota in mice. *Exp Anim* (2021) 70:73–83. doi: 10.1538/expanim.20-0094

13. Zhang CY, Peng XX, Shao HQ, Li XY, Wu Y, Tan ZJ. Gut microbiota comparison between intestinal contents and mucosa in mice with repeated stress-related diarrhea provides novel insight. *Front Microbiol* (2021) 12:626691. doi: 10.3389/fmicb.2021.626691

14. Liu J, Kong L, Shao M, Sun C, Li C, Wang Y, et al. Seabuckthorn polysaccharide combined with astragalus polysaccharide ameliorate alcoholic fatty liver by regulating intestinal flora. *Front Endocrinol (Lausanne)* (2022) 13:1018557. doi: 10.3389/fendo.2022.1018557

15. Li X, Zhang C, Hui H, Tan Z. Effect of gegenqinlian decoction on intestinal mucosal flora in mice with diarrhea induced by high temperature and humidity treatment. *Biotech* (2021) 11:83. doi: 10.1007/s13205-020-02628-0

16. Guo K, Yan Y, Zeng C, Shen L, He Y, Tan Z. Study on baohe pills regulating intestinal microecology and treating diarrhea of high-fat and high-protein diet mice. *Biomed Res Int* (2022) 2022:6891179. doi: 10.1155/2022/6891179

17. Zhu B, Zhang QL, Hua JW, Cheng WL, Qin LP. The traditional uses, phytochemistry, and pharmacology of atractylodes macrocephala koidz.: A review. *J J Ethnopharmacol* (2018) 226:143–67. doi: 10.1016/j.jep.2018.08.023

18. Ping Y, Li C, Wang L, Zhao H. Effects of atractylodes macrocephala rhizoma polysaccharide on intestinal microbiota composition in rats with mammary gland hyperplasia. *Front Endocrinol* (2023) 13:1102605. doi: 10.3389/fendo.2022.1102605

19. Lu W, Zhu H, Huang Y, Yang X, Hu Y, Luo H. Development key points of improved transdermal drug delivery system. *Chin J Pharm* (2022) 53:621–8. doi: 10.16522/j.cnki.cjph.2022.05.004

20. Shen R, Zhu Z, Zhang J, Luo H. Development progress of soluble microneedles in transdermal drug delivery systems. *J World Clin Drug* (2017) 45:460–6. doi: 10.13683/j.wph.2017.09.013

21. Waghule T, Singhvi G, Dubey SK, Pandey MM, Gupta G, Singh M, et al. Microneedles: A smart approach and increasing potential for transdermal drug delivery system. *J Biomed Pharmacother* (2019) 109:1249–58. doi: 10.1016/j.biopha.2018.10.078

22. Chen J, Huang W, Huang Z, Liu S, Ye Y, Li Q, et al. Fabrication of tip-dissolving microneedles for transdermal drug delivery of meloxicam. *J AAPS PharmSciTech* (2018) 19:1141–51. doi: 10.1208/s12249-017-0926-7

23. Alqam M, Wamsley CE, Hitchcock T, Jones BC, Akgul Y, Kenkel JM. Efficacy and tolerability of a microneedling device for treating wrinkles on the neck. *J Aesthet Surg J* (2022) 42:1154–60. doi: 10.1093/asj/sjac085

24. Bailey AJM, Li HO, Tan MG, Cheng W, Dover JS. Microneedling as an adjuvant to topical therapies for melasma: A systematic review and meta-analysis. *J Am Acad Dermatol* (2022) 86:797–810. doi: 10.1016/j.jaad.2021.03.116

25. Yang B, Dong Y, Shen Y, Hou A, Quan G, Pan X, et al. Bilayer dissolving microneedle array containing 5-fluorouracil and triamcinolone with biphasic release profile for hypertrophic scar therapy. *J Bioact Mater* (2021) 6:2400–11. doi: 10.1016/j.bioactmat.2021.01.014

26. Zong Q, Guo R, Dong N, Ling G, Zhang P. Design and development of insulin microneedles for diabetes treatment. *J Drug Delivery Transl Res* (2022) 12:973–80. doi: 10.1007/s13346-021-00981-y

27. Vora LK, Courtenay AJ, Tekko IA, Larrañeta E, Donnelly RF. Pullulan-based dissolving microneedle arrays for enhanced transdermal delivery of small and large biomolecules. *J Int J Biol Macromol* (2020) 146:290–8. doi: 10.1016/j.ijbiomac.2019.12.184

28. Park CO, Kim HL, Park JW. Microneedle transdermal drug delivery systems for allergen-specific immunotherapy, skin disease treatment, and vaccine development. *J Yonsei Med J* (2022) 63:881–91. doi: 10.3349/ymj.2022.0092

29. Wang X, Zhou Y. Clinical effect of interventional single microneedle radiofrequency technique in the treatment of lower eyelid wrinkles with pouch. *J China Med Cosmetology* (2021) 11:5–8. doi: 10.19593/j.issn.2095-0721.2021.11.003

30. Xing M, Liu H, Meng F, Ma Y, Zhang S, Gao Y. Design and evaluation of complex polypeptide-loaded dissolving microneedles for improving facial wrinkles in different areas. *J Polymers (Basel)* (2022) 14:4475–87. doi: 10.3390/polym14214475

31. You Z, Sun J, Xie F, Chen Z, Zhang S, Chen H, et al. Modulatory effect of fermented papaya extracts on mammary gland hyperplasia induced by estrogen and progestin in female rats. *J Oxid Med Cell Longev* (2017), 8235069. doi: 10.1155/2017/8235069

32. Wang X, Chen Y-G, Ma L, Li ZH, Li JY, Liu XG, et al. Effect of Chinese medical herbs-huiru yizeng yihao on hyperprolactinemia and hyperplasia of mammary gland in mice. *J Afr J Traditional Complementary Altern Medicines* (2013) 10:24–35. doi: 10.4314/ajtcam.v10i4.5

33. Wu Y, Peng X, Li X, Li D, Tan Z, Yu R. Sex hormones influence the intestinal microbiota composition in mice. *Front Microbiol* (2022) 13:964847. doi: 10.3389/fmicb.2022.964847

34. Wen W, Cheng Z, Hou K. Research progress of action mechanism of baizhu powder based on intestinal microecology. *Microbiol China* (2022) 49:769–80. doi: 10.13344/j.microbiol.china.210589

35. Raftogianis R, Creveling C, Weinshilboum R, Weisz J. Estrogen metabolism by conjugation. *J JNCI Monogr* (2000) 27:113–24. doi: 10.1093/oxfordjournals.jncimonographs.a024234

36. Kwa M, Plottel CS, Blaser MJ, Adams S. The intestinal microbiome and estrogen receptor-positive female breast cancer. *J J Natl Cancer Inst* (2016) 108:djw029. doi: 10.1093/jnci/djw029

37. Shimizu K, Muranaka Y, Fujimura R, Ishida H, Tazume S, Shimamura T. Normalization of reproductive function in germfree mice following bacterial contamination. *J Exp Anim* (1998) 47:151–8. doi: 10.1538/expanim.47.151

frontiers | Frontiers in Endocrinology

TYPE Review
PUBLISHED 01 March 2023
DOI 10.3389/fendo.2023.1149751



OPEN ACCESS

EDITED BY
Zhoujin Tan,
Hunan University of Chinese Medicine, China

REVIEWED BY
Yingchun Zeng,
Chengdu Medical College, China
Yan Liu,
Heilongjiang University of Chinese Medicine, China
Su Min,
Changsha Medical University, China

*CORRESPONDENCE
Hong Zhao
zhaohong1981@jmsu.edu.cn

†These authors contributed equally to this work and share first authorship

SPECIALTY SECTION
This article was submitted to Gut Endocrinology, a section of the journal Frontiers in Endocrinology

RECEIVED 23 January 2023
ACCEPTED 14 February 2023
PUBLISHED 01 March 2023

CITATION
Li D, Tang W, Wang Y, Gao Q, Zhang H, Zhang Y, Wang Y, Yang Y, Zhou Y, Zhang Y, Li H, Li S and Zhao H (2023) An overview of traditional Chinese medicine affecting gut microbiota in obesity.
*Front. Endocrinol.* 14:1149751.
doi: 10.3389/fendo.2023.1149751



# An overview of traditional Chinese medicine affecting gut microbiota in obesity

Donghui Li[1†], Weiwei Tang[1†], Yanyan Wang[1], Qi Gao[1], Hongwei Zhang[2], Yu Zhang[1], Yuliang Wang[1], Yongyi Yang[1], Yingming Zhou[1], Yike Zhang[1], Haonan Li[1], Shuo Li[1] and Hong Zhao[1*]

[1]College of Pharmacy, Jiamusi University, Jiamusi, China, [2]Department of Emergency Surgery, The First Affiliated Hospital of Jiamusi University, Jiamusi, China

Obesity, a chronic metabolic disease with a complex pathophysiology, is caused by several variables. High-fat diets lead to the disruption of the gut microbiota and impaired gut barrier function in obese people. The dysbiosis and its metabolites through the intestinal barrier lead to an imbalance in energy metabolism and inflammatory response, which eventually contributes to the development of chronic diseases such as diabetes, hypertension, and cardiovascular disease. Current medicines are therapeutic to obesity in the short term; however, they may bring significant physical and emotional problems to patients as major side effects. Therefore, it is urgent to explore new therapeutic methods that have definite efficacy, can be taken for a long time, and have mild adverse effects. Numerous studies have demonstrated that traditional Chinese medicine (TCM) can control the gut microbiota in a multi-targeted and comprehensive manner, thereby restoring flora homeostasis, repairing damaged intestinal mucosal barriers, and eventually curbing the development of obesity. The active ingredients and compounds of TCM can restore the normal physiological function of the intestinal mucosal barrier by regulating gut microbiota to regulate energy metabolism, inhibit fat accumulation, affect food appetite, and reduce intestinal mucosal inflammatory response, thereby effectively promoting weight loss and providing new strategies for obesity prevention and treatment. Although there are some studies on the regulation of gut microbiota by TCM to prevent and treat obesity, all of them have the disadvantage of being systematic and comprehensive. Therefore, this work comprehensively describes the molecular mechanism of obesity mediated by gut microbiota based on the research state of obesity, gut microbiota, and TCM. A comprehensive and systematic summary of TCM targeting the regulation of gut microbiota for the treatment of obesity should be conducted in order to provide new strategies and ideas for the treatment of obesity.

KEYWORDS

**traditional Chinese medicine, gut microbiota, obesity, short-chain fatty acids (SCFAs), active ingredients**

# 1 Introduction

Obesity is a chronic metabolic disease that is caused by excessive accumulation and abnormal distribution of body fat due to the imbalance of energy intake and consumption (1). Research shows that obesity has become a worldwide public health problem. More than 2 billion adults are overweight or obese worldwide, and the prevalence of obesity continues to rise globally (2, 3). Obesity will increase the risk of heart disease, diabetes, digestive disorders, and several types of cancer (4). At present, there are two main types of drugs that have been clinically proven to help with weight loss. One type is the central nervous system drugs, such as cloxacillin, but these drugs have side effects including insomnia, constipation, and anxiety (5). Another type of drug works on the non-central nervous system, such as orlistat, which has the same side effects (insomnia, constipation, and anxiety) (6). According to modern medicine, the pathogenesis of obesity is complex and involves dietary habits, genetic factors, and environmental factors (7). An increasing number of studies have shown that gut microbiota, as a key environmental factor, could contribute to the occurrence and development of obesity (8).

The gut microbiota refers to the microorganisms inhabiting the human gastrointestinal tract. The gut microbiota consists of many interacting symbiotic bacteria, which is considered to be an endocrine organ involved in maintaining energy homeostasis and host immunity. The bioactive metabolites of the gut microbiota can affect the physiological effects of the host (9–12). In humans, the gut microbiota is a complex and dynamic ecosystem that represents approximately 1 kg of our body weight (13). Under normal conditions, the gut microbiota works in harmony with the host and participates in the regulation of many physiological functions of the host, such as nutrient and substance metabolism, food digestion and absorption, the formation of a biological barrier in the intestinal mucosal epithelium, and boosting host immune function (14, 15). Furthermore, healthy gut microbiota produces short-chain fatty acids (SCFAs) to repair and promote intestinal function, and to effectively inhibit the growth of spoiled bacteria in the gut and improve the intestinal environment (16). However, dietary habits or environmental factors affect the composition of gut microbiota, and long-term consumption of improper diet may affect metabolism (17). Several studies have found that antibiotics can change the intestinal mucosa bacterial composition, reduce colonization resistance, and damage the intestinal mucosal barrier by reducing the abundance of gut microbiota (18–20). The high-fat and high-protein diet altered the community structure of lactase bacteria in the intestinal mucosa and decreased the abundance of the critical lactase bacteria (21). The dysbiosis of the gut microbiota may be involved in the pathogenesis of obesity through multiple mechanisms, including disruption of energy homeostasis, lipid synthesis, and storage, central regulation of appetite and feeding behavior, and chronic low-grade inflammation (13, 22, 23). Therefore, regulation of gut microbiota and improvement of intestinal dysbiosis are regarded as key directions for the treatment of obesity, as shown in Figure 1.

Traditional Chinese medicine (TCM) has thousands of years of clinical experience in the treatment of obesity, and its benefits are safe, mild, and long-lasting. The majority of TCM is taken orally, and the active ingredients in the TCM interact with the gut microbiota as they enter the gastrointestinal tract. The growth and proliferation of certain microbiota can be stimulated or inhibited by TCM. For example, the Wu et al. study found that *Lilium lancifolium* can promote the growth of *Lactobacillus* spp. and *Bifidobacteria* spp., and inhibit the growth of total bacteria in the intestines of normal mice (24). Qiweibaizhu powder could overcome the influence of dysbacteriosis and could lead to the recovery of intestinal mucosal microbiota homeostasis (25). Folium senna decoction gavage increased intestinal microbiota diversity; *Bacteroides vulgatus*, *Helicobacter ganmani*, *Lactobacillus murinus*, *Microbacterium dextranolyticum*, and *Klebsiella pneumoniae* were significantly enriched, while *Candidatus arthromitus* sp. and *Lactobacillus johnsonii* were significantly depleted (26, 27). Qiweibaizhu powder has a positive effect on the recovery of

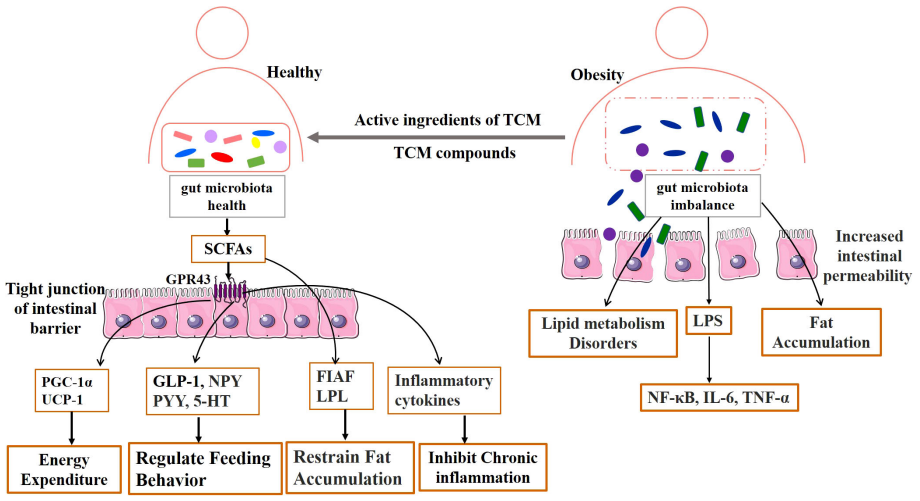


FIGURE 1
Mechanism diagram of TCM affecting gut microbiota in obesity.

bacterial lactase gene diversity to normal levels and increases the abundance of *Lysobacter* and *Eukaryota* (28). The Qiwei Baizhu Powder decoction and QWBZP-TG promoted the proliferation of *Lactobacillus* and inhibited the growth of *Proteus*, *Clostridium*, *Eubacterium*, *Facklamia*, and *Escherichia* (29). The active ingredients in the Gegenqinlian decoction may increase the microbial activity of the intestinal mucosa of mice and reduce the microbial activity of the intestinal contents through multiple targets (30). This review will focus on recent advances in the connection between gut microbiota and obesity, and the role of gut microbiota in the treatment of obesity is clarified, in order to find new ideas and research directions for the treatment of obesity and related diseases.

# 2 Mechanisms of obesity mediation by gut microbiota

The gut microbiota colonizes the intestines and has important physiological functions. Studies have shown that obesity is associated with a decrease in gut microbiota diversity, gene expression of gut microbiota, and alteration of metabolic pathways (31, 32). Compared with healthy people, the gut microbiota of obese people usually shows changes at the phylum, family, and genus levels (33, 34). The imbalance of gut microbiota may lead to obesity, which may be related to energy balance, regulation of feeding behavior, fat storage, and inflammation. The mechanisms of gut microbiota-mediated obesity are discussed in this review.

## 2.1 Characteristics of obese gut microbiota

The first evidence for a link between gut microbiota and obesity was from studies of germ-free mice. In 1983, Wostmann et al. first discovered that germ-free rats needed more energy to maintain their body weight compared to wild rats, but the precise mechanism was unknown at the time (35). In 2004, Gordon et al. observed that gut microbiota can affect energy absorption from the diet and energy storage in mice, and found that the proportion of *Firmicutes* was higher and the proportion of *Bacteroidetes* was lower in the guts of obese people (36). Numerous studies have demonstrated that the structure and abundance of gut microbiota are altered in obese people compared to healthy people. Obese people show lower gut microbiota diversity than healthy people and show significant overall obesity and dyslipidemia (37–39).

Numerous studies have demonstrated that the meat-based Western diet has a negative impact on the richness and function of gut microbiota. Being high in animal-derived protein and low in vegetables and fruits, the Western-style diet leads to a significant decrease in the numbers of total bacteria and commensal *Bifidobacterium* and *Eubacterium* species (40). A diet rich in fat, with high consumption of red meat and refined carbohydrates, may have a direct effect on the immune system causing a structural and functional modification of the gut microbiota (41). Lard and vegetable blend oil diet affected the composition of the intestinal microorganisms and the functions of digestive enzymes (42). It was found that more *Firmicutes* than *Bacteroidetes* caused the body to absorb more calories from food and more easily convert calories into fat to accumulate under the skin (43, 44). The gut of obese people is rich in archaea, which can oxidize hydrogen produced by *Prevotella*, thus accelerating the fermentation of polysaccharides and causing the body to absorb more energy (45). According to Petersen et al. (46), *Clostridium* was reduced in obese people and some of the *Clostridium* were able to absorb fat and reduce obesity in mice. The levels of *Ackermanella* are significantly decreased in obese people, which reduces metabolic disturbances caused by high-fat diets, improves fat accumulation, and reduces inflammatory responses (47). In summary, the gut microbiota changes in obese people are mainly shown as the increase in bacteria that cause inflammation and fat production and the decrease in bacteria that inhibit obesity and inflammation. Therefore, it can play a role in the treatment of obesity by regulating the diversity and abundance of the dominant gut microbiota, inhibiting adipogenesis, and the inflammatory response.

## 2.2 Regulation of energy absorption

Gut microbiota participates in energy metabolism and absorption under normal and pathological conditions. The obesity-associated gut microbiome can increase the capacity for energy harvest from the diet, thus contributing to increased adipose tissue storage of the host, especially the white adipose tissue (WAT) (48). SCFAs, mainly acetate, propionate, and butyrate, are produced by the gut microbiota through the metabolism of complex dietary plant polysaccharides (49, 50). As one of the primary metabolites of the intestinal microbiota, SCFAs can lower intestinal pH to a certain extent, thereby inhibiting the viability of pathogenic microbiota from promoting intestinal microecological balance and maintaining the integrity of the intestinal mucosal barrier (51). SCFAs are an important source of energy for the host, contributing up to 70% of the daily energy supply for herbivores and 10% of the total daily energy needed for omnivores (13). Among them, butyric acid is a significant source of energy for the epithelial cells of the human colon and cecum (52). As depicted in Figure 2, SCFAs not only provide direct energy but also raise energy expenditure and encourage lipolysis. Acetate can have a beneficial effect on host energy metabolism by reducing levels of pro-inflammatory cytokines, increasing energy expenditure and lipid oxidation, and promoting lipolysis (53). Butyrate promotes fatty acid oxidation and increases energy consumption by acting on G protein-coupled receptor 43 (GPR43) and upregulating the expression of peroxisome proliferator-activated receptor coactivator-1 alpha (PGC-1α) and uncoupling protein 1 (UCP-1) expression in brown adipose tissue (BAT) (54). SCFAs are typically considered to have beneficial effects on the body. However, some research suggests that excessive SCFAs may have a negative impact on the body. Clinical studies by Tirosh et al. (55) showed that consuming a propionate-containing diet causes the levels of glucagon in the blood, which raises the risk of obesity. Therefore, gut microbiota metabolites can have both positive and negative effects on the host.

10.3389/fendo.2023.1149751

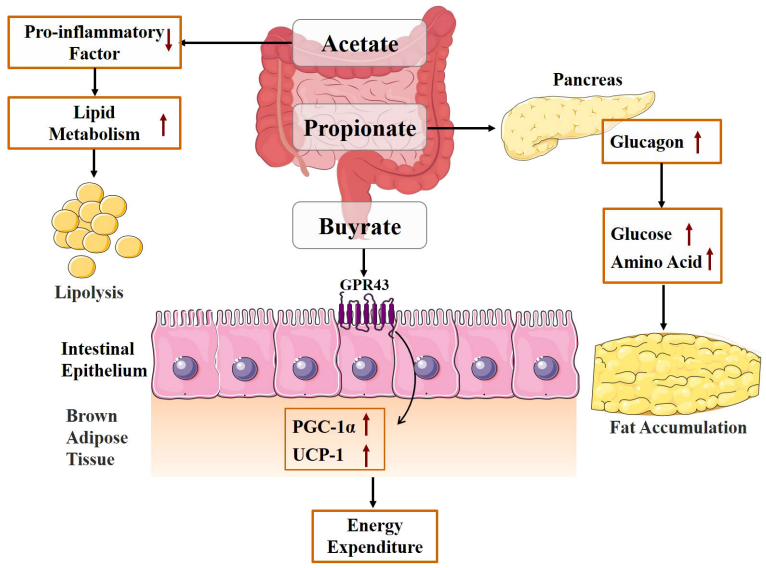


FIGURE 2
Mechanism diagram of energy absorption mediated by gut microbiota metabolites.

If we want to regulate the energy absorption of the body by regulating the metabolites of the intestinal flora, the concentration should be taken into consideration.

## 2.3 Regulation of feeding behavior

The brain is the main part of the appetite regulation neural pathway, which directly regulates feeding behavior. Gut microbiota produces specific metabolic compounds, which interact with the central nervous system, such as glutamic acid, bile acids, 5-hydroxytryptamine (5-HT), SCFAs, and GABA (Glu) (Figure 3) (56, 57). These neuroendocrine components and their receptors have a role in controlling central appetite and feeding behavior by mediating the bidirectional communication between the brain and the digestive system (58). Through the "brain–gut–bacteria" axis, SCFAs can control the body's energy metabolism to control the GPRs pathway, activate the MAPK signal pathway in intestinal epithelial cells, promote the secretion of 5-HT and gastrointestinal peptides (GIPs) in the intestine, increase satiety, decrease gastric emptying and intestinal movement, affect energy intake, and decrease body weight (53). Propionate in SCFAs activates GPR41, increases leptin (LP) levels, reduces the content of neuropeptide Y (NPY), which has the effect of enhancing appetite, and inhibits the secretion of peptide YY (PYY), which has the effect of appetite (59, 60). Butyrate reduces obesity by acting on GPR43 to increase plasma GLP-1 levels, controlling appetite through the central nervous system, and reducing food intake (60, 61). In addition, oral butyric acid also inhibits the hypothalamic expression of NPY and pro-appetitive neural activity, and decreases food intake (62).

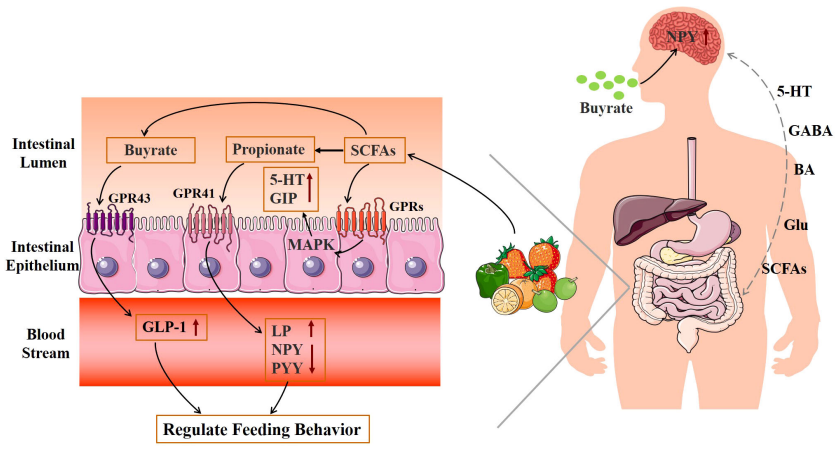


FIGURE 3
Mechanism diagram of gut microbiota metabolites regulating feeding behavior.

According to Frost et al. (63), acetate can reduce hunger by increasing the amount of GABA in mice's brains. Therefore, the production of SCFAs can be controlled by regulating the structure and activity of the intestinal flora to achieve obesity treatment.

## 2.4 Regulation of fat accumulation

The regulation of genes related to fat accumulation is greatly influenced by intestinal flora and its metabolites (Figure 4) (64). Fasting-induced adipokines (FIAFs) inhibit adipose tissue storage by inhibiting lipoprotein lipase (LPL) activity, reducing extracellular triglyceride hydrolysis and fatty acid uptake (65, 66). Studies have shown that SCFAs can inhibit fat accumulation in the body, which may be related to their ability to activate the expression of FIAF and inhibit the expression of LPL, thus preventing the triglyceride cycle (67). In addition, acetate also prevents fat accumulation by stimulating GLP-1 production and activating GPR43 in the gut (68). Propionate regulates glucose and lipid metabolism by binding to and activating neuronal GPRs, causing the release of vasoactive intestinal peptide (VIP) from the submucosal plexus, activating adenylate cyclase (AC), and reducing cAMP levels (69).

## 2.5 The chronic mild inflammatory response

At present, obesity and obesity-related diseases are recognized as systemic chronic low inflammation by the medical community. Recent research has demonstrated that Gram-negative bacteria in the gut microbiota of obese people can create lipopolysaccharides (LPS) and bind to toll-like receptor 4 (TLR-4), activating nearby and distant pro-inflammatory cascades and releasing inflammatory factors (70, 71). TLR4 is an important binding regulator of LPS, which is overexpressed in intestinal mucosal epithelial cells after stimulation of activation, inducing the production of various pro-inflammatory factors and causing and maintaining obesity-type low-level inflammation in the body (72). In addition, damage to the intestinal mucosal barrier can also lead to inflammation. The changes in intestinal flora increase intestinal permeability and promote LPS to enter the blood to activate the NF-κB signal pathway, which leads to chronic inflammation, endotoxemia, and increased fat accumulation, and ultimately leads to metabolic syndrome and obesity (73). The high-fat diet could induce the interactions between *Thermoactinomyces*, *Staphylococcus*, and intestinal inflammation (74).

Gut microbiota and its metabolites mediate the chronic inflammatory response and inhibit obesity (Figure 5). The main mechanisms are as follows: (1) Promote the proliferation of intestinal epithelial cells, reduce the apoptosis of intestinal epithelial cells, and maintain the intestinal mucosal barrier. (2) Regulation of inflammation-related gene expression and reduction of inflammatory response. SCFAs are important signaling molecules to regulate intestinal mucosal immunity, inhibiting LPS or TNF-α-induced inflammatory responses, in which the mechanism is related to the regulation of NF-κB and MAPK signaling pathways (75). The study also discovered that additional SCFA supplementation could enhance mitochondrial activity in brown fat cells, inhibit chronic inflammation, increase the expression of G protein-coupled receptors (GPR43 and GPR41), promote the oxidation of free fatty acids and the hydrolysis of triglycerides, and decrease the body weight of obese mice (76). SCFAs inhibit the transport of toxic substances by maintaining the stability of the intestinal barrier, reducing the concentration of LPS in the blood, and reducing the inflammatory response (77). Acetate improves epithelial cell-mediated intestinal defense and enhances intestinal integrity, thereby protecting the host from lethal infections (78). Butyrate inhibits the activity of macrophages, dendritic cells, neutrophils, and T cells, which lessens inflammation of the intestinal tissue (79, 80). In addition, butyric acid can also block the activity of the transcription factor NF-B and decrease the expression of inflammatory factors like IL-6 and IL-12, which inhibits the inflammatory response in the intestine (81).

In conclusion, the development of obesity is closely correlated with gut microbiota. Human obesity and several numbers of other disorders are brought about by gut microbial dysbiosis. Healthy

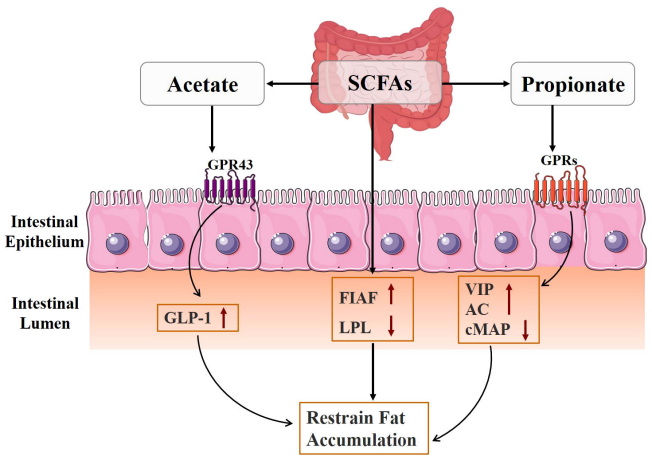


FIGURE 4
Mechanism diagram of gut microbiota metabolites regulating fat accumulation.

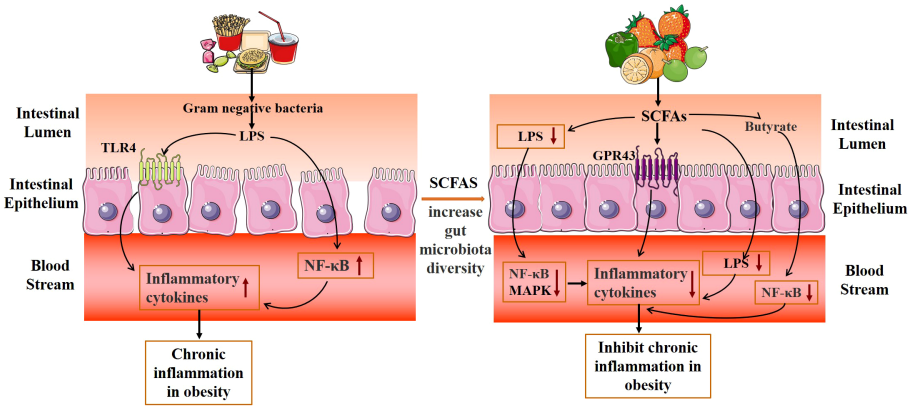


FIGURE 5
Mechanism diagram of gut microbiota metabolites inhibiting the chronic mild inflammatory response.

intestinal flora and its metabolites can play a potential role in preventing or treating obesity by regulating energy absorption, feeding behavior, fat accumulation, and inflammatory reaction.

## 3 The mechanism of TCM affecting gut microbiota to inhibit obesity

The role of regulation of gut microbiota by TCM in the treatment of obesity and related diseases has been confirmed. Several studies have found that the TCM compound, single Chinese medicine, and its active ingredients act on gut microbiota and its metabolites, and play a role in controlling energy metabolism absorption, feeding behavior, and fat storage, and in assuaging chronic delicate inflammation; therefore, it can be used in the treatment of obesity and other related diseases, as shown in Table 1.

### 3.1 Study on the mechanism of active ingredients of TCM affecting gut microbiota to inhibit obesity

#### 3.1.1 Regulation of energy metabolism and absorption

The anti-obesity effect of TCM and its active ingredients is closely related to the regulation of gut microbiota. The active ingredients of TCM can affect the absorption of energy metabolism in the body by improving the abundance of gut microbiota and the expression of related signal pathway proteins. Zhang et al. (82) found that ginsenosides, the active ingredient of ginseng, improved the structural composition of the gut microbiota, increased the concentration of SCFAs and receptor proteins (GPR41, GPR43, and GPR109A), and enhanced the gut barrier completeness. Song et al. (83) found that the root of *Atractylodes macrocephala* Koidzumi extract can prevent diet-induced obesity and glucose intolerance in mice. Its mechanisms are related to increasing the number of brown fat cells, increasing PGC-1 α and UCP1 expression, and promoting the energy metabolism of brown fat tissue. Propolis ethanol extract reduced high-fat diet-induced obesity by regulating the abundance of gut microbiota and improving glucose tolerance and lipid distribution in high-fat diet rats (84). According to Wang et al. (85), *Polygala tenuifolia* extract inhibits high-fat diet-induced lipid accumulation in obese mice by modulating the composition of gut microbiota and regulating the levels of transcription factors of lipid oxidation. Li et al. (106) found that *Dendrobium officinale* can improve the diversity of intestinal mucosal flora and influence the gut microbiota to positively affect high-fat diet-induced negative effects in mice. Asparagus can affect the diversity of bacteria in the intestinal mucosa of mice fed a high-fat diet, and achieve a lipid-lowering effect by regulating the intestinal microecology of mice fed a high-fat diet (107). Baohe pills can restore the number of intestinal flora to a certain extent and improve the activities of various digestive enzymes including protease and amylase in mice fed a high-fat and high-protein diet (108).

#### 3.1.2 Regulation of feeding behavior

The active components of TCM can improve the abundance of gut microbiota and the expression of associated signaling pathway protein in obese mice to regulate feeding behavior and thus play a role in treating obesity. The active components of TCM can alter feeding behavior, increase microbiota abundance, and consequently increase the production of proteins involved in linked signaling pathways in obese mice. According to Neyrinck et al. (93), berberine and curcumin can improve intestinal barrier function, increase the number of intestinal probiotics, upregulate the expression of the innate immunity genes Pla2g2a and PYY, and decrease food intake in obese mice. Casanova-Martí et al. (94) discovered that grape seed proanthocyanidins can suppress appetite and promote weight reduction by controlling the quantity of gut microbiota in rats, raising serum GLP-1 levels, and upregulating GLP-1 mRNA and protein expression in ileum and colonic tissues. According to Lin et al. (95), diet-induced obese mice's appetites were suppressed and their weight was decreased because Rb1, the active component of

10.3389/fendo.2023.1149751

TABLE 1 Study on the intervention mechanism of TCM affecting gut microbiota in obesity.

| Mechanism | Chinese medicine and formula | Target/ medium | Reference |
|---|---|---|---|
| The expression of genes that control energy absorption such as GPR43, TC, and TG | Ginsenoside | SCFAs, GPR41, GPR43, GPR109A | (82) |
| | Root of *Atractylodes macrocephala* Koidzumi | PGC-1α, UCP1 | (83) |
| | Extract of propolis | IL-1β, IL-6, IL-10 | (84) |
| | Polygala tenuifolia extract | SREBP1C, TG, SAA1 | (85) |
| | *Cordyceps guangdongensis* | SCFAs, TC, TG, ALT | (86) |
| | Lingguizhugan formula | TC, TG, FFA | (87–89) |
| | Erchen decoction | IRS1, AKT, PKA, HSL | (90) |
| | Xiexin tang | SCFAs, ACK, BUT, PGC-1α, AMPK | (91) |
| | Shenlian decoction | / | (92) |
| The levels of PYY and GLP-1 increase, improve diversity of gut microbiota and the intestinal barrier function, and decrease food intake | Berberine Curcumin | Pla2g2a, PYY, Muc2 | (93) |
| | Grape seed proanthocyanidins | GLP-1 | (94) |
| | Ginsenoside | PYY, NPY, Y2 receptor | (95) |
| Increases the level of SCFA increase, regulates the abundance of gut microbiota, improves disorders of lipid metabolism, and inhibits fat accumulation | Ganoderma amboinense polysaccharide | SCFAs, TC, TG | (96) |
| | Rutin | IWAT, UCP1, SCFAs, BUT | (97) |
| | Heat-treated adzuki | SCFAs | (98) |
| Inhibits pathways leading to the production of pro-inflammatory cytokines; reduces LPS, thereby reducing chronic low-grade inflammation | Rhizoma Atractylodis Macrocephalae | HDL, IL-6, TNF-α | (99) |
| | Berberine | CD14, IL-1, IL-6, TNF-α | (100) |
| | Polysaccharide from the sclerotium of *Poria cocos* | PPAR-γ | (101) |
| | Polysaccharide from sporoderm-broken spore of *Ganoderma lucidum via* gut microbiota regulation | SCFAs, GPR43, GPR41, IL-1β | (102) |
| | Polysaccharide from Sijunzi decoction | SCFAs | (103) |
| | Effects of shenling baizhu | SCFAs, TLR4, IL-1, TNF-α | (104) |
| | JinQi Jiangtang | SCFAs, MCP-1, IL-6, TNF-α | (105) |

ginseng, was able to upregulate the expression of PYY mRNA in the intestine and downregulate the expression of NPY in the gut.

### 3.1.3 Regulation of fat accumulation

The active components of TCM effectively reduce fat formation by high-fat diets by controlling the homeostasis of gut microbiota and microbial metabolites. In mice given a high-fat diet, Ren et al. (96) discovered that *Ganoderma lucidum* polysaccharides efficiently lower blood lipid concentrations, regulate the abundance of gut bacteria and various critical pathways, and successfully relieve fat formation. According to Cheng et al. (97), Rubin may greatly raise the amounts of SCFAs and SCFA-producing enzymes in the feces of obese mice, prevent fat accumulation, treat glucolipid metabolic problems, and cause obese animals to lose weight. Heat-treated adzuki bean protein hydrolysates can assist to prevent and treat obesity and its associated consequences, as well as increase the diversity of gut bacteria in mice fed a high-fat diet (98).

### 3.1.4 Alleviation of chronic mild inflammatory response

TCM and its active components can significantly improve the intestinal environment, enhance intestinal barrier function, and

control the production of inflammatory markers associated with obesity during intestinal metabolism. Wang et al. (99) showed that fermented Rhizoma Atractylodis Macrocephalae can regulate the gut microbiota, improve the growth of probiotics, alleviate the inflammatory response, and restore the intestinal epithelial barrier function and exert weight loss effects. According to Cao et al. (100), berberine may help people lose weight by controlling the abundance of their gut bacteria and lowering levels of pro-inflammatory cytokines like IL-1, IL-6, and TNF-α. Insoluble polysaccharides from *Poria cocos* sclerotium can significantly reduce the weight of obese mice by increasing the abundance of intestinal flora, improving the integrity of intestinal mucosa, and activating the intestinal PPAR-γ pathway to reduce inflammatory response (101). *G. lucidum* polysaccharides improve dysbiosis of the gut microbiota and maintain intestinal barrier function to inhibit TLR4/Myd88/NF-κB signaling pathway expression in adipose tissue, thereby exerting treatment of obesity (102).

## 3.2 Mechanism of TCM compounds affecting gut microbiota to control obesity

### 3.2.1 Regulation of gut microbiota abundance and lipid metabolism

The TCM compounds can regulate the abundance of gut microbiota and lipid metabolism to treat obesity. In the mechanism involving the regulation of gut microbiota abundance, SCFAs, and genes involved in lipid metabolism, the Cordyceps guangdongensis lipid-lowering formula dramatically reduced weight and fat accumulation in high-fat diet mice (86). By lowering total cholesterol (TC) and triglyceride (TG) levels and increasing the quantity and variety of gut microbiota, the Jian Pi Tiao Gan Yin medicine helps mice with obesity (109). By controlling the distribution and relative abundance of gut microbiota, enhancing the small intestinal villi, and altering the metabolic pathways linked to obesity, the Lingguizhugan decoction (consisting of Poria, Ramulus Cinnamomi, Rhizoma Atractylodis Macrocephalae, and Radix Glycyrrhizae) aids in weight loss (87–89). By changing the composition of the gut microbiota and the relative abundance of bacteria in obese rats, the Erchen decoction (consisting of Radix et Rhizoma Panax, Radix tangerine, Poria, and Radix Glycyrrhizae) can improve lipid metabolism disorders and change the function of the gut microbiota and cause weight loss (90). In addition to improving obesity, Xiexin Tang (a combination of rhubarb, Huang Lian, and Scutellaria) increases the activity of crucial enzymes involved in the synthesis of SCFAs, enhances the gut microbiota's capacity to metabolize SCFAs, and decreases energy intake while increasing energy expenditure (91). The Shenlian (SL) decoction (composed of Coptis and ginseng) is considered a potential drug for weight loss, which can decrease the expression of flora associated with LPS biosynthesis, increase the diversity and abundance of gut microbiota, and regulate metabolic disorders (92). Daesiho-Tang is an effective herbal formulation in attenuation of obesity in HFD-fed mice through the alteration of gene expressions and modulation of intestinal microbiota (110). The TCM formula (CoTOL) (composed of Glabrous Greenbrier Rhizome, Dioscorea septemloba Thunb, Curcuma Longa, and so on) has beneficial effects on hyperuricemia and overweight, which may be attributed to regulating material metabolism and improving the structure or function of gut microbiota (111). The TCM Formula Kang Shuai Lao Pian (composed of glutinosa, ginseng, japonicas, and so on) could improve HFD-induced obesity, glucose tolerance disorder, and gut dysbiosis (112).

### 3.2.2 Regulation of gut microbiota abundance and reduction of chronic inflammation

The Sijunzi decoction, which contains ginseng, *Atractylodes macrocephala*, Poria, and Glycyrrhiza glabra, can have immunomodulatory effects by regulating the number of gut microbiota and SCFA levels (103). The shenling baizhu powder herbal formula (composed of lotus seed meat, coix kernel, sand kernel, bellflower, poria, ginseng, and licorice) reduced weight and serum total cholesterol levels and repaired intestinal mucosa in high-fat diet rats, and the mechanism may be related to reducing TLR4-related protein expression, decreasing the levels of inflammatory factors such as TNF-α and IL-1, and increasing the relative abundance of gut microbiota (104). Jinqi Hypoglycemic Tablets (composed of Huang Lian, Huang Qi, and Jin Yin Hua) regulate the gut microbiota and promote the production of SCFAs in HFD mice by a mechanism related to enhancing intestinal barrier function and reducing host inflammatory response (105). The Shen-Yan-Fang-Shuai formula (composed of Astragali Radix, Radix Angelicae Sinensis, Rheum Officinale Baill, and four other herbs) treatment prevented weight gain, low-grade inflammation, and insulin resistance in HFD mice (113). The Gegenqinlian decoction could intervene from inflammatory response through multiple targets and multiple channels to adjust the balance of intestinal mucosa flora (114).

# 4 Conclusion

Gut microbiota is closely related to the occurrence and development of obesity and related metabolic diseases. TCM can improve the metabolic disorder of obesity by regulating the imbalance of gut microbiota. Gut microbiota can be used as a new target for the prevention and treatment of obesity and to improve obesity and its metabolic diseases by correcting gut microbiota disorders. This study primarily summarizes how TCM treats obesity by regulating the flora in the intestines. The active ingredients of TCM and its compound can lower blood lipid levels and fat accumulation in patients by controlling the distribution of gut microbiota, enhancing the capacity of gut microbiota metabolism to generate SCFAs, reducing inflammatory damage, and improving the energy metabolism of the body, thereby improving obesity. Further study of the relationship between TCM and gut microbiota will help to enrich the theory of TCM and develop TCM preparations that target the gut microbiota. However, the research on the interaction between TCM and gut microbiota is complex and still in the initial stage. Many key scientific issues need to be further explored. The internal

environment of gut microbiota is complex, and different types of bacteria produce different metabolic enzymes, which makes it difficult to explain the biotransformation of active ingredients of TCM and gut microbiota. In the future, the molecular mechanism of gut microbiota regulation should be further explored. It is helpful for us to understand that TCM directly acts on gut microbiota or indirectly regulates the structure of gut microbiota and maintains the balance of intestinal micro-ecology, in order to promote the use of herbal medicine in the prevention and treatment of difficult-to-treat diseases such as obesity.

## Author contributions

DL and WT reviewed a large amount of literature, conducted relevant data analysis, and drafted the manuscript. YYW and QG completed the mechanism diagram. YY, HWZ, YMZ and YW analyzed the relevance of the literature and provided the analysis report. YZ supervised the project and revised the manuscript. YKZ, HL and SL analyzed the data and revised the manuscript. HZ reviewed the article and provided revisions, formal analysis, and manuscript drafting. All authors contributed to the article and approved the submitted version.

## Funding

This study was supported by the Heilongjiang Province in Special Funding for Postdoctoral (LBH-Q20185), the Heilongjiang Provincial North Medicine and Function Food for Featured Discipline of Heilongjiang Province (2018-TSXK-02), the Technological Innovation Team Construction Project of Heilongjiang Provincial Department of Education (2021-KYYEF-0638), the Key Program of the Natural Science Foundation of Heilongjiang Province of China (ZD2022H006), the Joint Guidance Project of the Natural Science Foundation of Heilongjiang Province (LH2022H093), and the Basic Research Project of Fundamental Research Business Expenses of Education Department in Heilongjiang Province (No. 2022-KYYWF-0615).

## Conflict of interest

The authors declare that the research was conducted in the absence of any commercial or financial relationships that could be construed as a potential conflict of interest.

## Publisher's note



## References

1. Zhang C, Sheng J, Xie W, Luo X, Xue Y, Xu G, et al. Mechanism and basis of traditional Chinese medicine against obesity: Prevention and treatment strategies. *Front Pharmacol* (2021) 12:615895. doi: 10.3389/fphar.2021.615895

2. Aaseth J, Ellefsen S, Alehagen U, Sundfør T, Alexander J. Diets and drugs for weight loss and health in obesity - an update. *BioMed Pharmacother* (2021) 140:111789. doi: 10.1016/j.biopha.2021.111789

3. Wang L, Yu C, Li J, Tian Q, Du Y. Mechanism of action of acupuncture in obesity: A perspective from the hypothalamus. *Front Endocrinol (Lausanne)* (2021) 12:632324. doi: 10.3389/fendo.2021.632324

4. Piché M, Tchernof A, Després J. Obesity phenotypes, diabetes, and cardiovascular diseases. *Circ Res* (2020) 126(11):1477–500. doi: 10.1161/circresaha.120.316101

5. Fan Q, Xu F, Liang B, Zou X. The anti-obesity effect of traditional Chinese medicine on lipid metabolism. *Front Pharmacol* (2021) 12:696603. doi: 10.3389/fphar.2021.696603

6. Krentz A, Fujioka K, Hompesch M. Evolution of pharmacological obesity treatments: Focus on adverse side-effect profiles. *Diabetes Obes Metab* (2016) 18 (6):558–70. doi: 10.1111/dom.12657

7. Lin X, Li H. Obesity: Epidemiology, pathophysiology, and therapeutics. *Front Endocrinol (Lausanne)* (2021) 12:706978. doi: 10.3389/fendo.2021.706978

8. Cheng Z, Zhang L, Yang L, Chu H. The critical role of gut microbiota in obesity. *Front Endocrinol (Lausanne)* (2022) 13:1025706. doi: 10.3389/fendo.2022.1025706

9. Clarke G, Stilling R, Kennedy P, Stanton C, Cryan J, Dinan T. Minireview: Gut microbiota: the neglected endocrine organ. *Mol Endocrinol* (2014) 28(8):1221–38. doi: 10.1210/me.2014-1108

10. Jia Q, Xie Y, Lu C, Zhang A, Lu Y, Lv S, et al. Endocrine organs of cardiovascular diseases: Gut microbiota. *J Cell Mol Med* (2019) 23(4):2314–23. doi: 10.1111/jcmm.14164

11. Chen Y, Zhou J, Wang L. Role and mechanism of gut microbiota in human disease. *Front Cell Infect Microbiol* (2021) 11:625913. doi: 10.3389/fcimb.2021.625913

12. Wu Y, Peng X, Li X, Li D, Tan Z, Yu R. Sex hormones influence the intestinal microbiota composition in mice. *Front Microbiol* (2022) 13:964847. doi: 10.3389/fmicb.2022.964847

13. Gérard P. Gut microbiota and obesity. *Cell Mol Life Sci* (2016) 73(1):147–62. doi: 10.1007/s00018-015-2061-5

14. Thursby E, Juge N. Introduction to the human gut microbiota. *Biochem J* (2017) 474(11):1823–36. doi: 10.1042/bcj20160510

15. Fan Y, Pedersen O. Gut microbiota in human metabolic health and disease. *Nat Rev Microbiol* (2021) 19(1):55–71. doi: 10.1038/s41579-020-0433-9

16. Li C, Zhou K, Xiao N, Peng M, Tan Z. The effect of qiweibaizhu powder crude polysaccharide on antibiotic-associated diarrhea mice is associated with restoring intestinal mucosal bacteria. *Front Nutr* (2022) 9:952647. doi: 10.3389/fnut.2022.952647

17. Qiao B, Li X, Peng M, Hui H, Tan Z. Alteration of intestinal mucosal microbiota in mice with Chinese dampness-heat syndrom diarrhea by improper diet combined with high temperature and humidity environments. *Front Cell Infect Microbiol* (2022) 12:1096202. doi: 10.3389/fcimb.2022.1096202

18. He L, Long C, Liu Y, Guo Y, Xiao N, Tan Z. Effects of debaryomyces hansenii treatment on intestinal microorganisms in mice with antibiotics-induced diarrhea. *3 Biotech* (2017) 7(5):347. doi: 10.1007/s13205-017-0953-9

19. Long C, Liu Y, He L, Tan Q, Yu Z, Xiao N, et al. Bacterial lactase genes diversity in intestinal mucosa of mice with dysbacterial diarrhea induced by antibiotics. *3 Biotech* (2018) 8(3):176. doi: 10.1007/s13205-018-1191-5

20. Xie G, Tan K, Peng M, Long C, Li D, Tan Z. Bacterial diversity in intestinal mucosa of antibiotic-associated diarrhea mice. *3 Biotech* (2019) 9(12):444. doi: 10.1007/s13205-019-1967-2

21. Zhou K, Peng M, Deng N, Tan Z, Xiao N. Lactase bacteria in intestinal mucosa are associated with diarrhea caused by high-fat and high-protein diet. *BMC Microbiol* (2022) 22(1):226. doi: 10.1186/s12866-022-02647-2

22. Liu B, Liu X, Liang Z, Wang J. Gut microbiota in obesity. *World J Gastroenterol* (2021) 27(25):3837–50. doi: 10.3748/wjg.v27.i25.3837

23. Li X, Deng N, Zheng T, Qiao B, Peng M, Xiao N, et al. Importance of dendrobium officinale in improving the adverse effects of high-fat diet on mice associated with intestinal contents microbiota. *Front Nutr* (2022) 9:957334. doi: 10.3389/fnut.2022.957334

24. Wu Y, Zhang C, Shao H, Luo H, Tan Z. Characteristics of intestinal microbiota and enzyme activities in mice fed with lily bulb. *3 Biotech* (2021) 11(1):17. doi: 10.1007/s13205-020-02597-4

25. Shao H, Zhang C, Wang C, Tan Z. Intestinal mucosal bacterial diversity of antibiotic-associated diarrhea (AAD) mice treated with debaryomyces hansenii and qiweibaizhu powder. *3 Biotech* (2020) 10(9):392. doi: 10.1007/s13205-020-02383-2

26. Yuan Z, Zhang C, Peng X, Shu L, Long C, Tan Z. Intestinal microbiota characteristics of mice treated with folium senna decoction gavage combined with restraint and tail pinch stress. *3 Biotech* (2020) 10(4):180. doi: 10.1007/s13205-020-02172-x

27. Zhang C, Shao H, Peng X, Liu T, Tan Z. Microbiotal characteristics colonized in intestinal mucosa of mice with diarrhoea and repeated stress. *3 Biotech* (2020) 10(8):372. doi: 10.1007/s13205-020-02368-1

28. Long C, Liu Y, He L, Yu R, Li D, Tan Z, et al. Bacterial lactase genes diversity in intestinal mucosa of dysbacterial diarrhea mice treated with qiweibaizhu powder. *3 Biotech* (2018) 8(10):423. doi: 10.1007/s13205-018-1460-3

29. Xie G, Deng N, Zheng T, Peng X, Zhang S, Tan Z. Total glycosides contribute to the anti-diarrheal effects of qiwei baizhu powder *via* regulating gut microbiota and bile acids. *Front Cell Infect Microbiol* (2022) 12:945263. doi: 10.3389/fcimb.2022.945263

30. Li X, Zhang C, Tan Z, Yuan J. Network pharmacology-based analysis of gegenqinlian decoction regulating intestinal microbial activity for the treatment of diarrhea. *Evid Based Complement Alternat Med* (2021) 2021:5520015. doi: 10.1155/2021/5520015

31. Turnbaugh P, Hamady M, Yatsunenko T, Cantarel B, Duncan A, Ley R, et al. A core gut microbiome in obese and lean twins. *Nature* (2009) 457(7228):480–4. doi: 10.1038/nature07540

32. Wang P, Gao J, Ke W, Wang J, Li D, Liu R, et al. Resveratrol reduces obesity in high-fat diet-fed mice *via* modulating the composition and metabolic function of the gut microbiota. *Free Radic Biol Med* (2020) 156:83–98. doi: 10.1016/j.freeradbiomed.2020.04.013

33. Gomes A, Hoffmann C, Mota J. The human gut microbiota: Metabolism and perspective in obesity. *Gut Microbes* (2018) 9(4):308–25. doi: 10.1080/19490976.2018.1465157

34. Muscogiuri G, Cantone E, Cassarano S, Tuccinardi D, Barrea L, Savastano S, et al. Gut microbiota: A new path to treat obesity. *Int J Obes Suppl* (2019) 9(1):10–9. doi: 10.1038/s41367-019-0011-7

35. Wostmann B, Larkin C, Moriarty A, Bruckner-Kardoss E. Dietary intake, energy metabolism, and excretory losses of adult male germfree wistar rats. *Lab Anim Sci* (1983) 33(1):46–50.

36. Bäckhed F, Ding H, Wang T, Hooper L, Koh G, Nagy A, et al. The gut microbiota as an environmental factor that regulates fat storage. *Proc Natl Acad Sci U.S.A.* (2004) 101(44):15718–23. doi: 10.1073/pnas.0407076101

37. Le Chatelier E, Nielsen T, Qin J, Prifti E, Hildebrand F, Falony G, et al. Richness of human gut microbiome correlates with metabolic markers. *Nature* (2013) 500(7464):541–6. doi: 10.1038/nature12506

38. Liu R, Hong J, Xu X, Feng Q, Zhang D, Gu Y, et al. Gut microbiome and serum metabolome alterations in obesity and after weight-loss intervention. *Nat Med* (2017) 23(7):859–68. doi: 10.1038/nm.4358

39. Vallianou N, Stratigou T, Christodoulatos G, Dalamaga M. Understanding the role of the gut microbiome and microbial metabolites in obesity and obesity-associated metabolic disorders: Current evidence and perspectives. *Curr Obes Rep* (2019) 8(3):317–32. doi: 10.1007/s13679-019-00352-2

40. Moszak M, Szulińska M, Bogdański P. You are what you eat-the relationship between diet, microbiota, and metabolic disorders-a review. *Nutrients* (2020) 12(4):1096. doi: 10.3390/nu12041096

41. Merra G, Noce A, Marrone G, Cintoni M, Tarsitano M, Capacci A, et al. Influence of Mediterranean diet on human gut microbiota. *Nutrients* (2020) 13(1):7. doi: 10.3390/nu13010007

42. Qiao B, Li X, Zheng T, Tan Z. Different effects of lard and vegetable blend oil on intestinal microorganisms, enzyme activity and blood routine in mice. *J Oleo Sci* (2022) 71(2):301–10. doi: 10.5650/jos.ess21247

43. Turnbaugh P, Ley R, Mahowald M, Magrini V, Mardis E, Gordon J. An obesity-associated gut microbiome with increased capacity for energy harvest. *Nature* (2006) 444(7122):1027–31. doi: 10.1038/nature05414

44. Meijnikman A, Aydin O, Prodan A, Tremaroli V, Herrema H, Levin E, et al. Distinct differences in gut microbial composition and functional potential from lean to morbidly obese subjects. *J Intern Med* (2020) 288(6):699–710. doi: 10.1111/joim.13137

45. Kobyliak N, Virchenko O, Falalyeyeva T. Pathophysiological role of host microbiota in the development of obesity. *Nutr J* (2016) 15:43. doi: 10.1186/s12937-016-0166-9

46. Petersen C, Bell R, Klag K, Lee S, Soto R, Ghazaryan A, et al. T Cell-mediated regulation of the microbiota protects against obesity. *Science* (2019) 365(6451):eaat9351. doi: 10.1126/science.aat9351

47. Everard A, Belzer C, Geurts L, Ouwerkerk J, Druart C, Bindels L, et al. Cross-talk between akkermansia muciniphila and intestinal epithelium controls diet-induced obesity. *Proc Natl Acad Sci U.S.A.* (2013) 110(22):9066–71. doi: 10.1073/pnas.1219451110

48. Wu D, Wang H, Xie L, Hu F. Cross-talk between gut microbiota and adipose tissues in obesity and related metabolic diseases. *Front Endocrinol (Lausanne)* (2022) 13:908868. doi: 10.3389/fendo.2022.908868

49. Koh A, De Vadder F, Kovatcheva-Datchary P, Bäckhed F. From dietary fiber to host physiology: Short-chain fatty acids as key bacterial metabolites. *Cell* (2016) 165(6):1332–45. doi: 10.1016/j.cell.2016.05.041

50. Canfora E, Meex R, Venema K, Blaak E. Gut microbial metabolites in obesity, NAFLD and T2DM. *Nat Rev Endocrinol* (2019) 15(5):261–73. doi: 10.1038/s41574-019-0156-z

51. Li C, Xiao N, Deng N, Li D, Tan Z, Peng M. Dose of sucrose affects the efficacy of qiweibaizhu powder on antibiotic-associated diarrhea: Association with intestinal mucosal microbiota, short-chain fatty acids, IL-17, and MUC2. *Front Microbiol* (2023) 14:1108398. doi: 10.3389/fmicb.2023.1108398

52. Zhang L, Liu C, Jiang Q, Yin Y. Butyrate in energy metabolism: There is still more to learn. *Trends Endocrinol Metab* (2021) 32(3):159–69. doi: 10.1016/j.tem.2020.12.003

53. Cani P, Van Hul M, Lefort C, Depommier C, Rastelli M, Everard A. Microbial regulation of organismal energy homeostasis. *Nat Metab* (2019) 1(1):34–46. doi: 10.1038/s42255-018-0017-4

54. Lu Y, Fan C, Li P, Lu Y, Chang X, Qi K. Short chain fatty acids prevent high-fat-diet-induced obesity in mice by regulating G protein-coupled receptors and gut microbiota. *Sci Rep* (2016) 6:37589. doi: 10.1038/srep37589

55. Tirosh A, Calay E, Tuncman G, Claiborn K, Inouye K, Eguchi K, et al. The short-chain fatty acid propionate increases glucagon and FABP4 production, impairing insulin action in mice and humans. *Sci Transl Med* (2019) 11(489):eaav0120. doi: 10.1126/scitranslmed.aav0120

56. Engevik M, Luck B, Visuthranukul C, Ihekweazu F, Engevik A, Shi Z, et al. Human-derived bifidobacterium dentium modulates the mammalian serotonergic system and gut-brain axis. *Cell Mol Gastroenterol Hepatol* (2021) 11(1):221–48. doi: 10.1016/j.jcmgh.2020.08.002

57. Generoso J, Giridharan V, Lee J, Macedo D, Barichello T. The role of the microbiota-gut-brain axis in neuropsychiatric disorders. *Braz J Psychiatry* (2021) 43(3):293–305. doi: 10.1590/1516-4446-2020-0987

58. Torres-Fuentes C, Schellekens H, Dinan T, Cryan J. The microbiota-gut-brain axis in obesity. *Lancet Gastroenterol Hepatol* (2017) 2(10):747–56. doi: 10.1016/s2468-1253(17)30147-4

59. Oduro-Donkor D, Turner M, Farnaud S, Renshaw D, Kyrou I, Hanson P, et al. Modification of fecal microbiota as a mediator of effective weight loss and metabolic benefits following bariatric surgery. *Expert Rev Endocrinol Metab* (2020) 15(5):363–73. doi: 10.1080/17446651.2020.1801412

60. Cunningham A, Stephens J, Harris D. A review on gut microbiota: a central factor in the pathophysiology of obesity. *Lipids Health Dis* (2021) 20(1):65. doi: 10.1186/s12944-021-01491-z

61. Naraoka Y, Yamaguchi T, Hu A, Akimoto K, Kobayashi H. Short chain fatty acids upregualte adipokine production in type 2 diabetes-derived human adipocytes. *Acta Endocrinol (Buchar)* (2018) 14(3):287–93. doi: 10.4183/aeb.2018.287

62. Li Z, Yi C, Katiraei S, Kooijman S, Zhou E, Chung C, et al. Butyrate reduces appetite and activates brown adipose tissue *via* the gut-brain neural circuit. *Gut* (2018) 67(7):1269–79. doi: 10.1136/gutjnl-2017-314050

63. Frost G, Sleeth M, Sahuri-Arisoylu M, Lizarbe B, Cerdan S, Brody L, et al. The short-chain fatty acid acetate reduces appetite *via* a central homeostatic mechanism. *Nat Commun* (2014) 5:3611. doi: 10.1038/ncomms4611

64. Jing N, Liu X, Jin M, Yang X, Hu X, Li C, et al. Fubrick tea attenuates high-fat diet induced fat deposition and metabolic disorder by regulating gut microbiota and caffeine metabolism. *Food Funct* (2020) 11(8):6971–86. doi: 10.1039/d0fo01282c

65. Villaret A, Galitzky J, Decaunes P, Estève D, Marques MA, Sengenès C, et al. Adipose tissue endothelial cells from obese human subjects: Differences among depots in angiogenic, metabolic, and inflammatory gene expression and cellular senescence. *Diabetes* (2010) 59(11):2755–63. doi: 10.2337/db10-0398

66. Goldberg I. 2017 George Lyman duff memorial lecture: Fat in the blood, fat in the artery, fat in the heart: Triglyceride in physiology and disease. *Arterioscler Thromb Vasc Biol* (2018) 38(4):700–6. doi: 10.1161/atvbaha.117.309666

67. Jiao A, Yu B, He J, Yu J, Zheng P, Luo Y, et al. Sodium acetate, propionate, and butyrate reduce fat accumulation in mice *via* modulating appetite and relevant genes. *Nutrition* (2021) 87-88:111198. doi: 10.1016/j.nut.2021.111198

68. Cuevas-Sierra A, Ramos-Lopez O, Riezu-Boj J, Milagro F, Martinez J. Diet, gut microbiota, and obesity: Links with host genetics and epigenetics and potential applications. *Adv Nutr* (2019) 10(suppl_1):S17–s30. doi: 10.1093/advances/nmy078

69. Steinert R, Beglinger C, Langhans W. Intestinal GLP-1 and satiation: from man to rodents and back. *Int J Obes (Lond)* (2016) 40(2):198–205. doi: 10.1038/ijo.2015.172

70. Bäckhed F, Manchester J, Semenkovich C, Gordon J. Mechanisms underlying the resistance to diet-induced obesity in germ-free mice. *Proc Natl Acad Sci U.S.A.* (2007) 104(3):979–84. doi: 10.1073/pnas.0605374104

71. Al Bander Z, Nitert M, Mousa A, Naderpoor N. The gut microbiota and inflammation: An overview. *Int J Environ Res Public Health* (2020) 17(20):7618. doi: 10.3390/ijerph17207618

72. Soltani N, Esmaeil N, Marandi S, Hovsepian V, Momen T, Shahsanai A, et al. Assessment of the effect of short-term combined high-intensity interval training on TLR4, NF-κB and IRF3 expression in young overweight and obese girls. *Public Health Genomics* (2020) 23(1-2):26–36. doi: 10.1159/000506057

73. Ridaura V, Faith J, Rey F, Cheng J, Duncan A, Kau A, et al. Gut microbiota from twins discordant for obesity modulate metabolism in mice. *Science* (2013) 341 (6150):1241214. doi: 10.1126/science.1241214

74. Liu J, Qiao B, Deng N, Wu Y, Li D, Tan Z. The diarrheal mechanism of mice with a high-fat diet in a fatigued state is associated with intestinal mucosa microbiota. *3 Biotech* (2023) 13(3):77. doi: 10.1007/s13205-023-03491-5

75. Li M, van Esch B, Wagenaar G, Garssen J, Folkerts G, Henricks P. Pro- and anti-inflammatory effects of short chain fatty acids on immune and endothelial cells. *Eur J Pharmacol* (2018) 831:52–9. doi: 10.1016/j.ejphar.2018.05.003

76. Vatanen T, Franzosa E, Schwager R, Tripathi S, Arthur T, Vehik K, et al. The human gut microbiome in early-onset type 1 diabetes from the TEDDY study. *Nature* (2018) 562(7728):589–94. doi: 10.1038/s41586-018-0620-2

77. Kelly C, Zheng L, Campbell E, Saeedi B, Scholz C, Bayless A, et al. Crosstalk between microbiota-derived short-chain fatty acids and intestinal epithelial HIF augments tissue barrier function. *Cell Host Microbe* (2015) 17(5):662–71. doi: 10.1016/j.chom.2015.03.005

78. Fukuda S, Toh H, Hase K, Oshima K, Nakanishi Y, Yoshimura K, et al. Bifidobacteria can protect from enteropathogenic infection through production of acetate. *Nature* (2011) 469(7331):543–7. doi: 10.1038/nature09646

79. Park J, Kim M, Kang S, Jannasch A, Cooper B, Patterson J, et al. Short-chain fatty acids induce both effector and regulatory T cells by suppression of histone deacetylases and regulation of the mTOR-S6K pathway. *Mucosal Immunol* (2015) 8 (1):80–93. doi: 10.1038/mi.2014.44

80. Iyengar N, Gucalp A, Dannenberg A, Hudis C. Obesity and cancer mechanisms: Tumor microenvironment and inflammation. *J Clin Oncol* (2016) 34(35):4270–6. doi: 10.1200/jco.2016.67.4283

81. Aguilar E, Leonel A, Teixeira L, Silva A, Silva J, Pelaez J, et al. Butyrate impairs atherogenesis by reducing plaque inflammation and vulnerability and decreasing NFκB activation. *Nutr Metab Cardiovasc Dis* (2014) 24(6):606–13. doi: 10.1016/j.numecd.2014.01.002

82. Zhang M, Zhao J, Deng J, Duan Z, Zhu C, Fan D. The protective effect of protopanaxatriol-type saponin on intestinal health in antibiotic-treated mice. *Food Funct* (2019) 10(7):4124–33. doi: 10.1039/c9fo00242a

83. Song M, Lim S, Wang J, Kim H. The root of atractylodes macrocephala koidzumi prevents obesity and glucose intolerance and increases energy metabolism in mice. *Int J Mol Sci* (2018) 19(1):278. doi: 10.3390/ijms19010278

84. Cai W, Xu J, Li G, Liu T, Guo X, Wang H, et al. Ethanol extract of propolis prevents high-fat diet-induced insulin resistance and obesity in association with modulation of gut microbiota in mice. *Food Res Int* (2020) 130:108939. doi: 10.1016/j.foodres.2019.108939

85. Wang C, Yen J, Cheng Y, Lin C, Hsieh C, Gau R, et al. Polygala tenuifolia extract inhibits lipid accumulation in 3T3-L1 adipocytes and high-fat diet-induced obese mouse model and affects hepatic transcriptome and gut microbiota profiles. *Food Nutr Res* (2017) 61(1):1379861. doi: 10.1080/16546628.2017.1379861

86. Wang G, Sun C, Xie B, Wang T, Liu H, Chen X, et al. Cordyceps guangdongensis lipid-lowering formula alleviates fat and lipid accumulation by modulating gut microbiota and short-chain fatty acids in high-fat diet mice. *Front Nutr* (2022) 9:1038740. doi: 10.3389/fnut.2022.1038740

87. Liu M, Huang Y, Zhang T, Tan L, Lu X, Qin J. Lingguizhugan decoction attenuates diet-induced obesity and hepatosteatosis *via* gut microbiota. *World J Gastroenterol* (2019) 25(27):3590–606. doi: 10.3748/wjg.v25.i27.3590

88. Wu R, Zhao D, An R, Wang Z, Li Y, Shi B, et al. Linggui zhugan formula improves glucose and lipid levels and alters gut microbiota in high-fat diet-induced diabetic mice. *Front Physiol* (2019) 10:918. doi: 10.3389/fphys.2019.00918

89. Ning Y, Gong Y, Zheng T, Xie Y, Yuan S, Ding W. Lingguizhugan decoction targets intestinal microbiota and metabolites to reduce insulin resistance in high-fat diet rats. *Diabetes Metab Syndr Obes* (2022) 15:2427–42. doi: 10.2147/dmso.S370492

90. Zhao T, Zhan L, Zhou W, Chen W, Luo J, Zhang L, et al. The effects of erchen decoction on gut microbiota and lipid metabolism disorders in zucker diabetic fatty rats. *Front Pharmacol* (2021) 12:647529. doi: 10.3389/fphar.2021.647529

91. Xiao S, Zhang Z, Chen M, Zou J, Jiang S, Qian D, et al. Xiexin tang ameliorates dyslipidemia in high-fat diet-induced obese rats *via* elevating gut microbiota-derived short chain fatty acids production and adjusting energy metabolism. *J Ethnopharmacol* (2019) 241:112032. doi: 10.1016/j.jep.2019.112032

92. Sun R, Huang W, Xiao Y, Wang D, Mu G, Nan H, et al. Shenlian (SL) decoction, a traditional Chinese medicine compound, may ameliorate blood glucose *via* mediating the gut microbiota in db/db mice. *J Diabetes Res* (2022) 2022:7802107. doi: 10.1155/2022/7802107

93. Neyrinck A, Sánchez C, Rodriguez J, Cani P, Bindels L, Delzenne N. Prebiotic effect of berberine and curcumin is associated with the improvement of obesity in mice. *Nutrients* (2021) 13(5):1436. doi: 10.3390/nu13051436

94. Casanova-Martí À, Serrano J, Portune K, Sanz Y, Blay M, Terra X, et al. Grape seed proanthocyanidins influence gut microbiota and enteroendocrine secretions in female rats. *Food Funct* (2018) 9(3):1672–82. doi: 10.1039/c7fo02028g

95. Lin N, Cai D, Jin D, Chen Y, Shi J. Ginseng panaxoside Rb1 reduces body weight in diet-induced obese mice. *Cell Biochem Biophys* (2014) 68(1):189–94. doi: 10.1007/s12013-013-9688-3

96. Ren F, Meng C, Chen W, Chen H, Chen W. Ganoderma amboinense polysaccharide prevents obesity by regulating gut microbiota in high-fat-diet mice. *Food Biosci* (2021) 42:101107. doi: 10.1016/j.fbio.2021.101107

97. Cheng L, Shi L, He C, Wang C, Lv Y, Li H, et al. Rutin-activated adipose tissue thermogenesis is correlated with increased intestinal short-chain fatty acid levels. *Phytother Res* (2022) 36(6):2495–510. doi: 10.1002/ptr.7462

98. Zhao Q, Fu Y, Zhang F, Wang C, Yang X, Bai S, et al. Heat-treated adzuki bean protein hydrolysates reduce obesity in mice fed a high-fat diet *via* remodeling gut microbiota and improving metabolic function. *Mol Nutr Food Res* (2022) 66(8): e2100907. doi: 10.1002/mnfr.202100907

99. Wang J, Bose S, Kim H, Han K, Kim H. Fermented rhizoma atractylodis macrocephalae alleviates high fat diet-induced obesity in association with regulation of intestinal permeability and microbiota in rats. *Sci Rep* (2015) 5:8391. doi: 10.1038/srep08391

100. Cao Y, Pan Q, Cai W, Shen F, Chen G, Xu L, et al. Modulation of gut microbiota by berberine improves steatohepatitis in high-fat diet-fed BALB/C mice. *Arch Iran Med* (2016) 19(3):197–203. doi: 10.1088/1475-7516/2016/03/008

101. Sun S, Wang K, Ma K, Bao L, Liu H. An insoluble polysaccharide from the sclerotium of poria cocos improves hyperglycemia, hyperlipidemia and hepatic steatosis in ob/ob mice *via* modulation of gut microbiota. *Chin J Nat Med* (2019) 17 (1):3–14. doi: 10.1016/s1875-5364(19)30003-2

102. Sang T, Guo C, Guo D, Wu J, Wang Y, Wang Y, et al. Suppression of obesity and inflammation by polysaccharide from sporoderm-broken spore of ganoderma lucidum *via* gut microbiota regulation. *Carbohydr Polymers* (2021) 256:117594. doi: 10.1016/j.carbpol.2020.117594

103. Gao B, Wang R, Peng Y, Li X. Effects of a homogeneous polysaccharide from sijunzi decoction on human intestinal microbes and short chain fatty acids *in vitro*. *J Ethnopharmacol* (2018) 224:465–73. doi: 10.1016/j.jep.2018.06.006

104. Zhang Y, Tang K, Deng Y, Chen R, Liang S, Xie H, et al. Effects of shenling baizhu powder herbal formula on intestinal microbiota in high-fat diet-induced NAFLD rats. *BioMed Pharmacother* (2018) 102:1025–36. doi: 10.1016/j.biopha.2018.03.158

105. Cao Y, Yao G, Sheng Y, Yang L, Wang Z, Yang Z, et al. JinQi jiangtang tablet regulates gut microbiota and improve insulin sensitivity in type 2 diabetes mice. *J Diabetes Res* (2019) 2019:1872134. doi: 10.1155/2019/1872134

106. Li X, Peng X, Guo K, Tan Z. Bacterial diversity in intestinal mucosa of mice fed with dendrobium officinale and high-fat diet. *3 Biotech* (2021) 11(1):22. doi: 10.1007/s13205-020-02558-x

107. Guo K, Xu S, Zhang Q, Peng M, Yang Z, Li W, et al. Bacterial diversity in the intestinal mucosa of mice fed with asparagus extract under high-fat diet condition. *3 Biotech* (2020) 10(5):228. doi: 10.1007/s13205-020-02225-1

108. Guo K, Yan Y, Zeng C, Shen L, He Y, Tan Z. Study on baohe pills regulating intestinal microecology and treating diarrhea of high-fat and high-protein diet mice. *BioMed Res Int* (2022) 2022:6891179. doi: 10.1155/2022/6891179

109. Dong W, Mao Y, Xiang Z, Zhu J, Wang H, Wang A, et al. Traditional Chinese medicine formula jian pi tiao gan yin reduces obesity in mice by modulating the gut microbiota and fecal metabolism. *Evid Based Complement Alternat Med* (2022) 2022:9727889. doi: 10.1155/2022/9727889

110. Hussain A, Yadav M, Bose S, Wang J, Lim D, Song Y, et al. Daesiho-tang is an effective herbal formulation in attenuation of obesity in mice through alteration of gene expression and modulation of intestinal microbiota. *PloS One* (2016) 11(11):e0165483. doi: 10.1371/journal.pone.0165483

111. Gao Y, Sun J, Zhang Y, Shao T, Li H, Wang M, et al. Effect of a traditional Chinese medicine formula (CoTOL) on serum uric acid and intestinal flora in obese hyperuricemic mice inoculated with intestinal bacteria. *Evid Based Complement Alternat Med* (2020) 2020:8831937. doi: 10.1155/2020/8831937

112. Gong S, Ye T, Wang M, Wang M, Li Y, Ma L, et al. Traditional Chinese medicine formula kang shuai lao pian improves obesity, gut dysbiosis, and fecal metabolic disorders in high-fat diet-fed mice. *Front Pharmacol* (2020) 11:297. doi: 10.3389/fphar.2020.00297

113. Wang Z, Lu J, Zhou J, Sun W, Qiu Y, Chen W, et al. Modulation of the gut microbiota by shen-Yan-Fang-Shuai formula improves obesity induced by high-fat diets. *Front Microbiol* (2020) 11:564376. doi: 10.3389/fmicb.2020.564376

114. Li X, Zhang C, Hui H, Tan Z. Effect of gegenqinlian decoction on intestinal mucosal flora in mice with diarrhea induced by high temperature and humidity treatment. *3 Biotech* (2021) 11(2):83. doi: 10.1007/s13205-020-02628-0

frontiers | Frontiers in Endocrinology

TYPE Review
PUBLISHED 09 March 2023
DOI 10.3389/fendo.2023.1151723



OPEN ACCESS

EDITED BY
Zhoujin Tan,
Hunan University of Chinese Medicine, China

REVIEWED BY
Zipeng Gong,
Guizhou Medical University, China
Dahong Li,
Shenyang Pharmaceutical University, China
Su Min,
Changsha Medical University, China

*CORRESPONDENCE
Xiaoliang Li
lixiaoliang-1984@163.com

SPECIALTY SECTION
This article was submitted to Gut Endocrinology, a section of the journal Frontiers in Endocrinology

RECEIVED 26 January 2023
ACCEPTED 20 February 2023
PUBLISHED 09 March 2023

CITATION
Liu J, Liu Y and Li X (2023) Effects of intestinal flora on polycystic ovary syndrome.
*Front. Endocrinol.* 14:1151723.
doi: 10.3389/fendo.2023.1151723



# Effects of intestinal flora on polycystic ovary syndrome

Jiayue Liu[1,2,3], Ying Liu[1,2,3] and Xiaoliang Li[1,2,3]*

[1]Key Laboratory of Tropical Translational Medicine of Ministry of Education, Hainan Provincial Key Laboratory for Research and Development of Tropical Herbs, Haikou Key Laboratory of Li Nationality Medicine, School of Pharmacy, Hainan Medical University, Haikou, China, [2]Key Laboratory of Tropical Cardiovascular Diseases Research of Hainan Province, Cardiovascular Diseases Institute of the First Affiliated Hospital, Hainan Medical University, Haikou, China, [3]College of Pharmacy, Heilongjiang Provincial Key Laboratory of New Drug Development and Pharmacotoxicological Evaluation, Jiamusi University, Jiamusi, Heilongjiang, China

Polycystic ovary syndrome (PCOS) is a common endocrine disorder in women of reproductive age. Its clinical characteristics are mainly oligo-ovulation or anovulation, hyperandrogenemia (HA) and insulin resistance (IR). PCOS is considered to be one of the main causes of infertility in women of childbearing age, and its pathogenesis is still unclear. Intestinal flora, known as the "second genome" of human beings, is closely related to metabolic diseases, immune diseases and infectious diseases. At the same time, mounting evidence suggests that intestinal flora can regulate insulin synthesis and secretion, affect androgen metabolism and follicular development, and is involved in the occurrence of chronic inflammation and obesity. The imbalance of intestinal flora is caused by the abnormal interaction between intestinal flora and host cells caused by the change of intestinal microbial diversity, which is related to the occurrence and development of PCOS. The adjustment of intestinal flora may be a potential direction for the treatment of PCOS.

KEYWORDS

**intestinal flora, polycystic ovary syndrome, hyperandrogenemia, insulin resistance, chronic inflammation, obesity**

## 1 Introduction

PCOS is a common endocrine disorder in women. The prevalence rate of PCOS among women of childbearing age is 5% ~ 10% globally, and it is increasing year by year (1–3). PCOS are mainly manifested by irregular menstruation or infertility, hirsutism, acne, obesity, HA, IR, enlargement and polycystic changes of the ovaries (4–6). Currently, the Rotterdam criteria are commonly used for the diagnosis of PCOS in clinical practice. According to this criteria, the serum androgen level of patients with PCOS is remarkable increased, ovulation is significantly decreased, and polycystic ovary appear. If two of the above criteria are met, they can be classified as PCOS (7). Besides, PCOS is a high risk factor for diabetes, metabolic syndrome, endometrial cancer, cardiovascular and cerebrovascular diseases and other diseases, which seriously affects the health of women (8–10). Up to now, it is generally believed that PCOS is a disease caused by multiple factors. Its etiology and pathogenesis usually involve genetics, inflammatory factors,

intestinal flora, endocrine hormones and IR (11–13). In recent years, the study of intestinal flora in patients with PCOS has attracted widespread attention, and it has been found that intestinal flora plays a key role in the occurrence and development of PCOS (14, 15).

The human gut is home to trillions of microorganisms, including bacteria, archaea, fungi, protists and viruses, of which bacteria are the main "residents" (16, 17). These bacteria contain 800 species and more than 7,000 strains, about 1014, with a total mass of 1 ~ 2 kg, which is known as the second genome of human (18). The microorganisms living in the gastrointestinal system of the host mainly rely on the digestion of the food residues in the host body to provide energy for themselves, and these microorganisms together with their living environment constitute the intestinal microecosystem (19–21). When the number of harmful bacteria in the gut increases, it will cause physical discomfort, and even cause serious inflammatory and immune responses (22). When the body's metabolic dysfunction, it is easy to lead to the loss of bacteria with protective effect in the intestinal tract, which will cause changes in the composition of microorganisms in the intestine, and finally, the intestinal barrier is destroyed. Recent studies have shown that changes in intestinal flora are common in patients with PCOS. Moreover, the imbalance of intestinal microecology is related to the occurrence and progression of PCOS, and intestinal flora is involved in the pathological links of PCOS, such as HA, IR, chronic inflammation, obesity, etc (23–26). Based on the etiology and pathogenesis of PCOS in recent years, this article reviewed the research progress of the relationship between intestinal flora and PCOS.

# 2 Relationship between intestinal microecological disorders and HA in PCOS

## 2.1 HA and PCOS

The abnormality of sex hormones is an important feature of PCOS, in which the clinical or biochemical manifestations of HA are the main, which is also belong to the core pathological manifestations of PCOS. Hormonal abnormalities in PCOS patients are mainly manifested by elevated testosterone levels (27). Some scholars pointed out that the possibility of PCOS caused by excessive androgen secretion is 82% through the study of more than 1200 women with high androgen levels (3). The synthesis of androgens in women is closely related to the hypothalamus-pituitary-ovarian axis. The hypothalamus secretes gonadotropin-releasing hormone (GnRH), which leads to the release of luteinizing hormone (LH) and follicle-stimulating hormone (FSH). LH acts on theca cells to synthesize androgen, while FSH acts on granulosa cells to convert androgen into estrogen (28). The mechanism of androgen increase is that LH stimulates the transformation of cholesterol in the follicular membrane cells into pregnenolone through cytochrome P450 side chain lyase, which in turn synthesizes androstenedione, and then finally convert into testosterone *via* 17P-hydroxysteroid dehydrogenase (29). The androgen in thecal cells diffuses to granulosa cells, FSH stimulates aromatase activity located in granulosa cells, and eventually converts it into estradiol. The increase of LH level can not only increase the androgen from the ovary, but also reduce the FSH level through the negative feedback effect of estrogen, resulting in leads to the decrease of aromatase activity and the reduction of androgen to estrogen conversion. However, the exposure of immature oocytes to high androgen levels will cause follicular growth arrest or even atresia, which is the occurrence of ovulation disorder (30). Similarly, low level of FSH and insufficient conversion of estradiol also lead to the occurrence of this process (31). In addition, in the occurrence and development of PCOS, HA and IR are closely connected and promote each other, eventually forming a vicious cycle (32).

## 2.2 Relationship between intestinal flora and HA in PCOS

Gut microbiota can change in response to changes in hormone levels, which in turn affect sex hormone levels in the body. The research on the relationship between sex hormones and intestinal flora mostly focused on the serum testosterone. It was found that serum testosterone and hirsutism were negatively correlated with α diversity of flora (33, 34), while the level of free testosterone was correlated to the ratio of *Firmicutes/Bacteroidetes* (35). In the study of PCOS mouse model induced by letrozole, HA was found to reduce the species and the number of bacteria in the large intestine of mice. The main results showed that the number of *Bacteroides* decreased, the number of *Firmicutes* increased, body mass, fat mass and blood glucose level increased compared with the control group, indicating that HA can significantly change the intestinal flora (36). In a non-obese diabetic mouse model, it was found that the microbial changes in the intestinal flora could affect the sex hormone level of mice. Transplanting the intestinal flora of mature male mice into the body of immature female mice increased testosterone levels in the female mice (37). In another study, the serum testosterone level of mice fed with lactobacillus was remarkably higher than that of untreated mice. At the same time, the testis of mice was significantly enlarged, the number of spermatogenesis and testicular interstitial cells increased. This study indicated that the change of intestinal flora can regulate the serum testosterone level, affect the change of metabonomics, and promote the occurrence of islet inflammation (38). The above studies showed that HA may interact with intestinal flora in the pathophysiological process of PCOS. The intestinal flora not only affects the level of androgen, but is regulated by androgen in turn, as shown in Figure 1.

# 3 Relationship between intestinal microecological disorders and IR in PCOS

## 3.1 IR and PCOS

IR is one of the pathophysiological mechanisms leading to PCOS. 50%-70% of PCOS patients are accompanied by IR and compensatory hyperinsulinemia (32, 39, 40). Insulin is a polypeptide secreted by pancreatic β cells, consisting of 51 amino acids. Its physiological function is to regulate the metabolism and gene expression of the

body by activating PI3K/PKB and MAPK/Ras signal pathways after binding to insulin receptor (41). When the insulin receptor and corresponding signal pathway are interfered, the sensitivity of peripheral tissue to insulin decreases, which leads to the obstruction of glucose utilization in peripheral tissues. In order to regulate the body's blood sugar level, the body will secrete insulin compensatively, resulting in high blood insulin level, that is, IR. Glucose metabolism can directly provide energy for follicular growth. Therefore, abnormal glucose metabolism caused by IR will affect follicular growth and ovulation in PCOS (40), which inevitably affects the normal physiological function of ovary. The increase of fasting insulin level can trigger the insulin receptor of the pituitary gland and stimulate the secretion of LH by the pituitary. In addition, IR can also enhance the effect of cytochrome P450C17a enzyme in theca cells through insulin-like growth factor to improve the level of androgen (42). The elevated androgen can cause symptoms such as hirsutism, acne and alopecia in PCOS patients. More seriously, the increase of local androgen in the ovary can cause premature follicular atresia and the formation of dominant follicles, resulting in ovulation dysfunction. Meanwhile, the increase of androgen level further promotes the development of IR, thus forming a vicious cycle and aggravating the process of PCOS.

## 3.2 Relationship between intestinal flora and IR in PCOS

In 2004, Gordon research team in the United States transplanted intestinal flora of conventional mouse into germ-free mouse. In the same feeding conditions, the body fat of sterile mice increased and IR appeared, which was the first evidence that intestinal flora was related to IR (43). The study showed (44) that compared with normal adult women, PCOS patients had intestinal flora disorder, intestinal mucosal barrier damage, increased intestinal wall permeability, and significantly increased endotoxemia related indicators. Insulin sensitivity is increased in patients with metabolic syndrome who are transplanted with healthy human flora (45). One study showed that the degree of tyrosine phosphorylation of insulin receptors in PCOS patients with IR was significantly lower than that in PCOS patients without IR, which indicated that PCOS patients with IR had defects in their own insulin receptor phosphorylation (46). It has also been suggested that intestinal flora can also affect insulin sensitivity through the inflammatory response mediated by branched amino acids (BCAAs) (15). Some scholars (47) revealed the relationship between intestinal flora and BCAAs, and found that *Prevotella* in human gut was involved in the synthesis of BCAAs. Zhang CM et al. (48) found that the levels of leucine and valine in follicular fluid of PCOS patients with IR were significantly increased. In this regard, they speculated that the disorder of amino acid metabolism would aggravate IR by altering glucose metabolism or inducing inflammation. All the above studies suggest that IR is correlated with the disruption of intestinal flora. Changes in intestinal flora can lead to increased permeability of the intestinal wall and the production of endotoxin factors, which enter the systemic circulation to activate the immune system. Furthermore, the c-jun amino-terminal kinase signaling pathway can be activated by nuclear factor κB and mitogen-activated protein kinases signaling pathways. And then, it causes the increase of serine phosphorylation of insulin receptor substrate and the decrease of tyrosine phosphorylation, leading to the disorder of insulin metabolism and triggering IR (49). IR caused by intestinal flora disturbance leads to abnormal glucose metabolism, HA and follicular dysplasia of PCOS. IR, in turn, exacerbates the disruption of the intestinal flora, which eventually causes the ovaries to produce more androgens, affecting the normal development of follicles, as shown in Figure 2.

# 4 Relationship between intestinal microecological disorders and chronic inflammation in PCOS

## 4.1 Chronic inflammation and PCOS

The view that the patients with PCOS have chronic low-grade inflammation was first put forward by Kelly et al. (50), who believed

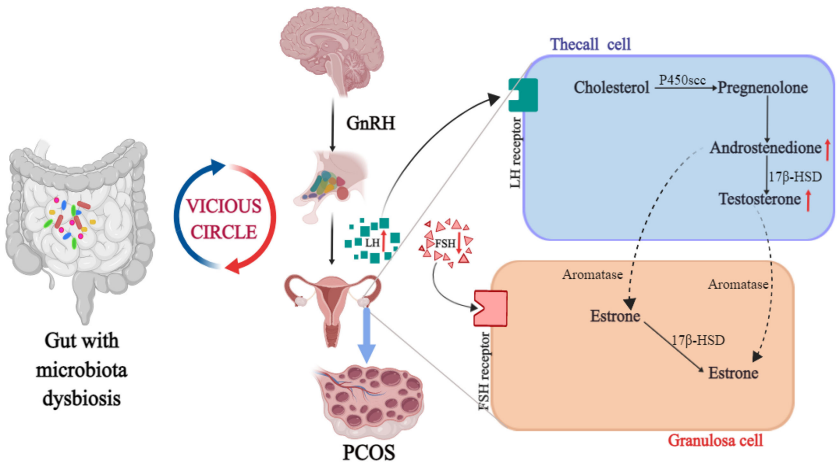


FIGURE 1
The intrinsic relationship between HA, intestinal flora and PCOS.

that it was related to IR and abdominal obesity. In recent years, studies have shown that the chronic inflammatory state of PCOS is not only manifested in the infiltration of macrophages and lymphocytes in the local pathology of ovary of patients with PCOS, but also the changes in the level of relevant inflammatory factors *in vivo*, such as hypersensitive C-reactive protein, interleukin-6, tumor necrosis factor, etc (50, 51). Inflammatory factors can affect insulin signal transduction by activating JNK, changing the phosphorylation level of insulin receptors, and blocking the expression of glucose transporter 4 (52, 53). In addition, the activation of JNK also promotes NF-κB signaling pathway in the islet, which in turn stimulates the production of more pro-inflammatory cytokines. Therefore, this vicious cycle of inflammatory cytokines will lead to islet β-cell dysfunction (54). In addition to inducing IR through a common signaling pathway, inflammatory factors can also stimulate the body to produce a large number of reactive oxygen species, which directly damage the insulin beta-cell sensitive to ROS, resulting in the reduction of the number of insulin beta cells or loss of function, and then lead to the occurrence of IR (55). Some studies have confirmed that the degree of oxidative stress and the level of inflammatory factors in patients with PCOS are positively correlated with the level of androgen (56). More directly, various inflammatory factors can trigger the production of excessive ovarian androgens or inhibit the aromatization of androgen into estrogen (57, 58). Obesity is a metabolic state characterized by chronic inflammation. In obese women with PCOS, the levels of some inflammatory mediators such as TNF-α, IL-6 and CRP are high, and they aggravate the inflammatory state of patients with PCOS by activating IKK signaling pathway (59, 60). In conclusion, the increased expression levels of some pro-inflammatory cytokines in patients with PCOS are also closely related to metabolic disorders such as IR, HA and obesity. Therefore, the pro-inflammatory cytokines have a certain influence on patients with PCOS directly or indirectly, and interact with other factors to aggravate the disease of PCOS.

## 4.2 Relationship between intestinal flora and chronic inflammation in PCOS

The occurrence of chronic inflammation is related to the changes of intestinal flora to some extent. The inflammatory factors generated by chronic inflammation may directly act on the hypothalamic-pituitary-gonadal axis, thus affecting the process of follicular development, maturation and ovulation in patients with PCOS. Cani et al. (61) proposed for the first time that "endotoxemia" produced by intestinal flora may be an important factor to initiate inflammatory activities. Xue et al. (62) found that in the PCOS mouse model induced by DHEA and high fat, the ovarian inflammatory indexes including TNF-α, IL-6 and IL-17A in the inulin group were significantly reduced compared with the model group. According to the sequencing and analysis of intestinal flora, compared with the model group, the number of *bifidobacterium* in the inulin group was increased. The correlation analysis also proved that intestinal flora was related to inflammatory factors, and inulin can alleviate the inflammatory state of PCOS by anti-inflammatory and improving intestinal microflora. A high fat diet for 4 weeks increased plasma LPS concentrations by two to three times, and this critical point is called metabolic endotoxemia. Endotoxemia caused by intestinal flora imbalance may be an important factor in the development of inflammation-mediated obesity and IR (61). When the ecosystem of intestinal flora is unbalanced, the intestinal permeability will increase, which enables LPS to enter the systemic circulation through the damaged intestinal mucosal barrier (63). Then, the carrier protein transports LPS to the membrane and binds with CD14. It stimulates the expression and production of various inflammatory factors by activating TLR4, resulting in IR, which then participates in the HA and metabolic abnormalities of PCOS (64). In conclusion, the inflammation state mediated by intestinal flora plays a significant role in the pathological process of IR and PCOS. There is a cross action between inflammatory signaling

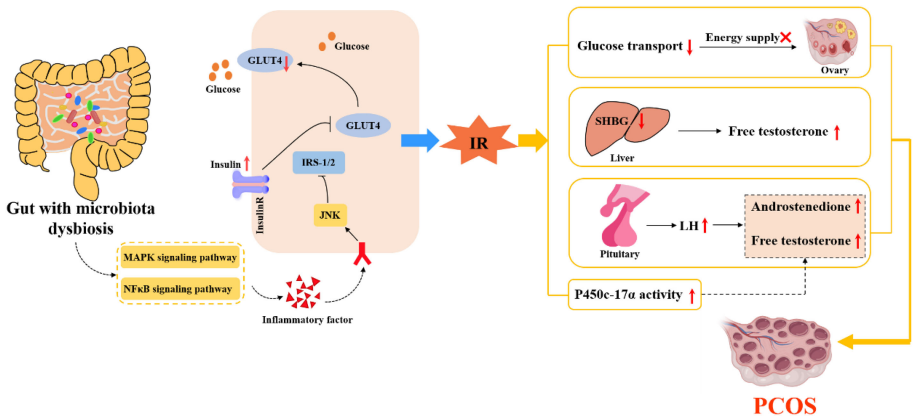


FIGURE 2
The internal relationship between IR, intestinal flora and PCOS.

pathway and insulin signaling pathway. Endotoxemia caused by intestinal flora imbalance may be the key cause of inflammation, IR, HA and obesity (65), and the possible mechanism is shown in Figure 3.

# 5 Relationship between intestinal microecological disorders and obesity in PCOS

## 5.1 Obesity and PCOS

Obesity is a disease with excessive body fat, which is closely related to IR and increases the risk of metabolic diseases, including type 2 diabetes and cardiovascular disease (39, 66, 67). Obesity is not unique to PCOS, but women with PCOS are at a higher risk of overweight, obesity, central obesity and weight gain compared to non-PCOS women (68). Compared with overall obesity, obesity in PCOS is mostly abdominal obesity, that is, fat mainly accumulates in the abdominal wall and omentum. In the case of obesity and other metabolic disorders, the production and secretion of various fat factors (such as leptin) are significantly changed, and their functions are also substantially impaired. Obesity usually exacerbates PCOS through the production of adipokines and the reduction of SHBG (66). On the one hand, adipose tissue secretes adipokines that directly induce IR and adrenal androgen overload, leading to HA and hyperinsulinemia, or abnormal release of gonadotropin (elevated LH/FSH ratio) from the hypothalamus, leading to ovarian dysfunction, which in turn leads to PCOS-related HA and ovulation dysfunction. On the other hand, obesity can inhibit the synthesis of SHBG in the liver, thus promoting the secretion of androgen and insulin, which leads to IR, while high levels of insulin and androgen further aggravate the abnormal fat distribution. At the same time, obesity aggravates the metabolic dysfunction of PCOS patients, which leads to more prone to IR (69–71). Hence, obesity and PCOS are mutually causal. Obesity in adolescence can cause irregular menstruation and thin ovulation, thus promoting the occurrence of PCOS, while obesity in PCOS patients can lead to more serious HA, IR and other endocrine disorders (72).

## 5.2 Relationship between intestinal flora and obesity in PCOS

The imbalance of intestinal flora will directly affect the metabolism and immunity of the host and induce metabolic diseases of the host. Intestinal flora plays an important role in the development of obesity (73). By observing the changes in the weight of mice fed with sterile high-fat diet and normal low-fat diet, it was found that the weight increase of mice fed with high-fat diet was significantly lower than that of normal mice, which indicated that intestinal flora played a key role in the process of diet-induced obesity (74). A study found that leptin can reduce the weight of mice fed with high-fat diet, and its mechanism was mainly related to the increase of the diversity of intestinal flora and the reduction of endotoxin content, thus reducing the inflammatory state (74). The occurrence of obesity is mainly related to the high-fat diet. The intestinal flora is disturbed under the high-fat diet, resulting in the increase of LPS production and the decrease of SCFAs production (75). Modern research has found that the imbalance of intestinal flora may lead to obesity and lipid metabolism disorder through the SCFAs and G protein coupling, bile acid metabolism (76) and LPS pathway (65). The content of SCFAs in obese patients with PCOS is lower than that in healthy women. SCFAs coupled with GPR41 and GPR43 can promote the secretion of PYY and GLP-1 by intestinal L cells, which can delay gastric emptying and increase satiety, thus controlling the intake of diet and improving the abnormality of glucose and lipid metabolism (77). Therefore, the disturbance of intestinal flora will lead to the decrease of GLP-1 secretion, accelerate gastric emptying through the stimulation of gut-brain axis, improve the appetite for food, and then affect glucose and lipid metabolism, causing IR and obesity. Meanwhile, the disturbance of intestinal flora in PCOS patients increases LPS with endotoxin function and changes intestinal permeability. The increased LPS in the blood causes endotoxemia and chronic

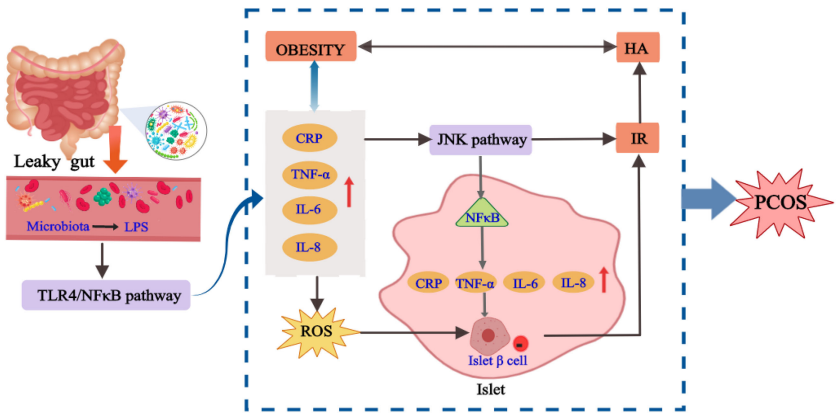


FIGURE 3
The internal relationship between chronic inflammation, intestinal flora and PCOS.

inflammation of the body, affects the function of insulin receptor, and then leads to IR and obesity (78). In addition, some intestinal flora, such as *Firmicutes* and *Bacteroidetes* (79), can encode bile brine hydrolyzase, which can metabolize primary bile acid into secondary bile acid. The composition of bile acid pool is changed by the farnesoid X receptor and the G protein-coupled bile acid receptor 1, or by dehydrogenation, dehydroxylation and epimerization, thus affecting the lipid metabolism and glucose homeostasis (80). The high-fat diet will lead to the imbalance of intestinal flora in patients, which will further affect the metabolism of glucose and lipid in patients and promote metabolic diseases such as obesity. Obesity can aggravate the IR and androgen level of PCOS patients, which may further exacerbate the metabolic disorder in PCOS patients, as shown in Figure 4. Therefore, weight loss through improving diet structure, exercise, surgery and other methods can effectively correct intestinal flora disorders (81). Improving intestinal permeability and alleviating IR can ameliorate the symptoms of HA and metabolic disorders in PCOS to a certain extent.

## 6 Discussion

The relationship between intestinal flora and PCOS has gradually become the focus of many studies in recent years. In 2012, Tremellen et al. (63) first proposed the hypothesis that PCOS is related to intestinal flora, suggesting that the imbalance of intestinal flora is associated with various manifestations of PCOS, such as HA, multiple ovarian cysts, and anovulation. Since then, the research on the relationship between intestinal flora and PCOS has started. Some studies have found that the overall diversity of intestinal flora is significantly different between patients with PCOS and healthy people, mainly reflected in the reduction of α diversity (82). Other studies have found that in the intestinal flora of patients with PCOS, specific microflora have changed, such as the change of the balance between *Bacteroides* and *Firmicutes* (83, 84), which will affect the production of short-chain fatty acids and have a negative impact on metabolism, intestinal barrier integrity and immunity. Liu et al. (85) conducted a controlled study of patients with PCOS and healthy subjects to explore the correlation between PCOS and intestinal flora. The 16SrRNA sequencing data showed that the intestinal flora diversity of patients with PCOS was lower than that of healthy people. The increase of relative abundance of *Firmicutes* and *Bacteroidetes* was positively correlated with androgen, body mass index and IR (86). In addition, after transplanting the intestinal flora of adult male mice into juvenile female mice, Markle et al. (37) found that the testosterone level in juvenile female mice increased. This indicated that the change of intestinal flora will affect the level of androgen in the serum of female mice, and indirectly participate in the occurrence and development of PCOS. Thus, intestinal flora may become a new therapeutic target for PCOS.

Although the relationship between the change of intestinal flora and PCOS has been found, there is no consensus on which bacteria are most relevant to PCOS, and the causal relationship between the two is not yet clear (87). Intestinal flora is the "endocrine organ" to maintain human health. The microbiota in the gut affects the reproductive endocrine system by interacting with estrogen, androgen, insulin, etc (63). A prospective study (88) involving 24 patients with PCOS and 19 healthy women confirmed that endotoxemia caused by gastrointestinal leakage was related to chronic inflammation, IR, fat accumulation and HA through 16S rRNA gene amplification and sequencing analysis. Kimural et al. (89) found that the body fat rate of GPR43-deficient mice was greatly increased, whereas the mice with increased GPR43 were still thin even after being fed a high-fat diet. This suggested that after ingestion of food, the body transmits signals through GPR43, a G-protein-coupled receptor for short-chain fatty acids (SCFAs), to produce and release energy to various tissues. As a protective barrier of intestinal microecology, SCFAs trigger the secretion of glucagon-like peptide through GPR43 and act on pancreatic islet P cells to regulate the production of insulin in the body, thus affecting the metabolism of PCOS. Bile acid, as a compound synthesized from cholesterol, can effectively help the utilization and digestion of lipids in the body's lipid metabolism to improve the accumulation of lipids. However, bile acid in the gut, under the stimulation of SCFAs, can promote the synthesis and secretion of incretin by intestinal cells to participate in the regulation of blood glucose (90). Zhang J et al. (91) found that the patients with PCOS have a positive effect on the production of butyric acid by improving the

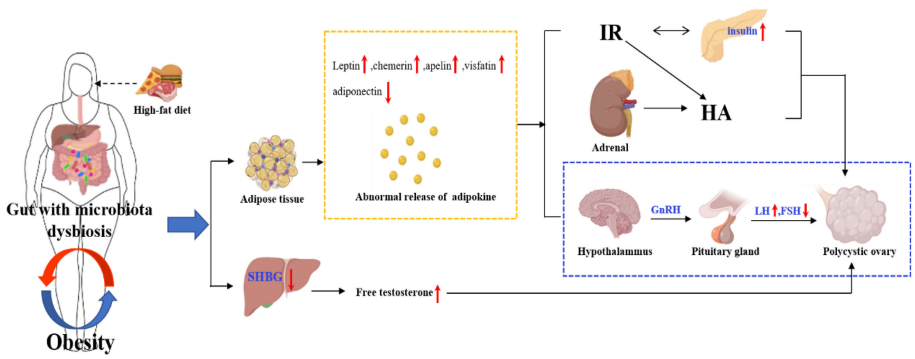


FIGURE 4
The internal relationship between obesity, intestinal flora and PCOS.

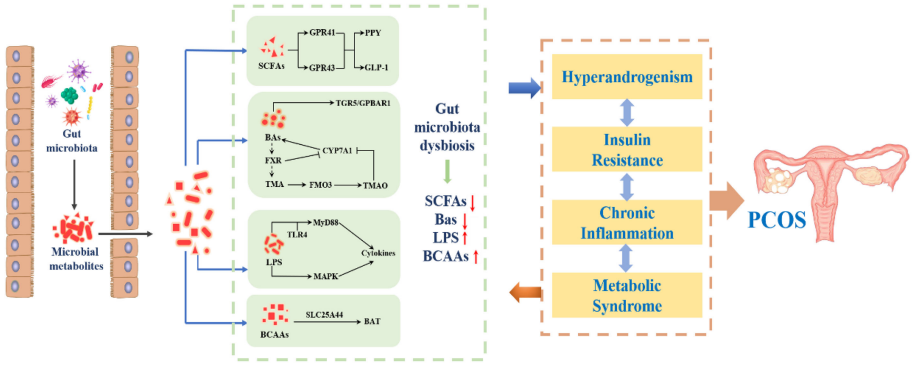


FIGURE 5
The internal relationship between intestinal flora and PCOS.

homeostasis of intestinal flora and stimulating the secretion of lactic acid, which promotes the regulation of intestinal microorganisms and improves metabolic disorders. Intestinal flora can act on the gut brain axis through gastrointestinal hormones and other mediators, and regulate the central nervous system by mediating the release of hypothalamic gonadotrophin releasing hormone (GnRH), which can aggravate the progression of PCOS (92). Currently, more than 20 of the 50 gastrointestinal hormones are known to be involved in brain-gut axis interactions (93). In conclusion, intestinal flora disorders are involved in endotoxemia, the production of SCFAs, bile acid metabolism, brain-gut axis and other processes, which are related to HA, IR, chronic inflammatory response, obesity and other manifestations of PCOS (94). Therefore, intestinal flora may participate in the pathogenesis of PCOS by influencing follicular development, sex hormone and metabolic level through HA, IR, chronic inflammation and obesity, as shown in Figure 5.

## 7 Conclusion

As a complex endocrine and metabolic disorder, PCOS is closely related to HA, IR, chronic inflammatory, obesity, etc. The intestinal flora not only affects the metabolism of androgen, but also leads to IR, inflammatory reaction and obesity, which plays a key role in the occurrence and development of PCOS. In the past, genetic factors were considered to be one of the important causes of PCOS, but so far, no exact pathogenic genes have been found. As exogenous genetic material, intestinal flora will inevitably communicate with the host's own genetic information, which will change the expression of host genes and trigger PCOS. It is precisely because the pathogenesis of PCOS is still unclear, so the treatment of PCOS is limited to the improvement of clinical symptoms such as IR, HA and ovulation disorders, rather than the radical treatment. However, with the deepening of research, the role of intestinal flora in PCOS will be gradually revealed, which is bound to provide new therapeutic strategies for PCOS.

## Author contributions

JL prepared the first draft of the manuscript. YL supervised the work and reviewed the manuscript. XL conceived the paper and revised the manuscript. All authors reviewed the manuscript and approved the submitted version.

## Funding

This study was supported by Hainan Provincial Natural Science Foundation of China (819MS061), Scientific Research Support Project of Colleges and Universities in Hainan Province (Hnky2019ZD-24), Research and Cultivation Foundation of Hainan Medical University (HYPY201910), National Natural Science Foundation of China (82160702), Academician workstation of Hainan province and the specific research fund of The Innovation Platform for Academicians of Hainan Province (No. YSPTZX202132).

## Conflict of interest

The authors declare that the research was conducted in the absence of any commercial or financial relationships that could be construed as a potential conflict of interest.

## Publisher's note

# References


1. Escobar-Morreale HF. Polycystic ovary syndrome: definition, aetiology, diagnosis and treatment. *Nat Rev Endocrinol* (2018) 14(5):270–84. doi: 10.1038/nrendo.2018.24

2. Aversa A, La Vignera S, Rago R, Gambineri A, Nappi RE, Calogero AE, et al. Fundamental concepts and novel aspects of polycystic ovarian syndrome: Expert consensus resolutions. *Front Endocrinol (Lausanne)* (2020) 11:516. doi: 10.3389/fendo.2020.00516

3. Azziz R, Sanchez LA, Knochenhauer ES, Moran C, Lazenby J, Stephens KC, et al. Androgen excess in women: experience with over 1000 consecutive patients. *J Clin Endocrinol Metab* (2004) 89(2):453–62. doi: 10.1210/jc.2003-031122

4. Armanini D, Boscaro M, Bordin L, Sabaddin C. Controversies in the pathogenesis, diagnosis and treatment of PCOS: Focus on insulin resistance, inflammation, and hyperandrogenism. *Int J Mol Sci* (2022) 23(8):4110. doi: 10.3390/ijms23084110

5. Sirmans SM, Pate KA. Epidemiology, diagnosis, and management of polycystic ovary syndrome. *Clin Epidemiol* (2013) 6:1–13. doi: 10.2147/CLEP.S37559

6. Palomba S, de Wilde MA, Falbo A, Koster MPH, Battista La Sala G, Fauser BC. Pregnancy complications in women with polycystic ovary syndrome. *Hum Reprod Update* (2015) 21(5):575–92. doi: 10.1093/humupd/dmv029

7. Lizneva D, Suturina L, Walker W, Brakta S, Gavrilova-Jordan L, Azziz R. Criteria, prevalence, and phenotypes of polycystic ovary syndrome. *Fertil Steril* (2016) 106(1):6–15. doi: 10.1016/j.fertnstert.2016.05.003

8. Sangaraju SL, Yepez D, Grandes XA, Manjunatha RT, Habib S. Cardio-metabolic disease and polycystic ovarian syndrome (PCOS): A narrative review. *Cureus* (2022) 14(5):e25076. doi: 10.7759/cureus.25076

9. Teede H, Deeks A, Moran L. Polycystic ovary syndrome: a complex condition with psychological, reproductive and metabolic manifestations that impacts on health across the lifespan. *BMC Med* (2010) 8:41. doi: 10.1186/1741-7015-8-41

10. Shawky NM. Cardiovascular disease risk in offspring of polycystic ovary syndrome. *Front Endocrinol (Lausanne)* (2022) 13:977819. doi: 10.3389/fendo.2022.977819

11. Giampaolino P, Foreste V, Di Filippo C, Gallo A, Mercorio A, Serafino P, et al. Microbiome and PCOS: State-of-Art and future aspects. *Int J Mol Sci* (2021) 22(4):2048. doi: 10.3390/ijms22042048

12. Sadeghi HM, Adeli I, Calina D, Docea AO, Mousavi T, Daniali M, et al. Polycystic ovary syndrome: A comprehensive review of pathogenesis, management, and drug repurposing. *Int J Mol Sci* (2022) 23(2):583. doi: 10.3390/ijms23020583

13. Stener-Victorin E, Padmanabhan V, Walters KA, Li XY, Wu Y, Tan ZJ, et al. Animal models to understand the etiology and pathophysiology of polycystic ovary syndrome. *Endocr Rev* (2020) 41(4):bnaa010. doi: 10.1210/endrev/bnaa010

14. Wang L, Zhou J, Gober HJ, Leung WT, Huang ZS, Pan XY, et al. Alterations in the intestinal microbiome associated with PCOS affect the clinical phenotype. *BioMed Pharmacother* (2021) 133:110958. doi: 10.1016/j.biopha.2020.110958

15. He FF, Li YM. Role of gut microbiota in the development of insulin resistance and the mechanism underlying polycystic ovary syndrome: a review. *J Ovarian Res* (2020) 13(1):73. doi: 10.1186/s13048-020-00670-3

16. Zhou B, Yuan Y, Zhang S, Guo G, Li XL, Li GY, et al. Intestinal flora and disease mutually shape the regional immune system in the intestinal tract. *Front Immunol* (2020) 11:575. doi: 10.3389/fimmu.2020.00575

17. Guo K, Xu S, Zhang Q, Peng MJ, Yang ZY, Li WG, et al. Bacterial diversity in the intestinal mucosa of mice fed with asparagus extract under high-fat diet condition. *3 Biotech* (2020) 10(5):228. doi: 10.1007/s13205-020-02225-1

18. Fassarella M, Blaak EE, Penders J, Nauta A, Smidt H, Zoetendal EG. Gut microbiome stability and resilience: elucidating the response to perturbations in order to modulate gut health. *Gut* (2021) 70(3):595–605. doi: 10.1136/gutjnl-2020-321747

19. Adelman MW, Woodworth MH, Langelier C, Busch LM, Kempker JA, Kraft CS, et al. The gut microbiome's role in the development, maintenance, and outcomes of sepsis. *Crit Care* (2020) 24(1):278. doi: 10.1186/s13054-020-02989-1

20. Mousa WK, Chehadeh F, Husband S. Microbial dysbiosis in the gut drives systemic autoimmune diseases. *Front Immunol* (2022) 13:906258. doi: 10.3389/fimmu.2022.906258

21. Zhang CY, Peng XX, Shao HQ, Li XY, Wu Y, Tan ZJ. Gut microbiota comparison between intestinal contents and mucosa in mice with repeated stress-related diarrhea provides novel insight. *Front Microbiol* (2021) 12:626691. doi: 10.3389/fmicb.2021.626691

22. Li C, Zhou K, Xiao N, Peng MJ, Tan ZJ. The effect of qiweibaizhu powder crude polysaccharide on antibiotic-associated diarrhea mice is associated with restoring intestinal mucosal bacteria. *Front Nutr* (2022) 9:952647. doi: 10.3389/fnut.2022.952647

23. He F, Li Y. The gut microbial composition in polycystic ovary syndrome with insulin resistance: findings from a normal-weight population. *J Ovarian Res* (2021) 14(1):50. doi: 10.1186/s13048-021-00799-9

24. Jeanes YM, Reeves S. Metabolic consequences of obesity and insulin resistance in polycystic ovary syndrome: diagnostic and methodological challenges. *Nutr Res Rev* (2017) 30(1):97–105. doi: 10.1017/S0954422416000287

25. Fox CW, Zhang L, Sohni A, Doblado M, Wilkinson MF, Chang RJ, et al. Inflammatory stimuli trigger increased androgen production and shifts in gene expression in theca-interstitial cells. *Endocrinology* (2019) 160(12):2946–58. doi: 10.1210/en.2019-00588

26. Chen W, Pang Y. Metabolic syndrome and PCOS: Pathogenesis and the role of metabolites. *Metabolites* (2021) 11(12):869. doi: 10.3390/metabo11120869

27. Sanchez-Garrido MA, Tena-Sempere M. Metabolic dysfunction in polycystic ovary syndrome: Pathogenic role of androgen excess and potential therapeutic strategies. *Mol Metab* (2020) 35:100937. doi: 10.1016/j.molmet.2020.01.001

28. Rosenfield RL, Ehrmann DA. The pathogenesis of polycystic ovary syndrome (PCOS): The hypothesis of PCOS as functional ovarian hyperandrogenism revisited. *Endocr Rev* (2016) 37(5):467–520. doi: 10.1210/er.2015-1104

29. Lebbe M, Woodruff TK. Involvement of androgens in ovarian health and disease. *Mol Hum Reprod* (2013) 19(12):828–37. doi: 10.1093/molehr/gat065

30. Laven JSE. Follicle stimulating hormone receptor (FSHR) polymorphisms and polycystic ovary syndrome (PCOS). *Front Endocrinol (Lausanne)* (2019) 10:23. doi: 10.3389/fendo.2019.00023

31. Dumesic DA, Oberfield SE, Stener-Victorin E, Marshall JC, Laven JS, Legro RS. Scientific statement on the diagnostic criteria, epidemiology, pathophysiology, and molecular genetics of polycystic ovary syndrome. *Endocr Rev* (2015) 36(5):487–525. doi: 10.1210/er.2015-1018

32. Wang J, Wu D, Guo H, Li MX. Hyperandrogenemia and insulin resistance: The chief culprit of polycystic ovary syndrome. *Life Sci* (2019) 236:116940. doi: 10.1016/j.lfs.2019.116940

33. Jobira B, Frank DN, Pyle L, Silveira LJ, Kelsey MM, Garcia-Reyes Y, et al. Obese adolescents with PCOS have altered biodiversity and relative abundance in gastrointestinal microbiota. *J Clin Endocrinol Metab* (2020) 105(6):e2134-44. doi: 10.1210/clinem/dgz263

34. Torres PJ, Siakowska M, Banaszewska B, Pawelczyk L, Duleba AJ, Kelley ST, et al. Gut microbial diversity in women with polycystic ovary syndrome correlates with hyperandrogenism. *J Clin Endocrinol Metab* (2018) 103(4):1502–11. doi: 10.1210/jc.2017-02153

35. Zeng B, Lai Z, Sun L, Zhang Z, Yang J, Li Z, et al. Structural and functional profiles of the gut microbial community in polycystic ovary syndrome with insulin resistance (IR-PCOS): a pilot study. *Res Microbiol* (2019) 170(1):43–52. doi: 10.1016/j.resmic.2018.09.002

36. Kelley ST, Skarra DV, Rivera AJ, Thackray VG. The gut microbiome is altered in a letrozole-induced mouse model of polycystic ovary syndrome. *PloS One* (2016) 11(1):e0146509. doi: 10.1371/journal.pone.0146509

37. Markle JG, Frank DN, Mortin-Toth S, Robertson CE, Feazel LM, Rolle-Kampczyk U, et al. Sex differences in the gut microbiome drive hormone-dependent regulation of autoimmunity. *Science* (2013) 339(6123):1084–8. doi: 10.1126/science.1233521

38. Xie F, Anderson CL, Timme KR, Kurz SG, Fernando SC, Wood JR, et al. Obesity-dependent increases in oocyte mRNAs are associated with increases in proinflammatory signaling and gut microbial abundance of lachnospiraceae in female mice. *Endocrinology* (2016) 157(4):1630–43. doi: 10.1210/en.2015-1851

39. Calcaterra V, Verduci E, Cena H, Magenes VC, Todisco CF, Tenuta E, et al. Polycystic ovary syndrome in insulin-resistant adolescents with obesity: The role of nutrition therapy and food supplements as a strategy to protect fertility. *Nutrients* (2021) 13(6):1–32. doi: 10.3390/nu13061848

40. Li M, Chi X, Wang Y, Setrerrahmane S, Xie WW, Xu HM, et al. Trends in insulin resistance: insights into mechanisms and therapeutic strategy. *Signal Transduct Target Ther* (2022) 7(1):216. doi: 10.1038/s41392-022-01073-0

41. Xu Y, Fu JF, Chen JH, Zhang ZW, Zou ZQ, Han LY, et al. Sulforaphane ameliorates glucose intolerance in obese mice *via* the upregulation of the insulin signaling pathway. *Food Funct* (2018) 9(9):4695–701. doi: 10.1039/C8FO00763B

42. Ding H, Zhang J, Zhang F, Zhang SG, Chen XZ, Liang WQ, et al. Resistance to the insulin and elevated level of androgen: A major cause of polycystic ovary syndrome. *Front Endocrinol (Lausanne)* (2021) 12:741764. doi: 10.3389/fendo.2021.741764

43. Bäckhed F, Ding H, Wang T, Hooper LV, Koh GY, Nagy A, et al. The gut microbiota as an environmental factor that regulates fat storage. *Proc Natl Acad Sci U.S.A.* (2004) 101(44):15718–23. doi: 10.1073/pnas.0407076101

44. Dubey P, Reddy S, Boyd S, Bracamontes C, Sanchez S, Chattopadhyay M, et al. Effect of nutritional supplementation on oxidative stress and hormonal and lipid profiles in PCOS-affected females. *Nutrients* (2021) 13(9):2938. doi: 10.3390/nu13092938

45. Vrieze A, Van Nood E, Holleman F, Salojärvi J, Kootte RS, Bartelsman JFWM, et al. Transfer of intestinal microbiota from lean donors increases insulin sensitivity in individuals with metabolic syndrome. *Gastroenterology* (2012) 143(4):913–6.e7. doi: 10.1053/j.gastro.2012.06.031

46. Mor E, Zograbyan A, Saadat P, Bayrak A, Tourgeman DE, Zhang C, et al. The insulin resistant subphenotype of polycystic ovary syndrome: clinical parameters and pathogenesis. *Am J Obstet Gynecol* (2004) 190(6):1654–60. doi: 10.1016/j.ajog.2004.02.052

47. Pedersen HK, Gudmundsdottir V, Nielsen HB, Hyotylainen T, Nielsen T, Jensen BAH, et al. Human gut microbes impact host serum metabolome and insulin sensitivity. *Nature* (2016) 535(7612):376–81. doi: 10.1038/nature18646

48. Zhang CM, Zhao Y, Li R, Yu Y, Yan L-Y, Li L, et al. Metabolic heterogeneity of follicular amino acids in polycystic ovary syndrome is affected by obesity and related to pregnancy outcome. *BMC Pregnancy Childbirth* (2014) 14:11. doi: 10.1186/1471-2393-14-11

49. Bremer AA, Miller WL. The serine phosphorylation hypothesis of polycystic ovary syndrome: a unifying mechanism for hyperandrogenemia and insulin resistance. *Fertil Steril* (2008) 89(5):1039–48. doi: 10.1016/j.fertnstert.2008.02.091

50. Kelly CC, Lyall H, Petrie JR, Gould GW, Connell JMC, Sattar N. Low grade chronic inflammation in women with polycystic ovarian syndrome. *J Clin Endocrinol Metab* (2001) 86(6):2453–5. doi: 10.1210/jcem.86.6.7580

51. Alanbay I, Ercan CM, Sakinci M, Coksuer H, Ozturk M, Tapan S. A macrophage activation marker chitotriosidase in women with PCOS: does low-grade chronic inflammation in PCOS relate to PCOS itself or obesity? *Arch Gynecol Obstet* (2012) 286(4):1065–71. doi: 10.1007/s00404-012-2425-0

52. Solinas G, Becattini B. JNK at the crossroad of obesity, insulin resistance, and cell stress response. *Mol Metab* (2017) 6(2):174–84. doi: 10.1016/j.molmet.2016.12.001

53. Hameed I, Masoodi SR, Mir SA, Nabi M, Ghazanfar K, Ganai BA, et al. Type 2 diabetes mellitus: From a metabolic disorder to an inflammatory condition. *World J Diabetes* (2015) 6(4):598–612. doi: 10.4239/wjd.v6.i4.598

54. Tak PP, Firestein GS. NF-kappaB: a key role in inflammatory diseases. *J Clin Invest* (2001) 107(1):7–11. doi: 10.1172/JCI11830

55. Gong Y, Luo S, Fan P, Zhu H, Li Y, Huang W. Growth hormone activates PI3K/Akt signaling and inhibits ROS accumulation and apoptosis in granulosa cells of patients with polycystic ovary syndrome. *Reprod Biol Endocrinol* (2020) 18(1):121. doi: 10.1186/s12958-020-00677-x

56. Pandey AK, Gupta A, Tiwari M, Prasad S, Pandey AN, Yadav PK, et al. Impact of stress on female reproductive health disorders: Possible beneficial effects of shatavari (Asparagus racemosus). *BioMed Pharmacother* (2018) 103:46–9. doi: 10.1016/j.biopha.2018.04.003

57. Schiffer L, Bossey A, Kempegowda P, Taylor AE, Akerman I, Scheel-Toellner D, et al. Peripheral blood mononuclear cells preferentially activate 11-oxygenated androgens. *Eur J Endocrinol* (2021) 184(3):353–63. doi: 10.1530/EJE-20-1077

58. González F, Nair KS, Daniels JK, Basal E, Schimke JM. Hyperandrogenism sensitizes mononuclear cells to promote glucose-induced inflammation in lean reproductive-age women. *Am J Physiol Endocrinol Metab* (2012) 302(3):E297–306. doi: 10.1152/ajpendo.00416.2011

59. Engin A. The pathogenesis of obesity-associated adipose tissue inflammation. *Adv Exp Med Biol* (2017) 960:221–45. doi: 10.1007/978-3-319-48382-5_9

60. Jarrett BY, Lujan ME. Impact of hypocaloric dietary intervention on ovulation in obese women with PCOS. *Reproduction* (2016), REP–16-0385. doi: 10.1530/REP-16-0385

61. Cani PD, Amar J, Iglesias MA, Poggi M, Knauf C, Bastelica D, et al. Metabolic endotoxemia initiates obesity and insulin resistance. *Diabetes* (2007) 56(7):1761–72. doi: 10.2337/db06-1491

62. Xue J, Li X, Liu P, Li K, Sha L, Yang X, et al. Inulin and metformin ameliorate polycystic ovary syndrome *via* anti-inflammation and modulating gut microbiota in mice. *Endocr J* (2019) 66(10):859–70. doi: 10.1507/endocrj.EJ18-0567

63. Tremellen K, Pearce K. Dysbiosis of gut microbiota (DOGMA)–a novel theory for the development of polycystic ovarian syndrome. *Med Hypotheses* (2012) 79(1):104–12. doi: 10.1016/j.mehy.2012.04.016

64. Boutagy NE, McMillan RP, Frisard MI, Hulver MW. Metabolic endotoxemia with obesity: Is it real and is it relevant? *Biochimie* (2016) 124:11–20. doi: 10.1016/j.biochi.2015.06.020

65. Sjögren YM, Tomicic S, Lundberg A, Böttcher MF, Björkstén B, Sverremark-Ekström E, et al. Influence of early gut microbiota on the maturation of childhood mucosal and systemic immune responses. *Clin Exp Allergy* (2009) 39(12):1842–51. doi: 10.1111/j.1365-2222.2009.03326.x

66. Glueck CJ, Goldenberg N. Characteristics of obesity in polycystic ovary syndrome: Etiology, treatment, and genetics. *Metabolism* (2019) 92:108–20. doi: 10.1016/j.metabol.2018.11.002

67. Xu Y, Zhu H, Li W, Chen D, Xu Y, Xu A, et al. Targeting adipokines in polycystic ovary syndrome and related metabolic disorders: from experimental insights to clinical studies. *Pharmacol Ther* (2022) 240:108284. doi: 10.1016/j.pharmthera.2022.108284

68. Wang Z, Groen H, Cantineau AEP, van Elten TM, Karsten MDA, van Oers AM, et al. Dietary intake, eating behavior, physical activity, and quality of life in infertile women with PCOS and obesity compared with non-PCOS obese controls. *Nutrients* (2021) 13(10):3526. doi: 10.3390/nu13103526

69. Pasquali R, Casimirri F, Venturoli S, Antonio M, Morselli L, Reho S, et al. Body fat distribution has weight-independent effects on clinical, hormonal, and metabolic features of women with polycystic ovary syndrome. *Metabolism* (1994) 43(6):706–13. doi: 10.1016/0026-0495(94)90118-X

70. Motta AB. The role of obesity in the development of polycystic ovary syndrome. *Curr Pharm Des* (2012) 18(17):2482–91. doi: 10.2174/13816128112092482

71. Barber TM, Hanson P, Weickert MO, Franks S. Obesity and polycystic ovary syndrome: Implications for pathogenesis and novel management strategies. *Clin Med Insights Reprod Health* (2019) 13:1179558119874042. doi: 10.1177/1179558119874042

72. Simon S, Rahat H, Carreau AM, Garcia-Reyes Y, Halbower A, Pyle L, et al. Poor sleep is related to metabolic syndrome severity in adolescents with PCOS and obesity. *J Clin Endocrinol Metab* (2020) 105(4):e1827–34. doi: 10.1210/clinem/dgz285

73. Xu Y, Wang N, Tan HY, Zhang C, Feng Y. Function of akkermansia muciniphila in obesity: Interactions with lipid metabolism, immune response and gut systems. *Front Microbiol* (2020) 11:219. doi: 10.3389/fmicb.2020.00219

74. Bäckhed F, Manchester JK, Semenkovich CF, Gordon JI. Mechanisms underlying the resistance to diet-induced obesity in germ-free mice. *Proc Natl Acad Sci U.S.A.* (2007) 104(3):979–84. doi: 10.1073/pnas.0605374104

75. Kimura I, Ichimura A, Ohue-Kitano R, Igarashi M. Free fatty acid receptors in health and disease. *Physiol Rev* (2020) 100(1):171–210. doi: 10.1152/physrev.00041.2018

76. Ridaura VK, Faith JJ, Rey FE, Cheng J, Duncan AE, Kau AL, et al. Gut microbiota from twins discordant for obesity modulate metabolism in mice. *Science* (2013) 341(6150):1241214. doi: 10.1126/science.1241214

77. Lin W, Wen L, Wen J, Xiang GD. Effects of sleeve gastrectomy on fecal gut microbiota and short-chain fatty acid content in a rat model of polycystic ovary syndrome. *Front Endocrinol (Lausanne)* (2021) 12:747888. doi: 10.3389/fendo.2021.747888

78. González F, Considine RV, Abdelhadi OA, Acton AJ. Saturated fat ingestion promotes lipopolysaccharide-mediated inflammation and insulin resistance in polycystic ovary Syndrome[J]. *J Clin Endocrinol Metab* (2019) 104(3):934–46. doi: 10.1210/jc.2018-01143

79. Jones BV, Begley M, Hill C, Gahan CGM, Marchesi JR. Functional and comparative metagenomic analysis of bile salt hydrolase activity in the human gut microbiome. *Proc Natl Acad Sci U.S.A.* (2008) 105(36):13580–5. doi: 10.1073/pnas.0804437105

80. Romo-Vaquero M, Cortés-Martín A, Loria-Kohen V, Ramírez-de-Molina A, García-Mantrana I, Collado MC, et al. Deciphering the human gut microbiome of urolithin metabotypes: Association with enterotypes and potential cardiometabolic health implications. *Mol Nutr Food Res* (2019) 63(4):e1800958. doi: 10.1002/mnfr.201800958

81. Cincione RI, Losavio F, Ciolli F, Valenzano A, Cibelli G, Messina G, et al. Effects of mixed of a ketogenic diet in overweight and obese women with polycystic ovary syndrome. *Int J Environ Res Public Health* (2021) 18(23):12490. doi: 10.3390/ijerph182312490

82. Thackray VG. Sex, microbes, and polycystic ovary syndrome. *Trends Endocrinol Metab* (2019) 30(1):54–65. doi: 10.1016/j.tem.2018.11.001

83. Wang T, Sha L, Li Y, Zhu LL, Wang Z, Li K, et al. Dietary α-linolenic acid-rich flaxseed oil exerts beneficial effects on polycystic ovary syndrome through sex steroid hormones-Microbiota-Inflammation axis in rats. *Front Endocrinol (Lausanne)* (2020) 11:284. doi: 10.3389/fendo.2020.00284

84. Jobira B, Frank DN, Silveira LJ, Pyle L, Kelsey MM, Garcia-Reyes Y, et al. Hepatic steatosis relates to gastrointestinal microbiota changes in obese girls with polycystic ovary syndrome. *PloS One* (2021) 16(1):e0245219. doi: 10.1371/journal.pone.0245219

85. Liu R, Zhang C, Shi Y, Zhang F, Li LX, Wang XJ, et al. Dysbiosis of gut microbiota associated with clinical parameters in polycystic ovary syndrome. *Front Microbiol* (2017) 8:324. doi: 10.3389/fmicb.2017.00324

86. Zeng X, Xie YJ, Liu YT, Long SL, Mo ZC. Polycystic ovarian syndrome: Correlation between hyperandrogenism, insulin resistance and obesity. *Clin Chim Acta* (2020) 502:214–21. doi: 10.1016/j.cca.2019.11.003

87. Qi X, Yun C, Sun L, Xia JL, Wu Q, Wang Y, et al. Gut microbiota-bile acid-interleukin-22 axis orchestrates polycystic ovary syndrome. *Nat Med* (2019) 25(8):1225–33. doi: 10.1038/s41591-019-0509-0

88. Lindheim L, Bashir M, Münzker J, Trummer C, Zachhuber V, Leber B, et al. Alterations in gut microbiome composition and barrier function are associated with reproductive and metabolic defects in women with polycystic ovary syndrome (PCOS): A pilot study. *PloS One* (2017) 12(1):e0168390. doi: 10.1371/journal.pone.0168390

89. Kimura I, Ozawa K, Inoue D, Imamura T, Kimura K, Maeda T, et al. The gut microbiota suppresses insulin-mediated fat accumulation *via* the short-chain fatty acid receptor GPR43. *Nat Commun* (2013) 4:1829. doi: 10.1038/ncomms2852

90. Cicione C, Degirolamo C, Moschetta A. Emerging role of fibroblast growth factors 15/19 and 21 as metabolic integrators in the liver. *Hepatology* (2012) 56(6):2404–11. doi: 10.1002/hep.25929

91. Zhang J, Sun Z, Jiang S, Bai XY, Ma CC, Peng QN, et al. Probiotic bifidobacterium lactis V9 regulates the secretion of sex hormones in polycystic ovary syndrome patients through the gut-brain axis. *mSystems* (2019) 4(2):e00017–19. doi: 10.1128/mSystems.00017-19

92. Liao B, Qiao J, Pang Y. Central regulation of PCOS: Abnormal neuronal-Reproductive-Metabolic circuits in PCOS pathophysiology. *Front Endocrinol (Lausanne)* (2021) 12:667422. doi: 10.3389/fendo.2021.667422

93. Lach G, Schellekens H, Dinan TG, Cryan JF. Anxiety, depression, and the microbiome: A role for gut peptides. *Neurotherapeutics* (2018) 15(1):36–59. doi: 10.1007/s13311-017-0585-0

94. Rudnicka E, Suchta K, Grymowicz M, et al. Chronic Low Grade Inflammation in Pathogenesis of PCOS. *Int J Mol Sci* (2021) 22(7):3789. doi: 10.3390/ijms22073789

# Frontiers in Endocrinology

**Explores the endocrine system to find new therapies for key health issues**

The second most-cited endocrinology and metabolism journal, which advances our understanding of the endocrine system. It uncovers new therapies for prevalent health issues such as obesity, diabetes, reproduction, and aging.

---

## Discover the latest Research Topics

See more →

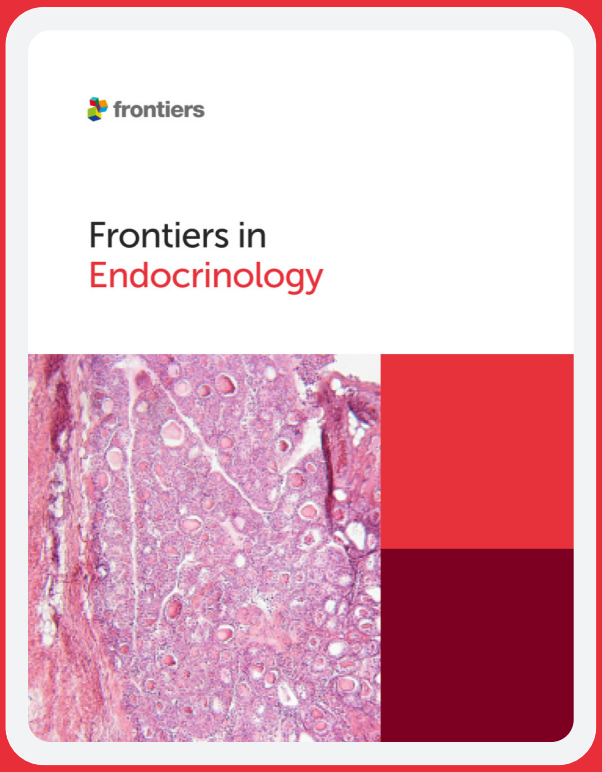


**Frontiers**

Avenue du Tribunal-Fédéral 34
1005 Lausanne, Switzerland
frontiersin.org

**Contact us**

+41 (0)21 510 17 00
frontiersin.org/about/contact